frontiers | Research Topics

Gliomas microenvironment: New drug entities, mechanisms of action, molecular biomarkers and drug delivery strategies

Edited by
Célia Cabral, Mariana Magalhães, Diana Matias and Claudia Carbone

Published in
Frontiers in Pharmacology
Frontiers in Oncology

FRONTIERS EBOOK COPYRIGHT STATEMENT

The copyright in the text of individual articles in this ebook is the property of their respective authors or their respective institutions or funders. The copyright in graphics and images within each article may be subject to copyright of other parties. In both cases this is subject to a license granted to Frontiers.

The compilation of articles constituting this ebook is the property of Frontiers.

Each article within this ebook, and the ebook itself, are published under the most recent version of the Creative Commons CC-BY licence. The version current at the date of publication of this ebook is CC-BY 4.0. If the CC-BY licence is updated, the licence granted by Frontiers is automatically updated to the new version.

When exercising any right under the CC-BY licence, Frontiers must be attributed as the original publisher of the article or ebook, as applicable.

Authors have the responsibility of ensuring that any graphics or other materials which are the property of others may be included in the CC-BY licence, but this should be checked before relying on the CC-BY licence to reproduce those materials. Any copyright notices relating to those materials must be complied with.

Copyright and source acknowledgement notices may not be removed and must be displayed in any copy, derivative work or partial copy which includes the elements in question.

All copyright, and all rights therein, are protected by national and international copyright laws. The above represents a summary only. For further information please read Frontiers' Conditions for Website Use and Copyright Statement, and the applicable CC-BY licence.

ISSN 1664-8714
ISBN 978-2-8325-4987-2
DOI 10.3389/978-2-8325-4987-2

About Frontiers

Frontiers is more than just an open access publisher of scholarly articles: it is a pioneering approach to the world of academia, radically improving the way scholarly research is managed. The grand vision of Frontiers is a world where all people have an equal opportunity to seek, share and generate knowledge. Frontiers provides immediate and permanent online open access to all its publications, but this alone is not enough to realize our grand goals.

Frontiers journal series

The Frontiers journal series is a multi-tier and interdisciplinary set of open-access, online journals, promising a paradigm shift from the current review, selection and dissemination processes in academic publishing. All Frontiers journals are driven by researchers for researchers; therefore, they constitute a service to the scholarly community. At the same time, the *Frontiers journal series* operates on a revolutionary invention, the tiered publishing system, initially addressing specific communities of scholars, and gradually climbing up to broader public understanding, thus serving the interests of the lay society, too.

Dedication to quality

Each Frontiers article is a landmark of the highest quality, thanks to genuinely collaborative interactions between authors and review editors, who include some of the world's best academicians. Research must be certified by peers before entering a stream of knowledge that may eventually reach the public - and shape society; therefore, Frontiers only applies the most rigorous and unbiased reviews. Frontiers revolutionizes research publishing by freely delivering the most outstanding research, evaluated with no bias from both the academic and social point of view. By applying the most advanced information technologies, Frontiers is catapulting scholarly publishing into a new generation.

What are Frontiers Research Topics?

Frontiers Research Topics are very popular trademarks of the *Frontiers journals series*: they are collections of at least ten articles, all centered on a particular subject. With their unique mix of varied contributions from Original Research to Review Articles, Frontiers Research Topics unify the most influential researchers, the latest key findings and historical advances in a hot research area.

Find out more on how to host your own Frontiers Research Topic or contribute to one as an author by contacting the Frontiers editorial office: frontiersin.org/about/contact

Gliomas microenvironment: New drug entities, mechanisms of action, molecular biomarkers and drug delivery strategies

Topic editors

Célia Cabral — University of Coimbra, Portugal
Mariana Magalhães — University of Coimbra, Portugal
Diana Matias — Universidade de Lisboa, Portugal
Claudia Carbone — University of Catania, Italy

Citation

Cabral, C., Magalhães, M., Matias, D., Carbone, C., eds. (2024). *Gliomas microenvironment: New drug entities, mechanisms of action, molecular biomarkers and drug delivery strategies*. Lausanne: Frontiers Media SA.
doi: 10.3389/978-2-8325-4987-2

Table of contents

frontiers | Frontiers in Pharmacology

TYPE Editorial
PUBLISHED 05 June 2024
DOI 10.3389/fphar.2024.1431975

Check for updates

OPEN ACCESS

EDITED AND REVIEWED BY
Olivier Feron,
Université catholique de Louvain, Belgium

*CORRESPONDENCE
Mariana Magalhães,
mmagalhaes@cnc.uc.pt

RECEIVED 13 May 2024
ACCEPTED 23 May 2024
PUBLISHED 05 June 2024

CITATION
Magalhães M, Matias D, Carbone C and Cabral C (2024), Editorial: Gliomas microenvironment: new drug entities, mechanisms of action, molecular biomarkers and drug delivery strategies.
Front. Pharmacol. 15:1431975.
doi: 10.3389/fphar.2024.1431975

COPYRIGHT
© 2024 Magalhães, Matias, Carbone and Cabral. This is an open-access article distributed under the terms of the Creative Commons Attribution License (CC BY). The use, distribution or reproduction in other forums is permitted, provided the original author(s) and the copyright owner(s) are credited and that the original publication in this journal is cited, in accordance with accepted academic practice. No use, distribution or reproduction is permitted which does not comply with these terms.

Editorial: Gliomas microenvironment: new drug entities, mechanisms of action, molecular biomarkers and drug delivery strategies

Mariana Magalhães[1,2,3]*, Diana Matias[4], Claudia Carbone[5] and Célia Cabral[2,3,6]

[1]University of Coimbra, Institute for Interdisciplinary Research (IIIUC), Center for Neuroscience and Cell Biology (CNC), Coimbra, Portugal, [2]University of Coimbra, Coimbra Institute for Clinical and Biomedical Research (iCBR), Clinic Academic Center of Coimbra (CACC), Faculty of Medicine, Coimbra, Portugal, [3]University of Coimbra, Center for Innovative Biomedicine and Biotechnology (CIBB), Coimbra, Portugal, [4]Faculdade de Medicina, Instituto de Medicina Molecular João Lobo Antunes, Universidade de Lisboa, Lisbon, Portugal, [5]Department of Drug and Health Sciences, University of Catania, Catania, Italy, [6]University of Coimbra, Centre for Functional Ecology, Department of Life Sciences, Coimbra, Portugal

KEYWORDS

gliomas, glioblastoma, tumor microenvironment, drug repurposing, drug delivery, biomarkers, nanotechnology

Editorial on the Research Topic
Gliomas microenvironment: new drug entities, mechanisms of action, molecular biomarkers and drug delivery strategies

This Research Topic explores the tumor microenvironment of gliomas, highlighting the importance of understanding their molecular and cellular mechanisms for the development of personalized therapies with enhanced efficacy and tolerability. We have invited authors to contribute with original research and review articles, each providing insight into the experimental validation of novel bioactive molecules and the discovery of potential molecular biomarkers for tumor-specific therapies.

Among the submissions, we have selected 10 manuscripts of exceptional quality that include articles in the following categories: original research, review, systematic review, hypothesis and theory, perspective, and technology and code. These contributions cover a spectrum of human research methodologies, offering diverse perspectives on common themes.

Li et al. explored the molecular mechanisms underlying the potential efficacy of imipramine, an antidepressant, in the treatment of glioblastoma (GB). Using bioinformatics tools and human databases, the authors analyzed 77 samples from GB patients and 23 samples from healthy individuals. Their study identified the neuron-derived epidermal growth factor receptor (EGFR) as a potential target of imipramine, suggesting its role in modulating interactions between neurons, myeloid cells, and macrophages. Furthermore, they proposed the ability of imipramine to target EGFR mutants, potentially influencing GB treatment and drug resistance. These findings unveil novel avenues for targeted GB therapies.

Li and Xu conducted a comprehensive review on harnessing mitochondria as a therapeutic target in GB. The researchers explored natural bioactive compounds that target mitophagy and induce apoptosis via the mitochondrial pathway in GB models. Additionally, they discussed nanomedicine and sonodynamic therapy strategies to overcome biological barriers, including the blood-brain barrier (BBB), to improve drug delivery for targeted GB therapy. Their work highlights the potential of novel targeted therapies based on natural lead compounds to target mitochondria for improved GB treatment outcomes.

Wang and He conducted a comprehensive analysis of low-grade gliomas (LGGs), focusing on molecular subtypes, immune responses, and a prognostic signature linked to epithelial-mesenchymal transition (EMT) genes. Their study aimed to design new therapeutic strategies and discover new drugs for the treatment of LGGs. Employing a multi-omics approach and validating their findings *in vitro*, they revealed tumor heterogeneity driven by EMT-related gene expression variations. They categorized LGG-EMT into two subtypes with distinct clinical outcomes, clinicopathological features, mutational profiles, immune cell infiltration, and tumor microenvironment characteristics. This heterogeneity determines differential responses to immunotherapy and chemotherapy, guiding precise treatment decisions. Additionally, they developed a reliable EMT signature for LGG prognosis and identified potential small molecules to improve clinical outcomes. Their findings suggest a potential prognostic tool that is pivotal for personalized treatment strategies and prognostic assessment for LGGs.

Wang and He investigated the role of chloride intracellular channel 1 (CLIC1) in gliomas. Through a multi-omics approach and *in vitro* studies, they uncovered the therapeutic potential of targeting CLIC1 and elucidated its molecular mechanisms in low-grade gliomas (LGGs) and GB progression. Their findings suggest that elevated CLIC1 levels correlate with poorer survival outcomes in glioma patients. Knockdown experiments revealed CLIC1 as a potential treatment vulnerability and actionable target in gliomas, providing insights into prognostic factors and therapeutic avenues for glioma management.

Laws et al. have provided a fascinating insight into the potential mechanism by which primary cilia contribute to tumor-induced immunosuppression in GB. Their research, conducted with GB cell models and molecular techniques, revealed that suppressing CCRK, KIF3A, and IFT88 proteins led to the loss of primary cilia and decreased IL-6 levels. This study not only highlighted the involvement of primary cilia in IL-6 release and immunosuppression but also suggested a possible role in extracellular vesicle (EV) release. These findings could potentially revolutionize our understanding of GB and open new avenues for innovative therapeutic strategies targeting cilia.

Yang et al. delved into the connection between glioma and glycosylation. By employing bioinformatics methodologies alongside *in vitro* experiments, they elucidated the role of glycosylation modification in tumor progression, which is strongly correlated with glioma prognosis. The authors identified five prognosis-related genes implicated in glycosylation. Subsequently, they developed a predictive model using a glycosylation signature, which demonstrated high accuracy in predicting survival outcomes for glioma patients, validated through external datasets. Moreover, the glycosylation signature exhibited associations with immune infiltration in the glioma microenvironment, potentially indicating variable efficacy levels of immunotherapy. These insights promise significant contributions to future glioma research and clinical applications.

Zhang et al. investigated the prognostic significance of TGFB-induced factor homeobox 2 (TGIF2) in glioma, a study that holds potential implications for the fields of cancer biology and immunology. They examined TGIF2 expression in normal tissues and gliomas using public databases and analyzed its correlation with clinicopathologic features, prognosis, and potential biological functions in glioma patients, as well as its impact on tumor immune infiltration. *In vitro* studies further confirmed these findings. The results indicated that increased TGIF2 expression is strongly correlated with malignant phenotypes and a poor prognosis in glioma patients. Importantly, the knockdown of TGIF2 *in vitro* was shown to inhibit glioma invasion and migration and suppress the EMT phenotype. Thereby, these results suggest TGIF2 as a potential glioma biomarker linked to tumor immune infiltration and EMT, which may have direct implications for the development of novel therapeutic strategies for glioma.

Tripathy et al. conducted a review of the evolution of GB research, encompassing insights into GB biology and approved treatments over time. They explored the pivotal players within the GB microenvironment and the regulation of critical mechanisms involved in GB progression and survival. Furthermore, they examined the diverse array of potential therapeutic agents used for GB patients. This review underscores the imperative need for molecular targets and mechanisms that are specific to GB, particularly in the context of advancing personalized medicine, which holds immense potential for the future of GB treatment.

Li et al. developed a novel integrative stacking ensemble model framework (ecGBMsub), aimed at improving the classification of molecular subtypes in *IDH*-wild-type GB. Leveraging machine learning techniques, the researchers constructed an ensemble model using extrachromosomal circular DNA (eccDNA) molecular profiling. Additionally, they developed a user-friendly web tool that provides clinicians with a robust resource to discern molecular subtypes and explore potential links between GB subtypes and eccDNA biology. This advancement holds promise for helping clinicians predict molecular subtypes in GB patients, thereby facilitating more personalized treatment selection.

Jajin et al. conducted a systematic review and meta-analysis to investigate the effectiveness of vaccines in the treatment of GB. Their study examined the efficacy and safety of existing vaccines, including personalized vaccines, and compared them with conventional treatments for GB patients. The findings revealed that personalized vaccines exhibited superior efficacy in the treatment of GB, leading to improved overall survival, progression-free survival, and time to survival. Notably, AFTV, peptide, and dendritic cell-based vaccines emerged as effective options for glioma.

Taken together, these promising studies lay the groundwork for a better understanding of the molecular networks of GB, potentially refining the selection of personalized therapies for GB patients. This

progress holds great promise for improving patient survival and overall wellbeing.

Author contributions

MM: Writing–original draft. DM: Writing–review and editing. ClC: Writing–review and editing. CéC: Writing–review and editing.

Conflict of interest

The authors declare that the research was conducted in the absence of any commercial or financial relationships that could be construed as a potential conflict of interest.

Publisher's note

All claims expressed in this article are solely those of the authors and do not necessarily represent those of their affiliated organizations, or those of the publisher, the editors and the reviewers. Any product that may be evaluated in this article, or claim that may be made by its manufacturer, is not guaranteed or endorsed by the publisher.

frontiers | Frontiers in Pharmacology

TYPE Hypothesis and Theory
PUBLISHED 30 May 2023
DOI 10.3389/fphar.2023.1156492

Check for updates

OPEN ACCESS

EDITED BY
Mariana Magalhães,
University of Coimbra, Portugal

REVIEWED BY
Sree Deepthi Muthukrishnan,
University of California, Los Angeles, United States
Qian Liu,
Capital Medical University, China

*CORRESPONDENCE
Zesheng Li,
lizesheng20190820@163.com
Lei Han,
superhanlei@hotmail.com

†These authors have contributed equally to this work

RECEIVED 01 February 2023
ACCEPTED 18 May 2023
PUBLISHED 30 May 2023

CITATION
Li Z, Wang B, Wu J and Han L (2023), Will EGFRvIII and neuronal-derived EGFR be targets for imipramine?
Front. Pharmacol. 14:1156492.
doi: 10.3389/fphar.2023.1156492

COPYRIGHT
© 2023 Li, Wang, Wu and Han. This is an open-access article distributed under the terms of the Creative Commons Attribution License (CC BY). The use, distribution or reproduction in other forums is permitted, provided the original author(s) and the copyright owner(s) are credited and that the original publication in this journal is cited, in accordance with accepted academic practice. No use, distribution or reproduction is permitted which does not comply with these terms.

Will EGFRvIII and neuronal-derived EGFR be targets for imipramine?

Zesheng Li[1†]*, Bo Wang[1†], Jianjian Wu[2†] and Lei Han[1]*

[1]Tianjin Neurological Institute, Key Laboratory of Post-Neuroinjury Neuro-repair and Regeneration in Central Nervous System, Ministry of Education and Tianjin City, Tianjin Medical University General Hospital, Tianjin, China, [2]Department of Environment, College of Environment and Resources, Xiangtan University, Xiangtan, China

Tricyclic antidepressant is an old and well-established therapeutic agent with a good safety profile, making them an excellent candidate for repurposing. In light of the growing understanding of the importance of nerves in the development and progression of cancer, attention is now being turned to using nerve-targeting drugs for the treatment of cancer, particularly TCAs. However, the specific mechanism by which antidepressants affect the tumor microenvironment of glioblastoma (GBM) is still unclear. Here, we combined bulk RNA sequencing, network pharmacology, single-cell sequencing, molecular docking and molecular dynamics simulation to explore the potential molecular mechanism of imipramine in the treatment of GBM. We first revealed that the imipramine treatment is presumed to target EGFRvIII and neuronal-derived EGFR, which may play a pivotal role in treating GBM by reducing the GABAergic synapse and vesicle-mediated release and other processes thereby modulating immune function. The novel pharmacological mechanisms might provide further research directions.

KEYWORDS

glioblastoma, tricyclic antidepressant (TCA), cancer biology, neuroscience < neuropharmacology, translational medicine, EGFR

Introduction

Glioblastoma (GBM) is known as the most aggressive type of intracranial tumor. High morbidity and recurrence rates represent poor prognosis in GBM patients. Treatments involving monotherapy are often not effective enough to suppress GBM tumor cells. First-line treatment of GBM patients is usually a combination therapy, including maximal safe surgical resection, postoperative radiotherapy, and chemotherapy with temozolomide. Although advances have been made in the field of surgery, radiotherapy, and chemotherapy, the median survival time (15–16 months) for GBM patients remains below expectations (Ostrom et al., 2018). Thus, novel therapeutic approaches for improving the survival of GBM patients are urgently needed.

Tricyclic antidepressants (TCAs) were originally developed and marketed for the treatment of depression, but have been used to treat a wide range of conditions, most commonly off-label. Long-term use of TCAs is associated with a lower incidence of gliomas (Walker et al., 2011). A previous study found that imipramine, a TCA, increased autophagy and resulted in therapeutic benefits in animals bearing GBM tumors (Shchors et al., 2015). Bielecka-Wajdman et al. reported that several antidepressants, including imipramine and amitriptyline, promoted the conversion of glioma stem cells to non-glioma stem cells, thereby reversing the malignant phenotype (Bielecka-Wajdman et al., 2017). Recently, Chryplewicz et al. describe imipramine increases autophagic flux

within cancer cells, thereby recruiting T cells, as well as reprogramming macrophages as pro-inflammatory cells by inhibiting the histamine receptor on the membrane (Chryplewicz et al., 2022). Considering the psychological pressure of GBM patients, as well as the resulting anxiety and depression, using imipramine to treat GBM patients can kill two birds with one stone. Since depression is a frequent occurrence in GBM patients as well as there are overlaps between molecular and cellular mechanisms involved in both diseases' pathogenesis, antidepressants that act as antitumor agents are an attractive treatment option for GBM patients (Abadi et al., 2022). However, how imipramine regulates crosstalk between various cells in the GBM microenvironment deserves further exploration.

As a strategy, network pharmacology is a powerful tool for examining the complex mechanisms that cause disease and the effects of drugs. Molecular Docking is the process of predicting the structure of molecules using computer modeling. This method is widely used to discover new medicines and mechanisms of action for pharmaceuticals (Pinzi and Rastelli, 2019). In this study, we aim to use bulk RNA sequencing, network pharmacology, single-cell RNA-seq analysis, molecular docking and molecular dynamics simulation to explore the mechanism of imipramine in treating GBM. We uncovered the crucial role of imipramine in GABA (Gamma-aminobutyric acid) and immune function regulation in GBM patients. We hypothesize that imipramine may target neuronal cell-derived EGFR, thereby modulating the immune microenvironment. We also found that imipramine has a strong binding ability to EGFRvIII, which may provide a new potential drug for clinical treatment.

Methods

Dataset collection and preprocessing

RNA-seq data from GSE4290 was downloaded from Gene Expression Omnibus (GEO, https://www.ncbi.nlm.nih.gov/gds) database. The screening criteria were as follows: First, the dataset including GBM samples and non-tumor samples. Second, both non-tumor samples and GBM samples should be greater than 20 to ensure the quality of WGCNA. The GSE4290 dataset includes 81 samples from patients with GBM as well as 23 normal samples from healthy individuals (Sun et al., 2006). After preprocessing, we finally obtained 77 GBM samples and 23 normal samples with clinical data.

Obtaining targets for imipramine

The detailed information of imipramine was obtained from PubChem (https://pubchem.ncbi.nlm.nih.gov/). The SwissTargetPrediction database (http://www.swisstargetprediction.ch/) (Daina et al., 2019) and the TargetNet database (http://targetnet.scbdd.com/home/index/) (Yao et al., 2016) as well as CTD (https://ctdbase.org/) (Davis et al., 2023), and BindingDB (https://bindingdb.org/bind) (Chen et al., 2002) were utilized for identifying potential target genes. A further search was conducted to access target proteins names using the UniProt database (https://www.uniprot.org/uploadlists/).

Gene Ontology and pathway analysis

Gene Ontology (GO) and Kyoto Encyclopedia of Genes and Genomes (KEGG) pathway analysis was performed by clusterProfiler R package with a threshold of adjusted p-value <0.05 (Wu et al., 2021).

Identification of DEGs

The R package "limma" was used to identify the differentially expressed genes (DEGs) between the GBM samples and healthy controls (Ritchie et al., 2015). |log2 (foldchange)| > 2 and the adjusted p-value <0.05 were used as screening criteria.

Gene set enrichment analysis

GSEA is used to determine whether a defined set of genes shows a statistically significant difference in two different traits. Pathways that may play a role in the pathogenesis of GBM were explored using GSEA. The R package clusterProfiler was used for GSEA analysis. The following settings were used for the analysis: false discovery rate (FDR) < 0.25, adjusted p-value <0.05, |normalized enrichment score (NES)| > 1, which to be considered significant.

WGCNA analysis of GEO

All genes were selected to construct the weighted gene co-expression network. First, a hierarchical clustering analysis was conducted to exclude the outlier samples. The Pearson correlation value was computed for each pair of genes. Then, an adjacency matrix was conducted. The WGCNA package's "pickSoftThreshold" function was utilized to select the optimal β that satisfies the scale-free distribution (Langfelder and Horvath, 2008). The adjacency matrix was converted into two matrices: the topological overlap matrix (TOM) and 1-TOM. The TOM reflects the similarity between genes, while 1-TOM reflects the dissimilarity among them. Last, hierarchical clustering was used to classify genes into distinct modules. The module eigengene (ME) was computed to reflecting the gene expression profiles for each module. The settings of parameters were as follows. The soft threshold β = 6, minModuleSize = 50, mergeCutHeight = 0.25.

Generation of protein-protein interaction (PPI) networks

Screened genes were analyzed in STRING (version 11.5, https://string-db.org/) to investigate protein-protein interactions (PPI) (Szklarczyk et al., 2019). PPI was constructed and visualized using Cytoscape software (version 3.9.1) (Shannon et al., 2003). A Molecular Complex Detection algorithm (MCODE) was used to detect dense regions of tightly bound proteins or PPI. The MCODE algorithm is used to identify critical sub-networks that contribute to the development of GBM and to identify critical subpopulation genes. The parameters of MCODE were all set using default settings.

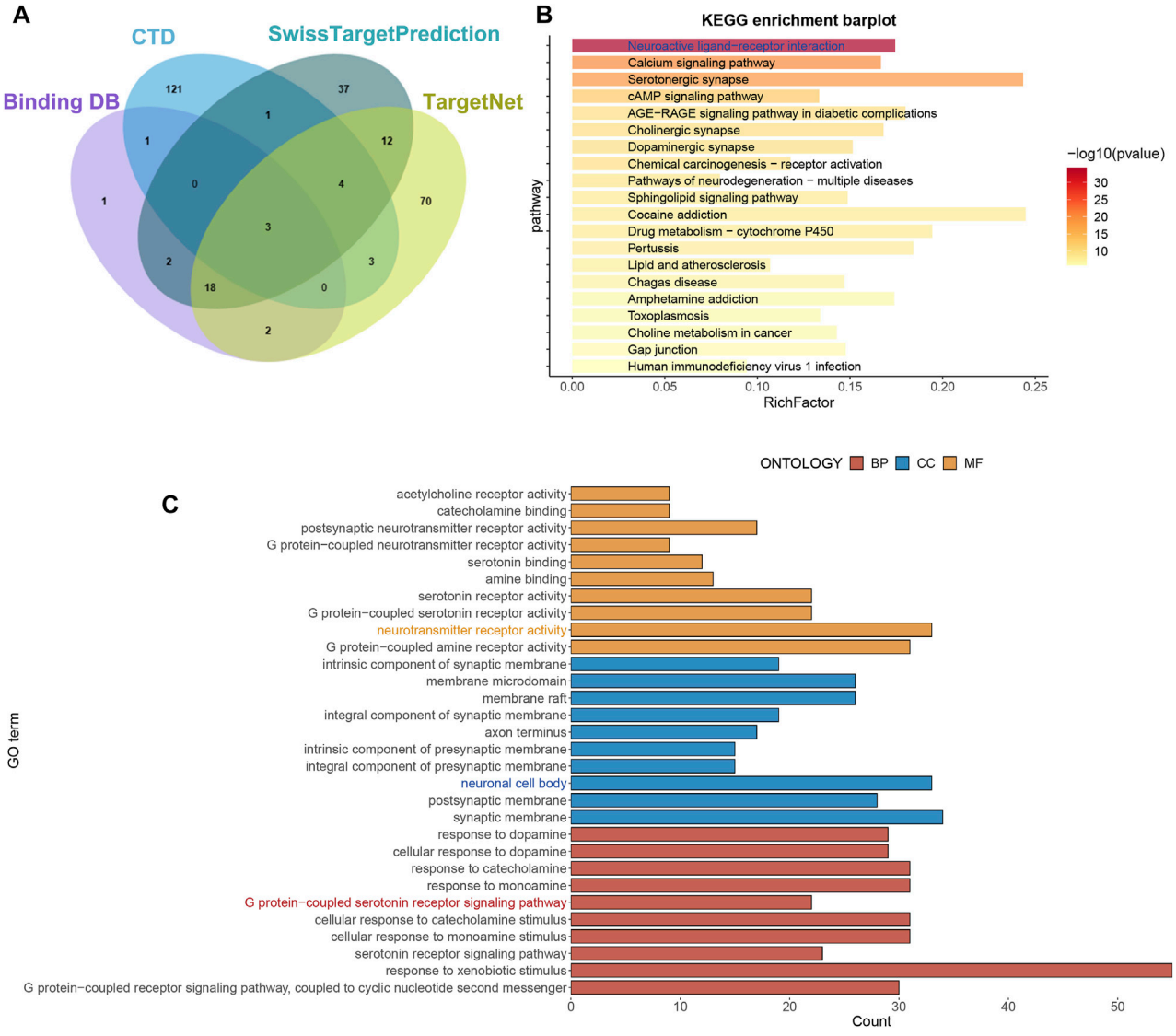

FIGURE 1
Obtain drug targets and functional analysis. **(A)** The drug targets were obtained from four databases. **(B)** KEGG analysis of drug targets. **(C)** GO analysis of drug targets.

Single-cell RNA sequencing data analysis

TISCH2 is a database that utilizes single-cell RNA sequencing (scRNA-seq) technology to concentrate on the tumor microenvironment (TME) and its immune response against tumors (Han et al., 2023).

For a single gene, TISCH2 supports exploring its expression level across different single-cell datasets or cancer types. We explored the expression level of EGFR gene in different single-cell datasets with TISCH2.

The scTIME Portal is a database and a portal for single cell transcriptomes of tumor immune microenvironment (Hong et al., 2021). We employed it to obtain the expression of pathway genes in all cell types in GSE84465. We also used scTIME Portal to perform the cell-to-cell communication analysis in GSE84465.

Analysis related to wild-type EGFR and mutant EGFR

CAMOIP is a tool for analyzing the expression data and mutation data from the TCGA. All analyzes related to wild-type EGFR and mutant EGFR were performed on CAMOIP (http://www.camoip.net/) (Lin et al., 2022).

Molecular docking and molecular dynamics simulation

Firstly, the protein was optimized before docking using the Protein Preparation Wizard, and the ligand was prepared with LigPrep tool. We utilized the OPLS-2005 force field to provide partial atomic charge attribution, protonation states generation, and energy minimization. Grid-Based Ligand Docking with Energetics (Glide v11.5,

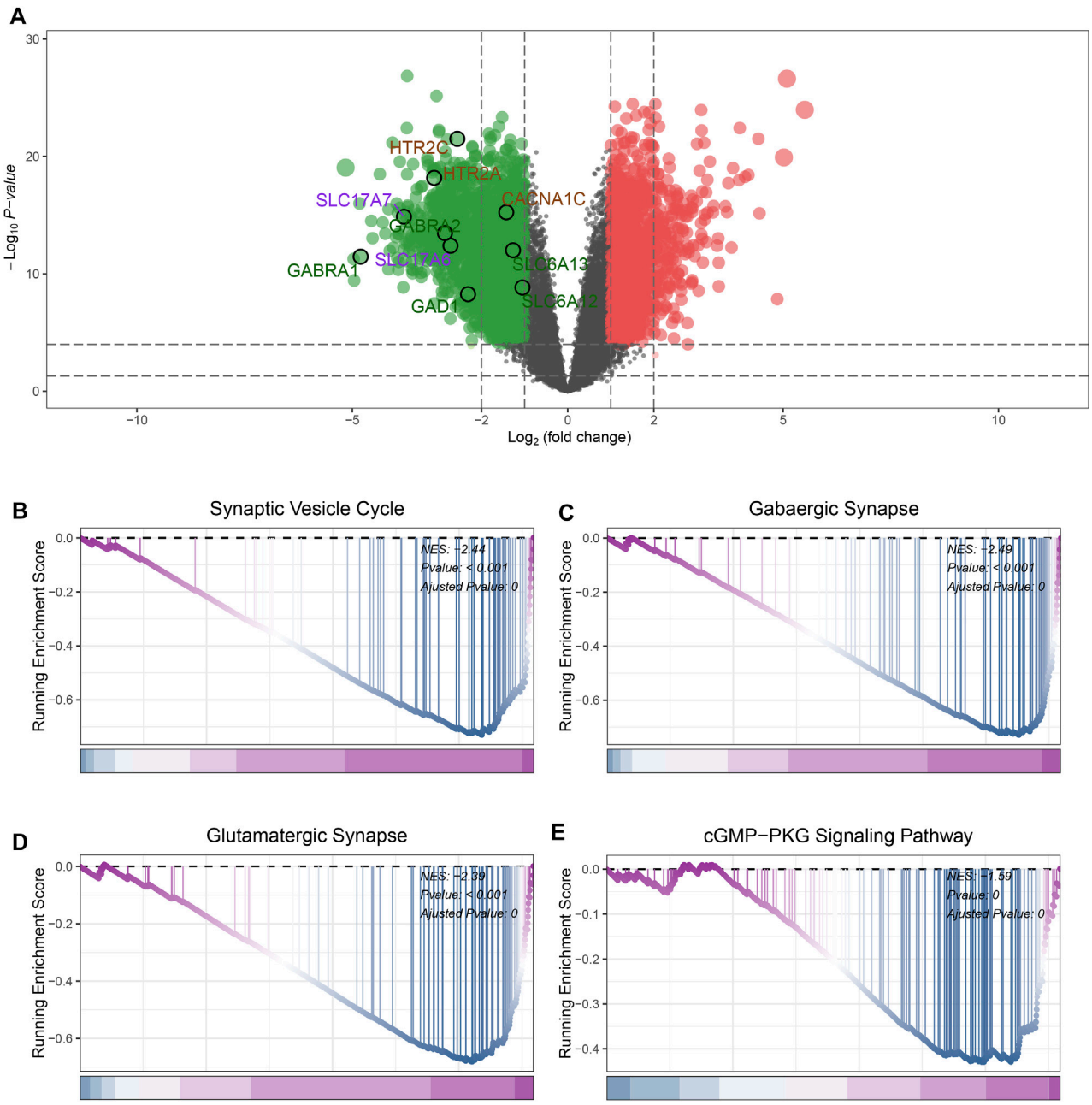

FIGURE 2
Identification of DEGs and GSEA analysis. **(A)** The volcano plot of DEGs expression. **(B)** GSEA results of Synaptic Vesicle Cycle pathway. **(C)** GSEA results of GABAergic Synapse pathway. **(D)** GSEA results of Glutamatergic Synapse pathway. **(E)** GSEA results of cGMP-PKG Signaling Pathway.

Schrödinger) was used to dock all ligands into the catalytic pocket of the RPT protein in "extra precision mode" without applying any constraints. Finally, the complex with the lowest score was selected for further study. The molecular dynamics simulation protocol can be found in previous article (Wu et al., 2023).

Statistical analysis

R software (version 4.2.0) (http://www.r-project.org) was used for statistical analysis. Wilcoxon tests were used to analyze subgroup differences. $p < 0.05$ was used as the threshold for statistical significance.

Result

Target genes for imipramine

The SwissTargetPrediction, CTD, BindingDB, and TargetNet databases were used to identify target genes associated with imipramine. Finally, 275 target genes associated with

10.3389/fphar.2023.1156492

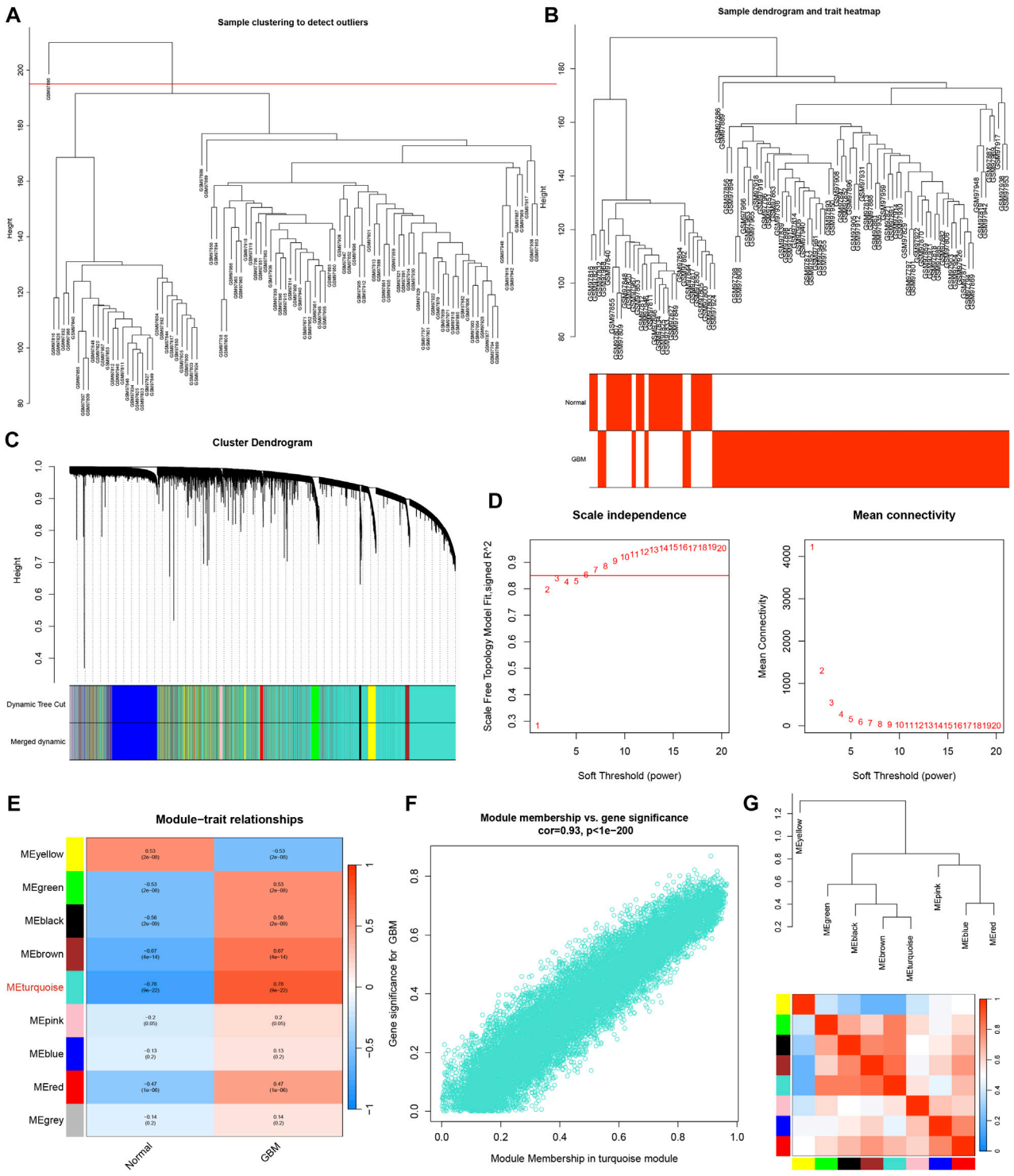

FIGURE 3
WGCNA analysis. **(A)** Raw cluster tree. **(B)** Sample dendrogram and trait heatmap. **(C)** The cluster dendrogram of WGCNA. **(D)** The soft threshold power and mean connectivity of WGCNA. **(E)** Correlations between gene modules and GBM status. **(F)** The correlation between the turquoise module memberships and the gene significance. **(G)** The correlation between modules.

imipramine were identified and retrieved from these databases (Figure 1A; Supplementary Table S1). KEGG enrichment analysis shows that drug target genes were mainly enriched in neuroactive ligand−receptor interaction, serotonergic synapse, and calcium signaling pathway (Figure 1B). GO enrichment analysis shows that the enriched pathways were mainly involved in BP: response

FIGURE 4
Identification of intersect genes and functional analysis. **(A)** The intersection of DEGs and WGCNA turquoise module genes were named GBM genes. **(B)** The intersection of GBM genes and drug targets genes were named intersect genes. **(C)** KEGG analysis of intersect genes.

to xenobiotic stimulus, cellular response to catecholamine stimulus; CC: synaptic membrane, neuronal cell body; MF: neurotransmitter receptor activity, G protein−coupled amine receptor activity (Figure 1C). In total, the enrichment results showed that imipramine might be affecting neurotransmitter signaling circuits.

Identification of DEGs between GBM and control

In GSE4290 datasets, first, we removed the batch effect between the samples (Supplementary Figure S1). According to the filtering criteria (|log2 (foldchange)| > 2 and the adjusted

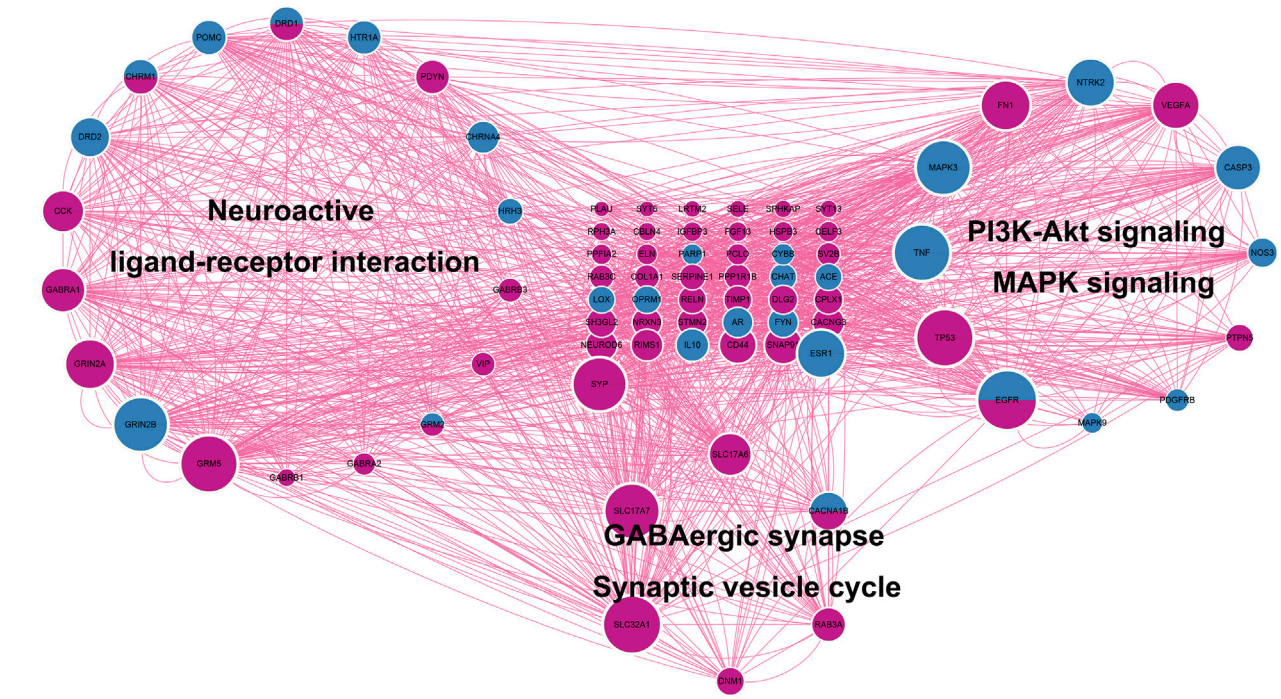

FIGURE 5
Identification of key cluster proteins and functional analysis. **(A)** The PPI network of key cluster proteins. DeepPink: GBM genes. Blue: drug targets genes. DeepPink and blue: both GBM gene and drug target.

p-value <0.05), a total of 777 DEGs were screened, of which 207 DEGs were upregulated and 570 DEGs were downregulated (Supplementary Table S2). The result of the differential analysis was visualized in Figure 2A. Some genes participated in the pathways including Gabaergic Synapse, Synaptic Vesicle Cycle were significantly downregulated in GBM samples (Figures 2A–C). This phenomenon is consistent with previous reports (Jung et al., 2019).

GSEA analysis

GSEA analysis was performed to investigate the differences in pathway landscapes between GBM and normal samples. We noticed that Synaptic Vesicle Cycle, GABAergic synapse, Glutamatergic Synapse and cGMP–PKG Signaling Pathway were significantly downregulated in GBM group (Figures 2B–E). These results indicate synthesis and vesicle-mediated release of the neurotransmitter GABA as well as signal transduction activities may be closely related to the pathogenesis of GBM.

Construction of the weighted gene co-expression network

The GBM samples and healthy control subjects from the GSE4290 dataset were analyzed utilizing the WGCNA package in R software. The outlier samples were removed (Figure 3A). The sample dendrogram and trait heatmap was shown in Figure 3B. The cluster dendrogram was shown in Figure 3C. The matrix was transformed into an adjacency matrix using the soft-thresholding parameter, denoted as β. The R^2 achieved more than 0.85 when β = 6, which became the power of our adjacency matrix (Figure 3D). After merging modules with similarity >0.75, nine co-expression modules were identified using the hierarchical clustering method of which the turquoise module exhibits the highest correlation with GBM (R = 0.78, $p < 0.001$), as shown in Figure 3E. Meanwhile, the scatter plot of MM relative to GS showed a good correlation between GS and MM within the turquoise module (R = 0.93, $p < 0.001$) (Figure 3F). Thus, the turquoise module could be a pivotal module closely associated with GBM. Additionally, the network heatmap was shown in Figure 3G.

Functional enrichment analysis

The overlap between the DEGs and hub genes in the turquoise module was shown in Figure 4A, which was named GBM genes (Supplementary Table S3). The overlap between the GBM genes and Drug targets was shown in Figure 4B, which was named intersect genes. Then, we performed KEGG analysis on intersect genes. KEGG enrichment analysis showed that the enriched pathways were also mainly involved in Calcium signaling pathway, Gap junction, Glutamatergic synapse, Neuroactive ligand–receptor interaction, Serotonergic synapse, Glioma, GABAergic synapse (Figure 4C).

10.3389/fphar.2023.1156492

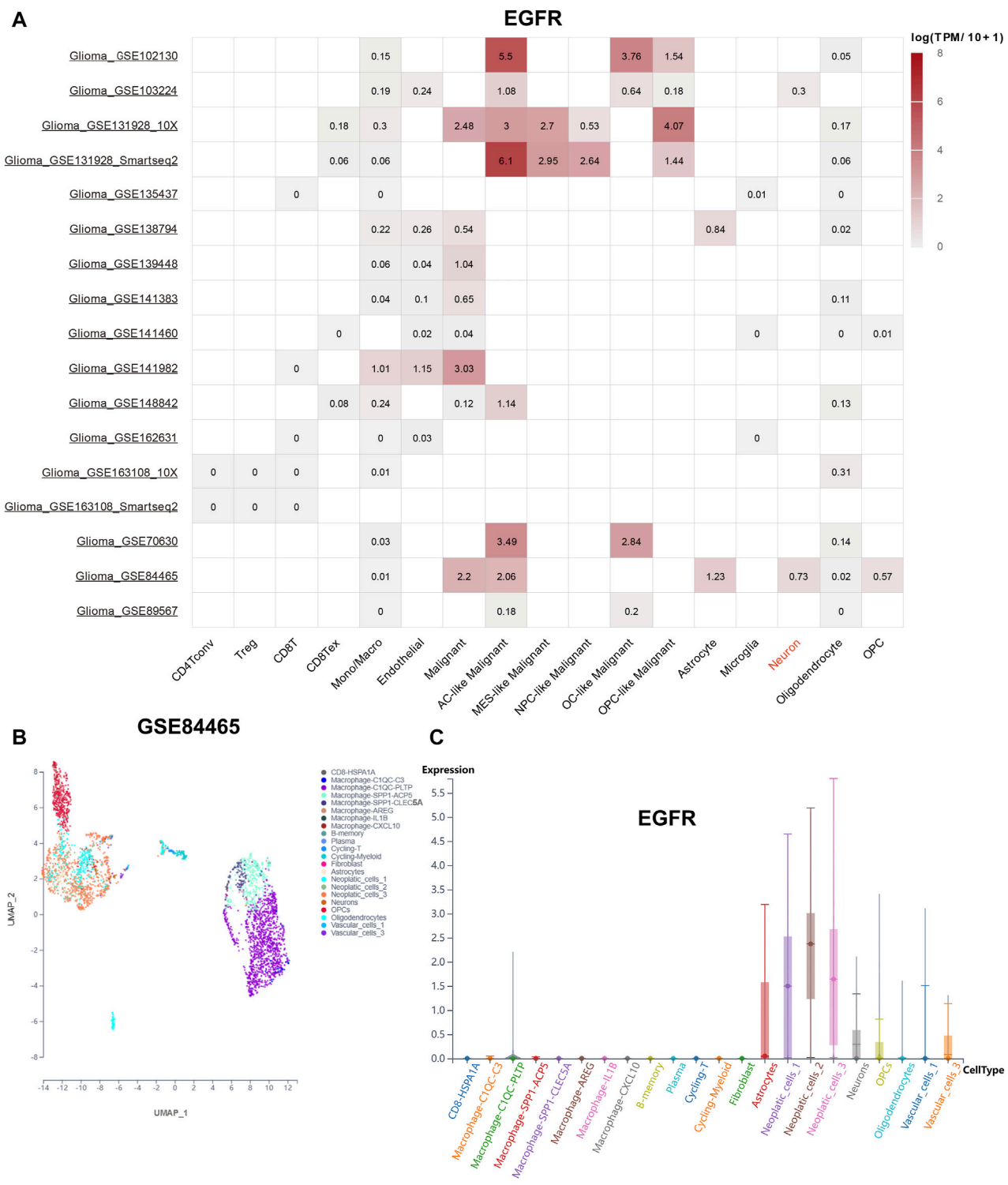

FIGURE 6
EGFR distribution landscape. **(A)** the distribution of EGFR in the different single-cell datasets. **(B)** the UMAP plot of GSE84465. **(C)** the distribution of EGFR in GSE84465.

Selection of key target genes

It is widely recognized that drugs elicit diverse effects on their target genes or target proteins. These effects may encompass the inhibition or upregulation of target gene expression, as well as the enhancement or suppression of target protein activity. Importantly, the precise regulatory effect of a drug on its target requires experimental validation. In this study, we solely analyze and predict the regulatory

10.3389/fphar.2023.1156492

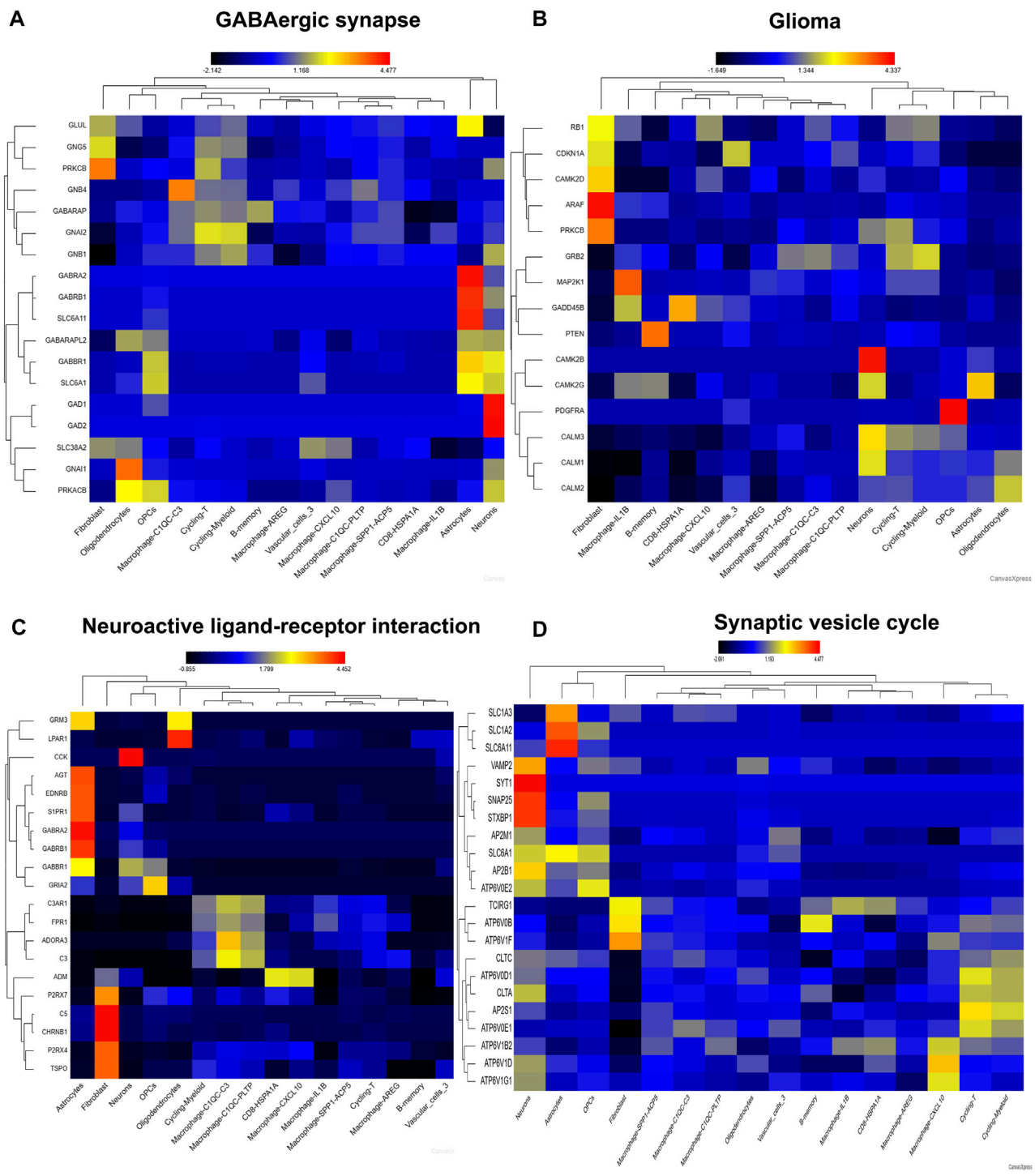

FIGURE 7
The distribution of pathway signatures in GSE84465. **(A)** GABAergic synapse pathway **(B)** Glioma pathway **(C)** Neuroactive ligand-receptor interaction pathway **(D)** Synaptic vesicle cycle pathway.

impact based on existing literature reports, with the aim of offering theoretical insights for subsequent researchers.

Traditional network pharmacology articles construct PPI with the intersect genes of drug targets and disease-related targets. However, this approach may not be entirely accurate, because there is a regulatory effect between proteins, and the drug targeting its own target protein may also affect the activity of other proteins. So, we do not only focus on the intersect genes and we selected all drug target genes and GBM genes to perform a large-scale PPI network and screen the key cluster with most interactions to explore the regulatory relationship between drug targets and disease-related targets.

10.3389/fphar.2023.1156492

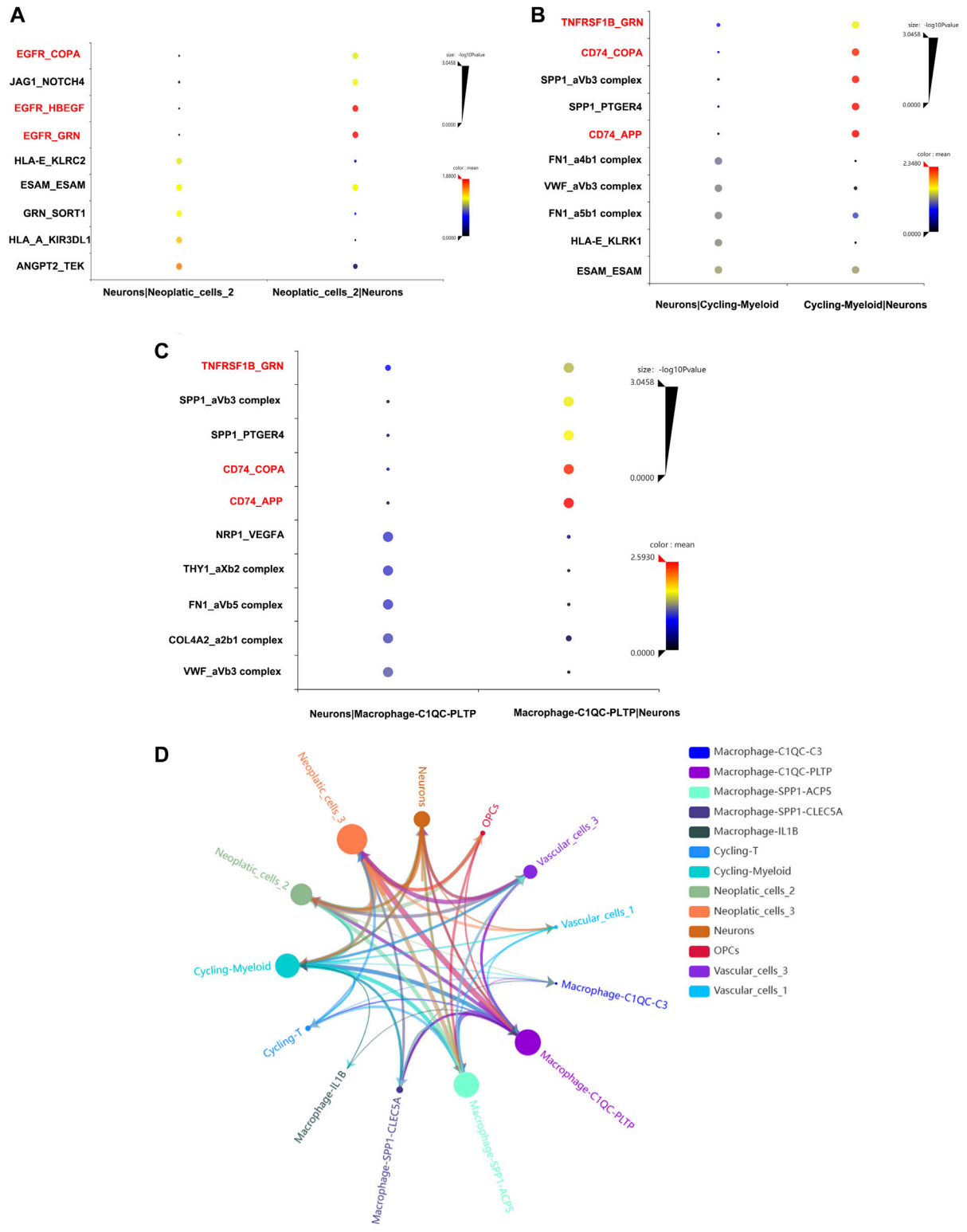

FIGURE 8
Cell-to-cell communication analysis. **(A)** The ligands and receptors interaction between neurons and neoplastic. **(B)** The ligands and receptors interaction between neurons and cycling-myeloid. **(C)** The ligands and receptors interaction between neurons and macrophages. **(D)** The cell-to-cell communication between all cell types.

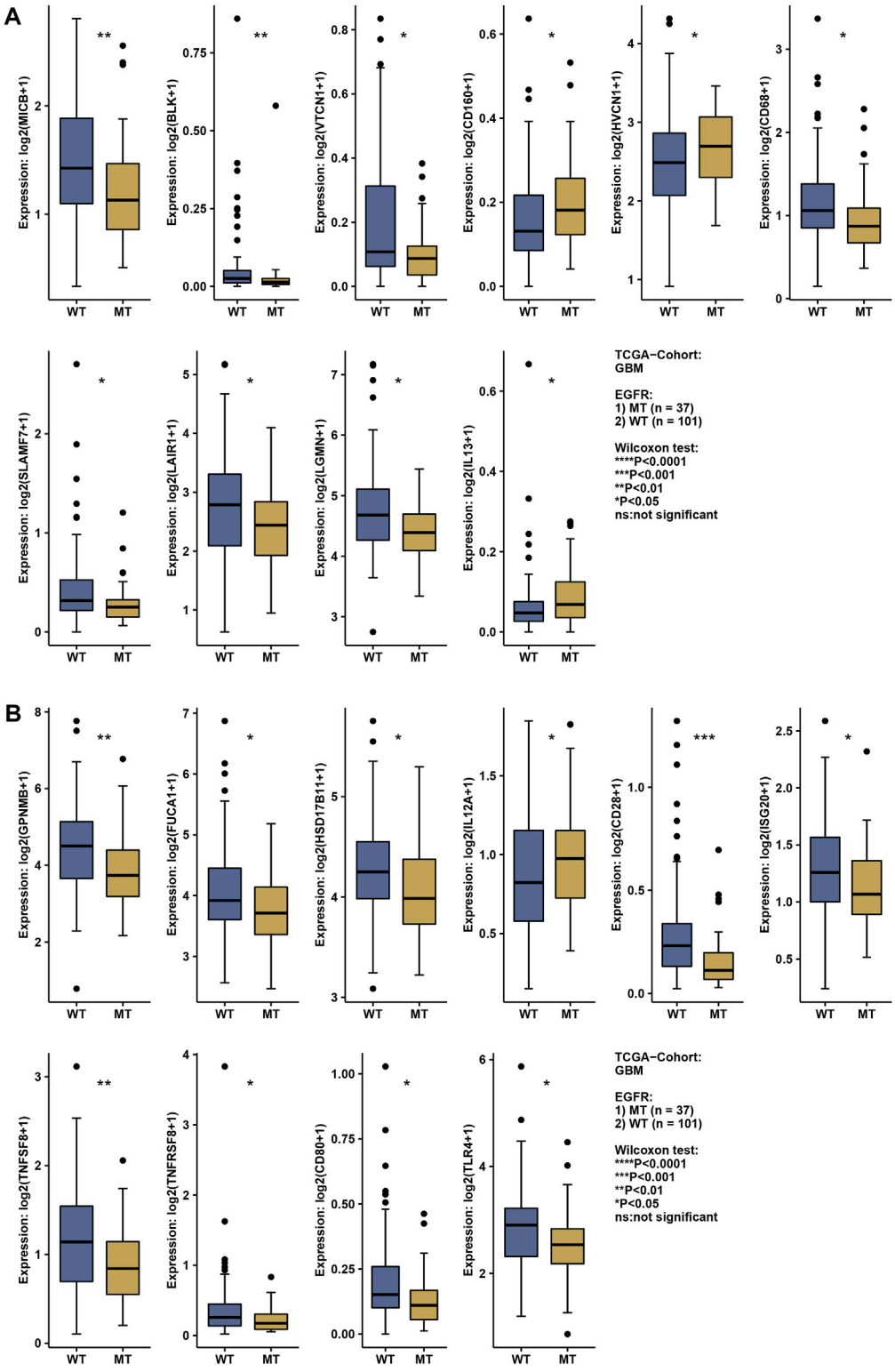

FIGURE 9
The expression level of the immune-related gene in EGFR wildtype and mutation patients **(A,B)**. * represents a significant difference ($p < 0.05$), ** represents a significant difference ($p < 0.01$), *** represents a significant difference ($p < 0.001$).

A total of 883 drug target genes and GBM genes were imported into the STRING online database (version 11.5) to construct the PPI network. Then, the key cluster proteins were identified by Cytoscape's plugin code "MCODE". The key cluster proteins with the most interactions were visualized in Figure 5A. It is not difficult to infer that imipramine affects the progression of GBM by

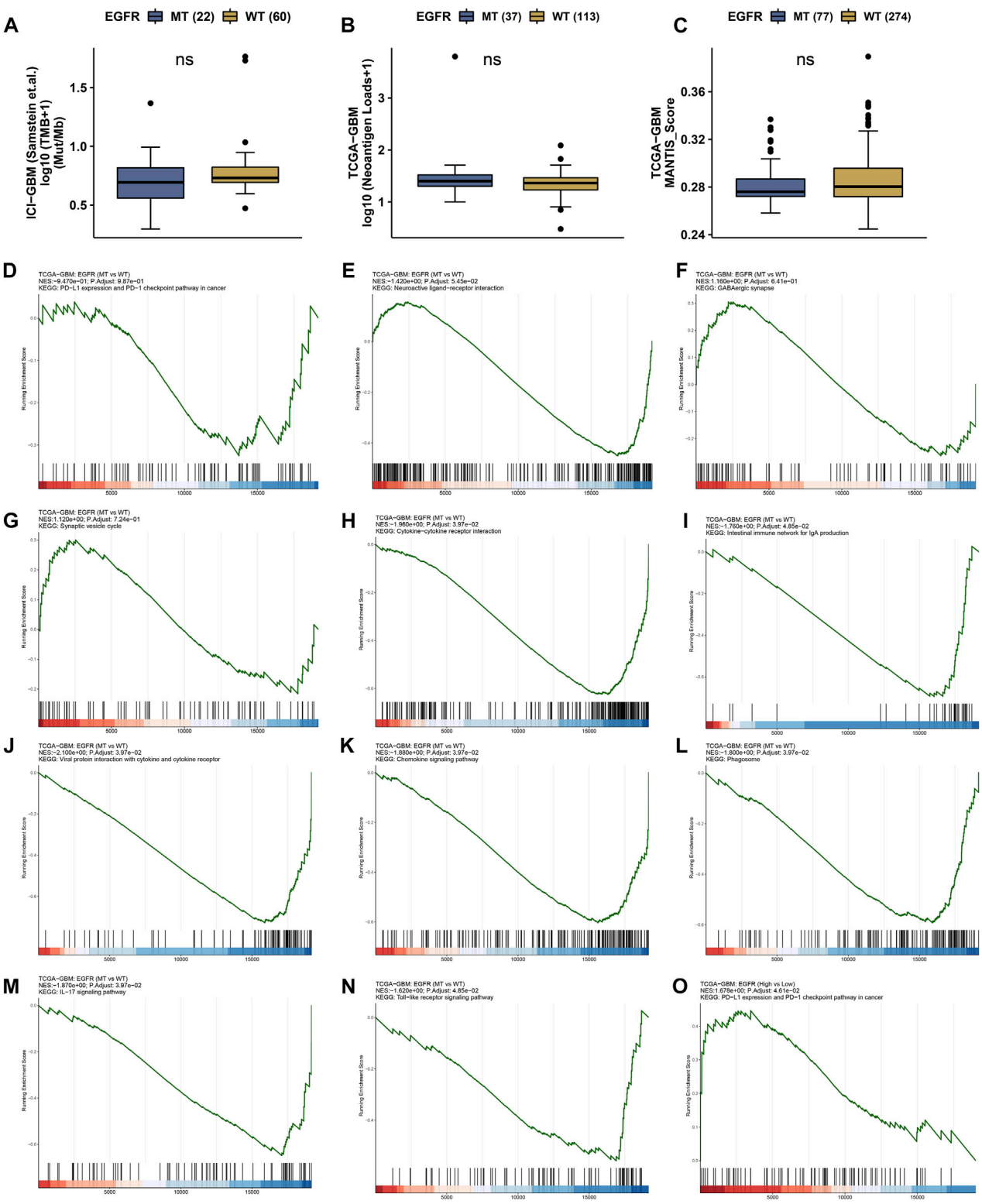

FIGURE 10
Immune landscape in EGFR wildtype and mutation patients. **(A)** Tumor mutation burden (TMB) status in EGFR wildtype and mutation groups. **(B)** Neoantigen status in EGFR wildtype and mutation groups. **(C)** MANTIS_Score in EGFR wildtype and mutation groups. ns represents no significant difference. **(D–O)** GSEA results in TCGA-GBM cohort.

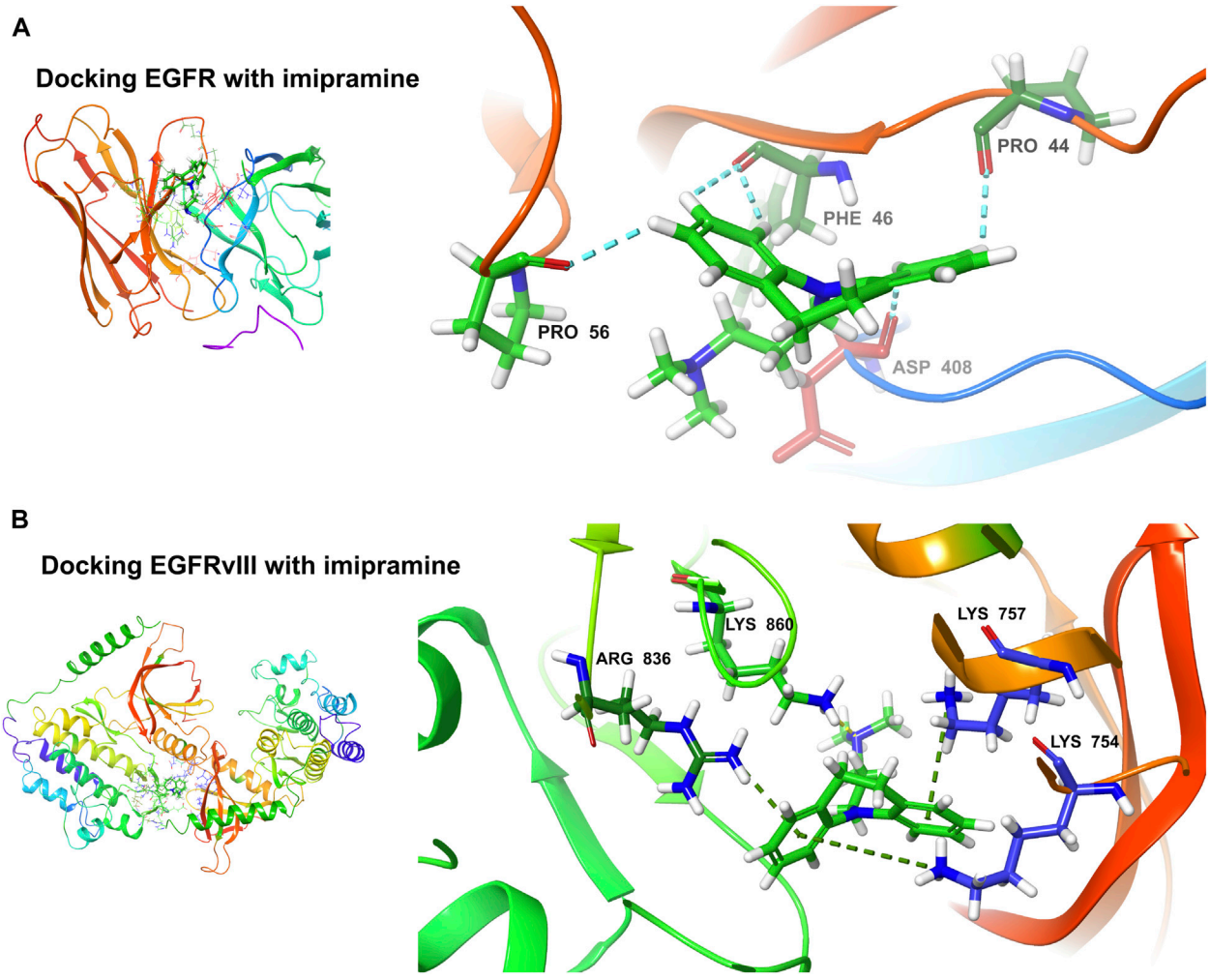

FIGURE 11
Molecular docking. **(A)** Docking EGFR with imipramine (−4.291 kcal/mol). **(B)** Docking EGFRvIII with imipramine (−5.242 kcal/mol).

regulating the release and transmission of the neurotransmitter, such as GABA, thereby affecting MAPK signaling and PI3K-AKT signaling. In Figure 5A, the size of protein represents the degree of the protein, we noticed that EGFR is both a drug target and a GBM gene, while also exhibits a high degree. So, we infer EGFR as a key target for imipramine, which plays important role in MAPK signaling, PI3K-AKT signaling, Neuroactive ligand–receptor interaction, Synaptic Vesicle Cycle and GABAergic synapse.

Single-cell analysis

To explore the distribution of EGFR genes in tumor microenvironment (TME), online datasets TISCH2 was utilized. The expression level of EGFR in different cells was shown in Figure 6A. Interestingly, we noticed that EGFR was expressed on neurons with a relative high level in GSE84465. In this way, the GBM single-cell RNA-seq dataset GSE84465 was chosen for further analysis. The Uniform Manifold Approximation and Projection (UMAP) plot of GSE84465 was shown in Figure 6B. The distribution of EGFR in different cell types was shown in Figure 6C. We can see that EGFR was expressed in neurons and astrocytes, implicating its potential role in the regulation of neurotransmitter.

Then, we visualize four pathways involving in neurotransmitter activity (Figures 7A–D). Genes involving in GABAergic synapse mainly distributed in fibroblast, neurons, astrocytes, cycling-T, cycling-Myeloid, macrophage, implicating these genes may play important role in immune cell fate (Figure 7A). Genes involving in Glioma pathway were also distributed in neurons, fibroblast, and macrophage, B-memory, which confirmed the importance of neurons, stromal cells and immune cell in the pathogenesis of glioma (Figure 7B). Consistently, the genes involving in Neuroactive ligand–receptor interaction were also distributed in astrocytes, neurons, fibroblast, macrophage and CD8 cells (Figure 7C). Genes involving in Synaptic Vesicle Cycle mainly distributed in neurons, astrocytes, cycling-T, cycling-Myeloid, macrophage (Figure 7D). So, the neurons might play a pivotal role in reshape TME by regulating crosstalk between tumor cell, immune cell and stromal cell.

10.3389/fphar.2023.1156492

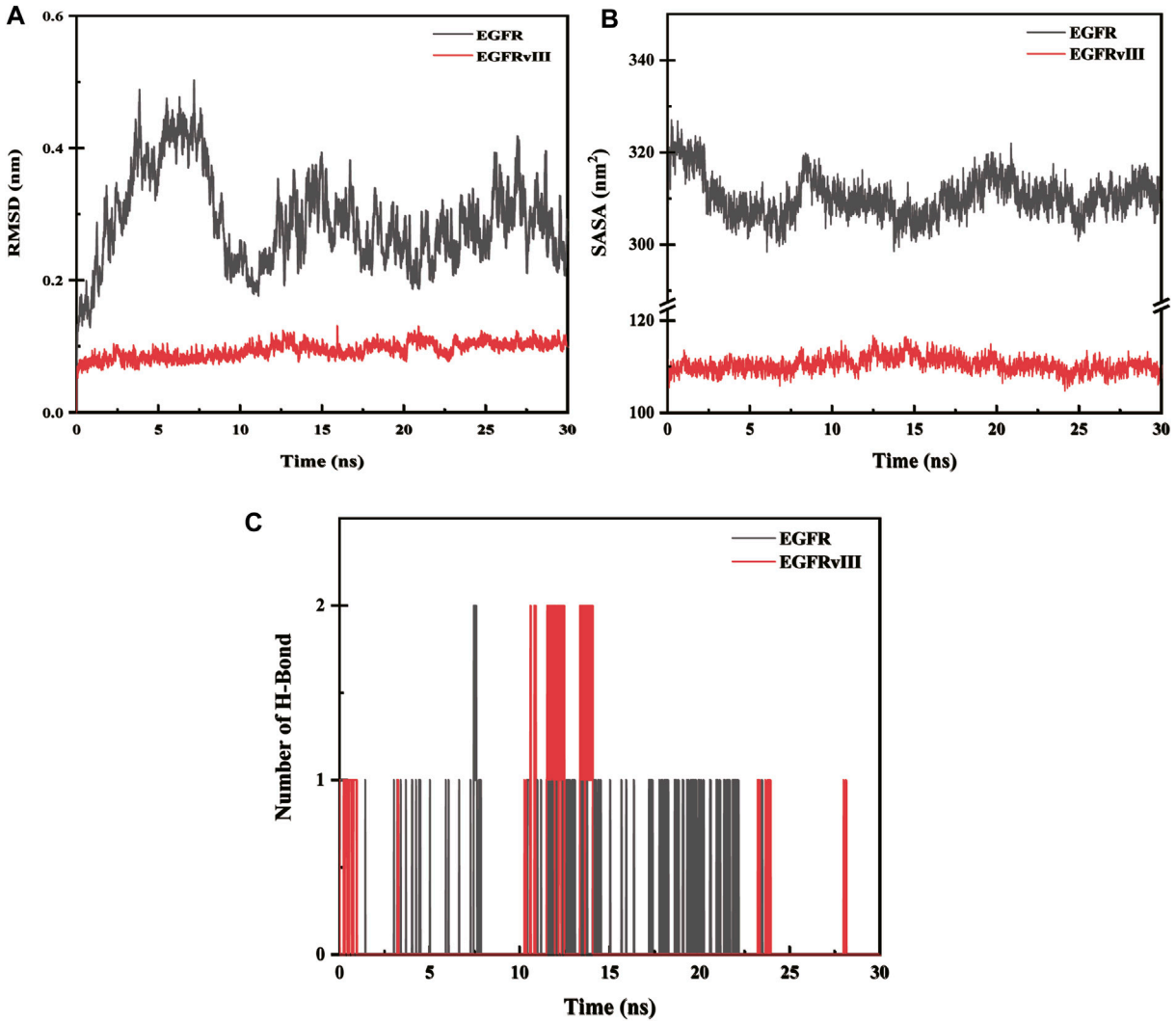

FIGURE 12
(A) Root-mean-square deviation (RMSD) analysis. **(B)** The solvent-accessible surface areas. **(C)** Hydrogen bond interaction.

TABLE 1 Analysis of MMPBSA.

Energy	EGFR - imipramine	EGFRvIII - imipramine
Van der Waals Energy (KJ/mol)	−98.372	−134.599
Electrostatic energy (KJ/mol)	−29.479	−26.148
Polar solvation energy (KJ/mol)	73.338	99.033
Nonpolar solvation Energy (KJ/mol)	−15.879	−17.653
Total Binding Energy (KJ/mol)	−70.392	−79.368
TΔS(KJ/mol)	14.510	14.582
Total Binding Free Energy (KJ/mol)	−55.882	−64.786

To confirmed our conjecture, cell-to-cell communication analysis was conducted. The ligand and receptor pair strength was shown in Figures 8A–C. We noticed that EGFR gene plays important role in the communication between neurons and neoplastic cells (Figure 8A). Additionally, neurons and cycling-myeloid, neurons and macrophage also exhibit communications. Surprisingly, EGFR,

COPA, GRN, TNFRSF1B were key ligands and receptors participant in communications between neurons, macrophage and neopaltic cells. So, we confirmed the key role of EGFR again, which may play an important role in regulating the crosstalk between neurons and TME. The communications between all cells were shown in Figure 8D.

The effects of EGFR and EGFR mutation on immune function

The status of EGFR plays a dominant role in the therapeutic effect, which might attribute to the immune function difference. Here, we explore the landscape of immune genes in TCGA-GBM cohort (Figures 9A, B). We noticed that CD160, HVCN1, IL13, IL12A were upregulated in EGFR mutated samples. However, EGFR status might not affect the aspect of immunogenicity in GBM (Figures 10A–C). Additionally, the pathways including PD-L1 expression and PD-1 checkpoint pathway, Neuroactive ligand–receptor interaction, GABAergic Synapse and Synaptic vesicle cycle showed no difference between the EGFR-mutated patients and EGFR-wildtype patients (Figures 10D–G). Interestingly, we noticed that some immune-related pathways were downregulated in the EGFR-mutated group, including Cytokine-cytokine receptor interaction, Intestinal immune network for IgA production, Viral protein interaction with cytokine and cytokine receptor, Chemokine signaling pathway, Phagosome, IL-17 signaling pathway and Toll-like receptor signaling pathway (Figures 10H–N). So, EGFR-mutated patients might suffer a worse immune status. In addition to mutation status, EGFR expression also affects immune checkpoint-related pathways. The PD-L1 expression and PD-1 checkpoint pathway was upregulated in the patients with high EGFR expression level (Figure 10O). In conclusion, if imipramine can target EGFR and EGFR mutants, it may improve the immune microenvironment of patients.

Molecular docking

The binding ability of the key targets was predicted using molecular docking technology. According to the general consensus, binding energies below −4.25 kcal/mol indicate specific binding between the ligand and the receptor. A binding energy below −5.0 kcal/mol indicates enhanced binding capability. Through molecular docking, we found that both EGFR (−4.291 kcal/mol) and EGFRvIII (−5.242 kcal/mol) have an excellent binding ability to the imipramine (Figures 11A, B).

Root-mean-square deviation (RMSD) analyses

The root-mean-square deviation (abbreviated as RMSD) is a measure of the deviation of atomic coordinates relative to a reference structure, and it is often used to evaluate whether a simulation system has reached stability. A stable RMSD indicates that the corresponding atoms have become stable, while a fluctuating RMSD implies fluctuations. The RMSD value of EGFR-imipramine is higher than that of EGFRvIII-imipramine, which indicates that the stability of the EGFRvIII-imipramine composite system is higher than that of the EGFR-imipramine composite system (Figure 12A).

The solvent-accessible surface areas

The solvent accessible surface area (SASA) is calculated by considering the interactions between van der Waals forces and solvent molecules on the solute surface. The SASA of a protein decreases as the compactness of the protein increases, so changes in SASA can be used to predict alterations in protein structure. The fluctuations in SASA values for EGFR-imipramine are greater than those for EGFRvIII-imipramine, indicating that the stability of the EGFRvIII-imipramine composite system is higher than that of the EGFR-imipramine composite system (Figure 12B).

Hydrogen bond interaction

To investigate the interactions between proteins and ligands, we first performed a hydrogen bond analysis on the protein-ligand complexes. We found that the average number of hydrogen bonds for EGFR-imipramine and EGFRvIII-imipramine were 0.09 and 0.13, respectively. This indicates that the hydrogen bond interaction strength between EGFRvIII and imipramine is greater than that between EGFR and imipramine (Figure 12C).

MMPBSA the free energy

To better explain the interaction energy between ligands and receptors, we used the gmx_mmpbsa script (https://jerkwin.github.io/gmxtool/) to determine the binding energies of all protein-ligand complexes during the equilibrium phase. In the application of the MMPBSA method, the total binding energy is decomposed into four independent parts (electrostatic interactions, van der Waals interactions, and polar and nonpolar solvation interactions). The results of the protein-ligand binding energies are shown in Table 1. In the protein-ligand complex systems, the main interaction energies are van der Waals and electrostatic energy. The binding free energies of EGFR and EGFRvIII proteins with imipramine are −55.882 and −64.786 kJ/mol, respectively, further indicating that the interaction strength between EGFRvIII and imipramine is greater than that between EGFR and imipramine.

Conclusion

Many studies have focused on imipramine acting directly on tumor cells to exert a therapeutic effect. However, the therapeutic mechanism of imipramine exerted on other cells in the GBM tumor microenvironment has not been fully elucidated. In this study, two main hypotheses with clinical significance were established. First, based on network pharmacology, single-cell sequencing and molecular docking, we identified neuron-derived EGFR as a possible key target of imipramine. In this way, imipramine might play a key role in

regulating crosstalk between neurons, circulating myeloid cells, and macrophages by target neuron-derived EGFR. Next, since EGFR mutations play an important role in the treatment and drug resistance of GBM, we compared the differences in immune-related genes in wild-type EGFR and mutant EGFR samples to confirm whether the status of EGFR affects the immune system, thus supporting the regulation of EGFR on immune cells mentioned above. We found differences in the expression of immune-related genes between wild-type EGFR patients and mutant EGFR patients. GSEA analysis showed that the immune-related pathways were significantly down-regulated in patients with EGFR mutations, while the PD1 pathway was significantly up-regulated in patients with high EGFR expression. Therefore, if imipramine can be used to simultaneously target EGFR mutants and inhibit the expression level of EGFR, it will be a promising therapeutic strategy.

Since EGFRvIII has pivotal clinical guiding significance in the diagnosis and treatment of GBM, we continued to explore the binding ability of imipramine and EGFRvIII. We found that the binding ability of EGFRvIII and imipramine is stronger. Combined with previous GSEA analysis of mutant EGFR *versus* wild-type EGFR, this finding demonstrates that imipramine may target EGFRvIII, thereby altering its function, which may benefit immune microenvironment, such as downregulation of PD1 and PDL1. Last, whether EGFRvIII derived from extrachromosomal DNA can be bound and blocked by imipramine may be an interesting question (Li et al., 2022).

Perspective

In recent years, more and more intersections between neuroscience and glioma biology were revealed. Venkataramani et al. have demonstrated that some glioma cells are capable of forming functional synapses with nearby neurons. In addition, these glioma cells with functional synapses are able to form electrically active tissues that can signal to other cells as well to stimulate glioma cells' migration and growth (Venkataramani et al., 2019). Targeting specific types of postsynaptic signal processing processes, or synapse formation mechanisms might be a promising therapeutic approach. Frank et al. found that the invasion of glioblastoma cells is controlled by a variety of neuronal mechanisms (Venkataramani et al., 2022). Consistently, Monje et al. found that the integration of synapses and electrical signals into neural circuits contributes to the progression of gliomas (Venkatesh et al., 2019). Innovative therapeutic advancements will be developed in the convergence between neuroscience and neuro-oncology.

The role of GABA in immune regulation is emerging. GABA, which is transformed from intracellular glutamine by glutamic acid decarboxylases (GAD1/2). GABA transport signaling through two receptors, GABAAR and GABABR. Elevated levels of GABA in late-stage human tumors are inversely associated with prognosis, as are the expressions of GAD1 and GABABR, which are usually co-expressed in cancer cells, creating an autocrine signaling loop (Hanahan and Monje, 2023). Previous studies have shown that GABA-mediated signaling contributes to the maintenance of cancer cell proliferation and immune evasion. Additionally, GABA influences tumor-promoting inflammation, affecting the balance between the two opposing aspects of the immune response to tumors. When GABA signaling is inhibited, this balance shifts towards favoring T cell attack on the tumor. Meanwhile, previous studies uncovered a mechanism for this immune evasion: GABA/GABABR/β-catenin signaling in cancer cells suppresses the expression of pro-inflammatory chemokines CCL4/5 (Huang et al., 2022). Additionally, GABA regulates pro-inflammatory macrophage responses associated with metabolic reprogramming and protein succinylation (Fu et al., 2022). In the future, exploring the role of GABA signaling in maintaining the balance between tumor-promoting inflammation and anti-tumor immune responses will be an intriguing area of study. Moreover, with the development of technologies such as spatial transcriptomics and spatial metabolomics, in some specific brain regions, such as the hippocampus or other regions, neuron-related transcription and metabolic signals will be more deciphered.

Limitations

The hypothesis proposed in this paper still has limitations, the following are some aspects that need to be further improved. First, due to the limitation of current single-cell sequencing technology, it is difficult to effectively capture a sufficient number of neurons in GBM tissue samples, which is caused by the large cell body and axonal structure of neurons. This poses a barrier to dissecting neuronal-tumor microenvironment communication at the single-cell level. Second, our study has a single-cohort bias, and the differences in the GABA pathway between normal and GBM samples, as well as the differences in immune function between wild-type EGFR and mutant EGFR, need to be verified in large-scale external cohorts. Third, further validation of molecular biology and pharmacology experiments is needed.

Data availability statement

The datasets presented in this study can be found in online repositories. The names of the repository/repositories and accession number(s) can be found in the article/Supplementary Material.

Author contributions

LH, ZL, and BW conceived the article. ZL and LH drafted the manuscript and revised it before submission. BW and JW collected the references. ZL and JW performed the analysis. JW performed molecular docking and molecular dynamics simulations. All authors contributed to the article and approved the submitted version.

Acknowledgments

We thank the paper of Douglas Hanahan's lab for the inspiration (PMID: 36113478). We also thank Yun Hak Kim's lab for the R code support (PMID: 36329504).

Conflict of interest

The authors declare that the research was conducted in the absence of any commercial or financial relationships that could be construed as a potential conflict of interest.

Publisher's note

All claims expressed in this article are solely those of the authors and do not necessarily represent those of their affiliated organizations, or those of the publisher, the editors and the reviewers. Any product that may be evaluated in this article, or claim that may be made by its manufacturer, is not guaranteed or endorsed by the publisher.

Supplementary material

The Supplementary Material for this article can be found online at: https://www.frontiersin.org/articles/10.3389/fphar.2023.1156492/full#supplementary-material

SUPPLEMENTARY FIGURE S1
The batch effect has been removed.

References

Abadi, B., Shahsavani, Y., Faramarzpour, M., Rezaei, N., and Rahimi, H.-R. (2022). Antidepressants with anti-tumor potential in treating glioblastoma: A narrative review. *Fundam. Clin. Pharmacol.* 36, 35–48. doi:10.1111/fcp.12712

Bielecka-Wajdman, A. M., Lesiak, M., Ludyga, T., Sieroń, A., and Obuchowicz, E. (2017). Reversing glioma malignancy: A new look at the role of antidepressant drugs as adjuvant therapy for glioblastoma multiforme. *Cancer Chemother. Pharmacol.* 79, 1249–1256. doi:10.1007/s00280-017-3329-2

Chen, X., Lin, Y., Liu, M., and Gilson, M. K. (2002). The binding database: Data management and interface design. *Bioinformatics* 18, 130–139. doi:10.1093/bioinformatics/18.1.130

Chryplewicz, A., Scotton, J., Tichet, M., Zomer, A., Shchors, K., Joyce, J. A., et al. (2022). Cancer cell autophagy, reprogrammed macrophages, and remodeled vasculature in glioblastoma triggers tumor immunity. *Cancer Cell* 40, 1111–1127.e9. doi:10.1016/j.ccell.2022.08.014

Daina, A., Michielin, O., and Zoete, V. (2019). SwissTargetPrediction: Updated data and new features for efficient prediction of protein targets of small molecules. *Nucleic Acids Res.* 47, W357–W364. doi:10.1093/nar/gkz382

Davis, A. P., Wiegers, T. C., Johnson, R. J., Sciaky, D., Wiegers, J., and Mattingly, C. J. (2023). Comparative toxicogenomics database (CTD): Update 2023. *Nucleic Acids Res.* 51, D1257–D1262. doi:10.1093/nar/gkac833

Fu, J., Han, Z., Wu, Z., Xia, Y., Yang, G., Yin, Y., et al. (2022). GABA regulates IL-1β production in macrophages. *Cell Rep.* 41, 111770. doi:10.1016/j.celrep.2022.111770

Han, Y., Wang, Y., Dong, X., Sun, D., Liu, Z., Yue, J., et al. (2023). TISCH2: Expanded datasets and new tools for single-cell transcriptome analyses of the tumor microenvironment. *Nucleic Acids Res.* 51, D1425–D1431. doi:10.1093/nar/gkac959

Hanahan, D., and Monje, M. (2023). Cancer hallmarks intersect with neuroscience in the tumor microenvironment. *Cancer Cell* 41, 573–580. doi:10.1016/j.ccell.2023.02.012

Hong, F., Meng, Q., Zhang, W., Zheng, R., Li, X., Cheng, T., et al. (2021). Single-cell analysis of the pan-cancer immune microenvironment and scTIME portal. *Cancer Immunol. Res.* 9, 939–951. doi:10.1158/2326-6066.CIR-20-1026

Huang, D., Wang, Y., Thompson, J. W., Yin, T., Alexander, P. B., Qin, D., et al. (2022). Cancer-cell-derived GABA promotes β-catenin-mediated tumour growth and immunosuppression. *Nat. Cell Biol.* 24, 230–241. doi:10.1038/s41556-021-00820-9

Jung, E., Alfonso, J., Osswald, M., Monyer, H., Wick, W., and Winkler, F. (2019). Emerging intersections between neuroscience and glioma biology. *Nat. Neurosci.* 22, 1951–1960. doi:10.1038/s41593-019-0540-y

Langfelder, P., and Horvath, S. (2008). Wgcna: an R package for weighted correlation network analysis. *BMC Bioinforma.* 9, 559. doi:10.1186/1471-2105-9-559

Li, Z., Wang, B., Liang, H., and Han, L. (2022). Pioneering insights of extrachromosomal DNA (ecDNA) generation, action and its implications for cancer therapy. *Int. J. Biol. Sci.* 18, 4006–4025. doi:10.7150/ijbs.73479

Lin, A., Qi, C., Wei, T., Li, M., Cheng, Q., Liu, Z., et al. (2022). Camoip: A web server for comprehensive analysis on multi-omics of immunotherapy in pan-cancer. *Brief. Bioinform* 23, bbac129. doi:10.1093/bib/bbac129

Ostrom, Q. T., Gittleman, H., Truitt, G., Boscia, A., Kruchko, C., and Barnholtz-Sloan, J. S. (2018). CBTRUS statistical report: Primary brain and other central nervous system tumors diagnosed in the United States in 2011-2015. *Neuro Oncol.* 20, iv1. doi:10.1093/neuonc/noy131

Pinzi, L., and Rastelli, G. (2019). Molecular docking: Shifting paradigms in drug discovery. *Int. J. Mol. Sci.* 20, 4331. doi:10.3390/ijms20184331

Ritchie, M. E., Phipson, B., Wu, D., Hu, Y., Law, C. W., Shi, W., et al. (2015). Limma powers differential expression analyses for RNA-sequencing and microarray studies. *Nucleic Acids Res.* 43, e47. doi:10.1093/nar/gkv007

Shannon, P., Markiel, A., Ozier, O., Baliga, N. S., Wang, J. T., Ramage, D., et al. (2003). Cytoscape: A software environment for integrated models of biomolecular interaction networks. *Genome Res.* 13, 2498–2504. doi:10.1101/gr.1239303

Shchors, K., Massaras, A., and Hanahan, D. (2015). Dual targeting of the autophagic regulatory circuitry in gliomas with repurposed drugs elicits cell-lethal autophagy and therapeutic benefit. *Cancer Cell* 28, 456–471. doi:10.1016/j.ccell.2015.08.012

Sun, L., Hui, A.-M., Su, Q., Vortmeyer, A., Kotliarov, Y., Pastorino, S., et al. (2006). Neuronal and glioma-derived stem cell factor induces angiogenesis within the brain. *Cancer Cell* 9, 287–300. doi:10.1016/j.ccr.2006.03.003

Szklarczyk, D., Gable, A. L., Lyon, D., Junge, A., Wyder, S., Huerta-Cepas, J., et al. (2019). STRING v11: Protein-protein association networks with increased coverage, supporting functional discovery in genome-wide experimental datasets. *Nucleic Acids Res.* 47, D607–D613. doi:10.1093/nar/gky1131

Venkataramani, V., Tanev, D. I., Strahle, C., Studier-Fischer, A., Fankhauser, L., Kessler, T., et al. (2019). Glutamatergic synaptic input to glioma cells drives brain tumour progression. *Nature* 573, 532–538. doi:10.1038/s41586-019-1564-x

Venkataramani, V., Yang, Y., Schubert, M. C., Reyhan, E., Tetzlaff, S. K., Wißmann, N., et al. (2022). Glioblastoma hijacks neuronal mechanisms for brain invasion. *Cell* 185, 2899–2917.e31. doi:10.1016/j.cell.2022.06.054

Venkatesh, H. S., Morishita, W., Geraghty, A. C., Silverbush, D., Gillespie, S. M., Arzt, M., et al. (2019). Electrical and synaptic integration of glioma into neural circuits. *Nature* 573, 539–545. doi:10.1038/s41586-019-1563-y

Walker, A. J., Card, T., Bates, T. E., and Muir, K. (2011). Tricyclic antidepressants and the incidence of certain cancers: A study using the GPRD. *Br. J. Cancer* 104, 193–197. doi:10.1038/sj.bjc.6605996

Wu, J., Ge, F., Zhu, L., and Liu, N. (2023). Potential toxic mechanisms of neonicotinoid insecticides in rice: Inhibiting auxin-mediated signal transduction. *Environ. Sci. Technol.* 57, 4852–4862. doi:10.1021/acs.est.2c09352

Wu, T., Hu, E., Xu, S., Chen, M., Guo, P., Dai, Z., et al. (2021). clusterProfiler 4.0: A universal enrichment tool for interpreting omics data. *Innov. (Camb)* 2, 100141. doi:10.1016/j.xinn.2021.100141

Yao, Z.-J., Dong, J., Che, Y.-J., Zhu, M.-F., Wen, M., Wang, N.-N., et al. (2016). TargetNet: A web service for predicting potential drug-target interaction profiling via multi-target SAR models. *J. Comput. Aided Mol. Des.* 30, 413–424. doi:10.1007/s10822-016-9915-2

frontiers | Frontiers in Pharmacology

TYPE Review
PUBLISHED 30 June 2023
DOI 10.3389/fphar.2023.1211719

Check for updates

OPEN ACCESS

EDITED BY
David A. Gewirtz,
Virginia Commonwealth University,
United States

REVIEWED BY
Kui Zhang,
The University of Chicago, United States
Mariana Magalhães,
University of Coimbra, Portugal

*CORRESPONDENCE
Xia Xu,
xu.bertha@csu.edu.cn

RECEIVED 25 April 2023
ACCEPTED 23 June 2023
PUBLISHED 30 June 2023

CITATION
Li W and Xu X (2023), Advances in mitophagy and mitochondrial apoptosis pathway-related drugs in glioblastoma treatment.
Front. Pharmacol. 14:1211719.
doi: 10.3389/fphar.2023.1211719

COPYRIGHT
© 2023 Li and Xu. This is an open-access article distributed under the terms of the Creative Commons Attribution License (CC BY). The use, distribution or reproduction in other forums is permitted, provided the original author(s) and the copyright owner(s) are credited and that the original publication in this journal is cited, in accordance with accepted academic practice. No use, distribution or reproduction is permitted which does not comply with these terms.

Advances in mitophagy and mitochondrial apoptosis pathway-related drugs in glioblastoma treatment

Weiping Li and Xia Xu*

Department of General Practice, Xiangya Hospital of Central South University, Changsha, Hunan, China

Glioblastoma (GBM) is the most common malignant tumor of the central nervous system (CNS). It is a leading cause of death among patients with intracranial malignant tumors. GBM exhibits intra- and inter-tumor heterogeneity, leading to drug resistance and eventual tumor recurrence. Conventional treatments for GBM include maximum surgical resection of glioma tissue, temozolomide administration, and radiotherapy, but these methods do not effectively halt cancer progression. Therefore, development of novel methods for the treatment of GBM and identification of new therapeutic targets are urgently required. In recent years, studies have shown that drugs related to mitophagy and mitochondrial apoptosis pathways can promote the death of glioblastoma cells by inducing mitochondrial damage, impairing adenosine triphosphate (ATP) synthesis, and depleting large amounts of ATP. Some studies have also shown that modern nano-drug delivery technology targeting mitochondria can achieve better drug release and deeper tissue penetration, suggesting that mitochondria could be a new target for intervention and therapy. The combination of drugs targeting mitochondrial apoptosis and autophagy pathways with nanotechnology is a promising novel approach for treating GBM.This article reviews the current status of drug therapy for GBM, drugs targeting mitophagy and mitochondrial apoptosis pathways, the potential of mitochondria as a new target for GBM treatment, the latest developments pertaining to GBM treatment, and promising directions for future research.

KEYWORDS

drugs, glioblastoma, mitochondrial apoptosis, mitophagy, new developments

1 Introduction

Glioblastoma (GBM) is a malignant tumor that develops from astrocytes, which are cells that support nerve cells in the brain(Watson et al., 2023). It can also develop from mutations in specific pathways related to cell death and proliferation in different cells of the brain(Louis et al., 2021). Unfortunately, it has the lowest 5-year relative survival rate among central nervous system tumors (6.8%) (Ostrom et al., 2019). The first-line treatment for GBM includes maximal surgical resection followed by concomitant chemoradiotherapy and adjuvant chemotherapy (TMZ). (Szklener et al., 2022). After standard-of-care surgery and adjuvant chemotherapy, the approximate median survival is 14–16 months. It is mainly induced by its high resistance to radiotherapy and chemotherapy and the inability to remove the tumor tissue completely (Ohgaki and Kleihues, 2005; Lah et al., 2020). GBM-initiating cells (GICs), also known as GBM stem cells (GSCs), have the potential for self-renewal, multi-directional differentiation, and tumor initiation,

TABLE 1 Summary of main mitophagy and mitochondrial apoptosis pathway-related drugs in GBM treatment.

Classification	Drugs
Mitophagy pathway-related drugs	Silibinin
	Cannabidiol
	Gossypol (AT-101)
Apoptosis pathway-related drugs	Xanthohumol
	Pterostilbene
	Chrysophanol
	Shikonin
	Grape seeds
Mitophagy and mitochondrial apoptosis pathway-related drugs	Sinomenine

which are associated with treatment resistance and relapse and are considered to be the cause of relapse in most patients with this devastating disease (He et al., 2021; Yi et al., 2019, Osuka and Van Meir, 2017). Temozolomide (TMZ) is a currently the first-line drug used for GBM treatment independent of the methylation state of O6-methylguanine methyltransferase(MGMT), which can induce DNA strand breaks during cell replication and thus promotes cell apoptosis(Hegi et al., 2019). Owing to the overexpression of MGMT and the lack of DNA repair pathways in GMB, TMZ-resistance is a major obstacle in improving the prognosis of patients with GBM (Chen et al., 2018; Lin et al., 2022a). Furthermore, phenotypic and genotypic heterogeneity (Banelli et al., 2017), hypoxic tumor environment (Ho et al., 2022), the presence of glioblastoma stem cells (Huang et al., 2020), abnormal signaling pathways (Yu et al., 2019; Liu et al., 2020a; Lee et al., 2022a), and notably, the existence of the blood–brain barrier (BBB) (Zou et al., 2022) result in a need for increased chemotherapeutic drug doses to reach effective concentrations of the drugs, which worsens the systemic side effects of the drugs (Oberoi et al., 2016). Therefore, further research, drug development, and identification of novel and effective drugs are urgently needed.

In recent years, natural products, synthetic drugs, and cytokines targeting the mitochondria have increasingly been applied for the prevention and treatment of various tumors, and their promising results in anti-tumor research and application are becoming evident. This review focuses on research progress into potential natural drug leads for inducing mitophagy or apoptotic pathways that may be relevant to GBM (Tab.1).

2 Mitophagy and GBM

2.1 Mitophagy

Mitochondria are important organelles that play important roles in cellular metabolism, including but not limited to the production of ATP via electron transport coupled with oxidative phosphorylation, tricarboxylic acid cycle, fatty acid β-oxidation, amino acid synthesis, calcium homeostasis, and iron metabolism (biosynthesis of heme and iron-sulfur clusters) (Zhang et al., 2022a). According to the International Cancer Genome Consortium and The Cancer Genome Atlas Program, mutations in mitochondrial DNA (mtDNA) can be detected in approximately 60% of solid tumors, and the accumulation of mutations in mtDNA can result in mitochondrial dysfunction(Leao et al., 2021). In glioma, mitochondrial function is impaired by marked alterations in the mitochondrial genome, resulting in altered morphology and abnormal bioenergetics, including increased ROS production(Lu and Ho, 2020). Mitochondrial dysfunction plays a crucial role in the regulation of several cancer intrinsic pathways related to tumor metabolism, survival, proliferation, and cell death in GBM (Lu and Ho, 2020).

Autophagy, morphologically characterized by the formation of autophagosomes or autolysosomes in the cytoplasm, is a degradation pathway through which intracellular materials or impaired organelles are transported to lysosomes for clearance (Levy et al., 2017). Autophagy has a dual function in GBM. As a tumor suppressor, it can destroy harmful unfolded proteins, oncogenic protein substrates, and damaged organelles (Batara et al., 2021). For instance, according to recent studies, breast cancer patients with brain metastases may benefit from therapeutic strategies aimed at targeting autophagy (Maiti and Hait, 2021).It may also have a role in protecting GBM cells by eliminating misfolded proteins generated during oxidative stress (Di Rita et al., 2018). Combining standard cancer treatment with the regulation of autophagy activity, by promoting or preventing autophagy using inducers or inhibitors based on tumorigenesis and cancer stages, has the potential to be a promising anti-cancer therapy (Li et al., 2020). Mitophagy refers to the selective removal of damaged mitochondria through the autophagy mechanism to maintain mitochondrial quality and rescue cells from death (Bravo-San et al., 2017; Wang et al., 2018).

These pathways can be classified into typical and atypical. The typical pathway mainly includes PINK1/parkin-, BNIP3/NIX-, and FUNDC1-mediated mitophagy, whereas the atypical pathway mainly includes lipid-, AMBRA1-, BCL2L13-, FKBP8-, and RAB-mediated mitophagy (Vara-Perez et al., 2019). Of note, the autophagy/lysosomal pathway that removes damaged mitochondria (i.e., mitophagy) is impaired in patients with Alzheimer's disease, which leads to the accumulation of dysfunctional mitochondria, leading to synaptic dysfunction and cognitive deficits (Kerr et al., 2017). Dopaminergic neurons selectively fail to execute mitophagy, which promotes their survival(Bernardini et al., 2017; Katayama et al., 2020) within lesions in a mouse model of Parkinson's disease. Rapamycin reduces cisplatin-mediated nephrotoxicity by stimulating PINK1/parkin-mediated mitophagy in renal tubular cells, reducing tissue damage caused by chemotherapy (Wang et al., 2018). Accordingly, mitophagy plays a crucial role in maintaining cellular homeostasis and is a major pathway for the degradation of dysfunctional or damaged mitochondria. Moreover, mitophagy is also a programmed event involved in developmental and differentiation processes, including the elimination of paternal mitochondria from fertilized eggs (Song et al., 2021), as well as the removal of mitochondria during erythropoiesis and muscle differentiation (Senft and Ronai, 2016; Panigrahi et al., 2020) (Figure 1).

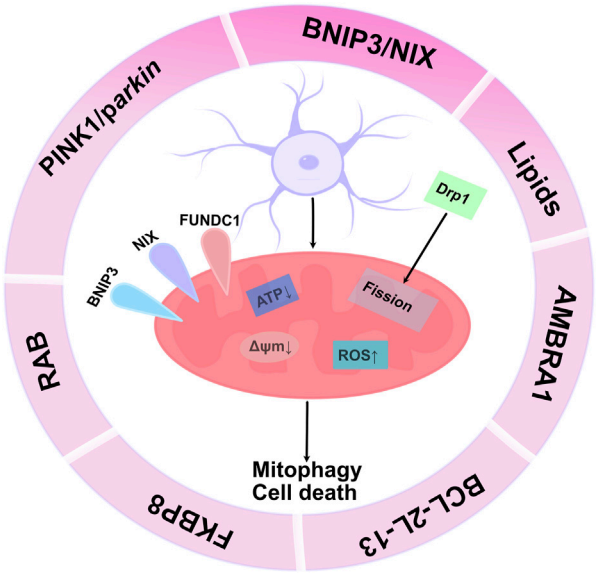

FIGURE 1
Molecular mechanism of mitophagy: The figure reflects mitophagy mediated by receptors (mainly BINP3, NIX, PINK1/parkin, FUNDC1, BCL-2L-13, lipids, RAB, FKBP8). These mitochondrial receptors mediate mitophagy by directly binding to LC3 on autophagosomes via a conserved LIR motif in their N-terminal region. Lipid accumulation on the mitochondrial outer membrane maintains cellular homeostasis, thereby regulating the mitophagy machinery. Hypoxia is an important stimulus that induces this process. PINK1/parkin-mediated mitophagy occurs in a ubiquitination-dependent manner, and ubiquitination of specific mitochondrial proteins enhances phosphorylation of ubiquitin on mitochondrial proteins by PINK1 to recruit mitophagy receptors and mediate the process of mitophagy. After further polyubiquitination, parkin recruits adapter proteins (such as p62/SQSTM1, OPTN) and interacts with LC3 on the membrane surface of autophagosomes to promote mitophagy.

2.2 Relationship between mitophagy and GBM

Activation of mitophagy has been used in the treatment of GBM(Zhou et al., 2020; Wang et al., 2022; Cammarata et al., 2023).It can relieve stress and suppressing tumors by eliminating dysfunctional mitochondria, and mitophagy-mediated clearance of pro-apoptotic mitochondria may provide cytoprotective benefits(Panigrahi et al., 2020). In recent years, studies have shown that drugs related to mitophagy pathways can promote the death of GBM cells by inducing mitochondrial damage, impairing ATP synthesis, and depleting ATP in large quantities. The induction of lethal autophagy has become a strategy to eliminate GBM cells, which is reportedly an effective method to eradicate cancer cells(Maiti et al., 2019; Meng et al., 2022; Rademaker et al., 2022).

2.3 Drugs related to mitophagy

2.3.1 Silibinin

Silibinin is a flavonoid extracted and isolated from the fruit of the chrysanthemum plant Silybum marianum (Tuli et al., 2021). It has been widely used for the treatment and prevention of various hepatobiliary disorders, including alcoholic liver disease, non-alcoholic fatty liver disease, and mushroom poisoning (Abenavoli et al., 2018; Hosseinabadi et al., 2019; Wang et al., 2020a). Recent studies have demonstrated the broad-spectrum anti-cancer effects of silibinin against most types of cancer cells(Jahanafrooz et al., 2018). For example, it can inhibit the migration and invasion of breast cancer MDA-MB-231 cells through induction of mitochondrial fusion(Si et al., 2020). In hepatocellular carcinoma, silibinin has been found to effectively abate hepatocarcinogenesis and hepatocellular carcinoma growth by regulating various signaling pathways including HGF/c-Met, Wnt/β-catenin and PI3K/Akt/mTOR(Yassin et al., 2022). In cholangiocarcinoma, silibinin has the ability to inhibit cholangiocarcinoma through the ERK/mitochondrial apoptotic pathway, which makes silibinin a potential anti-tumor drug candidate for cholangiocarcinoma treatment(Bai et al., 2022).

Considering that silibinin has extremely high antioxidant and anti-tumor properties, it has drawn our attention to its potential use in the treatment of GBM.BNIP3, a member of the Bcl-2 family of pro-apoptotic proteins and a receptor for mitophagy, exhibits context-dependent roles in cancer(Gorbunova et al., 2020; Gorbunova et al., 2020; Vara-Perez et al., 2021).It targets mitochondria and could induce mitochondrial damage and nuclear translocation of AIF6 (Su et al., 2016). A study using GBM cell lines and nude mice with xenografted GBM has confirmed that silibinin could induce mitophagy in GBM, and that autophagy can promote silibinin-induced BNIP3 overexpression and its accumulation in the mitochondria, thereby triggering AIF-dependent death in GBM cells (Wang et al., 2020b). Moreover, silibinin has also been shown to inhibit GBM cell migration by inhibiting MMP-2 and -9 and improving TMZ-resistance in GBM cells (Zhai et al., 2021; Wong et al., 2023). Silibinin have potential uses for patients with GBM. However, like other polyphenols, faces the challenge of low bioavailability, which impedes its potential as a transformative chemotherapeutic drug(Tuli et al., 2021). At the same time, further clinical research is also needed to better understand the potential toxicity and risks associated with the drug's use in treating GBM. This will provide more reliable evidence to support clinical treatment of GBM.

2.3.2 Cannabidiol

Cannabidiol (CBD), the main active component of medical cannabis, is extracted from the wild hemp (Karimi-Haghighi et al., 2022). It easily passes through the BBB, is highly safe, and has anti-proliferation and anti-invasion activities against various cancers (Valenti et al., 2022; Ammendolia et al., 2023). The literature indicates that in many animal cancer models, CBD has shown potential in inhibiting the progression of various types of cancers, including in GBM, breast(Kiskova et al., 2019; Valenti et al., 2022), lung(Milian et al., 2022; Misri et al., 2022), prostate(Mahmoud et al., 2023), colon cancer(Jeong et al., 2019; Lee et al., 2022b; Yuksel et al., 2023), and melanoma(Bachari et al., 2020). CBD has emerged as a promising agent in the treatment of glioma cells due to its ability to inhibit their proliferation and promote cell death. This effect is mainly achieved by targeting the mitophagy pathway, which has gained significant attention in recent research.

Transient receptor potential vanilloid 4 (TRPV4) is a widely expressed multimodal-gated ion channel that plays a pivotal role in many physiological and pathophysiological processes (Grace et al., 2017; Muller and Reggio, 2020). Its expression in human brain basement membrane tissue is closely related to tumor grade and prognosis (Yang et al., 2020). CBD can induce mitophagy by activating endoplasmic reticulum stress via the TRPV4–ATF4–DDIT3–TRIB3–AKT–MTOR axis. TRPV4 expression in human GBM tissues correlates with both tumor grade and poor survival, suggesting that TRPV4 could be an attractive therapeutic target and biomarker for GBM (Huang et al., 2021a). CBD can also lead to abnormal stability of the plasma membrane by affecting the homeostasis of GBM lipid metabolism, thereby promoting the phagocytosis of tumor cells by macrophages and exerting an anti-GBM effect (Khodadadi et al., 2021; Genovese et al., 2022). These two mechanisms synergistically inhibit the formation and development of GBM, indicating that CBD has great clinical application prospects as an anti-GBM medicine et al., 2021).

Simultaneously, compared with single drug treatment alone, the combined treatment of CBD and TMZ more effectively targeted GBM patients, significantly inhibiting the growth of GBM cells and prolonging survival time, suggesting that CBD can effectively enhance the anti-tumor effect of TMZ in GBM (Lopez-Valero et al., 2018; Huang et al., 2021b). Furthermore, in the first study on the CBD-induced anti-tumor effects of RELA Ser311 phosphorylation, ROS was shown to serve as a biomarker for stratifying patients who may benefit from CBD treatment (Volmar et al., 2021).

2.3.3 Gossypol (AT-101)

Gossypol (2,2′-bis-(formyl-1,6,7-trihydroxy-5-isopropyl-3-methylnaphthalene), a BH3-mimetic compound naturally present in cottonseed, exerts anti-tumor effects by targeting various signal transduction pathways. It has been extensively studied in clinical trials, where it has shown good tolerability and safety (Benvenuto et al., 2018; Yurekli et al., 2018). However, recent studies have found that it is the (-)-enantiomer of gossypol, namely (-)-gossypol (also known as AT-101), rather than (+)-gossypol or racemic gossypol, that has significant anti-cancer properties (Benvenuto et al., 2018). Therefore, the development of single-isomer pharmaceutical preparations can avoid potential adverse reactions. Thus far, AT-101 has been considered a promising anti-cancer drug for the treatment of various tumors, including multiple myeloma (Ailawadhi et al., 2023), adrenal cortical carcinoma (Yurekli et al., 2018), esophagus cancer (Que et al., 2019), breast cancer (Bulut et al., 2020), lung cancer (Ahmad et al., 2021; Renner et al., 2022), and prostate cancer (Aktepe and Yukselten, 2022).

HMOX1 is an inducible enzyme that catalyzes the degradation of oxidized preheme and is also involved in mitochondrial biogenesis and mitophagy (Constantin et al., 2012; Hull et al., 2016). AT-101 can promote GBM cell death by inducing overactivation of HMOX1 and the autophagy receptors BNIP3 and BNIP3L, causing early mitochondrial dysfunction and marked loss of mitochondrial mass/protein (Meyer et al., 2018). It also suppresses the growth of TMZ-resistant glioblastoma (Kim et al., 2019). Mitochondrial respiration and mitochondrial permeability transition pore opening were impaired after AT-101 treatment, suggesting that mitochondrial dysfunction is a key driver of AT-101-induced cell demise (Meyer et al., 2018). Because the AT-101 molecule is hydrophobic, oral administration greatly reduces its bioavailability, and gastrointestinal side effects can easily be caused. Therefore, the cyclic RGD (cRGD)-decorated mixed liposome (cRGD-LP) nanopreparation for the tumor-targeted delivery of AT-101 (abbreviated as Gos hereafter) came into being (Xie et al., 2019a; Liu et al., 2022). This nanoformulation enhanced tumor engraftment *in vivo*, possibly due to cRGD binding to the αvβ3 integrin on tumors and tumor cells, enhancing tumor targeting (Liu et al., 2022). Moreover, some studies have also shown that arsenic trioxide-mediated hedgehog/notch inhibition can interfere with DNA double-stranded break repair by reducing the expression of CHEK1 and CHEK2, synergistically targeting GSC along with AT-101 (Linder et al., 2019). AT-101 combined with demethoxycurcumin can enhance the inhibitory effect on the proliferation of glioblastoma cells (Mehner et al., 2020), suggesting that combination therapy with different agents may be an option to overcome drug resistance in GBM cells effectively, in a long-term treatment strategy.

3 Mitochondrial apoptosis and GBM

3.1 Mitochondrial apoptosis

Mitochondria serve as vital organelles in diverse cellular functions, including oxidative phosphorylation, ROS, and calcium signaling, as well as intermediate metabolite synthesis required for cell growth and motility(Bhargava and Schnellmann, 2017). ROS are a crucial class of molecules directly involved in the regulation of mitochondrial function, mainly produced by mitochondrial oxidative phosphorylation. Various cellular metabolic processes are associated with ROS, including transcription factor activation, gene expression, and cell differentiation and proliferation (Thannickal and Fanburg, 2000). Apoptosis is a type of programmed cell death that maintains the homeostasis of the internal environment, which is mainly regulated by the activation of the caspase cascade (Zimmermann et al., 2001). Caspase-3 is considered as the most important regulator of apoptosis, while caspase-9 is considered to be the master regulator of mitochondria-mediated apoptosis (Batoon et al., 2023; Cao et al., 2023). Apoptosis is controlled by intrinsic (mitochondrial pathway) and extrinsic pathways, and the intrinsic pathway is regulated by the BCL-2 family, including the anti-apoptotic activator BCL-xL and proapoptotic effector BAX(Lindenboim et al., 2000). Cell stress induces the proapoptotic effector BAX to induce cell apoptosis by inducing the release of cytochrome-c (Cyt-C), a key component of the mitochondrial electron transport chain, into the cytoplasm (Finucane et al., 1999; Desagher and Martinou, 2000). In the extrinsic pathway, caspase-8 cleaves and activates procaspase-3 (Boatright and Salvesen, 2003). However, the result of both pathways is caspase activation and the cleavage of specific cellular substrates, leading to morphological and biochemical changes associated with an apoptotic phenotype (Lee et al., 2020). In this process, apoptosis is characterized by the formation of apoptotic bodies, containing the contents of dead cells, which will be engulfed by the surrounding cells without

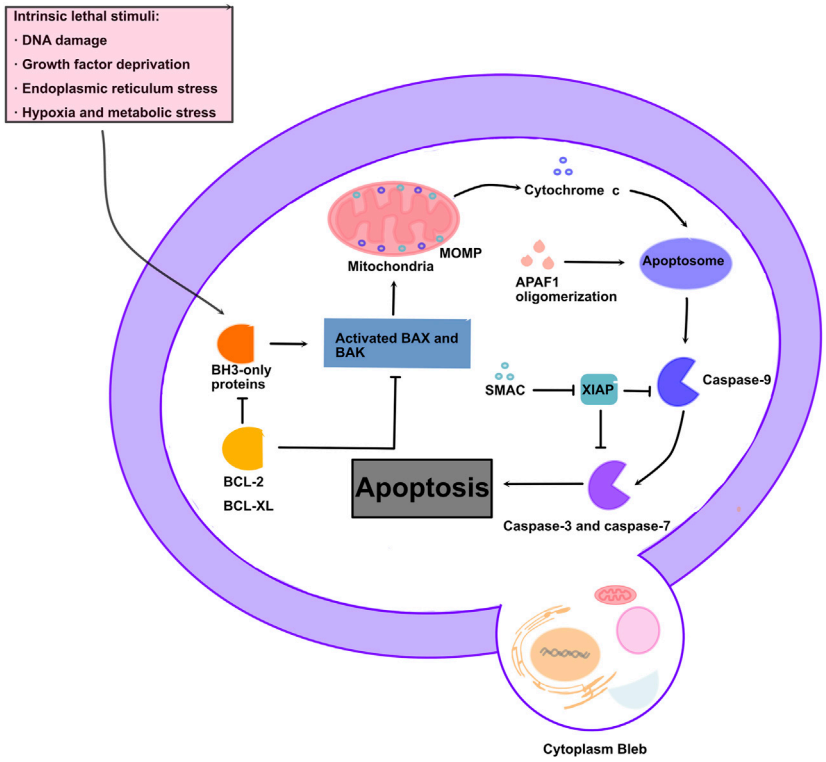

FIGURE 2
Molecular mechanism of mitochondrial apoptosis: Apoptotic stresses promote accumulation of BH3-only proteins leading to BAX/BAK oligomerization, MOMP, and release of intermembrane space proteins. Cytochrome c leads to apoptosome formation, which results in caspase activation and apoptosis.

causing content leakage or damage to the surrounding cells (Li et al., 2021) (Figure 2).

3.2 Relationship between mitochondrial apoptosis and GBM

The accumulation of intracellular ROS can cause carcinogenesis. In GBM cells that require high levels of ROS, if ROS are lower than the minimum level for GBM cell survival, it may induce intracellular signaling disturbances and apoptosis (Huang et al., 2021a; Huangfu et al., 2021). The accumulation of mutations in mitochondrial DNA (mtDNA) contributes to mitochondrial dysfunction, which plays a crucial role in the pathogenesis of GBM. This dysfunction leads to abnormal energy and reactive oxygen species production, as well as resistance to apoptosis and chemotherapeutic agents(Leao et al., 2021).While many chemotherapeutic drugs play a tumor-killing role by inducing ROS and enhancing oxidative stress, they can also damage the mitochondria and DNA of normal cells and even induce carcinogenesis in other cells (Kleih et al., 2019). Therefore, regulating the level of ROS in tumor and normal tissues and selectively killing tumor cells has great clinical significance (Di Meo et al., 2022). Mitochondria are considered to be novel targets for cancer intervention and therapy (Xu et al., 2009). It can induce apoptosis in GBM cells by disrupting the balance in the anti-oxidant system, which are important mechanisms in the research of anti-tumor therapies (Benlloch et al., 2016; Feng et al., 2016).

3.3 Drugs related to mitochondrial apoptosis

3.3.1 Xanthohumol

Xanthohumol (XN), a natural compound found in hops, is an isoprene flavonoid with a wide range of biological activities, including anti-inflammatory, anti-oxidant, anti-cancer, antibacterial, and lipid lowering (Lin et al., 2022c; Neumann et al., 2022). Since flavonoids readily cross the BBB *in vivo*, they are considered potential drug leads for treating disease. Several studies have shown that XN has anti-GBM effects. It can not only inhibit the IGFBP2/AKT/BCL-2 pathway and activate the P53 signaling pathway to participate in XN-induced GBM cell apoptosis (Chen et al., 2016), but it also induces apoptosis of glial pathway cells by increasing ROS and activating MAPK pathways (Festa et al., 2011). Hou et al. confirmed that XN can inhibit C6 proliferation, trigger mitochondrial stress, and induce cell death in a concentration- and time-dependent manner (Hou et al., 2021). Following treatment of GBM cells with XN, the cell cycle was blocked at the G0/G1 phase, and XN induced AIF-mediated apoptosis, which was accompanied by mitochondrial structure and function impairment, as well as mitophagy blockage (Hou et al., 2021). In contrast, mitochondrial injury not only disrupts

ATP synthesis in cells but also consumed large amounts of ATP to maintain intracellular stability. This vicious cycle exacerbates cellular energy consumption. The DNA repair machinery is a tool to remove DNA damage for the maintenance of genomic integrity in normal cells and paradoxically plays a crucial role in driving the development of drug resistance and tumor recurrence (Huang and Zhou, 2021). The results of Ho et al. showed that XN could enhance the cytotoxicity of TMZ by inhibiting the DNA repair system and could be used as an adjuvant drug in the treatment of patients with GBM with DNA repair activation (Ho et al., 2020). Moreover, XN also reduces the invasiveness of GBM cells by inhibiting the signaling of stromal interacting molecule 1 (STIM1), indicating that XN may be a good GBM therapeutic agent (Ho et al., 2018). Elucidating the XN-mediated molecular mechanism may provide novel strategies for future drug development and tumor research.

3.3.2 Pterostilbene

As a methylated derivative of resveratrol, pterostilbene (PTE) has higher biological activity and safety than resveratrol and is mainly found in blueberries and grapes (Rimando et al., 2004; Ruiz et al., 2009; Chang et al., 2012). PTE has a wide range of biological functions, including anti-tumor, anti-oxidation, anti-inflammatory, apoptosis, cardiovascular protection, anti-proliferation, and antibacterial activities (Chen et al., 2020), gallbladder (Tong et al., 2021), breast (Harandi-Zadeh et al., 2021; Kumar et al., 2021), colon (Wawszczyk et al., 2022), cervical (Shin et al., 2020), prostate (Hemani et al., 2022), and lung cancers (Bracht et al., 2019). In GBM, PTE can induce the loss of mitochondrial membrane potential and production of reactive oxygen species (ROS) (Gao et al., 2021) and activate the FAS/FASL pathway and caspase-3, thereby inhibiting proliferation and inducing GBM cell apoptosis (Tan et al., 2019; Gao et al., 2021). Moreover, given that PTE presents highly bioavailability and easily crosses the BBB, PTE administration can serve as a novel treatment for patients with GBM (Ma et al., 2019). Based on the abovementioned experimental results, PTE has a high research value and development prospects in the field of GBM drug treatment.

3.3.3 Chrysophanol

Chrysophanol (1, 8-dihydroxy-3-methyl-9, 10-anthraquinone) is a phytochemical extracted from Rheum officinale (rhubarb), which has been utilized as a traditional Chinese herbal medicine (Yusuf et al., 2019; Su et al., 2020). It has various pharmacological effects, including anti-cancer, antioxidant, neuroprotective, antibacterial, antiviral, and blood lipid-regulation effects. Studies have shown that chrysophanol can attenuate hepatic stellate cell-induced endoplasmic reticulum fibrosis by regulating hepatitis B virus stress and iron concentration (Kuo et al., 2020). Moreover, it can inhibit the growth and metastasis of T-cell acute lymphoblastic leukemia through the miR-9/PD-L1 axis (Yin et al., 2021), regulating the effect of the microRNA-27b-3p/peroxisome proliferator-activated receptor γ axis on sepsis-induced acute myocardium damage protection (Park et al., 2022).

Moreover, the application of chrysophanol for cancer treatment is also increasing. For instance, chrysophanol promotes cell morphological changes, induces cell apoptosis through DNA damage, and arrests S phase cell cycle among patients with liver cancer (Ni et al., 2012). In patients with lung cancer, chrysophanol expresses anti-cancer activity by regulating the ROS/HIF-1a/VEGF signaling pathway (Zhang et al., 2020a; Zhang et al., 2021a). In patients with GBM, it has been discovered that chrysophanol increased the accumulation of ROS in the mitochondria of GBM cells, promoting the release of Cyt-C from the mitochondria to the cytoplasm and, thereby, causing GBM cell apoptosis (Gu et al., 2021). Chrysophanol regulates the anti-cancer effect on GBM cells by activating the mitochondrial apoptosis pathway, indicating that it may serve as an innovative chemotherapeutic agent for GBM. However, chrysophanol has obvious hepatotoxicity and nephrotoxicity. Nevertheless, pharmacokinetics has shown that chrysophanol combined with other drugs can reduce toxicity and improve efficacy (Xie et al., 2019b).

3.3.4 Shikonin

Shikonin is the main bioactive component extracted from the root of Lithospermum erythrorhizon, which has various bioactivities related to cancer treatment, inflammation, and wound healing. Many studies have shown that shikonin has strong anti-cancer effects on leukemia, gastrointestinal cancer, pancreatic cancer, lung cancer, breast cancer, and urogenital organ cancer, by inhibiting cell proliferation and migration, and inducing apoptosis and necroptosis (Guo et al., 2019). A clinical trial conducted by Guo et al. reported that, among 19 patients suffering from late-stage lung cancer who were not subjected to surgery, chemotherapy, or radiotherapy, the tumor diameter decreased by more than 25% after treatment with shikonin, posing a remission rate of 37% and a 1-year survival rate of 47% (Boulos et al., 2019). Shikonin is a potent inducer of necrotizing apoptosis in cancer cells. In terms of pharmacological mechanism, anti-glioma effect of shikonin by interfering with endoplasmic reticulum stress-mediated tumor apoptosis targeting Caspase-3, and Bax/Bak-induced mitochondrial outer membrane permeabilization (MOMP) triggering cancer cell apoptosis (Ma et al., 2020). ROS is the executor of necrotizing apoptosis. Shikonin increases intracellular ROS levels by targeting both NOX1 and the mitochondrial respiratory chain complex (Yang et al., 2014). RIP1 and RIP3 can modulate shikonin-induced ROS overproduction by targeting the mitochondria and promoting RIP1/RIP3-dependent necroptosis in GBM cells (Lu et al., 2017). Shikonin has shown great promise as a potential drug for treating glioma by targeting the mitochondrial apoptosis pathway. In order to achieve greater precision and efficacy in treating glioma, it is necessary to consider the shikonin's ability to cross the blood-brain barrier. Wang et al. developed an AS1411 aptamer/hyaluronic acid-bifunctionalized microemulsion co-loading shikonin and docetaxel (AS1411/SKN&DTX-M), which has the ability to penetrate the BBB according to their research report. The codelivery of shikonin and docetaxel through bifunctionalization with hyaluronic acid and AS1411 aptamer presents a promising approach for anti-GBM therapy using dual-drug therapy (Wang et al., 2019).

3.3.5 Grape seeds

Grape seeds are the seeds of Vitis vinifera. Grape seed proanthocyanidins (GSP) is a general term for a large class of polyphenolic compounds that have antioxidant activity. GSP has

various biological activities and has been proven to have good anti-tumor effects, as well as certain inhibitory effects on cervical cancer (Li et al., 2022a), carcinoma of the urinary bladder (Yang et al., 2021a), lung cancer (Xu et al., 2021a; Zhang et al., 2021; Mao et al., 2023), colon cancer (Aiello et al., 2019; Zhang et al., 2019), liver cancer (Feng et al., 2019), prostate cancer (Chen and Yu, 2019), among others. In a study on liver cancer cells, GSP was found to trigger ROS production, decrease matrix-metalloproteinases (MMPs), and increase caspase-3 activity in HepG2 cells (Wang et al., 2020), proving that GSPs may induce ROS production and, consequently, lead to MMP reduction and caspase-3 activation. This ultimately induces HepG2 cell apoptosis. GSP can reverse EMT by inhibiting the TGF-β signaling pathway, effectively inhibiting the migration and invasion of bladder cancer (BC) cells (Yang et al., 2021b), suggesting that GSP can be used as a potential chemotherapy drug for BC. GSP can also reduce the proliferation activity of cancer cells (Habib et al., 2022). The mechanism of GSP pertaining to GBM is related to the inhibition of proliferation, induction of apoptosis, arrest of the cell cycle, and inhibition of angiogenesis and metastasis (Yang et al., 2021b). Grape seed, as a natural anti-cancer drug, holds great promise for the treatment of glioma. However, further clinical research is necessary to fully elucidate its role in the treatment mechanism.

3.4 Drugs related to mitochondrial apoptosis and mitophagy

3.4.1 Sinomenine

The alkaloid sinomenine (SIN), namely 7,8-didehydro-4-hydroxy-3,7-dimethoxy-17-methylmorphinan-6-one (C19H23NO4), is extracted from the rhizome of the traditional Chinese medicine plant Sinomenium acutum (Zheng et al., 2021). SIN has anti-inflammatory effects and has been used to treat rheumatoid diseases in humans (Lin et al., 2022b; Chen et al., 2022). In recent years, SIN and its derivatives have been reported to have strong anti-tumor activity against various tumors, including BC (Xu et al., 2021b), prostate (Xu et al., 2019), papillary thyroid (Zhang et al., 2022b), breast (Li et al., 2022b; Gao et al., 2022), ovarian (Qu et al., 2021), and lung cancers (Bai et al., 2021). SIN can inhibit cell proliferation (Sun et al., 2018a; He et al., 2018), induce apoptosis (Liu et al., 2019) and arrest the cell cycle at the G0/G1 phase in various cancers (Yang et al., 2021a). SINI-WCJ-33 (SW33, C33H51NO5), a SIN-derivative obtained by the acylation of 4-hydroxyl and 14-carboxylic acid, can inhibit the proliferation, migration, invasion, and colony formation of human glioblastoma cell lines (Zheng et al., 2021). This derivative has higher anti-GBM activity and safety than its parent compound (Liu et al., 2019). The CCNB1/CDC2 complex is a key mediator of the G2/M checkpoint (Park et al., 2000; Taylor and Stark, 2001; Cheng et al., 2016). The polo-like kinase (PLK1)-dependent phosphorylation of CDC25C is required for normal cell cycle progression from the G2/M phase (Liu et al., 2020b; Tang et al., 2020). SW33 can reduce the expression of P-CDC2, CDC2, and CCNB1, as well as the protein levels of P-PLK1 and PCDC25C in GBM cells. It can also increase the expression of P53 and its transcriptional target P21, finally leading to the arrest of the GBM cell cycle in the G2/M phase, causing mitochondrial dysfunction, consequently releasing Cyt-C, activating caspase 3/9, and inducing mitochondrial apoptosis (Zheng et al., 2021).

In addition, PI3K/AKT/MTOR, MAPK/MTOR, and AMPK/MTOR have been widely reported to activate mitophagy (Zhang et al., 2020b; Liu et al., 2021). Zheng et al. have shown that SW33 can induce autophagy through the PI3K/AKT/MTOR and AMPK/MTOR signaling pathways in patients with GBM, thus playing an anti-GBM role, significantly inhibiting tumorigenesis, without having obvious adverse effects on the body (Zheng et al., 2021). Taken together, all these results suggest that SW33 may be a promising drug for the treatment of GBM.

4 New advances in drug therapy for GBM

4.1 The application of nanotechnology in GBM

The BBB comprises multiple components with barrier functions, including polarized endothelial cells connected by continuous adhesive and tight junctions, endothelial and parenchymal basement membranes, pericytes, and astrocyte foot processes (endfeet) (Steeg, 2021). As a barrier between circulating blood and brain parenchyma, it can prevent blood-borne pathogens or toxic substances from entering the CNS, maintain the dynamic balance of the CNS, and prevent the effective passage of cancer treatment drugs, including antibodies and miRNAs (Sarkaria et al., 2018). The concept of the BBB was first proposed by Edwin Goldman in 1913, who observed the limited transport of dye between the blood and brain. After injecting dye into the veins and CSF of animals, dye was distributed in almost all organs, except the brain (Langen et al., 2019). The disruption of the BBB during tumor progression results in the formation of the blood-tumor barrier (BTB) (Steeg, 2021). While the BTB is more permeable than the BBB, its uneven permeability to molecules of different sizes and uneven blood flow can lead to less than ideal drug accumulation in brain tumors(Arvanitis et al., 2020; Steeg, 2021).With significant advances in nanotechnology, various inorganic/organic/natural nanomaterials that target ligands and/or cell-penetrating peptide (CPP) surface modifications through the BBB have been created to help drugs cross the BBB to induce mitochondrial dysfunction for highly precise therapy (Tang et al., 2019).

4.1.1 Resveratrol

Resveratrol (3,5,4′-trihydroxystilbene) (RES) is a naturally occurring polyphenol and phytoalexin that is abundant in red wine, berries, peanuts, and soybeans and has anti-inflammatory, anti-oxidant, anti-cancer, cardioprotective, and neuroprotective effects (Baur and Sinclair, 2006; Catalgol et al., 2012; Neves et al., 2012). Resveratrol is effective in the treatment of GBM through various mechanisms, but its bioavailability is severely reduced due to its poor water solubility, short biological half-life (approximately 9–14 min for primary molecules), chemical instability (oxidation and photosensitivity), and rapid metabolism and elimination (Jhaveri et al., 2018). If its shortcomings as a free drug can be overcome, its *in vitro* activity could be enhanced, and the relevant

therapeutic effect could be improved. Triphenylphosphine (TPP+) is a lipophilic cation that can couple many bioactive molecules to achieve mitochondrial targeting (Wang et al., 2021). According to a report, paclitaxel-loaded liposomes prepared using TPP- modified polyethylene glycol-phosphatidylethanolamine (PEGPE) have been shown to be effective in targeting mitochondria in cancer cells (Biswas et al., 2012). Loading RES into PEGylated liposomes (RES-Ls) has been reported to overcome its drawbacks as a free drug (Fu et al., 2021). Furthermore, transferrin is overexpressed on most cancer cells, and transferrin-targeted RES-Ls may be an effective nanomedicine for the treatment of various cancers, including GBM, even though their biodistribution *in vivo* and ability to cross the BBB remain unknown.

4.1.2 Berberine

Berberine (BBR) is a natural compound isolated from Chinese herbal medicine, including the Coptis root (Huang Lian) and Amur corktree (Huang Bai). It has a wide range of pharmacological effects, including antidiarrheal, antibacterial, antioxidant, anti-inflammatory, and anti-tumor aspects (Li-Weber, 2013; Li et al., 2015). BBR can inhibit GBM cell growth, reduce cellular viability, and induce oncosis-like death (cell swelling, cytoplasmic vacuoles, and plasma membrane blebbing) (Sun et al., 2018b). We also found that BBR induces autophagy as a protective effect and decreases the oxygen consumption rate, which could inhibit mitochondrial aerobic respiration by repressing phosphorylated extracellular regulated protein kinases (p-ERK1/2), reducing its energy production efficiency and, thereby, reducing metabolic activity (Sun et al., 2018b). The most challenging aspect related to BBR or other therapeutics in GBM is crossing the BBB. Glucose-coated nanodrugs and fructose-coated nanoparticles can provide 10–100-times more uptake by tumor cells in various models (Hu et al., 2015). The formation of nanoshapes by simply dissolving BBR into 5% glucose solution provides a promising strategy for drugs to cross the BBB (Wang et al., 2020).

4.2 Sonodynamic therapy

Sonodynamic therapy (SDT) is a technique that involves using focused ultrasound (FUS) to increase the sensitivity of tumors to sonosensitizers during sonication (Mess et al., 2023).It has shown promise as a cancer therapeutic modality for GBM due to its high tissue penetration and minimal radiation damage to normal tissues (Zhang et al., 2021c). Despite the potential of SDT in eliminating tumor cells, its effectiveness is limited by the BBB and the low accumulation rate of sonosensitizers (Guo et al., 2022). As a result, complete eradication of tumor cells cannot be guaranteed through SDT.Therefore, to improve the efficiency of drug delivery and further reduce adverse reactions, ultrasound-targeted microbubble destruction has been developed. It is a non-invasive technology that combines low-intensity FUS and microbubbles (MBs), which can transiently and reversibly destroy the BBB and promote drug delivery in the brain with a high degree of spatial and temporal specificity (Gorick et al., 2018). Low-intensity FUS has been explored as a drug delivery platform for the treatment of brain diseases (Landhuis, 2017), which can promote the deep penetration of SDT and the accumulation of tumor-specific sonosensitizing agents (Yeshurun and Azhari, 2016). SDT often concomitantly initiates an autophagic response during tumor cell apoptosis induction (Zhao et al., 2011). Excessive ROS production by ACL-SDT induces mitochondrial dysfunction and leads to MAPK/p38-PINK1-PRKN-dependent mitophagy (Qu et al., 2020). Mitophagy plays a protective role under oxidative stress, and inhibition of the degradation pathway significantly enhances the SDT-induced apoptosis of GBM cells (Qu et al., 2020). The lysosomal chemoattractor hydroxychloroquine (HCQ) is the only clinically available autophagy inhibitor (Cook et al., 2014). Qu et al. designed an "all-in-one" nanosensitization platform incorporating Ce6 and HCQ into angiopeptide-2 peptide-modified liposomes and designated a smart nanosensitizer, that can be used to treat GBMs *in situ* (Qu et al., 2020). Combining autophagy inhibitors with non-invasive SDT therapy provides a promising anti-GBM strategy, and the "all-in-one" nanosensitization platform is expected to be extended to other sonotheranostics in future.Besides, the efficiency of SDT can be enhanced by using a nano-platform biodegradation technology called CSI. This involves encapsulating catalase (CAT) into silica nanoparticles (CAT@SiO2) to alleviate tumor hypoxia, and then loading it with the sonosensitizer indocyanine green, which significantly improves the efficacy of SDT(Wu et al., 2022). The combination of SDT and natural drugs targeted to mitochondria can significantly enhance the therapeutic efficacy against glioma, which holds great importance for precise treatment of this disease.

5 Summary

GBM is the most common primary malignant brain tumor with high metabolic activity. Currently, GBM is treated by removing the tumor to the maximum extent and combining it with chemotherapy (Molinaro et al., 2022). However, due to its invasiveness, the total resection rate is low, the residual tumor tissue has obvious resistance to radiotherapy and chemotherapy, and the long-term survival rate of patients with GBM is low (Yi et al., 2019). The presence of the BBB further complicates the treatment process. Despite significant progress in the standard of care for GBM, including surgery, radiation therapy, and medical therapy such as chemotherapy with TMZ, patient outcomes remain extremely poor with a low median overall survival rate. GBM is still considered a fatal disease with limited treatment options.Given the extremely low survival rates of currently approved treatments for GBM, new therapeutic strategies are urgently needed. The clinical reality of the BBB contribution to GBM treatment failure suggests that renewed efforts to optimize BBB disruption techniques, develop BBB penetrators, and perfect impenetrable drug delivery technologies that bypass the BBB are the focus of current GBM treatment research. With the development of comprehensive treatment for glioblastoma in recent years, the anti-cancer effects of natural products and phytochemicals commonly used in traditional Chinese medicine continue to attract widespread attention. But the BBB presents a challenge for the effective delivery of anticancer drugs to the brain, limiting their curative effects.Modern nano-drug delivery technology targeting mitochondria can achieve better drug release and deeper tissue penetration, suggesting that mitochondria could be a new target for intervention and therapy. The combination of drug targeting mitochondrial apoptosis and autophagy pathways with

nanotechnology is a promising novel approach for treating GBM. However, it is a particularly challenging task to engineer nanoformulations that can perfectly target mitochondrial abnormalities in tumor cells without causing toxic effects on nearby normal cells. Since most of our experiments were carried out on animal models, further research is needed to explore the safety parameters of ultrasound in GBM.With the rapid advances in knowledge and nanomedicine for GBM, increasing numbers of molecular targets have been identified, providing a solid foundation for the development of precise nanotherapeutic systems in future.We look forward to the development of more effective drugs for GBM treatment, focused on the mitochondrial pathway, and the emergence of more mature nanoagents combined with nanotechnology to kill tumor cells specifically, improving the therapeutic effects of medicine for GBM.

Author contributions

WL: Writing-original draft, writing-review and editing; XX: writing-review and editing. All authors contributed to the article and approved the submitted version.

Funding

This study was supported by the Outstanding Postdoctoral Innovative Talent Project of Hunan Province (No. 2021RC203), China.

Conflict of interest

The authors declare that the research was conducted in the absence of any commercial or financial relationships that could be construed as a potential conflict of interest.

Publisher's note

All claims expressed in this article are solely those of the authors and do not necessarily represent those of their affiliated organizations, or those of the publisher, the editors and the reviewers. Any product that may be evaluated in this article, or claim that may be made by its manufacturer, is not guaranteed or endorsed by the publisher.

References

Abenavoli, L., Izzo, A. A., Milic, N., Cicala, C., Santini, A., and Capasso, R. (2018). Milk thistle (Silybum marianum): A concise overview on its chemistry, pharmacological, and nutraceutical uses in liver diseases. *Phytother. Res.* 32 (11), 2202–2213. doi:10.1002/ptr.6171

Ahmad, I., Irfan, S., Ali, B. M., Kamli, H., Ali, S. P., Begum, N., et al. (2021). The SMAC mimetic AT-101 exhibits anti-tumor and anti-metastasis activity in lung adenocarcinoma cells by the IAPs/caspase-dependent apoptosis and p65-NFκB cross-talk. *Iran. J. Basic Med. Sci.* 24 (7), 969–977. doi:10.22038/ijbms.2021.56400.12586

Aiello, P., Sharghi, M., Mansourkhani, S. M., Ardekan, A. P., Jouybari, L., Daraei, N., et al. (2019). Medicinal plants in the prevention and treatment of colon cancer. *Oxid. Med. Cell Longev.* 2019, 2075614. doi:10.1155/2019/2075614

Ailawadhi, S., Parrondo, R. D., Dutta, N., Han, B., Ciccio, G., Cherukuri, Y., et al. (2023). AT-101 enhances the antitumor activity of lenalidomide in patients with multiple myeloma. *Cancers (Basel)* 15 (2), 477. doi:10.3390/cancers15020477

Aktepe, N., and Yukselten, Y. (2022). Induction of apoptosis in human hormone-refractory prostate cancer cell lines by using resveratrol in combination with AT-101. *Andrologia* 54 (1), e14267. doi:10.1111/and.14267

Ammendolia, I., Mannucci, C., Cardia, L., Calapai, G., Gangemi, S., Esposito, E., et al. (2023). Pharmacovigilance on cannabidiol as an antiepileptic agent. *Front. Pharmacol.* 14, 1091978. doi:10.3389/fphar.2023.1091978

Arvanitis, C. D., Ferraro, G. B., and Jain, R. K. (2020). The blood-brain barrier and blood-tumour barrier in brain tumours and metastases. *Nat. Rev. Cancer* 20 (1), 26–41. doi:10.1038/s41568-019-0205-x

Bachari, A., Piva, T. J., Salami, S. A., Jamshidi, N., and Mantri, N. (2020). Roles of cannabinoids in melanoma: Evidence from *in vivo* studies. *Int. J. Mol. Sci.* 21 (17), 6040. doi:10.3390/ijms21176040

Bai, S., Wen, W., Hou, X., Wu, J., Yi, L., Zhi, Y., et al. (2021). Inhibitory effect of sinomenine on lung cancer cells via negative regulation of α7 nicotinic acetylcholine receptor. *J. Leukoc. Biol.* 109 (4), 843–852. doi:10.1002/JLB.6MA0720-344RRR

Bai, Y., Chen, J., Hu, W., Wang, L., Wu, Y., and Yu, S. (2022). Silibinin therapy improves cholangiocarcinoma outcomes by regulating ERK/mitochondrial pathway. *Front. Pharmacol.* 13, 847905. doi:10.3389/fphar.2022.847905

Banelli, B., Forlani, A., Allemanni, G., Morabito, A., Pistillo, M. P., and Romani, M. (2017). MicroRNA in glioblastoma: An overview. *Int. J. Genomics* 2017, 7639084. doi:10.1155/2017/7639084

Batara, D., Choi, M. C., Shin, H. U., Kim, H., and Kim, S. H. (2021). Friend or foe: Paradoxical roles of autophagy in gliomagenesis. *Cells* 10 (6), 1411. doi:10.3390/cells10061411

Batoon, L., Koh, A. J., Kannan, R., Mccauley, L. K., and Roca, H. (2023). Caspase-9 driven murine model of selective cell apoptosis and efferocytosis. *Cell Death Dis.* 14 (1), 58. doi:10.1038/s41419-023-05594-6

Baur, J. A., and Sinclair, D. A. (2006). Therapeutic potential of resveratrol: The *in vivo* evidence. *Nat. Rev. Drug Discov.* 5 (6), 493–506. doi:10.1038/nrd2060

Benlloch, M., Obrador, E., Valles, S. L., Rodriguez, M. L., Sirerol, J. A., Alcacer, J., et al. (2016). Pterostilbene decreases the antioxidant defenses of aggressive cancer cells *in vivo*: A physiological glucocorticoids- and nrf2-dependent mechanism. *Antioxid. Redox Signal* 24 (17), 974–990. doi:10.1089/ars.2015.6437

Benvenuto, M., Mattera, R., Sticca, J. I., Rossi, P., Cipriani, C., Giganti, M. G., et al. (2018). Effect of the BH3 mimetic polyphenol (-)-Gossypol (AT-101) on the *in vitro* and *in vivo* growth of malignant mesothelioma. *Front. Pharmacol.* 9, 1269. doi:10.3389/fphar.2018.01269

Bernardini, J. P., Lazarou, M., and Dewson, G. (2017). Parkin and mitophagy in cancer. *Oncogene* 36 (10), 1315–1327. doi:10.1038/onc.2016.302

Bhargava, P., and Schnellmann, R. G. (2017). Mitochondrial energetics in the kidney. *Nat. Rev. Nephrol.* 13 (10), 629–646. doi:10.1038/nrneph.2017.107

Biswas, S., Dodwadkar, N. S., Deshpande, P. P., and Torchilin, V. P. (2012). Liposomes loaded with paclitaxel and modified with novel triphenylphosphonium-PEG-PE conjugate possess low toxicity, target mitochondria and demonstrate enhanced antitumor effects *in vitro* and *in vivo*. *J. Control Release* 159 (3), 393–402. doi:10.1016/j.jconrel.2012.01.009

Boatright, K. M., and Salvesen, G. S. (2003). Mechanisms of caspase activation. *Curr. Opin. Cell Biol.* 15 (6), 725–731. doi:10.1016/j.ceb.2003.10.009

Boulos, J. C., Rahama, M., Hegazy, M. F., and Efferth, T. (2019). Shikonin derivatives for cancer prevention and therapy. *Cancer Lett.* 459, 248–267. doi:10.1016/j.canlet.2019.04.033

Bracht, J., Karachaliou, N., Berenguer, J., Pedraz-Valdunciel, C., Filipska, M., Codony-Servat, C., et al. (2019). Osimertinib and pterostilbene in EGFR-mutation-positive non-small cell lung cancer (NSCLC). *Int. J. Biol. Sci.* 15 (12), 2607–2614. doi:10.7150/ijbs.32889

Bravo-San, P. J., Kroemer, G., and Galluzzi, L. (2017). Autophagy and mitophagy in cardiovascular disease. *Circ. Res.* 120 (11), 1812–1824. doi:10.1161/circresaha.117.311082

Bulut, G., Atmaca, H., and Karaca, B. (2020). Trastuzumab in combination with AT-101 induces cytotoxicity and apoptosis in Her2 positive breast cancer cells. *Future Oncol.* 16 (3), 4485–4495. doi:10.2217/fon-2019-0521

Cammarata, F. P., Torrisi, F., Vicario, N., Bravata, V., Stefano, A., Salvatorelli, L., et al. (2023). Proton boron capture therapy (PBCT) induces cell death and mitophagy in a heterotopic glioblastoma model. *Commun. Biol.* 6 (1), 388. doi:10.1038/s42003-023-04770-w

Cao, W., Chen, G., Wu, L., Yu, K. N., Sun, M., Yang, M., et al. (2023). Ionizing radiation triggers the antitumor immunity by inducing gasdermin E-mediated

pyroptosis in tumor cells. *Int. J. Radiat. Oncol. Biol. Phys.* 115 (2), 440–452. doi:10.1016/j.ijrobp.2022.07.1841

Catalgol, B., Batirel, S., Taga, Y., and Ozer, N. K. (2012). Resveratrol: French paradox revisited. *Front. Pharmacol.* 3141, 141. doi:10.3389/fphar.2012.00141

Chang, J., Rimando, A., Pallas, M., Camins, A., Porquet, D., Reeves, J., et al. (2012). Low-dose pterostilbene, but not resveratrol, is a potent neuromodulator in aging and Alzheimer's disease. *Neurobiol. Aging* 33 (9), 2062–2071. doi:10.1016/j.neurobiolaging.2011.08.015

Chen, M., and Yu, S. (2019). Lipophilic grape seed proanthocyanidin exerts anti-proliferative and pro-apoptotic effects on PC3 human prostate cancer cells and suppresses PC3 xenograft tumor growth *in vivo*. *J. Agric. Food Chem.* 67 (1), 229–235. doi:10.1021/acs.jafc.8b05936

Chen, P. H., Chang, C. K., Shih, C. M., Cheng, C. H., Lin, C. W., Lee, C. C., et al. (2016). The miR-204-3p-targeted IGFBP2 pathway is involved in xanthohumol-induced glioma cell apoptotic death. *Neuropharmacology* 110, 362–375. doi:10.1016/j.neuropharm.2016.07.038

Chen, X., Lu, C., Duan, Y., and Huang, Y. (2022). Recent advancements in drug delivery of sinomenine, A disease-modifying anti-rheumatic drug. *Pharmaceutics* 14, 2820. doi:10.3390/pharmaceutics14122820

Chen, X., Zhang, M., Gan, H., Wang, H., Lee, J. H., Fang, D., et al. (2018). A novel enhancer regulates MGMT expression and promotes temozolomide resistance in glioblastoma. *Nat. Commun.* 9 (1), 2949. doi:10.1038/s41467-018-05373-4

Chen, Y. T., Huang, Z. Y., Tang, H. H., Kuo, W. T., Wu, S. Y., Lan, S. H., et al. (2020). Pterostilbene sensitizes cisplatin-resistant human bladder cancer cells with oncogenic HRAS. *Cancers (Basel)* 12 (10), 2869. doi:10.3390/cancers12102869

Cheng, Y. M., Tsai, C. C., and Hsu, Y. C. (2016). Sulforaphane, a dietary isothiocyanate, induces G2/M arrest in cervical cancer cells through CyclinB1 downregulation and gadd45β/CDC2 association. *Int. J. Mol. Sci.* 17 (9), 1530. doi:10.3390/ijms17091530

Constantin, M., Choi, A. J., Cloonan, S. M., and Ryter, S. W. (2012). Therapeutic potential of heme oxygenase-1/carbon monoxide in lung disease. *Int. J. Hypertens.* 2012, 859235. doi:10.1155/2012/859235

Cook, K. L., Warri, A., Soto-Pantoja, D. R., Clarke, P. A., Cruz, M. I., Zwart, A., et al. (2014). Hydroxychloroquine inhibits autophagy to potentiate antiestrogen responsiveness in ER+ breast cancer. *Clin. Cancer Res.* 20 (12), 3222–3232. doi:10.1158/1078-0432.CCR-13-3227

Desagher, S., and Martinou, J. C. (2000). Mitochondria as the central control point of apoptosis. *Trends Cell Biol.* 10 (9), 369–377. doi:10.1016/s0962-8924(00)01803-1

Di Meo, S., Venditti, P., and Napolitano, G. (2022). Physiological and pathological role of ROS: Benefits and limitations of antioxidant treatment 2.0. *Int. J. Mol. Sci.* 23 (16), 9437. doi:10.3390/ijms23169437

Di Rita, A., D'Acunzo, P., Simula, L., Campello, S., Strappazzon, F., and Cecconi, F. (2018). AMBRA1-Mediated mitophagy counteracts oxidative stress and apoptosis induced by neurotoxicity in human neuroblastoma SH-SY5Y cells. *Front. Cell Neurosci.* 12, 92. doi:10.3389/fncel.2018.00092

Feng, J., Wang, C., Liu, T., Li, J., Wu, L., Yu, Q., et al. (2019). Procyanidin B2 inhibits the activation of hepatic stellate cells and angiogenesis via the Hedgehog pathway during liver fibrosis. *J. Cell Mol. Med.* 23 (9), 6479–6493. doi:10.1111/jcmm.14543

Feng, Y., Yang, Y., Fan, C., Di, S., Hu, W., Jiang, S., et al. (2016). Pterostilbene inhibits the growth of human esophageal cancer cells by regulating endoplasmic reticulum stress. *Cell Physiol. Biochem.* 38 (3), 1226–1244. doi:10.1159/000443071

Festa, M., Capasso, A., D'Acunto, C. W., Masullo, M., Rossi, A. G., Pizza, C., et al. (2011). Xanthohumol induces apoptosis in human malignant glioblastoma cells by increasing reactive oxygen species and activating MAPK pathways. *J. Nat. Prod.* 74 (12), 2505–2513. doi:10.1021/np200390x

Finucane, D. M., Bossy-Wetzel, E., Waterhouse, N. J., Cotter, T. G., and Green, D. R. (1999). Bax-induced caspase activation and apoptosis via cytochrome c release from mitochondria is inhibitable by Bcl-xL. *J. Biol. Chem.* 274 (4), 2225–2233. doi:10.1074/jbc.274.4.2225

Fu, G., Yin, G., Niu, T., Wu, W., Han, H., Chen, H., et al. (2021). A novel ratiometric fluorescent probe for the detection of mitochondrial pH dynamics during cell damage. *Analyst* 146 (2), 620–627. doi:10.1039/d0an01240h

Gao, H., Liu, Z., Xu, W., Wang, Q., Zhang, C., Ding, Y., et al. (2021). Pterostilbene promotes mitochondrial apoptosis and inhibits proliferation in glioma cells. *Sci. Rep.* 11 (1), 6381. doi:10.1038/s41598-021-85908-w

Gao, X., Sun, B., Hou, Y., Liu, L., Sun, J., Xu, F., et al. (2022). Anti-breast cancer sinomenine derivatives via mechanisms of apoptosis induction and metastasis reduction. *J. Enzyme Inhib. Med. Chem.* 37 (1), 1870–1883. doi:10.1080/14756366.2022.2096020

Genovese, T., Cordaro, M., Siracusa, R., Impellizzeri, D., Caudullo, S., Raffone, E., et al. (2022). Molecular and biochemical mechanism of cannabidiol in the management of the inflammatory and oxidative processes associated with endometriosis. *Int. J. Mol. Sci.* 23 (10), 5427. doi:10.3390/ijms23105427

Gorbunova, A. S., Yapryntseva, M. A., Denisenko, T. V., and Zhivotovsky, B. (2020). BNIP3 in lung cancer: To kill or rescue? *Cancers (Basel)* 12 (11), 3390. doi:10.3390/cancers12113390

Gorick, C. M., Sheybani, N. D., Curley, C. T., and Price, R. J. (2018). Listening in on the microbubble crowd: Advanced acoustic monitoring for improved control of blood-brain barrier opening with focused ultrasound. *Theranostics* 8 (11), 2988–2991. doi:10.7150/thno.26025

Grace, M. S., Bonvini, S. J., Belvisi, M. G., and Mcintyre, P. (2017). Modulation of the TRPV4 ion channel as a therapeutic target for disease. *Pharmacol. Ther.* 177, 9–22. doi:10.1016/j.pharmthera.2017.02.019

Gu, J., Rauniyar, S., Wang, Y., Zhan, W., Ye, C., Ji, S., et al. (2021). Chrysophanol induced glioma cells apoptosis via activation of mitochondrial apoptosis pathway. *Bioengineered* 12 (1), 6855–6868. doi:10.1080/21655979.2021.1972079

Guo, C., He, J., Song, X., Tan, L., Wang, M., Jiang, P., et al. (2019). Pharmacological properties and derivatives of shikonin-A review in recent years. *Pharmacol. Res.* 149, 104463. doi:10.1016/j.phrs.2019.104463

Guo, Q. L., Dai, X. L., Yin, M. Y., Cheng, H. W., Qian, H. S., Wang, H., et al. (2022). Nanosensitizers for sonodynamic therapy for glioblastoma multiforme: Current progress and future perspectives. *Mil. Med. Res.* 9 (1), 26. doi:10.1186/s40779-022-00386-z

Habib, H. M., El-Fakharany, E. M., Kheadr, E., and Ibrahim, W. H. (2022). Grape seed proanthocyanidin extract inhibits DNA and protein damage and labile iron, enzyme, and cancer cell activities. *Sci. Rep.* 12 (1), 12393. doi:10.1038/s41598-022-16608-2

Harandi-Zadeh, S., Boycott, C., Beetch, M., Yang, T., Martin, B., Ren, K., et al. (2021). Pterostilbene changes epigenetic marks at enhancer regions of oncogenes in breast cancer cells. *Antioxidants (Basel)* 10 (8), 1232. doi:10.3390/antiox10081232

He, X., Maimaiti, M., Jiao, Y., Meng, X., and Li, H. (2018). Sinomenine induces G1-phase cell cycle arrest and apoptosis in malignant glioma cells via downregulation of sirtuin 1 and induction of p53 acetylation. *Technol. Cancer Res. Treat.* 17, 1533034618770305. doi:10.1177/1533034618770305

Hegi, M. E., Genbrugge, E., Gorlia, T., Stupp, R., Gilbert, M. R., Chinot, O. L., et al. (2019). MGMT promoter methylation cutoff with safety margin for selecting glioblastoma patients into trials omitting temozolomide: A pooled analysis of four clinical trials. *Clin. Cancer Res.* 25 (6), 1809–1816. doi:10.1158/1078-0432.CCR-18-3181

Hemani, R., Patel, I., Inamdar, N., Campanelli, G., Donovan, V., Kumar, A., et al. (2022). Dietary pterostilbene for MTA1-targeted interception in high-risk premalignant prostate cancer. *Cancer Prev. Res. (Phila)* 15 (2), 87–100. doi:10.1158/1940-6207.CAPR-21-0242

Ho, K. H., Chang, C. K., Chen, P. H., Wang, Y. J., Chang, W. C., and Chen, K. C. (2018). miR-4725-3p targeting stromal interacting molecule 1 signaling is involved in xanthohumol inhibition of glioma cell invasion. *J. Neurochem.* 146 (3), 269–288. doi:10.1111/jnc.14459

Ho, K. H., Kuo, T. C., Lee, Y. T., Chen, P. H., Shih, C. M., Cheng, C. H., et al. (2020). Xanthohumol regulates miR-4749-5p-inhibited RFC2 signaling in enhancing temozolomide cytotoxicity to glioblastoma. *Life Sci.* 254, 117807. doi:10.1016/j.lfs.2020.117807

Ho, K. H., Shih, C. M., Liu, A. J., and Chen, K. C. (2022). Hypoxia-inducible lncRNA MIR210HG interacting with OCT1 is involved in glioblastoma multiforme malignancy. *Cancer Sci.* 113 (2), 540–552. doi:10.1111/cas.15240

Hosseinabadi, T., Lorigooini, Z., Tabarzad, M., Salehi, B., Rodrigues, C. F., Martins, N., et al. (2019). Silymarin antiproliferative and apoptotic effects: Insights into its clinical impact in various types of cancer. *Phytother. Res.* 33 (11), 2849–2861. doi:10.1002/ptr.6470

Hou, S., Song, Y., Sun, D., Zhu, S., and Wang, Z. (2021). Xanthohumol-induced rat glioma C6 cells death by triggering mitochondrial stress. *Int. J. Mol. Sci.* 22 (9), 4506. doi:10.3390/ijms22094506

Hu, C., Niestroj, M., Yuan, D., Chang, S., and Chen, J. (2015). Treating cancer stem cells and cancer metastasis using glucose-coated gold nanoparticles. *Int. J. Nanomedicine* 10, 2065–2077. doi:10.2147/IJN.S72144

Huang, H., Zhang, S., Li, Y., Liu, Z., Mi, L., Cai, Y., et al. (2021a). Suppression of mitochondrial ROS by prohibitin drives glioblastoma progression and therapeutic resistance. *Nat. Commun.* 12 (1), 3720. doi:10.1038/s41467-021-24108-6

Huang, M., Zhang, D., Wu, J. Y., Xing, K., Yeo, E., Li, C., et al. (2020). Wnt-mediated endothelial transformation into mesenchymal stem cell-like cells induces chemoresistance in glioblastoma. *Sci. Transl. Med.* 12, eaay7522. doi:10.1126/scitranslmed.aay7522

Huang, R., and Zhou, P. K. (2021). DNA damage repair: Historical perspectives, mechanistic pathways and clinical translation for targeted cancer therapy. *Signal Transduct. Target Ther.* 6 (1), 254. doi:10.1038/s41392-021-00648-7

Huang, T., Xu, T., Wang, Y., Zhou, Y., Yu, D., Wang, Z., et al. (2021b). Cannabidiol inhibits human glioma by induction of lethal mitophagy through activating TRPV4. *Autophagy* 17 (11), 3592–3606. doi:10.1080/15548627.2021.1885203

Huangfu, M., Wei, R., Wang, J., Qin, J., Yu, D., Guan, X., et al. (2021). Osthole induces necroptosis via ROS overproduction in glioma cells. *FEBS Open Bio* 11 (2), 456–467. doi:10.1002/2211-5463.13069

Hull, T. D., Boddu, R., Guo, L., Tisher, C. C., Traylor, A. M., Patel, B., et al. (2016). Heme oxygenase-1 regulates mitochondrial quality control in the heart. *JCI Insight* 1 (2), e85817. doi:10.1172/jci.insight.85817

Jahanafrooz, Z., Motamed, N., Rinner, B., Mokhtarzadeh, A., and Baradaran, B. (2018). Silibinin to improve cancer therapeutic, as an apoptotic inducer, autophagy modulator, cell cycle inhibitor, and microRNAs regulator. *Life Sci.* 213, 236–247. doi:10.1016/j.lfs.2018.10.009

Jeong, S., Yun, H. K., Jeong, Y. A., Jo, M. J., Kang, S. H., Kim, J. L., et al. (2019). Cannabidiol-induced apoptosis is mediated by activation of Noxa in human colorectal cancer cells. *Cancer Lett.* 447, 12–23. doi:10.1016/j.canlet.2019.01.011

Jhaveri, A., Deshpande, P., Pattni, B., and Torchilin, V. (2018). Transferrin-targeted, resveratrol-loaded liposomes for the treatment of glioblastoma. *J. Control Release* 277, 89–101. doi:10.1016/j.jconrel.2018.03.006

Karimi-Haghighi, S., Razavi, Y., Iezzi, D., Scheyer, A. F., Manzoni, O., and Haghparast, A. (2022). Cannabidiol and substance use disorder: Dream or reality. *Neuropharmacology* 207, 108948. doi:10.1016/j.neuropharm.2022.108948

Katayama, H., Hama, H., Nagasawa, K., Kurokawa, H., Sugiyama, M., Ando, R., et al. (2020). Visualizing and modulating mitophagy for therapeutic studies of neurodegeneration. *Cell* 181 (5), 1176–1187.e16. doi:10.1016/j.cell.2020.04.025

Kerr, J. S., Adriaanse, B. A., Greig, N. H., Mattson, M. P., Cader, M. Z., Bohr, V. A., et al. (2017). Mitophagy and Alzheimer's disease: Cellular and molecular mechanisms. *Trends Neurosci.* 40 (3), 151–166. doi:10.1016/j.tins.2017.01.002

Khodadadi, H., Salles, E. L., Alptekin, A., Mehrabian, D., Rutkowski, M., Arbab, A. S., et al. (2021). Inhalant cannabidiol inhibits glioblastoma progression through regulation of tumor microenvironment. *Cannabis Cannabinoid Res.* doi:10.1089/can.2021.0098

Kim, H. Y., Lee, B. I., Jeon, J. H., Kim, D. K., Kang, S. G., Shim, J. K., et al. (2019). Gossypol suppresses growth of temozolomide-resistant glioblastoma tumor spheres. *Biomolecules* 9 (10), 595. doi:10.3390/biom9100595

Kiskova, T., Mungenast, F., Suvakova, M., Jager, W., and Thalhammer, T. (2019). Future aspects for cannabinoids in breast cancer therapy. *Int. J. Mol. Sci.* 20 (7), 1673. doi:10.3390/ijms20071673

Kleih, M., Bopple, K., Dong, M., Gaissler, A., Heine, S., Olayioye, M. A., et al. (2019). Direct impact of cisplatin on mitochondria induces ROS production that dictates cell fate of ovarian cancer cells. *Cell Death Dis.* 10 (11), 851. doi:10.1038/s41419-019-2081-4

Kumar, V., Haldar, S., Das, N. S., Ghosh, S., Dhankhar, P., Sircar, D., et al. (2021). Pterostilbene-isothiocyanate inhibits breast cancer metastasis by selectively blocking IKK-β/NEMO interaction in cancer cells. *Biochem. Pharmacol.* 192, 114717. doi:10.1016/j.bcp.2021.114717

Kuo, C. Y., Chiu, V., Hsieh, P. C., Huang, C. Y., Huang, S. J., Tzeng, I. S., et al. (2020). Chrysophanol attenuates Hepatitis B virus X protein-induced hepatic stellate cell fibrosis by regulating endoplasmic reticulum stress and ferroptosis. *J. Pharmacol. Sci.* 144 (3), 172–182. doi:10.1016/j.jphs.2020.07.014

Lah, T. T., Novak, M., and Breznik, B. (2020). Brain malignancies: Glioblastoma and brain metastases. *Semin. Cancer Biol.* 60, 262–273. doi:10.1016/j.semcancer.2019.10.010

Landhuis, E. (2017). Ultrasound for the brain. *Nature* 551 (7679), 257–259. doi:10.1038/d41586-017-05479-7

Langen, U. H., Ayloo, S., and Gu, C. (2019). Development and cell biology of the blood-brain barrier. *Annu. Rev. Cell Dev. Biol.* 35, 591–613. doi:10.1146/annurev-cellbio-100617-062608

Leao, B. M., Pinheiro, D., and Borges, B. (2021). Mitochondrial DNA alterations in glioblastoma (GBM). *Int. J. Mol. Sci.* 22 (11), 5855. doi:10.3390/ijms22115855

Lee, H. S., Tamia, G., Song, H. J., Amarakoon, D., Wei, C. I., and Lee, S. H. (2022a). Cannabidiol exerts anti-proliferative activity via a cannabinoid receptor 2-dependent mechanism in human colorectal cancer cells. *Int. Immunopharmacol.* 108, 108865. doi:10.1016/j.intimp.2022.108865

Lee, J., Kim, E., Chong, K., Ryu, S. W., Kim, C., Choi, K., et al. (2022b). Atypical induction of HIF-1α expression by pericellular Notch1 signaling suffices for the malignancy of glioblastoma multiforme cells. *Cell Mol. Life Sci.* 79 (10), 537. doi:10.1007/s00018-022-04529-2

Lee, J. Y., Park, J. Y., Kim, D. H., Kim, H. D., Ji, Y. J., and Seo, K. H. (2020). Erigeron annuus protects PC12 neuronal cells from oxidative stress induced by ROS-mediated apoptosis. *Evid. Based Complement. Altern. Med.* 2020, 3945194. doi:10.1155/2020/3945194

Levy, J., Towers, C. G., and Thorburn, A. (2017). Targeting autophagy in cancer. *Nat. Rev. Cancer* 17 (9), 528–542. doi:10.1038/nrc.2017.53

Li, C., Zhang, L., Liu, C., He, X., Chen, M., and Chen, J. (2022a). Roles of hydrogen gas in plants under abiotic stress: Current knowledge and perspectives. *Antioxidants (Basel)* 11 (2), 1999. doi:10.3390/antiox11101999

Li, S., Zhang, J., Liu, C., Wang, Q., Yan, J., Hui, L., et al. (2021). The role of mitophagy in regulating cell death. *Oxid. Med. Cell Longev.* 2021, 6617256. doi:10.1155/2021/6617256

Li, W., Hua, B., Saud, S. M., Lin, H., Hou, W., Matter, M. S., et al. (2015). Berberine regulates AMP-activated protein kinase signaling pathways and inhibits colon tumorigenesis in mice. *Mol. Carcinog.* 54 (10), 1096–1109. doi:10.1002/mc.22179

Li, X., Chen, W., Huang, L., Zhu, M., Zhang, H., Si, Y., et al. (2022b). Sinomenine hydrochloride suppresses the stemness of breast cancer stem cells by inhibiting Wnt signaling pathway through down-regulation of WNT10B. *Pharmacol. Res.* 179, 106222. doi:10.1016/j.phrs.2022.106222

Li, X., He, S., and Ma, B. (2020). Autophagy and autophagy-related proteins in cancer. *Mol. Cancer* 19 (1), 12. doi:10.1186/s12943-020-1138-4

Li-Weber, M. (2013). Targeting apoptosis pathways in cancer by Chinese medicine. *Cancer Lett.* 332 (2), 304–312. doi:10.1016/j.canlet.2010.07.015

Lin, J. H., Yang, K. T., Lee, W. S., Ting, P. C., Luo, Y. P., Lin, D. J., et al. (2022a). Xanthohumol protects the rat myocardium against ischemia/reperfusion injury-induced ferroptosis. *Oxid. Med. Cell Longev.* 2022, 9523491. doi:10.1155/2022/9523491

Lin, K., Gueble, S. E., Sundaram, R. K., Huseman, E. D., Bindra, R. S., and Herzon, S. B. (2022b). Mechanism-based design of agents that selectively target drug-resistant glioma. *Science* 377 (6605), 502–511. doi:10.1126/science.abn7570

Lin, Y., Yi, O., Hu, M., Hu, S., Su, Z., Liao, J., et al. (2022c). Multifunctional nanoparticles of sinomenine hydrochloride for treat-to-target therapy of rheumatoid arthritis via modulation of proinflammatory cytokines. *J. Control Release* 348, 42–56. doi:10.1016/j.jconrel.2022.05.016

Lindenboim, L., Yuan, J., and Stein, R. (2000). Bcl-xS and Bax induce different apoptotic pathways in PC12 cells. *Oncogene* 19 (14), 1783–1793. doi:10.1038/sj.onc.1203495

Linder, B., Wehle, A., Hehlgans, S., Bonn, F., Dikic, I., Rodel, F., et al. (2019). Arsenic trioxide and (-)-Gossypol synergistically target glioma stem-like cells via inhibition of hedgehog and notch signaling. *Cancers (Basel)* 11 (3), 350. doi:10.3390/cancers11030350

Liu, B., Cao, Y., Wang, D., Zhou, Y., Zhang, P., Wu, J., et al. (2021). Zhen-Wu-Tang induced mitophagy to protect mitochondrial function in chronic glomerulonephritis via PI3K/AKT/mTOR and AMPK pathways. *Front. Pharmacol.* 12, 777670. doi:10.3389/fphar.2021.777670

Liu, B., Zhou, J., Wang, C., Chi, Y., Wei, Q., Fu, Z., et al. (2020a). LncRNA SOX2OT promotes temozolomide resistance by elevating SOX2 expression via ALKBH5-mediated epigenetic regulation in glioblastoma. *Cell Death Dis.* 11 (5), 384. doi:10.1038/s41419-020-2540-y

Liu, H., Zhang, R., Zhang, D., Zhang, C., Zhang, Z., Fu, X., et al. (2022). Cyclic RGD-decorated liposomal gossypol AT-101 targeting for enhanced antitumor effect. *Int. J. Nanomedicine* 17, 227–244. doi:10.2147/IJN.S341824

Liu, K., Zheng, M., Lu, R., Du, J., Zhao, Q., Li, Z., et al. (2020b). The role of CDC25C in cell cycle regulation and clinical cancer therapy: A systematic review. *Cancer Cell Int.* 20, 213. doi:10.1186/s12935-020-01304-w

Liu, Y., Liu, C., Tan, T., Li, S., Tang, S., and Chen, X. (2019). Sinomenine sensitizes human gastric cancer cells to cisplatin through negative regulation of PI3K/AKT/Wnt signaling pathway. *Anticancer Drugs* 30 (10), 983–990. doi:10.1097/CAD.0000000000000834

Lopez-Valero, I., Saiz-Ladera, C., Torres, S., Hernandez-Tiedra, S., Garcia-Taboada, E., Rodriguez-Fornes, F., et al. (2018). Targeting Glioma Initiating Cells with A combined therapy of cannabinoids and temozolomide. *Biochem. Pharmacol.* 157, 266–274. doi:10.1016/j.bcp.2018.09.007

Louis, D. N., Perry, A., Wesseling, P., Brat, D. J., Cree, I. A., Figarella-Branger, D., et al. (2021). The 2021 WHO classification of tumors of the central nervous system: A summary. *Neuro Oncol.* 23 (8), 1231–1251. doi:10.1093/neuonc/noab106

Lu, B., Gong, X., Wang, Z. Q., Ding, Y., Wang, C., Luo, T. F., et al. (2017). Shikonin induces glioma cell necroptosis *in vitro* by ROS overproduction and promoting RIP1/RIP3 necrosome formation. *Acta Pharmacol. Sin.* 38 (11), 1543–1553. doi:10.1038/aps.2017.112

Lu, R. O., and Ho, W. S. (2020). Mitochondrial dysfunction, macrophage, and microglia in brain cancer. *Front. Cell Dev. Biol.* 8, 620788. doi:10.3389/fcell.2020.620788

Ma, X., Yu, M., Hao, C., and Yang, W. (2020). Shikonin induces tumor apoptosis in glioma cells via endoplasmic reticulum stress, and Bax/Bak mediated mitochondrial outer membrane permeability. *J. Ethnopharmacol.* 263, 113059. doi:10.1016/j.jep.2020.113059

Ma, Z., Zhang, X., Xu, L., Liu, D., Di, S., Li, W., et al. (2019). Pterostilbene: Mechanisms of its action as oncostatic agent in cell models and *in vivo* studies. *Pharmacol. Res.* 145, 104265. doi:10.1016/j.phrs.2019.104265

Mahmoud, A. M., Kostrzewa, M., Marolda, V., Cerasuolo, M., Maccarinelli, F., Coltrini, D., et al. (2023). Cannabidiol alters mitochondrial bioenergetics via VDAC1 and triggers cell death in hormone-refractory prostate cancer. *Pharmacol. Res.* 189, 106683. doi:10.1016/j.phrs.2023.106683

Maiti, A., and Hait, N. C. (2021). Autophagy-mediated tumor cell survival and progression of breast cancer metastasis to the brain. *J. Cancer* 12 (4), 954–964. doi:10.7150/jca.50137

Maiti, P., Scott, J., Sengupta, D., Al-Gharaibeh, A., and Dunbar, G. L. (2019). Curcumin and solid lipid curcumin particles induce autophagy, but inhibit mitophagy and the PI3K-Akt/mTOR pathway in cultured glioblastoma cells. *Int. J. Mol. Sci.* 20 (2), 399. doi:10.3390/ijms20020399

Mao, J. T., Xue, B., Lu, Q. Y., Lundmark, L., Burns, W., Yang, J., et al. (2023). Combinations of grape seed procyanidin extract and milk thistle silymarin extract against lung cancer - the role of MiR-663a and FHIT. *Life Sci.* 318, 121492. doi:10.1016/j.lfs.2023.121492

Mehner, M., Kubelt, C., Adamski, V., Schmitt, C., Synowitz, M., and Held-Feindt, J. (2020). Combined treatment of AT101 and demethoxycurcumin yields an enhanced anti-proliferative effect in human primary glioblastoma cells. *J. Cancer Res. Clin. Oncol.* 146 (1), 117–126. doi:10.1007/s00432-019-03107-7

Meng, Y., Qiu, L., Zeng, X., Hu, X., Zhang, Y., Wan, X., et al. (2022). Targeting CRL4 suppresses chemoresistant ovarian cancer growth by inducing mitophagy. *Signal Transduct. Target Ther.* 7 (1), 388. doi:10.1038/s41392-022-01253-y

Mess, G., Anderson, T., Kapoor, S., Thombre, R., Liang, R., Derin, E., et al. (2023). Sonodynamic therapy for the treatment of glioblastoma multiforme in a mouse model using a portable benchtop focused ultrasound system. *J. Vis. Exp.* No. 192. doi:10.3791/65114

Meyer, N., Zielke, S., Michaelis, J. B., Linder, B., Warnsmann, V., Rakel, S., et al. (2018). AT 101 induces early mitochondrial dysfunction and HMOX1 (heme oxygenase 1) to trigger mitophagic cell death in glioma cells. *Autophagy* 14 (10), 1693–1709. doi:10.1080/15548627.2018.1476812

Milian, L., Monleon-Guinot, I., Sancho-Tello, M., Galbis, J. M., Cremades, A., Almenar-Ordaz, M., et al. (2022). *In vitro* effect of d9-tetrahydrocannabinol and cannabidiol on cancer-associated fibroblasts isolated from lung cancer. *Int. J. Mol. Sci.* 23 (12), 6766. doi:10.3390/ijms23126766

Misri, S., Kaul, K., Mishra, S., Charan, M., Verma, A. K., Barr, M. P., et al. (2022). Cannabidiol inhibits tumorigenesis in cisplatin-resistant non-small cell lung cancer via TRPV2. *Cancers (Basel)* 14 (5), 1181. doi:10.3390/cancers14051181

Molinaro, A. M., Wiencke, J. K., Warrier, G., Koestler, D. C., Chunduru, P., Lee, J. Y., et al. (2022). Interactions of age and blood immune factors and noninvasive prediction of glioma survival. *J. Natl. Cancer Inst.* 114 (3), 446–457. doi:10.1093/jnci/djab195

Muller, C., and Reggio, P. H. (2020). An analysis of the putative CBD binding site in the ionotropic cannabinoid receptors. *Front. Cell Neurosci.* 14, 615811. doi:10.3389/fncel.2020.615811

Neumann, H. F., Frank, J., Venturelli, S., and Egert, S. (2022). Bioavailability and cardiometabolic effects of xanthohumol: Evidence from animal and human studies. *Mol. Nutr. Food Res.* 66 (6), e2100831. doi:10.1002/mnfr.202100831

Neves, A. R., Lucio, M., Lima, J. L., and Reis, S. (2012). Resveratrol in medicinal chemistry: A critical review of its pharmacokinetics, drug-delivery, and membrane interactions. *Curr. Med. Chem.* 19 (11), 1663–1681. doi:10.2174/092986712799945085

Ni, C. H., Chen, P. Y., Lu, H. F., Yang, J. S., Huang, H. Y., Wu, S. H., et al. (2012). Chrysophanol-induced necrotic-like cell death through an impaired mitochondrial ATP synthesis in Hep3B human liver cancer cells. *Arch. Pharm. Res.* 35 (5), 887–895. doi:10.1007/s12272-012-0514-z

Oberoi, R. K., Parrish, K. E., Sio, T. T., Mittapalli, R. K., Elmquist, W. F., and Sarkaria, J. N. (2016). Strategies to improve delivery of anticancer drugs across the blood-brain barrier to treat glioblastoma. *Neuro Oncol.* 18 (1), 27–36. doi:10.1093/neuonc/nov164

Ohgaki, H., and Kleihues, P. (2005). Population-based studies on incidence, survival rates, and genetic alterations in astrocytic and oligodendroglial gliomas. *J. Neuropathol. Exp. Neurol.* 64 (6), 479–489. doi:10.1093/jnen/64.6.479

Ostrom, Q. T., Cioffi, G., Gittleman, H., Patil, N., Waite, K., Kruchko, C., et al. (2019), CBTRUS statistical report: Primary brain and other central nervous system tumors diagnosed in the United States in 2012-2016. *Neuro Oncol.* 21, v1-v100. doi:10.1093/neuonc/noz150

Panigrahi, D. P., Praharaj, P. P., Bhol, C. S., Mahapatra, K. K., Patra, S., Behera, B. P., et al. (2020). The emerging, multifaceted role of mitophagy in cancer and cancer therapeutics. *Semin. Cancer Biol.* 66, 45–58. doi:10.1016/j.semcancer.2019.07.015

Park, D. B., Park, B. S., Kang, H. M., Kim, J. H., and Kim, I. R. (2022). Chrysophanol-induced autophagy disrupts apoptosis via the PI3K/Akt/mTOR pathway in oral squamous cell carcinoma cells. *Med. Kaunas.* 59 (1), 42. doi:10.3390/medicina59010042

Park, M., Chae, H. D., Yun, J., Jung, M., Kim, Y. S., Kim, S. H., et al. (2000). Constitutive activation of cyclin B1-associated cdc2 kinase overrides p53-mediated G2-M arrest. *Cancer Res.* 60 (3), 542–545.

Qu, F., Wang, P., Zhang, K., Shi, Y., Li, Y., Li, C., et al. (2020). Manipulation of Mitophagy by "All-in-One" nanosensitizer augments sonodynamic glioma therapy. *Autophagy* 16 (8), 1413–1435. doi:10.1080/15548627.2019.1687210

Qu, X., Yu, B., Zhu, M., Li, X., Ma, L., Liu, C., et al. (2021). Sinomenine inhibits the growth of ovarian cancer cells through the suppression of mitosis by down-regulating the expression and the activity of CDK1. *Onco Targets Ther.* 14, 823–834. doi:10.2147/OTT.S284261

Que, F., Dai, L., Zhou, D., Lin, Q., Zeng, X., Yu, L., et al. (2019). AT-101 induces G1/G0 phase arrest via the beta-catenin/cyclin D1 signaling pathway in human esophageal cancer cells. *Oncol. Rep.* 41 (2), 1415–1423. doi:10.3892/or.2018.6876

Rademaker, G., Boumahd, Y., Peiffer, R., Anania, S., Wissocq, T., Liegeois, M., et al. (2022). Myoferlin targeting triggers mitophagy and primes ferroptosis in pancreatic cancer cells. *Redox Biol.* 53, 102324. doi:10.1016/j.redox.2022.102324

Renner, O., Mayer, M., Leischner, C., Burkard, M., Berger, A., Lauer, U. M., et al. (2022). Preclinical efficacy and toxicity analysis of the pan-histone deacetylase inhibitor gossypol for the therapy of colorectal cancer or hepatocellular carcinoma. *Pharm. (Basel)* 15 (2), 438. doi:10.3390/ph15040438

Rimando, A. M., Kalt, W., Magee, J. B., Dewey, J., and Ballington, J. R. (2004). Resveratrol, pterostilbene, and piceatannol in vaccinium berries. *J. Agric. Food Chem.* 52 (15), 4713–4719. doi:10.1021/jf040095e

Ruiz, M. J., Fernandez, M., Pico, Y., Manes, J., Asensi, M., Carda, C., et al. (2009). Dietary administration of high doses of pterostilbene and quercetin to mice is not toxic. *J. Agric. Food Chem.* 57 (8), 3180–3186. doi:10.1021/jf803579e

Sarkaria, J. N., Hu, L. S., Parney, I. F., Pafundi, D. H., Brinkmann, D. H., Laack, N. N., et al. (2018). Is the blood-brain barrier really disrupted in all glioblastomas? A critical assessment of existing clinical data. *Neuro Oncol.* 20 (2), 184–191. doi:10.1093/neuonc/nox175

Senft, D., and Ronai, Z. A. (2016). Regulators of mitochondrial dynamics in cancer. *Curr. Opin. Cell Biol.* 39, 3943–3952. doi:10.1016/j.ceb.2016.02.001

Shin, H. J., Han, J. M., Choi, Y. S., and Jung, H. J. (2020). Pterostilbene suppresses both cancer cells and cancer stem-like cells in cervical cancer with superior bioavailability to resveratrol. *Molecules* 25 (1), 228. doi:10.3390/molecules25010228

Si, L., Fu, J., Liu, W., Hayashi, T., Nie, Y., Mizuno, K., et al. (2020). Silibinin inhibits migration and invasion of breast cancer MDA-MB-231 cells through induction of mitochondrial fusion. *Mol. Cell Biochem.* 463 (1-2), 189–201. doi:10.1007/s11010-019-03640-6

Song, W. H., Zuidema, D., Yi, Y. J., Zigo, M., Zhang, Z., Sutovsky, M., et al. (2021). Mammalian cell-free system recapitulates the early events of post-fertilization sperm mitophagy. *Cells* 10 (9), 2450. doi:10.3390/cells10092450

Steeg, P. S. (2021). The blood-tumour barrier in cancer biology and therapy. *Nat. Rev. Clin. Oncol.* 18 (11), 696–714. doi:10.1038/s41571-021-00529-6

Su, S., Wu, J., Gao, Y., Luo, Y., Yang, D., and Wang, P. (2020). The pharmacological properties of chrysophanol, the recent advances. *Biomed. Pharmacother.* 125, 110002. doi:10.1016/j.biopha.2020.110002

Su, Y. C., Davuluri, G. V., Chen, C. H., Shiau, D. C., Chen, C. C., Chen, C. L., et al. (2016). Galectin-1-Induced autophagy facilitates cisplatin resistance of hepatocellular carcinoma. *PLoS One* 11 (2), e0148408. doi:10.1371/journal.pone.0148408

Sun, Y., Yu, J., Liu, X., Zhang, C., Cao, J., Li, G., et al. (2018a). Oncosis-like cell death is induced by berberine through ERK1/2-mediated impairment of mitochondrial aerobic respiration in gliomas. *Biomed. Pharmacother.* 102, 699–710. doi:10.1016/j.biopha.2018.03.132

Sun, Z., Zheng, L., Liu, X., Xing, W., and Liu, X. (2018b). Sinomenine inhibits the growth of melanoma by enhancement of autophagy via PI3K/AKT/mTOR inhibition. *Drug Des. Devel Ther.* 12, 2413–2421. doi:10.2147/DDDT.S155798

Szklener, K., Mazurek, M., Wieteska, M., Waclawska, M., Bilski, M., and Mandziuk, S. (2022). New directions in the therapy of glioblastoma. *Cancers (Basel)* 14 (21), 5377. doi:10.3390/cancers14215377

Tan, K. T., Chen, P. W., Li, S., Ke, T. M., Lin, S. H., and Yang, C. C. (2019). Pterostilbene inhibits lung squamous cell carcinoma growth *in vitro* and *in vivo* by inducing S phase arrest and apoptosis. *Oncol. Lett.* 18 (2), 1631–1640. doi:10.3892/ol.2019.10499

Tang, Q., Li, W., Zheng, X., Ren, L., Liu, J., Li, S., et al. (2020). MELK is an oncogenic kinase essential for metastasis, mitotic progression, and programmed death in lung carcinoma. *Signal Transduct. Target Ther.* 5 (1), 279. doi:10.1038/s41392-020-00288-3

Tang, W., Fan, W., Lau, J., Deng, L., Shen, Z., and Chen, X. (2019). Emerging blood-brain-barrier-crossing nanotechnology for brain cancer theranostics. *Chem. Soc. Rev.* 48 (11), 2967–3014. doi:10.1039/c8cs00805a

Taylor, W. R., and Stark, G. R. (2001). Regulation of the G2/M transition by p53. *Oncogene* 20 (15), 1803–1815. doi:10.1038/sj.onc.1204252

Thannickal, V. J., and Fanburg, B. L. (2000). Reactive oxygen species in cell signaling. *Am. J. Physiol. Lung Cell Mol. Physiol.* 279 (6), L1005–L1028. doi:10.1152/ajplung.2000.279.6.L1005

Tong, C., Wang, Y., Li, J., Cen, W., Zhang, W., Zhu, Z., et al. (2021). Pterostilbene inhibits gallbladder cancer progression by suppressing the PI3K/Akt pathway. *Sci. Rep.* 11 (1), 4391. doi:10.1038/s41598-021-83924-4

Tuli, H. S., Mittal, S., Aggarwal, D., Parashar, G., Parashar, N. C., Upadhyay, S. K., et al. (2021). Path of silibinin from diet to medicine: A dietary polyphenolic flavonoid having potential anti-cancer therapeutic significance. *Semin. Cancer Biol.* 73, 196–218. doi:10.1016/j.semcancer.2020.09.014

Valenti, C., Billi, M., Pancrazi, G. L., Calabria, E., Armogida, N. G., Tortora, G., et al. (2022). Biological effects of cannabidiol on human cancer cells: Systematic review of the literature. *Pharmacol. Res.* 181, 106267. doi:10.1016/j.phrs.2022.106267

Vara-Perez, M., Felipe-Abrio, B., and Agostinis, P. (2019). Mitophagy in cancer: A tale of adaptation. *Cells* 8 (5), 493. doi:10.3390/cells8050493

Vara-Perez, M., Rossi, M., Van den Haute, C., Maes, H., Sassano, M. L., Venkataramani, V., et al. (2021). BNIP3 promotes HIF-1α-driven melanoma growth by curbing intracellular iron homeostasis. *EMBO J.* 40 (10), e106214. doi:10.15252/embj.2020106214

Volmar, M., Cheng, J., Alenezi, H., Richter, S., Haug, A., Hassan, Z., et al. (2021). Cannabidiol converts NF-κB into a tumor suppressor in glioblastoma with defined antioxidative properties. *Neuro Oncol.* 23 (11), 1898–1910. doi:10.1093/neuonc/noab095

Wang, C., He, C., Lu, S., Wang, X., Wang, L., Liang, S., et al. (2020). Autophagy activated by silibinin contributes to glioma cell death via induction of oxidative stress-mediated BNIP3-dependent nuclear translocation of AIF. *Cell Death Dis.* 11 (8), 630. doi:10.1038/s41419-020-02866-3

Wang, H., Fang, B., Peng, B., Wang, L., Xue, Y., Bai, H., et al. (2021). Recent advances in chemical biology of mitochondria targeting. *Front. Chem.* 9, 683220. doi:10.3389/fchem.2021.683220

Wang, H., Zhu, Z., Zhang, G., Lin, F., Liu, Y., Zhang, Y., et al. (2019). AS1411 aptamer/hyaluronic acid-bifunctionalized microemulsion Co-loading shikonin and docetaxel for enhanced antiglioma therapy. *J. Pharm. Sci.* 108 (11), 3684–3694. doi:10.1016/j.xphs.2019.08.017

Wang, J., Qiu, X., Huang, J., Zhuo, Z., Chen, H., Zeng, R., et al. (2022). Development and validation of a novel mitophagy-related gene prognostic signature for glioblastoma multiforme. *BMC Cancer* 22 (1), 644. doi:10.1186/s12885-022-09707-w

Wang, L., Zhan, J., and Huang, W. (2020a). Grape seed proanthocyanidins induce apoptosis and cell cycle arrest of HepG2 cells accompanied by induction of the MAPK pathway and NAG-1. *Antioxidants (Basel)* 9 (12), 1200. doi:10.3390/antiox9121200

Wang, S., An, J., Dong, W., Wang, X., Sheng, J., Jia, Y., et al. (2020b). Glucose-coated berberine nanodrug for glioma therapy through mitochondrial pathway. *Int. J. Nanomedicine* 15, 7951–7965. doi:10.1038/s41419-020-02866-3

Wang, Y., Tang, C., Cai, J., Chen, G., Zhang, D., Zhang, Z., et al. (2018). PINK1/Parkin-mediated mitophagy is activated in cisplatin nephrotoxicity to protect against kidney injury. *Cell Death Dis.* 9 (11), 1113. doi:10.1038/s41419-018-1152-2

Watson, D. C., Bayik, D., Storevik, S., Moreino, S. S., Sprowls, S. A., Han, J., et al. (2023). GAP43-dependent mitochondria transfer from astrocytes enhances glioblastoma tumorigenicity. *Nat. Cancer* 4 (5), 648–664. doi:10.1038/s43018-023-00556-5

Wawszczyk, J., Jesse, K., Smolik, S., and Kapral, M. (2022). Mechanism of pterostilbene-induced cell death in HT-29 colon cancer cells. *Molecules* 27 (2), 369. doi:10.3390/molecules27020369

Wong, S. C., Kamarudin, M., and Naidu, R. (2023). Anticancer mechanism of flavonoids on high-grade adult-type diffuse gliomas. *Nutrients* 15 (4), 797. doi:10.3390/nu15040797

Xie, H., Yin, J., Shah, M. H., Menefee, M. E., Bible, K. C., Reidy-Lagunes, D., et al. (2019a). A phase II study of the orally administered negative enantiomer of gossypol (AT-101), a BH3 mimetic, in patients with advanced adrenal cortical carcinoma. *Invest. New Drugs* 37 (4), 755–762. doi:10.1007/s10637-019-00797-1

Xie, L., Tang, H., Song, J., Long, J., Zhang, L., and Li, X. (2019b). Chrysophanol: A review of its pharmacology, toxicity and pharmacokinetics. *J. Pharm. Pharmacol.* 71 (10), 1475–1487. doi:10.1111/jphp.13143

Xu, F., Li, Q., Wang, Z., and Cao, X. (2019). Sinomenine inhibits proliferation, migration, invasion and promotes apoptosis of prostate cancer cells by regulation of miR-23a. *Biomed. Pharmacother.* 112, 108592. doi:10.1016/j.biopha.2019.01.053

Xu, H., Dong, J., Hou, J., and Gao, R. (2021a). Sinomenine inhibits the progression of bladder cancer cells by downregulating LncRNA-HEIH expression. *Evid. Based Complement. Altern. Med.* 2021, 4699529. doi:10.1155/2021/4699529

Xu, X., Liu, Y., Wang, L., He, J., Zhang, H., Chen, X., et al. (2009). Gambogic acid induces apoptosis by regulating the expression of Bax and Bcl-2 and enhancing caspase-3 activity in human malignant melanoma A375 cells. *Int. J. Dermatol* 48 (2), 186–192. doi:10.1111/j.1365-4632.2009.03946.x

Xu, Y., Huang, Y., Chen, Y., Cao, K., Liu, Z., Wan, Z., et al. (2021b). Grape seed proanthocyanidins play the roles of radioprotection on normal lung and radiosensitization on lung cancer via differential regulation of the MAPK signaling pathway. *J. Cancer* 12 (10), 2844–2854. doi:10.7150/jca.49987

Yang, J. T., Li, Z. L., Wu, J. Y., Lu, F. J., and Chen, C. H. (2014). An oxidative stress mechanism of shikonin in human glioma cells. *PLoS One* 9 (4), e94180. doi:10.1371/journal.pone.0094180

Yang, N., Gao, J., Hou, R., Xu, X., Yang, N., and Huang, S. (2021a). Grape seed proanthocyanidins inhibit migration and invasion of bladder cancer cells by reversing EMT through suppression of TGF-beta signaling pathway. *Oxid. Med. Cell Longev.* 2021, 5564312. doi:10.1155/2021/5564312

Yang, W., Feng, Q., Li, M., Su, J., Wang, P., Wang, X., et al. (2021b). Sinomenine suppresses development of hepatocellular carcinoma cells via inhibiting MARCH1 and AMPK/STAT3 signaling pathway. *Front. Mol. Biosci.* 8, 684262. doi:10.3389/fmolb.2021.684262

Yang, W., Wu, P. F., Ma, J. X., Liao, M. J., Xu, L. S., and Yi, L. (2020). TRPV4 activates the Cdc42/N-wasp pathway to promote glioblastoma invasion by altering cellular protrusions. *Sci. Rep.* 10 (1), 14151. doi:10.1038/s41598-020-70822-4

Yassin, N., Abouzid, S. F., El-Kalaawy, A. M., Ali, T. M., Almehmadi, M. M., and Ahmed, O. M. (2022). Silybum marianum total extract, silymarin and silibinin abate hepatocarcinogenesis and hepatocellular carcinoma growth via modulation of the HGF/c-Met, Wnt/β-catenin, and PI3K/Akt/mTOR signaling pathways. *Biomed. Pharmacother.* 145, 112409. doi:10.1016/j.biopha.2021.112409

Yeshurun, L., and Azhari, H. (2016). Non-invasive measurement of thermal diffusivity using high-intensity focused ultrasound and through-transmission ultrasonic imaging. *Ultrasound Med. Biol.* 42 (1), 243–256. doi:10.1016/j.ultrasmedbio.2015.09.004

Yi, L., Zhou, X., Li, T., Liu, P., Hai, L., Tong, L., et al. (2019). Notch1 signaling pathway promotes invasion, self-renewal and growth of glioma initiating cells via modulating chemokine system CXCL12/CXCR4. *J. Exp. Clin. Cancer Res.* 38 (1), 339. doi:10.1186/s13046-019-1319-4

Yin, J., Yin, Q., Liang, B., Mi, R., Ai, H., Chen, L., et al. (2021). Retraction Note: Chrysophanol suppresses growth and metastasis of T cell acute lymphoblastic leukemia via miR-9/PD-L1 axis. *Naunyn Schmiedeb. Arch. Pharmacol.* 394 (3), 571. doi:10.1007/s00210-020-02026-6

Yu, X., Wang, M., Zuo, J., Wahafu, A., Mao, P., Li, R., et al. (2019). Nuclear factor I A promotes temozolomide resistance in glioblastoma via activation of nuclear factor κB pathway. *Life Sci.* 236, 116917. doi:10.1016/j.lfs.2019.116917

Yuksel, B., Hizli, D. A., Sahin, F., Sahin, K., and Turkel, N. (2023). Cannabinoid compounds in combination with curcumin and piperine display an anti-tumorigenic effect against colon cancer cells. *Front. Pharmacol.* 14, 1145666. doi:10.3389/fphar.2023.1145666

Yurekli, B. S., Karaca, B., Kisim, A., Bozkurt, E., Atmaca, H., Cetinkalp, S., et al. (2018). AT-101 acts as anti-proliferative and hormone suppressive agent in mouse pituitary corticotroph tumor cells. *J. Endocrinol. Invest.* 41 (2), 233–240. doi:10.1007/s40618-017-0733-8

Yusuf, M. A., Singh, B. N., Sudheer, S., Kharwar, R. N., Siddiqui, S., Abdel-Azeem, A. M., et al. (2019). Chrysophanol: A natural anthraquinone with multifaceted biotherapeutic potential. *Biomolecules* 9 (2), 68. doi:10.3390/biom9020068

Zhai, K., Mazurakova, A., Koklesova, L., Kubatka, P., and Busselberg, D. (2021). Flavonoids synergistically enhance the anti-glioblastoma effects of chemotherapeutic drugs. *Biomolecules* 11 (12), 1841. doi:10.3390/biom11121841

Zhang, C., Wu, J., Liu, W., Zheng, X., Zhang, W., Lee, C. S., et al. (2021a). A novel hypocrellin-based assembly for sonodynamic therapy against glioblastoma. *J. Mater Chem. B* 10 (1), 57–63. doi:10.1039/d1tb01886h

Zhang, J., Wang, Q., Wang, Q., Guo, P., Wang, Y., Xing, Y., et al. (2020a). Chrysophanol exhibits anti-cancer activities in lung cancer cell through regulating ROS/HIF-1a/VEGF signaling pathway. *Naunyn Schmiedeb. Arch. Pharmacol.* 393 (3), 469–480. doi:10.1007/s00210-019-01746-8

Zhang, J., Wang, Q., Wang, Q., Guo, P., Wang, Y., Xing, Y., et al. (2021b). Retraction Note to: Chrysophanol exhibits anti-cancer activities in lung cancer cell through regulating ROS/HIF-1a/VEGF signaling pathway. *Naunyn Schmiedeb. Arch. Pharmacol.* 394 (3), 577–578. doi:10.1007/s00210-020-02019-5

Zhang, J., Zhao, A., Jia, X., Li, X., Liang, Y., Liu, Y., et al. (2022a). Sinomenine hydrochloride promotes TSHR-dependent redifferentiation in papillary thyroid cancer. *Int. J. Mol. Sci.* 23 (18), 10709. doi:10.3390/ijms231810709

Zhang, Q., Wang, X., Cao, S., Sun, Y., He, X., Jiang, B., et al. (2020b). Berberine represses human gastric cancer cell growth *in vitro* and *in vivo* by inducing cytostatic autophagy via inhibition of MAPK/mTOR/p70S6K and Akt signaling pathways. *Biomed. Pharmacother.* 128, 110245. doi:10.1016/j.biopha.2020.110245

Zhang, R., Yu, Q., Lu, W., Shen, J., Zhou, D., Wang, Y., et al. (2019). Grape seed procyanidin B2 promotes the autophagy and apoptosis in colorectal cancer cells via regulating PI3K/Akt signaling pathway. *Onco Targets Ther.* 12, 4109–4118. doi:10.2147/OTT.S195615

Zhang, T., Liu, Q., Gao, W., Sehgal, S. A., and Wu, H. (2022b). The multifaceted regulation of mitophagy by endogenous metabolites. *Autophagy* 18 (6), 1216–1239. doi:10.1080/15548627.2021.1975914

Zhang, Z., Shi, J., Nice, E. C., Huang, C., and Shi, Z. (2021c). The multifaceted role of flavonoids in cancer therapy: Leveraging autophagy with a double-edged sword. *Antioxidants (Basel)* 10 (7), 1138. doi:10.3390/antiox10071138

Zhao, P., Liu, Q., Wang, P., Li, T., Wang, X., Su, S., et al. (2011). Autophagic and apoptotic response to sonodynamic therapy induced cell damage in leukemia l1210 cells *in vitro*. *Cancer Biother Radiopharm.* 26 (2), 209–218. doi:10.1089/cbr.2010.0807

Zheng, X., Li, W., Xu, H., Liu, J., Ren, L., Yang, Y., et al. (2021). Sinomenine ester derivative inhibits glioblastoma by inducing mitochondria-dependent apoptosis and autophagy by PI3K/AKT/mTOR and AMPK/mTOR pathway. *Acta Pharm. Sin. B* 11 (11), 3465–3480. doi:10.1016/j.apsb.2021.05.027

Zhou, Y., Wang, Y., Wu, S., Yan, Y., Hu, Y., Zheng, Z., et al. (2020). Sulforaphane-cysteine inhibited migration and invasion via enhancing mitophagosome fusion to lysosome in human glioblastoma cells. *Cell Death Dis.* 11 (9), 819. doi:10.1038/s41419-020-03024-5

Zimmermann, K. C., Bonzon, C., and Green, D. R. (2001). The machinery of programmed cell death. *Pharmacol. Ther.* 92 (1), 57–70. doi:10.1016/s0163-7258(01)00159-0

Zou, Y., Wang, Y., Xu, S., Liu, Y., Yin, J., Lovejoy, D. B., et al. (2022). Brain Co-delivery of temozolomide and cisplatin for combinatorial glioblastoma chemotherapy. *Adv. Mater* 34 (33), e2203958. doi:10.1002/adma.202203958

frontiers | Frontiers in Pharmacology

TYPE Original Research
PUBLISHED 08 November 2023
DOI 10.3389/fphar.2023.1279370

Check for updates

OPEN ACCESS

EDITED BY
Mariana Magalhães,
University of Coimbra, Portugal

REVIEWED BY
Zhi-Bin Wang,
Central South University, China
Wantao Wu,
Central South University, China

*CORRESPONDENCE
Zheng He,
friends1200@163.com

RECEIVED 17 August 2023
ACCEPTED 24 October 2023
PUBLISHED 08 November 2023

CITATION
Wang C and He Z (2023), Multi-omics analysis reveals CLIC1 as a therapeutic vulnerability of gliomas.
Front. Pharmacol. 14:1279370.
doi: 10.3389/fphar.2023.1279370

COPYRIGHT
© 2023 Wang and He. This is an open-access article distributed under the terms of the Creative Commons Attribution License (CC BY). The use, distribution or reproduction in other forums is permitted, provided the original author(s) and the copyright owner(s) are credited and that the original publication in this journal is cited, in accordance with accepted academic practice. No use, distribution or reproduction is permitted which does not comply with these terms.

Multi-omics analysis reveals CLIC1 as a therapeutic vulnerability of gliomas

Chengcheng Wang [1] and Zheng He [2]*

[1]Department of Pharmacy, Qilu Hospital, Cheeloo College of Medicine, Shandong University, Qingdao, Shandong, China, [2]Department of Neurosurgery, Qilu Hospital, Cheeloo College of Medicine, Shandong University, Qingdao, Shandong, China

Introduction: Despite advances in comprehending cancer biology, malignant gliomas remain incurable. The present work conducted a multi-omics analysis for investigating the significance of chloride intracellular channel 1 (CLIC1) in gliomas.

Methods: Multi-omics data of glioma covering transcriptomics, genomics, DNA methylation and single-cell transcriptomics from multiple public cohorts were enrolled for analyzing CLIC1. *In vitro* experiments were conducted to measure apoptosis and cell mobility in U251 and U373 glioma cells following transfection of CLIC1 siRNAs.

Results: Elevated CLIC1 expression was proven to stably and independently estimate worse survival outcomes. CLIC1 expression was higher in more advanced stage, wild-type IDH and unmethylated MGMT samples. Tumorigenic and anticancer immunity pathways were remarkably enriched in CLIC1-up-regulated tumors. Additionally, CLIC1 was positively linked with cancer-immunity cycle, stromal activation, DNA damage repair and cell cycle. Suppressing CLIC1 resulted in apoptosis and attenuated cell motility of glioma cells. More frequent genomic alterations were found in CLIC1-up-regulated tumors. CLIC1 expression presented a remarkably negative connection to DNA methylation. High CLIC1 expression samples were more sensitive to camptothecin, cisplatin, doxorubicin, erlotinib, paclitaxel, rapamycin, clofarabine, tanespimycin, methotrexate, everolimus, TAK-733, trametinib and AZD8330. Tumors with upregulated CLIC1 presented abundant immune cell infiltration, higher expression of immune-checkpoints and -modulators and similar transcriptome profiling, indicative of well response to immune-checkpoint blockade (ICB). Nevertheless, due to elevated TIDE score, tumors with CLIC1 upregulation appeared to be resistant to ICB. Single-cell analysis unveiled that CLIC1 was expressed ubiquitously in tumor cells and tumor microenvironment.

Abbreviations: AUC, area under the curve; CGGA, the Chinese Glioma Genome Atlas; CLIC1, Chloride intracellular channel 1; DSS, disease-specific survival; ESCC, esophageal squamous cell carcinoma; GBM, glioblastoma multiforme; GSEA, gene set enrichment analysis; HCC, hepatocellular carcinoma; HGG, high-grade glioma; IC50, half-maximal inhibitory concentration; ICB, immune-checkpoint blockade; LGG, low-grade glioma; MGMT, O6-methylguanine DNA methyltransferase; OS, overall survival; PFS, progression-free survival; ROCs, receiver operating characteristic curves; RT-qPCR, Real-time quantitative PCR; ssGSEA, single-sample GSEA; TCGA, the Cancer Genome Atlas; TIDE, Tumor Immune Dysfunction and Exclusion; TMB, tumor mutational burden; WHO, World Health Organization.

Conclusions: Overall, CLIC1 was a promising treatment vulnerability in glioma.

KEYWORDS

low-grade gliomas, tumor microenvironment, CLIC1, anticancer immunity, immune-checkpoint blockade, therapeutic vulnerability

Introduction

Gliomas account for nearly 80% of primary malignant brain tumors within the central nervous system (Yang et al., 2022). The most recent 2021 update by the World Health Organization (WHO) has integrated histological, molecular, and genomic characteristics into the systematic classification of gliomas (Louis et al., 2021). As per this classification, gliomas are stratified into four grades, with Grades 1 and 2 categorized as low-grade gliomas (LGG) and Grades 3 and 4 designated as high-grade gliomas (HGG) (Baumert et al., 2016; Buckner et al., 2016; Louis et al., 2021). LGG (Grade 1/2) constitute around 6% of primary brain tumors in the adult population, characterized by a relatively favorable overall survival (OS) of approximately 7 years (McClellan et al., 2023). It is noteworthy, however, that Grade 2 LGG frequently demonstrate a propensity for recurrence and progression to HGG (Stupp et al., 2017). Among HGG, glioblastoma multiforme (GBM) stands out as the most common and clinically aggressive Grade 4 glioma, with a median survival of only 12–15 months, despite standard-of-care therapy (Yu et al., 2022). Hence, the exploration of potential therapeutic vulnerabilities targeting gliomas assumes critical importance.

Chloride channels are a diverse group of proteins, which modulate basic cellular processes, e.g., stabilization of cellular membrane potential, transepithelial transport, maintenance of intracellular pH and cellular volume (Sarkar, 2022; Pressey et al., 2023). Chloride channels have been demonstrated to be responsible for glioma progression (Ozaki et al., 2021). Chloride intracellular channel 1 (CLIC1) is a member of the p64 family. The protein is primarily localized in the nucleus and displays chloride channel activity both in the nuclear and plasma membrane (Hossain et al., 2023). The role of CLIC1 in glioma has been proposed. Increased expression of CLIC1 correlates to unfavorable prognostic outcomes of gliomas (Wang et al., 2012). While CLIC1 activity itself may not be a determinant in the development of GBM (Barbieri et al., 2022), its suppression appears to influence the characteristics of glioma stem cells and their response to novel biguanide derivatives (Peretti et al., 2018). Nevertheless, the formation and activation mechanisms of functional CLIC1 in glioma remains indistinct.

To address these gaps in knowledge, the present study has conducted a comprehensive multi-omics analysis. Our aim is to determine the therapeutic potential of targeting CLIC1 and to unveil the molecular mechanisms underlying its role in gliomas. This research seeks to contribute to a better understanding of the intricate relationship between chloride channels, specifically CLIC1, and glioma progression, which may open doors to new treatment strategies.

Materials and methods

Multi-omics data acquisition

RNA sequencing data of LGG and GBM tumors from the Cancer Genome Atlas (TCGA) were retrieved via the Genomic Data Commons (https://portal.gdc.cancer.gov/) by use of TCGAbiolinks package (Colaprico et al., 2016). LGG (n = 530) and GBM (n = 168) samples were combined and batch effects were corrected utilizing sva package (Leek et al., 2012). Four glioma cohorts: CGGA_325 (n = 313) and CGGA_693 (n = 657) from the Chinese Glioma Genome Atlas (CGGA; http://www.cgga.org.cn/) (Zhao et al., 2021) and GSE16011 (n = 261) (Gravendeel et al., 2009) and GSE43378 (n = 50) (Kawaguchi et al., 2013) from the Gene Expression Omnibus (https://www.ncbi.nlm.nih.gov/geo/) were utilized as external verification. Supplementary Table S1 summarizes the clinical traits of above cohorts. GSE138794 dataset from GEO was used for the Single-cell RNA sequencing (ScRNA-seq) analysis. Copy number variations, somatic mutation and DNA methylation data were also curated from the UCSC Xena database (http://xena.ucsc.edu/).

Functional enrichment analysis

On the basis of the "c5.go.v7.4.symbols" and "c2.cp.kegg.v7.4.symbols" gene sets from the Molecular Signatures Database (Liberzon et al., 2015), gene set enrichment analysis (GSEA) was carried out (Xu et al., 2018). Enrichment values of specific well-established pathways (Tian et al., 2023) were quantified utilizing GSVA package (Xu et al., 2018).

Cell culture and transfection

Human glioma cell lines U251 and U373 (Cell Bank of the Chinese Academy of Sciences, Shanghai, China) were grown in RPMI-1640 medium (SEVEN, California, United States) with 10% fetal bovine serum (Hyclone, Utah, United States) in a humidified incubator with 5% CO_2 at 37°C. SiRNAs of CLIC1 (si-CLIC1) and negative control (si-NC) were synthesized by GenePharma (Shanghai, China), which were transfected into cells based upon X-tremeGENE™ siRNA transfection reagent (Roche, New Jersey, United States).

Real-time quantitative PCR (RT-qPCR)

Total RNA was extracted via Trizol (Yeasen, Shanghai, China). RNA quality was evaluated in line with OD260/OD280 ratio. The extracted RNA was reversely transcribed into cDNA. RT-qPCR was conducted based upon the ABI QuantStudio™ 12K Flex (ABI, Connecticut, United States). Primer sequences included: CLIC1, 5'-AGTCCCAGCAACCCAGAATTT-3' (forward), 5'-CACGAA CAATTCGACCTGCG-3' (reverse); GAPDH, 5'-GAATGGGCA GCCGTTAGGAA-3' (forward), 5'-AAAAGCATCACCCGGAGG AG-3' (reverse). Relative expression of CLIC1 was computed with $2^{-\Delta\Delta CT}$.

Western blotting

Whole-cell protein was extracted from U251 and U373 in RIPA buffer (Thermo Fisher Scientific, United States) and centrifuged at 12,000 rpm for 20 min. A BCA kit (Thermo, Waltham, MA, 23228) was used to measure the protein concentration. After immunoblotting, the proteins were transferred to a nitrocellulose membrane and incubated with specific antibodies. The following primary antibodies were used: β-actin (Proteintech,60008-1-lg), CLIC1 (Cell Signaling Technology, D7D6H Rabbit mAb #53424).

Flow cytometry

Cell apoptosis was measured via cell apoptosis detection kit (Abbkine, Wuhan, China). The supernatant was absorbed from the culture plate and transfered it to the centrifuge tube for preservation. The cells were washed twice with PBS, and the cleaning solution was collected for preservation. Appropriate amount of PBS was used to blow down the cells, the cell suspension was transferred to the centrifuge tube, and the supernatant of step 1 and cleaning solution of step 2 were added together. Following centrifugation at 1,000 rpm for 5 min and discard the supernatant. After adding PBS, centrifuge at 1,000 rpm for 5 min, the supernatant was discarded. This step was repeated. A cell suspension of 1 × 10*6 cells/ml was prepared via adding the pre-prepared 1× Annexin V buffer. 100 μl of cell suspension was taken and added to the new tube. The cell suspension was added with 5 μl Annexin V-AbFluor ™ 488 binding and 2 μl PI, and incubated at room temperature away from light for 15 min. 400 μl 1×Annexin V buffer was added, and apoptosis was tested within 1 h.

Wound healing assay

Cell motility was detected via wound healing assay. Cells were seeded in 6-well plates. When the cell confluence reached 100%, wounds were produced utilizing a 200-μL micropipette tip. The scratched cells were discarded and serum-free medium was added. Photographs were acquired at 0 and 48 h by use of an inverted microscope (Olympus, Japan).

Genomic alteration evaluation

Copy number gains and losses were estimated by use of GISTIC 2.0 (Mermel et al., 2011). Somatically mutated genes were assessed via maftools computational approach (Mayakonda et al., 2018). Tumor mutational burden (TMB), aneuploidy score, cancer testis antigen (CTA), fraction of genome altered and number of segments of glioma specimens were also analyzed.

Drug sensitivity estimation

By pRRophetic package (Geeleher et al., 2014), half-maximal inhibitory concentration (IC50) values of commonly applied drugs were estimated in accordance with the Genomics of Drug Sensitivity in Cancer cell line expression spectrum (Yang et al., 2013). After gathering drug sensitivity data from the CTRP and PRISM datasets, response to small molecular compounds was evaluated based upon area under the curve (AUC) (Ghandi et al., 2019).

Anticancer immunity assessment

Activity of steps in the cancer-immunity cycle (Chen and Mellman) was estimated by use of GSVA package (Xu et al., 2018). Expression of chemokine, receptor, immuno-stimulator, MHC and immune checkpoint molecules was computed (Chen et al., 2021). Through single-sample GSEA (ssGSEA) (Hanzelmann et al., 2013), infiltration of immune cell types was estimated. Response to PD-1 or CTLA4 antibody (Chen et al., 2016; Balar et al., 2017) was inferred based upon subclass mapping (Submap) algorithm (Hoshida et al., 2007). Tumor Immune Dysfunction and Exclusion (TIDE) (Jiang et al., 2018) was employed for estimation of immune-checkpoint blockade (ICB) efficacy.

ScRNA-seq analysis

ScRNA-seq data from nine glioma specimens were acquired from the GSE138794 dataset (Wang et al., 2019). Quality control was implemented, with subsequent removal of cells with >10% mitochondrial UMI counts. The analysis was achieved through Seurat package (Butler et al., 2018). The top 2,000 genes with high variability were chosen. Cell types were then clustered and recognized based upon known cell markers that were gathered from the CellMarker database (Zhang et al., 2019). Function role of CLIC1 in the single cell level was investigate through GSVA R package (Hanzelmann et al., 2013). The CellChat R package (v1.6.1) was used for cell-cell communication analysis. Glioma cells were isolated from all cells and categorized into “astrocyte,” “oligodendrocyte,” “macrophage,” “glial cell,” “monocyte,” and “endothelial cell.” A CellChat object was then created with the CellChat function (Jin et al., 2021). The computeCommunProbPathway function yielded cell-to-cell interactions for each cell signaling pathway. The CytoTRACE algorithm assessed cell differentiation and developmental potential by analyzing factors like mRNA feature expression and distribution (Gulati et al., 2020). To identify the initial stage of cellular differentiation, we used the CytoTRACE R package (v0.3.3). Additionally, we employed pseudotime analysis from the monocle2 R package (v2.24.0) (26) to determine the direction of cellular differentiation (Qiu et al., 2017).

Statistical analysis

All the analyses were achieved via appropriate R packages (version 4.2.1). OS, disease-specific survival (DSS) and progression-free survival (PFS) analyses were conducted through Kaplan–Meier curves and log-rank test utilizing survival package. Receiver operating characteristic curves (ROCs) were drawn for appraising the prediction efficiency via pROC package, and AUC values were computed. Continuous data between two groups were compared utilizing student’s t or Wilcoxon rank-sum test, with one-way analysis of variance for comparing ≥3 groups. Through uni- and multivariate cox regression methods, association of variables with

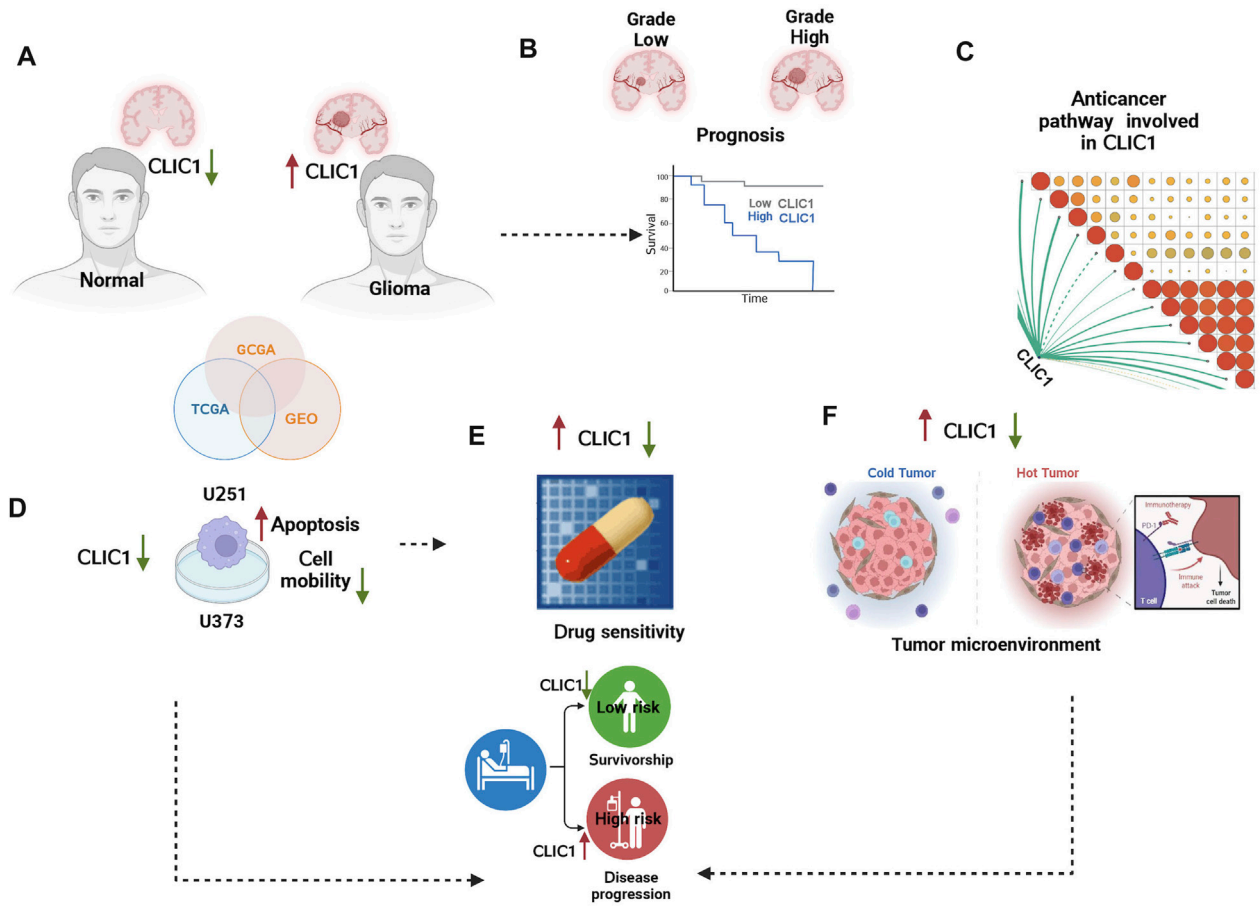

FIGURE 1
The graphical abstract and analysis flow chart of present study. **(A)** Multi-omics data acquisition. Gliomas present high expression of CLIC1. **(B)** Prognostic implication of CLIC1 was investigated in gliomas. **(C)** Signaling pathways involved in CLIC1. **(D)** Experiments validated CLIC1 as a therapeutic vulnerability of gliomas. **(E)** Association of CLIC1 with drug sensitivity. **(F)** Anticancer immunity assessment of CLIC1.

survival was investigated. Pearson's test was adopted for correlation analysis. Statistical significance was set as $p < 0.05$. Figure 1 presents the whole analysis flow chart.

Results

Upregulated CLIC1 correlates to undesirable prognostic outcomes of glioma

The study integrated TCGA-GBM and TCGA-LGG samples and corrected batch effects for analyzing CLIC1 in glioma (Supplementary Figures S1A, B). Prognostic implication of CLIC1 was firstly investigated in glioma. Patients with CLIC1 upregulation presented poorer OS outcomes versus those with CLIC1 downregulation (Figure 2A). ROCs were utilized for verifying the efficacy of CLIC1 in prognostication. AUC values at one-, three- and 5-year OS exceeded 0.65, demonstrating that CLIC1 enabled to potentially estimate OS. Association of CLIC1 with DSS and PFS was also evaluated. Worse DSS and PFS outcomes were found in patients with high CLIC1 expression (Figures 2B, C). AUC values of one-, three- and 5-year DSS and PFS were found to be more than 0.65, indicative of the efficacy of CLIC1 in estimation of DSS and PFS. For verifying the reliability and reproducibility of CLIC1 in prognostication, four cohorts: CGGA_325, CGGA_693, GSE16011 and GSE43378 were adopted. Consistently, upregulated CLIC1 was connected to terrible OS outcomes and presented the satisfactory efficiency of CLIC1 in survival estimation in above cohorts (Supplementary Figures S2A–D).

CLIC1 is linked with glioma patients' clinicopathological traits

Although CLIC1 is expressed ubiquitously in human tissues (Wang et al., 2012), CLIC1 was found to present aberrant overexpression in glioma versus normal tissues (Figure 3A). Association of CLIC1 with clinicopathological features was subsequently assessed. CLIC1 expression was remarkably higher in age ≥45 than <45 (Figure 3B). No significant difference was detected in male and female specimens (Figure 3C). CLIC1 was also detected to exhibit higher expression in grade III versus II (Figure 3D), indicating that CLIC1 upregulation was connected to more advanced grade. Mutant IDH1 and O^6-methylguanine DNA methyltransferase (MGMT) promoter methylation associate with

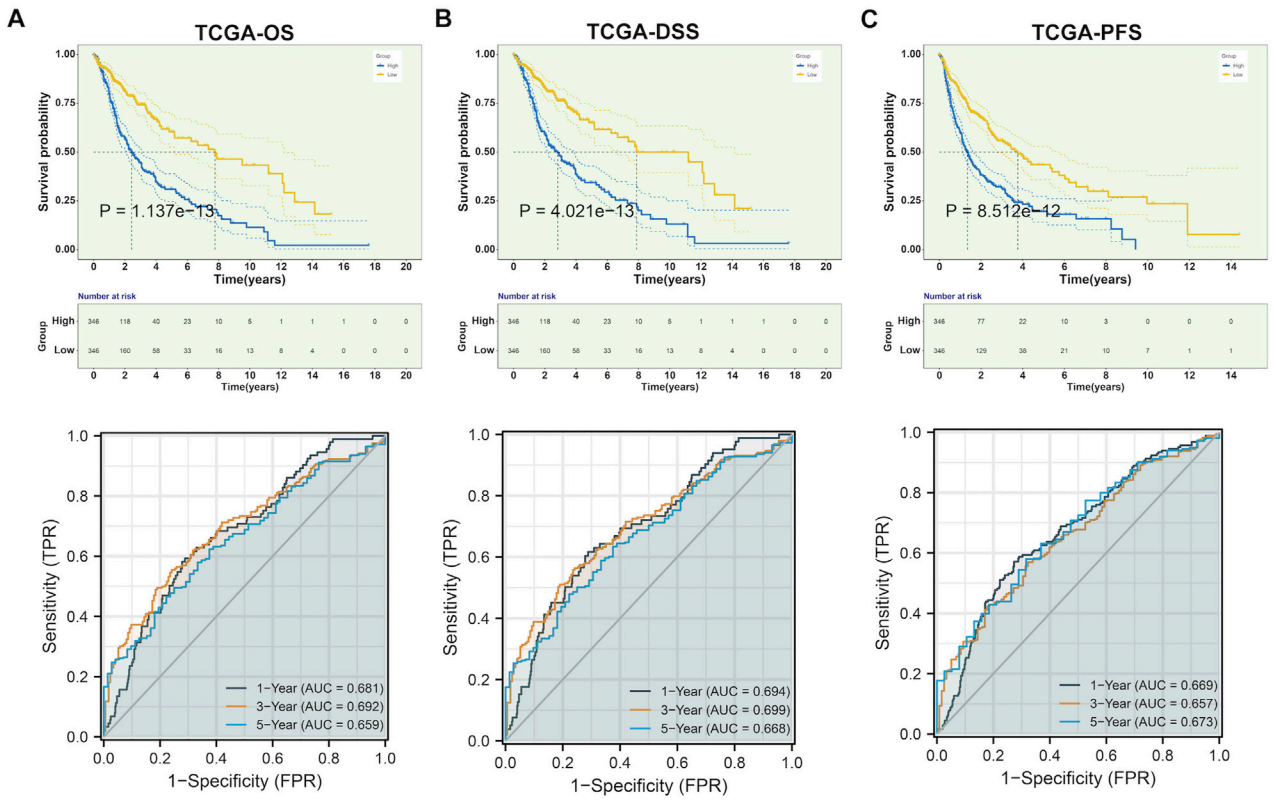

FIGURE 2
Upregulated CLIC1 correlates to undesirable prognostic outcomes of glioma. **(A–C)** Different OS, DSS and PFS outcomes in lowly and highly expressed CLIC1 patients as well as one-, three- and 5-year ROCs in TCGA cohort. OS, DSS and PFS analyses were conducted through Kaplan–Meier curves and log-rank test utilizing survival package. OS, overall survival; DSS, disease-specific survival; PFS, progression-free survival; ROC, receiver operating characteristic.

well prognostic outcomes of glioma patients (Della Monica et al., 2022). CLIC1 expression was notably higher in wild-type than mutant IDH1 tumors (Figure 3E). Additionally, unmethylated MGMT tumors displayed higher CLIC1 expression versus those with methylated MGMT (Figure 3F).

CLIC1 independently estimates glioma patients' prognosis

Integration of uni- and multivariate cox regression analyses showed that CLIC1 was independently predictive of patient survival in TCGA cohort (Supplementary Figures S3A, B). The independency of CLIC1 in prognostication was proven in the CGGA_325 and CGGA_693 datasets (Supplementary Figures S3C–F).

Signaling pathways and anticancer immunity involved in CLIC1

Tumorigenic and immunity-relevant signaling pathways: B cell receptor, chemokine, cytokine-cytokine receptor, JAK-STAT, T cell receptor and Toll-like receptor exhibited the remarkable enrichment in upregulated CLIC1 tumors (Figure 4A). Physiological processes, e.g., calcium signaling pathway, cardiac muscle contraction, long-term potentiation and neuroactive ligand receptor interaction were enriched in downregulated CLIC1 tumors (Figure 4B). In addition, CLIC1 was identified to positively associate with anticancer immunity (e.g., CD8 T effector, antigen processing machinery and immune checkpoint), cell cycle, stromal activation (pan-fibroblast TGFβ response signature (Pan-F-TBRS), epithelial-mesenchymal transition (EMT)1~3 and angiogenesis) and DNA damage repair mechanisms (DNA replication, nucleotide excision repair, homologous recombination and mismatch repair) (Figure 4C). Interrupting one or more steps within the cancer immune cycle allows the tumor to evade immune surveillance (Somarribas Patterson and Vardhana, 2021). CLIC1 presented positive interactions with all steps in the cancer immune cycle (Figure 4C), proving the significance of CLIC1 in modulating anticancer immunity.

CLIC1 is a therapeutic vulnerability of glioma

The study then assessed the potential of CLIC1 as a therapeutic vulnerability of glioma. U251 and U373 glioma cells were transfected with si-CLIC1 to silence CLIC1 expression (Figures 5A, B). The protein level of the CLIC1 in glioma cells transfected

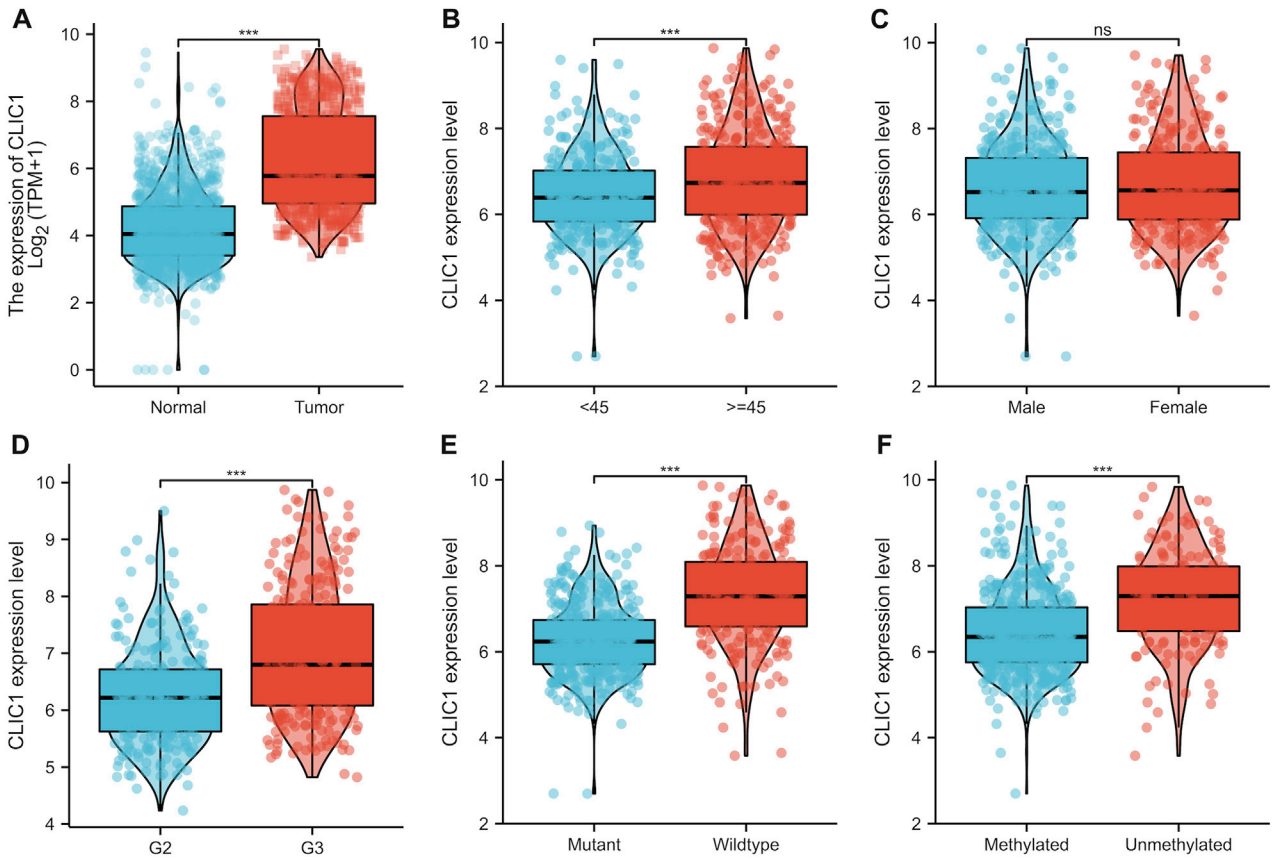

FIGURE 3
CLIC1 is linked with glioma patients' clinicopathological traits. **(A)** Comparison of CLIC1 expression in glioma and normal tissues. **(B–F)** Comparison of CLIC1 expression in age <45 versus ≥45; male versus female; grade II (G2) versus grade III (G3); wild-type versus mutant IDH1; methylated versus unmethylated MGMT specimens. The Student's t-test was used to compare the statistical difference between two groups. ***p-value < 0.001; ns: no significance.

with si-CLIC1 and a control sequence were assessed by Western blotting (Figure 5C). Based upon flow cytometry results, CLIC1-silent U251 and U373 cells presented remarkable enhancement in apoptosis (Figures 5D–F). In addition, wound healing results demonstrated that CLIC1 knockdown prominently alleviated cell mobility of U251 and U373 cells (Figures 5G–I). Overall, CLIC1 was regarded as a therapeutic vulnerability of glioma.

Genomic alterations and DNA methylation associated with CLIC1

More frequent gene gains and losses were detected in CLIC1 upregulation tumors (Figures 6A, B) in comparison to those with CLIC1 downregulation (Figures 6C, D). In addition, heterogeneous somatic mutations were observed in CLIC1 low and high tumors, e.g., IDH1 (78.8% versus 43.4%), CIC (26.6% versus 6%), NOTCH1 (9.3% versus 2.8%) and FUBP1 (9.6% versus 4.1%) occurred more frequent mutations in low CLIC1 tumors, and EGFR (6.6% versus 18.4%), RYR2 (2.1% versus 9.2%), with more frequently mutant NF1 (3.3% versus 10.4%), KEL (0.9% versus 5.4%), PTEN (6.9% versus 14.2%) and COL6A3 (1.5% versus 5.1%) in high CLIC1 tumors (Figure 6E). TMB and aneuploidy score were detected to be notably higher in CLIC1-up-regulated tumors, indicative of more mutations (Figures 6F, G). Additionally, high CLIC1 expression tumors presented lower CTA score (Figure 6H) as well as higher fraction of genome altered and number of segments (Figures 6I, J) versus those with lowly expressed CLIC1. Thus, CLIC1 upregulation was connected to more frequently genomic alterations. It was also found the prominently negative interaction of CLIC1 methylation with its expression (Figure 6K), indicating that CLIC1 overexpression was potentially affected by its hypomethylation.

Association of CLIC1 with drug sensitivity

Tumors with high CLIC1 expression displayed prominently lower IC50 values of camptothecin, cisplatin, doxorubicin, erlotinib, paclitaxel and rapamycin in comparison to those with lowly expressed CLIC1 (Figures 7A–G), suggesting that CLIC1 upregulation was linked with sensitivity to these drugs. CLIC1 was found to negatively correlate to AUC of CTRP compounds: clofarabine, tanespimycin and methotrexate; furthermore, highly expressed CLIC1 tumors exhibited lower AUC (Figure 7H). CLIC1 was also negatively connected to AUC of PRISM compounds: everolimus, TAK-733, trametinib and AZD8330, with lower AUC in high CLIC1 expression tumors

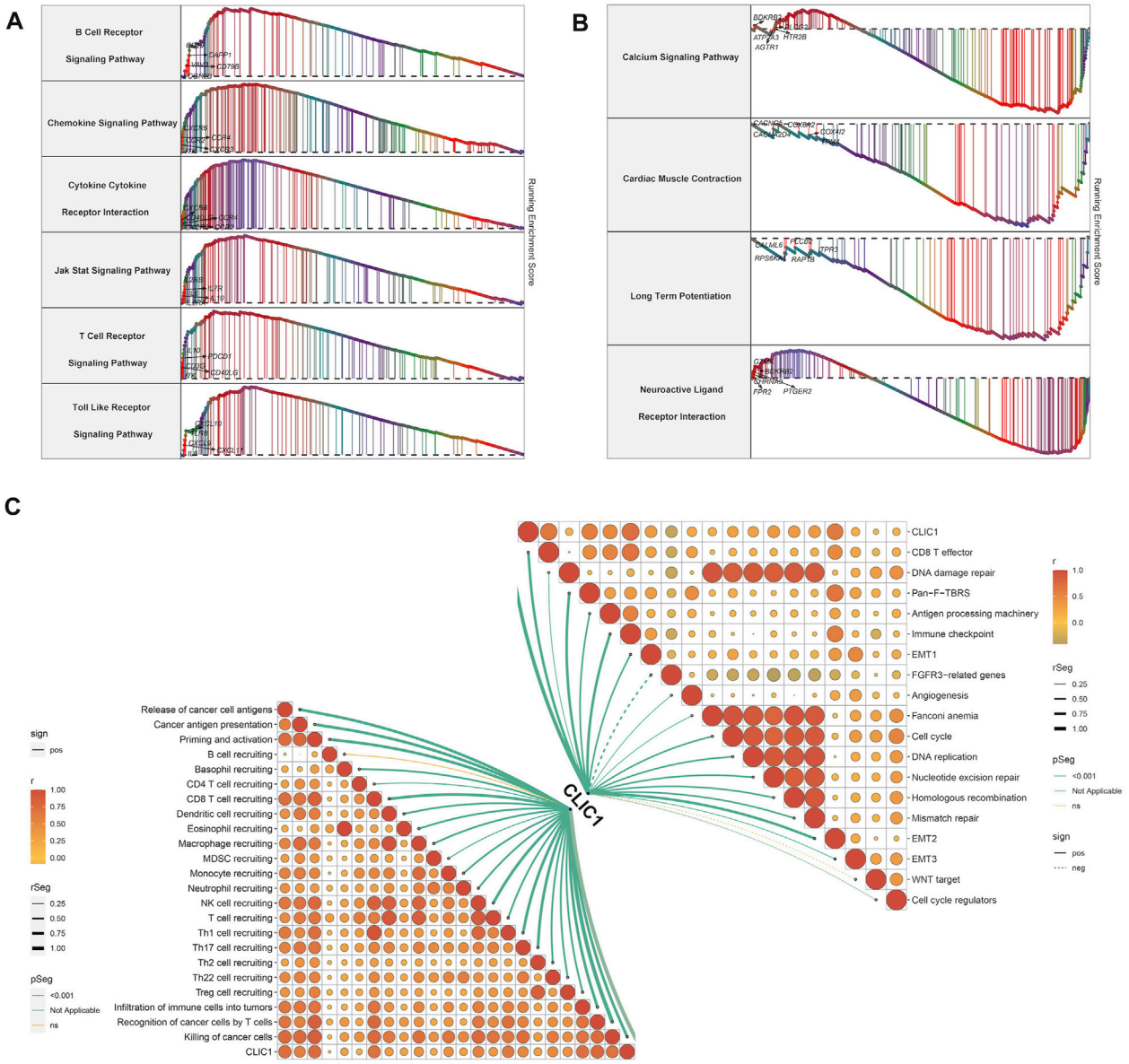

FIGURE 4
Signaling pathways involved in CLIC1. **(A)** Enrichment of GO and KEGG pathways in high CLIC1 expression tumors. **(B)** Enrichment of GO and KEGG pathways in low CLIC1 expression tumors. **(C)** Correlation of CLIC1 with cancer-immunity cycle and well-established pathways.

(Figure 7I). Above compounds might be appropriate for patients with overexpressed CLIC1.

CLIC1 upregulation is linked with hot tumors

Nearly all immune cell types (notably T cells) showed richer infiltration in CLIC1-up-regulated tumors (Supplementary Figure S4A). In addition, CLIC1 was positively connected to immune cell infiltration (Supplementary Figure S4B). With the increase in CLIC1 expression, expression of chemokine, receptor, immunostimulator and MHC molecules was gradually elevated (Supplementary Figures S4C–F). These data unveiled that CLIC1 upregulation was in relation to hot tumors.

Upregulated CLIC1 associates with response to ICB

Samples with highly expressed CLIC1 exhibited remarkably higher levels of almost all immune checkpoints (such as CD40/CD40LG, PDCD1/PDCD1LG2, CTLA4, CD276 and IDO1) versus those with low CLIC1 expression (Figure 8A). In addition, high CLIC1 expression tumors presented the similar expression profiling to patients who responded to PD-1 antibody (Figure 8B). TIDE approach was utilized for estimating the efficacy of ICB. Consequently, dysfunction, IFNG and TIDE scores were prominently higher in CLIC1-up-regulated tumors, without difference in exclusion score (Figures 8C–F), indicative of resistance to ICB. Hence, although tumors with

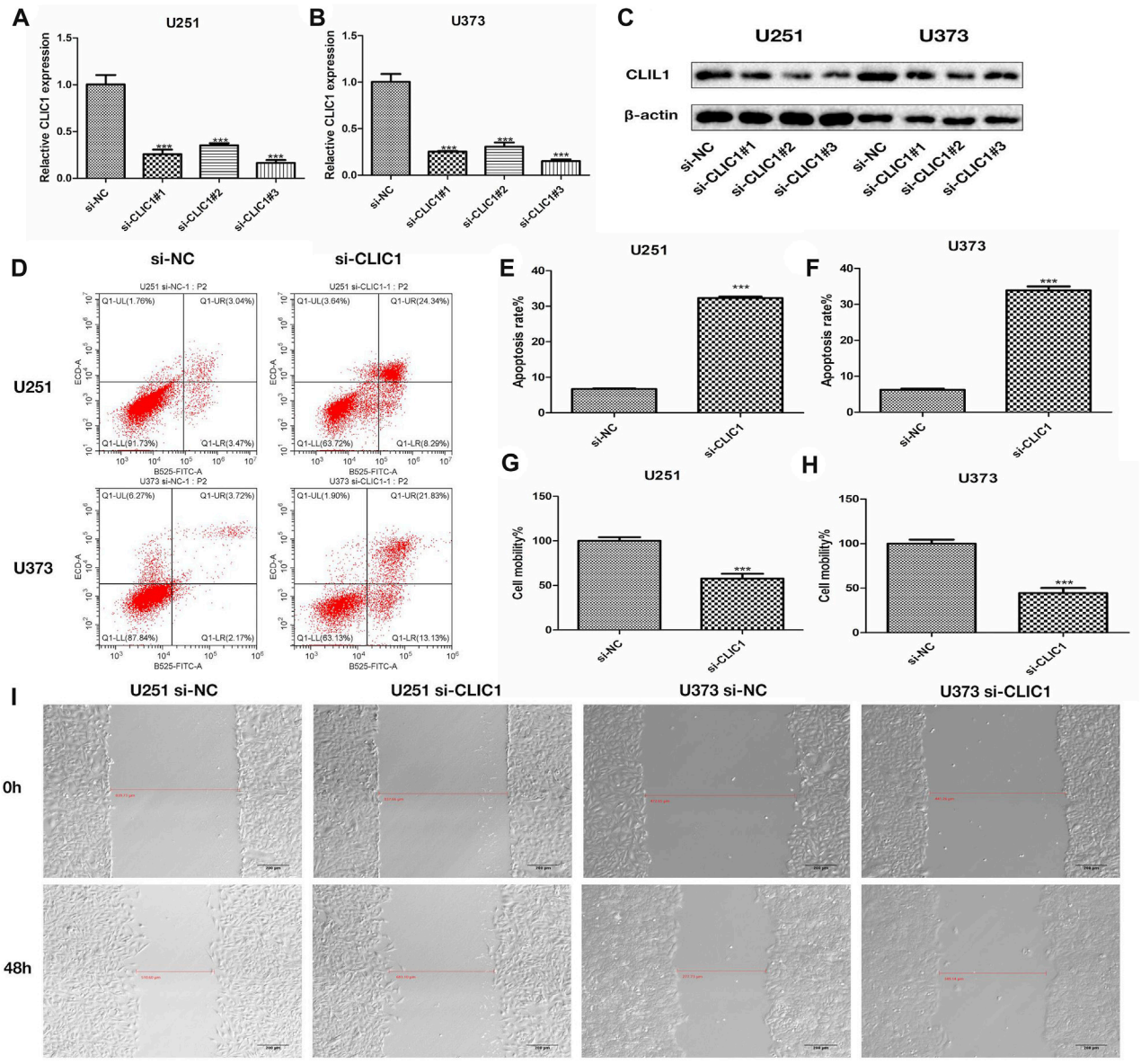

FIGURE 5
CLIC1 is a therapeutic vulnerability of glioma. **(A,B)** RT-qPCR for measurement of CLIC1 expression in U251 and U373 cells transfected with si-NC or si-CLIC1. **(C)** The protein level of the CLIC1 in glioma cells transfected with si-CLIC1 and a control sequence were assessed by Western blotting. β-actin was the loading control. **(D–F)** Flow cytometry for detection of apoptosis of si-NC or si-CLIC1-transfected U251 and U373 cells. **(G–I)** Wound healing for evaluation of cell mobility of si-NC- or si-CLIC1-transfected U251 and U373 cells. The Student's t-test and one-way analysis of variance (ANOVA) were respectively used to compare the statistical differences between two groups and three or more groups. Bar, 200 μm. ***p-value < 0.001.

CLIC1 upregulation had highly expressed immune checkpoints and abundant immune cells, they were resistant to ICB.

Single-cell analysis of CLIC1 in glioma tumors

The single-cell dataset GSE138794 comprised of nine samples, which contains 19,315 cells. The number of sequence genes, sequencing depth, and proportion of mitochondrial content were visualized in Supplementary Figure S5A. The sequencing depth and gene numbers presented a strong positive correlation (r = 0.92), while showed a weak correlation with mitochondrial content (Supplementary Figure S5B). Then, 2000 highly variable genes were selected from standardized expression matrix and top 10 genes were labeled (Supplementary Figure S5C). Based upon scRNA profiles, single cells from nine glioma specimens were clustered into 32 cell clusters (Supplementary Figure S5D). In line with known markers of cell types, six cell populations were identified, composed of astrocytes, endothelial cells, glial cell, monocytes (Mono)/macrophages (Macro) and oligodendrocytes (Figure 9A). CLIC1 was found to be expressed ubiquitously in distinct cell types, such as macrophages, astrocytes (Figure 9B). Moreover, we categorized cells into high and low CLIC1 group based on the median expression level of CLIC1. In

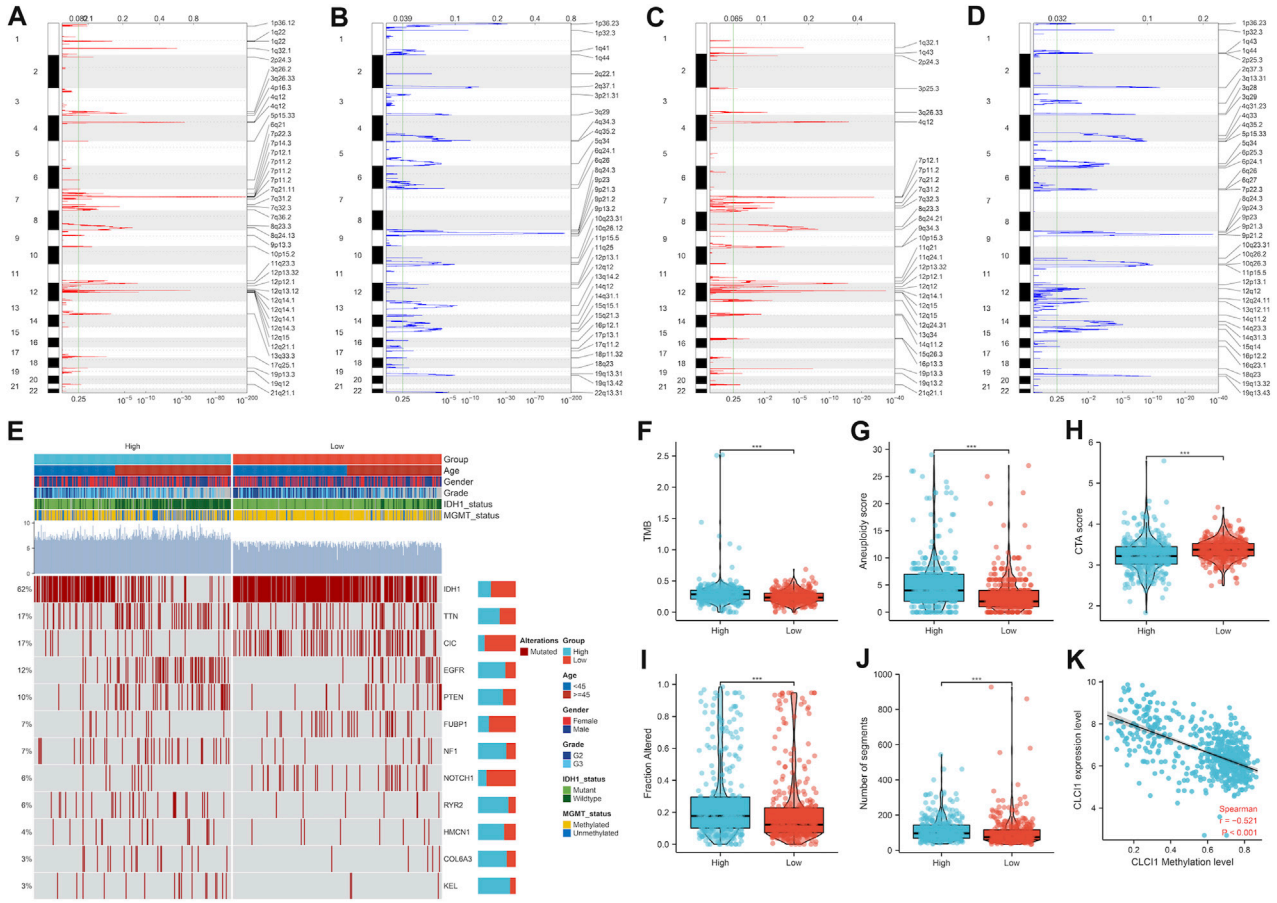

FIGURE 6
Genomic alterations and DNA methylation associated with CLIC1. **(A,B)** Gene gains and losses in glioma tumors with upregulated CLIC1. Red, gains; blue, losses. The significant cutoff was set as q-value of 0.25. **(C,D)** Gene gains and losses in tumors with downregulated CLIC1. **(E)** Somatically mutant genes in highly or lowly expressed CLIC1 tumors. Genes are ranked by mutant frequency. **(F–J)** Different TMB, aneuploidy score, CTA score, fraction of genome altered and number of segments in two groups. **(K)** Correlation between CLIC1 methylation and its expression across glioma tumors. The Student's t-test was used to compare the differences between two groups in terms of TMB, aneuploidy score, CTA score, fraction of genome altered, and the number of segments. The correlation between CLIC1 methylation and its expression across glioma tumors was assessed using the Spearman test. ***p-value < 0.001.

comparison to the high CLIC1 group, the low expression group has a greater quantity of cells (Figure 9C). The cells in high expression group were mostly concentrated on the macrophages and endothelial cells (Figure 9D). The cell - cell communication indicated that astrocytes and oligodendrocytes showed a strong interaction with other cell types (Figures 9E, F). In addition, the total number of interactions and interaction strength of the inferred cell-cell communication networks were compared between high and low CLIC1 group and revealed that high group showed a higher cell-cell interaction strength (Figure 9G). Then, we identified context-specific signaling pathways by comparing the interaction strength between high and low CLIC1 groups. Specifically, signaling pathways like MHC–II and NOTCH were found to be active in the high CLIC1 group (Figure 9H). Pathway enrichment analysis revealed that IL6_JAK_STAT pathway, TNFA signaling pathway, inflammatory response and KRAS signaling pathway were significantly enriched in high CLIC1 group, revealed that the oncogene role in golima (Figure 9I). To gain a deeper understanding of the differences between cell statuses, we monitored the movement trajectories of different cells. The findings indicated that all cells categorized into one root and three states, names 1, 2 and 3 (Supplementary Figures S6A–C). Moreover, we observed that CLIC1 was highly expressed in beginning of the trajectory (Supplementary Figure S6D). We subsequently using the cytotrace software to infer stemness (less differentiation) of the six cell types. As showed in Supplementary Figure S6E, astrocytes and oligodendrocytes have relative high cytotrace score, indicated that higher stemness of them.

Discussion

The present work demonstrated that elevated CLIC1 was linked with worse survival outcomes of gliomas. IDH-mutant gliomas usually exhibit low histologic grade with desirable prognostic outcomes and median survival of exceeding 12 years (Nicholson and Fine, 2021). Nevertheless, they usually transition to higher grade and clinical behaviors later in the natural history of this malignancy. Oppositely, IDH–wild-type gliomas often present as GBM (Ostrom

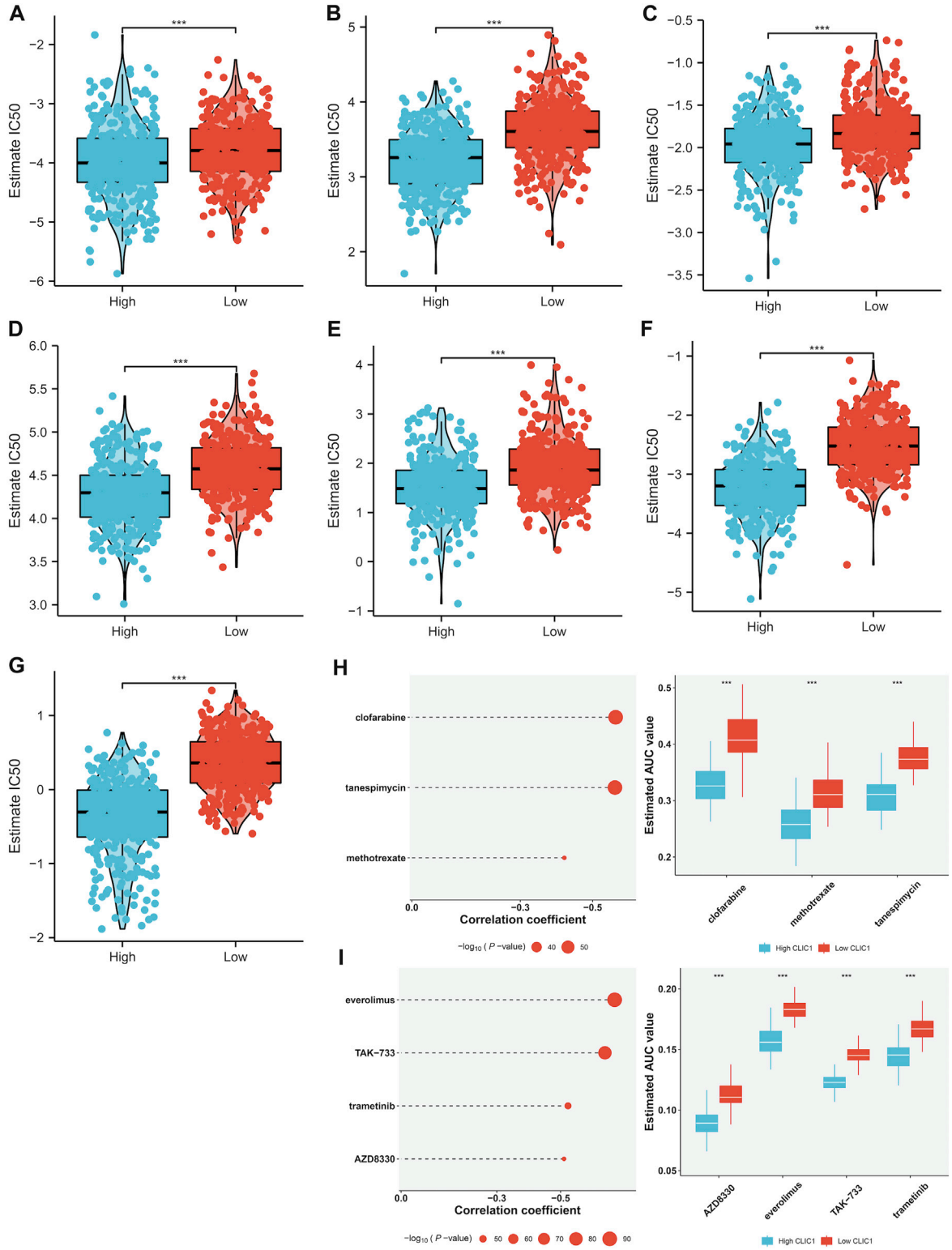

FIGURE 7
Association of CLIC1 with drug sensitivity. **(A–G)** Different IC50 values of **(A)** camptothecin, **(B)** cisplatin, **(C)** doxorubicin, **(D)** erlotinib, **(E)** etoposide, **(F)** paclitaxel and **(G)** rapamycin in highly and lowly expressed CLIC1 tumors. **(H,I)** Association of CLIC1 with AUC values of **(H)** CTRP- and **(I)** PRISM-derived drugs and different AUC values between down- and upregulated CLIC1 samples. The Student's t-test was used to compare the statistical difference between two groups. ***p-value < 0.001.

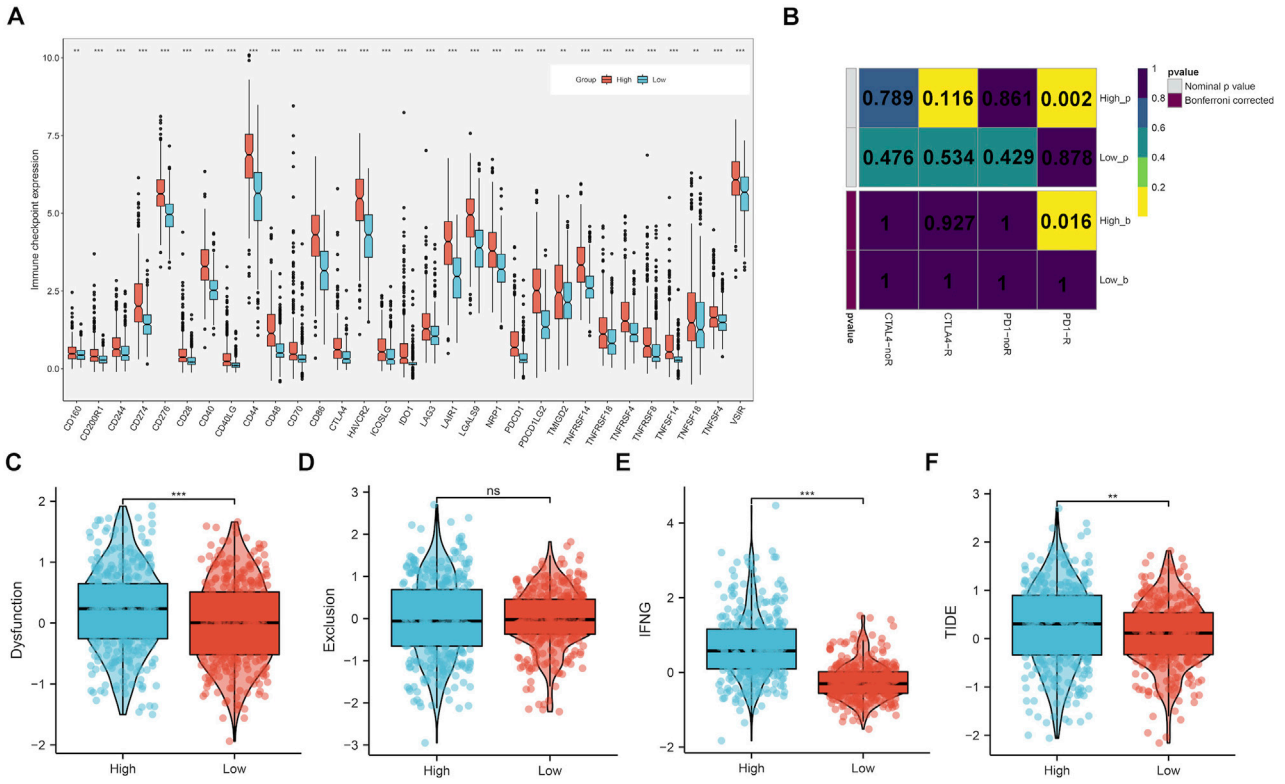

FIGURE 8
Upregulated CLIC1 associates with response to ICB. **(A)** Expression of immune checkpoints in lowly and highly expressed CLIC1 tumors. **(B)** Submap for evaluating the similarity in expression profiles between low or high CLIC1 expression samples and response to PD-1 or CTLA4 antibody. **(C–F)** Comparison of dysfunction, exclusion, IFNG and TIDE scores in tumors with up- and downregulated CLIC1. The Wilcoxon rank-sum test was used to compare the differences between two groups. ***p*-value < 0.01; ****p*-value < 0.001; ns, not significant.

et al., 2023). MGMT methylation status represents another molecular feature of gliomas. Herein, CLIC1 expression was elevated in more advanced tumors and IDH–wild-type and MGMT unmethylation status. Thus, CLIC1 was a possible prognostic factor of gliomas.

CLIC1, a member of the CLIC protein family, has emerged as a pivotal player in cancer progression across various malignancies (Ozaki et al., 2022). It exists in both soluble and membrane forms, and its multifaceted involvement in cancer biology has garnered significant attention, particularly in the context of diagnosis and therapeutic targeting. In a multitude of cancer types, CLIC1 has exhibited its potential as a diagnostic indicator and a therapeutic target. It influences fundamental cellular processes, including cell viability and mitochondrial function modulation. In ovarian cancer, CLIC1 has been identified as a promising biomarker (Ye et al., 2015; Singha et al., 2018) with prognostic value (Yu et al., 2018), impacting patient survival and possibly serving in conjunction with CLIC4. Additionally, CLIC1 may have implications in lymphoblastic leukemia (Dehghan-Nayeri et al., 2017). Breast cancer shows heightened CLIC1 expression, correlating with tumor characteristics such as size, TNM classification, pathological grade, lymph node metastasis, and Ki67, while lower expression levels associate with extended overall survival and progression-free survival. This indicates CLIC1's potential as a diagnostic marker for breast cancer (Xia et al., 2022). In esophageal squamous cell carcinoma (ESCC), CLIC1's elevated expression aligns with clinical TNM classifications, and its inhibition may promote the mTOR signaling pathway, impacting cell proliferation (Geng et al.). High CLIC1 expression in lung adenocarcinoma has been linked to reduced overall survival, establishing it as an independent prognostic factor (Yasuda et al., 2022). In gastric cancer, the absence of CLIC1 impedes invasion and migration, likely by increasing the expression of AMOT-p130 (Qiu et al., 2021). Hepatocellular carcinoma (HCC) exhibits upregulated CLIC1 expression, associated with tumor invasiveness, metastasis, and poor prognosis (Peng et al., 2021). CLIC1 plays a role in creating a microdomain that facilitates integrin-mediated adhesions and cytoskeletal extension, further contributing to HCC progression.

GBM presents high CLIC1 expression (Wang et al., 2012; Setti et al.), and its suppression reduces proliferation and self-renewal capabilities in glioma stem cells (Setti et al.). GBM aggressiveness correlates with CLIC1-mediated channel activity, suggesting a potential membrane-associated role for CLIC1 in tumor settings. CLIC1's ability to modulate reactive oxygen species and pH fluctuations influences GBM stem cell motility and proliferation, making it a promising therapeutic target (Peretti et al., 2018). Notably, CLIC1 alterations have been observed in solid tumors and vascular malformations, particularly in GBM and bladder cancers (Bia et al., 2016). Moreover, CLIC1 expression has been linked to the drug-resistant protein MRP1, emphasizing its potential relevance in drug resistance mechanisms (Wu and Wang, 2017).

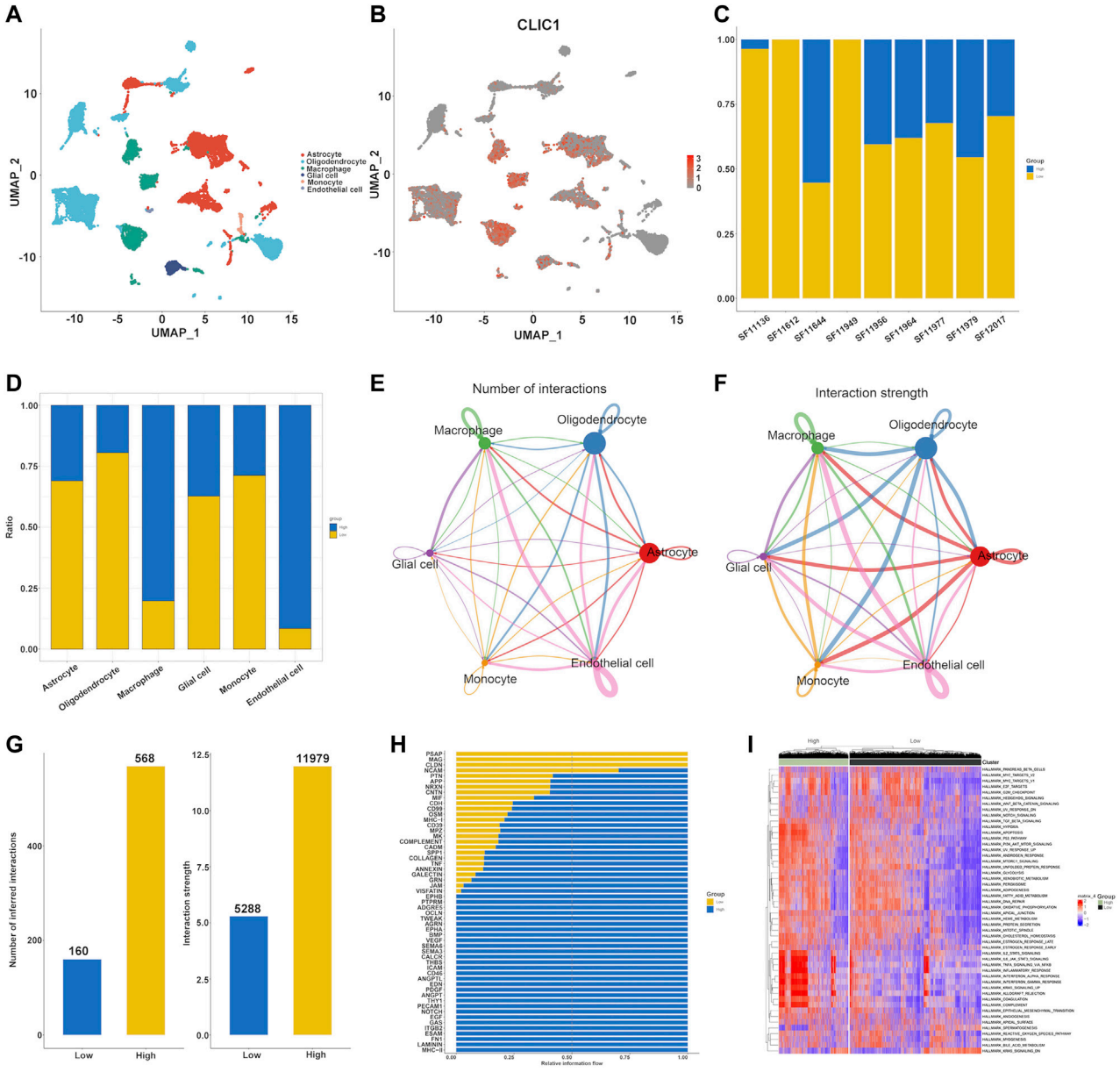

FIGURE 9
Single cell analysis of CLIC1 in Golima tumors. **(A)** Identification of cell types in line with well-established markers. **(B)** Expression distribution of CLIC1 in distinct cell types. **(C)** Proportion of high and low CLIC1 group in golima patients. **(D)** Proportion of high and low CLIC1 group in cell types. The landscape of golima's intercellular communication between each cell type is represented by the thickness of the line, which symbolizes the number of ligand-receptor pairs **(E)** or interaction weight **(F)**. **(G)** Comparisons of inferred interactions in high and low CLIC1 group. **(H)** A barplot reveals the ratio of interaction strength between high and low CLIC1 groups for each signaling pathway. **(I)** Pathway exploration between high and low CLIC1 group through GSVA analysis.

In summary, CLIC1 plays a pivotal role in various cancer types, affecting proliferation, migration, invasion, and metastasis. Targeting CLIC1 holds promise for malignant tumor treatment, although comprehensive mechanistic understanding and targeted therapies necessitate further research. CLIC1's significance in cancer and glioma progression, as well as its impact on patient survival, present exciting avenues for future cancer research.

Consistent with prior studies (Barbieri et al., 2022; Peretti et al., 2018; Setti et al.), CLIC1 was connected to physiological processes, tumorigenic and immunity-relevant signaling pathways. More importantly, suppressing CLIC1 notably induced glioma cell apoptosis and alleviated cell motility, proving that CLIC1 as a treatment vulnerability of glioma. Glioma progression is shaped by genetic evolution and microenvironment crosstalk (Varn et al., 2022). Detailed characterization of genomic alterations has not determined subtype-specific vulnerabilities in glioma patients (Feng et al., 2023). Heterogeneous genomic alterations were found in low and high CLIC1 expression tumors. Epigenetic

remodeling is a molecular hallmark of glioma, which has been regarded as a pivotal mediator of glioma pathogenesis (McClellan et al., 2023). CLIC1 overexpression was potentially affected by altered DNA methylation.

Malignant gliomas remain very difficult to cure because full surgical excision is not biologically feasible owing to the aggressive nature and the proximity of the tumor to functionally sensitive regions (Siegelin et al., 2021). In addition, adjuvant therapy faces frequent treatment resistance because the central nervous system is a protective environment and tumor cells exhibit large intratumor genetic and epigenetic variations. Consequently, novel treatments are urgently required, but the development processes of novel drugs that eventually achieve clinical applications are time-consuming and expensive. High CLIC1 expression was detected to associate with improved sensitivity to chemotherapy and targeted agents (camptothecin, cisplatin, doxorubicin, erlotinib, paclitaxel and rapamycin) as well as small molecular compounds clofarabine, tanespimycin, methotrexate, everolimus, TAK-733, trametinib and AZD8330.

ICB has revolutionized modern cancer treatment, arousing great interest in the field of neuro-oncology. ICB can unleash or redirect the function of T lymphocytes, carrying out cell-mediated immune response that directly kills tumor cells and enhances the anticancer abilities of other immune cell types. For complete anticancer immunity, T cells must have both effector function and the capacity to infiltrate the microenvironmental niche. Despite the well establishment of predictive biomarkers of response to ICB in several cancer types, they are limited to immunogenic cancer types, and malignant gliomas are largely refractory to ICB (Liu et al., 2023). Possible causes contain intrinsic characteristics of glioma cells, e.g., extensive genomic heterogeneity and poor mutation burden, extrinsic characteristics of immunosuppressive microenvironment and microvascular niches (Wu et al., 2023). CLIC1 overexpression was linked with most immune cell populations (notably T cells) and elevated expression of immune-modulators, indicative of a positive interaction of CLIC1 with hot tumors. Based upon high expression of immune checkpoints and similar transcriptome profiling to patients who responded to anti-PD-1, increased expression of CLIC1 indicated well response to ICB. Nevertheless, tumors with CLIC1 upregulation presented elevated TIDE score, indicating that they were resistant to ICB.

Single-cell transcriptomics shows the capacity to resolve whole transcriptomes of single cells with substantial throughput, which has revolutionized research of gene expression (Stuart et al., 2019). CLIC1 was expressed ubiquitously in astrocytes, endothelial cells, malignant cells, Mono/Macro and oligodendrocytes. CLIC1 is required for beta-amyloid-induced production of neurotoxic reactive oxygen species by microglia (Milton et al., 2008). Intracellular CLIC1 modulates macrophage function via mediating phagosomal acidification (Jiang et al., 2012). CLIC1 mediates endothelial S1P receptor to promote Rac1 and RhoA activity and functions (Mao et al., 2021). Thus, CLIC1 not only facilitates glioma tumor growth but also affects the tumor microenvironment.

Altogether, CLIC1 overexpression served as a prognostic factor of glioma patients and mediated malignant progression. It was also linked with genomic alterations, anticancer immunity and immune response as well as drug sensitivity. Our findings revealed that CLIC1 possessed the potential as a treatment vulnerability and actionable target in gliomas.

Data availability statement

The original contributions presented in the study are included in the article/Supplementary Material, further inquiries can be directed to the corresponding author.

Author contributions

CW: Writing–original draft, Writing–review and editing. ZH: Conceptualization, Data curation, Formal Analysis, Funding acquisition, Methodology, Validation, Visualization, Writing–original draft, Writing–review and editing.

Funding

The author(s) declare financial support was received for the research, authorship, and/or publication of this article. This research was supported by Qingdao Clinical Research Center for Rare Diseases of Nervous System (22-3-7-lczx-3-nsh), and Qingdao Key Health Discipline Development Fund.

Acknowledgments

We sincerely acknowledge TCGA, CGGA, GEO and the developers of these datasets.

Conflict of interest

The authors declare that the research was conducted in the absence of any commercial or financial relationships that could be construed as a potential conflict of interest.

Publisher's note

All claims expressed in this article are solely those of the authors and do not necessarily represent those of their affiliated organizations, or those of the publisher, the editors and the reviewers. Any product that may be evaluated in this article, or claim that may be made by its manufacturer, is not guaranteed or endorsed by the publisher.

Supplementary material

The Supplementary Material for this article can be found online at: https://www.frontiersin.org/articles/10.3389/fphar.2023.1279370/full#supplementary-material

SUPPLEMENTARY FIGURE S1
Combination of TCGA-GBM and TCGA-LGG samples and correction of batch effects. **(A, B)** PCA plots of TCGA-GBM and TCGA-LGG samples before and after correcting batch effects.

SUPPLEMENTARY FIGURE S2
Verification of OS difference and ROCs in the **(A)** CGGA_325, **(B)** CGGA_693, **(C)** GSE16011 and **(D)** GSE43378 cohorts.

SUPPLEMENTARY FIGURE S3
CLIC1 independently estimates glioma patients' prognosis. **(A, B)** Uni- and multivariate cox regression results on CLIC1, age, gender, grade, IDH1 and MGMT status with patient survival in TCGA dataset. **(C–F)** Verification of prognostic significance of CLIC1 and these clinicopathological parameters in the **(C, D)** CGGA_325 and **(E, F)** CGGA_693 datasets. Cox univariate regression analysis and multivariate Cox regression analysis were implemented to define the independent prognostic factor for OS.

SUPPLEMENTARY FIGURE S4
CLIC1 up-regulation is linked with hot tumors. **(A)** Different infiltration of immune cells in low and high CLIC1 expression tumors. **(B)** Interactions of CLIC1 with immune cell infiltration. **(C–F)** Expression patterns of **(C)** chemokine, **(D)** receptor, **(E)** immuno-stimulator and **(F)** MHC molecules in two groups. Blue to red denotes lowly to highly expressed molecules. The Student's t-test was used to compare the statistical difference between two groups. ***p-value < 0.001.

SUPPLEMENTARY FIGURE S5
Quality control and normalization of GSE138794 dataset. **(A)** Quality assurance of scRNA-Seq data derived from 9 golima samples. **(B)** Correlation between the detected gene numbers, mitochondrial content, and sequencing depth **(C)** Characterization of top 2,000 highly variable genes in scRNA-seq data. **(D)** TSNE and UMAP for single cell clustering analysis based upon scRNA data from the GSE138794.

SUPPLEMENTARY FIGURE S6
Differentiation trajectory analysis of scRNA-Seq data from the GSE138794. **(A)** Visualization of the trophoblast states throughout the trajectory analysis. **(B)** The biaxial scatter plot illustrates the development of trophoblastic cells, with darker shades denoting the earlier stages. **(C)** A sequence of cell clusters is plotted along pseudo-time, with each point representing a cell and each color representing a state. The cell sequence can be determined by examining the expression of the most dispersed genes in the cell cluster. **(D)** The expression of CLIC1 is plotted along pseudo-time, with each point representing a cell. **(D)** Trajectories of differentiation and distribution of six cell type were derived by CytoTRACE.

SUPPLEMENTARY TABLE S1
Clinical traits of glioma patients in TCGA, CGGA_325, CGGA_693, GSE16011 and GSE43378.

References

Balar, A. V., Galsky, M. D., Rosenberg, J. E., Powles, T., Petrylak, D. P., Bellmunt, J., et al. (2017). Atezolizumab as first-line treatment in cisplatin-ineligible patients with locally advanced and metastatic urothelial carcinoma: a single-arm, multicentre, phase 2 trial. *Lancet* 389, 67–76. doi:10.1016/S0140-6736(16)32455-2

Barbieri, F., Bosio, A. G., Pattarozzi, A., Tonelli, M., Bajetto, A., Verduci, I., et al. (2022). Chloride intracellular channel 1 activity is not required for glioblastoma development but its inhibition dictates glioma stem cell responsivity to novel biguanide derivatives. *J. Exp. Clin. Cancer Res.* 41, 53. doi:10.1186/s13046-021-02213-0

Baumert, B. G., Hegi, M. E., van den Bent, M. J., von Deimling, A., Gorlia, T., Hoang-Xuan, K., et al. (2016). Temozolomide chemotherapy versus radiotherapy in high-risk low-grade glioma (EORTC 22033-26033): a randomised, open-label, phase 3 intergroup study. *Lancet Oncol.* 17, 1521–1532. doi:10.1016/S1470-2045(16)30313-8

Biasiotta, A., D'Arcangelo, D., Passarelli, F., Nicodemi, E. M., and Facchiano, A. (2016). Ion channels expression and function are strongly modified in solid tumors and vascular malformations. *J. Transl. Med.* 14, 285. doi:10.1186/s12967-016-1038-y

Buckner, J. C., Shaw, E. G., Pugh, S. L., Chakravarti, A., Gilbert, M. R., Barger, G. R., et al. (2016). Radiation plus procarbazine, CCNU, and vincristine in low-grade glioma. *N. Engl. J. Med.* 374, 1344–1355. doi:10.1056/NEJMoa1500925

Butler, A., Hoffman, P., Smibert, P., Papalexi, E., and Satija, R. (2018). Integrating single-cell transcriptomic data across different conditions, technologies, and species. *Nat. Biotechnol.* 36, 411–420. doi:10.1038/nbt.4096

Chen, D. S., and Mellman, I. (2013). Oncology meets immunology: the cancer-immunity cycle. *Immunity* 39, 1–10. doi:10.1016/j.immuni.2013.07.012

Chen, L., Niu, X., Qiao, X., Liu, S., Ma, H., Shi, X., et al. (2021). Characterization of interplay between autophagy and ferroptosis and their synergistical roles on manipulating immunological tumor microenvironment in squamous cell carcinomas. *Front. Immunol.* 12, 739039. doi:10.3389/fimmu.2021.739039

Chen, P. L., Roh, W., Reuben, A., Cooper, Z. A., Spencer, C. N., Prieto, P. A., et al. (2016). Analysis of immune signatures in longitudinal tumor samples yields insight into biomarkers of response and mechanisms of resistance to immune checkpoint blockade. *Cancer Discov.* 6, 827–837. doi:10.1158/2159-8290.CD-15-1545

Colaprico, A., Silva, T. C., Olsen, C., Garofano, L., Cava, C., Garolini, D., et al. (2016). TCGAbiolinks: an R/Bioconductor package for integrative analysis of TCGA data. *Nucleic Acids Res.* 44, e71. doi:10.1093/nar/gkv1507

Dehghan-Nayeri, N., Eshghi, P., Pour, K. G., Rezaei-Tavirani, M., Omrani, M. D., and Gharehbaghian, A. (2017). Differential expression pattern of protein markers for predicting chemosensitivity of dexamethasone-based chemotherapy of B cell acute lymphoblastic leukemia. *Cancer Chemother. Pharmacol.* 80, 177–185. doi:10.1007/s00280-017-3347-0

Della Monica, R., Cuomo, M., Buonaiuto, M., Costabile, D., Franca, R. A., Del Basso De Caro, M., et al. (2022). MGMT and whole-genome DNA methylation impacts on diagnosis, prognosis and therapy of glioblastoma multiforme. *Int. J. Mol. Sci.* 23, 7148. doi:10.3390/ijms23137148

Feng, J., Zhao, Z., Wei, Y., Bao, Z., Zhang, W., Wu, F., et al. (2023). Temporal and spatial stability of the EM/PM molecular subtypes in adult diffuse glioma. *Front. Med.* 17, 240–262. doi:10.1007/s11684-022-0936-z

Geeleher, P., Cox, N., and Huang, R. S. (2014). pRRophetic: an R package for prediction of clinical chemotherapeutic response from tumor gene expression levels. *PLoS One* 9, e107468. doi:10.1371/journal.pone.0107468

Geng, H., Feng, C., Sun, Z., Fan, X., Xie, Y., Gu, J., et al. (2023). Chloride intracellular channel 1 promotes esophageal squamous cell carcinoma proliferation via mTOR signalling. *Transl. Oncol.* 27, 101560. doi:10.1016/j.tranon.2022.101560

Ghandi, M., Huang, F. W., Jané-Valbuena, J., Kryukov, G. V., Lo, C. C., McDonald, E. R., 3rd, et al. (2019). Next-generation characterization of the cancer cell line encyclopedia. *Nature* 569, 503–508. doi:10.1038/s41586-019-1186-3

Gravendeel, L. A., Kouwenhoven, M. C., Gevaert, O., de Rooi, J. J., Stubbs, A. P., Duijm, J. E., et al. (2009). Intrinsic gene expression profiles of gliomas are a better predictor of survival than histology. *Cancer Res.* 69, 9065–9072. doi:10.1158/0008-5472.CAN-09-2307

Gulati, G. S., Sikandar, S. S., Wesche, D. J., Manjunath, A., Bharadwaj, A., Berger, M. J., et al. (2020). Single-cell transcriptional diversity is a hallmark of developmental potential. *Science* 367, 405–411. doi:10.1126/science.aax0249

Hanzelmann, S., Castelo, R., and Guinney, J. (2013). GSVA: gene set variation analysis for microarray and RNA-seq data. *BMC Bioinforma.* 14, 7. doi:10.1186/1471-2105-14-7

Hoshida, Y., Brunet, J. P., Tamayo, P., Golub, T. R., and Mesirov, J. P. (2007). Subclass mapping: identifying common subtypes in independent disease data sets. *PLoS One* 2, e1195. doi:10.1371/journal.pone.0001195

Hossain, K. R., Turkewitz, D. R., Holt, S. A., Le Brun, A. P., and Valenzuela, S. M. (2023). Sterol structural features' impact on the spontaneous membrane insertion of CLIC1 into artificial lipid membranes. *Langmuir* 39, 3286–3300. doi:10.1021/acs.langmuir.2c03129

Jiang, L., Salao, K., Li, H., Rybicka, J. M., Yates, R. M., Luo, X. W., et al. (2012). Intracellular chloride channel protein CLIC1 regulates macrophage function through modulation of phagosomal acidification. *J. Cell Sci.* 125, 5479–5488. doi:10.1242/jcs.110072

Jiang, P., Gu, S., Pan, D., Fu, J., Sahu, A., Hu, X., et al. (2018). Signatures of T cell dysfunction and exclusion predict cancer immunotherapy response. *Nat. Med.* 24, 1550–1558. doi:10.1038/s41591-018-0136-1

Jin, S., Guerrero-Juarez, C. F., Zhang, L., Chang, I., Ramos, R., Kuan, C. H., et al. (2021). Inference and analysis of cell-cell communication using CellChat. *Nat. Commun.* 12, 1088. doi:10.1038/s41467-021-21246-9

Kawaguchi, A., Yajima, N., Tsuchiya, N., Homma, J., Sano, M., Natsumeda, M., et al. (2013). Gene expression signature-based prognostic risk score in patients with glioblastoma. *Cancer Sci.* 104, 1205–1210. doi:10.1111/cas.12214

Leek, J. T., Johnson, W. E., Parker, H. S., Jaffe, A. E., and Storey, J. D. (2012). The sva package for removing batch effects and other unwanted variation in high-throughput experiments. *Bioinformatics* 28, 882–883. doi:10.1093/bioinformatics/bts034

Liberzon, A., Birger, C., Thorvaldsdóttir, H., Ghandi, M., Mesirov, J. P., and Tamayo, P. (2015). The Molecular Signatures Database (MSigDB) hallmark gene set collection. *Cell Syst.* 1, 417–425. doi:10.1016/j.cels.2015.12.004

Liu, H., Zhao, Q., Tan, L., Wu, X., Huang, R., Zuo, Y., et al. (2023). Neutralizing IL-8 potentiates immune checkpoint blockade efficacy for glioma. *Cancer Cell* 41, 693–710.e8. doi:10.1016/j.ccell.2023.03.004

Louis, D. N., Perry, A., Wesseling, P., Brat, D. J., Cree, I. A., Figarella-Branger, D., et al. (2021). The 2021 WHO classification of tumors of the central nervous system: a summary. *Neuro Oncol.* 23 (2021), 1231–1251. doi:10.1093/neuonc/noab106

Mao, Y., Kleinjan, M. L., Jilishitz, I., Swaminathan, B., Obinata, H., Komarova, Y. A., et al. (2021). CLIC1 and CLIC4 mediate endothelial S1P receptor signaling to facilitate Rac1 and RhoA activity and function. *Sci. Signal* 14, eabc0425. doi:10.1126/scisignal.abc0425

Mayakonda, A., Lin, D. C., Assenov, Y., Plass, C., and Koeffler, H. P. (2018). Maftools: efficient and comprehensive analysis of somatic variants in cancer. *Genome Res.* 28, 1747–1756. doi:10.1101/gr.239244.118

McClellan, B. L., Haase, S., Nunez, F. J., Alghamri, M. S., Dabaja, A. A., Lowenstein, P. R., et al. (2023). Impact of epigenetic reprogramming on antitumor immune responses in glioma. *J. Clin. Invest.* 133, e163450. doi:10.1172/JCI163450

Mermel, C. H., Schumacher, S. E., Hill, B., Meyerson, M. L., Beroukhim, R., and Getz, G. (2011). GISTIC2.0 facilitates sensitive and confident localization of the targets of focal somatic copy-number alteration in human cancers. *Genome Biol.* 12, R41. doi:10.1186/gb-2011-12-4-r41

Milton, R. H., Abeti, R., Averaimo, S., DeBiasi, S., Vitellaro, L., Jiang, L., et al. (2008). CLIC1 function is required for beta-amyloid-induced generation of reactive oxygen species by microglia. *J. Neurosci.* 28, 11488–11499. doi:10.1523/JNEUROSCI.2431-08.2008

Nicholson, J. G., and Fine, H. A. (2021). Diffuse glioma heterogeneity and its therapeutic implications. *Cancer Discov.* 11, 575–590. doi:10.1158/2159-8290.CD-20-1474

Ostrom, Q. T., Shoaf, M. L., Cioffi, G., Waite, K., Kruchko, C., Wen, P. Y., et al. (2023). National-level overall survival patterns for molecularly-defined diffuse glioma types in the United States. *Neuro Oncol.* 25, 799–807. doi:10.1093/neuonc/noac198

Ozaki, S., Mikami, K., Kunieda, T., and Tanaka, J. (2022). Chloride intracellular channel proteins (CLICs) and malignant tumor progression: a focus on the preventive role of CLIC2 in invasion and metastasis. *Cancers (Basel)* 14, 4890. doi:10.3390/cancers14194890

Ozaki, S., Umakoshi, A., Yano, H., Ohsumi, S., Sumida, Y., Hayase, E., et al. (2021). Chloride intracellular channel protein 2 is secreted and inhibits MMP14 activity, while preventing tumor cell invasion and metastasis. *Neoplasia* 23, 754–765. doi:10.1016/j.neo.2021.06.001

Peng, J. M., Lin, S. H., Yu, M. C., and Hsieh, S. Y. (2021). CLIC1 recruits PIP5K1A/C to induce cell-matrix adhesions for tumor metastasis. *J. Clin. Invest.* 131, e133525. doi:10.1172/JCI133525

Peretti, M., Raciti, F. M., Carlini, V., Verduci, I., Sertic, S., Barozzi, S., et al. (2018). Mutual influence of ROS, pH, and CLIC1 membrane protein in the regulation of G(1)-S phase progression in human glioblastoma stem cells. *Mol. Cancer Ther.* 17, 2451–2461. doi:10.1158/1535-7163.MCT-17-1223

Pressey, J. C., de Saint-Rome, M., Raveendran, V. A., and Woodin, M. A. (2023). Chloride transporters controlling neuronal excitability. *Physiol. Rev.* 103, 1095–1135. doi:10.1152/physrev.00025.2021

Qiu, X., Mao, Q., Tang, Y., Wang, L., Chawla, R., Pliner, H. A., et al. (2017). Reversed graph embedding resolves complex single-cell trajectories. *Nat. Methods* 14, 979–982. doi:10.1038/nmeth.4402

Qiu, Y., Mao, Y. T., Zhu, J. H., Zhao, K., Wang, J. F., Huang, J. M., et al. (2021). CLIC1 knockout inhibits invasion and migration of gastric cancer by upregulating AMOT-p130 expression. *Clin. Transl. Oncol.* 23, 514–525. doi:10.1007/s12094-020-02445-0

Sarkar, S. (2022). Microglial ion channels: Key players in non-cell autonomous neurodegeneration. *Neurobiol. Dis.* 174, 105861. doi:10.1016/j.nbd.2022.105861

Setti, M., Savalli, N., Osti, D., Richichi, C., Angelini, M., Brescia, P., et al. (2013). Functional role of CLIC1 ion channel in glioblastoma-derived stem/progenitor cells. *J. Natl. Cancer Inst.* 105, 1644–1655. doi:10.1093/jnci/djt278

Siegelin, M. D., Schneider, E., Westhoff, M. A., Wirtz, C. R., and Karpel-Massler, G. (2021). Current state and future perspective of drug repurposing in malignant glioma. *Semin. Cancer Biol.* 68, 92–104. doi:10.1016/j.semcancer.2019.10.018

Singha, B., Harper, S. L., Goldman, A. R., Bitler, B. G., Aird, K. M., Borowsky, M. E., et al. (2018). CLIC1 and CLIC4 complement CA125 as a diagnostic biomarker panel for all subtypes of epithelial ovarian cancer. *Sci. Rep.* 8, 14725. doi:10.1038/s41598-018-32885-2

Somarribas Patterson, L. F., and Vardhana, S. A. (2021). Metabolic regulation of the cancer-immunity cycle. *Trends Immunol.* 42, 975–993. doi:10.1016/j.it.2021.09.002

Stuart, T., Butler, A., Hoffman, P., Hafemeister, C., Papalexi, E., Mauck, W. M., 3rd, et al. (2019). Comprehensive integration of single-cell data. *Cell* 177, 1888–1902. doi:10.1016/j.cell.2019.05.031

Stupp, R., Taillibert, S., Kanner, A., Read, W., Steinberg, D., Lhermitte, B., et al. (2017). Effect of tumor-treating fields plus maintenance temozolomide vs maintenance temozolomide alone on survival in patients with glioblastoma: a randomized clinical trial. *Jama* 318, 2306–2316. doi:10.1001/jama.2017.18718

Tian, Y., Xiao, H., Yang, Y., Zhang, P., Yuan, J., Zhang, W., et al. (2023). Crosstalk between 5-methylcytosine and N(6)-methyladenosine machinery defines disease progression, therapeutic response and pharmacogenomic landscape in hepatocellular carcinoma. *Mol. Cancer* 22, 5. doi:10.1186/s12943-022-01706-6

Varn, F. S., Johnson, K. C., Martinek, J., Huse, J. T., Nasrallah, M. P., Wesseling, P., et al. (2022). Glioma progression is shaped by genetic evolution and microenvironment interactions. *Cell* 185, 2184–2199.e16. doi:10.1016/j.cell.2022.04.038

Wang, L., Babikir, H., Müller, S., Yagnik, G., Shamardani, K., Catalan, F., et al. (2019). The phenotypes of proliferating glioblastoma cells reside on a single Axis of variation. *Cancer Discov.* 9, 1708–1719. doi:10.1158/2159-8290.CD-19-0329

Wang, L., He, S., Tu, Y., Ji, P., Zong, J., Zhang, J., et al. (2012). Elevated expression of chloride intracellular channel 1 is correlated with poor prognosis in human gliomas. *J. Exp. Clin. Cancer Res.* 31, 44. doi:10.1186/1756-9966-31-44

Wu, J., and Wang, D. (2017). CLIC1 induces drug resistance in human choriocarcinoma through positive regulation of MRP1. *Oncol. Res.* 25, 863–871. doi:10.3727/096504016X14772315906527

Wu, M., Wu, L., Wu, W., Zhu, M., Li, J., Wang, Z., et al. (2023). Phagocytosis of glioma cells enhances the immunosuppressive phenotype of bone marrow-derived macrophages. *Cancer Res.* 83, 771–785. doi:10.1158/0008-5472.CAN-22-1570

Xia, J., Wang, Q., Ju, F., Luo, X., Wang, F., Zhou, Y., et al. (2022). Chloride intracellular channel 1 is a potential biomarker for breast cancer. *Breast Cancer (Dove Med. Press)* 14, 247–258. doi:10.2147/BCTT.S367519

Xu, L., Deng, C., Pang, B., Zhang, X., Liu, W., Liao, G., et al. (2018). TIP: a web server for resolving tumor immunophenotype profiling. *Cancer Res.* 78, 6575–6580. doi:10.1158/0008-5472.CAN-18-0689

Yang, W., Soares, J., Greninger, P., Edelman, E. J., Lightfoot, H., Forbes, S., et al. (2013). Genomics of Drug Sensitivity in Cancer (GDSC): a resource for therapeutic biomarker discovery in cancer cells. *Nucleic Acids Res.* 41, D955–D961. doi:10.1093/nar/gks1111

Yang, Z., Hu, N., Wang, W., Hu, W., Zhou, S., Shi, J., et al. (2022). Loss of FBXW7 correlates with increased IDH1 expression in glioma and enhances IDH1-mutant cancer cell sensitivity to radiation. *Cancer Res.* 82, 497–509. doi:10.1158/0008-5472.CAN-21-0384

Yasuda, Y., Nagano, T., Jimbo, N., Kiriu, T., Suraya, R., Hazama, D., et al. (2022). Chloride intracellular channel 1 expression is associated with poor prognosis of lung adenocarcinoma. *Anticancer Res.* 42, 271–277. doi:10.21873/anticanres.15482

Ye, Y., Yin, M., Huang, B., Wang, Y., Li, X., and Lou, G. (2015). CLIC1 a novel biomarker of intraperitoneal metastasis in serous epithelial ovarian cancer. *Tumour Biol.* 36, 4175–4179. doi:10.1007/s13277-015-3052-8

Yu, S., Chen, L., Xu, H., Long, S., Jiang, J., Wei, W., et al. (2022). Application of nanomaterials in diagnosis and treatment of glioblastoma. *Front. Chem.* 10, 1063152. doi:10.3389/fchem.2022.1063152

Yu, W., Cui, R., Qu, H., Liu, C., Deng, H., and Zhang, Z. (2018). Expression and prognostic value of CLIC1 in epithelial ovarian cancer. *Exp. Ther. Med.* 15, 4943–4949. doi:10.3892/etm.2018.6000

Zhang, X., Lan, Y., Xu, J., Quan, F., Zhao, E., Deng, C., et al. (2019). CellMarker: a manually curated resource of cell markers in human and mouse. *Nucleic Acids Res.* 47, D721–d728. doi:10.1093/nar/gky900

Zhao, Z., Zhang, K. N., Wang, Q., Li, G., Zeng, F., Zhang, Y., et al. (2021). Chinese glioma genome Atlas (CGGA): a comprehensive resource with functional genomic data from Chinese glioma patients. *Genomics Proteomics Bioinforma.* 19, 1–12. doi:10.1016/j.gpb.2020.10.005

frontiers | Frontiers in Pharmacology

TYPE Original Research
PUBLISHED 20 November 2023
DOI 10.3389/fphar.2023.1276466

Check for updates

OPEN ACCESS

EDITED BY
Diana Matias,
Universidade de Lisboa, Portugal

REVIEWED BY
Rui Cruz Pereira,
Universidade do Porto, Portugal
Fanen Yuan,
University of Pittsburgh, United States

*CORRESPONDENCE
Zheng He,
friends1200@163.com

RECEIVED 12 August 2023
ACCEPTED 06 November 2023
PUBLISHED 20 November 2023

CITATION
Wang C and He Z (2023), Integrating bulk and single-cell RNA sequencing data reveals epithelial-mesenchymal transition molecular subtype and signature to predict prognosis, immunotherapy efficacy, and drug candidates in low-grade gliomas. *Front. Pharmacol.* 14:1276466. doi: 10.3389/fphar.2023.1276466

COPYRIGHT
© 2023 Wang and He. This is an open-access article distributed under the terms of the Creative Commons Attribution License (CC BY). The use, distribution or reproduction in other forums is permitted, provided the original author(s) and the copyright owner(s) are credited and that the original publication in this journal is cited, in accordance with accepted academic practice. No use, distribution or reproduction is permitted which does not comply with these terms.

Integrating bulk and single-cell RNA sequencing data reveals epithelial-mesenchymal transition molecular subtype and signature to predict prognosis, immunotherapy efficacy, and drug candidates in low-grade gliomas

Chengcheng Wang[1] and Zheng He[2]*

[1]Department of Pharmacy, Qilu Hospital (Qingdao), Cheeloo College of Medicine, Shandong University, Qingdao, Shandong, China, [2]Department of Neurosurgery, Qilu Hospital (Qingdao), Cheeloo College of Medicine, Shandong University, Qingdao, Shandong, China

Objective: Epithelial-mesenchymal transition (EMT) is a tightly regulated and dynamic process occurring in both embryonic development and tumor progression. Our study aimed to comprehensively explore the molecular subtypes, immune landscape, and prognostic signature based on EMT-related genes in low-grade gliomas (LGG) in order to facilitate treatment decision-making and drug discovery.

Methods: We curated EMT-related genes and performed molecular subtyping with consensus clustering algorithm to determine EMT expression patterns in LGG. The infiltration level of diverse immune cell subsets was evaluated by implementing the single-sample gene set enrichment analysis (ssGSEA) and ESTIMATE algorithms. The distinctions in clinical characteristics, mutation landscape, and immune tumor microenvironment (TME) among the subtypes were subjected to further investigation. Gene Set Variation Analysis (GSVA) was performed to explore the biological pathways that were involved in subtypes. The chemo drug sensitivity and immunotherapy of subtypes were estimated through GDSC database and NTP algorithm. To detect EMT subtype-related prognostic gene modules, the analysis of weighted gene co-expression network (WGCNA) was performed. The LASSO algorithm was utilized to construct a prognostic risk model, and its efficacy was verified through an independent CGGA dataset. Finally, the expression of the hub genes from the prognostic model was evaluated through the single-cell dataset and *in-vitro* experiment.

Results: The TCGA-LGG dataset revealed the creation of two molecular subtypes that presented different prognoses, clinical implications, TME, mutation landscapes, chemotherapy, and immunotherapy. A three-gene signature (SLC39A1, CTSA and CLIC1) based on EMT expression pattern were established through WGCNA analysis. Low-risk patients showed a positive outlook, increased immune cell presence, and higher expression of immune checkpoint proteins. In addition, several promising drugs, including birinapant, fluvastatin, clofarabine, dasatinib, tanespimycin, TAK–733, GDC–0152, AZD8330, trametinib and ingenol-

mebutate had great potential to the treatment of high risk patients. Finally, CTSA and CLIC1 were highly expressed in monocyte cell through single-cell RNA sequencing analysis.

Conclusion: Our research revealed non-negligible role of EMT in the TME diversity and complexity of LGG. A prognostic signature may contribute to the personalized treatment and prognostic determination.

KEYWORDS

low-grade gliomas, Epithelial-mesenchymal transition (EMT), molecular subtypes, tumor microenvironment, immunotherpapy, signature, single cell RNA analysis

1 Introduction

The efficacy of cancer chemotherapy and immunotherapy is often impeded by inter-patient and intra-tumor heterogeneity, as well as multifactorial drug resistance. Low-grade gliomas (LGGs), being a form of malignant brain tumor, are also confronted with the challenge of tumor heterogeneity and resistance to treatment (Weller et al., 2015). Even after undergoing standard surgical resection followed by radiotherapy and chemotherapy, individuals diagnosed with low-grade gliomas continue to have a bleak prognosis, with an average survival rate ranging from 2 to 10 years (Golub et al., 2019). Despite extensive efforts to improve clinical outcomes, more than half of LGG cases progress and evolve into therapy-resistant high-grade aggressive glioma over time (Claus et al., 2015). One of the primary objectives of precision medicine is to precisely identify patients who are likely to benefit from personalized treatment and to prescribe treatments that are tailored to the unique characteristics of their tumors, with the aim of achieving optimal therapeutic outcomes. Hence, in the realm of precision medicine, it is imperative to establish a more precise categorization of tumors to eradicate the heterogeneity and resistance to treatment associated with LGGs.

The process of epithelial-mesenchymal transition (EMT) is an essential differentiation program that is necessary for the development of tissues during embryogenesis. During this process, cells lose their epithelial characteristics and acquire mesenchymal migration properties (Yang et al., 2020). Aberrant activation of the EMT process is frequently observed in tumor proliferation, leading to the development of resistance towards conventional therapeutic interventions (Lambert et al., 2017; Shibue and Weinberg, 2017). EMT has the capability to enhance the potential of tumor cells for invasion and metastasis by facilitating their migration, disturbing cell-cell connections, disintegrating the basement membrane, and restructuring the extracellular matrix (ECM) (Miyoshi et al., 2004). Moreover, the process of EMT is linked with a higher percentage of cancer stem cells, reduced immune response against tumors and the development of resistance towards treatment (Akalay et al., 2013; Rhim et al., 2014), the study of therapeutic resistance from the perspective of EMT is one of cancer research focus. Thus, the presence of EMT, which is a hallmark of cancer, has been shown to be intimately linked with tumor invasion, metastasis, and the acquisition of chemotherapy resistance, all of which are critical biological processes in cancer development (van Staalduinen et al., 2018; Loret et al., 2019). Despite the existence of variations among tumor subtypes, the EMT process in LGG could potentially hold significant prognostic and molecular typing value. As a result of the highly hostile and intrusive characteristics of gliomas, it has been progressively acknowledged that the occurrence of EMT in gliomas may hold significant significance in the progression of glioma and the restructuring of the glioma microenvironment (Lu et al., 2012). Given the emergence of innovative immunotherapy techniques that offer groundbreaking cancer treatment alternatives, it is crucial to ascertain the immune profile of distinct EMT expression patterns, and their responsiveness to immunotherapy (Yamaguchi, 2016). In our study, while we have primarily relied on computational analyses of existing datasets, we have also performed experimental validation of the identified key genes. This approach underscores the critical role of EMT-related genes in the context of low-grade gliomas (LGG) and further highlights their significance in future research. By combining computational insights with experimental evidence, we aim to provide a more comprehensive understanding of the role of EMT in the expression, prognosis, immune tumor microenvironment (TME), clinical implications, and personalized treatment strategies for LGG.

2 Materials and methods

2.1 Data acquisition

Transcriptome data, mutation data and clinicopathologic characteristics of LGG samples were retrieved from the Cancer Genome Atlas (TCGA; https://www. cancer. gov/tcga/) through the Genomic Data Commons data portal (GDC; https://portal.gdc.cancer.gov/). In addition, the aforementioned information were obtained from two cohorts (mRNAseq_693, Illumina HiSeq Platform; mRNAseq_325, Illumina HiSeq (2000) and (2,500) platforms) in Chinese Glioma Genome Atlas (CGGA; http://www.cgga.org.cn), and serve as an external dataset. "SVA" (Leek et al., 2012) package was then used to merged the two cohorts after removing the batch effects ("ComBat" algorithm). After converting the raw read count, the values were expressed as transcripts per kilobase million (TPM). The Molecular signatures database (MSigDB; http://www.broadinstitute.org/msigdb) (Liberzon et al., 2015) provided a collection of 200 genes related to EMT, obtained from the gene set named "HALLMARK_EPITHELIAL_MESENCHYMAL_TRANSITION". Figure 1 showed the graphical abstract and analysis flow chart of present study.

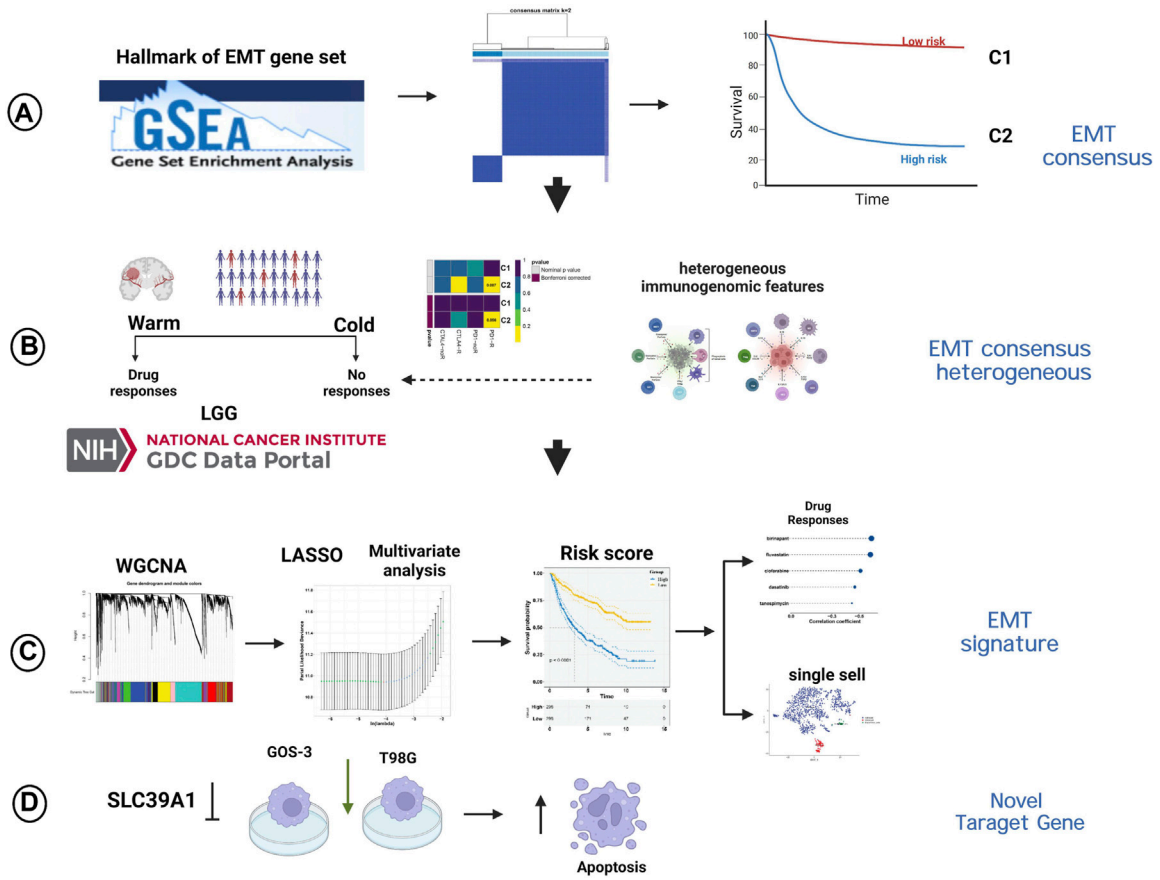

FIGURE 1
The graphical abstract and analysis flow chart of present study. **(A)** Construction of EMT-related consensus clusters. **(B)** Evaluation of immunotherapy of EMT-related consensus clusters. **(C)** Construction of EMT-related signature. **(D)** Experimental validation of SLC39A1.

2.2 Unsupervised clustering analysis

To perform an unsupervised cluster analysis on mRNA expression profiles of genes associated with EMT, the "ConsensusClusterPlus" R package was created (Wilkerson and Hayes, 2010). The optimal number of clusters was determined using the cumulative distribution function (CDF) and consensus matrix through resampling analysis to achieve the best performance. To assess the disparity in survival among clusters, the Kaplan-Meier (KM) analysis was employed. The results displayed the top 20 mutated genes in each cluster after visualizing single-nucleotide polymorphisms (SNP) variations using the R package "maftools" (Mayakonda et al., 2018). The GISTIC2.0 tool from Genome Data Analysis Center (GDAC) Firehose (https://gdac.broadinstitute.org) was used to analyze the copy number alterations (CNA) data among subtypes.

2.3 Landscape of immune TME

To calculate the ratio of immune cells in LGG samples, the Estimation of Stromal and Immune cells in Malignant Tumours using Expression (ESTIMATE) data method was utilized to compute the stromal and immune scores (Yoshihara et al., 2013). The estimation of tumor purity was done by combining stromal and immune scores. The violin plot displayed variations in immune score, stromal score, and tumor purity across various subtypes.

The single-sample gene set enrichment analysis (ssGSEA) algorithm was utilized to measure the proportion of immune cell infiltration in the immune TME of LGG samples through the computation of enrichment scores. To compute the abundance of 28 tumor infiltrating immune cells (TIICs), a sum of 782 marker genes was collected from Bindea et al. (Bindea et al., 2013) and Broad Institute (http://software.broadinstitute.org/gsea/msigdb/index.jsp). Boxplots were used to present the results of ssGSEA analysis, which compared the level and function of immune infiltration among different subtypes using the gene set variation analysis (GSVA) software "GSVA" R package.

2.4 GSVA and functional annotation

To evaluate dissimilarities in biological processes among various clusters, the R software package "GSVA" was utilized for conducting GSVA analysis. Based on transcriptome data, GSVA is an unsupervised and nonparametric gene enrichment method that estimates alterations in the activity of biological processes and pathways in samples (Hänzelmann et al., 2013). To run GSVA

analysis, the gene set of "C2. cp.kegg.v7.1″was downloaded from MSigDB database. The "clusterProfiler" R software package was utilized to conduct functional annotation of genes related to EMT. Significantly enriched pathways were identified through screening for those with an adjusted p-value < 0.05 and false discovery rate (FDR) < 0.05.

2.5 Therapy response prediction of subtype

The tumor immune dysfunction and exclusion (TIDE) algorithm (Jiang et al., 2018) was utilized to approximate the efficacy of immunotherapy based on tumor immune dysfunction and exclusion. According to the Genomics of Drug Sensitivity in Cancer (GDSC) database (https://www.cancerrxgene.org/) (Yang et al., 2012), we predict chemotherapy response of each LGG sample. After performing simple processing of data (such as elimination of low-variation genes and summarize duplicated gene expression data into averages), we estimated the sensitivity of eight chemotherapeutic agents (cisplatin, erlotinib, methotrexate, vincristine, carmustine, temozolomide (TMZ), rapamycin, and doxorubicin) currently under study or widely applied in gliomas by SubMap analysis (Gene Pattern) of GDSC data (Hoshida et al., 2007). The ridge regression was performed to estimate the half-maximal inhibitory concentration (IC50) for LGG by "pRRophetic" R software package (Geeleher et al., 2014a), and the quantitative prediction accuracy was verified by 10-fold cross validation based on the GDSC training set (Geeleher et al., 2014b).

2.6 Weighted correlation network analysis (WGCNA) to identify hub genes from subtypes

For the purpose of identifying subtype associated genes, we adopted WGCNA algorithm through the "WGCNA" R package (Version: 1.71) (Langfelder et al., 2009). At first, genes that exhibited a variance value exceeding 25% were selected for the construction of the coexpression network (Yang and Xu, 2021; Zhou et al., 2021; Feng et al., 2022). Subsequently, the outlier samples were excluded through the "goodSampleGenes" function, and the soft-thresholding value $\beta = 5$ (scale free = 0.85) was applied to ensure a scale-free network. Then, a gene clustering tree was generated based on the computed adjacency among genes, followed by the categorization of genes into distinct modules comprising no less than 100 genes exhibiting similar characteristics within each module. The modules that exhibited most correlation with subtypes were selected to the downstream analysis, such as KEGG analysis. Moreover, the hub genes were screened based on the cutoff gene significance (GS) > 0.6 and module membership (MM) > 0.8. Pathway enrichment analysis on the modules was performed via the "clusterProfiler" R package (Wu et al., 2021).

2.7 Development of EMT-related signature

The "glmnet" package was employed to conduct a LASSO regression analysis on genes associated with prognostic EMT subtyping to evaluate their effect on prognosis. The analysis was subjected to ten-fold cross-validation, and the genes were chosen based on the point with the lowest error rate. Patients were categorized into low or high EMT score subgroups using the median score, which was calculated by merging gene expression and coefficients to compute the EMT risk score. KM survival curves were generated by performing survival analysis with the aid of the "survival" and "survminer" packages. To generate receiver operating characteristic (ROC) curves the "timeROC" package was employed. Prognostic variables were subjected to uni- and multivariate-cox regression analyses. A nomogram was constructed using the "rms" package to estimate survival probability, and calibration curves were used to evaluate the accuracy of the predictions.

2.8 Drug discovery of EMT-related signature

The response of human cancer cell lines to small molecule compounds was estimated using drug sensitivity profiles obtained from either the Cancer Therapeutics Response Portal (CTRP) (Basu et al., 2013) or the PRISM project (Corsello et al., 2020).

2.9 Single cell RNA-sequencing (scRNA-seq) revealed the expression level of genes

The GSE202096 dataset provided scRNA-seq data for one LGG samples (GSM6094425) (Chen et al., 2022). After conducting quality control, cells that had more than 20% mitochondrial UMI counts were eliminated using the "Seurat" package (Cao et al., 2022). The selection process involved choosing the top 1,500 genes with high variability, followed by clustering cell populations via the FindClusters function and then mapping them into t-distributed stochastic neighbor embedding (t-SNE). Using the FindAllMarkers function, the markers for each cell cluster were determined. Then, the CellMarker database was utilized to annotate cells based on their cell markers (Hu et al., 2022).

2.10 Cell culture and transfection

The cultivation of HMC3, GOS-3, T98G, and LN-18 cells (ATCC) was carried out in DMEM supplemented with 10% fetal bovine serum (Sigma Aldrich) under an atmosphere of 5% CO2 at 37°C. After cloning siRNA targeting SLC39A1 into lentiviral vectors, the vectors were transfected into GOS-3 and T98G cells for 3 days and then exposed to 4 μg/mL puromycin for 1 week.

2.11 Real-time quantitative PCR (RT-qPCR)

Total RNA was extracted using TRIzol (Beyotime) and cDNA was synthesized with the PrimeScript RT reagent kit after gDNA Eraser (Takara) treatment. SYBR Green II Mixture (TaKaRa) was used for RT-qPCR, and GAPDH was used as an internal reference to calculate the expression using the $2^{-\Delta\Delta CT}$ method.

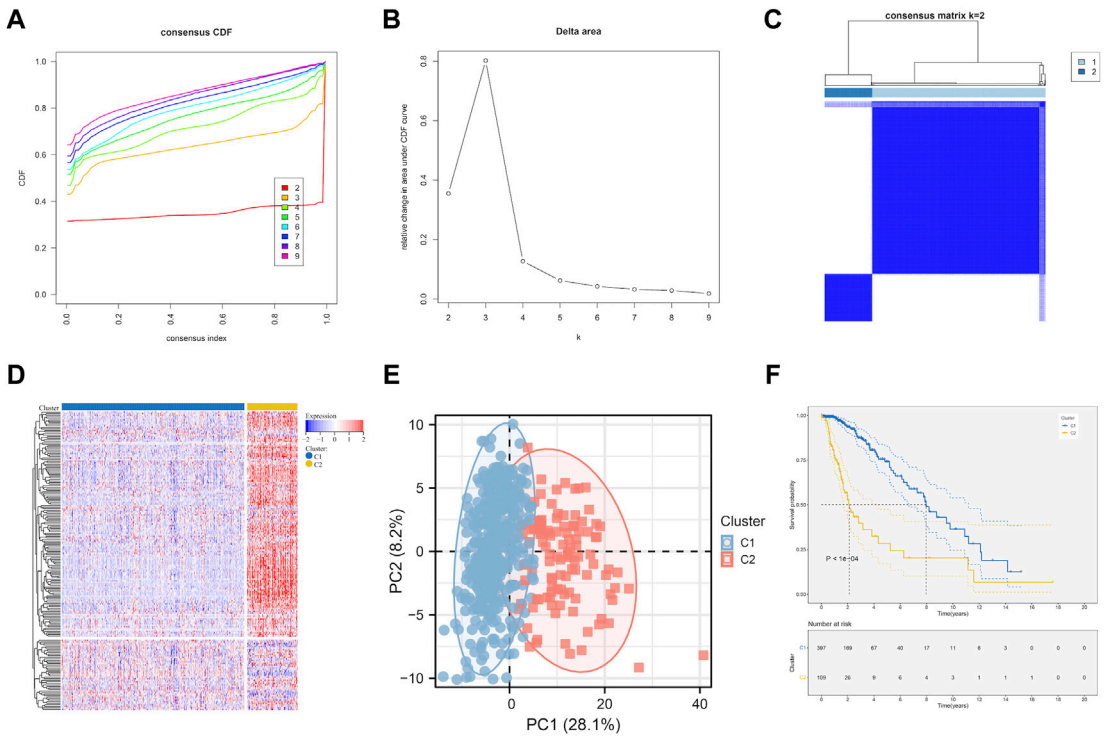

FIGURE 2
EMT-related genes could distinguish LGG in TCGA with different clinical and molecular features. **(A)** Relative change in area under CDF curve for k = 2 to k = 9. **(B)** Delta curve analysis from k = 2 to k = 9. **(C)** Consensus clustering matrix heatmap plots of 506 samples from TCGA datasets for k = 2. **(D)** Expression of EMT-related genes in molecular subtypes. **(E)** PCA analysis of the EMT-related genes expression when k = 2. **(F)** Kaplan-Meier analysis of patients between two subtypes. CDF, cumulative distribution function; PCA, principal components analysis.

2.12 Flow cytometry

Cell apoptosis was detected through flow cytometry and the Cell Apoptosis Detection Kit (KTA0002; Abbkine) was utilized. To summarize, a group of cells was exposed to 5 μL of Annexin V-AbFluor™ 488 binding and 2 μL of PI for 15 min at room temperature while being shielded from light. After adding 400 μL of 1 x Annexin V buffer, the level of apoptosis was assessed using a Beckman Flow cytometer.

2.13 Statistical analysis

The R language (R-project.org) platform and software package from the Bioconductor project (www.bioconductor.org) (R Core Team, Version 4.0.2) were used for statistical analysis and visualization of results in the current study. To compare the two groups and more groups, the Wilcoxon and Kruskal–Wallis tests were utilized, respectively (Hazra and Gogtay, 2016). To detect the differentially expressed genes (DEGs) between the two subtypes, the one-way ANOVA and Tukey's test were conducted with a q-value of less than 0.05 and an absolute value of log2FC greater than 2. The KM curve, analyzed by log-rank test, exhibited the variations in operating systems among different groups. Bilateral p values were used, with a statistically significant difference defined as $p < 0.05$.

3 Results

3.1 Clinicopathological characteristics of two LGG molecular subtypes based on EMT related genes

Based on the prognostic EMT gene expression profile, LGG samples was divided into two molecular subtypes by unsupervised clustering analysis (Figures 2A–C). The EMT gene expression were presented a significant divergence between two subtypes (Figure 2D). Figure 2E showed that the principal components analysis (PCA) distribution patterns were mostly in agreement with the two subtypes designations. Figure 2F suggested the overall prognosis of C2 is worse than that of C1 ($p < 0.0001$). Moreover, we further explore the relationship between subtypes and clinical traits.

As Figures 3A–G showed, the patients survival status (Figure 3A), age (Figure 3B), grade (Figure 3D), IDH status (Figure 3E), 1p19q status (Figure 3F) and methylation status (Figure 3G) were showed a significant difference ($p < 0.05$) between C1 and C2, while no difference was observed in gender (Figure 3C). Subtype C2 corresponding to more deaths, elderly patients, higher grade, 1p19q non-codel, IDH wild type, and unmethylated cases.

We assessed the function of each subtype through GSVA analysis (Supplementary Figure S1) to delve deeper into the potential biological process of the two clusters. Results suggested

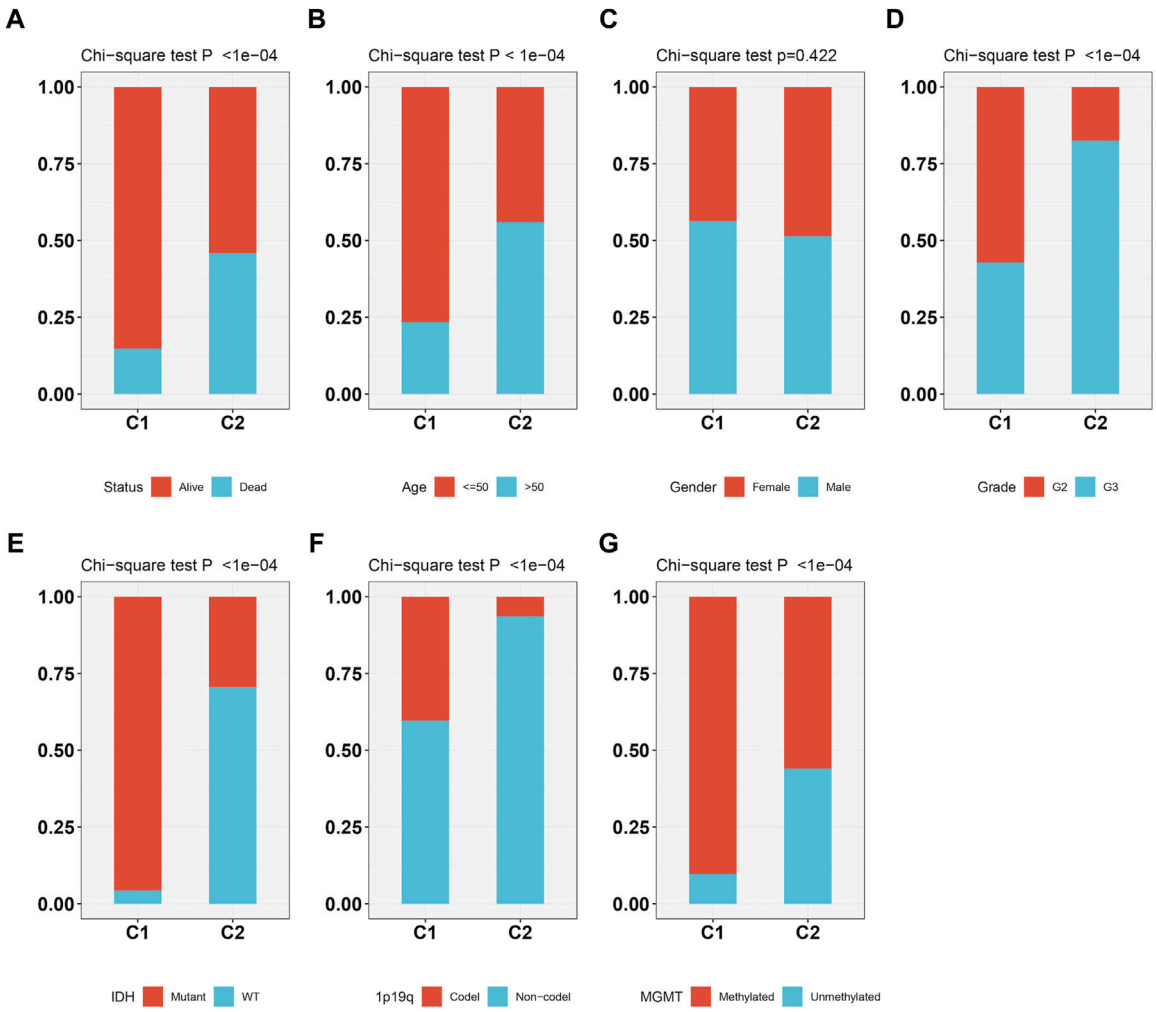

FIGURE 3
The relationship between two molecular subtypes, survival status **(A)**, age **(B)**, gender **(C)**, grade **(D)**, IDH mutation status **(E)**, 1p19q status **(F)** and methylation status **(G)**.

that C1 mainly enriched metabolism-related signaling pathways, such as butanoate metabolism and propanoate metabolism pathways. The primary routes of C2 that were enriched consist of cell adhesion molecules (CAMs), interaction with ECM receptors, the p53 signaling pathway, interaction between cytokines and cytokine receptors, focal adhesion, the JAK-stat signaling pathway, and apoptosis. These pathways were significantly correlated with tumor cell genesis, proliferation, invasion and migration. Furthermore, the GSVA outcomes indicated that C2 was linked to pathways related to DNA damage repair (such as Nucleotide excision repair, DNA replication, and Mismatch_ repair) as well as immune functions (including Natural killer cell mediated cytotoxicity, Toll like receptor signaling pathway, and Antigen processing and presentation). In conclusion, C2 showed more malignant biological behaviors and enrichment signaling pathways than C1.In addition, SNP analysis of the two clusters in TCGA uncovered that C1 had a higher mutation proportion than C2 of IDH1, TP53, ATRX, CIC, FUBP1, NOTCH1 (Rotin et al., 2015) and IDH2 (Supplementary Figure S1A). However, EGFR, PTEN and NF1 (Verhaak et al., 2010; Marques et al., 2019; Koptyra et al., 2023), the mutations that were common in glioblastoma (GBM), were more frequent in C2 than C1 (Supplementary Figure S2B). Therefore, EMT related genes are important references for LGG molecular subtype. Our cluster-specific CNAs analysis presented chromosome deletions and amplifications, for example, deletion of 9p21.3 were significantly enriched in the C2. The 9p21.3 deletions is associated with the poor survival outcome in LGG (Xia et al., 2021). In addition, gene duplication/amplification at 7p11.2 activates EGFR expression through the formation of new topological associating domain (TAD) and the emergence of new enhancer-promoter interactions between LINC01446 and EGFR, and EGFR amplification and/or mutations are directly associated with poor prognosis of gliomas (Yang et al., 2022).

3.2 Disparity in immune tumor microenvironment between subtypes

We delved deeper into the dissimilarities in the immune tumor microenvironment between the two LGG EMT

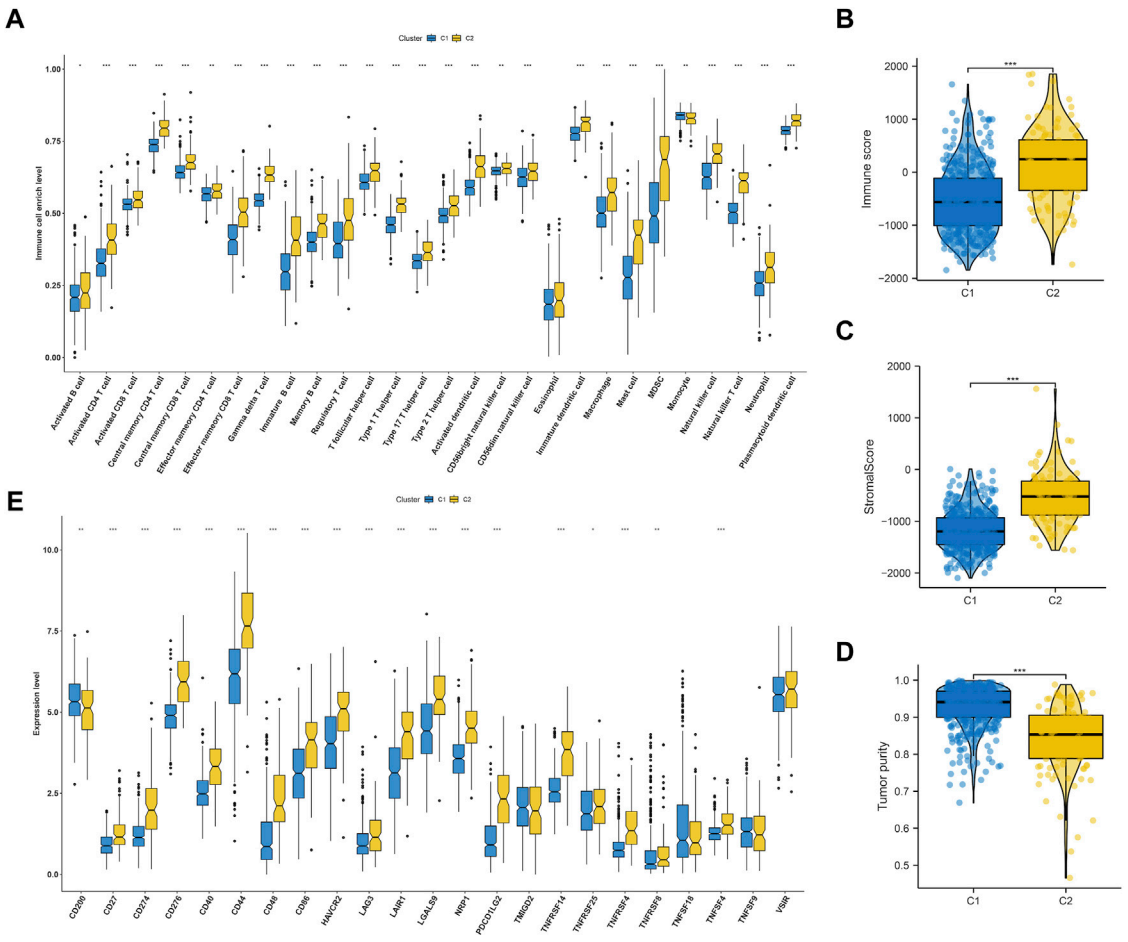

FIGURE 4
Immune landscape of subtypes in LGG. **(A)** Comparisons of 28 immune cells infiltration level in two molecular subtypes. Evaluation of the immune score **(B)**, stromal score **(C)** and tumor purity **(D)** in two molecular subtypes. **(E)** Comparisons of key immune checkpoints expression level in two molecular subtypes.

subtypes, given their notable clinicopathologic distinctions. According to Figure 4A, C2 had a higher degree of immune cell infiltration than C1, which included various types of immune cells such as Activated $CD8^+$ T cells, effector memory $CD4^+$ T cells, Regulatory T cells, CD56bright natural Killer cells, Type-1 T-helper 1 cells, Central memory $CD4^+$ T cells, Activated Dendritic cells, Activated $CD4^+$ T cells, CD56dim natural killer cells, myeloid-derived suppressor cells, Immature Dendritic cells, Central memory $CD8^+$ T cells, Effector memory $CD8^+$ T cells, immature B cells, macrophages, mast cells, memory B cells, natural killer cells, natural killer T cells, neutrophils, plasmacytoid dendritic cells, follicular helper T cells, Gamma delta T cells, Type-17 T helper cells, Type-2 T helper cells, activated B cells, eosinophils and monocytes. The findings from analyzing various cluster immune TME in TCGA and CGGA datasets indicated a strong correlation between the EMT molecular subtype and immune TME. It was noticed that C2 had higher stromal and immune scores compared to C1 (both $p < 0.0001$) as shown in Figures 4B,C. On the other hand, the tumor purity in C2 was lower than that in C1 ($p < 0.0001$) as depicted in Figure 4D. Figure 4E showed that C2 had significantly higher expression levels of most checkpoints compared to C1.

3.3 Sensitivity prediction of different clusters to chemotherapy and immunotherapy

Immunotherapy has shown a potential application prospect in the treatment of glioma. We evaluated the response of two clusters to immunotherapy through TIDE analysis. The findings revealed that patients belonging to C1 exhibit a higher number of responders in comparison to C2 ($p < 0.05$) (Figure 5A), and individuals with a lower TIDE score are more likely to experience benefits from immunotherapy. The TIDE, Dysfunction, and Exclusion scores in the C1 group were lower, which implies that they could benefit more from immunotherapy (Figures 5B–D). Immune checkpoint blockade (ICB) is one of the most promising therapeutic approaches to change the current pessimistic situation in the treatment of glioma. Therefore, SubMap module analysis was used to compare the expression profile of LGG cluster with other published ICB-therapy datasets. As showed in Figure 5E, Subtype

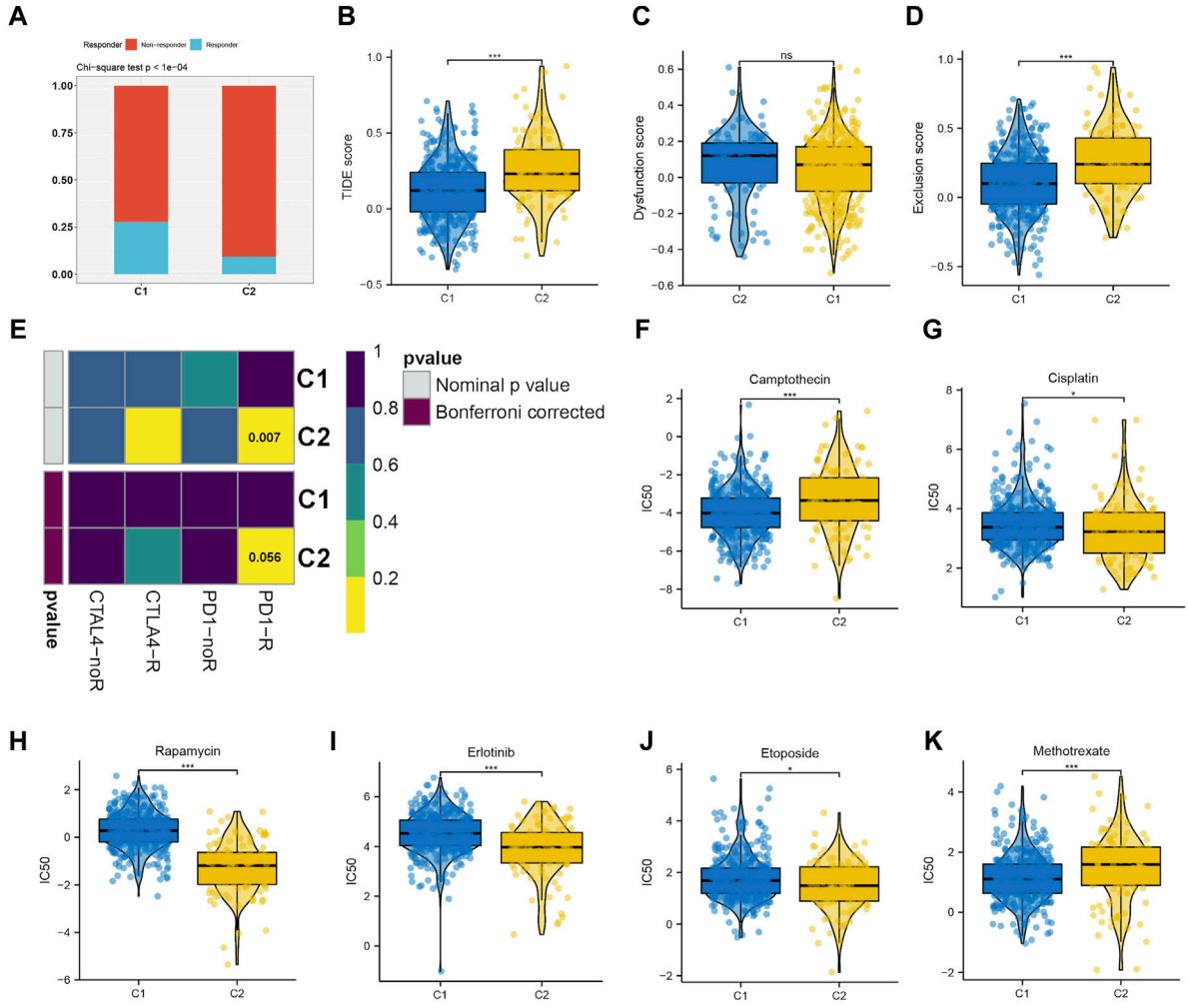

FIGURE 5
(A–D) The immune response, TIDE score, dysfunction score and exclusion score of the C1 and C2 subtype. **(E)** Submap analysis revealing that C2 would be more sensitive to immunotherapy, especially checkpoints PD-1 immunotherapy (Bonferroni-corrected $p < 0.05$). Drug sensitivity evaluation of the Camptothecin **(F)**, Cisplatin **(G)**, Rapamycin **(H)**, Erlotinib **(I)**, Etoposide **(J)**, Methotrexate **(K)** in C1 and C2 subtypes.

C2 is similar to the melanoma patients who reacted positively to anti-PD-1 therapy.

We then evaluated the different responses of two clusters to drug chemotherapy. The regimen of combined treatment for gliomas includes maximum safe surgical resection and postoperative chemotherapy with radiotherapy. Glioma can be treated with chemotherapy, which is considered a fundamental therapy. The GDSC database was utilized to predict the efficacy of 8 frequently used drugs in LGG chemotherapy, including cisplatin, erlotinib, methotrexate, camptothecin, etoposide, rapamycin, and doxorubicin. According to the findings, camptothecin (Figure 5F) and methotrexate (Figure 5K) were found to be more effective on C1, whereas cisplatin (Figure 5G), rapamycin (Figure 5H), erlotinib (Figure 5I), and etoposide (Figure 5J) were more effective on C2.

Genomic instability is a hallmark of cancer, particularly LGG, which facilitates its growth and the ability to withstand treatments (Dionellis et al., 2021). In our result, we found that Aneuploidy score, fraction altered, number of segments, tumor mutation burden (TMB) were elevated in C2, while Cancer Testicular Antigens (CTA) score were lower in C2, which consistent with previously reports (Nie et al., 2020) (Figure 6).

3.4 Identification of EMT-related genes through WGCNA analysis

We utilized WGCNA to build correlation networks in order to identify genes associated with EMT. The optimal soft threshold was set to 5, based on a chosen R2 of 0.90 (Figures 7A,B). Eleven modules were identified based on their connectivity in Figure 7C, each containing at least 100 genes. The "module-trait" relationship heatmap revealed that brown module have the highest correlation associated with molecular subtypes (R = 0.70) (Figure 7D). In addition, six hub genes were identified, namely, SLC39A1, CTSA, TMSB4X, CAST, S100A11, and Chloride Intracellular Channel 1 (CLIC1), based on their GS being greater than 0.6 and their MM being greater than 0.8, as shown in Figure 7E. Further function enrichment of the brown module indicated that

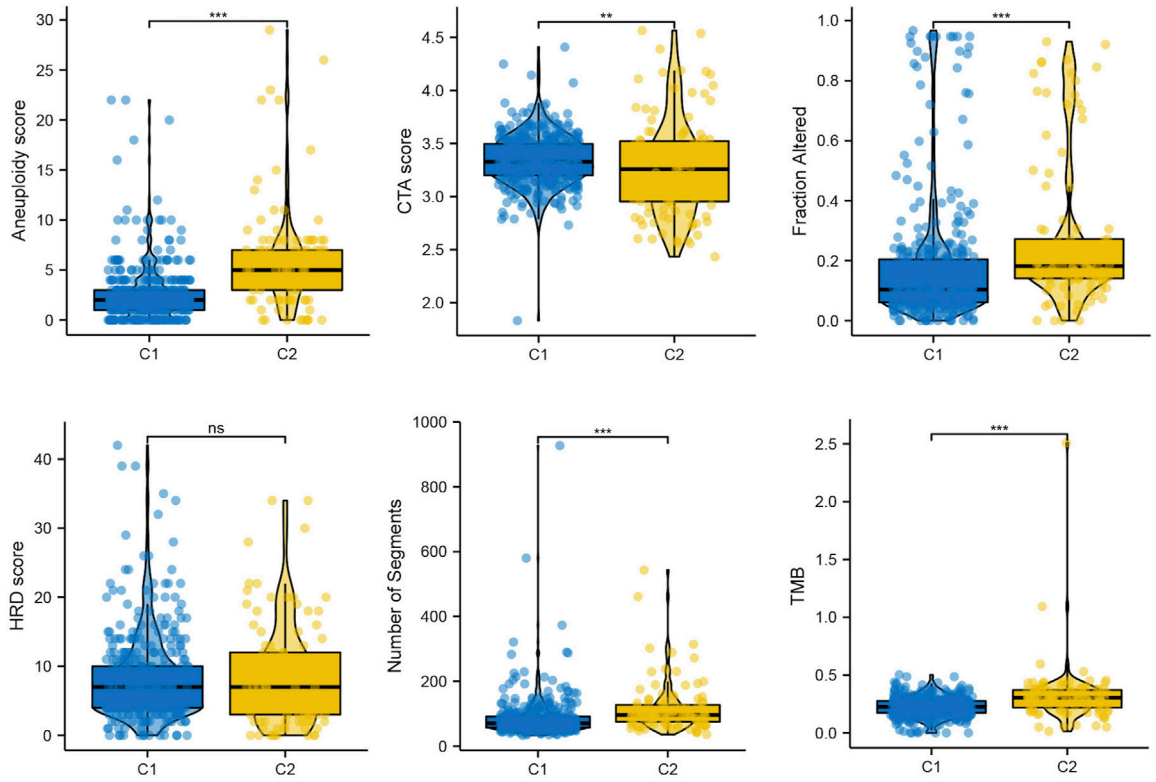

FIGURE 6
The mutation profile in subtypes, including Aneuploidy score, CTA score, Fraction altered, HRD score, Number of segments, and TMB.

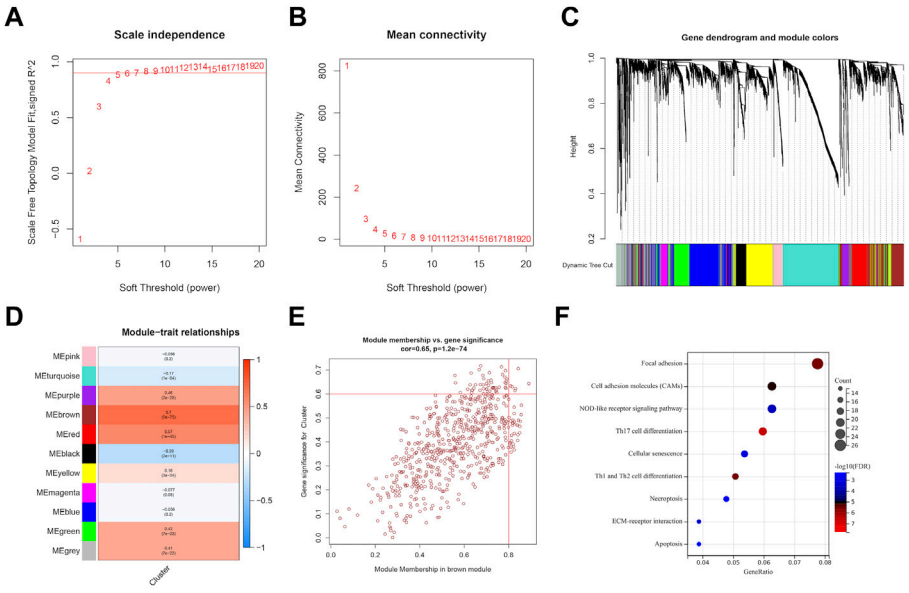

FIGURE 7
Identification of EMT-related genes through WGCNA analysis. **(A, B)** soft threshold determination through scale-free network analysis. **(C)** Clustering dendrograms were used to classify genes with similar expression patterns in LGG into co-expression modules. **(D)** module-traits heatmap showed the correlation between Cluster and gene modules. **(E)** hub genes were characterized by brown module with module membership >0.8 and gene significance >0.6. **(F)** Pathway enrichment analysis.

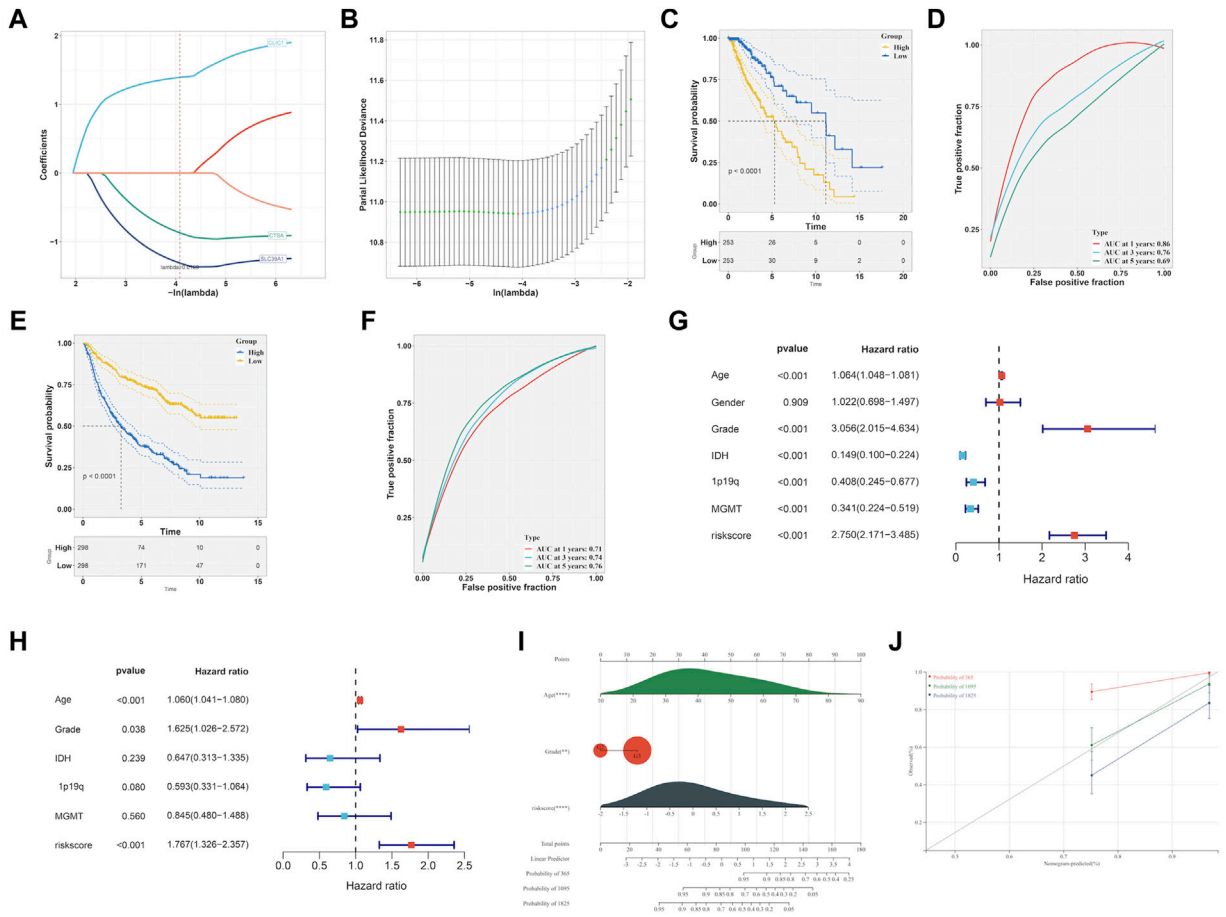

FIGURE 8
Development of EMT-related signature. **(A, B)** LASSO analysis to determine the EMT-related signature. **(C)** K-M curve survival analysis between high- and low-risk group in TCGA-LGG dataset. **(D)** ROC curve analysis of the EMT-related signature in TCGA-LGG dataset. **(E)** K-M curve survival analysis between high- and low-risk group in CGGA dataset. **(F)** ROC curve analysis of the of EMT-related signature in CGGA dataset. Determination of the independence of Univariate cox regression **(G)** and multivariate cox regression **(H)** analysis of the EMT-related signature. **(I)** Construction of nomogram on the basis of independent prognostic factors. **(J)** Calibration plot for the nomogram in 1-year, 3-year and 5-year OS.

genes may involve in focal adhesion, Th17 cell differentiation, necroptosis, etc (Figure 7F).

To identify prognostic genes related to EMT from six hub genes, we performed lasso analysis and found three genes, namely, CLIC1, CTSA, and SLC39A1, based on the optimal lambda value (Figures 8A,B). The CGGA dataset was used as an external validation cohort to guarantee its reliability. The score for the risk model was computed utilizing the risk equation Risk score = (SLC39A1exp * −1.559) + (CTSAexp* −1.139) + (CLIC1exp * 1.474). After analyzing the TCGA and CGGA datasets, patients were divided into two groups: high-risk and low-risk, with the median score serving as the differentiating factor for each group. Figure 8C and Figure 8E demonstrated that patients who had a high-risk score in both TCGA and CGGA datasets had a poor survival outcome, whereas those with a low risk score had a favorable survival. Furthermore, the precision of the risk model was assessed using ROC curve analysis, yielding a score of 0.86, 0.76, and 0.69 for 1-, 3-, and 5-year periods in the TCGA and CGGA datasets, as shown in Figure 8D and 0.71, 0.74, and 0.76 in Figure 8F, respectively. The independent prognostic factors were identified through the results of both univariate and multivariate Cox regression analyses, demonstrating that the risk score can function in this manner, as depicted in Figures 8G,H. Then, the independent factors including risk score, grade were including to construct nomogram to predict patients overall survival (OS) (Figure 8I). According to Figure 8J, the calibration curves indicated that the estimated OS values were consistent with the real values, particularly for the 3-year OS.

3.5 Immune infiltration landscape and drug discovery of EMT-related model

Though the immune cell infiltration analysis, we evaluated the divergence of immune cells between risk groups. The result of Figure 9A revealed that most of immune cells infiltration level in high risk group were elevated compared to low risk group, such as Activated $CD8^+$ T cells ($CD8^+$ Ta), effector memory $CD4^+$ T cells, Regulatory T cells, CD56bright natural Killer cells, Type-1 T-helper 1 cells, Central memory $CD4^+$ T cells, Activated

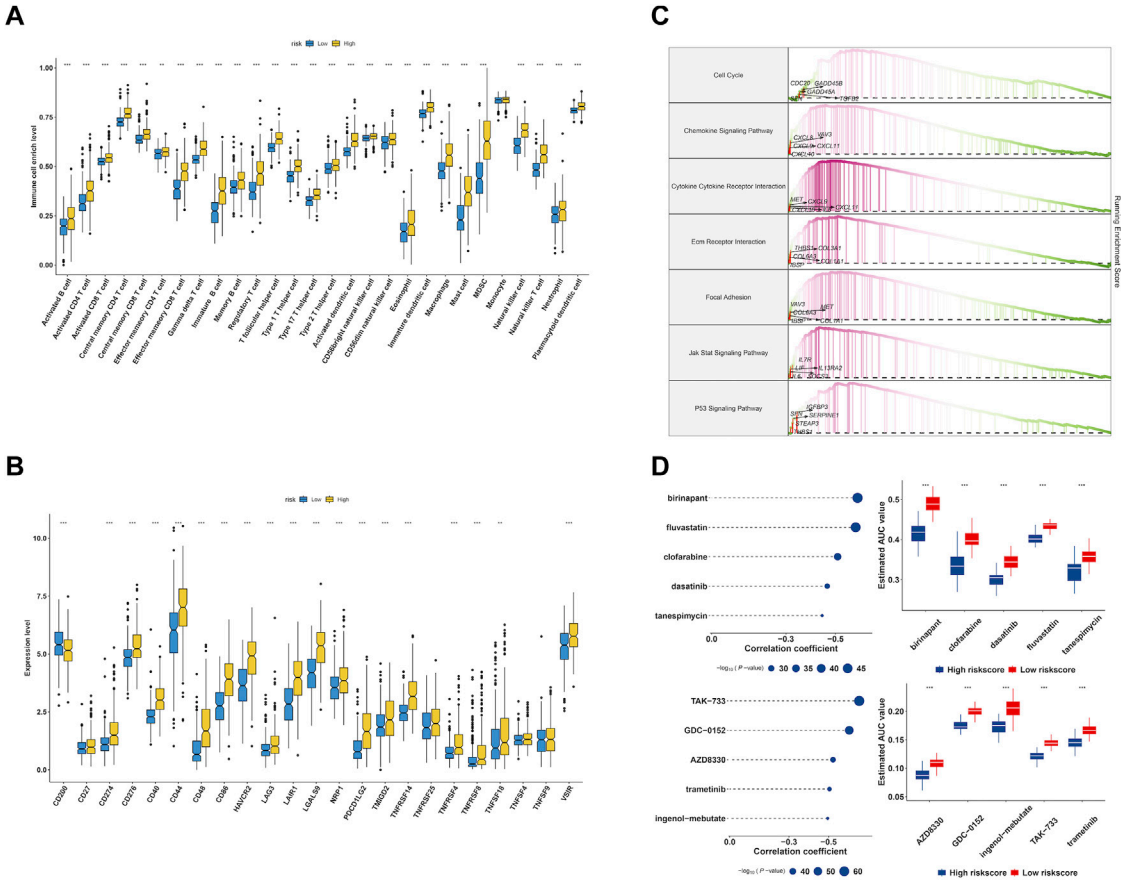

FIGURE 9
Characterization of immune infiltration and drug discovery of EMT-related signature. **(A)** Evaluation of 28 immune cells infiltration in high- and low-risk group. **(B)** The expression level of immune checkpoints in high- and low-risk group. **(C)** GSEA enrichment analysis of EMT signature. **(D)** Identification of molecular compounds in the high-risk groups based on CTRP and PRISM drug database.

Dendritic cells, Activated CD4$^+$ T cells, CD56dim natural killer cells, myeloid-derived suppressor cells, Immature Dendritic cells, Central memory CD8$^+$ T cells, Effector memory CD8$^+$ T cells, immature B cells, macrophages, mast cells, memory B cells, natural killer cells, natural killer T cells, neutrophils, plasmacytoid dendritic cells, follicular helper T cells, Gamma delta T cells, Type-17 T helper cells, Type-2 T helper cells, activated B cells, eosinophils and monocytes. We further checked the expression of immune checkpoint between groups and found that the genes showed a high expression level in high risk group (Figure 9B). Accumulative evidence have demonstrated that anti-tumor effects of a high T cell infiltration are counteracted by the immunosuppressive pathways that are triggered by the over-expression of immune checkpoint proteins (Vuong et al., 2019; Dionellis et al., 2021). The GSEA analysis was performed between groups, and found cell cycle, chemokine signaling pathway, cytokine-cytokine receptor interaction, ECM receptor interaction, p53 signaling pathway were significantly enriched in high risk group (Figure 9C).

To explore potential molecular drugs to the treatment of LGG in high risk group, we integrated CTRP and PRISM drug database. As showed in Figure 9D, the top panel of CTRP result revealed five drugs including birinapant, fluvastatin, clofarabine, dasatinib and tanespimycin may have the potential value to the treatment of high risk LGG patients, and the bottom panel of PRISM results indicated five drugs including TAK−733, GDC−0152, AZD8330, trametinib and ingenol−mebutate were identified.

3.6 Evaluation of gene expression level through single cell analysis

In order to estimate the gene expression level of hub genes, we retrieved LGG single cell sample from GSE202096 dataset (Figures 10A–E). Following data filtering and standardization, 1,500 genes exhibiting the most variance were selected for cell classification (Figures 10F,G). Dimensionality reduction of the expression levels of 1,500 genes was done by PCA analysis, resulting in PC1 to PC20. T-SNE was then applied to the PC1-20 to classify all cells into 9 clusters (Figure 10H). Afterwards, we annotated the cells in each cluster. The main cell types identified were astrocyte, monocyte, and endothelial cells (Figure 10I). The expression level of hub genes (CTSA, CLIC1) in cell clusters were showed in Figures 10J,K, of which CTSA was highly expressed in monocyte, and CLIC1 highly expressed in monocyte and endothelial cells.

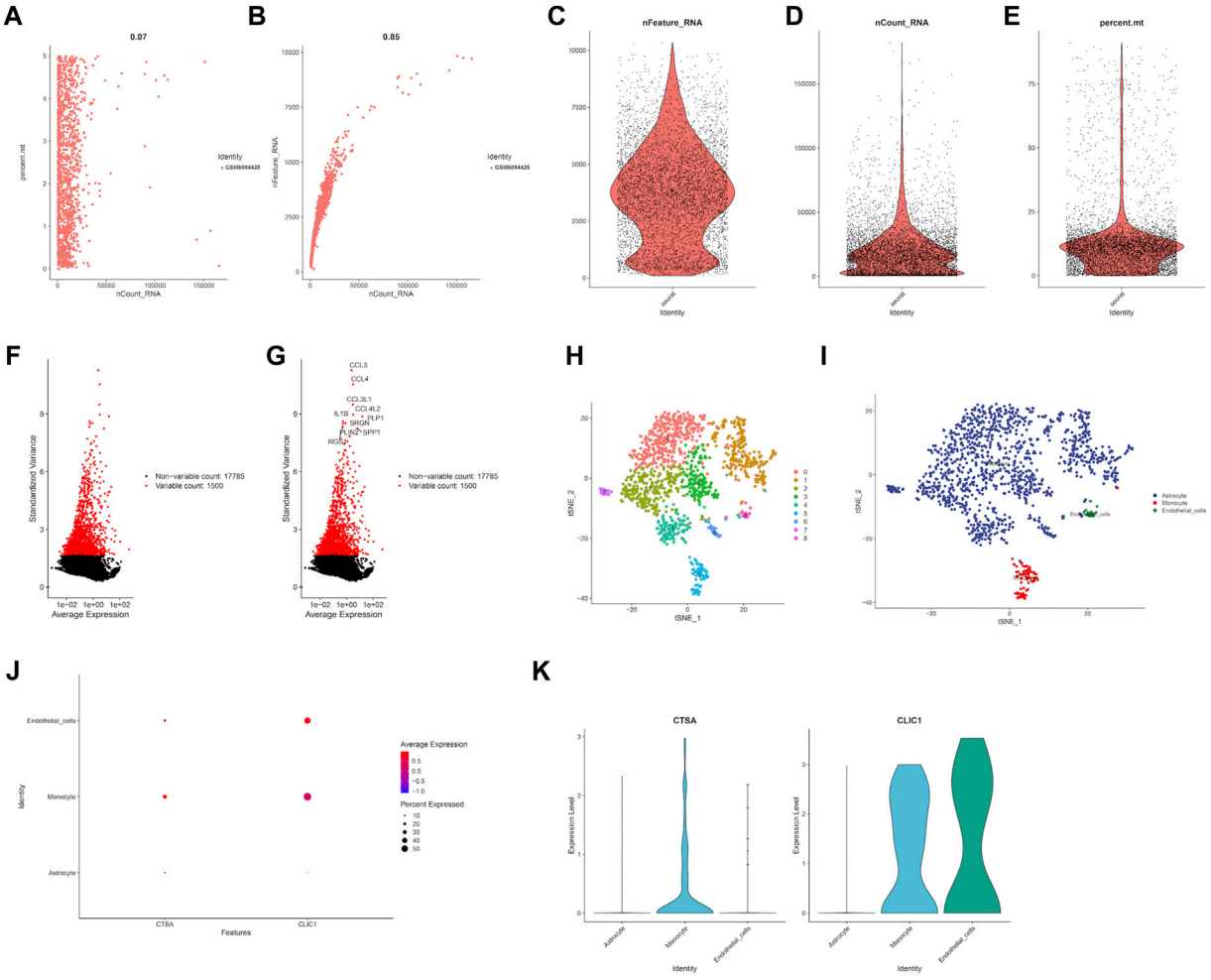

FIGURE 10
Single cell RNA analysis of LGG samples. **(A)** Evaluation of relationship between percentage of mitochondrial genes and mRNA readings. **(B)** Evaluation of relationship between percentage of mRNA quantity and mRNA readings. **(C–E)** A scatter plot illustrates the quantity of genes, UMI, and the percentage of mitochondrial genes in each cell type from the single LGG sample before quality control. **(F–G)** The red dots show the 1,500 genes that have the highest variability. **(H)** tSNE plot showed the cell population of LGG samples. **(I)** Cell annotation using cell markers for each cell. Expression level of prognostic genes in each cell type through dot plot **(J)** and violine plot **(K)**.

3.7 Experiment validation of the hub genes

As depicted in the previously result, we obtained six hub genes (CAST, CLIC1, CTSA, S100A1, SLC39A1 and TMSB4X) associated with EMT from WGCNA result. Next, we investigated the level of expression of the six genes in four LGG cell lines, namely, HMC3, GOS-3, T98G, and LN-18. Figure 11A demonstrates that the majority of genes were expressed at high levels in both COS-3 and T98G cell lines, as indicated by the RT-PCR results. Using the gene expression profiling interactive analysis (GEPIA) database, we delved deeper into the expression levels of normal and tumor tissue. Our findings revealed that CLIC1, S100A1, and SLC39A1 were significantly highly expressed in tumor tissue compared to normal tissue. However, CAST, CTSA, and TMSB4X showed no significant difference (Supplementary Figure S3). Prior research indicated that CLIC1 and S100A1 are involved in the advancement of LGG, thus our focus shifted to examining the function of SLC39A1 in LGG. Firstly, we examined the expression level through the RT-PCR experiment. Two LGG cell lines, GOS-3 and T98G, were treated with si-SLC39A1 #one to three, resulting in a notable reduction in SLC39A1 expression as determined by RT-qPCR analysis (Figure 11B). Meanwhile, we screened the stably transfected cell lines with puromycin after transfection of si-SLC39A1 #one to three, and the construction of stably transfected cell lines was observed by light microscopy 1 week after screening. The results showed that the stable-transformed cell line of si-SLC39A1 was successfully constructed by puromycin screening (Figure 11C). Flow cytometry was conducted to assess the apoptosis of GOS-3 and T98G cells, by comparing the number of cells distributed in early apoptosis and late apoptosis, the results showed that the apoptotic cell number in Q2 and Q3 regions of the si-SLC39A1 group was much higher than that of the si-NC group in both GOS-3 and T98G cell lines, revealing that the apoptosis rate was greater in cells with SLC39A1 knockout, indicating that the reduction of SLC39A1 significantly induced apoptosis of LGG cells (Figures 11D,E).

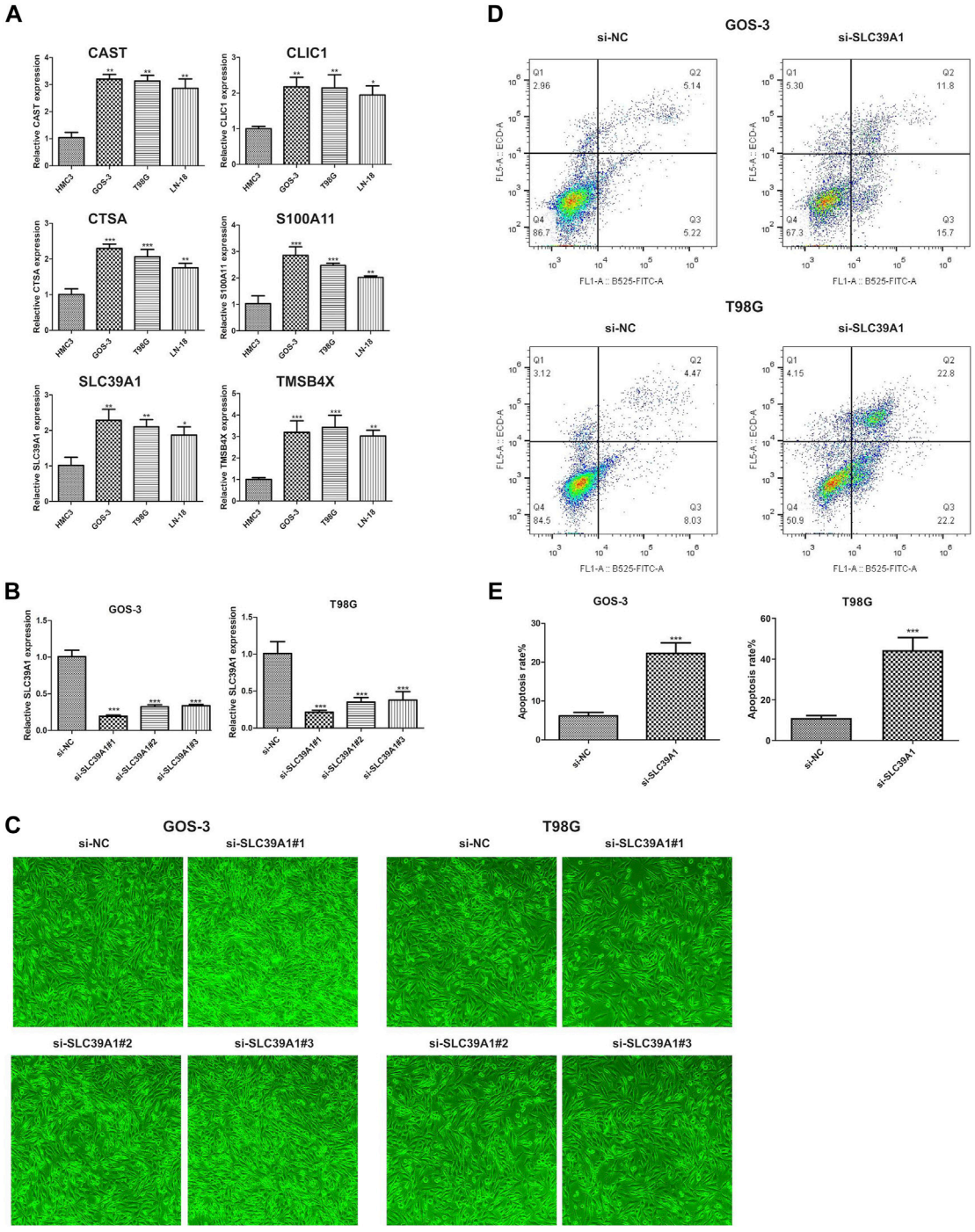

FIGURE 11
Validation of hub gene through *in-vitro* experiment. **(A)** Six hub genes expression level in HMC3, GOS-3, T98G, LN-18 cell lines. **(B)** SLC39A1 expression level in GOS-3 and T98G cell lines with SLC39A1 silence. **(C)** Transfection of si-SLC39A1 was filtered with puromycin for 1 week, and the expression of si-NC and si-SLC39A1 was observed by light microscopy. **(D, E)** Apoptotic level of SLC39A1-knockout GOS-3 and T98G cells.

4 Discussion

In the present study, a comprehensive analysis of LGG in TCGA and CGGA datasets was conducted based on EMT-related genes. By data mining analysis, we identified two clusters with markedly different prognosis and clinical phenotype in LGG. Further analysis showed that the two clusters were significantly different in TME immune cell infiltration and functional pathways, and presented inconsistent sensitivity to chemotherapy and immunotherapy. Finally, we developed a EMT-related signature and screen small molecule compounds with potential therapeutic effect targeting EMT. Additionally, we have undertaken further experimental validation of the identified EMT-related genes and their role in LGG. To some extent, our research contributed to

improving the current LGG treatment dilemma in precision therapy such as molecular classification, drug development, chemotherapy and immunotherapy.

The ESTIMATE and ssGSEA algorithms were used to measure the number of immune cells and stromal cells in every LGG sample from the TCGA and CGGA datasets. According to our data, immune and stromal scores as well as tumor purity vary among various LGG-EMT subtypes. Furthermore, our findings indicate that C2, which represents the LGG-EMT subtype with unfavorable prognosis, is associated with a greater level of infiltration of various immune cells such as CD56bright and CD56dim natural killer cells, eosinophils, monocytes, plasmacytoid dendritic cells, and others. Monocytes, which are believed to have tumor-promoting and immunosuppressive effects, are the primary infiltrating immune cells (Filipazzi et al., 2012; Marvel and Gabrilovich, 2015). It is anticipated that directing attention towards monocytes or other stromal components will alter the gliomas "cold" TME to a more "hot" TME phenotype. The efficiency of conventional first-line immunotherapy for glioma may be enhanced by this alteration (Tomaszewski et al., 2019). It may be possible to develop more effective therapeutic strategies if we understand the interaction between LGG and immune cells. Our findings using the TIDE algorithm supported the conclusion that C2 exhibited greater responsiveness to immunotherapy compared to C1. Furthermore, the SubMap method was employed to juxtapose the expression patterns of the LGG group with other previously published immune checkpoint datasets, which additionally validates the heightened susceptibility of C2 to immunotherapy, particularly PD-1.

The EMT-related survival prognosis model constructed by WGCNA and LASSO algorithm contains a series of hub genes, such as CLIC1, CTSA and SLC39A1. Multiple studies underscored the tumor-driver roles of the hub genes identified in present study. These hub genes were potential to be novel therapeutic targets and prognostic predictors in LGG. CLIC1, extensively studied within the CLIC family concerning tumors, has potential as a diagnostic indicator and therapeutic target. It has been linked to various cancers, influencing cell processes, including cell viability and mitochondrial function (Dehghan-Nayeri et al., 2017; Singha et al., 2018). In breast cancer, elevated CLIC1 expression correlates with tumor characteristics like size, TNM classification, grade, lymph node metastasis, and Ki67, while lower expression associates with extended OS and progression-free survival, suggesting its diagnostic potential (Xia et al., 2022). In esophageal squamous cell carcinoma (ESCC), CLIC1 is linked to clinical TNM classifications (Geng et al., 2022). CLIC1 knockdown in ESCC cell lines inhibits mTOR signaling, affecting cell proliferation and protein expression (Geng et al., 2022). High CLIC1 expression in lung adenocarcinoma predicts shorter overall survival and functions as an independent prognostic factor (Yasuda et al., 2022). In gastric cancer, CLIC1 absence impedes invasion and migration by affecting AMOT-p130 expression, possibly contributing to metastasis (Qiu et al., 2020). In hepatocellular carcinoma (HCC), upregulated CLIC1 is associated with aggressiveness, metastasis, and poor prognosis (Peng et al., 2020). GBM exhibits high CLIC1 expression (Setti et al., 2013). Reducing CLIC1 expression impairs cell proliferation and self-renewal in GBM, while CLIC1-mediated channel activity correlates with tumor aggressiveness (Setti et al., 2013). CLIC1 modulates reactive oxygen species and pH in human GBM stem cells, impacting motility and proliferation, making it a potential therapeutic target (Peretti et al., 2018). The study by Biasiotta et al. identified CLIC1 among nine genes with significant alterations in ion channels in solid tumors and vascular malformations, particularly in GBM and bladder cancers (Biasiotta et al., 2016). CLIC1 expression is correlated with the drug-resistant protein MRP1. Knockdown of CLIC1 in human choriocarcinoma cell lines reduces MRP1 expression (Wu and Wang, 2016). Additionally, CLIC1 has been found to transfer from GBM cells to microvascular epithelial cells through extracellular vesicles, potentially impacting metastasis (Thuringer et al., 2018). In summary, CLIC1 plays a crucial role in various cancers, including breast cancer, ESCC, lung adenocarcinoma, gastric cancer, and HCC, making it a potential target for cancer treatment due to its influence on cell proliferation, migration, invasion, and metastasis. Research into CLIC1's role in cancer and glioma progression and patient survival is promising, but further studies are needed to fully understand the mechanisms of action and develop targeted therapies.

Research on HCC has shown that SLC39A1 overexpression is linked to immune infiltration and promotes tumor progression (Zhang et al., 2021). Yuan et al. (2022) conducted a study to explore SLC39A1's potential as a tumor suppressor in renal cell carcinoma (RCC) using integrated omics analyses. They found that SLC39A1 significantly impacts various metabolic pathways and triggers communication among multiple signaling pathways. This research provides valuable insights into RCC development and the molecular changes induced by SLC39A1 (Yuan et al., 2022). Furthermore, glioma tissues exhibit increased SLC39A1 expression, strongly associated with clinical features like grade, IDH mutation status, and 1p19q co-deletion status. Elevated SLC39A1 levels are linked to reduced survival chances and contribute to glioma malignancy by promoting cell growth, inhibiting cell death, and influencing immune cell infiltration in the tumor microenvironment (Wang et al., 2020). SLC39A1 shows promise as a novel prognostic biomarker and therapeutic target for gliomas.

CTSA, a lysosomal protease, is upregulated in various cancers, including HCC and prostate cancer (Park et al., 2020; Wang et al., 2021; Luo et al., 2022). Its role as a potential diagnostic and prognostic biomarker has been explored. Petrera et al. (2016) demonstrated that inhibiting CTSA in a mouse model improved cardiac functionality in heart failure (Petrera et al., 2016). High CTSA levels can differentiate HCC from healthy liver tissue and are linked to poorer survival rates (Wang et al., 2021). Luo et al. (2022) found high CTSA expression correlated with poor HCC patient outcomes, reinforcing its prognostic value (Luo et al., 2022). In prostate cancer, Park et al. (2020) showed that suppressing CTSA gene expression reduced proliferation, migration, and tumorigenesis (Park et al., 2020). CTSA is a potential therapeutic target and prognostic biomarker in various cancers. Hu et al., Zhang et al., Toss et al., and Kim et al. explored CTSA's role in lung adenocarcinoma (Hu et al., 2020), glioma (Zhang et al., 2022), breast ductal carcinoma *in situ* (Toss et al., 2019), and canine inflammatory mammary adenocarcinoma (Kim et al., 2020), respectively. Hu et al. found that CTSA promotes lung adenocarcinoma progression and may be a promising target for treatment (Hu et al., 2020). Zhang et al. linked CTSA to poor prognosis in glioma (Zhang et al., 2022). Toss et al. associated CTSA with unfavorable outcomes in breast ductal carcinoma *in situ* (Toss et al., 2019). Kim et al. demonstrated the impact of leptin on inflammatory mammary adenocarcinoma in dogs by modulating

CTSA expression (Kim et al., 2020). In summary, CTSA is significant in different cancers as a potential treatment target and predictor. Further research is needed to elucidate its precise molecular mechanisms and develop tailored treatments.

5 Conclusion

In conclusion, the present study comprehensively demonstrated the difference in molecular subtype of LGG based on EMT-related genes, thus revealing the tumor heterogeneity of LGG. We identified two distinct subtypes of LGG-EMT with varying clinical prognoses, clinicopathological characteristics, mutation statuses, immune cell infiltration, tumor microenvironment, and signaling pathway activities. The heterogeneity among LGG-EMT subtypes leads to divergent responses to immunotherapy and chemotherapy, guiding the precision treatment of LGG. Moreover, we developed and validated a reliable EMT-signature for LGG prognosis, and speculated about several small molecule compounds that could enhance the clinical practical value of LGG. Further experimental studies can help us understand the underlying mechanisms of EMT in LGG, thereby providing additional support for the clinical utility of the prognostic signature.

Data availability statement

The original contributions presented in the study are included in the article/Supplementary Material, further inquiries can be directed to the corresponding author.

Author contributions

CW: Writing–original draft. ZH: Conceptualization, Data curation, Formal Analysis, Methodology, Visualization, Writing–original draft.

Funding

The authors declare financial support was received for the research, authorship, and/or publication of this article. This research was supported by Qingdao Clinical Research Center for Rare Diseases of Nervous System (22-3-7-lczx-3-nsh), and Qingdao Key Health Discipline Development Fund.

Acknowledgments

We sincerely acknowledge TCGA, CGGA, GEO and the developers of these datasets.

Conflict of interest

The authors declare that the research was conducted in the absence of any commercial or financial relationships that could be construed as a potential conflict of interest.

Publisher's note

All claims expressed in this article are solely those of the authors and do not necessarily represent those of their affiliated organizations, or those of the publisher, the editors and the reviewers. Any product that may be evaluated in this article, or claim that may be made by its manufacturer, is not guaranteed or endorsed by the publisher.

Supplementary material

The Supplementary Material for this article can be found online at: https://www.frontiersin.org/articles/10.3389/fphar.2023.1276466/full#supplementary-material

References

Akalay, I., Janji, B., Hasmim, M., Noman, M. Z., Andre, F., Cremoux, P., et al. (2013). Epithelial-to-Mesenchymal transition and autophagy induction in breast carcinoma promote escape from T-cell-mediated lysis. *Cancer Res.* 73, 2418–2427. doi:10.1158/0008-5472.CAN-12-2432

Basu, A., Bodycombe, N., Cheah, J., Price, E., Liu, K., Schaefer, G., et al. (2013). An interactive resource to identify cancer genetic and lineage dependencies targeted by small molecules. *Cell.* 154, 1151–1161. doi:10.1016/j.cell.2013.08.003

Biasiotta, A., D'Arcangelo, D., Passarelli, F., Nicodemi, E., and Facchiano, A. (2016). Ion channels expression and function are strongly modified in solid tumors and vascular malformations. *J. Transl. Med.* 14, 285. doi:10.1186/s12967-016-1038-y

Bindea, G., Mlecnik, B., Tosolini, M., Kirilovsky, A., Waldner, M., Obenauf, A., et al. (2013). Spatiotemporal dynamics of intratumoral immune cells reveal the immune landscape in human cancer. *Immunity* 39, 782–795. doi:10.1016/j.immuni.2013.10.003

Cao, Y., Fu, L., Wu, J., Peng, Q., Nie, Q., Zhang, J., et al. (2022). Integrated analysis of multimodal single-cell data with structural similarity. *Nucleic Acids Res.* 50, e121. doi:10.1093/nar/gkac781

Chen, X. Y., Chen, Y., Fang, W. H., Wu, Z. Y., Wang, D. L., Xu, Y. W., et al. (2022). Integrative and comparative single-cell analysis reveals transcriptomic difference between human tumefactive demyelinating lesion and glioma. *Commun. Biol.* 5, 941. doi:10.1038/s42003-022-03900-0

Claus, E., Walsh, K., Wiencke, J., Molinaro, A., Wiemels, J., Schildkraut, J., et al. (2015). Survival and low-grade glioma: the emergence of genetic information. *Neurosurg. focus* 38, E6. doi:10.3171/2014.10.FOCUS12367

Corsello, S., Nagari, R., Spangler, R., Rossen, J., Kocak, M., Bryan, J., et al. (2020). Discovering the anticancer potential of non-oncology drugs by systematic viability profiling. *Nat. Cancer* 1, 235–248. doi:10.1038/s43018-019-0018-6

Dehghan-Nayeri, N., Eshghi, P., Pour, K., Rezaei tavirani, M., Omrani, m.d., and Gharehbaghian, A. (2017). Differential expression pattern of protein markers for predicting chemosensitivity of dexamethasone-based chemotherapy of B cell acute lymphoblastic leukemia. *Cancer Chemother. Pharmacol.* 80, 177–185. doi:10.1007/s00280-017-3347-0

Dionellis, V., Norkin, M., Karamichali, A., Rossetti, G., Huelsken, J., Ordóñez-Morán, P., et al. (2021). Genomic instability profiles at the single cell level in mouse colorectal cancers of defined genotypes. *Cancers* 13, 1267. doi:10.3390/cancers13061267

Feng, S., Xu, Y., Dai, Z., Yin, H., Zhang, K., and Shen, Y. (2022). Integrative analysis from multicenter studies identifies a WGCNA-derived cancer-associated fibroblast signature for ovarian cancer. *Front. Immunol.* 13, 951582. doi:10.3389/fimmu.2022.951582

Filipazzi, P., Huber, V., and Rivoltini, L. (2012). Phenotype, function and clinical implications of myeloid-derived suppressor cells in cancer patients. *Cancer Immunol. Immunother.* 61, 255–263. doi:10.1007/s00262-011-1161-9

Geeleher, P., Cox, N., and Huang, R. (2014a). pRRophetic: an R package for prediction of clinical chemotherapeutic response from tumor gene expression levels. *PloS one* 9, e107468. doi:10.1371/journal.pone.0107468

Geeleher, P., Cox, N., and Huang, R. (2014b). Abstract 5561: clinical drug response can be predicted using baseline gene expression levels and *in vitro* drug sensitivity in cell lines. *Genome Biol.* 15, R47. doi:10.1186/gb-2014-15-3-r47

Geng, H., Feng, C., Sun, Z., Fan, X., Xie, Y., Gu, J., et al. (2022). Chloride intracellular channel 1 promotes esophageal squamous cell carcinoma proliferation via mTOR signalling. *Transl. Oncol.* 27, 101560. doi:10.1016/j.tranon.2022.101560

Golub, D., Iyengar, N., Dogra, S., Wong, T., Bready, D., Tang, K., et al. (2019). Mutant isocitrate dehydrogenase inhibitors as targeted cancer therapeutics. *Front. Oncol.* 9, 417. doi:10.3389/fonc.2019.00417

Hänzelmann, S., Castelo, R., and Guinney, J. (2013). GSVA: gene set variation analysis for microarray and RNA-Seq data. *BMC Bioinforma.* 14, 7. doi:10.1186/1471-2105-14-7

Hazra, A., and Gogtay, N. (2016). Biostatistics series module 3: comparing groups: numerical variables. *Indian J. Dermatology* 61, 251–260. doi:10.4103/0019-5154.182416

Hoshida, Y., Brunet, J. P., Tamayo, P., Golub, T., and Mesirov, J. (2007). Subclass mapping: identifying common subtypes in independent disease data sets. *PloS one* 2, e1195. doi:10.1371/journal.pone.0001195

Hu, B., Zhu, X., and Lu, J. (2020). Cathepsin A knockdown decreases the proliferation and invasion of A549 lung adenocarcinoma cells. *Mol. Med. Rep.* 21, 2553–2559. doi:10.3892/mmr.2020.11068

Hu, C., Li, T., Xu, L., Zhang, X., Li, F., Bai, J., et al. (2022). CellMarker 2.0: an updated database of manually curated cell markers in human/mouse and web tools based on scRNA-seq data. *Nucleic acids Res.* 51, D870–D876. doi:10.1093/nar/gkac947

Jiang, P., Gu, S., Pan, D., Fu, J., Sahu, A., Hu, X., et al. (2018). Signatures of T cell dysfunction and exclusion predict cancer immunotherapy response. *Nat. Med.* 24, 1550–1558. doi:10.1038/s41591-018-0136-1

Kim, J., Mahiddine, F., and Kim, G. (2020). Leptin modulates the metastasis of canine inflammatory mammary adenocarcinoma cells through downregulation of lysosomal protective protein cathepsin A (CTSA). *Int. J. Mol. Sci.* 21, 8963. doi:10.3390/ijms21238963

Koptyra, M., Rahti, K., Zhu, Y., Farrow, B., Miller, D., Kraya, A., et al. (2023). Abstract 3566: expansion of the pediatric brain tumor Atlas: children's brain tumor network, kids first data resource and childhood cancer data initiative open science effort. *Cancer Res.* 83, 3566. doi:10.1158/1538-7445.am2023-3566

Lambert, A., Pattabiraman, D., and Weinberg, R. (2017). Emerging biological principles of metastasis. *Cell.* 168, 670–691. doi:10.1016/j.cell.2016.11.037

Langfelder, P., Horvath, S., Langfelder, P., and Horvath, S. (2009). WGCNA: an R package for weighted correlation network analysis. *BMC Bioinforma.* 9, 559. doi:10.1186/1471-2105-9-559

Leek, J., Johnson, W., Parker, H., Jaffe, A., and Storey, J. (2012). The SVA package for removing batch effects and other unwanted variation in high-throughput experiments. *Bioinforma. Oxf. Engl.* 28, 882–883. doi:10.1093/bioinformatics/bts034

Liberzon, A., Birger, C., Thorvaldsdóttir, H., Ghandi, M., Mesirov, J. P., and Tamayo, P. (2015). The Molecular Signatures Database (MSigDB) hallmark gene set collection. *Cell. Syst.* 1, 417–425. doi:10.1016/j.cels.2015.12.004

Loret, N., Denys, H., Tummers, P., and Berx, G. (2019). The role of epithelial-to-mesenchymal plasticity in ovarian cancer progression and therapy resistance. *Cancers* 11, 838. doi:10.3390/cancers11060838

Lu, K., Chang, J., Parachoniak, C., Pandika, M., Aghi, M., Meyronet, D., et al. (2012). VEGF inhibits tumor cell invasion and mesenchymal transition through a MET/VEGFR2 complex. *Cancer Cell.* 22, 21–35. doi:10.1016/j.ccr.2012.05.037

Luo, L., Wang, X., Wang, H., Yang, C., Zhang, Y., Li, X., et al. (2022). High cathepsin A protein expression predicts poor prognosis and tumor recurrence of hepatocellular carcinoma patients after curative hepatectomy. *Am. J. cancer Res.* 12, 3843–3856.

Marques, C., Unterkircher, T., Kroon, P., Izzo, A., Gargiulo, G., Kling, E., et al. (2019). NF1 regulates mesenchymal glioblastoma plasticity and aggressiveness through the AP-1 transcription factor FOSL1. *Elife* 10, e64846. doi:10.7554/eLife.64846

Marvel, D., and Gabrilovich, D. I. (2015). Myeloid-derived suppressor cells in the tumor microenvironment: expect the unexpected. *J. Clin. Invest.* 125, 3356–3364. doi:10.1172/JCI80005

Mayakonda, A., Lin, D., Assenov, Y., Plass, C., and Koeffler, H. (2018). Maftools: efficient and comprehensive analysis of somatic variants in cancer. *Genome Res* 28, 1747–1756. doi:10.1101/gr.239244.118

Verhaak, R. G., Hoadley, K. A., Purdom, E., Wang, V., Qi, Y., Wilkerson, M. D., et al. (2010). Integrated genomic analysis identifies clinically relevant subtypes of glioblastoma characterized by abnormalities in PDGFRA, IDH1, EGFR, and NF1. *Cancer cell* 17 (1), 98–110. doi:10.1016/j.ccr2009.12.020

Miyoshi, A., Kitajima, Y., Sumi, K., Sato, K., Hagiwara, A., Koga, Y., et al. (2004). Snail and SIP1 increase cancer invasion by upregulating MMP family in hepatocellular carcinoma cells. *Br. J. cancer* 90, 1265–1273. doi:10.1038/sj.bjc.6601685

Nie, W., Xu, M. D., Gan, L., Yi, Z., Qian, J., Gu, K., et al. (2020). Advanced non-small cell lung cancer patients with low tumor mutation burden might derive benefit from immunotherapy. *J. Immunother. Hagerst. Md, 1997)* 43, 189–195. doi:10.1097/CJI.0000000000000318

Park, S., Kwon, W., Park, J. K., Baek, S. M., Lee, S. W., Cho, G. J., et al. (2020). Suppression of cathepsin a inhibits growth, migration, and invasion by inhibiting the p38 MAPK signaling pathway in prostate cancer. *Archives Biochem. Biophysics* 688, 108407. doi:10.1016/j.abb.2020.108407

Peng, J. M., Lin, S. H., Yu, M. C., and Hsieh, S. Y. (2020). CLIC1 recruits PIP5K1A/C to induce cell-matrix adhesions for tumor metastasis. *J. Clin. Investigation* 131, e133525. doi:10.1172/JCI133525

Peretti, M., Raciti, F., Carlini, V., Verduci, I., Sertic, S., Barozzi, S., et al. (2018). Mutual influence of ROS, pH, and CLIC1 membrane protein in the regulation of G1-S phase progression in human glioblastoma stem cells. *Mol. Cancer Ther.* 17, 2451–2461. doi:10.1158/1535-7163.MCT-17-1223

Petrera, A., Gassenhuber, J., Ruf, S., Gunasekaran, D., Eßer, J., Shahinian, J., et al. (2016). Cathepsin A inhibition attenuates myocardial infarction-induced heart failure on the functional and proteomic levels. *J. Transl. Med.* 14, 153. doi:10.1186/s12967-016-0907-8

Qiu, Y., Mao, Y. T., Zhu, J. H., Zhao, K., Wang, J. F., Huang, J. M., et al. (2020). CLIC1 knockout inhibits invasion and migration of gastric cancer by upregulating AMOT-p130 expression. *Clin. Transl. Oncol.* 23, 514–525. doi:10.1007/s12094-020-02445-0

Rhim, A., Aiello-Couzo, N., Mirek, E., and Stanger, B. (2014). Abstract IA5: epigenetic genome control by heterochromatin machinery and non-coding RNAs. *Cancer Res.* 72, IA5. doi:10.1158/1538-7445.nonrna12-ia5

Rotin, D., Brat, D. J., Verhaak, R. G. W., Aldape, K. D., Yung, W. K. A., Salama, S. R., et al. (2015). Comprehensive, integrative genomic analysis of diffuse lower-grade gliomas. *N. Eng. J. Med.* 372, 2481–2498. doi:10.1056/NEJMoa1402121

Setti, M., Savalli, N., Osti, D., Richichi, C., Angelini, M., Brescia, P., et al. (2013). Functional role of CLIC1 ion channel in glioblastoma-derived stem/progenitor cells. *J. Natl. Cancer Inst.* 105, 1644–1655. doi:10.1093/jnci/djt278

Shibue, T., and Weinberg, R. (2017). EMT, CSCs, and drug resistance: the mechanistic link and clinical implications. *Nat. Rev. Clin. Oncol.* 14, 611–629. doi:10.1038/nrclinonc.2017.44

Singha, B., Harper, S., Goldman, A., Bitler, B., Aird, K., Borowsky, M., et al. (2018). CLIC1 and CLIC4 complement CA125 as a diagnostic biomarker panel for all subtypes of epithelial ovarian cancer. *Sci. Rep.* 8, 14725. doi:10.1038/s41598-018-32885-2

Thuringer, D., Chanteloup, G., Winckler, P., and Garrido, C. (2018). The vesicular transfer of CLIC1 from glioblastoma to microvascular endothelial cells requires TRPM7. *Oncotarget* 9, 33302–33311. doi:10.18632/oncotarget.26048

Tomaszewski, W., Sanchez-Perez, L., Gajewski, T., and Sampson, J. (2019). Brain tumor micro-environment and host state - implications for immunotherapy. *Clin. Cancer Res.* 25, 4202–4210. doi:10.1158/1078-0432.CCR-18-1627

Toss, M., Miligy, I., Haj-Ahmad, R., Gorringe, K., Al-Kawaz, A., Mittal, K., et al. (2019). The prognostic significance of lysosomal protective protein (Cathepsin A) in breast ductal carcinoma *in situ*. *Histopathology* 74, 1025–1035. doi:10.1111/his.13835

van Staalduinen, J., Baker, D., Dijke, P., and Dam, H. (2018). Epithelial–mesenchymal-transition-inducing transcription factors: new targets for tackling chemoresistance in cancer? *Oncogene* 37, 6195–6211. doi:10.1038/s41388-018-0378-x

Vuong, L., Kotecha, R., Voss, M., and Hakimi, A. (2019). Tumor microenvironment dynamics in clear-cell renal cell carcinoma. *Cancer Discov.* 9, 1349–1357. doi:10.1158/2159-8290.CD-19-0499

Wang, H., Xu, F., Yang, F., Lv, L., and Jiang, Y. (2021). Prognostic significance and oncogene function of cathepsin A in hepatocellular carcinoma. *Sci. Rep.* 11, 14611. doi:10.1038/s41598-021-93998-9

Wang, P., Zhang, J., He, S., Xiao, B., and Peng, X. (2020). SLC39A1 contribute to malignant progression and have clinical prognostic impact in gliomas. *Cancer Cell. Int.* 20, 573. doi:10.1186/s12935-020-01675-0

Weller, M., Weber, R., Willscher, E., Riehmer, V., Hentschel, B., Kreuz, M., et al. (2015). Molecular classification of diffuse cerebral WHO grade II/III gliomas using genome- and transcriptome-wide profiling improves stratification of prognostically distinct patient groups. *Acta neuropathol.* 129, 679–693. doi:10.1007/s00401-015-1409-0

Wilkerson, M., and Hayes, D. (2010). ConsensusClusterPlus: a class discovery tool with confidence assessments and item tracking. *Bioinforma. Oxf. Engl.* 26, 1572–1573. doi:10.1093/bioinformatics/btq170

Wu, J., and Wang, D. (2016). CLIC1 induces drug resistance in human choriocarcinoma through positive regulation of MRP1. *Oncol. Res.* 25, 863–871. doi:10.3727/096504016X14772315906527

Wu, T., Hu, E., Xu, S., Chen, M., Guo, P., Dai, Z., et al. (2021). clusterProfiler 4.0: a universal enrichment tool for interpreting omics data. *Innovation* 2, 100141. doi:10.1016/j.xinn.2021.100141

Xia, J., Wang, Q., Ju, F., Luo, X., Wang, F., Zhou, Y., et al. (2022). Chloride Intracellular Channel 1 is a potential biomarker for breast cancer. *Breast Cancer Targets Ther.* 14, 247–258. doi:10.2147/BCTT.S367519

Xia, Y., Liu, Y., Yang, C., Simeone, D., Sun, T. T., DeGraff, D., et al. (2021). Dominant role of CDKN2B/p15INK4B of 9p21.3 tumor suppressor hub in inhibition of cell-cycle and glycolysis. *Nat. Commun.* 12, 2047. doi:10.1038/s41467-021-22327-5

Yamaguchi, Y. (2016). *Immunotherapy of cancer: an innovative treatment comes of age*. Japan: Springer.

Yang, J., Antin, P., Berx, G., Blanpain, C., Brabletz, T., Bronner, M., et al. (2020). Guidelines and definitions for research on epithelial–mesenchymal transition. *Nat. Rev. Mol. Cell. Biol.* 21, 341–352. doi:10.1038/s41580-020-0237-9

Yang, Q., Jiang, N., Zou, H., Fan, X., Liu, T., Huang, X., et al. (2022). Alterations in 3D chromatin organization contribute to tumorigenesis of EGFR-amplified glioblastoma. *Comput. Struct. Biotechnol. J.* 20, 1967–1978. doi:10.1016/j.csbj.2022.04.007

Yang, W., Soares, J., Greninger, P., Edelman, E., Lightfoot, H., Forbes, S., et al. (2012). Genomics of Drug Sensitivity in Cancer (GDSC): a resource for therapeutic biomarker discovery in cancer cells. *Nucleic acids Res.* 41, D955–D961. doi:10.1093/nar/gks1111

Yang, Y., and Xu, X. (2021). Identification of key genes in coronary artery disease: an integrative approach based on weighted gene co-expression network analysis and their correlation with immune infiltration. *Aging (Albany NY)* 13, 8306–8319. doi:10.18632/aging.202638

Yasuda, Y., Nagano, T., Jimbo, N., Kiriu, T., Suraya, R., Hazama, D., et al. (2022). Chloride Intracellular Channel 1 expression is associated with poor prognosis of lung adenocarcinoma. *Anticancer Res.* 42, 271–277. doi:10.21873/anticanres.15482

Yoshihara, K., Shahmoradgoli, M., Martinez-Ledesma, J. E., Vegesna, R., Kim, H., Torres-García, W., et al. (2013). Inferring tumour purity and stromal and immune cell admixture from expression data. *Nat. Commun.* 4, 2612. doi:10.1038/ncomms3612

Yuan, Y., Liu, Z., Li, B., Gong, Z., Piao, C., Du, Y., et al. (2022). Integrated analysis of transcriptomics, proteomics and metabolomics data reveals the role of SLC39A1 in renal cell carcinoma. *Front. Cell. Dev. Biol.* 10, 977960. doi:10.3389/fcell.2022.977960

Zhang, M., Huang, J., Wang, Y., Nie, Q., Zhang, X., Yang, Y., et al. (2022). Cathepsin A upregulation in glioma: a potential therapeutic target associated with immune infiltration. *J. Med. Biochem.* 41, 459–465. doi:10.5937/jomb0-35677

Zhang, Q., Pan, J., An, F., Nie, H., and Zhan, Q. (2021). Decreased SLC39A1 (solute carrier family 39 member 1) expression predicts unfavorable prognosis in patients with early-stage hepatocellular carcinoma. *Bioengineered* 12, 8147–8156. doi:10.1080/21655979.2021.1987131

Zhou, H., Huang, L., Liang, L., Chen, L., Zou, C., Li, Z., et al. (2021). Identification of an miRNA regulatory network and candidate markers for ischemic stroke related to diabetes. *Int. J. Gen. Med.* 14, 3213–3223. doi:10.2147/IJGM.S319503

Glossary

CAMs	cell adhesion molecules
CDF	cumulative distribution function
CGGA	the Chinese Glioma Genome Atlas
CLIC1	Chloride Intracellular Channel 1
CNA	copy number alterations
CTA	Cancer Testicular Antigens
CTRP	Cancer Therapeutics Response Portal
DCIS	ductal carcinoma *in situ*
DEGs	differentially expressed genes
DSS	disease-specific survival
ECM	extracellular matrix
EMT	epithelial-mesenchymal transition
ESCC	esophageal squamous cell carcinoma
ESTIMATE	Estimation of Stromal and Immune cells in MAlignant Tumours using Expression
FDR	false discovery rate
GBM	glioblastoma
GDAC	Genome Data Analysis Center
GDSC	Genomics of Drug Sensitivity in Cancer
GEPIA	gene expression profiling interactive analysis
GS	gene significance
GSVA	gene set variation analysis
HCC	hepatocellular carcinoma
IC50	half-maximal inhibitory concentration
ICB	immune checkpoint blockade
KM	Kaplan-Meier
LGG	low-grade glioma
MM	module membership
MSigDB	Molecular signatures database
OS	overall survival
PCA	principal components analysis
RCC	renal cell carcinoma
ROC	receiver operating characteristic
RT-qPCR	Real-time quantitative PCR
scRNA-seq	single cell RNA-sequencing
SNP	single-nucleotide polymorphisms
ssGSEA	single-sample gene set enrichment analysis
TAD	topological associating domain
TCGA	the Cancer Genome Atlas
TIDE	tumor immune dysfunction and exclusion

TIICs	tumor infiltrating immune cells
TME	tumor microenvironment
TMZ	temozolomide
TNM	tumor node metastasis
TPM	transcripts per kilobase million
t-SNE	T-distributed stochastic neighbor embedding
WGCNA	weighted correlation network analysis

frontiers | Frontiers in Oncology

TYPE Perspective
PUBLISHED 18 December 2023
DOI 10.3389/fonc.2023.1279923

Check for updates

OPEN ACCESS

EDITED BY
Mariana Magalhães,
University of Coimbra, Portugal

REVIEWED BY
Prit Benny Malgulwar,
University of Texas MD Anderson Cancer Center, United States
Vrunda Trivedi,
Stanford University, United States
Sandeep Srivastava,
Children's National Hospital, United States

*CORRESPONDENCE
Desmond A. Brown
desmond.brown@nih.gov

†These authors have contributed equally to this work

RECEIVED 18 August 2023
ACCEPTED 20 November 2023
PUBLISHED 18 December 2023

CITATION
Laws MT, Walker EN, Cozzi FM, Ampie L, Jung M-Y, Burton EC and Brown DA (2023) Glioblastoma may evade immune surveillance through primary cilia-dependent signaling in an IL-6 dependent manner.
Front. Oncol. 13:1279923.
doi: 10.3389/fonc.2023.1279923

COPYRIGHT
© 2023 Laws, Walker, Cozzi, Ampie, Jung, Burton and Brown. This is an open-access article distributed under the terms of the Creative Commons Attribution License (CC BY). The use, distribution or reproduction in other forums is permitted, provided the original author(s) and the copyright owner(s) are credited and that the original publication in this journal is cited, in accordance with accepted academic practice. No use, distribution or reproduction is permitted which does not comply with these terms.

Glioblastoma may evade immune surveillance through primary cilia-dependent signaling in an IL-6 dependent manner

Maxwell T. Laws[1†], Erin N. Walker[1,2†], Francesca M. Cozzi[3], Leonel Ampie[1], Mi-Yeon Jung[1], Eric C. Burton[1,4] and Desmond A. Brown[1*]

[1]Neurosurgical Oncology Unit, Surgical Neurology Branch, National Institutes of Neurological Disorders and Stroke, National Institutes of Health, Bethesda, MD, United States, [2]University of South Carolina School of Medicine Greenville, Greenville, SC, United States, [3]Cambridge Brain Tumour Imaging Lab, Division of Neurosurgery, Department of Clinical Neurosciences, University of Cambridge, Addenbroke's Hospital, Cambridge, United Kingdom, [4]Neuro-Oncology Branch, Center for Cancer Research, National Cancer Institute, National Institutes of Health, Bethesda, MD, United States

Glioblastoma is the most common, malignant primary brain tumor in adults and remains universally fatal. While immunotherapy has vastly improved the treatment of several solid cancers, efficacy in glioblastoma is limited. These challenges are due in part to the propensity of glioblastoma to recruit tumor-suppressive immune cells, which act in conjunction with tumor cells to create a pro-tumor immune microenvironment through secretion of several soluble factors. Glioblastoma-derived EVs induce myeloid-derived suppressor cells (MDSCs) and non-classical monocytes (NCMs) from myeloid precursors leading to systemic and local immunosuppression. This process is mediated by IL-6 which contributes to the recruitment of tumor-associated macrophages of the M2 immunosuppressive subtype, which in turn, upregulates anti-inflammatory cytokines including IL-10 and TGF-β. Primary cilia are highly conserved organelles involved in signal transduction and play critical roles in glioblastoma proliferation, invasion, angiogenesis, and chemoradiation resistance. In this perspectives article, we provide preliminary evidence that primary cilia regulate intracellular release of IL-6. This ties primary cilia mechanistically to tumor-mediated immunosuppression in glioblastomas and potentially, in additional neoplasms which have a shared mechanism for cancer-mediated immunosuppression. We propose potentially testable hypotheses of the cellular mechanisms behind this finding.

KEYWORDS

glioblastoma, extracellular vesicles, primary cilia, glioblastoma-mediated immunosuppression, IL-6, CCRK

Introduction

Glioblastoma is the most common malignant brain tumor with mean survival of 15 months, and average 5-year survival of 6.9% (1). Despite significant effort to develop novel therapies, there has been little improvement in outcomes. The pathogenesis of glioblastoma involves myriad cellular adaptations which promote proliferation, invasion, angiogenesis, DNA repair, and immune suppression. Immunotherapies have garnered significant interest among the scientific community and have revolutionized treatment of several solid cancers. Glioblastoma is notorious for propagating an immunosuppressive tumor microenvironment (TME) through suppressing infiltrating immune cells via numerous pathways which work both locally and systemically. In the local tumor microenvironment, production of tryptophan metabolites, secretion of cytokines including IL-6 and IL-10, and an increase in membrane expression of checkpoint proteins like PD-L1 result in local immunosuppression. Contemporary evidence also implicate glioblastoma-derived extracellular vesicles (EVs) in upregulation of myeloid-derived suppressor cells (MDSCs) which contribute to systemic immunosuppression (2–5). While it is known that glioblastoma generates an immunosuppressive TME, the specific alterations in gene expression and cellular signaling which trigger this immunosuppressive phenotype remain enigmatic.

Primary cilia are non-motile, microtubule-based organelles which act in key signaling pathways, e.g. EGFR (6), Shh (7), WNT (8), TGF (9) and Notch (10). The primary cilium is anchored to the plasma membrane by the basal body. The basal body is important because it acts as a template for cilia construction and repurposes itself in cell division as the mother centriole (11). The implication of this juxtaposition with the centrosome, is that the primary cilia must be disassembled before the cell can transition from the G_0/G_1 phase to the cycling $S/G_2/M$ phase of mitosis (12). This "ciliary checkpoint" acts as a brake, confining the cell to the G_0/G_1 phase. Perhaps unsurprisingly, many systemic and CNS malignancies including glioblastoma, melanoma, pancreatic, liver, and prostate cancers demonstrate reduction in primary cilia frequency, though in each of these tumors, a ciliated cell population remains (13, 14). In this perspectives article, we present evidence for a potential role of primary cilia as master regulators of glioblastoma-mediated immunosuppression through the regulation of IL-6. This is a novel idea which may ultimately yield deeper understanding of the pathogenesis of glioblastoma and other cancers which all rely on this shared mechanism and may also allow for development of potentially novel and urgently needed therapeutic strategies.

Methods

Source of human glioblastoma cells and cell culture

Human glioblastoma cells (dBT114 and dBT116) were acquired from the Brain Tumor PDX National Resource Database by Sarkarias et al. from the Mayo Clinic (Mayo Clinic IRB312-003458). Cells were cultured in DMEM/F12 (Thermo Fisher Scientific, Waltham, MA) with 10% fetal bovine serum (FBS) and 1% Pen/Strep and incubated in 5% CO_2 at 37 degrees Celsius.

Protein knockdown by small interfering RNA

siRNA sequences targeting KIF3A (sc-270301), CCRK (sc-92544), IFT88 (sc-75329), or a nontargeting siRNA control (sc-37007) were acquired (Santa Cruz Inc, Dallas, TX). Each siRNA product consisted of pools of 3–5 target-specific 19–25 nucleotide siRNAs designed to knock down expression of the gene of interest. Glioblastoma cells (2.5×10^5) were incubated in DMEM with 10% FBS and siRNAs were transfected using Lipofectamine RNAiMAX (Thermo Fisher Scientific) per the manufacturer's instructions. Cells were then recovered in complete medium for 24 hours, and the efficacy of gene targeting at the mRNA and protein level was assessed by qRT-PCR and western blotting, respectively.

Immunoblotting and densitometric analysis

Whole-cell lysates (WCL) were prepared with RIPA buffer (50 mM Tris [pH 7.4], 1% Triton X-100, 0.25% sodium deoxycholate, 150 mM NaCl, 1 mM EDTA [pH 8], and 10 mM NaF) containing complete Protease Inhibitor (Roche, Basel, Switzerland). Protein concentration was determined with a BCA assay (Thermo Fisher Scientific) per the manufacturer's instructions. Proteins were then separated by electrophoresis on NuPAGE 4-20% gradient precast polyacrylamide gels (Life Technologies, Carlsbad, CA). Following membrane transfer, the proteins were probed using the following antibodies: HSP90 (4874S; Cell Signaling, Danvers, MA), KIF3A (PA5-121019), IFT88 (PA5-18467), CCRK (PA5-52464), and IL-6 (M620) all sourced from Thermo Fisher Scientific. Secondary antibody was horseradish peroxidase-conjugated goat anti-rabbit (Jackson ImmunoResearch, West Grove, PA). Detection was enhanced by chemiluminescence. Immunoreactive band density was then quantified using ImageJ software (NIH, Bethesda, MD).

RNA extraction and qRT-PCR

Total RNA was isolated from glioblastoma cells (3×10^5) using the RNeasy Plus Mini Kit (Qiagen, Valencia, CA). Isolated RNA (500 ng) was then utilized to perform a reverse-transcription reaction (30 µl) with random hexamers and SuperScript III RT (Thermo Fisher Scientific). The resulting cDNA (5 µl) was used for real-time PCR using the TaqMan gene-expression assay for KIF3A (Hs00199901_m1), CCRK (Hs01114921_m1), IFT88 (Hs00544051_m1), and actin (Hs00188792_m1), according to the manufacturer's instructions. $2^{-\Delta\Delta Ct}$ was used to determine the relative expression levels of the target genes. All experiments were performed in triplicate.

Enzyme-linked immunosorbent assay

The cellular levels of IL-6 were measured after knockdown of cilia proteins using ELISA. Specifically, the Millipore Human IL-6 ELISA kit (Millipore, Billerica, MA, Cat#RAB0306) was performed according to the manufacturer's instructions and analyzed at 450 nm using a plate reader (BioTek, Winooski, VT). Each sample was performed in triplicate from which the means and standard deviations were calculated.

Immunocytochemistry

Transfection of dBT116 was conducted by transferring 10 µL of shRNA transduction particles (Clone ID TRCN0000199977, SHCLNV, Sigma-Aldrich, St. Louis, MO) in polybrene (10 µg/mL) to a 6 well plate containing 1 x 10^6 bone marrow mononuclear cells in 3 mL of complete dBT116 cell medium. After 24 hours, the medium was changed to virus-free complete DMEM with 10% FBS medium, and puromycin selection was initiated (2 µg/mL, Sigma-Aldrich). Immunocytochemistry experiments were conducted on days 5-7 after antibiotic selection.

Two-well chamber slides were coated with collagen, type I solution (Sigma Aldrich, Burlington, MA) diluted in 70% ethanol per manufacturer protocol. Cultured cells were seeded and incubated overnight at 37 degrees Celsius. Cells were washed in filtered 1X PBS three times and fixed with 4% formaldehyde for 10 minutes at room temperature. Cells were washed three times in filtered 1X PBS, permeabilized in filtered 0.5% Triton X-100 in PBS for 15 minutes, washed four times and incubated with filtered blocking solution (PBS containing 0.15% Glycine and 0.5% BSA) for 60 minutes at room temperature. Cells were then incubated with primary antibodies in 1X PBS for 1 hour, washed three times with 1X PBS, and incubated in the dark with secondary antibodies conjugated to Alexa Fluor 488 and 549 for Arl13B and gamma tubulin, respectively, in 1X PBS for 1 hour at room temperature (1:300, Invitrogen, Waltham, MA). Primary antibodies used were mouse monoclonal Arl13B (1:300, Invitrogen), rabbit monoclonal gamma tubulin (1:300, Invitrogen). Antifade mounting medium with DAPI was used to coverslip the slides (Thermo Fisher, P36935). Images were collected using a Leica DMi8 widefield fluorescence microscope with a 20X objective for DAPI, Alexa 488, and Alexa 549 fluorophores (Leica Biosystems, Buffalo Grove, IL).

Statistical analysis

All data represent at least three individual experiments. For the direct comparison of three or more conditions a one-way analysis of variance was performed, with multiple comparisons analyzed via Newmans-Keuls multiple comparisons test. When directly comparing two conditions a two-tailed student-t test was performed. All comparisons were considered significant with p-values less than 0.05.

Results

Primary cilia loss reduces IL-6 expression in human glioblastoma cells

The function of primary cilia in cancer has been gaining interest over the past two decades, and is known to influence pathogenesis of some CNS neoplasms including medulloblastoma, choroid plexus papilloma, and ependymoma (15). *In vitro* and *in vivo* models of ciliary ablation including knockdown or knockout of *KIF3A* and *IFT88* have been invaluable tools for dissecting and understanding the myriad functions of the primary cilium. *KIF3A* is a microtubule plus end-directed kinesin motor that is required for ciliogenesis (16). Intraflagellar transport protein 88 (IFT88) is necessary for primary cilia assembly via the transport of essential components up the ciliary axoneme (17). Previous immunocytochemistry studies have shown loss of primary cilia following KIF3A or IFT88 knockdown (18, 19). Cell cycle-related kinase (CCRK) now known as CDK20 has been specifically implicated in tumor-mediated immunosuppression by induction of MDSC in response to IL-6 upregulation (20). However, we previously showed that CCRK is required for proper cilia morphogenesis in a knockout mouse model (21). As CCRK is highly overexpressed in glioblastoma and considered an oncogene, we questioned whether the elevated IL-6 expression and the resulting immunosuppressive phenotype was due to CCRK's role in cilia morphology versus other unrelated activity. To that end, we performed siRNA-mediated knockdown of *CCRK* as well as *KIF3A* and *IFT88*. Our hypothesis was that if IL-6 expression was dependent on primary cilia, then all three knockdowns would result in reduction of IL-6 expression. As demonstrated in Figure 1, siRNA targeted against *KIF3A*, *IFT88*, and *CCRK* resulted in robust knockdown of each protein (Figures 1A, B) as well as each corresponding mRNA (Figure 1C). Fluorescence immunocytochemistry confirmed primary cilia loss with CCRK suppression compared to control (Figures 1F, G). Loss of these essential ciliary genes each resulted in a similar loss of IL-6 protein levels through ELISA (Figures 1D, E).

Discussion

Glioblastoma remains a universally incurable and fatal disease. One important characteristic of glioblastoma is profound local and systemic immunosuppression. The latter is the result of a multitude of means by which glioblastoma hijacks the immune system including the kynurenine-tryptophan (IDO-TDO1) pathway, expression of pro-mitogenic, immunosuppressive EVs, the release of anti-inflammatory cytokines, and manipulation of checkpoint proteins (e.g., PD-1, CTLA-4). There is considerable interest in studying the biological roles of primary cilia in glioblastoma as a path for drug development. Prior studies established that cilia are present in glioblastoma cells, with one study finding 8-25% of glioblastoma cells bearing primary cilia at any point in time (22). The same group later found that 60-90% of single clones from patient-derived glioblastoma cell lines were able to generate ciliated offspring (23). While cilia-dependent signaling is present in

10.3389/fonc.2023.1279923

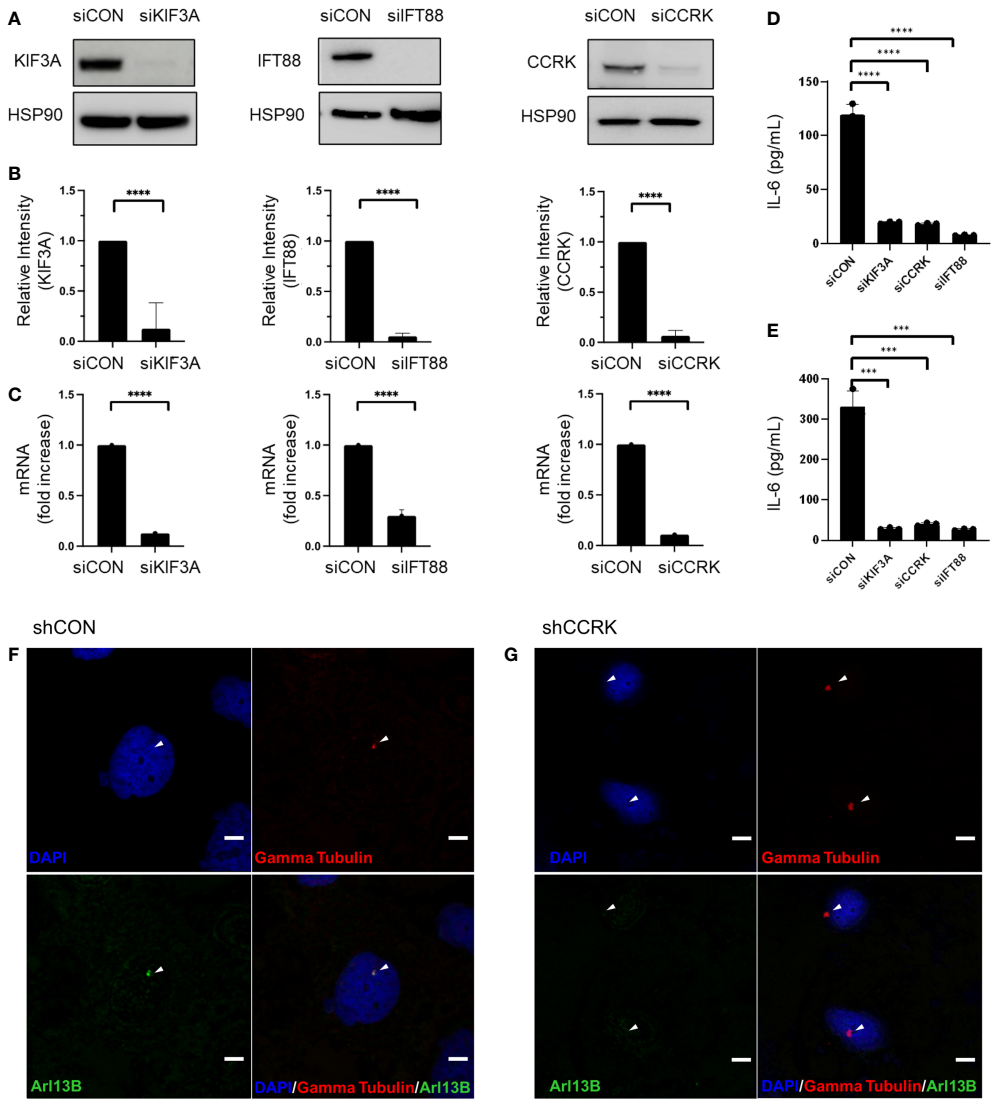

FIGURE 1
IL-6 expression is dependent on primary cilia. Ciliogenesis-required proteins KIF3A, IFT88, and CCRK were depleted via transfection using *siRNA* or a scrambled control (*siCON*). **(A)** dBT114 cell protein levels were assessed with immunoblotting assay with HSP90 serving as loading control. **(B)** Densitometric analysis of the bands are shown. **(C)** The effect of knockdown on *IL-6* mRNA transcription in dBT114 cells was assessed by qRT-PCR. Knockdown of genes required for ciliogenesis resulted in depletion of IL-6 as assessed by ELISA for cell lines **(D)** dBT116 and **(E)** dBT114. All experiments were performed in triplicate. Means were compared using the two-sided student's t-test. *** denotes a P-value <0.005. CCRK was suppressed using shRNA or a scrabbled control (shCON) and immunocytochemistry performed on dBT116 glioblastoma cells for the basal body with gamma tubulin and then primary cilia axoneme with Arl13B. Nuclei were stained with a DAPI counterstain. Representative images were obtained at 20X with DAPI, Alexa 488, and Alexa 549 fluorophores. Scale bar 20 μm. **(F)** Control dBT116 cells (shCON) demonstrating the presence of a basal body as well as an adjoining Arl13B-positive axoneme indicating the presence of a primary cilia. **(G)** CCRK suppressed dBT116 cells (shCCRK) have basal bodies revealed through gamma tubulin staining, but lack primary cilia, as evidenced by the absence of a Arl13B-positive axoneme. Arrows denote structures of interest. **** denotes a P-value <0.001.

glioblastoma, it is unclear how cilia-dependent signaling cascades act in a tumor-promoting or suppressing manner. For instance, disruption of cilia formation in glioblastoma cell lines through knockdown of essential ciliogenesis genes, such as KIF3A or IFT88, had variable effects on tumor growth *in vitro* and *in vivo* (23). There is evidence, however, that treatments aimed to reduce ciliogenesis could enhance conventional glioblastoma therapies. For instance, PCM1-mediated depletion of cilia in patient-derived glioblastoma cell lines led to decreased proliferation and increased sensitivity to temozolomide (TMZ) treatment (24). There is a preponderance of evidence that now links canonical pathways of glioblastoma immune evasion with primary cilia signaling. The objective of this perspectives article is to review evidence supporting potential mechanisms by which cilia-dependent signal transduction contributes to glioblastoma-mediated immunosuppression.

CCRK, IL-6 and the cilia connection

Cell cycle-related kinase (CCRK) plays an evolutionarily conserved role in the assembly of cilia and is highly overexpressed in gliomas where it is thought to play an oncogenic role (21, 25). CCRK knockout

mice display neural tube and skeletal defects identical to those seen in SHH deficient mice; embryonic fibroblasts derived from these mice showed dysmorphic, non-functional cilia (21). *In vitro*, CCRK overexpression reduces cilia frequency and promotes proliferation in the U-251 glioblastoma cell line (26). Conversely, CCRK silencing led to the inhibition of cell growth in high CCRK-expressing U-373 and U-87 cell lines (27). Interestingly, CCRK activity has been linked to cytokine expression in other tumor models. For instance, in the Hepa1-6 hepatocellular carcinoma model, CCRK is necessary for IL-6 expression which led to the expansion of MDSCs in peripheral blood (20). Whether this relationship between IL-6 and CCRK was related to the role of the latter in cilia structure and function has never been explored. We now show a similar statistically significant reduction in IL-6 intracellular concentrations following depletion of proteins required for ciliogenesis (Figure 1). The implication is that it is the primary cilia specifically, and not CCRK per se, that is important in driving IL-6 expression and that the relationship noted between CCRK, IL-6, and MDSC expansion is a direct result of the role of CCRK on primary ciliogenesis. We found a similar result with stable lentiviral transduction of shRNAs against essential ciliogenesis proteins and subsequently performed transcriptomic sequencing (data not shown). A potential mechanism in which cilia signaling may regulate IL-6 expression may be through the GLI1-SHH pathway–the best described cilia-dependent signaling cascade. The binding of SHH to the patched-1 receptor leads to the translocation and accumulation of Smoothened at the ciliary tip and activation of the GLI family of transcription factors, including GLI-1 (28). In a murine model of pancreatic cancer, GLI-1 binds to the IL-6 promoter and increase its expression, leading to a more aggressive phenotype (29). In the absence of activated GLI-1, mice developed only low-grade lesions and at a low frequency. Glioblastoma and pancreatic adenocarcinoma are reliant on EVs and IL-6 for immune modulation and cellular proliferation. Thus, the implication of primary cilia may have far-reaching implications across multiple cancers.

IL-6 has emerged as a potential therapeutic target in treatment of glioblastoma. Rolhion et al. found that glioblastomas displayed significantly higher IL-6 expression compared to other glioma types (3). IL-6 then orchestrates recruitment of tumor-associated macrophages of the M2 suppressive phenotype which produce anti-inflammatory cytokines like IL-10 and TGF-β, which in turn inhibit tumor-associated T-cell invasion and activation (30). Glioblastoma secretion of IL-6 increased PD-L1 expression on peripheral myeloid cells, promoting T cell anergy (31). Levels of IL-6 found in serum and cerebrospinal fluid corresponded to glioma grade, with significant reduction in levels following resection (32). Yang et al. found that knockout of IL-6 reduced the intra-tumoral population of myeloid cells and macrophages and enhanced the population of CD8+ T cells (30). Concomitantly, anti-IL-6 therapy improved overall survival by 30% in a GL261 murine glioblastoma model (30). Analysis of the TCGA dataset revealed that IL-6 and IL-6R mRNA levels were significantly higher in mesenchymal subtype and IDH-wildtype glioblastoma (33). As mentioned previously, the mesenchymal subtype has the highest infiltration of immune cells. The influx and subsequent reprogramming of resident immune cells is due in part to EVs and IL-6, both of which are likely dependent on cilia signaling.

Review of glioblastoma-mediated immunosuppression: EVs, MDSCs, and tumor-associated myeloid cells

Extracellular vesicles (EVs) are a heterogeneous group of lipid membrane-enclosed vesicles released ubiquitously from cells and contain proteins, nucleic acids, and other biological mediators (34). They allow for intercellular communication in both physiologic and pathophysiologic states. Several cancers including breast, pancreas, prostate, and brain produce high levels of EVs which operationalize the local cellular milieu (35–37). Glioblastoma-derived EVs were first described by Skog et al. in 2008 and actively promote glioblastoma cell proliferation and angiogenesis (38). There is now an abundance of contemporary evidence supporting a role for glioblastoma EVs in regulating multiple pathways that ultimately contribute to several key glioblastoma characteristics including tumor-mediated immunosuppression. Hoang-Minh et al. demonstrated that glioblastoma primary cilia produce vesicles that may have overlap with EVs. During G_0 phase, glioblastoma primary cilia had vesicles that appeared to bud from the tip and floated away out of the field of view (15). Furthermore, they found that these vesicles had mitogenic capacity, as their presence promoted tumor cell proliferation. It is possible that these same cilia-derived vesicles also contribute to the local and systemic immunosuppression which are hallmarks of glioblastomas and other cancers.

Local immunosuppression in the glioblastoma microenvironment is dependent on tumor-associated myeloid cells (microglia, macrophages, and monocytes) which constitute up to 30-50% of cells within glioblastoma tissues (39–41). These immune cells migrate via chemotaxis into the glioblastoma tumor microenvironment. Once within the tumor stroma, cells in the tumor microenvironment (including immune cells) are exposed to high EV levels and (and presumably EV content) as well as other soluble factors. Glioblastoma EVs in the tumor microenvironment then stimulate local astrocytes to produce cytokines including CSF2 and 3, IL-4, -6, -10, and -13, which together promote a T-helper type 2 immunosuppressive phenotype (42). The result is immune cell reprogramming into immunosuppressive regulatory cells. Furthermore, glioblastoma EVs enhance the phagocytic capacity of tumor-associated macrophages and enhance the expression of membrane type 1-matrix metalloproteinase in microglia (43). Tumor-derived EVs promote extracellular matrix remodeling (ECM), thus facilitating tumor migration and invasion (44, 45). There is evidence of heterogeneity in EV expression and effects among glioblastoma subtypes. Mesenchymal glioblastoma cells secrete EVs at higher levels compared to those of the classical and pro-neural subclass as identified by mass spectroscopy (43). Low glioma EV concentrations are associated with immune activation and increased migration capacity of peripheral blood mononuclear cells (PBMCs), while high EV concentrations impair PBMC migration (46). The mesenchymal glioblastoma subtype has been associated with the highest infiltration of tumor-associated lymphocytes (47).

Glioblastoma-derived EVs are also implicated in systemic immunosuppression in glioblastoma. These EVs induce monocytes into myeloid-derived suppressor cells (MDSCs) and

nonclassical monocytes (NCMs). Elevated levels of MDSCs are described in a number of cancers including melanoma, renal, gastric, bladder, pancreatic, and gliomas (48). The induction of MDSCs is particularly robust in glioblastomas with circulating MDSCs in glioblastoma patients estimated at up to 12 times greater than that seen in controls (49, 50). Predictably, there are resident NCMs and MDSCs identifiable in freshly resected glioblastoma tissue (5). Jung et al. showed that induction of MDSCs and NCMs was dependent on both PD-L1 and IDO1 expression within the EVs in a mechanism dependent on interferon-γ (51). Interestingly, there was no identifiable direct effect of glioblastoma EVs on T cells. Instead, there was evidence for production of IL-10 by MDSCs and NCMs with resulting T cell inhibition. Glioblastoma patients have higher proportions of tumor-infiltrating regulatory Tregs – an effect of high circulating MDSCs (52, 53). Compared to PBMCs, the ratio of exhausted CD4+ and CD8+ T cells are significantly higher in tumor regions (54). Glioblastoma-infiltrating NK cells show significantly lower cytolytic ability, owing to lower levels of interferon-γ (54). Treg-depletion in a murine glioma model revealed prolonged survival compared to control mice (55). EVs regulate additional key tumor characteristics including remodeling innate and adaptive immune cell behaviors, promoting therapy resistance, glioma stemness, and tissue invasion.

We present a theoretical framework in which primary cilia participate in glioblastoma immune programming (Figure 2) and to present preliminary data supporting this hypothesis. We have shown that through disruption of primary cilia via knockdown of CCRK, KIF3A, or IFT88, there is decreased IL-6 protein expression. It is evident that IL-6 is crucial for coordinating the M2 macrophage response in the glioblastoma microcompartment. Nonetheless, anti-IL-6 monotherapy only showed modest efficacy in *in vivo* preclinical glioblastoma models (30, 31). Glioblastoma EVs are central to intercellular communication among glioblastoma cells, the local milieu, and peripheral immune cells. Primary cilia are a major organelle in extracellular communication and microenvironment sensing, and we cannot exclude the possibility that primary cilia are involved in GBM EV release, especially considering that vesicles have been shown to be released from primary cilia (15). Whether these primary cilia-derived vesicles are indeed EVs and associated with tumor-mediated immunosuppression, is unknown, and should be an avenue for further investigation. Understanding the contribution of primary cilia to GBM tumor immunosuppression may be pivotal in the development of novel therapies.

Implications for glioblastoma immunotherapy

Immunotherapy has garnered interest in glioblastoma research in large part due to the revolutionary improvement in survival noted with several systemic cancers. Unfortunately, no immunotherapy treatments have met the efficacy and safety profiles to be adopted for

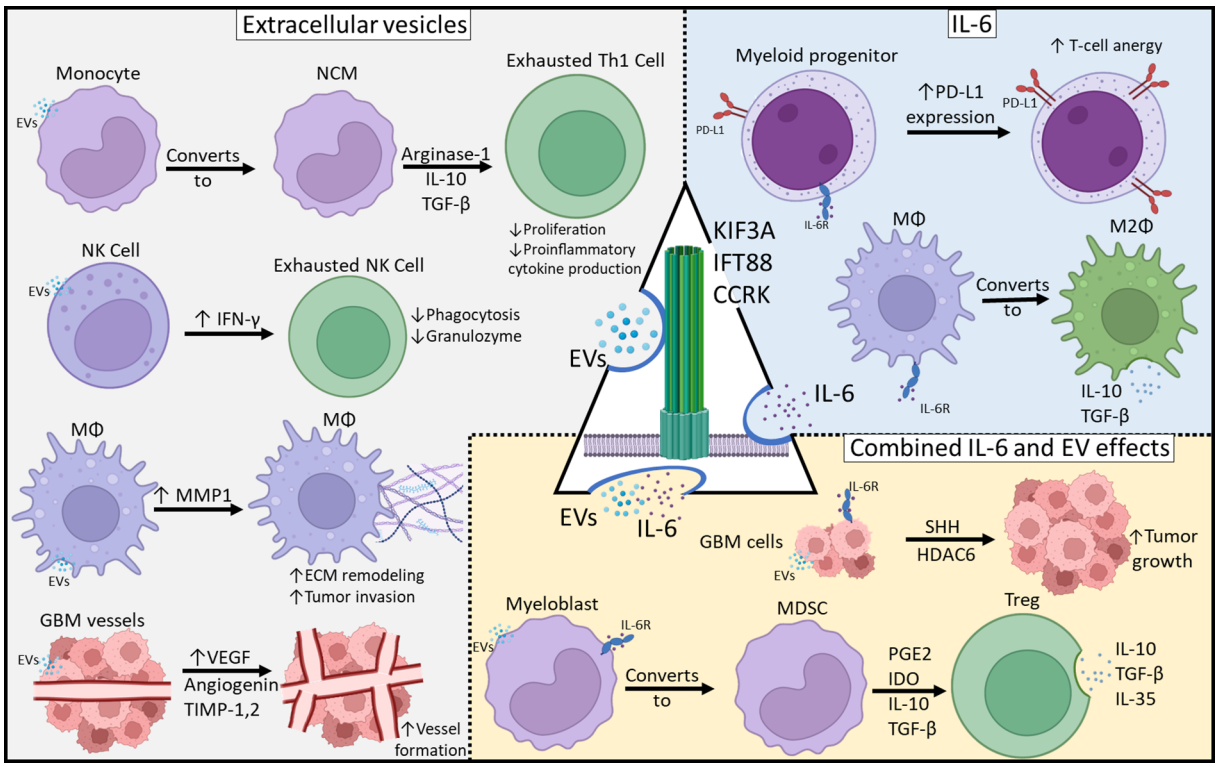

FIGURE 2
Mechanisms of Glioblastoma-Mediated Immunosuppression. Immunosuppressive effects can be categorized as those resulting from EVs, IL-6 or both. Primary cilia may be involved in both EV release as well as IL-6 expression and those may play a central role in tumor-mediated immunosuppression.

widespread clinical use or FDA approval. It is possible that primary cilia, as the principal organelle in microenvironment sensing and communication, is involved in regulation of both IL-6 and glioblastoma EVs. Primary cilia signaling could be therapeutically targeted, leading to suppression of IL-6, EV packaging and secretion, and other cellular cues such as proliferation and invasion. Thus, the immunosuppressive effects of these soluble factors could be potentially reversed, reconstituting antitumor immunity, rendering glioblastomas more amenable to immunotherapy. Further investigation into the interplay between primary cilia signaling and glioblastoma-mediated immunosuppression will be necessary and may lead to the development of novel 'ciliotherapeutic' approaches to glioblastomas.

Conclusions

Glioblastoma is the most common CNS malignancy. It remains universally fatal with only small gains in survival over the last 3 decades. The tumor is genetically complex with several simultaneously dysregulated pathways. There is also profound local and systemic immunosuppression which limit efficacy of immunotherapy. Understanding the interplay between glioblastoma and its microenvironment is key to developing effective immunotherapies. In this perspectives article, we provide evidence for a role of primary cilia in IL-6 release and immunosuppression. We also suggest a potential role of primary cilia in EV release. There is potential for novel cilia-related therapeutic strategies which would be welcomed addition in the armamentarium against this deadly disease.

Data availability statement

The raw data supporting the conclusions of the article will be made available by the authors upon request.

Ethics statement

Ethical approval was not required for the studies on humans in accordance with the local legislation and institutional requirements because only commercially available established cell lines were used.

Author contributions

ML: Writing – original draft, Writing – review & editing. EW: Data curation, Writing – original draft, Writing – review & editing. FG: Writing – review & editing. LA: Writing – review & editing. M-YJ: Data curation, Writing – review & editing. EB: Supervision, Writing – review & editing. DB: Conceptualization, Supervision, Writing – review & editing.

Funding

The author(s) declare financial support was received for the research, authorship, and/or publication of this article. This work was supported financially by the Intramural Research Program of the National Institute of Neurological Disorders and Stroke and the National Cancer Institute in Bethesda, Maryland.

Acknowledgments

The authors express gratitude to Michelle Moore and Lisa Martin for their tireless administrative support of the Neurosurgical Oncology Unit.

Conflict of interest

The authors declare that the research was conducted in the absence of any commercial or financial relationships that could be construed as a potential conflict of interest.

Publisher's note

All claims expressed in this article are solely those of the authors and do not necessarily represent those of their affiliated organizations, or those of the publisher, the editors and the reviewers. Any product that may be evaluated in this article, or claim that may be made by its manufacturer, is not guaranteed or endorsed by the publisher.

References

1. Ostrom QT, Price M, Neff C, Cioffi G, Waite KA, Kruchko C, et al. CBTRUS statistical report: primary brain and other central nervous system tumors diagnosed in the United States in 2015–2019. *Neuro-Oncology* (2022) 24:v1–v95. doi: 10.1093/neuonc/noac202

2. Hosseinalizadeh H, Mahmoodpour M, Samadani AA, Roudkenar MH. The immunosuppressive role of indoleamine 2, 3-dioxygenase in glioblastoma: mechanism of action and immunotherapeutic strategies. *Med Oncol* (2022) 39:130. doi: 10.1007/s12032-022-01724-w

3. Rolhion C, Penault-Llorca F, Kémény JL, Lemaire JJ, Jullien C, Labit-Bouvier C, et al. Interleukin-6 overexpression as a marker of Malignancy in human gliomas. *J Neurosurg* (2001) 94:97–101. doi: 10.3171/jns.2001.94.1.0097

4. Huettner C, Paulus W, Roggendorf W. Messenger RNA expression of the immunosuppressive cytokine IL-10 in human gliomas. *Am J Pathol* (1995) 146:317–22.

5. Himes BT, Peterson TE, de Mooij T, Garcia LMC, Jung M-Y, Uhm S, et al. The role of extracellular vesicles and PD-L1 in glioblastoma-mediated immunosuppressive monocyte induction. *Neuro-Oncology* (2020) 22:967–78. doi: 10.1093/neuonc/noaa029

6. Christensen ST, Clement CA, Satir P, Pedersen LB. Primary cilia and coordination of receptor tyrosine kinase (RTK) signalling. *J Pathol* (2012) 226:172–84. doi: 10.1002/path.3004

7. Rohatgi R, Milenkovic L, Scott MP. Patched1 regulates hedgehog signaling at the primary cilium. *Science* (2007) 317:372–6. doi: 10.1126/science.1139740

8. Simons M, Gloy J, Ganner A, Bullerkotte A, Bashkurov M, Krönig C, et al. Inversin, the gene product mutated in nephronophthisis type II, functions as a molecular switch between Wnt signaling pathways. *Nat Genet* (2005) 37:537–43. doi: 10.1038/ng1552

9. Ten Dijke P, Egorova AD, Goumans M-JT, Poelmann RE, Hierck BP. TGF-β signaling in endothelial-to-mesenchymal transition: the role of shear stress and primary cilia. *Sci Signaling* (2012) 5:pt2–2. doi: 10.1126/scisignal.2002722

10. Ezratty EJ, Stokes N, Chai S, Shah AS, Williams SE, Fuchs E. A role for the primary cilium in Notch signaling and epidermal differentiation during skin development. *Cell* (2011) 145:1129–41. doi: 10.1016/j.cell.2011.05.030

11. Lattao R, Kovács L, Glover DM, Centrioles T. Centrosomes, basal bodies, and cilia of drosophila melanogaster. *Genetics* (2017) 206:33–53. doi: 10.1534/genetics.116.198168

12. Seeley ES, Nachury MV. The perennial organelle: assembly and disassembly of the primary cilium. *J Cell Sci* (2010) 123:511–8. doi: 10.1242/jcs.061093

13. Seeley ES, Nachury MV. Constructing and deconstructing roles for the primary cilium in tissue architecture and cancer. *Methods Cell Biol* (2009) 94:299–313. doi: 10.1016/S0091-679X(08)94015-2

14. Zingg D, Debbache J, Peña-Hernández R, Antunes AT, Schaefer SM, Cheng PF, et al. EZH2-mediated primary cilium deconstruction drives metastatic melanoma formation. *Cancer Cell* (2018) 34:69–84.e14. doi: 10.1016/j.ccell.2018.06.001

15. Hoang-Minh LB, Dutra-Clarke M, Breunig JJ, Sarkisian MR. Glioma cell proliferation is enhanced in the presence of tumor-derived cilia vesicles. *Cilia* (2018) 7:6. doi: 10.1186/s13630-018-0060-5

16. Cullen CL, O'Rourke M, Beasley SJ, Auderset L, Zhen Y, Pepper RE, et al. Kif3a deletion prevents primary cilia assembly on oligodendrocyte progenitor cells, reduces oligodendrogenesis and impairs fine motor function. *Glia* (2021) 69:1184–203. doi: 10.1002/glia.23957

17. Wang W, Jack BM, Wang HH, Kavanaugh MA, Maser RL, Tran PV. Intraflagellar transport proteins as regulators of primary cilia length. *Front Cell Dev Biol* (2021) 9:661350. doi: 10.3389/fcell.2021.661350

18. Lee J, Yi S, Won M, Song YS, Yi H-S, Park YJ, et al. Loss-of-function of IFT88 determines metabolic phenotypes in thyroid cancer. *Oncogene* (2018) 37:4455–74. doi: 10.1038/s41388-018-0211-6

19. Chen J-L, Chang C-H, Tsai J-W. Gli2 rescues delays in brain development induced by Kif3a dysfunction. *Cereb Cortex* (2019) 29:751–64. doi: 10.1093/cercor/bhx356

20. Zhou J, Liu M, Sun H, Feng Y, Xu L, Chan AWH, et al. Hepatoma-intrinsic CCRK inhibition diminishes myeloid-derived suppressor cell immunosuppression and enhances immune-checkpoint blockade efficacy. *Gut* (2018) 67:931–44. doi: 10.1136/gutjnl-2017-314032

21. Snouffer A, Brown D, Lee H, Walsh J, Lupu F, Norman R, et al. Cell Cycle-Related Kinase (CCRK) regulates ciliogenesis and Hedgehog signaling in mice. *PloS Genet* (2017) 13:e1006912. doi: 10.1371/journal.pgen.1006912

22. Sarkisian MR, Siebzehnrubl D, Hoang-Minh L, Deleyrolle L, Silver DJ, Siebzehnrubl FA, et al. Detection of primary cilia in human glioblastoma. *J Neurooncol* (2014) 117:15–24. doi: 10.1007/s11060-013-1340-y

23. Hoang-Minh LB, Deleyrolle LP, Siebzehnrubl D, Ugartemendia G, Futch H, Griffith B, et al. Disruption of KIF3A in patient-derived glioblastoma cells: effects on ciliogenesis, hedgehog sensitivity, and tumorigenesis. *Oncotarget* (2016) 7:7029–43. doi: 10.18632/oncotarget.6854

24. Hoang-Minh LB, Deleyrolle LP, Nakamura NS, Parker AK, Martuscello RT, Reynolds BA, et al. PCM1 depletion inhibits glioblastoma cell ciliogenesis and increases cell death and sensitivity to temozolomide. *Trans Oncol* (2016) 9:392–402. doi: 10.1016/j.tranon.2016.08.006

25. Ng SS, Cheung Y-T, An X-M, Chen YC, Li M, Hoi-Yee Li G, et al. Cell cycle–related kinase: A novel candidate oncogene in human glioblastoma. *J Natl Cancer Institute* (2007) 99:936–48. doi: 10.1093/jnci/djm011

26. Yang Y, Roine N, Mäkelä TP. CCRK depletion inhibits glioblastoma cell proliferation in a cilium-dependent manner. *EMBO Rep* (2013) 14:741–7. doi: 10.1038/embor.2013.80

27. Ng SS, Cheung YT, An XM, Chen YC, Li M, Li GH, et al. Cell cycle-related kinase: a novel candidate oncogene in human glioblastoma. *J Natl Cancer Inst* (2007) 99:936–48. doi: 10.1093/jnci/djm011

28. Niewiadomski P, Kong JH, Ahrends R, Ma Y, Humke EW, Khan S, et al. Gli protein activity is controlled by multisite phosphorylation in vertebrate Hedgehog signaling. *Cell Rep* (2014) 6:168–81. doi: 10.1016/j.celrep.2013.12.003

29. Mills LD, Zhang Y, Marler RJ, Herreros-Villanueva M, Zhang L, Almada LL, et al. Loss of the transcription factor GLI1 identifies a signaling network in the tumor microenvironment mediating KRAS oncogene-induced transformation. *J Biol Chem* (2013) 288:11786–94. doi: 10.1074/jbc.M112.438846

30. Yang F, He Z, Duan H, Zhang D, Li J, Yang H, et al. Synergistic immunotherapy of glioblastoma by dual targeting of IL-6 and CD40. *Nat Commun* (2021) 12:3424. doi: 10.1038/s41467-021-23832-3

31. Lamano JB, Lamano JB, Li YD, DiDomenico JD, Choy W, Veliceasa D, et al. Glioblastoma-derived IL6 induces immunosuppressive peripheral myeloid cell PD-L1 and promotes tumor growth. *Clin Cancer Res* (2019) 25:3643–57. doi: 10.1158/1078-0432.CCR-18-2402

32. Shan Y, He X, Song W, Han D, Niu J, Wang J. Role of IL-6 in the invasiveness and prognosis of glioma. *Int J Clin Exp Med* (2015) 8:9114–20.

33. Jiang Y, Han S, Cheng W, Wang Z, Wu A. NFAT1-regulated IL6 signalling contributes to aggressive phenotypes of glioma. *Cell Communication Signaling* (2017) 15:1–11. doi: 10.1186/s12964-017-0210-1

34. Musatova OE, Rubtsov YP. Effects of glioblastoma-derived extracellular vesicles on the functions of immune cells. *Front Cell Dev Biol* (2023) 11:1060000. doi: 10.3389/fcell.2023.1060000

35. Nabet BY, Qiu Y, Shabason JE, Wu TJ, Yoon T, Kim BC, et al. Exosome RNA unshielding couples stromal activation to pattern recognition receptor signaling in cancer. *Cell* (2017) 170:352–366.e13. doi: 10.1016/j.cell.2017.06.031

36. Hinzman CP, Singh B, Bansal S, Li Y, Iliuk A, Girgis M, et al. A multi-omics approach identifies pancreatic cancer cell extracellular vesicles as mediators of the unfolded protein response in normal pancreatic epithelial cells. *J Extracellular Vesicles* (2022) 11:e12232. doi: 10.1002/jev2.12232

37. Clos-Garcia M, Loizaga-Iriarte A, Zuñiga-Garcia P, Sánchez-Mosquera P, Rosa Cortazar A, González E, et al. Metabolic alterations in urine extracellular vesicles are associated to prostate cancer pathogenesis and progression. *J Extracellular Vesicles* (2018) 7:1470442. doi: 10.1080/20013078.2018.1470442

38. Skog J, Würdinger T, Van Rijn S, Meijer DH, Gainche L, Curry WT Jr., et al. Glioblastoma microvesicles transport RNA and proteins that promote tumour growth and provide diagnostic biomarkers. *Nat Cell Biol* (2008) 10:1470–6. doi: 10.1038/ncb1800

39. Rossi M, Hughes J, Esiri M, Coakham H, Brownell D. Immunohistological study of mononuclear cell infiltrate in Malignant gliomas. *Acta neuropathologica* (1987) 74:269–77. doi: 10.1007/BF00688191

40. Morantz RA, Wood GW, Foster M, Clark M, Gollahon K. Macrophages in experimental and human brain tumors: Part 2: Studies of the macrophage content of human brain tumors. *J Neurosurg* (1979) 50:305–11. doi: 10.3171/jns.1979.50.3.0305

41. Badie B, Schartner JM. Flow cytometric characterization of tumor-associated macrophages in experimental gliomas. *Neurosurgery* (2000) 46:957–61;discussion 961-2. doi: 10.1097/00006123-200004000-00035

42. Harshyne LA, Nasca BJ, Kenyon LC, Andrews DW, Hooper DC. Serum exosomes and cytokines promote a T-helper cell type 2 environment in the peripheral blood of glioblastoma patients. *Neuro Oncol* (2016) 18:206–15. doi: 10.1093/neuonc/nov107

43. de Vrij J, Maas SLN, Kwappenberg KMC, Schnoor R, Kleijn A, Dekker L, et al. Glioblastoma-derived extracellular vesicles modify the phenotype of monocytic cells. *Int J Cancer* (2015) 137:1630–42. doi: 10.1002/ijc.29521

44. Atay S, Banskota S, Crow J, Sethi G, Rink L, Godwin AK. Oncogenic KIT-containing exosomes increase gastrointestinal stromal tumor cell invasion. *Proc Natl Acad Sci* (2014) 111:711–6. doi: 10.1073/pnas.1310501111

45. Mu W, Rana S, Zöller M. Host matrix modulation by tumor exosomes promotes motility and invasiveness. *Neoplasia* (2013) 15:875–87. doi: 10.1593/neo.13786

46. Hellwinkel JE, Redzic JS, Harland TA, Gunaydin D, Anchordoquy TJ, Graner MW. Glioma-derived extracellular vesicles selectively suppress immune responses. *Neuro-Oncology* (2015) 18:497–506. doi: 10.1093/neuonc/nov170

47. Rutledge WC, Kong J, Gao J, Gutman DA, Cooper LA, Appin C, et al. Tumor-infiltrating lymphocytes in glioblastoma are associated with specific genomic alterations and related to transcriptional class. *Clin Cancer Res* (2013) 19:4951–60. doi: 10.1158/1078-0432.CCR-13-0551

48. Serafini P, Borrello I, Bronte V. Myeloid suppressor cells in cancer: recruitment, phenotype, properties, and mechanisms of immune suppression. *Semin Cancer Biol* (2006) pp:53–65. doi: 10.1016/j.semcancer.2005.07.005

49. Raychaudhuri B, Rayman P, Huang P, Grabowski M, Hambardzumyan D, Finke JH, et al. Myeloid derived suppressor cell infiltration of murine and human gliomas is associated with reduction of tumor infiltrating lymphocytes. *J neuro-oncology* (2015) 122:293–301. doi: 10.1007/s11060-015-1720-6

50. Raychaudhuri B, Rayman P, Ireland J, Ko J, Rini B, Borden EC, et al. Myeloid-derived suppressor cell accumulation and function in patients with newly diagnosed glioblastoma. *Neuro-oncology* (2011) 13:591–9. doi: 10.1093/neuonc/nor042

51. Jung M-Y, Aibaidula A, Brown DA, Himes BT, Cumba Garcia LM, Parney IF. Superinduction of immunosuppressive glioblastoma extracellular vesicles by IFN-γ through PD-L1 and IDO1. *Neuro-Oncology Adv* (2022) 4:1–11. doi: 10.1093/noajnl/vdac017

52. Fecci PE, Mitchell DA, Whitesides JF, Xie W, Friedman AH, Archer GE, et al. Increased regulatory T-cell fraction amidst a diminished CD4 compartment explains cellular immune defects in patients with Malignant glioma. *Cancer Res* (2006) 66:3294–302. doi: 10.1158/0008-5472.CAN-05-3773

53. Andaloussi AE, Lesniak MS. An increase in CD4+ CD25+ FOXP3+ regulatory T cells in tumor-infiltrating lymphocytes of human glioblastoma multiforme. *Neuro-oncology* (2006) 8:234–43. doi: 10.1215/15228517-2006-006

54. Fu W, Wang W, Li H, Jiao Y, Huo R, Yan Z, et al. Single-cell atlas reveals complexity of the immunosuppressive microenvironment of initial and recurrent glioblastoma. *Front Immunol* (2020) 11:835. doi: 10.3389/fimmu.2020.00835

55. Poirier M-D, Haban H, El Andaloussi A. A combination of systemic and intracranial anti-CD25 immunotherapy elicits a long-time survival in murine model of glioma. *J Oncol* (2009) 2009:963037. doi: 10.1155/2009/963037

frontiers | Frontiers in Pharmacology

TYPE Original Research
PUBLISHED 16 January 2024
DOI 10.3389/fphar.2023.1259051

Check for updates

OPEN ACCESS

EDITED BY
Mariana Magalhães,
University of Coimbra, Portugal

REVIEWED BY
Wantao Wu,
Central South University, China
Peidong Liu,
First Affiliated Hospital of Zhengzhou University, China

*CORRESPONDENCE
Zhong Wang,
wangzhong761@163.com
Yanbing Yu,
yuyanbing123@126.com

RECEIVED 15 July 2023
ACCEPTED 11 December 2023
PUBLISHED 16 January 2024

CITATION
Yang Y, Teng H, Zhang Y, Wang F, Tang L, Zhang C, Hu Z, Chen Y, Ge Y, Wang Z and Yu Y (2024), A glycosylation-related gene signature predicts prognosis, immune microenvironment infiltration, and drug sensitivity in glioma.
Front. Pharmacol. 14:1259051.
doi: 10.3389/fphar.2023.1259051

COPYRIGHT
© 2024 Yang, Teng, Zhang, Wang, Tang, Zhang, Hu, Chen, Ge, Wang and Yu. This is an open-access article distributed under the terms of the Creative Commons Attribution License (CC BY). The use, distribution or reproduction in other forums is permitted, provided the original author(s) and the copyright owner(s) are credited and that the original publication in this journal is cited, in accordance with accepted academic practice. No use, distribution or reproduction is permitted which does not comply with these terms.

A glycosylation-related gene signature predicts prognosis, immune microenvironment infiltration, and drug sensitivity in glioma

Yanbo Yang[1], Haiying Teng[2,3], Yulian Zhang[4], Fei Wang[2,3], Liyan Tang[2], Chuanpeng Zhang[5,4], Ziyi Hu[2,3], Yuxuan Chen[2,3], Yi Ge[6], Zhong Wang[2]* and Yanbing Yu[1]*

[1]China-Japan Friendship Hospital, Chinese Academy of Medical Sciences and Peking Union Medical College, Beijing, China, [2]Department of Neurosurgery and Brain and Nerve Research Laboratory, The First Affiliated Hospital of Soochow University, Suzhou, Jiangsu, China, [3]Suzhou Medical College of Soochow University, Suzhou, Jiangsu, China, [4]Department of Neurosurgery, China-Japan Friendship Hospital, Beijing, China, [5]Department of Neurosurgery, Peking University China-Japan Friendship School of Clinical Medicine, Beijing, China, [6]The Affiliated Changzhou Second People's Hospital of Nanjing Medical University, Nanjing, Jiangsu, China

Glioma represents the most common primary cancer of the central nervous system in adults. Glycosylation is a prevalent post-translational modification that occurs in eukaryotic cells, leading to a wide array of modifications on proteins. We obtained the clinical information, bulk RNA-seq data, and single-cell RNA sequencing (scRNA-seq) from The Cancer Genome Atlas (TCGA), Chinese Glioma Genome Atlas (CGGA), Gene Expression Omnibus (GEO), and Repository of Molecular Brain Neoplasia Data (Rembrandt) databases. RNA sequencing data for normal brain tissues were accessed from the Genotype-Tissue Expression (GTEx) database. Then, the glycosylation genes that were differentially expressed were identified and further subjected to variable selection using a least absolute shrinkage and selection operator (LASSO)-regularized Cox model. We further conducted enrichment analysis, qPCR, nomogram, and single-cell transcriptome to detect the glycosylation signature. Drug sensitivity analysis was also conducted. A five-gene glycosylation signature (*CHPF2*, *PYGL*, *GALNT13*, *EXT2*, and *COLGALT2*) classified patients into low- or high-risk groups. Survival analysis, qPCR, ROC curves, and stratified analysis revealed worse outcomes in the high-risk group. Furthermore, GSEA and immune infiltration analysis indicated that the glycosylation signature has the potential to predict the immune response in glioma. In addition, four drugs (crizotinib, lapatinib, nilotinib, and topotecan) showed different responses between the two risk groups. Glioma cells had been classified into seven lines based on single-cell expression profiles. The five-gene glycosylation signature can accurately predict the prognosis of glioma and may offer additional guidance for immunotherapy.

KEYWORDS

glycosylation, glioma, tumor microenvironment, prognosis, immunity, drug sensitivity

Introduction

Histologically, there exist over 100 distinct primary brain and central nervous system tumors (Davis, 2018). Glioma is the most prevalent form of primary cancer in the central nervous system of adults, with an annual diagnosis rate of 2.96 cases per 100,000 individuals in the United States (Fogh et al., 2010), accounting for 15% of all brain tumors (Ostrom et al., 2018). However, despite surgery, radiotherapy, and chemotherapy, most gliomas inevitably recur (Barthel et al., 2019). Approximately 52%–62% of patients have a recurrence within 5 years. Patients with glioblastoma multiforme (GBM), the most malignant glioma (World Health Organization [WHO] grade IV), using the current standard of care, have an average lifespan of 14 months after diagnosis (Van Meir et al., 2010). There are still fatal prognoses and high rates of mortality and recurrence (Wang et al., 2017).

Glycosylation is one of the most abundant and diverse forms of post-translational modification of proteins in eukaryotic cells, where sugar molecules are attached to nascent proteins (Schjoldager et al., 2020). The formation of glycosidic bonds is a dynamic process regulated by various enzymes, such as glycosyltransferases and glycosidases. The nitrogen of asparagine (N-glycans) or the oxygen of serine or threonine (O-glycans) is usually responsible for attaching glycan chains to their polypeptide backbone in glycoproteins (Rodrigues et al., 2018). Glycosylation plays a crucial role in the molecular and cellular mechanisms of tumorigenesis. Tumor growth relies on cancer cells' ability to bypass cellular division checkpoints, evade immune surveillance and death signals, and migrate to metastatic sites. Glycosylation plays a critical role in all of these processes (Reily et al., 2019). Although glycosylation has been implicated in various biological processes and diseases, the specific role of glycosylation in glioma remains a relatively unexplored area. Investigating the functional roles of the identified gene signature can provide insights into the underlying mechanisms through which glycosylation influences glioma development, invasion, and therapeutic response. In this study, we investigated the roles of core glycosylation genes in glioma and established a glycosylation gene model to predict glioma patient survival and tumor immune microenvironment, elucidating that the underlying correlation is of great clinical significance. To the best of our knowledge, this is the first paper to investigate the relationship between glioma and glycosylation, and we hope our research can fill the research gap and inspire others.

Methods

Data collection

We retrieved clinical and mRNA sequencing data from The Cancer Genome Atlas (TCGA, https://portal.gdc.cancer.gov/), Chinese Glioma Genome Atlas (CGGA, http://www.cgga.org.cn/), and Repository of Molecular Brain Neoplasia Data (Rembrandt, https://gtexportal.org/home/) databases. RNA sequencing data for normal brain tissues were obtained from the Genotype-Tissue Expression (GTEx) database. Raw data were collected from the corresponding databases, filtered, and normalized using the EDASeq package (Bullard et al., 2010) (version 3.15). Batch effects were corrected using the R package ComBat (Martin et al., 2015) (version 3.15).

Univariate Cox regression analysis and differential expression analysis

We obtained 168 glycosyltransferase-related genes through public databases. Then, we performed univariate Cox regression with the genes of interest in TCGA and CGGA cohorts. Genes that showed an adjusted p-value of less than 0.05 were considered significantly correlated with survival. In addition, we conducted a differential expression analysis of gliomas and normal brain tissue using TCGA and GTEx datasets. The R package edgeR (Robinson et al., 2010) (version 3.15) was used to verify the expression fold change value (expressed as a logFC value) and statistical significance. Genes with an absolute logFC value greater than 1 and a false discovery rate less than 0.05 were regarded as differentially expressed.

Construction and validation of the model

The overlapping genes were subjected to variable selection using a least absolute shrinkage and selection operator (LASSO)-regularized Cox model. We randomly divided TCGA dataset into a training set and a testing set with a ratio of 4:1. The C-index was used for model performance evaluation. A bidirectional step-wise variable selection was performed. We used the R packages glmnet (Simon et al., 2011) (version 4.1-4), StepReg (Variyath and Brobbey, 2020) (version 1.4.3), and survival (Bair and Tibshirani, 2004) (version 3.3-1) for fitting and establishing the survival model. The forest plot was performed using the R package "survminer." The risk score for each patient was calculated as follows:

$$\boldsymbol{RiskScore} = \sum_{i=1}^{n} (\boldsymbol{Coef}^{*}\boldsymbol{xi}).$$

The median risk score served as the threshold for classifying patients into high- or low-risk groups. The model was then validated in TCGA testing set and externally validated through CGGA and Rembrandt sets. ROC curves and AUC values were generated using the R package timeROC (Blanche et al., 2013) (version 0.4).

Construction and evaluation of a nomogram

A nomogram was constructed to clarify whether the risk score was an independent prognostic predictor of glioma. Univariate and multivariate Cox regression analyses were performed to identify the independent prognostic factors for TCGA and CGGA datasets. We investigated the probability of 1-, 3-, and 5-year OS rates of patients with glioma based on the glycosylation score combined with clinical information including tumor grade, patient age, MGMT methylation, and IDH mutations. Then, we constructed a nomogram using the regplot package (version 1.1). The calibration plot and ROC curve were also performed to assess the accuracy of the nomogram for OS prediction.

Pathway enrichment analysis and GSEA

We conducted a differential analysis between high-risk and low-risk groups using edgeR. Genes that met the criteria of absolute logFC value > 1 and false discovery rate <0.05 were identified as differentially expressed. We then conducted Gene Ontology and KEGG pathway enrichment analyses for the top differentially expressed genes. In addition, GSEA was also conducted. The R package clusterProfiler (Wu et al., 2021) (version 3.15) was used for all the above-mentioned enrichment analyses. These enrichment analyses aimed to identify molecular mechanisms that indicate a worse prognosis between the two subgroups.

Cell line culture, qPCR, and IHC

We used quantitative polymerase chain reaction (qPCR) to detect glycosylation genes in cell lines. Glioma cell lines, namely, U87, T98G, A172, U251, HMC3 microglial cell line, and HA 1800 normal human astrocyte cell line, were obtained from ScienCell Research Laboratory, Cell Bank of the Chinese Academy of Sciences, and ATCC. The cells were cultured and maintained in DMEM supplemented with 10% fetal bovine serum. We extracted RNA using an mRNA extraction kit (Yeasen) following the instructions of the manufacturer. RNA was then reverse-transcribed. We used the qPCR SYBR Green Master Mix (Yeasen Biotechnology Co., Ltd., China) as a PCR indicator, and the qPCR process was performed using the QuantStudio Q5 Real-Time PCR System. The column plot was made using GraphPad Prism 8 software. After accessing the IHC images for each candidate glycosylation gene in glioma and normal tissue samples from The Human Protein Atlas database (HPA database, https://www.proteinatlas.org/), we assessed the staining intensity of each tissue according to the HPA database standards.

Mutation burden and waterfall plot

We acquired the single nucleotide variation data with aliquot ensemble somatic variant merging and masking workflow from TCGA database through the TCGAbiolinks package (Colaprico et al., 2016). The mutation burden was calculated and then plotted using the ggbetweenstats package. The GenVisR package (Skidmore et al., 2016) was used to produce waterfall plots with the top 15 most commonly mutated genes in each group.

Immune filtration

To study the immune infiltration level of gliomas, we applied the ESTIMATE algorithm (Yoshihara et al., 2013) to predict the immune fraction and stromal fraction for each sample. In addition, the fraction of each major immune cell was predicted and calculated through the xCell (Aran et al., 2017) algorithm. We created a heatmap to assess the differences between the high-risk and low-risk groups in the abundance of 32 immune cells and the stromal score, immune score, ESTIMATE score, and tumor purity.

Drug sensitivity analysis

Cancer Cell Line Encyclopedia (CCLE) and Drug Sensitivity in Cancer v2 (GDSC2) were downloaded through the "PharmacoGx" package (Smirnov et al., 2016). This package enables efficient implementation of curated annotations of compounds, cell lines, and molecular features, facilitating integration and comparisons between different pharmacogenomic datasets. *In vivo* drug responses in cancer patients were predicted using the "oncoPredict" package (Maeser et al., 2021). The calcPhenotype function is capable of predicting the half-maximal inhibitory concentration (IC_{50}) of drugs for glioma patients by fitting a ridge model, in which the testing sets are RNA-seq profiles of glioma patients in TCGA or CGGA and the training sets are the gene expression profiles of tissues and IC_{50} of the cancer cell lines to drugs from GDSC2 and CCLE. Drugs with the consistent direction of response (resistant or sensitive) in different combinations of training and testing sets were finally selected. The IC_{50} values from experiments of selected drugs between different tissues were then visualized using PharmacoDB 2.0 (https://pharmacodb.ca/) (Feizi et al., 2022).

scRNA-seq data processing and cell–cell communication of glioma samples

Single-cell transcriptomes of glioma samples were downloaded from the GEO database (https://www.ncbi.nlm.nih.gov/geo/) (GSE167960). One WHO grade IV glioma and five WHO grade III gliomas were used for the analysis of cell populations and the expression of the markers of glial lineage. A total of 28,298 cells were analyzed using the R package "Seurat." The FindIntegrationAnchors and IntegrateData functions were applied to remove the batch effect among different samples. Cells were clustered using FindNeighbors and FindClusters functions with a resolution of 0.5. The uniform manifold approximation and projection (UMAP) algorithm was used to reduce dimensionality. Cell types were identified through the use of marker genes from the CellMarker database (http://xteam.xbio.top/CellMarker). We used the "CellChat" packages to create CellChat objects. Then, the major ligand–receptor interactions in humans were evaluated using the "CellChatDB.human" database to perform the analysis of intercellular communication networks from annotated scRNA-seq data for seven cell clusters in all glioma samples. We then conducted intercellular communication networks on tumor-associated pathways.

Results

Identification and construction of a glycosylation gene prognostic model

The flow chart of our study is shown in Figure 1A. First, we chose genes that are differently expressed in normal brain tissue and glioma using normal brain tissue expression data from the GTEx dataset and glioma expression data from TCGA dataset. Genes with an absolute logFC value greater than 1 and a false discovery rate below 0.05 were identified as differentially expressed. The gene expression heatmap is shown in Figure 1B. Univariate Cox regression analysis was conducted to investigate prognostic-related gene analyses using TCGA dataset. We chose

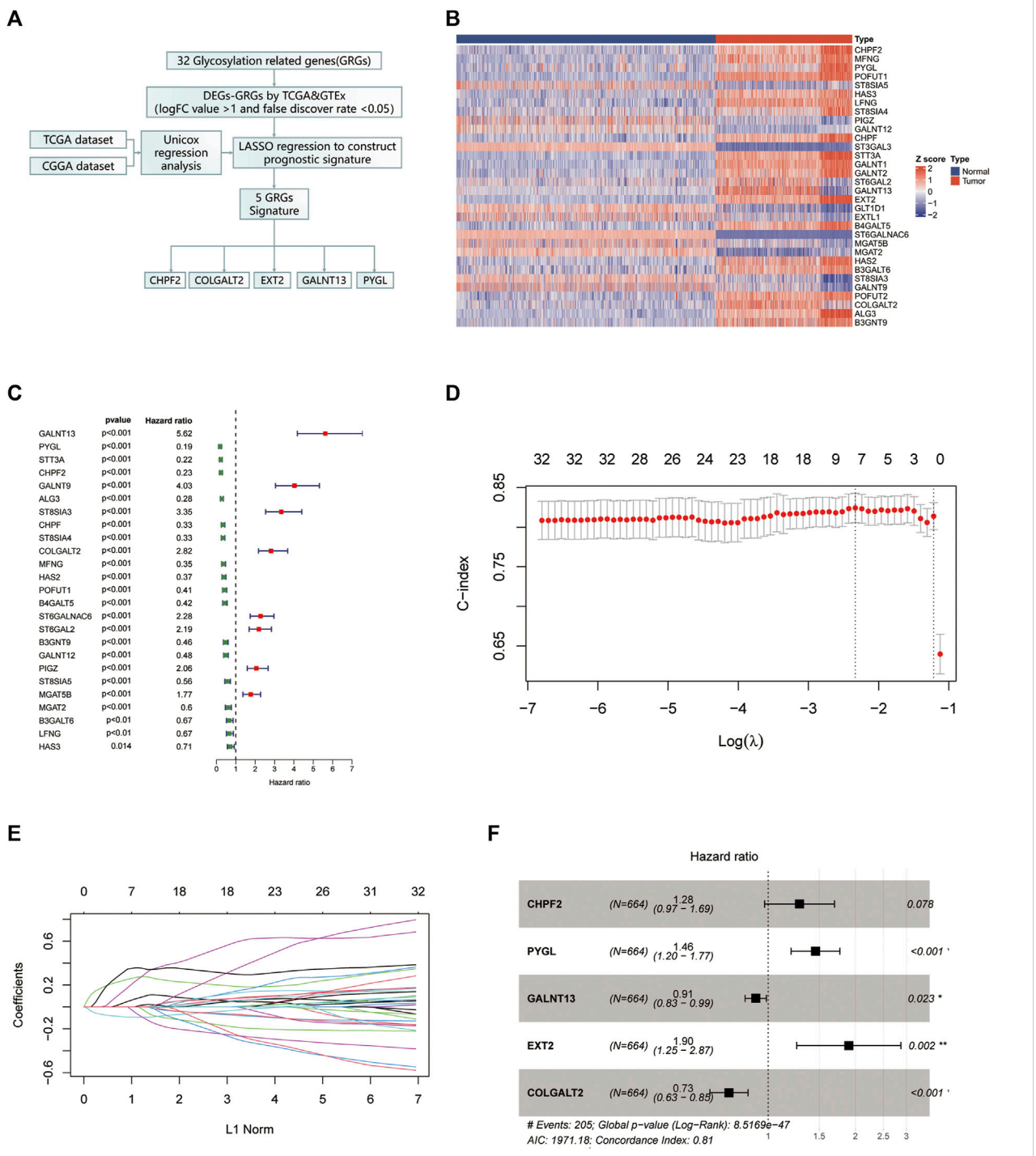

FIGURE 1
Identification of the glycosylation gene signature using LASSO-Cox regression. **(A)** Flow chart of our study. **(B)** The protein–protein interaction network was performed on the Metascape website. **(C)** Gene Ontology enrichment analysis was performed on the Metascape website. **(D)** Heatmap of all glycosylation genes between the normal brain and glioma tissues. **(E)** Forest plot of univariate Cox regression of differentially expressed glycosylation genes. **(F)** LASSO was used to conduct the log (lambda) sequence plot of glycosylation genes. **(G)** LASSO coefficient profiles of glycosylation genes in TCGA training dataset. **(H)** Forest plot of five glycosylation signature genes. LASSO, least absolute shrinkage and selection operator; TCGA, The Cancer Genome Atlas. $^{**}p < 0.01$, $^{***}p < 0.001$.

32 glycosylation genes shared by the three datasets. The forest plot of the selected genes is shown in Figure 1C. Then, we performed a LASSO regression with fit measured by the C-index. The model fit across different lambda values is shown in Figure 1D. The coefficient plot is shown in Figure 1E. The selected five-gene model with their corresponding HR value is plotted in Figure 1F. The Venn plot of overlapping genes between TCGA, CGGA, and GTEx datasets is shown in Supplementary Figure S1.

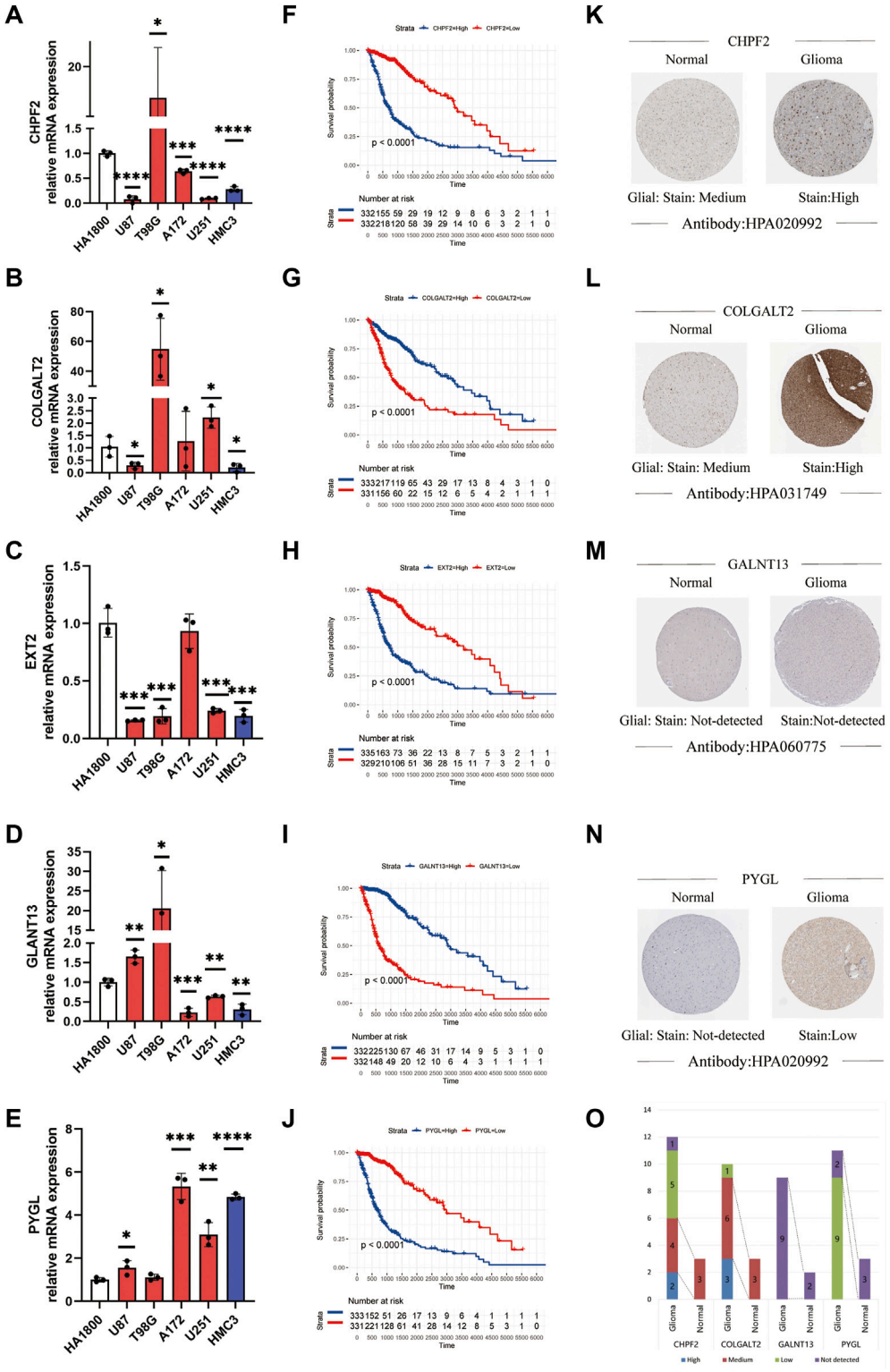

FIGURE 2
Relationship between the tumor grade and prognosis and the expression status of the glycosylation gene signature. **(A–E)** Expression level of mRNA of the glycosylation gene signature in different cell lines using qPCR. (*$p < 0.05$, **$p < 0.01$, ***$p < 0.001$, ****$p < 0.0001$, without label: no significant difference between the cell line and HA 1800). **(F–J)** Kaplan–Meier survival curves of different glycosylation gene signatures in glioma patients. **(K–N)** Protein expression images of different glycosylation gene signatures in the HPA database. **(O)** Histogram of glycosylation gene signature-related protein expression levels in the HPA database. qPCR, quantitative polymerase chain reaction; HPA, Human Protein Atlas.

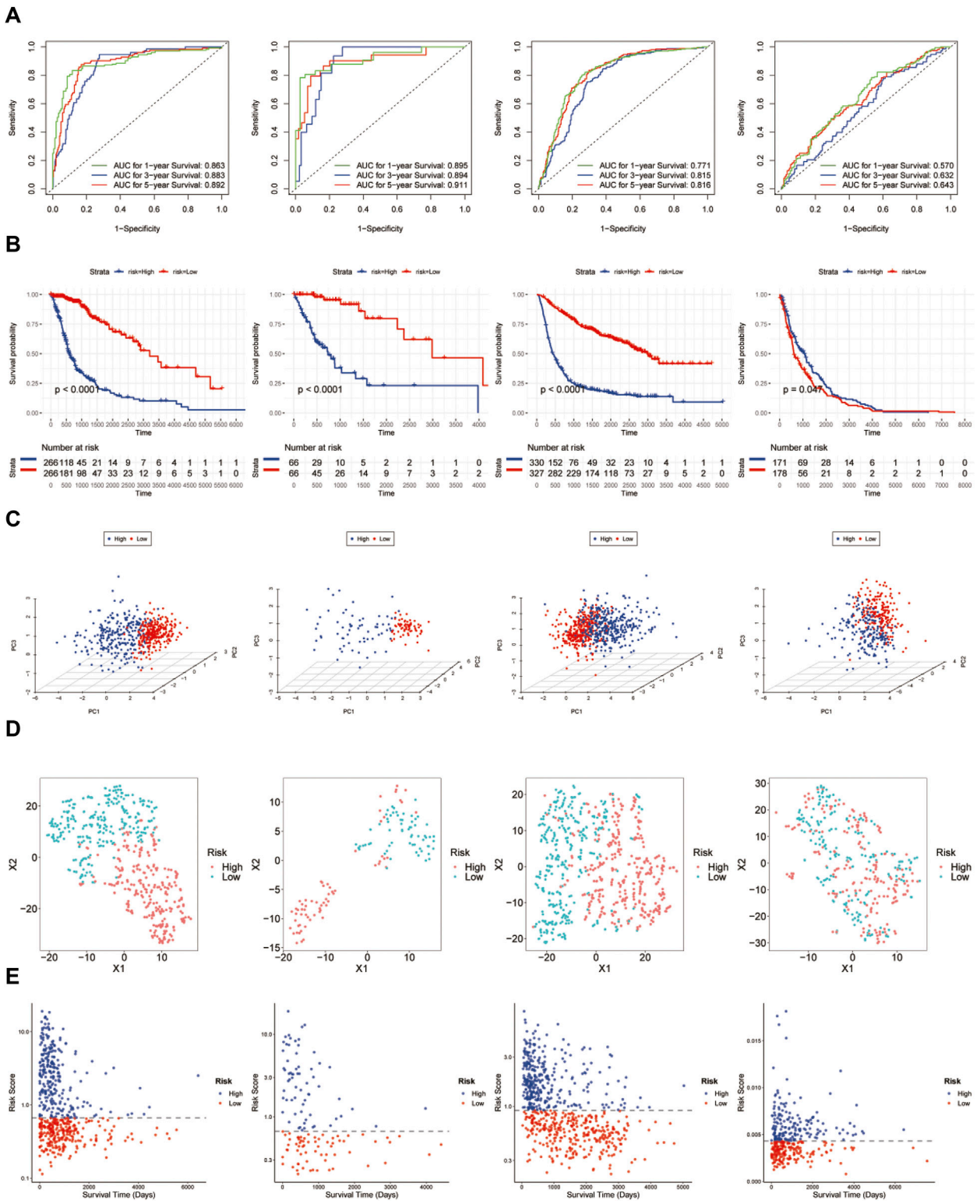

FIGURE 3
Prognostic risk model analysis of the glycosylation gene signature in TCGA-train, TCGA-test, CGGA, and Rembrandt datasets. **(A)** ROC curves demonstrate the predictive efficiency of the glycosylation gene signature on the 1-, 3-, and 5-year survival rates in TCGA-train, TCGA-test, CGGA, and Rembrandt datasets. **(B)** Survival curve of the glycosylation gene signature in these datasets. **(C)** PCA of the glycosylation gene signature in these datasets. **(D)** t-SNE analysis of the glycosylation gene signature in these datasets. **(E)** Distributions of survival time, survival status, and glycosylation risk score in these datasets. TCGA, The Cancer Genome Atlas; CGGA, Chinese Glioma Genome Atlas; PCA, principal component analysis; t-SNE, t-distributed stochastic neighbor embedding.

The relationship between the expression status of the glycosylation gene signature and the tumor grade and prognosis

We assessed the correlation between the expression status of the five genes and both tumor grade and prognosis. As to prognosis, higher expression of *CHPF2*, *PYGL*, and *EXT2* was associated with a worse prognosis, while that of *COLGALT2* and *GALNT13* was associated with a better prognosis. Furthermore, the mRNA expression of the five genes was measured in different cell lines using qPCR assays. The RNA expression levels were determined in glioma cell lines to verify our result. Five cell lines were used to replicate experiments and improve reliability. The results are shown in Figures 2A–E. The Kaplan–Meier survival curves of each gene in TCGA dataset are shown in Figures 2F–J. The Kaplan–Meier survival curves of the five genes are shown in Supplementary Figure S2. The Kaplan–Meier survival curves of each gene in the CGGA dataset (Supplementary Figures S3A–F) and REMx dataset (Supplementary Figures S4A–F) were made to further evaluate the relationship between the selected genes and prognosis. Moreover, we investigated the protein expression levels in glioma patients obtained from the Human Protein Atlas database and found greater staining intensity in glioma compared to normal brain tissues (Figures 2K–N). The corresponding statistical histogram is shown in Figure 2O.

Construction and validation of the prognostic glycosylation genes

Based on the constructed signature, which is the summing up of each selected glycosylation gene expression level and corresponding coefficients, all the glycosylation scores of patients were calculated. Afterward, the patients with glioma were divided into high- and low-risk categories using the median glycosylation score as the threshold value (Figure 3A). The heatmap of the five selected genes between the high- and low-risk groups at the CGGA (Supplementary Figure S5) and TCGA (Supplementary Figure S6) datasets was used to screen the differential gene expression. The Kaplan–Meier survival curves indicate that the overall survival (OS) of the low-risk group patients in the CGGA cohort was significantly longer than that of the high-risk group patients. ($p < 0.001$). Subsequently, the same analyses were performed on TCGA-test cohort as well as in Rembrandt databases. The study revealed a noteworthy difference ($p < 0.001$) between the low-risk and high-risk groups (Figure 3B). PCA (Figure 3C), t-SNE analysis (Figure 3D), and the distribution plot of survival time, survival status, and glycosylation risk score (Figure 3E) also confirmed that the prognostic glycosylation genes could stably and accurately predict the prognosis of glioma patients.

Evaluation of the correlation between glycosylation gene risk score and clinicopathologic characteristics

Heatmaps depict the correlation between risk groups of glycosylation genes and various clinical characteristics in TCGA (Figure 4A) and CGGA (Figure 4B) datasets. Violin plots indicate that the glycosylation risk score is highly related to these important clinicopathologic characteristics (Figures 4C–N), including age, gender, tumor grade, MGMT methylation, IDH mutation, and 1p19q co-deletion in TCGA and CGGA datasets.

Establishment and evaluation of a nomogram based on independent prognostic factors for OS

The study performed univariate and multivariate Cox regression analyses to identify glycosylation signatures as independent prognostic OS-related factors of glioma patients in TCGA database (Figures 5A–C). Then, a nomogram of TCGA cohort (Figure 5A) based on clinical characteristics, including WHO grade, IDH mutation, MGMT promoter methylation, age, and glycosylation score, was established. The calibration plots presented a concordance between the predicted probabilities from the nomogram and the observed 1-, 2-, and 3-year OS rates in TCGA cohort (Figures 5B, C). It is crucial that the nomogram has the ability to serve as a quantitative tool for forecasting survival outcomes in glioma patients. Our nomogram attained a greater net benefit than the single independent clinical feature. Meanwhile, the efficiency of the prognostic nomogram was clarified from multiple aspects.

Functional enrichment analyses

To further clarify the functional mechanism of glycosylation genes and prognosis of glioma patients, we performed GO and KEGG enrichment analyses to characterize the biological functions of DEGs between the low-risk and high-risk groups. GO analyses in TCGA database (Figure 6A) revealed significant enrichment of biological processes, including response to the bacterium and immune effector process, and that in the CGGA database presented gene enrichment in immune regulation, including cell activation and response to cytokine (Figure 6B). At the same time, the KEGG pathway analysis revealed the enrichment of immune-related pathways in both databases (Supplementary Figures S7, S8). To confirm these results, we conducted GSEA in both the CGGA and TCGA datasets. We identified significant enhancement of multiple immune processes in the high-risk group in both cohorts, for example, adaptive immune response and response to the bacterium in TCGA cohort (Figure 6C) and cell activation, response to the bacterium, and positive regulation of the immune system in the CGGA cohort (Figure 6D). In addition, multiple neuron-related signatures were enriched in the low-risk group (Figures 6E, F).

Immune filtration and tumor microenvironment

We used the xCell algorithm to eliminate the cellular component of tumor samples from bulk sequencing data and analyzed the immune cell types between the high- and low-risk groups. In general, the high-risk group showed an enrichment of immune

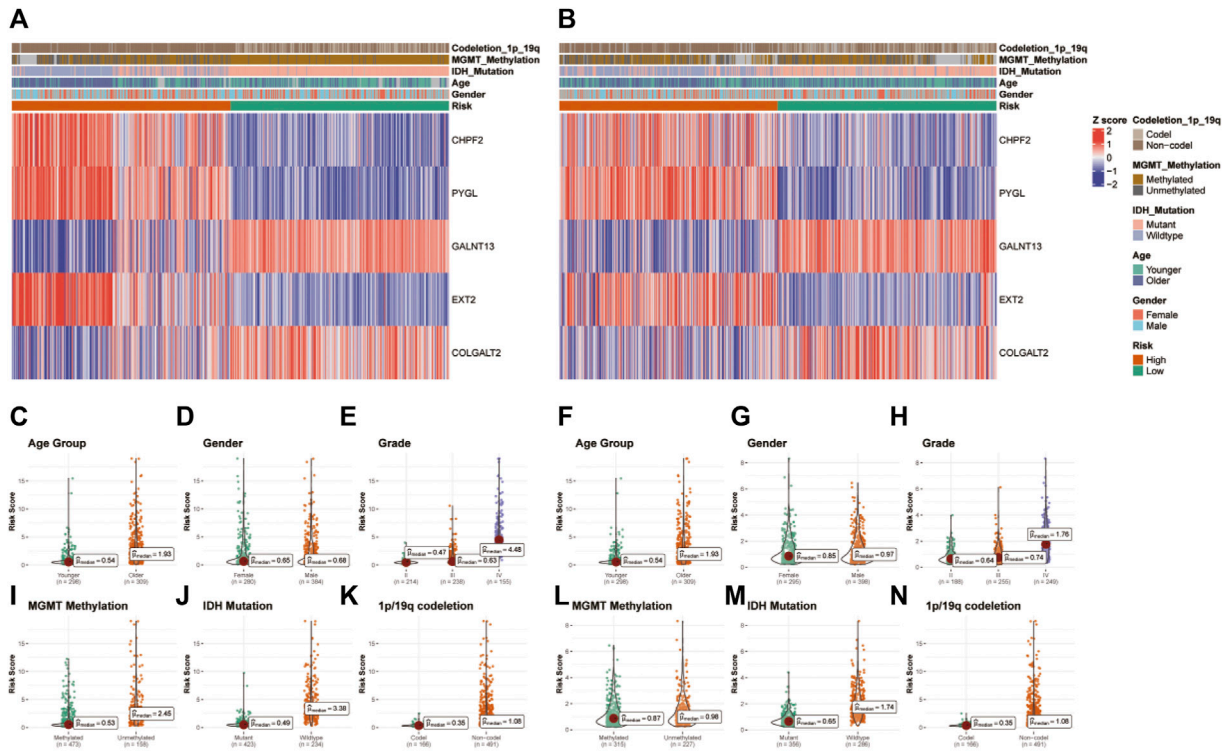

FIGURE 4
Correlation between the glycosylation gene risk score and clinicopathologic characteristics. **(A)** Heatmap of correlation between glycosylation gene risk groups with age, gender, tumor grade, MGMT methylation, IDH mutation, and 1p19q co-deletion and glycosylation signature gene expression in TCGA dataset. **(B)** Heatmap of correlation between glycosylation gene risk groups with age, gender, tumor grade, MGMT methylation, IDH mutation, and 1p19q co-deletion and glycosylation signature gene expression in the CGGA dataset. **(C–K)** Box and scatter plots of relationship between risk score and age **(C)**, gender **(D)**, tumor grade **(E)**, MGMT methylation **(I)**, IDH mutation **(J)**, and 1p19q co-deletion **(K)** in TCGA dataset and age **(F)**, gender **(G)**, tumor grade **(H)**, MGMT methylation **(L)**, IDH status **(M)**, and 1p19q co-deletion **(N)** in the CGGA dataset. TCGA, The Cancer Genome Atlas; CGGA, Chinese Glioma Genome Atlas; MGMT, O^6-methylguanine-DNA methyltransferase; IDH, isocitrate dehydrogenase.

cells related to innate immunity, while the low-risk group showed an enrichment of adaptive immune cells (see Figure 7A). Then, we examined the correlation between glycosylation score and immune infiltration via stromal score, immune score, ESTIMATE score, and tumor purity. We found that the glycosylation score was significantly positively related to the stromal score, immune score, and ESTIMATE score and negatively related to tumor purity (Figures 7B–I), indicating that the glycosylation score was strongly correlated with local immune cell infiltration.

Single nucleotide variation

First, we investigated the correlation between glycosylation score and mutation burden in glioma patients in TCGA cohort. As shown in Figure 8A, the glycosylation score was positively related to mutation burden. In addition, patients in the high-risk group have significantly increased mutation burden (Figure 8B). Then, we explored the specific mutation type and host genes in the high- and low-risk groups. In the low-risk group, the predominant mutation is the missense mutation of IDH1, which appeared in over 80% of all samples, followed by TP53 mutations, indicating a generally benign disease course (Figure 8C). However, in the high-risk group, the TP53 mutation is the most frequent mutation, accounting for only 40% of all mutations (Figure 8D).

Identification of appropriate drugs for glioma patients in different risk groups

To select appropriate drugs for patients in different risk groups, we used the oncoPredict algorithm to predict the IC_{50} value of glioma patients in TCGA and CGGA cohorts. In the GDSC2 pharmacogenomic dataset, 131 drugs were identified to show different responses in both TCGA and CGGA datasets, including 35 drugs that have been approved by the FDA (Figure 9A). Among them, 22 drugs were resistant in the high-risk group and 13 drugs were sensitive in the high-risk group. The pathways of these drug targets are shown in Figure 9A. Four drugs (crizotinib, lapatinib, nilotinib, and topotecan) have been identified after taking intersections in four databases (Figure 9B). To further explore the relationship between the predicted IC_{50} values of these four drugs and five glycosylation signatures, we performed Spearman's correlation analysis in the permutation and combination of these four datasets. (Figures 9C–F). The IC_{50} values from experiments of these four drugs in different cancer tissues were visualized using PharmacoDB 2.0 (Figures 9G–J).

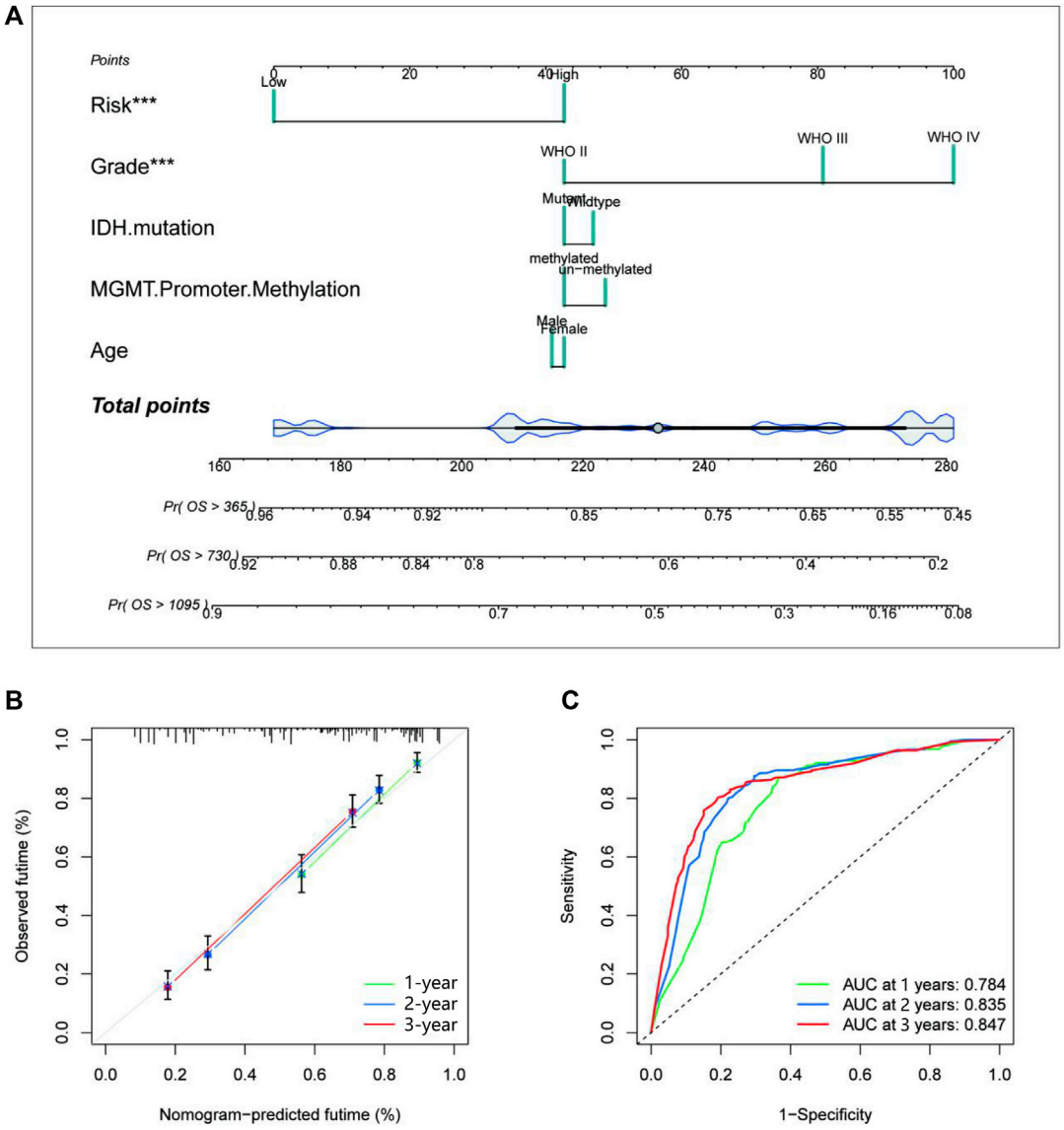

FIGURE 5
Establishment and evaluation of a nomogram in TCGA cohort. **(A)** The nomogram with glycosylation gene signature risk group for the prediction of OS of glioma patients was constructed based on TCGA dataset. **(B)** The time-dependent ROC analyses show the concordance between the predicted and observed 1-, 2-, and 3-year OS rates of the glycosylation gene nomogram in TCGA. **(C)** The calibration plots for predicting 1-, 2-, and 3-year survival using TCGA. TCGA, The Cancer Genome Atlas; OS, overall survival.

Single-cell transcriptomes and cell–cell communication of glioma samples

Glioma cells were classified into seven lines based on single-cell expression profiles: 1) astrocytes, 2) B cells, 3) endothelial cells, 4) glioma cells, 5) macrophages, 6) stem-like cells, and 7) T cells (Figure 10A). The expression features of marker genes of the seven major clusters are presented in Figure 10B. *GALNT13* was relatively highly expressed in stem-like cells and astrocytes. *COLGALT2* was highly found in glioma cells. *PYGL* was only highly found in macrophages. *CHPF2* and *EXT2* were relatively low in these seven cell lines (Figure 10C). We then explored the cell–cell interactions of glioma cells and different types of immune cells in glioma tissues (Figures 10D, E). The cell–cell communication networks showed that glioma cells do not have significant interactions with macrophages, T cells, and B cells. Heatmaps showed the communication probability for different cell populations on the CXCL signaling pathway (Figure 10F), CCL signaling pathway (Figure 10G), and IL1 signaling pathway (Figure 10H). Glioma may not have significant interactions with other cell types on these tumor-associated signaling pathways.

Discussion

Gliomas are a heterogeneous assemblage of brain tumors that originate from genetically/epigenetically abnormal cells with glial

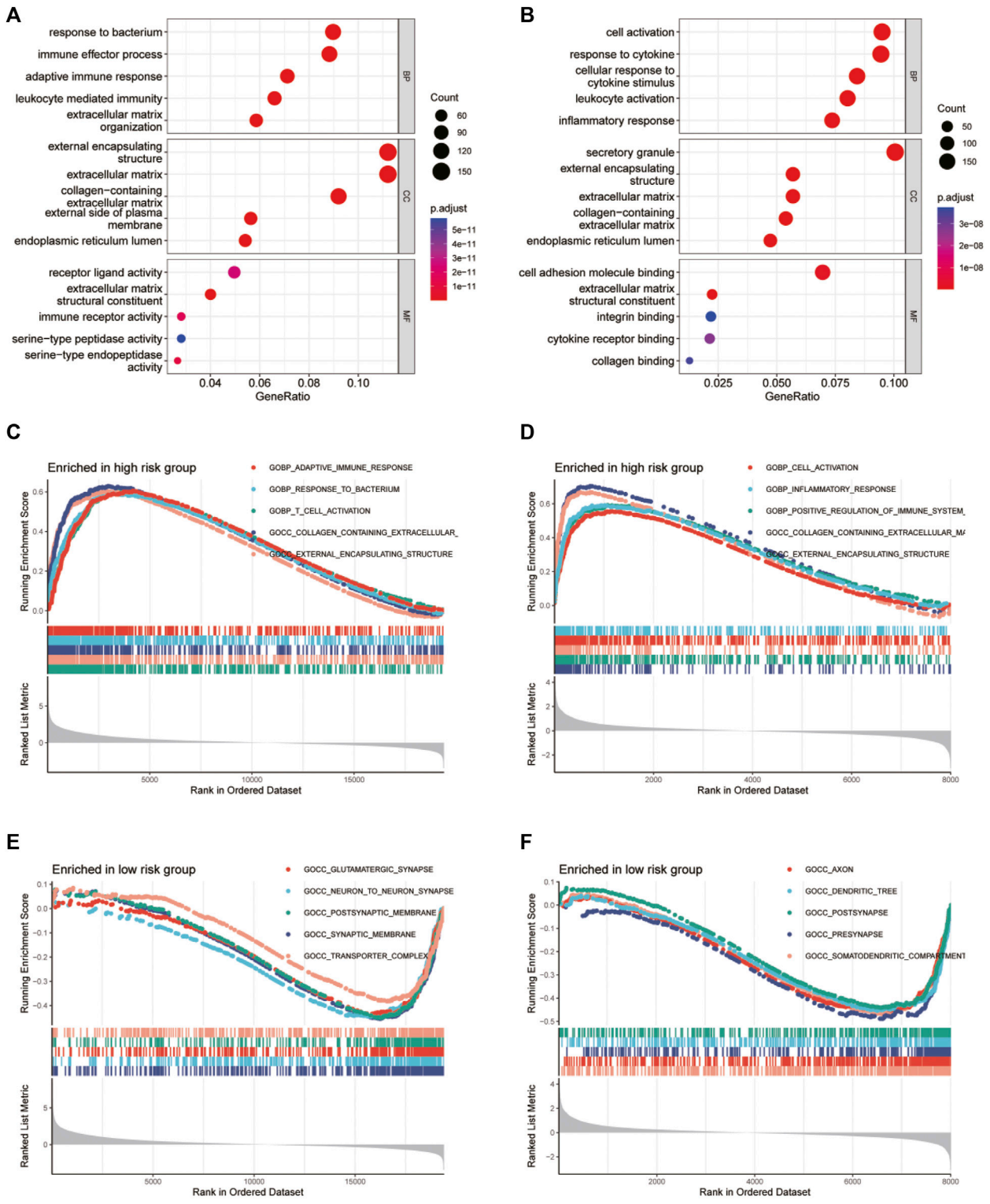

FIGURE 6
GO functional enrichment analyses between different glycosylation gene risk groups. **(A,B)** Bubble graph of GO enrichment analysis between high- and low-glycosylation gene risk group using TCGA **(A)** and CGGA **(B)**. **(C–F)** GSEA GO analyses of different glycosylation gene risk groups in TCGA or CGGA datasets. **(C)** high-risk, TCGA; **(D)** high-risk, CGGA; **(E)** low-risk, TCGA; **(F)** low-risk, CGGA. GO, Gene Ontology. TCGA, The Cancer Genome Atlas; CGGA, Chinese Glioma Genome Atlas; GSEA, gene set enrichment analysis.

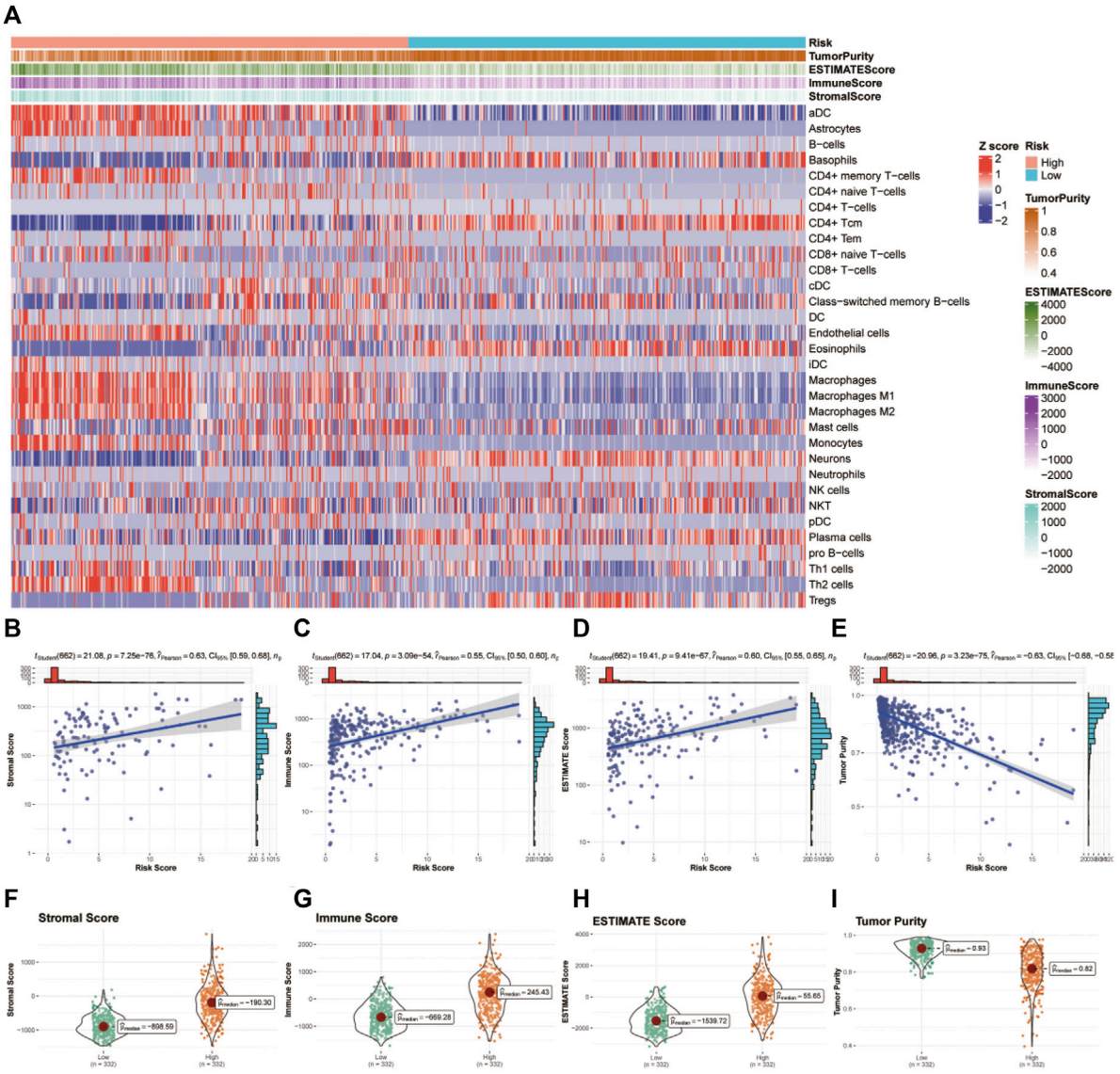

FIGURE 7
Tumor microenvironment and immunocorrelation analysis of glycosylation gene signature risk groups in glioma. **(A)** Heatmap of immune infiltration patterns between different risk groups in TCGA dataset. **(B–E)** Association of the risk score with the stromal score **(B)**, immune score **(C)**, ESTIMATE score **(D)**, and tumor purity **(E)**. **(F–I)** Correlation analysis between the risk score and stromal score **(F)**, immune score **(G)**, ESTIMATE score **(H)**, and tumor purity **(I)**.TCGA, The Cancer Genome Atlas.

stem/progenitor-like features (Nicholson and Fine, 2021). Although studies suggest that gliomas may be caused by mutations in genes such as TP53 (Pratt et al., 2022), their pathogenesis is not fully understood. Gliomas have traditionally been histopathologically classified as diffuse astrocytoma, oligodendrogliomas, and mixed astrocytoma/oligoastrocytoma based on the type of tumor cells (Lenting et al., 2017). In addition, gliomas are classified by malignancy grade (World Health Organization grades I–IV) based on marked mitotic activity, necrosis, and the presence or absence of erythematous microvascular hyperplasia (MVP) (Wesseling et al., 2015). Intratumoral heterogeneity is a well-known feature of gliomas and may result from selection pressures, such as nutritional limitation, clonal competition, and therapy (Sottoriva et al., 2013). The clinical manifestation of glioma depends on the anatomic sites, histopathology, and functional status. In newly diagnosed cases, the standard approach to treatment includes surgery, followed by concomitant radiotherapy with temozolomide and additional adjuvant temozolomide (Tan et al., 2020).

Glycosylation is a common, complex, and plastic post-translational modification of secreted and membrane-bound proteins. It is the outcome of a collaboration between nucleotide sugar transporters and biosynthesis pathways, along with glycosyltransferases and glycosidases present in the endoplasmic reticulum (ER) and the Golgi apparatus. Most of the final processing occurs in the cis-, medial-, and trans-Golgi compartments (Pinho and Reis, 2015). In these organelles, glycosyltransferases and glycosidases form carbohydrate structures through a series of

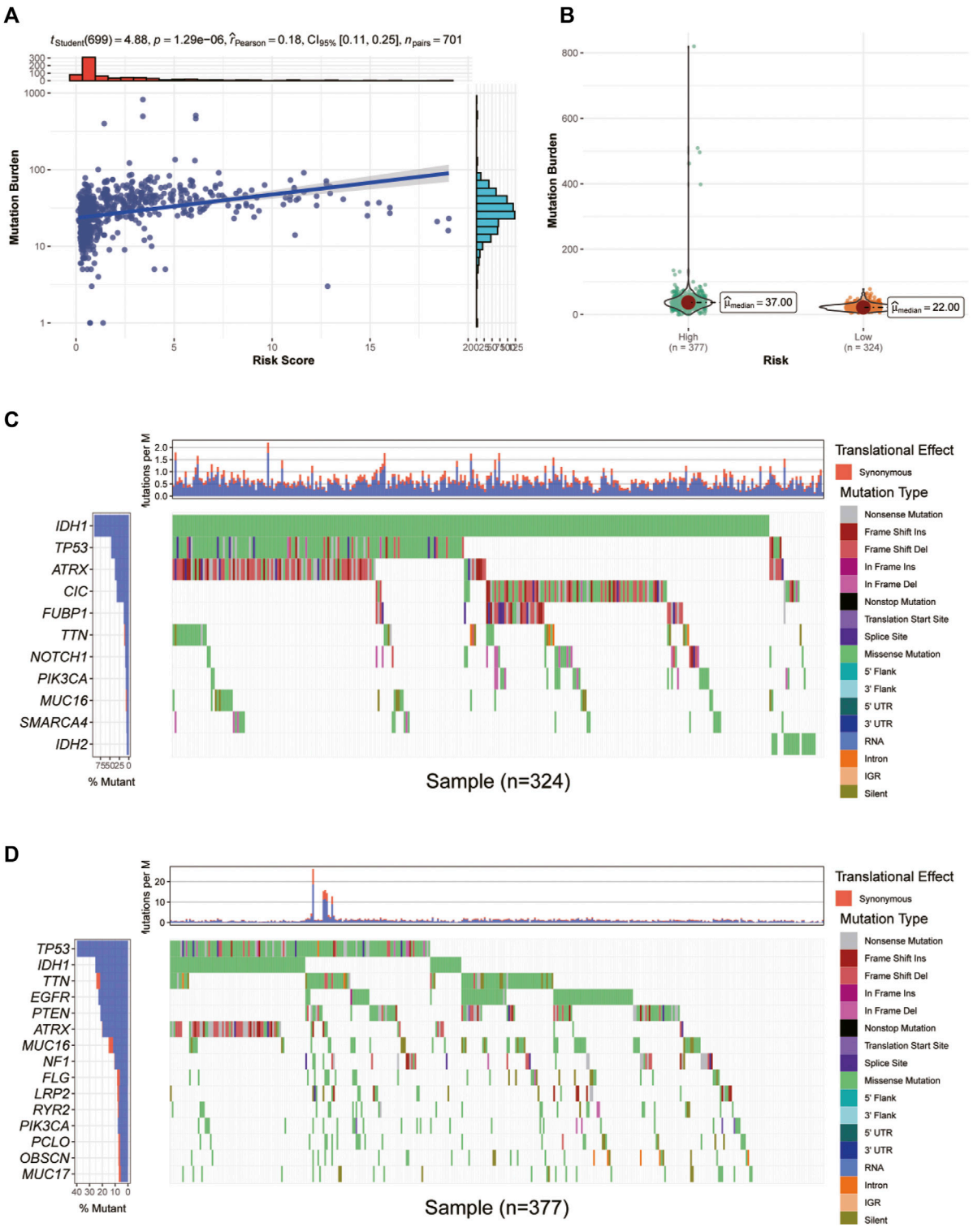

FIGURE 8
Correlation between glycosylation score and mutation burden in glioma patients in TCGA dataset. **(A,B)** Correlation analysis between glycosylation score and mutation burden. **(C,D)** The waterfall diagram demonstrates the top genes with the highest mutation frequency in the low- **(C)** and high-risk **(D)** groups. TCGA, The Cancer Genome Atlas.

stages that are controlled by enzyme activity, substrate availability, levels of gene transcription, and enzyme position within the organelles (Reily et al., 2019).

Glycans play a critical role in different stages of carcinogenesis, such as cancer cell dissociation and invasion, cell-to-cell adhesion, angiogenesis, immune modulation, and metastasis composition.

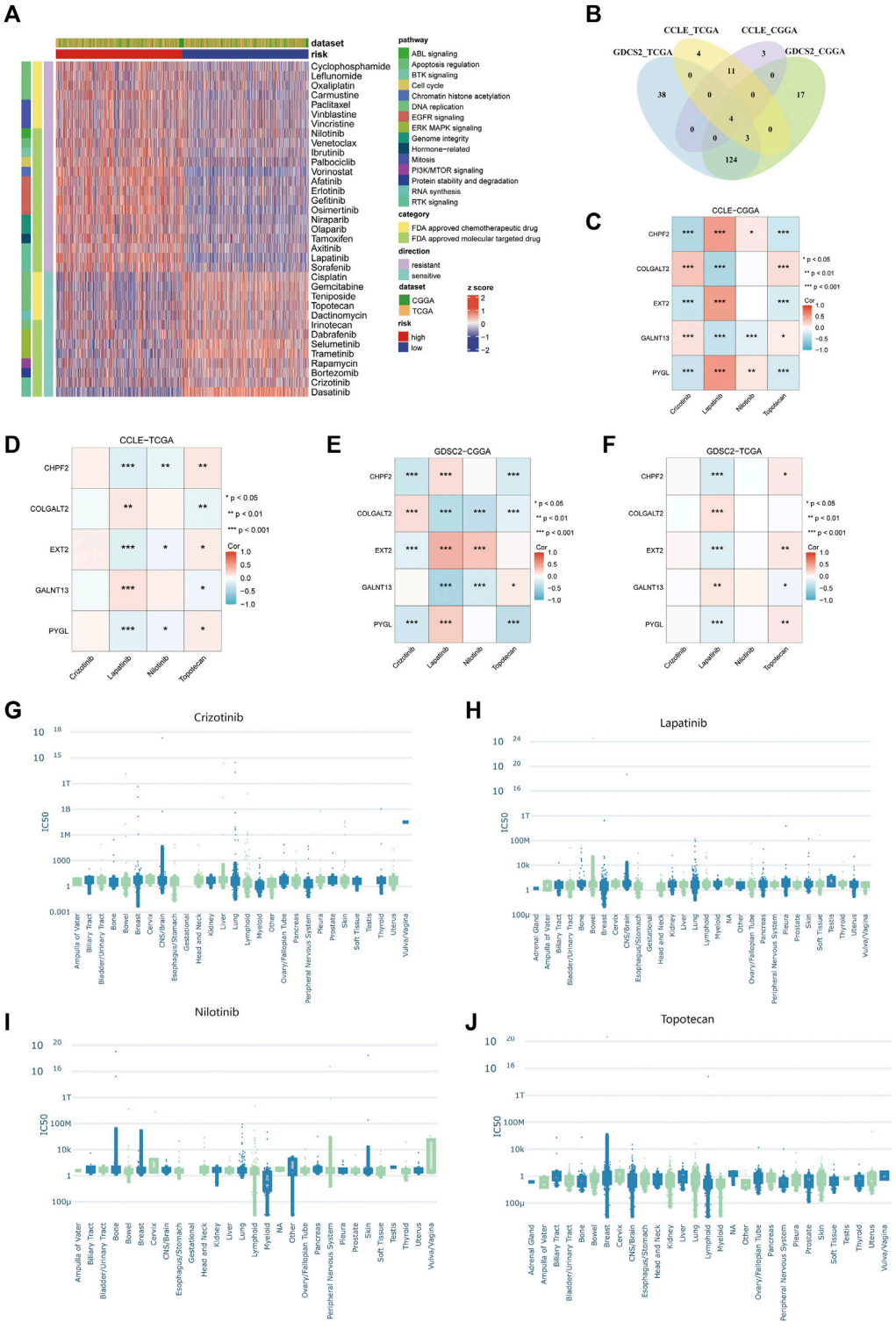

FIGURE 9
Prediction of drug sensitivity using the glycosylation signature in glioma patients. **(A)** The heatmap of predicted IC_{50} values of 35 FDA-approved drugs in GDSC2 between the high- and low-risk groups. **(B)** Venn diagram between different combinations of training and testing sets. **(C–F)** Correlation between the predicted IC_{50} values of four selected drugs and the expression of five glycosylation signatures among the combination of CCLE–CGGA **(C)**, CCLE–TCGA **(D)**, GDSC2–CGGA **(E)**, and GDSC2–TCGA **(F)**. **(G–J)**. The IC_{50} values from experiments of crizotinib **(G)**, lapatinib **(H)**, nilotinib **(I)**, and topotecan **(J)** among different cancer tissues in all available pharmacogenomic datasets in PharmacoDB.

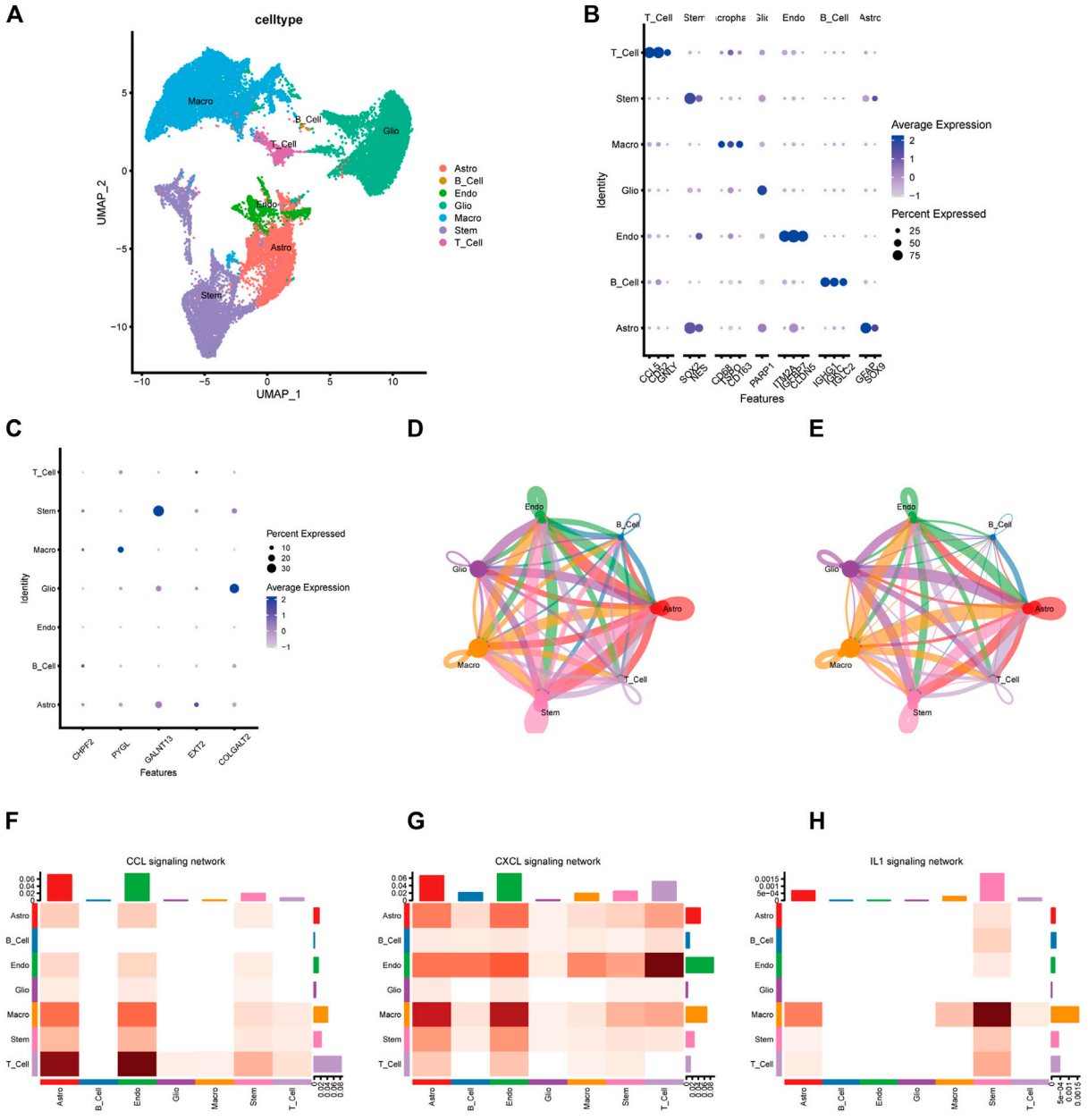

FIGURE 10
Single-cell transcriptome analysis of the five-gene glycosylation signature and cell–cell communication between different cell types. **(A)** Clustering and annotation of single-cell data. **(B)** Dot plot of the expression features of marker genes of the seven major clusters. **(C)** Identification of the five-gene glycosylation signature expression in seven cell types in glioma. **(D–E)** The circle interaction plots show the count **(D)** and weight **(E)** of inferred intercellular communication network analysis of glioma cells with the remaining several cell clusters. **(F–H)** The heatmaps show the communication probability on the CXCL signaling pathway **(F)**, CCL signaling pathway **(G)**, and IL1 signaling pathway **(H)** for different cell populations.

Glycosylation is critical in cell communication and signaling (Haltiwanger and Lowe, 2004). Incomplete synthesis and neosynthesis are two primary mechanisms that underlie carbohydrate-related structural changes in cancer, as identified by Kannagi et al. (2008), while the incomplete biosynthesis pathway is more common in the early stages of cancer. On the contrary, neosynthesis typically occurs in the advanced stages of a tumor and is relevant to the induction of several genes involved in the glycosylation pathway (Kannagi et al., 2008). Glycosylation changes are commonly observed in cancer cells, including increased sialyl Lewis structures, irregular core fucosylation, an increase in N-glycan branching, or exposure of the mucin-type O-glycan, which may result in the production of unique tumor antigens that could be promising targets for immune therapy (Holmes et al., 1987). In some cases, malignant tissues triggered the recurrence of glycosylated antigens that were expressed in fetal life. Possibly the most extensively researched tumor-associated glycans consist of variations arising from a premature termination of protein O-glycosylation called the Tn antigen (the most basic O-glycan), its sialylated counterpart sialyl-Tn (sTn;

Neu5Acα2-6GalNAcα-O-Ser/Thr), and the T or core 1 antigen which arises following the addition of a Gal residue to the Tn antigen (Galβ1-3GalNAc-Ser/Thr) (Julien et al., 2011). Both the sTn and sialylated T antigens are not present in normal healthy tissues but are overexpressed in many types of solid tumors (Marcos et al., 2011; Julien et al., 2012). The roles of glycans in the tumor have been highlighted by the fact that glycosylation variations are implicated in the growth and advancement of cancer, therefore serving as biomarkers and presenting a set of precise targets for therapy (Pinho and Reis, 2015). In our study, we found that the glycosylation score was positively correlated with immune infiltration, which may be interpreted by increased mutation burden for a high glycosylation score. This suggests that glycans play a role in immune infiltration in cancer cells.

Our study determined that glycosylation modification is crucial in tumor progression and has a strong correlation with glioma prognosis. The study selected prognostic-related genes based on univariate Cox regression across TCGA and CGGA and then filtered the overlapped genes through LASSO regression and step-wise Cox regression to build and validate a glycosylation-related gene signature through internal and external validation. The five genes are all involved in the glycosylation process. In the next paragraph, we will discuss the general function and the latest research progress of these genes through a systematic approach.

Chondroitin sulfate (CS) proteoglycan is a vital enzyme that is translated by the *CHPF2* gene. It exists in various tissues as a proteoglycan in which the disaccharide units of N-acetylgalactosamine and glucuronic acid residues are repeated, and the sulfate residues are distributed in different positions. This unique structure provides hyperosmolarity and water retention ability, and it may also play an important role in regulating cell adhesion to the extracellular matrix, thus acting as an important mediator for cell proliferation, cell migration, morphogenesis, and some cytokine signaling (Yada et al., 2003). Glycosaminoglycan plays a crucial role in morphogenesis and tissue development and contributes to tumor development and formation. The biosynthesis of CS is accomplished through a variety of enzymes, such as glycosyltransferases and sulfotransferases (Kalathas et al., 2011). Glycosaminoglycans are generally altered in tumors in qualitative and quantitative terms (Skandalis et al., 2007; Kalathas et al., 2009). In addition, the reduction in C-6 sulfation is more abrupt in cancer; the effect of C-4 sulfation is gradually diminished at the stage of advanced cancer. These changes may be caused by differences in core protein precursor biosynthesis, substrate pools, and expression level of the enzymes involved in chondroitin/dermatan sulfate biosynthesis (Kalathas et al., 2010). Compared to tumor tissues, adjacent macroscopic tissues have been observed to have lower levels of CS in many cancer types (Kalathas et al., 2011). A previous study found that the expression of *CHPF2* was positively correlated with the levels of macrophages and dendritic cells, which may influence drug sensitivity.

PYGL has been reported to have oncogenic effects in multiple tumors (Zhu et al., 2022). It has been reported to be a glycogenolysis-related gene whose expression is upregulated in various tumors (Zhao et al., 2021). The protein translated by *PYGL* is glycogen phosphorylase, liver form. Glycogen metabolism is considered a crucial pathway in cancer metabolism reprogramming (Yang et al., 2019). It was also believed that the degradation of glycogen, which is regulated by *PYGL*, could sustain proliferation and prevent premature senescence in cancer cells (Favaro et al., 2012). Zhu et al. (2022) revealed the relationship between the *PYGL* gene and the prognosis of glioma by analyzing the Chinese Glioma Genome Atlas database and using quantitative real-time PCR to verify the *PYGL* expression level in gliomas. Previous investigations have observed a comparatively sluggish rise in *PYGL* levels under hypoxic conditions. Further examination of *PYGL* expression in tumor cells has unveiled discernible patterns of induction in response to hypoxia (0.1% O_2), which have been consistently observed at both the mRNA and protein levels. The result of the research indicated that *PYGL* could be regarded as a new biomarker and molecular target for assessing the prognosis and immunotherapy of glioma. Zhao et al. (2021) returned the same result. They found that the mRNA expression level of *PYGL* showed a positive correlation with the glioma grade. Overall survival and Cox regression analyses showed that high *PYGL* expression is an independent risk factor for a worse prognosis in glioma patients ($p < 0.05$).

GALNT13 is one of the specialized glycosyltransferases termed polypeptide N-acetylgalactosaminyltransferases, which mediate the initial reaction in O-linked oligosaccharide biosynthesis. N-Acetylgalactosaminyltransferases catalyze the transfer of an N-acetyl-D-galactosamine (GalNAc) residue to a target protein at the serine or threonine residue, which will form the GalNAc-O-Ser/Thr structure, also known as Tn antigen (Raman et al., 2012). A prior study analyzed the expression levels of *GALNT13* mRNA in a variety of fetal and adult human tissues. The greatest expression level occurred in the fetal brain, trailed by the adult brain (Zhang et al., 2003). In the analysis of *GALNT13* mRNA expression levels among human cancer cell lines, Nogimori et al. (2016) discovered that the expression was higher only in neuroblastoma lines and lung tumors. Considering that *GALNT13* is basically expressed in the fetal brain, both *GALNT13* and its products of translation trimeric Tn may play an essential role in cell growth and proliferation and serve as a specific maker for malignant CNS tumors (Nogimori et al., 2016). Different exons in *GALNT13* mRNA exhibit distinct sequences in the lectin-like domain. Consequently, the contrasting outcomes observed in variant exon usages could potentially be attributed to variations in substrate recognition during O-glycan synthesis. Therefore, the utilization of tumor-specific and malignancy-associated variant exons may hold significance as targets for molecular therapy in cancer treatment, although further investigation is required to elucidate the precise mechanisms involved. Berois et al. (2006) found that *GALNT13* was the most highly expressed gene indicated by microarray gene expression analysis performed using a metastatic xenograft-derived cell model of human neuroblastoma, with a 12-fold upregulation in metastatic malignant neuroblasts compared to the primary cancer xenograft, suggesting that the *GALNT13* expression level could be potentially used to detect malignant neuroblasts at diagnosis or recurrence. However, it has not been investigated in clinical studies.

The exostosin (EXT) family of glycosyltransferases includes *EXT1* (located on chromosome 8q23-q24) and *EXT2* (located on chromosome 11p11-p12), which mediate the synthesis of heparan sulfate proteoglycans (HSPGs) (Busse-Wicher et al., 2014). HSPGs are ubiquitous component parts of the extracellular matrix and are involved in tissue homeostasis (Meneghetti et al., 2015). Numerous

research studies have shown that heparin sulfate is essential for signal transduction in a variety of processes, such as cell survival, migration, division, differentiation, and cancer progression (Li and Kusche-Gullberg, 2016). Both genes (*EXT1* and *EXT2*) encoding exocrine glycosyltransferases have tumor-suppressive functions, although the details of mechanisms and predictions of the prognostic value of exostosin in cancer remain unclear. Ushakov et al. (2017) demonstrated a significant decrease in both *EXT1* and *EXT2* expression levels in gliomas. However, according to Wade et al. (2013), the expression levels of these genes are upregulated in glioblastoma tissues. The mutations in *EXT1* and *EXT2* may have a significant correlation with hereditary multiple exostoses (HME), a disorder dominantly associated with a genetic disorder characterized by the formation of multiple cartilaginous tumors. *EXT2* expression levels showed significant associations with tumor purity as well as infiltration levels of $CD4^+$ T cells, macrophages, neutrophils, and dendritic cells in head and neck squamous cell carcinoma. The observed correlation between elevated *EXT2* expression and increased neutrophil infiltration in head and neck squamous cell carcinoma cases suggests that this phenomenon might be the most important factor associated with a poor prognosis. The germline heterozygous loss-of-function mutations in the tumor suppressor genes *EXT1* or *EXT2* shoulder the responsibility for over 70%–95% of HME cases. Al-Zayed et al. (2021) investigated genetic defects of *EXT2* in Saudi HME patients, and found that 77% of the patients had *EXT1* and *EXT2* mutations, while the *de novo EXT1* and *EXT2* mutations are popular.

The biological functions of human collagen beta (1-O) galactosyltransferase 2 (*COLGALT2*) in tumors have not been determined despite its significance in the collagen glycosylation process (Wang et al., 2020). Guo et al. (2021) found that compared with healthy ovary tissues, *COLGALT2* expression is significantly higher in both high-grade and low-grade serous ovarian cancer types, which are common subtypes of ovarian cancer. According to Wang et al. (2020), adipose-derived mesenchymal stem cell exosomes prompt the progression of osteosarcoma by increasing *COLGALT2* expression levels in osteosarcoma cells. The *COLGALT2* enzyme initiates post-translational glycosylation of collagen and is therefore a compelling target of osteosarcoma susceptibility (Kehayova et al., 2021). It was demonstrated that exosomes derived from adipose-derived mesenchymal stem cells promoted the invasion, migration, and proliferation of osteosarcoma cells. Furthermore, this effect was accompanied by an upregulation in the expression of *COLGALT2*.

Our study pooled multiple glioma datasets to build a universal model for all gliomas. However, the high degree of heterogeneity among different types of gliomas is one of the significant obstacles in the current treatment of glioma. Due to their shared origin in neuroepithelial-derived cells, LGG and GBM exhibit significant similarities in their malignant biological behavior. We tried to explore common biomarkers that can overcome this heterogeneity. Therefore, we included all types of gliomas in this study rather than focusing on specific types. In addition, combining the LGG and GBM datasets could increase the sample size in the predictive model, which may increase the overall accuracy and broaden the clinical usage of the model.

Functional enrichment analyses demonstrated differences in immune-related biological processes between the high- and low-risk groups. Additionally, the tumor immune microenvironment was investigated in both groups. It showed that the high-risk group had higher stromal, immune, and ESTIMATE scores and lower tumor purity. The high- and low-risk groups had different mutation burdens. Cancer-associated glycosylation may enhance the communication among tumor cells in a microenvironment through the glycan-binding receptor—lectin. Glycans are oligosaccharide structures discovered on proteins and lipids. Endogenous lectins are expressed on immune cells and additional cells in the stroma and facilitate cell–cell interactions and adhesion, thus contributing to homeostasis. During malignancy, alterations in the glycosylation of tumor cells may affect inflammatory responses, facilitate viral immune evasion, enhance cancer cell metastasis, or regulate apoptosis (Pinho and Reis, 2015). Crizotinib and topotecan were observed to be effective in the high-risk group, while lapatinib and nilotinib showed resistance in the same group. Notably, crizotinib, lapatinib, and nilotinib belong to the class of tyrosine kinase inhibitors (TKIs) that are commonly used in cancer therapy to target the epidermal growth factor receptor family (Roskoski, 2014). The application of TKIs to oncology was revolutionary. For instance, imatinib significantly increased the 5-year survival rate of Philadelphia chromosome-positive patients with chronic myelogenous leukemia (CML) from 11% to 90% (Bower et al., 2016). Topotecan is a water-soluble derivative of camptothecin that has antineoplastic activity in cell culture and xenograft systems. It has been approved as a second-line therapy in ovarian and small-cell lung cancer (SCLC). The drug disrupts the normal function of the nuclear enzyme topoisomerase I to inhibit the replication of rapidly dividing cells (Ormrod and Spencer, 1999).

Our study has several advantages. First, we constructed a glycosylation-related gene signature that includes only five genes yet shows high accuracy in the prognosis of glioma patients. Second, the gene signature was constructed based on a public database that contained a large number of patient samples. Third, no glycosylation-related gene signature has been found related to glioma; thus, this study fills the gap of glycosylation-related genes in the prognostic prediction of glioma. Our study built the predictive model based on high-throughput sequencing. Although it provided high-dimensional data with satisfying accuracy, it also limited the interpretation of our results. In clinical use, high-throughput sequencing of the tumor tissue is not widely used as a clinical routine. In addition, the use of normalization methods and the high tendency of batch effect may decrease the universal use of a model based on sequencing. In addition, the available samples for qPCR were not sufficient. Moreover, the underlying molecular mechanism has not been identified. Therefore, further investigations are required to study the interactions between glycosylation-related genes and glioma.

Conclusion

This study developed a predictive model using a glycosylation signature. This model can accurately predict the survival outcomes of glioma patients and has been validated using external sources of data. Additionally, the glycosylation signature correlated with immune infiltration in the glioma microenvironment and may suggest varying levels of effectiveness for immunotherapy. These

findings will offer valuable insights for future studies and clinical practice.

Data availability statement

The original contributions presented in the study are included in the article/Supplementary Material; further inquiries can be directed to the corresponding authors.

Author contributions

YY: formal analysis, software, and writing–review and editing. HT: investigation and writing–original draft. YZ: resources and writing–original draft. FW: conceptualization and writing–original draft. LT: methodology and writing–review and editing. CZ: formal analysis and writing–original draft. ZH: project administration and writing–original draft. YC: project administration and writing–review and editing. YG: visualization and writing–review and editing. ZW: supervision and writing–review and editing. YY: resources and writing–review and editing.

Funding

The author(s) declare that no financial support was received for the research, authorship, and/or publication of this article.

Acknowledgments

The authors appreciate the valuable and constructive suggestions and assistance from their Team of Neurosurgical Study.

Conflict of interest

The authors declare that the research was conducted in the absence of any commercial or financial relationships that could be construed as a potential conflict of interest.

Publisher's note

All claims expressed in this article are solely those of the authors and do not necessarily represent those of their affiliated organizations, or those of the publisher, the editors, and the reviewers. Any product that may be evaluated in this article, or claim that may be made by its manufacturer, is not guaranteed or endorsed by the publisher.

Supplementary material

The Supplementary Material for this article can be found online at: https://www.frontiersin.org/articles/10.3389/fphar.2023.1259051/full#supplementary-material

References

Al-Zayed, Z., Al-Rijjal, R. A., Al-Ghofaili, L., BinEssa, H. A., Pant, R., Alrabiah, A., et al. (2021). Mutation spectrum of EXT1 and EXT2 in the Saudi patients with hereditary multiple exostoses. *Orphanet J. Rare Dis.* 16 (1), 100. doi:10.1186/s13023-021-01738-z

Aran, D., Hu, Z., and Butte, A. J. (2017). xCell: digitally portraying the tissue cellular heterogeneity landscape. *Genome Biol.* 18 (1), 220. doi:10.1186/s13059-017-1349-1

Bair, E., and Tibshirani, R. (2004). Semi-supervised methods to predict patient survival from gene expression data. *PLoS Biol.* 2 (4), E108. doi:10.1371/journal.pbio.0020108

Barthel, F. P., Johnson, K. C., Varn, F. S., Moskalik, A. D., Tanner, G., Kocakavuk, E., et al. (2019). Longitudinal molecular trajectories of diffuse glioma in adults. *Nature* 576 (7785), 112–120. doi:10.1038/s41586-019-1775-1

Berois, N., Blanc, E., Ripoche, H., Mergui, X., Trajtenberg, F., Cantais, S., et al. (2006). ppGalNAc-T13: a new molecular marker of bone marrow involvement in neuroblastoma. *Clin. Chem.* 52 (9), 1701–1712. doi:10.1373/clinchem.2006.067975

Blanche, P., Dartigues, J. F., and Jacqmin-Gadda, H. (2013). Estimating and comparing time-dependent areas under receiver operating characteristic curves for censored event times with competing risks. *Stat. Med.* 32 (30), 5381–5397. doi:10.1002/sim.5958

Bower, H., Bjorkholm, M., Dickman, P. W., Hoglund, M., Lambert, P. C., and Andersson, T. M. (2016). Life expectancy of patients with chronic myeloid leukemia approaches the life expectancy of the general population. *J. Clin. Oncol.* 34 (24), 2851–2857. doi:10.1200/JCO.2015.66.2866

Bullard, J. H., Purdom, E., Hansen, K. D., and Dudoit, S. (2010). Evaluation of statistical methods for normalization and differential expression in mRNA-Seq experiments. *BMC Bioinforma.* 11, 94. doi:10.1186/1471-2105-11-94

Busse-Wicher, M., Wicher, K. B., and Kusche-Gullberg, M. (2014). The exostosin family: proteins with many functions. *Matrix Biol.* 35, 25–33. doi:10.1016/j.matbio.2013.10.001

Colaprico, A., Silva, T. C., Olsen, C., Garofano, L., Cava, C., Garolini, D., et al. (2016). TCGAbiolinks: an R/Bioconductor package for integrative analysis of TCGA data. *Nucleic Acids Res.* 44 (8), e71. doi:10.1093/nar/gkv1507

Davis, M. E. (2018). Epidemiology and overview of gliomas. *Semin. Oncol. Nurs.* 34 (5), 420–429. doi:10.1016/j.soncn.2018.10.001

Favaro, E., Bensaad, K., Chong, M. G., Tennant, D. A., Ferguson, D. J., Snell, C., et al. (2012). Glucose utilization via glycogen phosphorylase sustains proliferation and prevents premature senescence in cancer cells. *Cell Metab.* 16 (6), 751–764. doi:10.1016/j.cmet.2012.10.017

Feizi, N., Nair, S. K., Smirnov, P., Beri, G., Eeles, C., Esfahani, P. N., et al. (2022). PharmacoDB 2.0: improving scalability and transparency of *in vitro* pharmacogenomics analysis. *Nucleic Acids Res.* 50 (D1), D1348–D1357. doi:10.1093/nar/gkab1084

Fogh, S. E., Andrews, D. W., Glass, J., Curran, W., Glass, C., Champ, C., et al. (2010). Hypofractionated stereotactic radiation therapy: an effective therapy for recurrent high-grade gliomas. *J. Clin. Oncol.* 28 (18), 3048–3053. doi:10.1200/JCO.2009.25.6941

Guo, T., Li, B., Kang, Y., Gu, C., Fang, F., Chen, X., et al. (2021). *COLGALT2* is overexpressed in ovarian cancer and interacts with PLOD3. *Clin. Transl. Med.* 11 (3), e370. doi:10.1002/ctm2.370

Haltiwanger, R. S., and Lowe, J. B. (2004). Role of glycosylation in development. *Annu. Rev. Biochem.* 73, 491–537. doi:10.1146/annurev.biochem.73.011303.074043

Holmes, E. H., Ostrander, G. K., Clausen, H., and Graem, N. (1987). Oncofetal expression of Lex carbohydrate antigens in human colonic adenocarcinomas. Regulation through type 2 core chain synthesis rather than fucosylation. *J. Biol. Chem.* 262 (23), 11331–11338. doi:10.1016/s0021-9258(18)60963-9

Julien, S., Ivetic, A., Grigoriadis, A., QiZe, D., Burford, B., Sproviero, D., et al. (2011). Selectin ligand sialyl-Lewis x antigen drives metastasis of hormone-dependent breast cancers. *Cancer Res.* 71 (24), 7683–7693. doi:10.1158/0008-5472.CAN-11-1139

Julien, S., Videira, P. A., and Delannoy, P. (2012). Sialyl-tn in cancer: (how) did we miss the target? *Biomolecules* 2 (4), 435–466. doi:10.3390/biom2040435

Kalathas, D., Theocharis, D. A., Bounias, D., Kyriakopoulou, D., Papageorgakopoulou, N., Stavropoulos, M. S., et al. (2009). Alterations of glycosaminoglycan disaccharide content and composition in colorectal cancer: structural and expressional studies. *Oncol. Rep.* 22 (2), 369–375. doi:10.3892/or_00000447

Kalathas, D., Theocharis, D. A., Bounias, D., Kyriakopoulou, D., Papageorgakopoulou, N., Stavropoulos, M. S., et al. (2011). Chondroitin synthases I, II, III and chondroitin sulfate glucuronyltransferase expression in colorectal cancer. *Mol. Med. Rep.* 4 (2), 363–368. doi:10.3892/mmr.2011.431

Kalathas, D., Triantaphyllidou, I. E., Mastronikolis, N. S., Goumas, P. D., Papadas, T. A., Tsiropoulos, G., et al. (2010). The chondroitin/dermatan sulfate synthesizing and modifying enzymes in laryngeal cancer: expressional and epigenetic studies. *Head. Neck Oncol.* 2, 27. doi:10.1186/1758-3284-2-27

Kannagi, R., Yin J Fau - Miyazaki, K., Miyazaki, K., Fau - Izawa, M., and Izawa, M. (2008). Current relevance of incomplete synthesis and neo-synthesis for cancer-associated alteration of carbohydrate determinants--Hakomori's concepts revisited. *Biochim. Biophys. Acta* 1780, 525–531. doi:10.1016/j.bbagen.2007.10.007

Kehayova, Y. S., Watson, E., Wilkinson, J. M., Loughlin, J., and Rice, S. J. (2021). Genetic and epigenetic interplay within a *COLGALT2* enhancer associated with osteoarthritis. *Arthritis Rheumatol.* 73 (10), 1856–1865. doi:10.1002/art.41738

Lenting, K., Verhaak, R., Ter Laan, M., Wesseling, P., and Leenders, W. (2017). Glioma: experimental models and reality. *Acta Neuropathol.* 133 (2), 263–282. doi:10.1007/s00401-017-1671-4

Li, J. P., and Kusche-Gullberg, M. (2016). Heparan sulfate: biosynthesis, structure, and function. *Int. Rev. Cell Mol. Biol.* 325, 215–273. doi:10.1016/bs.ircmb.2016.02.009

Maeser, D., Gruener, R. F., and Huang, R. S. (2021). oncoPredict: an R package for predicting *in vivo* or cancer patient drug response and biomarkers from cell line screening data. *Brief. Bioinform* 22 (6), bbab260. doi:10.1093/bib/bbab260

Marcos, N. T., Bennett, E. P., Gomes, J., Magalhaes, A., Gomes, C., David, L., et al. (2011). ST6GalNAc-I controls expression of sialyl-Tn antigen in gastrointestinal tissues. *Front. Biosci. (Elite Ed.* 3 (4), 1443–1455. doi:10.2741/e345

Martin, T. C., Yet, I., Tsai, P. C., and Bell, J. T. (2015). coMET: visualisation of regional epigenome-wide association scan results and DNA co-methylation patterns. *BMC Bioinforma.* 16, 131. doi:10.1186/s12859-015-0568-2

Meneghetti, M. C., Hughes, A. J., Rudd, T. R., Nader, H. B., Powell, A. K., Yates, E. A., et al. (2015). Heparan sulfate and heparin interactions with proteins. *J. R. Soc. Interface* 12 (110), 0589. doi:10.1098/rsif.2015.0589

Nicholson, J. G., and Fine, H. A. (2021). Diffuse glioma heterogeneity and its therapeutic implications. *Cancer Discov.* 11 (3), 575–590. doi:10.1158/2159-8290.CD-20-1474

Nogimori, K., Hori, T., Kawaguchi, K., Fukui, T., Mii, S., Nakada, H., et al. (2016). Increased expression levels of ppGalNAc-T13 in lung cancers: significance in the prognostic diagnosis. *Int. J. Oncol.* 49 (4), 1369–1376. doi:10.3892/ijo.2016.3638

Ormrod, D., and Spencer, C. M. (1999). Topotecan: a review of its efficacy in small cell lung cancer. *Drugs* 58 (3), 533–551. doi:10.2165/00003495-199958030-00020

Ostrom, Q. T., Gittleman, H., Truitt, G., Boscia, A., Kruchko, C., and Barnholtz-Sloan, J. S. (2018). CBTRUS statistical report: primary brain and other central nervous system tumors diagnosed in the United States in 2011-2015. *Neuro Oncol.* 20 (Suppl. l_4), iv1–iv86. doi:10.1093/neuonc/noy131

Pinho, S. S., and Reis, C. A. (2015). Glycosylation in cancer: mechanisms and clinical implications. *Nat. Rev. Cancer* 15 (9), 540–555. doi:10.1038/nrc3982

Pratt, D., Abdullaev, Z., Papanicolau-Sengos, A., Ketchum, C., Panneer Selvam, P., Chung, H. J., et al. (2022). High-grade glioma with pleomorphic and pseudopapillary features (HPAP): a proposed type of circumscribed glioma in adults harboring frequent TP53 mutations and recurrent monosomy 13. *Acta Neuropathol.* 143 (3), 403–414. doi:10.1007/s00401-022-02404-9

Raman, J., Guan, Y., Perrine, C. L., Gerken, T. A., and Tabak, L. A. (2012). UDP-N-acetyl-alpha-D-galactosamine:polypeptide N-acetylgalactosaminyltransferases: completion of the family tree. *Glycobiology* 22 (6), 768–777. doi:10.1093/glycob/cwr183

Reily, C., Stewart, T. J., Renfrow, M. B., and Novak, J. (2019). Glycosylation in health and disease. *Nat. Rev. Nephrol.* 15 (6), 346–366. doi:10.1038/s41581-019-0129-4

Robinson, M. D., McCarthy, D. J., and Smyth, G. K. (2010). edgeR: a Bioconductor package for differential expression analysis of digital gene expression data. *Bioinformatics* 26 (1), 139–140. doi:10.1093/bioinformatics/btp616

Rodrigues, J. G., Balmana, M., Macedo, J. A., Pocas, J., Fernandes, A., de-Freitas-Junior, J. C. M., et al. (2018). Glycosylation in cancer: selected roles in tumour progression, immune modulation and metastasis. *Cell Immunol.* 333, 46–57. doi:10.1016/j.cellimm.2018.03.007

Roskoski, R., Jr. (2014). The ErbB/HER family of protein-tyrosine kinases and cancer. *Pharmacol. Res.* 79, 34–74. doi:10.1016/j.phrs.2013.11.002

Schjoldager, K. T., Narimatsu, Y., Joshi, H. J., and Clausen, H. (2020). Global view of human protein glycosylation pathways and functions. *Nat. Rev. Mol. Cell Biol.* 21 (12), 729–749. doi:10.1038/s41580-020-00294-x

Simon, N., Friedman, J., Hastie, T., and Tibshirani, R. (2011). Regularization paths for cox's proportional hazards model via coordinate descent. *J. Stat. Softw.* 39 (5), 1–13. doi:10.18637/jss.v039.i05

Skandalis, S. S., Stylianou, M., Vynios, D. H., Papageorgakopoulou, N., and Theocharis, D. A. (2007). The structural and compositional changes of glycosaminoglycans are closely associated with tissue type in human laryngeal cancer. *Biochimie* 89 (12), 1573–1580. doi:10.1016/j.biochi.2007.07.006

Skidmore, Z. L., Wagner, A. H., Lesurf, R., Campbell, K. M., Kunisaki, J., Griffith, O. L., et al. (2016). GenVisR: genomic visualizations in R. *Bioinformatics* 32 (19), 3012–3014. doi:10.1093/bioinformatics/btw325

Smirnov, P., Safikhani, Z., El-Hachem, N., Wang, D., She, A., Olsen, C., et al. (2016). PharmacoGx: an R package for analysis of large pharmacogenomic datasets. *Bioinformatics* 32 (8), 1244–1246. doi:10.1093/bioinformatics/btv723

Sottoriva, A., Spiteri, I., Piccirillo, S. G., Touloumis, A., Collins, V. P., Marioni, J. C., et al. (2013). Intratumor heterogeneity in human glioblastoma reflects cancer evolutionary dynamics. *Proc. Natl. Acad. Sci. U. S. A.* 110 (10), 4009–4014. doi:10.1073/pnas.1219747110

Tan, A. C., Ashley, D. M., Lopez, G. Y., Malinzak, M., Friedman, H. S., and Khasraw, M. (2020). Management of glioblastoma: state of the art and future directions. *CA Cancer J. Clin.* 70 (4), 299–312. doi:10.3322/caac.21613

Ushakov, V. S., Tsidulko, A. Y., de La Bourdonnaye, G., Kazanskaya, G. M., Volkov, A. M., Kiselev, R. S., et al. (2017). Heparan sulfate biosynthetic system is inhibited in human glioma due to EXT1/2 and HS6ST1/2 down-regulation. *Int. J. Mol. Sci.* 18 (11), 2301. doi:10.3390/ijms18112301

Van Meir, E. G., Hadjipanayis, C. G., Norden, A. D., Shu, H. K., Wen, P. Y., and Olson, J. J. (2010). Exciting new advances in neuro-oncology: the avenue to a cure for malignant glioma. *CA Cancer J. Clin.* 60 (3), 166–193. doi:10.3322/caac.20069

Variyath, A. M., and Brobbey, A. (2020). Variable selection in multivariate multiple regression. *PLoS One* 15 (7), e0236067. doi:10.1371/journal.pone.0236067

Wade, A., Robinson, A. E., Engler, J. R., Petritsch, C., James, C. D., and Phillips, J. J. (2013). Proteoglycans and their roles in brain cancer. *FEBS J.* 280 (10), 2399–2417. doi:10.1111/febs.12109

Wang, X., Jia, Y., Wang, P., Liu, Q., and Zheng, H. (2017). Current status and future perspectives of sonodynamic therapy in glioma treatment. *Ultrason. Sonochem* 37, 592–599. doi:10.1016/j.ultsonch.2017.02.020

Wang, Y., Chu, Y., Li, K., Zhang, G., Guo, Z., Wu, X., et al. (2020). Exosomes secreted by adipose-derived mesenchymal stem cells foster metastasis and osteosarcoma proliferation by increasing *COLGALT2* expression. *Front. Cell Dev. Biol.* 8, 353. doi:10.3389/fcell.2020.00353

Wesseling, P., van den Bent, M., and Perry, A. (2015). Oligodendroglioma: pathology, molecular mechanisms and markers. *Acta Neuropathol.* 129 (6), 809–827. doi:10.1007/s00401-015-1424-1

Wu, T., Hu, E., Xu, S., Chen, M., Guo, P., Dai, Z., et al. (2021). clusterProfiler 4.0: a universal enrichment tool for interpreting omics data. *Innov. (Camb)* 2 (3), 100141. doi:10.1016/j.xinn.2021.100141

Yada, T., Gotoh, M., Sato, T., Shionyu, M., Go, M., Kaseyama, H., et al. (2003). Chondroitin sulfate synthase-2. Molecular cloning and characterization of a novel human glycosyltransferase homologous to chondroitin sulfate glucuronyltransferase, which has dual enzymatic activities. *J. Biol. Chem.* 278 (32), 30235–30247. doi:10.1074/jbc.M303657200

Yang, W., Zhang, C., Li, Y., Jin, A., Sun, Y., Yang, X., et al. (2019). Phosphorylase kinase beta represents a novel prognostic biomarker and inhibits malignant phenotypes of liver cancer cell. *Int. J. Biol. Sci.* 15 (12), 2596–2606. doi:10.7150/ijbs.33278

Yoshihara, K., Shahmoradgoli, M., Martinez, E., Vegesna, R., Kim, H., Torres-Garcia, W., et al. (2013). Inferring tumour purity and stromal and immune cell admixture from expression data. *Nat. Commun.* 4, 2612. doi:10.1038/ncomms3612

Zhang, Y., Iwasaki, H., Wang, H., Kudo, T., Kalka, T. B., Hennet, T., et al. (2003). Cloning and characterization of a new human UDP-N-acetyl-alpha-D-galactosamine: polypeptide N-acetylgalactosaminyltransferase, designated pp-GalNAc-T13, that is specifically expressed in neurons and synthesizes GalNAc alpha-serine/threonine antigen. *J. Biol. Chem.* 278 (1), 573–584. doi:10.1074/jbc.M203094200

Zhao, C. Y., Hua, C. H., Li, C. H., Zheng, R. Z., and Li, X. Y. (2021). High PYGL expression predicts poor prognosis in human gliomas. *Front. Neurol.* 12, 652931. doi:10.3389/fneur.2021.652931

Zhu, Y., Liu, Z., Lv, D., Cheng, X., Wang, J., Liu, B., et al. (2022). Identification of PYGL as a key prognostic gene of glioma by integrated bioinformatics analysis. *Future Oncol.* 18 (5), 579–596. doi:10.2217/fon-2021-0759

frontiers | Frontiers in Immunology

TYPE Original Research
PUBLISHED 26 February 2024
DOI 10.3389/fimmu.2024.1356833

Check for updates

OPEN ACCESS

EDITED BY
Mariana Magalhães,
University of Coimbra, Portugal

REVIEWED BY
Shanqiang Qu,
Southern Medical University, China
Donatien Kamdem Toukam,
University of Cincinnati, United States

*CORRESPONDENCE
Hang Peng
hangpeng21@126.com
Long Zhang
longzhang@xjtu.edu.cn

RECEIVED 16 December 2023
ACCEPTED 09 February 2024
PUBLISHED 26 February 2024

CITATION
Zhang W, Zhang L, Dong H and Peng H (2024) TGIF2 is a potential biomarker for diagnosis and prognosis of glioma. *Front. Immunol.* 15:1356833. doi: 10.3389/fimmu.2024.1356833

COPYRIGHT
© 2024 Zhang, Zhang, Dong and Peng. This is an open-access article distributed under the terms of the Creative Commons Attribution License (CC BY). The use, distribution or reproduction in other forums is permitted, provided the original author(s) and the copyright owner(s) are credited and that the original publication in this journal is cited, in accordance with accepted academic practice. No use, distribution or reproduction is permitted which does not comply with these terms.

TGIF2 is a potential biomarker for diagnosis and prognosis of glioma

Wan Zhang[1,2], Long Zhang[3]*, Huanhuan Dong[4] and Hang Peng[1,5]*

[1]Health Science Center of Xi'an Jiaotong University, Xi'an, Shaanxi, China, [2]Bone and Joints Research Center, The First Affiliated Hospital of Xi'an Jiaotong University, Xi'an, Shaanxi, China, [3]Department of Respiratory and Critical Care Medicine, The Second Affiliated Hospital of Xi'an Jiaotong University, Xi'an, Shaanxi, China, [4]Department of Thoracic Surgery, The First Affiliated Hospital of Xi'an Jiaotong University, Xi'an, Shaanxi, China, [5]Second Department of General Surgery, Shaanxi Provincial People's Hospital, Xi'an, Shaanxi, China

Background: TGFB-induced factor homeobox 2 (TGIF2), a member of the Three-Amino-acid-Loop-Extension (TALE) superfamily, has been implicated in various malignant tumors. However, its prognostic significance in glioma, impact on tumor immune infiltration, and underlying mechanisms in glioma development remain elusive.

Methods: The expression of TGIF2 in various human normal tissues, normal brain tissues, and gliomas was investigated using HPA, TCGA, GTEx, and GEO databases. The study employed several approaches, including Kaplan-Meier analysis, ROC analysis, logistic regression, Cox regression, GO analysis, KEGG analysis, and GSEA, to explore the relationship between TGIF2 expression and clinicopathologic features, prognostic value, and potential biological functions in glioma patients. The impact of TGIF2 on tumor immune infiltration was assessed through Estimate, ssGSEA, and Spearman analysis. Genes coexpressed with TGIF2 were identified, and the protein-protein interaction (PPI) network of these coexpressed genes were constructed using the STRING database and Cytoscape software. Hub genes were identified using CytoHubba plugin, and their clinical predictive value was explored. Furthermore, *in vitro* experiments were performed by knocking down and knocking out TGIF2 using siRNA and CRISPR/Cas9 gene editing, and the role of TGIF2 in glioma cell invasion and migration was analyzed using transwell assay, scratch wound-healing assay, RT-qPCR, and Western blot.

Results: TGIF2 mRNA was found to be upregulated in 21 cancers, including glioma. High expression of TGIF2 was associated with malignant phenotypes and poor prognosis in glioma patients, indicating its potential as an independent prognostic factor. Furthermore, elevated TGIF2 expression positively correlated with cell cycle regulation, DNA synthesis and repair, extracellular matrix (ECM) components, immune response, and several signaling pathways that promote tumor progression. TGIF2 showed correlations with Th2 cells, macrophages, and various immunoregulatory genes. The hub genes coexpressed with TGIF2 demonstrated significant predictive value. Additionally, *in vitro* experiments revealed that knockdown and knockout of TGIF2 inhibited glioma cell invasion,

migration and suppressed the epithelial-mesenchymal transition (EMT) phenotype.

Conclusion: TGIF2 emerges as a potential biomarker for glioma, possibly linked to tumor immune infiltration and EMT.

KEYWORDS

TGIF2, biomarker, glioma, immune infiltration, EMT

1 Introduction

Glioma is the most prevalent primary brain tumor, accounting for approximately 80% of malignant primary brain tumors in adults (1). The World Health Organization (WHO) classifies gliomas into Grade II to IV based on malignancy, with Grade II representing low-grade gliomas and Grades III and IV representing high-grade gliomas. Low-grade gliomas have the potential to progress to high-grade gliomas (2, 3). Gliomas exhibit high invasiveness, heterogeneity, and poor marginal restriction, rendering them susceptible to recurrence. Consequently, controlling invasive lesions poses a significant challenge in glioma treatment. Despite the implementation of diverse treatment modalities, such as surgery, radiotherapy, chemotherapy, and immunotherapy, the overall prognosis for glioma patients remains bleak, with a median survival of only 15 months for the most malignant glioblastoma multiforme (Grade IV glioma) (4). Given these challenges, the identification of more sensitive molecular targets as biomarkers for glioma diagnosis, treatment, and prognosis assessment is imperative.

TGF-β-induced factor homeobox 2 (TGIF2) belongs to the three-amino-acid-loop extension (TALE) superfamily of homeodomain proteins (5). Operating as a transcriptional repressor, TGIF2 regulates the BMP/TGF-β pathway or directly binds to DNA (6–8). TGIF2 has been implicated in the development and progression of various cancers. For instance, in cervical cancer, TGIF2 downregulates FCMR by binding directly to its promoter, thereby promoting cervical cancer metastasis (9). In lung cancer, TGIF2 has been found to mediate the EGFR-RAS-ERK signaling pathway, enhancing the stemness of lung adenocarcinoma cells and facilitating LUAD progression and metastasis (10). MicroRNA-148a was found to inhibit ovarian cancer cell proliferation and invasion by suppressing TGIF2 (11). Additionally, TGIF2 is associated with the epithelial-mesenchymal transition (EMT) phenotype in various diseases, including lung adenocarcinoma (12), primary biliary cholangitis (13), chronic obstructive pulmonary disease (14), colon cancer (15), prostate cancer (16), hepatocellular carcinoma (17) *etc.* Notably, as a downstream target of multiple non-coding RNAs, TGIF2 regulates the progression of glioma (18–21). Previous *in vitro* experiments have suggested that TGIF2 promotes the EMT phenotype and migration in U87MG and A172 glioma cells (21), indicating the potential involvement of TGIF2 in regulating glioma cell invasion and tumor metastasis. However, whether TGIF2 can serve as a biomarker for tumor progression, diagnosis, and prognosis in glioma remains unclear.

In this study, we systematically analyzed transcriptomic data and clinicopathologic information of gliomas sourced from online databases. Our results revealed a significant overexpression of TGIF2 in gliomas compared to normal human brain tissues. Moreover, elevated TGIF2 expression correlated with malignant phenotypes and poor prognosis in glioma patients, establishing it as a potential independent prognostic indicator. Differentially expressed genes enrichment analysis uncovered positive associations between high TGIF2 expression and crucial biological processes, including cell cycle regulation, DNA synthesis and repair, extracellular matrix, immune response, and various signaling pathways implicated in tumor progression. Immune infiltration analysis revealed the association of TGIF2 with the infiltration status of multiple immune cells, including Th2 cells and macrophages. Furthermore, a comprehensive analysis of the TGIF2 coexpression gene network in glioma was conducted, shedding light on the expression patterns of genes interacting with TGIF2 and the potential clinical relevance of hub genes. Finally, knockdown and knockout of TGIF2 inhibited invasion, migration and EMT of U251 cells *in vitro*, suggesting its potential function in glioma invasion and migration. These findings collectively position TGIF2 as a promising candidate for a diagnostic and prognostic biomarker in glioma offering valuable insights into its multifaceted role in the regulation of glioma progression.

2 Materials and methods

2.1 Datasets collection

The RNA-seq data for the 33 cancers and normal tissue in this study were obtained from The Cancer Genome Atlas (TCGA) database (https://portal.gdc.cancer.gov/) and Genotype-Tissue Expression (GTEx) database (https://gtexportal.org/), in which contained 1152 normal human brain tissue and 706 glioma

samples. Clinicopathologic information of glioma patients were acquired from TCGA database (comprising 699 tumor samples). The raw data were normalized with the transcripts per million (TPM) and subsequent analyses were performed using log2 (TPM +1). Expression profiling microarray data of GSE14805 were downloaded from the Gene Expression Omnibus (GEO) database (http://www.ncbi.nlm.nih.gov/projects/geo/) (containing 34 tumor samples and 4 normal samples) and statistically analyzed by Xiantao database (https://www.xiantaozi.com/), an online bioinformatic analysis tool based on R software.

2.2 TGIF2 expression analysis

The mRNA expression data of TGIF2 in normal tissues and subcellular localization of TGIF2 protein in SH-SY5Y cell line were sourced from Human Protein Atlas (HPA) database (http://www.proteinatlas.org/). Statistical analysis of TGIF2 expression in normal, tumor, and various clinicopathologic characteristic groups was performed and visualized by Xiantao tool ("stats", "car" and "ggplot2" packages).

2.3 Survival analysis

Glioma patients were categorized into two groups based on the median expression of TGIF2 mRNA (low-expression group: 0%-50%; high-expression group: 50%-100%). Kaplan-Meier analysis and Cox regression analysis were employed for survival analysis. Overall survival (OS), disease-specific survival (DSS), and progression-free interval (PFI) were compared between the high and low TGIF2 expression groups by Xiantao tool ("Survival" package). Additionally, OS, DSS and PFI were compared in different clinicopathologic characteristic subgroups of glioma patients. Kaplan-Meier plots were generated by Xiantao tool ("Survminer" and "ggplot2" packages).

2.4 Receiver operator characteristic curve

Receiver Operator Characteristic (ROC) curves were utilized to assess the diagnostic value of TGIF2 and previously reported prognostic genes (IDH1, IDH2, EGFR, TP53, CDC6, CDC14B, and CHD5) in glioma. ROC analysis and visualized with Xiantao tool ("pROC", "timeROC" and "ggplot2" packages). The closer the area under the ROC curve (AUC) is to "1", the higher the diagnostic value of the gene.

2.5 Univariate logistic regression analysis

Univariate logistic regression analysis was performed using Xiantao tool ("stats" package). Glioma patients were divided into two groups according to the median mRNA expression of TGIF2, with the low-expression group serving as the control. Logistic regression models were constructed to assess the predictive effects of TGIF2 expression on different clinicopathologic characteristics. P value < 0.05 was considered statistically significant.

2.6 Univariate and multivariate cox regression analysis

Proportional hazards hypothesis testing was conducted using Xiantao tool ("survival" package), followed by univariate and multivariate Cox regression analyses to ascertain the independent prognostic significance of high TGIF2 expression and different clinicopathologic characteristics in the OS of glioma patients. Clinicopathologic factors with p value < 0.1 in the univariate Cox regression analysis were incorporated into the multivariate Cox regression analysis to further delineate their autonomous prognostic value. P value < 0.05 was considered as of statistical significance. Forest plots, risk score curve and point of survival chart were drawn using Xiantao tool ("ggplot2" package).

2.7 Prognostic model generation and prediction

Utilizing the independent prognostic factors identified post multivariate Cox regression analysis, Xiantao tool ("rms" package) was employed to construct nomogram model predicting 1-, 3-, and 5-year OS in glioma patients. Calibration analysis and visualization were carried out using Xiantao tool ("rms" package), depicting the differences between the predicted and actual probabilities corresponding to the model at different time points.

2.8 Differentially expressed genes analysis

For TCGA RNA-seq data, glioma patients were categorized into two groups (low-expression group: 0%-50%; high-expression group: 50%-100%) based on the median expression of TGIF2 mRNA. Differentially Expressed Genes (DEGs) of TCGA RNA-seq data and GSE14805 dataset statistically analyzed using Xiantao tool ("DEseq2" and "limma" packages respectively). Genes with an absolute log2 fold change (FC) > 1 and adjusted p value < 0.05 were considered DEGs and used for subsequent analysis. Volcano plots were generated by Xiantao tool ("ggplot2" package).

2.9 Gene ontology, Kyoto Encyclopedia of Genes and Genomes and gene set enrichment analysis

To determine the differences in biological functions and signaling pathways between high and low TGIF2 expression groups, the identified DEGs were analyzed for Gene Ontology (GO) and Kyoto Encyclopedia of Genes and Genomes (KEGG) enrichment using Xiantao tool ("clusterProfiler" package). Items with adjusted p value < 0.05 were considered as significant enrichment. The gene set "c2.cp.all.v2022.1.Hs.symbols.gmt [All

Canonical Pathways]" in Molecular Signatures Database (MSigDB) was chosen as the reference gene set for Gene Set Enrichment Analysis (GSEA), and the items with false discovery rate (FDR) < 0.25 and adjusted p value < 0.05 were considered significantly enriched. Results of GO, KEGG and GSEA enrichment analyses were used Xiantao tool ("ggplot2" package) for visualization.

2.10 Immune infiltration analysis

The "Estimate" package in R software (v 4.2.1) was applied to assess the stromal score, immune score, and estimate score in the glioma microenvironment grouped by high and low TGIF2 expression. Single sample Gene Set Enrichment Analysis (ssGSEA) was used to analyze the immune infiltration of 24 immune cells in glioma by calculating the enrichment score of each immune cell in the tumor samples according to the marker genes of the immune cells by Xiantao tool ("GSVA" package). Wilcoxon rank-sum test compared immune cell enrichment scores between high and low TGIF2 expression groups. Correlation between TGIF2 and various immune cells and immunoregulatory genes was implemented by Spearman analysis (22, 23). Visualization was performed using Xiantao tool ("ggplot2" package).

2.11 Screening of TGIF2-coexpressed genes in glioma

Spearman's correlation test was employed to analyze the correlation of each gene with TGIF2. Genes with adjusted p value < 0.05 were sorted by the correlation coefficient, and the top 50 genes positively or negatively correlated with TGIF2 were selected for subsequent analysis. The coexpression heatmap of the top 15 genes positively or negatively correlated with TGIF2 were visualized using Xiantao tool ("ggplot2" package).

2.12 Protein-protein interaction network construction and hub genes identification

To investigate the interaction relationships among coexpression genes correlated with TGIF2, the STRING database (https://string-db.org/) was used to establish a Protein-Protein Interaction (PPI) network based on default parameters. Subsequently, the network was visualized by the Cytoscape software, and the top 10 hub genes were identified using the CytoHubba plugin. Kaplan-Meier plots and ROC plots of these 10 hub genes were generated as previously described.

2.13 Cell culture, vector construction and transfection

U251 and 293T cells were cultured in DMEM (Cellmax, CGM102.05) medium supplemented with 10% FBS (Gibco, 2437694). To knockdown TGIF2, U251 cells were transfected with siRNA of TGIF2 (Sigma, SASI_Hs01_00107440) using Lipofectamine 3000 (Invitrogen, L3000015) at a final concentration of 100 pmol according to the manufacturer's instructions when the cells reached approximately 50% confluence. For TGIF2 knockout, guide RNAs (gRNAs) targeting exon 2 of TGIF2 were designed using the http://crispor.tefor.net/website. The double-stranded DNA formed after annealing gRNA33 and gRNA140 were inserted into the PX459 V2.0 plasmid. We transfected 293T cells with the cloned vectors, extracted genomic DNA and performed Sanger sequencing to determine the knockout efficiency of the vectors. The screened gRNA was transfected into U251 cells, and the monoclones that successfully knocked out TGIF2 were selected for expansion culture for subsequent experiments. The primer sequences for synthesizing gRNA were as follows: gRNA33, Forward: 5′- CACCGACCTA GATCACTGTCCGACA -3′;Reverse: 5′-AAACTGTCGGACAGT GATCTAGGTC -3′. gRNA140, Forward: 5′- CACCGCGGTGAA GATCCTCCGGGAC -3′;Reverse: 5′- AAACGTCCCG GAGGATCTTCACCGC -3′. The primer sequences for verifying knockout efficiency of gRNA were as follows: Forward: 5′- CATCCCCTGTGTCCCTTGTC -3′;Reverse: 5′- ACTTGCAG CACTGACAGGTT -3′.

2.14 RNA extraction, cDNA synthesis, and RT-qPCR

Total RNA was extracted with TsingZol total RNA extraction reagent (TSINGKE, TSP401) and cDNA was synthesized using 5× All-In-One RT Master Mix (Applied Biological Materials, G490) following the manufacturer's protocol. RT-qPCR was performed using PowerUp™ SYBR™ Green Master Mix (Applied Biosystems™, A25742) and PIKOREAL 96 Real-Time PCR System (ThermoFisher). GAPDH served as internal control for quantifying relative gene expression levels using the 2 −ΔΔCT method. The primer sequences were as follows: TGIF2, Forward: 5′- CTTCAACACGCCACCACCCACACC-3′; Reverse: 5′- CCTCT GTAGCGCCACCTCCACCAG -3′.CDH2, Forward: 5′- CCT CCAGAGTTTACTGCCATGAC -3′; Reverse: 5′- GTAGGA TCTCCGCCACTGATTC -3′. TWIST1, Forward: 5′- GCCAGGT ACATCGACTTCCTCT -3′; Reverse: 5′- TCCATCCTCC AGACCGAGAAGG -3′. TWIST2, Forward: 5′- GCAAG ATCCAGACGCTCAAGCT -3′; Reverse: 5′- ACACGGAG AAGGCGTAGCTGAG -3′. GAPDH, Forward: 5′- GGAGT CCACTGGCGTCTTCA -3′; Reverse: 5′- GTCATGAGTCCTT CCACGATACC -3′.

2.15 Transwell assay and scratch wound-healing assay

For transwell assay, $5x10^4$ cells were inoculated in transwell (Millicell, PI8P01250) upper chamber containing serum-free DMEM, and the lower chamber was layered with DMEM containing 10% FBS. After 24 h of incubation at 37°C, non-invasive cells on the upper surface of the membrane were wiped off with a cotton swab. Subsequently, invasive cells into the lower

surface of the membrane were fixed with 4% paraformaldehyde and stained with 0.1% crystalline violet (Solarbio, G1063), observed under the microscope and selected random fields were photographed. For scratch wound-healing assay, cells were plated into 12-well plates and cultured until 90% confluence, scratched using a 10 μL pipette tip, and washed with PBS to remove dropped cells. The cells migration distance was observed at 0 h and 24 h of scratching and photographed.

2.16 Western blot analysis

Cells were lysed with RIPA lysis buffer (Beyotime, P0013B) supplemented with 1 mM of the protease inhibitor phenylmethylsulfonyl fluoride (Beyotime, ST506) for 20 min on ice. After centrifugation at 12,000 rpm, the supernatant was collected, loaded onto a 10% polyacrylamide SDS gel, and subsequently transferred to a PVDF membrane (Millipore, IPVH00010). Membranes were blocked with TBST containing 5% skimmed milk (BD Pharmingen™, 232100) for 1 h at room temperature, followed by overnight incubation at 4°C with primary antibodies. After 5 washes with TBST, the membranes were incubated with secondary antibody at room temperature for 2 h. The membranes were then scanned and analyzed using the ChemiDoc™ system (Bio-Rad). The following antibodies were used: TGIF2 (11522-1-AP, Proteintech); GAPDH (EPR16891, Abcam); N-Cadherin (22018-1-AP, Proteintech); secondary antibody (AB0101, Abways).

2.17 Statistical analysis

Bioinformatics analysis was performed with Wilcoxon rank sum test to detect statistical significance between the two groups. The relationship between TGIF2 expression and baseline clinicopathologic characteristics of patients was evaluated using the chi-square test by Xiantao tool ("stats" package). Spearman's correlation coefficient assessed the correlation of TGIF2 expression with various immune cells and other genes. Statistical analysis of *in vitro* experiments were performed with GraphPad Prism 7.0 and comparisons between two conditions were applied by Student's t-test and the data were presented as mean ± standard deviation (SD). P value < 0.05 was considered statistically significant.

3 Results

3.1 TGIF2 expression is elevated in glioma and associated with worse prognosis

We explored the basal expression levels of TGIF2 across various tissues. Analysis of HPA database revealed higher TGIF2 mRNA expression in breast and female reproductive system, bone marrow, lymphoid, and muscle tissues, while lower expression was observed in brain tissues (Figure 1A). Subsequently, TGIF2 expression was assessed in 33 tumors from TCGA and GTEx databases. Notably, TGIF2 expression levels in 21 tumor tissues were significantly higher than in corresponding normal tissues (Figure 1B). Specifically, elevated TGIF2 expression was observed in low-grade glioma (LGG) and glioblastoma (GBM) compared to normal brain tissues (Figure 1B). Subcellular localization of TGIF2 protein is predominantly in the nucleus in the human glioma cell line SH-SY5Y (Figure 1C). Furthermore, in the GSE14805 dataset, we identified 2954 DEGs, including 1369 upregulated and 1585 downregulated genes, with TGIF2 significantly upregulated in the tumor group (Figure 1D). The ROC analysis indicated similar diagnostic ability for TGIF2 (AUC = 0.971) with established glioma prognostic genes (IDH1, IDH2, EGFR, TP53, CDC6, CDC14B, CHD5) (24–30) (Figure 1E). Kaplan-Meyer analysis demonstrated that glioma patients with high TGIF2 expression exhibited poor OS, DSS and PFI (Figures 1F–H). These findings suggest that TGIF2 expression is elevated in glioma and associated with worse prognosis, warranting further investigation.

3.2 High TGIF2 expression associated with malignant phenotypes of glioma

We investigated the association between TGIF2 expression and various clinicopathologic characteristics of glioma patients in the TCGA database. A total of 699 patients' clinicopathologic information was included in the statistics, and the chi-square test revealed that TGIF2 expression was significantly correlated with age, WHO grade, IDH status, 1p/19q codeletion, histological type, OS event, DSS event and PFI event in glioma patients (Table 1). Logistic regression analysis further confirmed significant associations between TGIF2 and age, WHO grade, IDH status, 1p/19q codeletion and histological type (Table 2). TGIF2 expression patterns in different clinicopathologic characteristics showed elevation in age > 60 years, IDH-wild type, 1p/19q non-codeletion, progressive disease and stable disease (PD&SD), OS events, DSS events, and PFI events subgroups (Figures 2A–G). TGIF2 expression increased with WHO grade classification, peaking in G4 glioma (Figure 2H). For histological type, glioblastoma exhibited significantly higher TGIF2 expression compared to other glioma types (Figure 2I). However, no statistically significant differences were observed among glioma patients of different genders and races (Figures 2J, K). These results suggest that high TGIF2 expression may be associated with malignant phenotypes of glioma and worsening clinical outcomes.

3.3 Prognostic value of TGIF2 expression in glioma

We assessed the prognostic value of TGIF2 expression for glioma patients in the TCGA database. Firstly, analysis of TGIF2 expression distribution, survival status, and risk scores indicated that higher TGIF2 expression in the high-risk group correlated with increased mortality rates compared to the low-risk group (Figure 3A). Time-dependent ROC analysis demonstrated

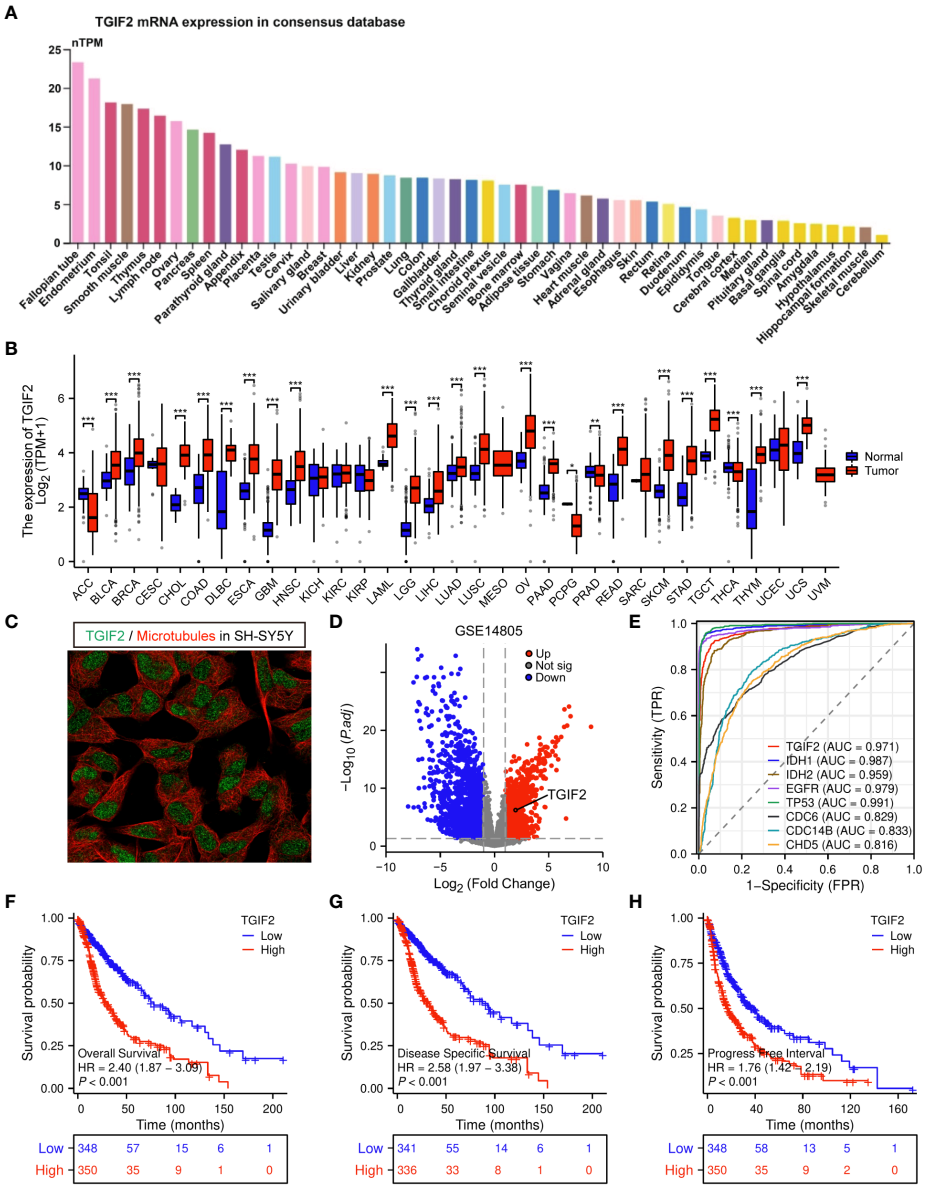

FIGURE 1
The expression level of TGIF2 in different human cancers and its relationship to glioma prognosis. **(A)** TGIF2 mRNA expression across various human organs and tissues based on consensus dataset in HPA database. **(B)** Comparison of TGIF2 expression between normal and tumor tissues across 33 cancers in TCGA and the GTEx database. **(C)** Subcellular localization of TGIF2 in SH-SY5Y cells from HPA datasets. **(D)** The volcano plot of DEGs in GSE14805. Red points represent upregulated, blue points represents downregulated genes. **(E)** ROC curve of TGIF2 and other established prognostic genes (IDH1, IDH2, EGFR, TP53, CDC6, CDC14B, CHD5) in glioma. **(F–H)** Survival curves for OS **(F)**, DSS **(G)** and PFI **(H)** in gliomas using TCGA database. ∗p < 0.05, ∗∗p < 0.01, ∗∗∗p < 0.001.

favorable predictive efficacy of TGIF2 expression for OS at 1-year (AUC = 0.653), 3-years (AUC = 0.715), and 5-years (AUC = 0.690) (Figure 3B). Univariate Cox regression analysis revealed an association between high TGIF2 expression and poorer OS (HR, 2.401; 95% confidence interval [CI], 1.867-3.089; p < 0.001) (Table 3). Multivariate Cox regression analysis, after confounding with other clinicopathologic variables, identified TGIF2 as an independent prognostic risk factor for glioma patients (HR, 2.366; 95% CI, 1.620-3.455; p < 0.001). Other clinicopathologic parameters, including age (HR, 5.203; 95% CI, 3.291-8.224; p < 0.001), 1p/19q codeletion (HR, 0.490; 95% CI, 0.298-0.807; p = 0.005), histological type (HR, 4.885; 95% CI, 1.709-13.959; p = 0.003), and primary therapy outcome (HR, 0.215; 95% CI, 1.620 -3.455; p < 0.001), also emerged as independent prognostic factors (Table 3; Figure 3C). A prognostic nomogram model, incorporating TGIF2 expression and other independent prognostic factors analyzed by Cox regression, was constructed for predicting OS at 1, 3, and 5 years (Figure 3D). Calibration curves assessed the predictive efficiency of the nomogram (Figure 3E).

Next, we explored the relationship between TGIF2 and prognosis (OS, DSS, and PFI) across different clinicopathologic subgroups of glioma. Kaplan-Meyer analysis revealed that higher

10.3389/fimmu.2024.1356833

TABLE 1 Clinical characteristics of glioma patients.

Characteristics	Low TGIF2	High TGIF2	P value
n	349	350	
Age, n (%)			**0.007**
<= 60	292 (41.8%)	264 (37.8%)	
> 60	57 (8.2%)	86 (12.3%)	
Gender, n (%)			0.519
Male	196 (28%)	205 (29.3%)	
Female	153 (21.9%)	145 (20.7%)	
WHO grade, n (%)			**< 0.001**
G2	143 (22.4%)	81 (12.7%)	
G3	128 (20.1%)	117 (18.4%)	
G4	45 (7.1%)	123 (19.3%)	
IDH status, n (%)			**< 0.001**
WT	69 (10%)	177 (25.7%)	
Mut	274 (39.8%)	169 (24.5%)	
1p/19q codeletion, n (%)			**< 0.001**
Non-codel	221 (31.9%)	299 (43.2%)	
Codel	127 (18.4%)	45 (6.5%)	
Histological type, n (%)			**< 0.001**
Astrocytoma	95 (13.6%)	101 (14.4%)	
Oligoastrocytoma	72 (10.3%)	63 (9%)	
Oligodendroglioma	137 (19.6%)	63 (9%)	
Glioblastoma	45 (6.4%)	123 (17.6%)	
Race, n (%)			0.629
Asian	7 (1%)	6 (0.9%)	
Black or African American	19 (2.8%)	14 (2%)	
White	316 (46.1%)	324 (47.2%)	
Primary therapy outcome, n (%)			0.065
PD	53 (11.4%)	59 (12.7%)	
SD	89 (19.1%)	59 (12.7%)	
PR	40 (8.6%)	25 (5.4%)	
CR	88 (18.9%)	52 (11.2%)	
OS event, n (%)			**< 0.001**
Alive	254 (36.3%)	173 (24.7%)	
Dead	95 (13.6%)	177 (25.3%)	
DSS event, n (%)			**< 0.001**
Yes	82 (12.1%)	162 (23.9%)	
No	260 (38.3%)	174 (25.7%)	
PFI event, n (%)			**< 0.001**
Yes	144 (20.6%)	202 (28.9%)	
No	205 (29.3%)	148 (21.2%)	

In order to clearly distinguish factors that are significantly different, we have bolded p values less than 0.05.

TABLE 2 Logistic analysis of the association between TGIF2 expression and clinical characteristics.

Characteristics	Total (N)	Odds Ratio (95% CI)	P value
Age (<= 60 vs. > 60)	699	0.599 (0.412 - 0.871)	**0.007**
Gender (Male vs. Female)	699	1.104 (0.818 - 1.490)	0.519
WHO grade (G2 vs. G3&G4)	637	0.408 (0.292 - 0.571)	**< 0.001**
IDH status (WT vs. Mut)	689	4.159 (2.967 - 5.830)	**< 0.001**
1p/19q codeletion (Codel vs. Non-codel)	692	0.262 (0.179 - 0.384)	**< 0.001**
Primary therapy outcome (PD&SD vs. PR&CR)	465	1.381 (0.951 - 2.007)	0.090
Race (White vs. Asian&Black or African American)	686	1.333 (0.729 - 2.436)	0.350
Histological type (Glioblastoma vs. Astrocytoma&Oligoastrocytoma&Oligodendroglioma)	699	3.660 (2.498 - 5.365)	**< 0.001**

In order to clearly distinguish factors that are significantly different, we have bolded p values less than 0.05.

TGIF2 expression associated with worse OS in subgroups including age >60, age ≤60, male, female, Race (White), WHO grade (G3), 1p/19q codeletion status (non-codel), histological type (astrocytoma), and primary therapy outcome (PD) (Figures 4A–I). For DSS, patients with higher TGIF2 expression had worse DSS in subgroups such as age >60, age ≤60, male, female, race (White), WHO grade (G3), 1p/19q codeletion status (non-codel), histological type (astrocytoma), primary therapy outcome (PD) and primary therapy outcome (SD) (Supplementary Figures S1A–J). For PFI, higher TGIF2 expression was associated with worse PFI in subgroups including age >60, age ≤60, male, female, race (White), WHO grade (G3), 1p/19q codeletion status (non-codel) (Supplementary Figures S2A–G).

3.4 Functional enrichment analysis of DEGs between TGIF2 high and low expression groups in glioma

We analyzed DEGs between TGIF2 high and low expression groups based on the median TGIF2 expression level. A total of 2696 DEGs were identified, comprising 1353 upregulated and 1343 downregulated genes (Figure 5A). In GO enrichment analysis, the biological process (BP) mainly contained embryonic organ development, regulation of membrane potential, extracellular matrix organization, calcium-mediated signaling and chemokine-mediated signaling pathway. The cellular component (CC) was

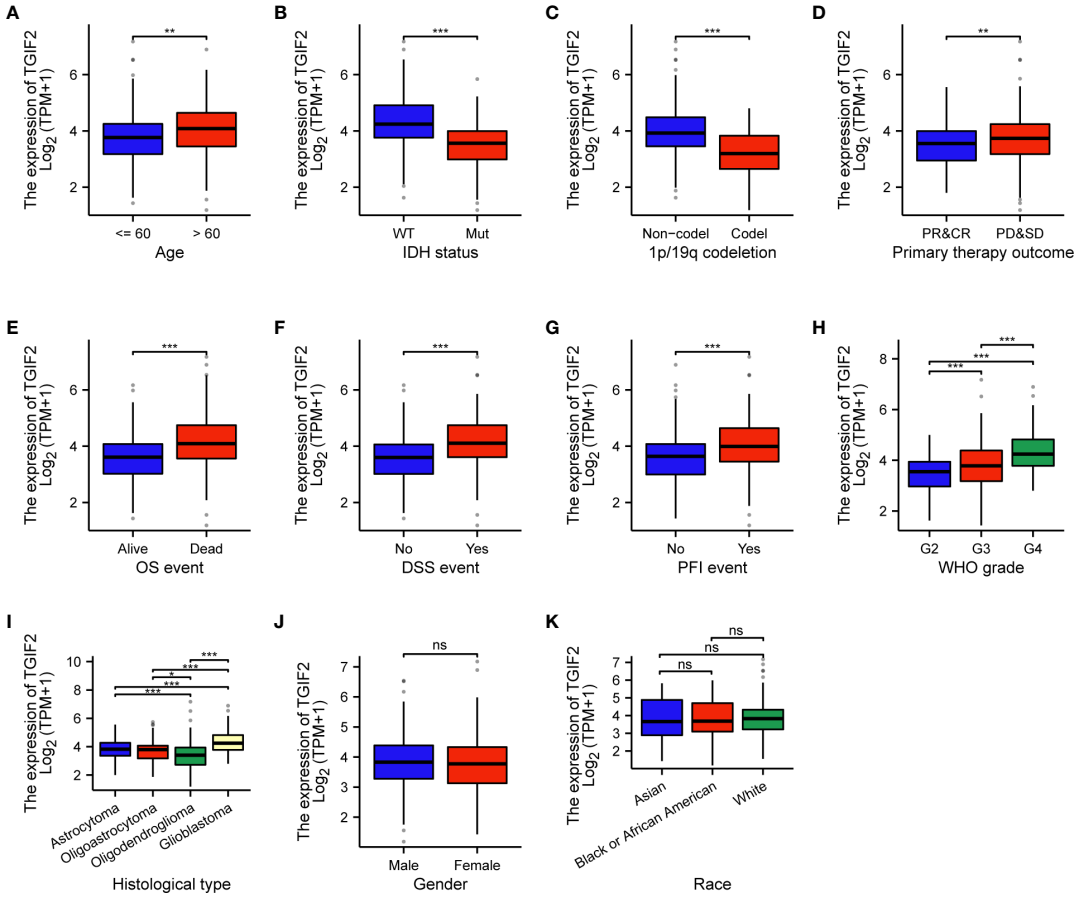

FIGURE 2
Associations between TGIF2 expression and various clinicopathologic characteristics in glioma. **(A)** Age. **(B)** IDH status. **(C)** 1p/19q codeletion status. **(D)** Primary therapy outcome. **(E)** OS events. **(F)** DSS events. **(G)** PFI events. **(H)** WHO grade. **(I)** Histological type. **(J)** Gender. **(K)** Race. $*p < 0.05$, $**p < 0.01$, $***p < 0.001$, ns, not significant.

enriched in ion channel complex, collagen-containing extracellular matrix, glutamatergic synapse, T cell receptor complex and voltage-gated potassium channel complex. The molecular function (MF) was mainly involved in DNA-binding transcription activator activity, extracellular matrix structural constituent, voltage-gated potassium channel activity, cytokine activity and chemokine activity. KEGG pathway enrichment analysis indicated that TGIF2 potential participation in the regulation of neuroactive ligand-receptor interaction, calcium signaling pathway, cAMP signaling pathway, glutamatergic synapse and ECM-receptor interaction (Figure 5B).

GSEA was applied to further investigate the biological functions of TGIF2. Upregulation of TGIF2 expression correlated with cell cycle and DNA replication pathways, including DNA replication, cell cycle, synthesis of DNA, DNA repair, and cell cycle checkpoints (Figure 5C). ECM-related functions, such as extracellular matrix organization, ECM receptor interaction, and collagens and laminin interactions, were enriched in the TGIF2 high-expression phenotype, suggesting involvement in ECM formation in glioma (Figure 5D). TGIF2 also impacted pathways related to tumor immunity, including cytokine cytokine receptor interaction, signaling by interleukins, inflam pathway, chemokine signaling pathway, toll-like receptor signaling pathway, and Pd-1 signaling (Figure 5E). Additionally, pathways related to tumor progression, such as Jak Stat signaling pathway, signaling by Notch, and Pi3kakt signaling pathway, were enriched (Figure 5F). Ion channel and glutamate signaling are facilitators of glioma cell invasion and migration (31, 32), yet they were negatively correlated with high TGIF2 expression (Figures 5G, H), which may be related to glioma grading (33, 34). These findings suggest that TGIF2 may play a role in glioma cell proliferation, invasion and migration, and tumor immunity, making it a promising target for glioma treatment.

3.5 Correlation between TGIF2 expression and immune cell infiltration in glioma

To unravel the intricate relationship between TGIF2 expression and the tumor immune response in glioma, we meticulously analyzed the disparities in the glioma immune microenvironment

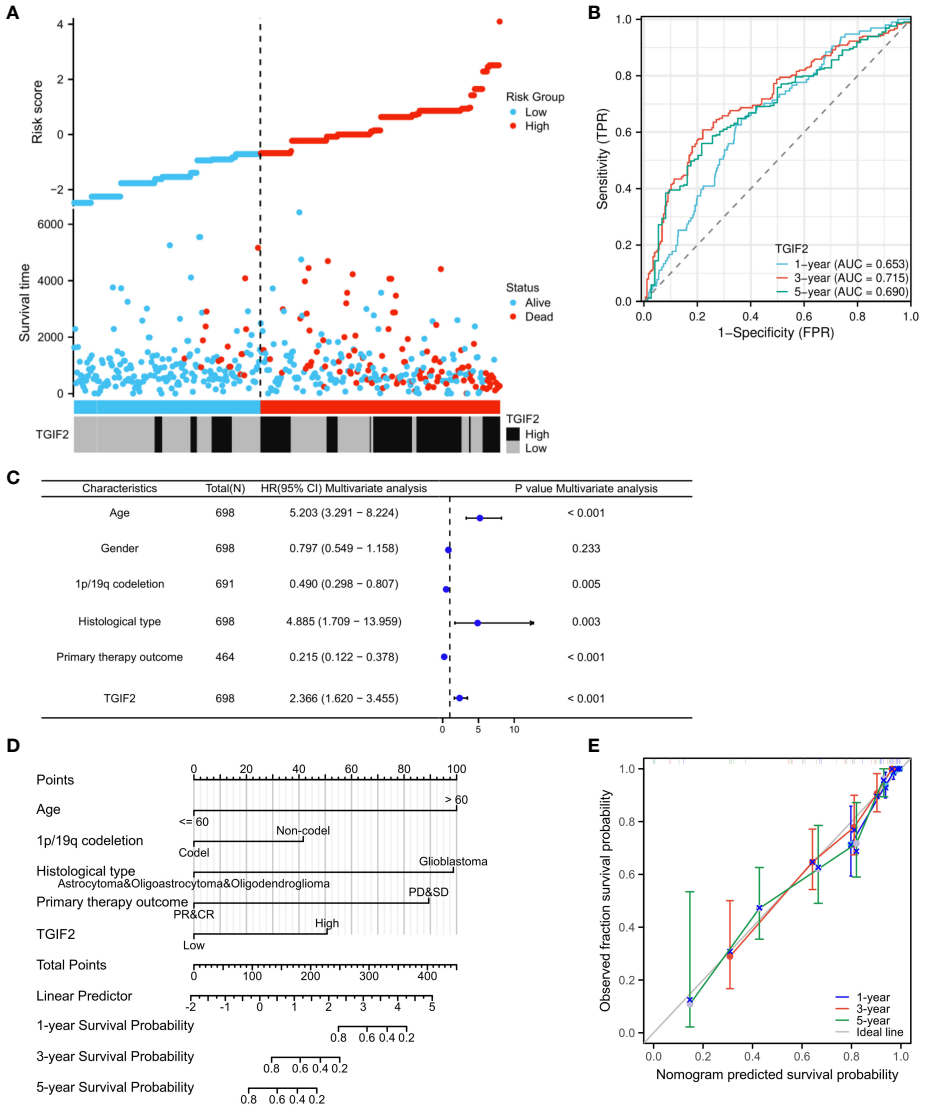

FIGURE 3
Prognostic value of TGIF2 expression level in glioma. **(A)** TGIF2 expression distribution and survival status. **(B)** Time-dependent ROC curves for TGIF2 expression in glioma. **(C)** Forest plot of OS by multivariate Cox regression analysis in glioma from TCGA database. **(D)** The nomogram for predicting 1-, 3-, or 5-year OS rates in patients with glioma. **(E)** The calibration curves for the nomogram.

TABLE 3 Univariate and multivariate cox regression analyses of clinical characteristics associated with overall survival.

Characteristics	Total(N)	Univariate analysis		Multivariate analysis	
		Hazard ratio (95% CI)	P value	Hazard ratio (95% CI)	P value
Age	698				
<= 60	555	Reference		Reference	
> 60	143	4.696 (3.620 - 6.093)	< **0.001**	5.203 (3.291 - 8.224)	< **0.001**
Gender	698				
Male	401	Reference		Reference	
Female	297	0.800 (0.627 - 1.021)	0.073	0.797 (0.549 - 1.158)	0.233

(Continued)

TABLE 3 Continued

Characteristics	Total(N)	Univariate analysis		Multivariate analysis	
		Hazard ratio (95% CI)	P value	Hazard ratio (95% CI)	P value
Race	685				
Asian&Black or African American	46	Reference			
White	639	0.817 (0.499 - 1.337)	0.421		
1p/19q codeletion	691				
Non-codel	520	Reference		Reference	
Codel	171	0.225 (0.147 - 0.346)	< **0.001**	0.490 (0.298 - 0.807)	**0.005**
Histological type	698				
Astrocytoma& Oligoastrocytoma& Oligodendroglioma	530	Reference		Reference	
Glioblastoma	168	9.172 (7.052 - 11.929)	< **0.001**	4.885 (1.709 - 13.959)	**0.003**
Primary therapy outcome	464				
PD&SD	260	Reference		Reference	
PR&CR	204	0.205 (0.117 - 0.359)	< **0.001**	0.215 (0.122 - 0.378)	< **0.001**
TGIF2	698				
Low	348	Reference		Reference	
High	350	2.401 (1.867 - 3.089)	< **0.001**	2.366 (1.620 - 3.455)	< **0.001**

In order to clearly distinguish factors that are significantly different, we have bolded p values less than 0.05.

between high and low TGIF2 expression groups. The outcomes unveiled a significant elevation in stromal scores (Figure 6A), immunity scores (Figure 6B), and estimated scores (Figure 6C) in glioma patients with high TGIF2 expression. Furthermore, multiple immune cell subtypes were significantly enriched in the TGIF2 high-expression group, including aDC, cytotoxic cells, eosinophils, iDC, macrophages, neutrophils, NK CD56dim cells, NK cells, T cells, T helper cells, Th17 cells, and Th2 cells (Figure 6D). In contrast, the TGIF2 low-expression group exhibited higher enrichment of DC, mast cells, NK CD56bright cells, pDC, TFH, TReg, and Tcm (Figure 6E). Subsequently, we further delved into the association between TGIF2 expression levels and the infiltration levels of different immune cells in gliomas. The results demonstrated a positive correlation between TGIF2 expression and the infiltration levels of Th2 cells, macrophages, eosinophils and neutrophils, *etc.* Nevertheless, there was a negative correlation with infiltration levels of mast cells, NK CD56bright cells, pDC and TFH, *etc.* (Figures 6F–N). In addition, we investigated the correlation between TGIF2 and various immunoregulatory molecules to further understand its immune modulating function. These immunoregulatory genes include antigen presentation, cell adhesion, co-inhibitory, co-stimulatory, ligand, receptor, and other according to the classification of Thorsson et al. (23). The findings indicated a positive correlation between TGIF2 expression and most immunoregulatory genes, implying a potential role for TGIF2 in regulating glioma immune infiltration (Supplementary Figure S3).

3.6 Analysis of genes coexpressed with TGIF2 in glioma

The analysis of genes coexpressed with TGIF2 in glioma provided valuable insights into potential regulatory networks and prognostic markers. The coexpression heatmap demonstrated the top 15 genes that were positively and negatively correlated with TGIF2 (Figure 7A). We performed PPI network analysis of the top 50 protein-coding genes positively and negatively correlated with TGIF2 using the STRING database and Cytoscape (Figure 7B) and identified the top 10 hub genes using the CytoHubba plugin (HDAC1, CASP3, REST, HMG20B, FZD7, GNAI3, FZD1, EPHB4, KCNJ9, SCRT1) (Table 4, Figure 7C). The top 10 hub genes highlighted potential central regulators in the context of TGIF2-associated glioma biology. Among these 10 genes HDAC1, CASP3, REST, HMG20B, FZD7,GNAI3, FZD1 and EPHB4 had elevated expression in tumor group compared to the normal group, while KCNJ9 and SCRT1 were decreased (Figure 7D). Kaplan-Meyer analysis showed that high expression of HDAC1, CASP3, REST, HMG20B, FZD7,GNAI3, FZD1 and EPHB4 was associated with worse OS, DSS and PFI, whereas high expression of KCNJ9 and SCRT1 suggested better OS, DSS and PFI (Figures 8A–J; Supplementary Figures S3A–J, S4A–J). ROC analysis further validated the good diagnostic capabilities of these 10 hub genes in glioma (Figures 9A–J). In summary, this comprehensive analysis not only revealed potential regulatory networks with TGIF2 in

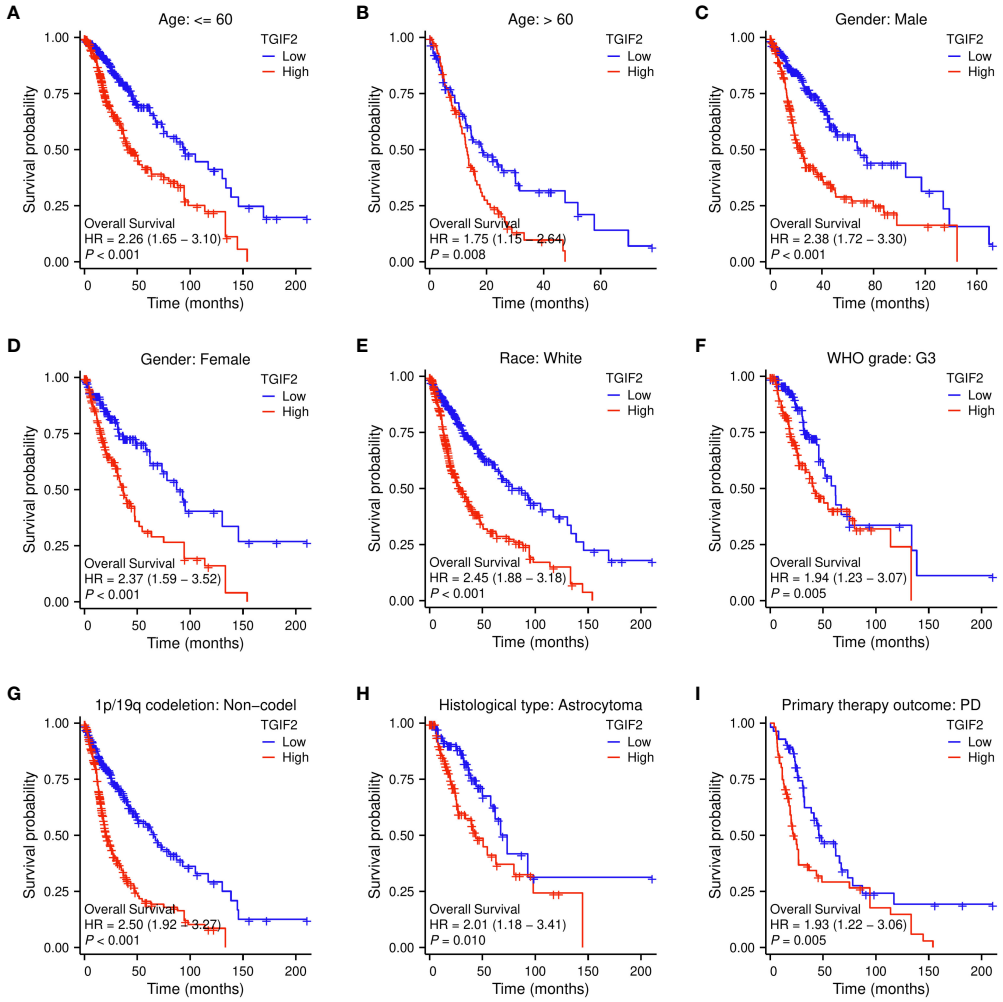

FIGURE 4
Correlations between TGIF2 expression level and OS in different clinicopathologic subgroups of glioma by Kaplan-Meier survival curve analysis. **(A)** Age ≤ 60. **(B)** Age > 60. **(C)** Gender: Male. **(D)** Gender: Female. **(E)** Race: White. **(F)** WHO grade: G3. **(G)** 1p/19q codeletion: non-codeletion. **(H)** Histological type: Astrocytoma. **(I)** Primary therapy outcome: PD.

glioma but also highlighted a promising gene cluster for prognostic assessment. Integrating these hub genes with TGIF2 may enhance the accuracy of prognostic predictions in glioma patients.

3.7 Knockdown and knockout of TGIF2 inhibits glioma cell invasion,migration and EMT *in vitro*

We explored the function of TGIF2 *in vitro*. Initially, we employed siRNA to knock down TGIF2 expression in the U251 glioma cell line. Both RT-qPCR and Western blot analyses confirmed the efficacy of TGIF2 knockdown, ensuring the reliability of subsequent experiments (Figures 10A, B). Subsequent transwell assays and scratch wound-healing assays revealed that TGIF2 inhibition suppressed the invasion and migration of U251 cells (Figures 10C, D). Furthermore, our investigations revealed a downregulation of N-Cadherin, a well-established marker of EMT, in the TGIF2-inhibited group (Figure 10B). This observation suggests that TGIF2 may play a role in promoting the EMT phenotype, thereby influencing glioma cell invasion and migration through the regulation of N-Cadherin expression. We used CRISPR/Cas9 gene editing to further validate the function of TGIF2. We designed gRNA sequences gRNA33 and gRNA140 targeting exon 2 of TGIF2, cloned them into the CRISPER Cas9 plasmid PX459 and verified the editing efficiency on TGIF2 (Figure 11A). Next, we transfected the PX459-gRNA33 plasmid, which was effective in editing TGIF2, into glioma U251 cells, and screened for TGIF2 knockout cell lines using Sanger sequencing (Figures 11B, C). Western blot analyses verified the knockout efficiency for TGIF2 of the PX459-gRNA33 plasmid in U251 cells (Figure 11D). Subsequently, transwell assays and scratch wound-healing assays showed that knockout of TGIF2 inhibited invasion and migration of U251 cells (Figures 11E, F). In addition, the expression of the signature genes of EMT (CDH2, TWIST1 and TWIST2) were also suppressed in the TGIF2-knockout group (Supplementary Figure S6). These results strengthen the evidence that TGIF2 promotes glioma cell invasion, migration and EMT.

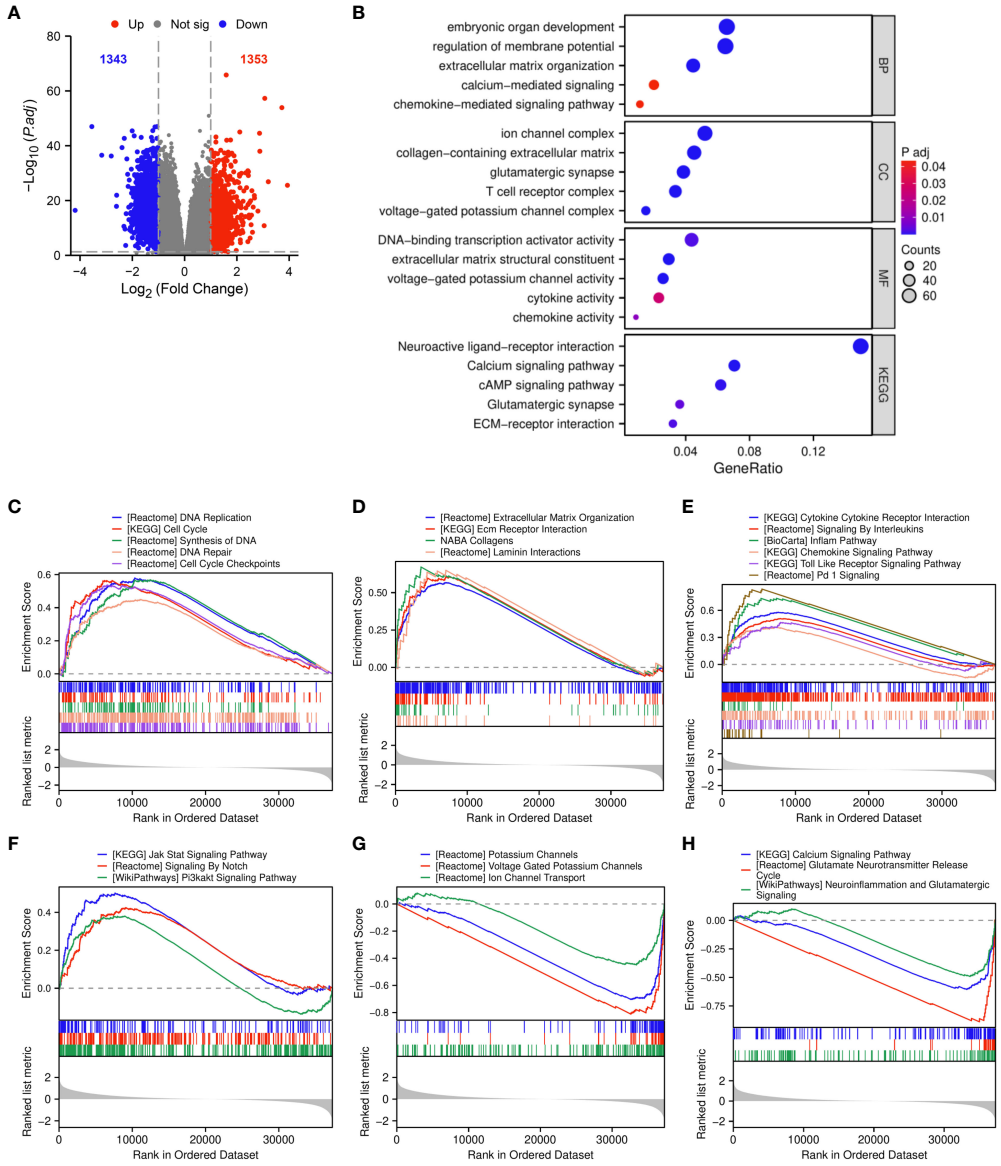

FIGURE 5
Functional enrichment analysis of DEGs between TGIF2 high and low expression groups. **(A)** The volcano plot of DEGs. Red represents upregulated, blue represents downregulated genes. **(B)** GO and KEGG pathway enrichment analysis of DEGs. **(C–H)** GSEA functional enrichment analysis.

4 Discussion

Glioma, recognized as the most lethal adult intracranial primary tumor with low overall survival rates (1), continues to pose formidable challenges despite advancements in treatment modalities (35). There is an imperative need for novel early diagnostic and prognostic targets to address the pressing need for glioma treatment. Numerous studies have been devoted to exploring biomarkers in order to open new avenues for glioma treatment (28–30, 36, 37). The 1p/19q codeletion and IDH mutation emerged as the initial biomarkers, widely employed in clinical glioma diagnosis and have been associated with a variety of prognostic factors to establish effective clinical prediction model (38–40). In this study, we focus on the transcription factor TGIF2 and propose for the first time its potential as a promising diagnostic and prognostic target for glioma. Our investigation demonstrated that TGIF2 expression significantly surpasses normal tissue levels in gliomas and correlates with adverse prognosis and malignant phenotypes. We established high TGIF2 expression as an independent risk factor for OS in glioma patients, as validated by multivariate Cox regression analysis. Moreover, we constructed a prognostic nomogram model of TGIF2 versus age, 1p/19q codeletion, histological type, and primary therapy outcome, enhancing the accuracy of predicting glioma risk factors for future clinical applications. Survival analysis across various clinicopathologic subgroups consistently demonstrated the significant association of TGIF2 with poor OS, DSS and PFI, underscoring its effective prognostic value. These findings collectively advocate TGIF2 as a promising biomarker for both diagnosing and predicting outcomes in glioma patients, offering

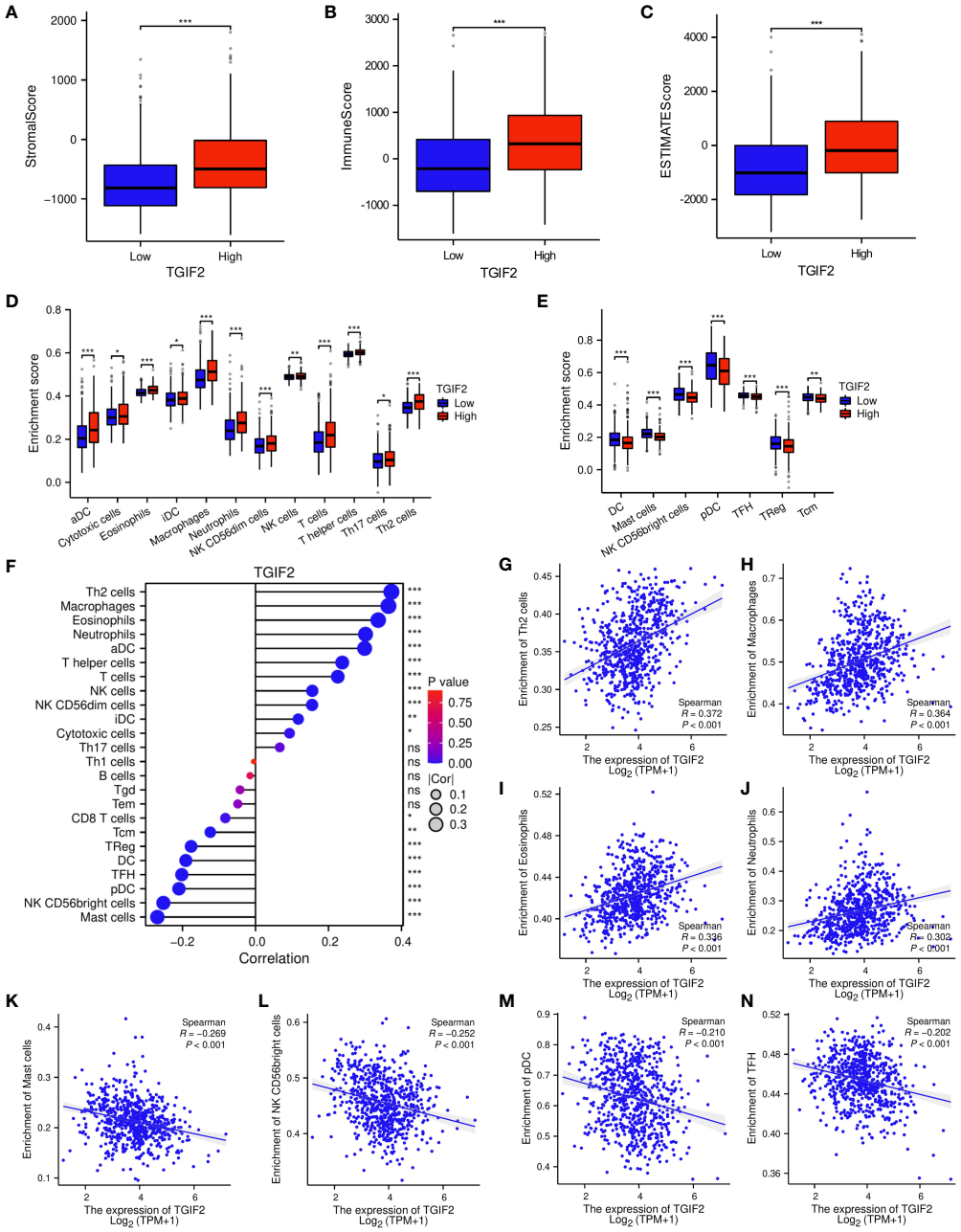

FIGURE 6
Correlations between TGIF2 expression and immune cell infiltration in glioma. **(A–C)** Comparison of StromalScore, ImmuneScore, and EstimateScore between TGIF2 high and low expression groups. **(D, E)** Comparison of immune cell enrichment scores in high and low TGIF2 expression groups. **(F)** The lollipop chart showing the correlations between the relative abundances of 24 immune cells and TGIF2 expression levels. **(G–N)** Scatterplots demonstrating the positive correlation of TGIF2 expression with Th2 cells, macrophages, eosinophils, and neutrophils, and the negative correlation with mast cells, NK CD56bright cells, pDC cells, and TFH cells. ∗p < 0.05, ∗∗p < 0.01, ∗∗∗p < 0.001, ns, not significant.

potential avenues for improved therapeutic strategies and patient care.

To further elucidate the biological function of TGIF2 in glioma development, we divided glioma patients into high and low expression groups based on the median TGIF2 expression, analyzed the differentially expressed genes in the two groups, and performed functional enrichment analysis. Cell hyperproliferation is a common characteristic of the vast majority of tumors, and consistently, we observed multiple items related to cell cycle and DNA synthesis and repair associated with high TGIF2 expression. In addition, our attention was drawn to several ECM-related items. Elevated expression of ECM components creates an impermeable microenvironment for glioma to evade drug and immune attacks, and contributes to tumor cell migration and invasion (41). The positive correlation between the high expression of ECM and TGIF2 suggests that TGIF2 may be involved in the formation of the ECM and thus promote the migration and invasion of glioma cells. In addition, signaling pathways closely related to

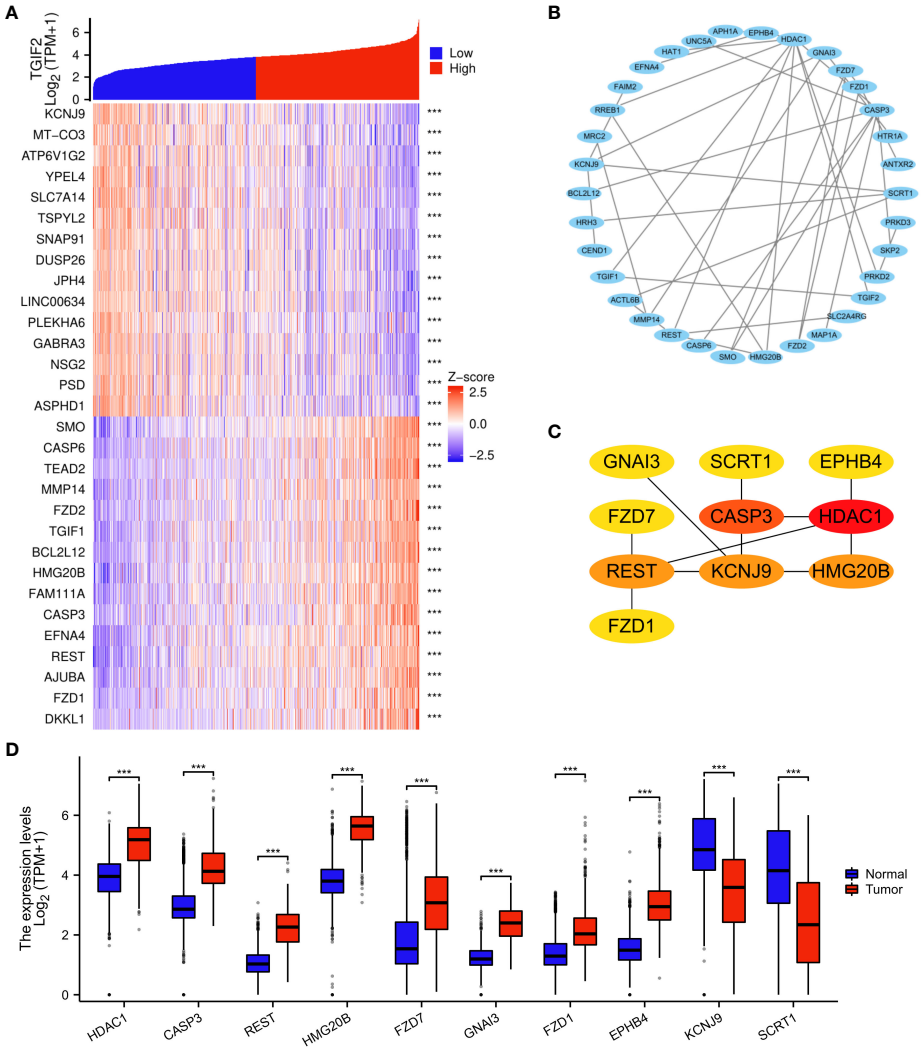

FIGURE 7
Analysis of genes coexpressed with TGIF2 in glioma. **(A)** Heatmap showing the 30 genes in glioma that were 15 positively and 15 negatively related to TGIF2. **(B)** PPI network of top 50 protein-coding genes positively and negatively correlated with TGIF2. **(C)** The top 10 hub genes of the PPI network in **(B)**. **(D)** The expression levels of the top 10 hub genes in normal and glioma tissues in TCGA and GTEx database. ***p < 0.001.

TABLE 4 The top 10 hub genes identified in the PPI network.

Gene symbol	Gene description
HDAC1	Histone deacetylase 1
CASP3	Caspase 3
REST	RE1 silencing transcription factor
HMG20B	High mobility group 20B
FZD7	Frizzled class receptor 7
GNAI3	G protein subunit alpha I3
FZD1	Frizzled class receptor 1
EPHB4	EPH receptor B4
KCNJ9	Potassium inwardly rectifying channel subfamily J member 9
SCRT1	Scratch family transcriptional repressor 1

tumorigenesis, such as Jak Stat signaling pathway (42), Notch signaling pathway (43), and Pi3k akt signaling pathway (44) were associated with increased expression of TGIF2. Notably, NOTCH signaling was reported to be associated with EMT, and the promotion of EMT in glioma cell by TGIF2 has been reported in glioma (21, 45), speculating a potential regulatory crosstalk between TGIF2 and NOTCH signaling. These findings suggest that TGIF2 may play a multifaceted role in glioma progression, influencing processes such as cell cycle regulation, ECM formation, and engagement with key signaling pathways. These insights contribute to a deeper understanding of TGIF2's impact on glioma development and progression.

The tumor immune microenvironment plays a crucial role in glioma progression and therapy response (46). Immune infiltration is intricately linked to the immune escape of tumor cells and exerts regulatory control over the remodeling of the tumor microenvironment. Immunotherapy, which removes tumor cells by altering or modulating the autoimmune system, has emerged as a

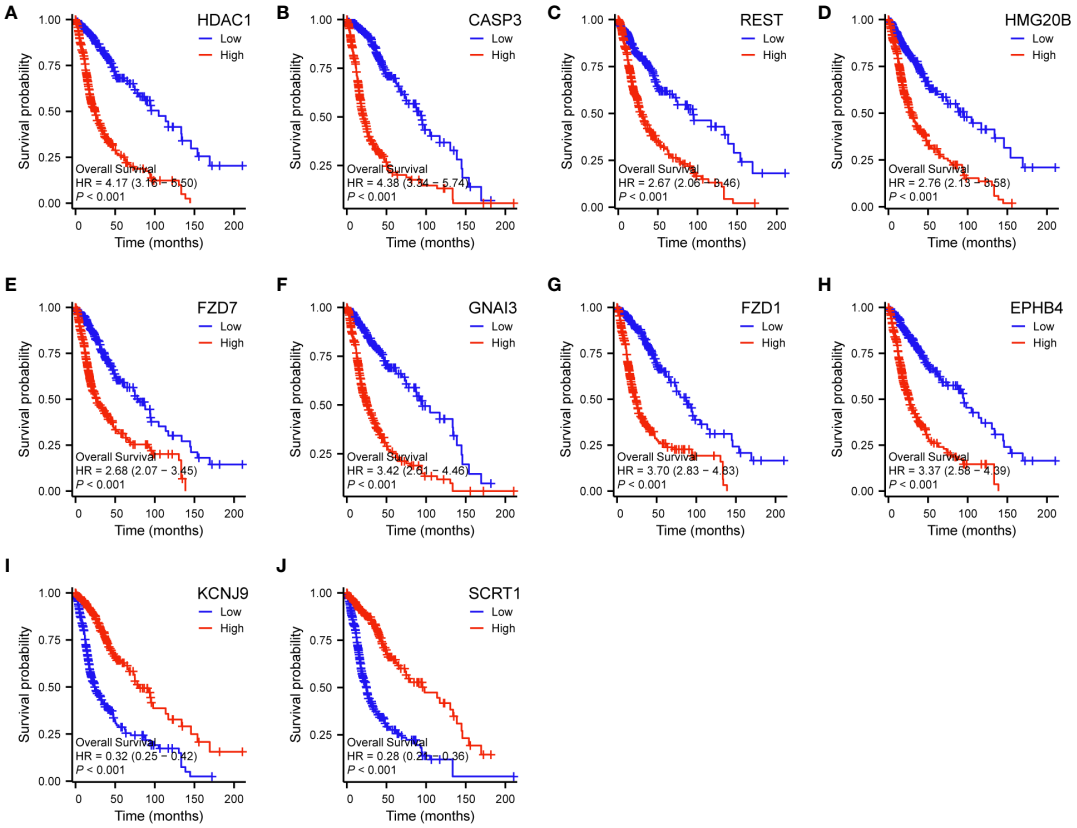

FIGURE 8
Correlations between the top 10 hub genes and OS of glioma patients in TCGA database by Kaplan-Meier survival curve analysis. **(A)** HDAC1. **(B)** CASP3. **(C)** REST. **(D)** HMG20B. **(E)** FZD7. **(F)** GNAI3. **(G)** FZD1. **(H)** EPHB4. **(I)** KCNJ9. **(J)** SCRT1.

powerful anticancer strategy compared to conventional therapies such as surgery, radiotherapy and chemotherapy. Several immunotherapeutic approaches have shown promise in glioma, including immune checkpoint inhibitors (ICIs), cancer vaccines, adoptive cell transfer (ACT), CAR-T cell therapy, and more (47). Additionally, the integration of nanomaterials, such as dendrimers, multifunctional nano-adjuvants, and nanoprobes, has expanded the possibilities in cancer immunotherapy (48–50). Approaches like near-infrared photoimmunotherapy have even progressed to the clinical study stage (51). Despite these advancements, each immunotherapeutic strategy has its limitations, and there is a continued need to explore and understand the intricate regulation of the glioma immune microenvironment. In this study, functional enrichment analysis showed that high TGIF2 expression was positively correlated with immune-related pathways such as chemokines, cytokines, interleukins, inflammation, toll like receptor and Pd 1. Notably, PD-L1 expression in glioma has been associated with WHO classification, positioning it as a potential biomarker (52, 53). The enrichment of the Pd-1 signaling pathway suggested a potential involvement of TGIF2 in the regulation of the PD-1/PD-L1 axis. This signaling axis is a critical component of immune checkpoint regulation and can influence the immune response against tumors. To further explore the relationship between TGIF2 and tumor immunity, we analyzed the infiltration level of immune cells in the microenvironment of glioma tumors. Our results showed that TGIF2 was positively correlated with Th2, macrophages, eosinophils and neutrophils, *etc.*, while displaying a negative correlation with mast cells, NK CD56bright cells, pDC, and TFH, *etc.* The balance of Th1/Th2 is an important mechanism leading to immune evasion of tumors (54, 55), therefore, TGIF2-mediated Th2 enrichment may be one of the potential factors for tumor cells to evade immune surveillance. On the contrary, TFH cells were associated with anti-tumor immunity (56), and the negative correlation observed between TGIF2 and TFH cells suggests a potential contribution of TGIF2 to tumor immune escape. The implications of these findings underscore the potential importance of TGIF2 in shaping the glioma immune microenvironment. However, the precise role and underlying mechanisms necessitate further elucidation through dedicated biological experiments.

We constructed a PPI network of the top 50 genes positively and negatively correlated with TGIF2 respectively and identified 10 hub genes (HDAC1, CASP3, REST, HMG20B, FZD7, GNAI3, FZD1, EPHB4, KCNJ9, SCRT1) which have good diagnostic ability in glioma. Among them, high expression of HDAC1, CASP3, REST, HMG20B, FZD7, GNAI3, FZD1 and EPHB4 were associated with worse OS, DSS and PFI, while high expression of KCNJ9 and SCRT1 suggested better OS, DSS and PFI. Consistent with our results, high expression of HDAC1, CASP3, REST, GNAI3, FZD1, EPHB4 was found to correlate with poor

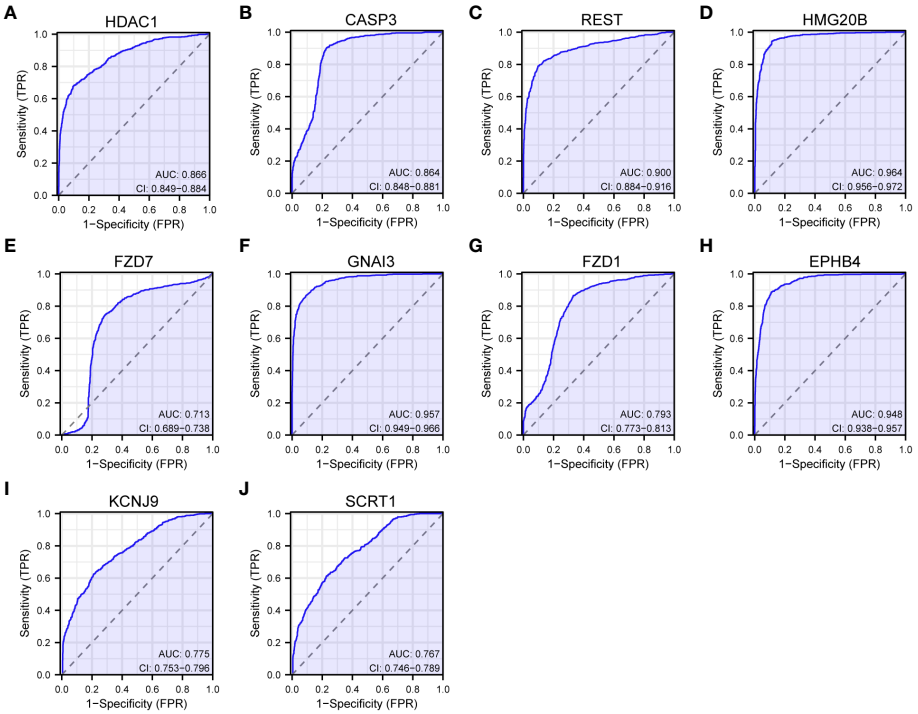

FIGURE 9
ROC curves of the top 10 hub genes. **(A)** HDAC1. **(B)** CASP3. **(C)** REST. **(D)** HMG20B. **(E)** FZD7. **(F)** GNAI3. **(G)** FZD1. **(H)** EPHB4. **(I)** KCNJ9. **(J)** SCRT1.

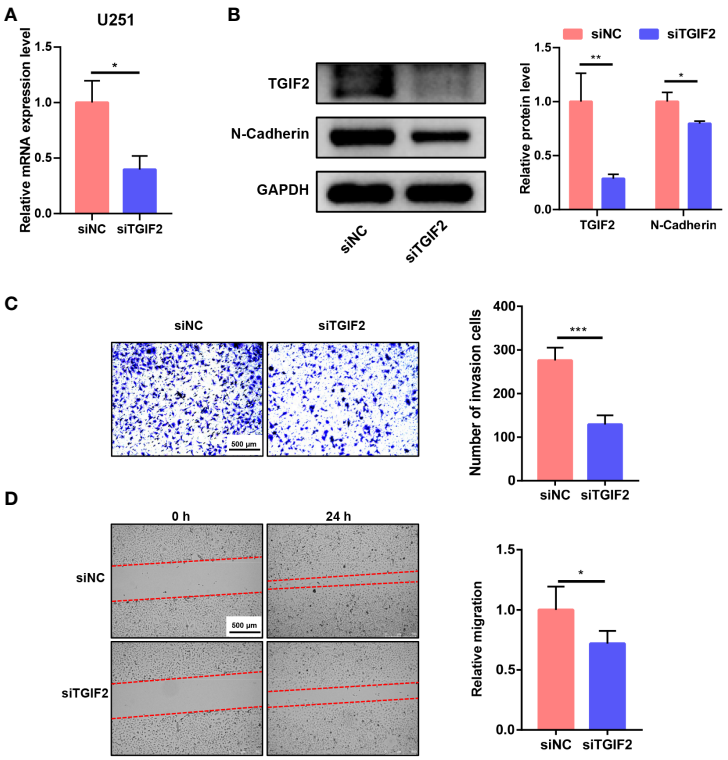

FIGURE 10
Knockdown of TGIF2 inhibits glioma cell invasion, migration and EMT *in vitro*. **(A)** Bar graph demonstrating the efficiency of siRNA knockdown of TGIF2 mRNA in U251 cells by RT-qPCR. **(B)** Western blot assay showing that siRNA effectively knocked down TGIF2 protein, and siTGIF2 downregulated N-cadherin protein expression in U251 cells. **(C)** Transwell assay demonstrating changes in the number of cells invaded after knockdown of TGIF2. Scale bar, 500 μm. **(D)** Scratch wound-healing assays were utilized to compare the distance of cell migration between TGIF2-inhibited group and control group at 0h and 24h after scratching. Scale bar, 500 μm. $*p < 0.05$, $**p < 0.01$, $***p < 0.001$.

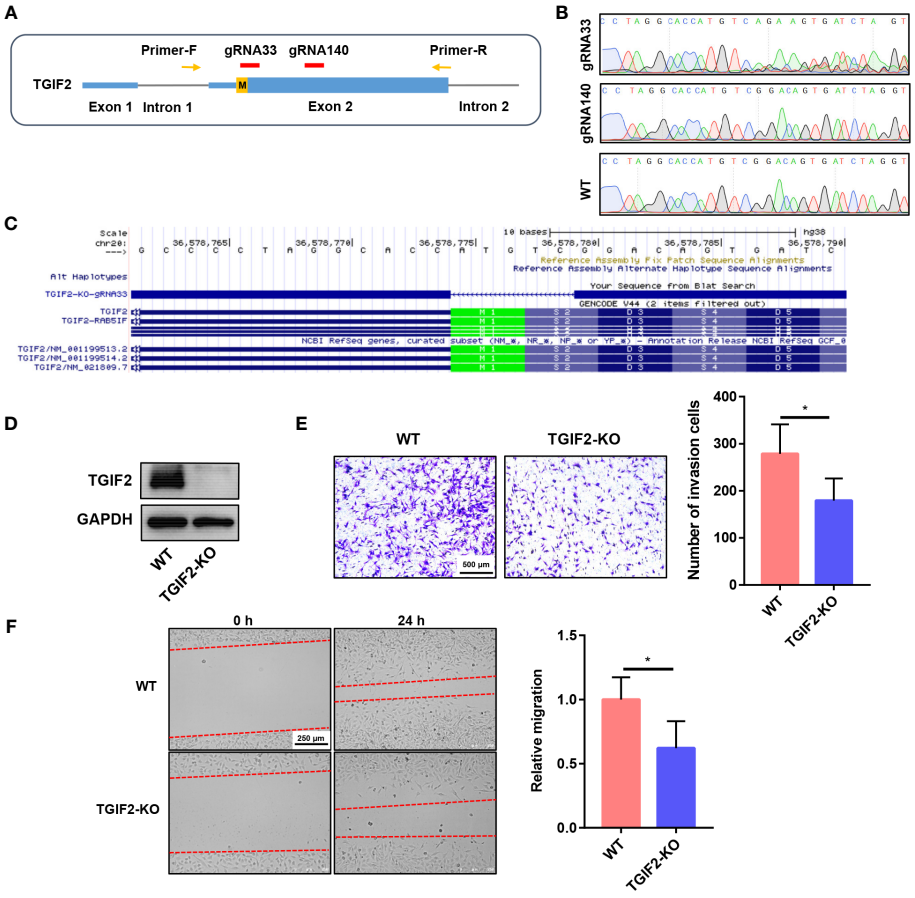

FIGURE 11
Knockout of TGIF2 suppresses glioma cell invasion, migration and EMT. **(A)** The gRNA sequences designed targeting exon 2 of TGIF2. **(B)** The editing efficiency of gRNA33 and gRNA140 on TGIF2 was verified in 293T cells utilizing Sanger sequencing. **(C)** TGIF2-gRNA33 in the UCSC browser. **(D)** Western blot assay showing the knockout efficiency of TGIF2 protein. WT, Wild type; KO, Knockout. **(E)** Transwell assays showing changes in the number of cells invaded after knockout of TGIF2. Scale bar, 500 μm. **(F)** Scratch wound-healing assays were utilized to compare the distance of cell migration between TGIF2-knockout group and control group at 0h and 24h after scratching. Scale bar, 250 μm. $*p < 0.05$.

prognosis of glioma, and inhibitors of HDAC1 inhibited the EMT process in glioma cells thereby affecting cell migration and invasion (57–62). FZD7, linked to glioma cell motility and invasiveness, aligns with our observation of TGIF2 promoting glioma cell migration (63). Collectively, these results suggest a potential co-regulation of migration and invasion in glioma by TGIF2 and these identified hub genes.

Although this study demonstrated an association between TGIF2 and glioma, there are still some limitations and shortcomings of this study. Since we utilized transcriptome sequencing data included in public databases and patients' clinicopathologic information for bioinformatics analysis, there were certain biases caused by confounding factors, and future prospective studies will be helpful in this regard. Meanwhile, our study needs more clinical samples to validate the aberrant expression of TGIF2 to improve reliability. In addition, combined with previous studies, our *in vitro* experiments have provided a preliminary exploration of the role of TGIF2 in glioma migration, invasion and EMT, and the specific mechanisms and more functions in glioma need to be further investigated.

In conclusion, our results suggest that TGIF2 can be used as a promising new indicator for predicting the malignant phenotypes and clinical prognosis of glioma patients, and correlates with immune infiltration and EMT phenotype.

Data availability statement

The datasets presented in this study can be found in online repositories. The names of the repository/repositories and accession number(s) can be found in the article/Supplementary Material.

Ethics statement

Ethical approval was not required for the studies on humans in accordance with the local legislation and institutional requirements because only commercially available established cell lines were used.

Author contributions

WZ: Writing – original draft, Conceptualization, Data curation, Investigation, Methodology, Project administration, Software, Visualization, Writing – review & editing. LZ: Writing – review & editing, Data curation, Supervision, Funding acquisition. HD: Writing – review & editing, Investigation, Methodology, Validation. HP: Conceptualization, Supervision, Validation, Visualization, Writing – original draft, Writing – review & editing, Project administration.

Funding

The author(s) declare financial support was received for the research, authorship, and/or publication of this article. This study was supported by the Fundamental Research Funds for the Central Universities (xzy012022114).

Acknowledgments

We thank Mr. An Yan for his contributions to some of the R code writing work.

Conflict of interest

The authors declare that the research was conducted in the absence of any commercial or financial relationships that could be construed as a potential conflict of interest.

Publisher's note

All claims expressed in this article are solely those of the authors and do not necessarily represent those of their affiliated organizations, or those of the publisher, the editors and the reviewers. Any product that may be evaluated in this article, or claim that may be made by its manufacturer, is not guaranteed or endorsed by the publisher.

Supplementary material

The Supplementary Material for this article can be found online at: https://www.frontiersin.org/articles/10.3389/fimmu.2024.1356833/full#supplementary-material

References

1. Saunders CN, Cornish AJ, Kinnersley B, Law PJ, Claus EB, Il'yasova D, et al. Lack of association between modifiable exposures and glioma risk: A mendelian randomization analysis. *Neuro Oncol.* (2020) 22:207–15. doi: 10.1093/neuonc/noz209

2. Lapointe S, Perry A, Butowski NA. Primary brain tumours in adults. *Lancet.* (2018) 392:432–46. doi: 10.1016/S0140-6736(18)30990-5

3. Zhang Y, Ni S, Huang B, Wang L, Zhang X, Li X, et al. Overexpression of sclip promotes growth and motility in glioblastoma cells. *Cancer Biol Ther.* (2015) 16:97–105. doi: 10.4161/15384047.2014.987037

4. Liu J, Guo S, Li Q, Yang L, Xia Z, Zhang L, et al. Phosphoglycerate dehydrogenase induces glioma cells proliferation and invasion by stabilizing forkhead box M1. *J Neurooncol.* (2013) 111:245–55. doi: 10.1007/s11060-012-1018-x

5. Hu Y, Yu H, Shaw G, Renfree MB, Pask AJ. Differential roles of tgif family genes in mammalian reproduction. *BMC Dev Biol.* (2011) 11:58. doi: 10.1186/1471-213X-11-58

6. Spagnoli FM, Brivanlou AH. The gata5 target, tgif2, defines the pancreatic region by modulating bmp signals within the endoderm. *Development.* (2008) 135:451–61. doi: 10.1242/dev.008458

7. Melhuish TA, Gallo CM, Wotton D. Tgif2 interacts with histone deacetylase 1 and represses transcription. *J Biol Chem.* (2001) 276:32109–14. doi: 10.1074/jbc.M103377200

8. Cerda-Esteban N, Naumann H, Ruzittu S, Mah N, Pongrac IM, Cozzitorto C, et al. Stepwise reprogramming of liver cells to a pancreas progenitor state by the transcriptional regulator tgif2. *Nat Commun.* (2017) 8:14127. doi: 10.1038/ncomms14127

9. Jiang J, Wu RH, Zhou HL, Li ZM, Kou D, Deng Z, et al. Tgif2 promotes cervical cancer metastasis by negatively regulating fcmr. *Eur Rev Med Pharmacol Sci.* (2020) 24:5953–62. doi: 10.26355/eurrev_202006_21488

10. Du R, Shen W, Liu Y, Gao W, Zhou W, Li J, et al. Tgif2 promotes the progression of lung adenocarcinoma by bridging egfr/ras/erk signaling to cancer cell stemness. *Signal Transduct Target Ther.* (2019) 4:60. doi: 10.1038/s41392-019-0098-x

11. Zhao M, Su Z, Zhang S, Zhuang L, Xie Y, Li X. Suppressive role of microrna-148a in cell proliferation and invasion in ovarian cancer through targeting transforming growth factor-beta-induced 2. *Oncol Res.* (2016) 24:353–60. doi: 10.3727/096504016X14685034103275

12. Du R, Wang C, Liu J, Wang K, Dai L, Shen W. Phosphorylation of tgif2 represents a therapeutic target that drives emt and metastasis of lung adenocarcinoma. *BMC Cancer.* (2023) 23:52. doi: 10.1186/s12885-023-10535-9

13. Pan Y, Wang J, He L, Zhang F. Microrna-34a promotes emt and liver fibrosis in primary biliary cholangitis by regulating tgf-beta1/smad pathway. *J Immunol Res.* (2021) 2021:6890423. doi: 10.1155/2021/6890423

14. Li D, Shen C, Liu L, Hu J, Qin J, Dai L, et al. Pkm2 regulates cigarette smoke-induced airway inflammation and epithelial-to-mesenchymal transition via modulating pink1/parkin-mediated mitophagy. *Toxicology.* (2022) 477:153251. doi: 10.1016/j.tox.2022.153251

15. Hamabe A, Konno M, Tanuma N, Shima H, Tsunekuni K, Kawamoto K, et al. Role of pyruvate kinase M2 in transcriptional regulation leading to epithelial-mesenchymal transition. *Proc Natl Acad Sci U.S.A.* (2014) 111:15526–31. doi: 10.1073/pnas.1407717111

16. Zhiping C, Shijun T, Linhui W, Yapei W, Lianxi Q, Qiang D. Mir-181a promotes epithelial to mesenchymal transition of prostate cancer cells by targeting tgif2. *Eur Rev Med Pharmacol Sci.* (2017) 21:4835–43.

17. Yang Y, Ren P, Liu X, Sun X, Zhang C, Du X, et al. Ppp1r26 drives hepatocellular carcinoma progression by controlling glycolysis and epithelial-mesenchymal transition. *J Exp Clin Cancer Res.* (2022) 41:101. doi: 10.1186/s13046-022-02302-8

18. Diao Y, Jin B, Huang L, Zhou W. Mir-129-5p inhibits glioma cell progression *in vitro* and *in vivo* by targeting tgif2. *J Cell Mol Med.* (2018) 22:2357–67. doi: 10.1111/jcmm.13529

19. Xu W, Xue R, Xia R, Liu WW, Zheng JW, Tang L, et al. Sevoflurane impedes the progression of glioma through modulating the circular rna has_Circ_0012129/mir-761/tgif2 axis. *Eur Rev Med Pharmacol Sci.* (2020) 24:5534–48. doi: 10.26355/eurrev_202005_21339

20. Zhang K, Wang Q, Zhao D, Liu Z. Circular rna circmmp1 contributes to the progression of glioma through regulating tgif2 expression by sponging mir-195-5p. *Biochem Genet.* (2022) 60:770–89. doi: 10.1007/s10528-021-10119-x

21. Vinchure OS, Sharma V, Tabasum S, Ghosh S, Singh RP, Sarkar C, et al. Polycomb complex mediated epigenetic reprogramming alters tgf-beta signaling via a novel ezh2/mir-490/tgif2 axis thereby inducing migration and emt potential in glioblastomas. *Int J Cancer.* (2019) 145:1254–69. doi: 10.1002/ijc.32360

22. Bindea G, Mlecnik B, Tosolini M, Kirilovsky A, Waldner M, Obenauf AC, et al. Spatiotemporal dynamics of intratumoral immune cells reveal the immune landscape in human cancer. *Immunity.* (2013) 39:782–95. doi: 10.1016/j.immuni.2013.10.003

23. Thorsson V, Gibbs DL, Brown SD, Wolf D, Bortone DS, Ou Yang TH, et al. The immune landscape of cancer. *Immunity.* (2018) 48:812–30 e14. doi: 10.1016/j.immuni.2018.03.023

24. Chang K, Bai HX, Zhou H, Su C, Bi WL, Agbodza E, et al. Residual convolutional neural network for the determination of idh status in low- and high-grade gliomas from mr imaging. *Clin Cancer Res.* (2018) 24:1073–81. doi: 10.1158/1078-0432.CCR-17-2236

25. Yan H, Parsons DW, Jin G, McLendon R, Rasheed BA, Yuan W, et al. Idh1 and idh2 mutations in gliomas. *N Engl J Med.* (2009) 360:765–73. doi: 10.1056/NEJMoa0808710

26. Saadeh FS, Mahfouz R, Assi HI. Egfr as a clinical marker in glioblastomas and other gliomas. *Int J Biol Markers*. (2018) 33:22–32. doi: 10.5301/ijbm.5000301

27. Cho SY, Park C, Na D, Han JY, Lee J, Park OK, et al. High prevalence of tp53 mutations is associated with poor survival and an emt signature in gliosarcoma patients. *Exp Mol Med*. (2017) 49:e317. doi: 10.1038/emm.2017.9

28. Wang F, Zhao F, Zhang L, Xiong L, Mao Q, Liu Y, et al. Cdc6 is a prognostic biomarker and correlated with immune infiltrates in glioma. *Mol Cancer*. (2022) 21:153. doi: 10.1186/s12943-022-01623-8

29. Zhu C, Zhao Y, Zheng W. Cdc14b is a favorable biomarker for recurrence and prognosis of gbm. *Clin Neurol Neurosurg*. (2023) 227:107665. doi: 10.1016/j.clineuro.2023.107665

30. Xu L, Shao F, Luo T, Li Q, Tan D, Tan Y. Pan-cancer analysis identifies chd5 as a potential biomarker for glioma. *Int J Mol Sci*. (2022) 23. doi: 10.3390/ijms23158489

31. Pei Z, Lee KC, Khan A, Erisnor G, Wang HY. Pathway analysis of glutamate-mediated, calcium-related signaling in glioma progression. *Biochem Pharmacol*. (2020) 176:113814. doi: 10.1016/j.bcp.2020.113814

32. Griffin M, Khan R, Basu S, Smith S. Ion channels as therapeutic targets in high grade gliomas. *Cancers (Basel)*. (2020) 12. doi: 10.3390/cancers12103068

33. Arvind S, Arivazhagan A, Santosh V, Chandramouli BA. Differential expression of a novel voltage gated potassium channel–kv 1.5 in astrocytomas and its impact on prognosis in glioblastoma. *Br J Neurosurg*. (2012) 26:16–20. doi: 10.3109/02688697.2011.583365

34. Wang R, Gurguis CI, Gu W, Ko EA, Lim I, Bang H, et al. Ion channel gene expression predicts survival in glioma patients. *Sci Rep*. (2015) 5:11593. doi: 10.1038/srep11593

35. Cheng Z, Li Z, Ma K, Li X, Tian N, Duan J, et al. Long non-coding rna xist promotes glioma tumorigenicity and angiogenesis by acting as a molecular sponge of mir-429. *J Cancer*. (2017) 8:4106–16. doi: 10.7150/jca.21024

36. Qu S, Huang C, Zhu T, Wang K, Zhang H, Wang L, et al. Olfml3, as a potential predictor of prognosis and therapeutic target for glioma, is closely related to immune cell infiltration. *VIEW*. (2023) 4:20220052. doi: 10.1002/VIW.20220

37. Liu Y, Yao R, Shi Y, Liu Y, Liu H, Liu J, et al. Identification of cd101 in glioma: A novel prognostic indicator expressed on M2 macrophages. *Front Immunol*. (2022) 13:845223. doi: 10.3389/fimmu.2022.845223

38. Qu S, Qiu O, Hu Z. The prognostic factors and nomogram for patients with high-grade gliomas. *Fundam Res*. (2021) 1:824–8. doi: 10.1016/j.fmre.2021.07.005

39. Ostrom QT, Gittleman H, Truitt G, Boscia A, Kruchko C, Barnholtz-Sloan JS. Cbtrus statistical report: primary brain and other central nervous system tumors diagnosed in the United States in 2011-2015. *Neuro Oncol*. (2018) 20:iv1–iv86. doi: 10.1093/neuonc/noy131

40. Wesseling P, Capper D. Who 2016 classification of gliomas. *Neuropathol Appl Neurobiol*. (2018) 44:139–50. doi: 10.1111/nan.12432

41. Mohiuddin E, Wakimoto H. Extracellular matrix in glioblastoma: opportunities for emerging therapeutic approaches. *Am J Cancer Res*. (2021) 11:3742–54.

42. Swiatek-MaChado K, Kaminska B. Stat signaling in glioma cells. *Adv Exp Med Biol*. (2020) 1202:203–22. doi: 10.1007/978-3-030-30651-9_10

43. Stockhausen MT, Kristoffersen K, Poulsen HS. Notch signaling and brain tumors. *Adv Exp Med Biol*. (2012) 727:289–304. doi: 10.1007/978-1-4614-0899-4_22

44. Shahcheraghi SH, Tchokonte-Nana V, Lotfi M, Lotfi M, Ghorbani A, Sadeghnia HR. Wnt/beta-catenin and pi3k/akt/mtor signaling pathways in glioblastoma: two main targets for drug design: A review. *Curr Pharm Des*. (2020) 26:1729–41. doi: 10.2174/1381612826666200131100630

45. Wang Z, Li Y, Kong D, Sarkar FH. The role of notch signaling pathway in epithelial-mesenchymal transition (Emt) during development and tumor aggressiveness. *Curr Drug Targets*. (2010) 11:745–51. doi: 10.2174/138945010791170860

46. Yang K, Wu Z, Zhang H, Zhang N, Wu W, Wang Z, et al. Glioma targeted therapy: insight into future of molecular approaches. *Mol Cancer*. (2022) 21:39. doi: 10.1186/s12943-022-01513-z

47. Rui R, Zhou L, He S. Cancer immunotherapies: advances and bottlenecks. *Front Immunol*. (2023) 14:1212476. doi: 10.3389/fimmu.2023.1212476

48. Gao Y, Shen M, Shi X. Interaction of dendrimers with the immune system: an insight into cancer nanotheranostics. *VIEW*. (2021) 2:20200120. doi: 10.1002/VIW.20200120

49. Zhu H, Yang C, Yan A, Qiang W, Ruan R, Ma K, et al. Tumor-targeted nano-adjuvants to synergize photomediated immunotherapy enhanced antitumor immunity. *VIEW*. (2023) 4:20220067. doi: 10.1002/VIW.20220067

50. Bian Y, Wang Y, Chen X, Zhang Y, Xiong S, Su D. Image-guided diagnosis and treatment of glioblastoma. *VIEW*. (2023) 4:20220069. doi: 10.1002/VIW.20220069

51. Monaco H, Yokomizo S, Choi HS, Kashiwagi S. Quickly evolving near-infrared photoimmunotherapy provides multifaceted approach to modern cancer treatment. *VIEW*. (2022) 3:20200110. doi: 10.1002/VIW.20200110

52. Chen RQ, Liu F, Qiu XY, Chen XQ. The prognostic and therapeutic value of pd-L1 in glioma. *Front Pharmacol*. (2018) 9:1503. doi: 10.3389/fphar.2018.01503

53. Wang Z, Zhang C, Liu X, Wang Z, Sun L, Li G, et al. Molecular and clinical characterization of pd-L1 expression at transcriptional level via 976 samples of brain glioma. *Oncoimmunology*. (2016) 5:e1196310. doi: 10.1080/2162402X.2016.1196310

54. Murakami H, Ogawara H, Hiroshi H. Th1/th2 cells in patients with multiple myeloma. *Hematology*. (2004) 9:41–5. doi: 10.1080/10245330310001652437

55. Zhao X, Liu J, Ge S, Chen C, Li S, Wu X, et al. Saikosaponin a inhibits breast cancer by regulating th1/th2 balance. *Front Pharmacol*. (2019) 10:624. doi: 10.3389/fphar.2019.00624

56. Cicalese MP, Salek-Ardakani S, Fousteri G. Editorial: follicular helper T cells in immunity and autoimmunity. *Front Immunol*. (2020) 11:1042. doi: 10.3389/fimmu.2020.01042

57. Cheng Z, Li S, Yuan J, Li Y, Cheng S, Huang S, et al. Hdac1 mediates epithelial-mesenchymal transition and promotes cancer cell invasion in glioblastoma. *Pathol Res Pract*. (2023) 246:154481. doi: 10.1016/j.prp.2023.154481

58. Chao B, Jiang F, Bai H, Meng P, Wang L, Wang F. Predicting the prognosis of glioma by pyroptosis-related signature. *J Cell Mol Med*. (2022) 26:133–43. doi: 10.1111/jcmm.17061

59. Li C, Wang Z, Tang X, Zeng L, Fan X, Li Z. Molecular mechanisms and potential prognostic effects of rest and rest4 in glioma (Review). *Mol Med Rep*. (2017) 16:3707–12. doi: 10.3892/mmr.2017.7071

60. Raza A, Yen MC, Anuraga G, Shahzadi I, Mazhar MW, Ta HDK, et al. Comparative analysis of the gnai family genes in glioblastoma through transcriptomics and single-cell technologies. *Cancers (Basel)*. (2023) 15. doi: 10.3390/cancers15205112

61. Huang K, Xu H, Han L, Xu R, Xu Z, Xie Y. Identification of therapeutic targets and prognostic biomarkers among frizzled family genes in glioma. *Front Mol Biosci*. (2022) 9:1054614. doi: 10.3389/fmolb.2022.1054614

62. Tu Y, He S, Fu J, Li G, Xu R, Lu H, et al. Expression of ephrinb2 and ephb4 in glioma tissues correlated to the progression of glioma and the prognosis of glioblastoma patients. *Clin Transl Oncol*. (2012) 14:214–20. doi: 10.1007/s12094-012-0786-2

63. Wald JH, Hatakeyama J, Printsev I, Cuevas A, Fry WHD, Saldana MJ, et al. Suppression of planar cell polarity signaling and migration in glioblastoma by nrdp1-mediated dvl polyubiquitination. *Oncogene*. (2017) 36:5158–67. doi: 10.1038/onc.2017.126

frontiers | Frontiers in Pharmacology

TYPE Review
PUBLISHED 08 March 2024
DOI 10.3389/fphar.2024.1355242

Check for updates

OPEN ACCESS

EDITED BY
Mariana Magalhães,
University of Coimbra, Portugal

REVIEWED BY
Hernando Lopez-Bertoni,
Johns Hopkins University, United States
Ramcharan Singh Angom,
Mayo Clinic Florida, United States

*CORRESPONDENCE
Kalpana Barhwal,
physio_kalpana@aiimsbhubaneswar.edu.in

†These authors have contributed equally to this work and share first authorship

RECEIVED 13 December 2023
ACCEPTED 07 February 2024
PUBLISHED 08 March 2024

CITATION
Tripathy DK, Panda LP, Biswal S and Barhwal K (2024), Insights into the glioblastoma tumor microenvironment: current and emerging therapeutic approaches.
Front. Pharmacol. 15:1355242.
doi: 10.3389/fphar.2024.1355242

COPYRIGHT
© 2024 Tripathy, Panda, Biswal and Barhwal. This is an open-access article distributed under the terms of the Creative Commons Attribution License (CC BY). The use, distribution or reproduction in other forums is permitted, provided the original author(s) and the copyright owner(s) are credited and that the original publication in this journal is cited, in accordance with accepted academic practice. No use, distribution or reproduction is permitted which does not comply with these terms.

Insights into the glioblastoma tumor microenvironment: current and emerging therapeutic approaches

Dev Kumar Tripathy[1†], Lakshmi Priya Panda[1†], Suryanarayan Biswal[2] and Kalpana Barhwal[1*]

[1]Department of Physiology, All India Institute of Medical Sciences (AIIMS), Bhubaneswar, India, [2]Department of Human Genetics and Molecular Medicine, Central University of Punjab, Bathinda, India

Glioblastoma (GB) is an intrusive and recurrent primary brain tumor with low survivability. The heterogeneity of the tumor microenvironment plays a crucial role in the stemness and proliferation of GB. The tumor microenvironment induces tumor heterogeneity of cancer cells by facilitating clonal evolution and promoting multidrug resistance, leading to cancer cell progression and metastasis. It also plays an important role in angiogenesis to nourish the hypoxic tumor environment. There is a strong interaction of neoplastic cells with their surrounding microenvironment that comprise several immune and non-immune cellular components. The tumor microenvironment is a complex network of immune components like microglia, macrophages, T cells, B cells, natural killer (NK) cells, dendritic cells and myeloid-derived suppressor cells, and non-immune components such as extracellular matrix, endothelial cells, astrocytes and neurons. The prognosis of GB is thus challenging, making it a difficult target for therapeutic interventions. The current therapeutic approaches target these regulators of tumor micro-environment through both generalized and personalized approaches. The review provides a summary of important milestones in GB research, factors regulating tumor microenvironment and promoting angiogenesis and potential therapeutic agents widely used for the treatment of GB patients.

KEYWORDS

glioblastoma, tumor microenvironment, angiogenesis, immunotherapy, blood-brain barrier, therapeutic approaches

1 Introduction

The most common CNS tumors in adults are meningioma (15%), glioblastoma (GB) (20%), and metastatic tumors (40%) (Bikfalvi et al., 2023). According to the World Health Organization (WHO) classification, astrocytomas are characterized according to their histopathology and molecular patterns (Table 1). Glial fibrillary acidic protein (GFAP) loss indicates malignancy and characteristic undifferentiated tumor cells. Molecular characterization includes IDH-mutant and IDH-wild type. GB is referred to as an IDH-wildtype astrocytoma with microvascular proliferation, high stemness, invasiveness and predisposition to necrosis (Louis et al., 2021). GB is mostly located in the frontal and temporal lobes of the brain and rarely found in the brainstem, cerebellum and spinal cord. It remains an irrepressible disease with a median survival of 15 months (Chang et al., 2016).

TABLE 1 Classification of astrocytomas according to WHO Guidelines (Louis et al., 2021).

Astrocytoma WHO Grade	WHO Grade 2	WHO Grade 3	WHO Grade 4	Glioblastoma
His topathology	Mild nuclear atypia, dense fibrillar background. Elongated nuclei, hyperchromatic irregular. Microcyst formation in the tumor storma	Cellularity, higher nuclear atypia, increased mitotic activity, round nuclei	Microvascular proliferation, accumulation of hyperplasticity endothelial cells, necrosis	Microvascular proliferation or necrosis. Lesions show higher degree of cellular and nuclear polymorphism, multinucleated giant cells. Astrocytic nature of the neoplasms
Criteria	IDH mutant, deletions of CDKN2A and CDKN2B absent	IDH mutant, loss of ATRX mutation , tp53 mutation	IDH mutant, homozygous deletion of CDKN2A and/or CDKN2B	IDH-wildtype, TERT promoter mutation, EGFR gene amplification, +7/-10 chromosome copy- number alterations
Proliferation index	Kr-67 proliferation index is 4%.	Ki-67 proliferation index ranges from 4- 10%	Vary considerably, not associated with survival	Elevated Ki-67 proliferation index
Molecular alterations	1p/19q intact	1p/19q intact	1p[1]19q intact	1p/19q intact?
Methylation status	G-CIMP high	G-GIMP high	0-CIMP high low?	G-CIMP low

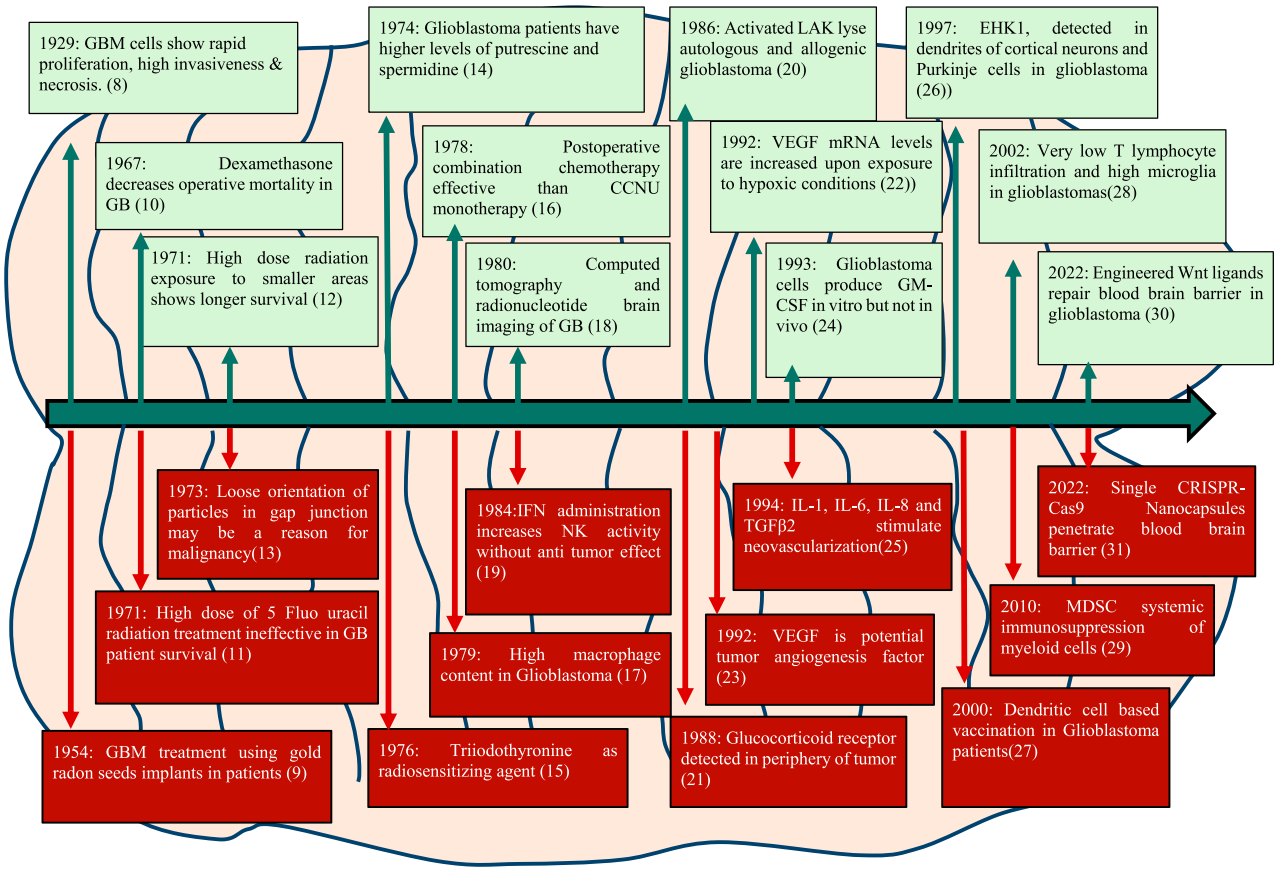

FIGURE 1
Major milestones in the management and treatment of GB since 1929.

Based on the CBTRUS Statistical Report: Primary Brain and Other Central Nervous System Tumors Diagnosed in the United States in 2012–2016 report incidence rate of GB is 3.22 per 100,000 persons in the United States with a median age of 64 years (Ostrom et al., 2019). In an Indian scenario, gliomas comprise 38.7% of tumors of the central nervous system (CNS), of which high-grade (grades III and IV) types constitute 59.5% and low-grade (grades I and II) account roughly 33.1%. In India, there were 23,000 cases of GBM incidence and 49000 widespread cases in 2016 (Rana et al., 2019).

GB is very uncommon in the pediatric population (Singla et al., 2021) and is found to be more prevalent in adult males (66.6% more) as compared to females. The gender-based age distribution in

glioblastoma patients shows 70.5% males in the age group below 18 years, 69.7% males in the age group between 19 and 50 years and 72.8% males above 50 years (Singh et al., 2021). The number of cases is expected to rise with the rise in the elderly population, particularly in developing countries like the United States. Notwithstanding rigorous therapeutic interventions that include surgical resection, radiation, and concurrent chemotherapy, the prognosis of GB continues to be poor due to its recurrence and poor survival outcomes.

Despite advances in the understanding of cancer biology, the heterogeneous makeup of the tumor microenvironment continues to be a challenge for treatment and management of GB across all age groups. The current experimental models GB cancer models fail to effectively mimic the tumor microenvironment comprising of tumor organismal milieu and niche that plays a key role in promoting and sustaining GB.

1.1 Milestones in glioblastoma research

Seminal publications in 1929 described the tissue structure of glioblastoma revealing its characteristic features like necrosis, abundant mitotic figures and invasive morphology with the large nucleus. Some important milestones in GB research in the last century are depicted in Figure 1.

2 Glioblastoma Microenvironment

The microenvironment of GB is highly complex and dynamic with various cross-interacting components that contribute towards the tumor formation and invasion. Some of the components of the tumor microenvironment and their roles are described as under.

2.1 Blood-brain barrier

The blood-brain barrier (BBB) is a unique and specialized structure that regulates the flow of molecules between the blood and the brain (Martin et al., 2022a). The BBB serves as a physical barrier between the vascular system and the central nervous system. The BBB is primarily made up of endothelial cells, pericytes, and astrocytes which create a tight barrier along the walls of blood vessels, specifically limiting the substances that can enter the parenchyma (Martin et al., 2022b).

GB is characterized by a high degree of vascularity, atypical structure, and decreased structural integrity. This leads to leakiness causing high interstitial fluid pressure, severe ischemia and necrosis, and edema (Rehman et al., 2018). GB tumor cells produce a variety of factors, including VEGF and matrix metalloproteinases (MMPs), which degrade tight junction proteins and basement membrane components, resulting in greater BBB permeability. VEGF is a powerful angiogenic factor that supports the formation of new blood vessels in the tumor microenvironment while also increasing BBB permeability by downregulating tight junction proteins and raising endothelial cell fenestration. MMPs are enzymes that help tumor cells invasion and angiogenesis by eroding the extracellular matrix and basement membrane, as well as disturbing the BBB through tight junction protein degradation (Gregoriadis, 2008; Daneman and Prat, 2015).

BBB is critical for shielding the brain from toxins and viruses while allowing nutrient flow and gaseous exchange. Increased permeability triggers inflammatory responses, fostering chronic inflammation that hampers anti-tumor immunity. Therapeutic delivery is also affected, challenging treatments targeting the immune response. BBB dysfunction contributes to tumor-induced immune suppression, allowing the influx of immunosuppressive factors. Lastly, compromised immune surveillance results from the BBB's failure, enabling tumor cells to evade detection and advance disease progression (Jain et al., 2007; Gomez-Zepeda et al., 2019). Increased BBB porosity allows immune cells and carcinogenic chemicals into the tumor microenvironment, encouraging tumor development and spread. Besides, it also limits therapeutic drug transport to the brain, reducing their effectiveness, and can contribute to cerebral edema, a frequent complication in GB (Louveau et al., 2015).

The increase in BBB permeability due to VEGF, MMPs and other by products formed during GB leads to remodeling of the BBB. Destruction of BBB leads to passage of large molecular weight substances into the extracellular fluid leading to passive diffusion of water resulting in cerebral edema. Progressive growth of tumor is often accompanied by overexpression of VEGF leading to neovascularization which further accelerates development of glioma. However, due to abnormal anatomy of new vascular tissue, the BBB permeability increases. The remodeled blood-brain tumor barrier (BTB) hinders the transport of therapeutic drugs due to the overexpression of extraneous (efflux) transporters on glioma cells. These efflux transporters belonging to the family of ABC transporters such as P-glycoprotein (P-GP), multidrug resistance associated protein (MRP), breast cancer resistance protein (BCRP) inhibiting the penetration of numerous therapeutic drugs by actively pumping these substrates out of the cells (Agarwal et al., 2011) resulting in poor efficacy of commonly used antitumor drugs against glioma (Parrish et al., 2015).

Development of new strategies to maintain the integrity of the BBB in GB, therefore, offers tremendous potential for improving patient outcomes. Although a spectrum of methodologies has been devised to navigate the complexities imposed by the blood-brain barrier, which includes direct drug delivery via intrathecal or intranasal routes, chemical modifications that target drugs or components of the BBB, suppression of efflux pumps, and physical disruption through techniques like radiofrequency electromagnetic radiation (EMP), laser-induced thermal therapy (LITT), focused ultrasounds (FUS) in combination with microbubbles, and convection-enhanced delivery (CED), but it frequently fails to reach therapeutic amounts in tumor in GB cells. (Wen et al., 2017; Quintero-Fabián et al., 2019; Mo et al., 2021).

2.2 The neuro-immune system in glioblastoma microenvironment

The permeability and cellular makeup of immune cells within the tumor microenvironment of GB are distinct, creating an extremely immunosuppressive microenvironment profile causing

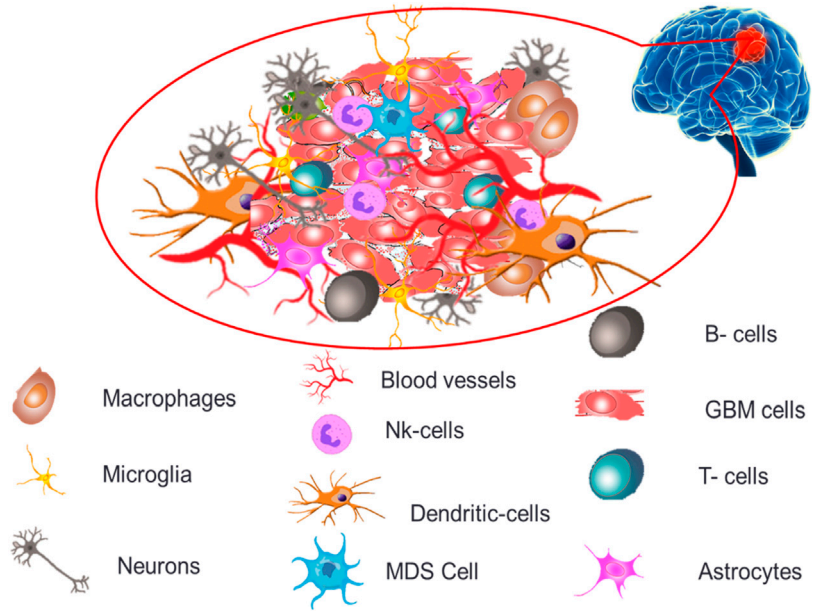

FIGURE 2
Diagrammatic illustration of the components of the GB microenvironment.

severe challenges for treatments and therapeutics (Zou et al., 2022). GB tumor microenvironment, as depicted in Figure 2 demonstrates both immune components (microglia, macrophages, T cells, B cells, NK cells, dendritic cells and myeloid-derived suppressor cells) and non-immune components (extracellular matrix, endothelial cells, astrocytes and neurons).

2.2.1 Macrophages

Macrophages, also known as tumor-associated macrophages (TAMs), are one of the most common immune cells in the GB tumor microenvironment. Macrophages have been demonstrated to have both pro- and anti-tumor effects in cancer, depending on their polarization state and the tumor microenvironment (Liu et al., 2017). TAMs are drawn to the cancer site by chemokines like C-C motif chemokine ligand 2 (CCL2), and aid tumor development and invasion by secreting cytokines and growth factors including interleukin-6 (IL-6), TGF-β, and VEGF. TAMs also promote tumor growth by inhibiting anti-tumor immune responses and increasing angiogenesis. TAMs with M2-like characteristics produce markers such as Cluster of Differentiation 206 (CD206) and arginase 1 (ARG1) (Lamszus et al., 2003).

The colony-stimulating factor-1 receptor (CSF-1R) is a tyrosine kinase receptor expressed on macrophages that controls GB-associated macrophage survival, proliferation, differentiation, and polarization. CSF-1R interacts to its ligands (IL-34 and CSF-1), resulting in activation of PI3K, ERK, NFκB and Src mediated macrophage survival and proliferation pathways. Targeting CSF-1R can reduce GB-associated macrophages in the tumor microenvironment and promote GB-associated macrophage repolarization, limiting tumor development, avoiding the recurrence of glioblastoma and promoting cytotoxic T-cell activation (Vegliante et al., 2022).

Several approaches have been proposed to target TAMs in GB, including the use of small molecule inhibitors, monoclonal antibodies, and cell-based therapies. Targeting CCL2 or its receptor CCR2 has been proven in experimental GB models to reduce TAM infiltration and enhance GB cell mortality. The use of chimeric antigen receptor T-cells (CAR-T) that target TAM-specific markers such as CD163 is also being investigated as a viable treatment for GB (Lamszus et al., 2003). TAMs in GB are known to promote angiogenesis as well as tumor growth and invasion. TAMs produce pro-angiogenic factors such as VEGF, which promote blood vessel growth and proliferation in the cancer microenvironment (Vegliante et al., 2022). This procedure is crucial for the tumor development and progression of GB by catering to blood flow requirements for absorbing nutrients and oxygen. The use of chimeric antigen receptor CAR-T cells that target TAM-specific markers such as CD163 is being investigated as a potential therapy for GB (Chen et al., 2017).

According to recent studies, GB has at least two distinct macrophage populations: one that promotes tumor development and another that suppresses tumor growth (Achkova and Maher, 2016). Understanding the diversity of macrophages in the GB microenvironment may lead to the development of targeted therapies.

2.2.2 Microglia

Microglia are brain immune cells that have been found to have an important role in the microenvironment of GB tumors. Microglia, in particular, are among the most abundant immune cells in the GB environment and are known as tumor-associated microglia. Tumor-associated microglia are drawn to the cancer site by chemokines such as CCL2, and help the tumor to expand and invade by secreting cytokines and growth factors such as IL-6, TGF-β, and VEGF. Tumor-associated microglia in GB are pro-tumor M2-like, as evidenced by the overexpression of markers such as CD206 and ARG1. These M2-like tumor-associated microglia

have been demonstrated to assist tumor growth and invasion by inhibiting anti-tumor immune responses and increasing angiogenesis (Kioi et al., 2010; Zhou et al., 2015; Achkova and Maher, 2016).

Furthermore, tumor-associated microglia play an important role in GB treatment resistance, including radiation and chemotherapy. Tumor-associated microglia, in particular, can protect cancer cells from radiation-induced apoptosis by secreting cytokines like IL-6 and TNF-β, as well as increasing chemotherapy tolerance by upregulating drug efflux pumps (Philipsen et al., 2023).

Targeting microglia in GB has been proposed using small chemical inhibitors, monoclonal antibodies, and cell-based therapies. Targeting CCL2 or its receptor CCR2 in preclinical GB models, for example, has been shown to reduce TAM infiltration and boost survival (Mantovani et al., 2004; Wang et al., 2013).

2.2.3 T cells

T cells are essential adaptive immune response mediators and play critical roles in anti-tumor immunity. T lymphocytes are present in the tumor microenvironment in GB. However, their activities are frequently compromised by a variety of mechanisms (Li et al., 2011) such as tumor-induced T cell fatigue, immunological checkpoint activation, and regulatory T cell (Treg) invasion. (Fecci et al., 2006). Tumor cells additionally release immunosuppressive cytokines such as transforming growth factor-beta (TGF-β), which inhibits T cell activity (Hussain et al., 2006). Depending on the subtype and functional state of the T cells, as well as the cytokine milieu inside the tumor microenvironment, infiltrating T cells can have both pro-tumorigenic and anti-tumorigenic effects (Wainwright et al., 2012).

Regulatory T cells (Tregs) Tregs, for example, have been demonstrated to promote glioblastoma development by inhibiting the anti-tumor immune response and establishing an immunosuppressive milieu (Berghoff et al., 2017). Effector T cells, on the other hand, have the ability to recognize and eliminate tumor cells but are frequently functionally impaired within the glioblastoma microenvironment due to factors such as the upregulation of immune checkpoint molecules and the accumulation of immunosuppressive cells (Alban, 2018).

2.2.4 B cells

B cells are immune cells that generate antibodies and play an important part in the adaptive immune response. In the GB microenvironment, B cells can induce immune suppression and angiogenesis. They can generate cytokines including interleukin-10 (IL-10) and transforming growth factor-beta (TGF-β), which suppress the activity of immune cells like T-cells and NK cells while promoting GB development and invasion (Garg et al., 2017; Jiao et al., 2017). Furthermore, B cells can secrete pro-angiogenic factors such as VEGF, CXC chemokine ligand 12 (CXCL12), and CXC chemokine ligand 13 (CXCL13), which stimulate the formation of new blood vessels, provide nutrients and oxygen to the tumor, and promote GB growth and invasion (Shonka et al., 2013).

B cells also play a role in GB therapeutic response by influencing responsiveness to immune checkpoint inhibitors (ICIs). B lymphocytes can express immunological checkpoints including programmed death-ligand 1 (PD-L1), which interacts with the T cell immune checkpoint programmed cell death protein 1 (PD-1) to cause T cell depletion and immune evasion by GB cells (Pellegatta et al., 2015). Several approaches, including the use of monoclonal antibodies targeting B cells and B cell-derived cytokines, as well as B cell function modulation have been proposed to target B cells in the GB microenvironment. Anti-CD20 monoclonal antibodies, such as rituximab, can reduce B cells and increase survival in GB patients. In addition, inhibitors of B cell-derived cytokines such as IL-10 and TGF-β may be a potential strategy for GB treatment (Cai et al., 2015).

B cells play a role in immune escape and have a direct impact on GB development and progression. B cells isolated from GB patient samples have been shown to promote tumor cell proliferation and migration through the secretion of growth factors such as insulin-like growth factor-1 (IGF-1) and hepatocyte growth factor (HGF). They can also influence the immunological milieu of GB by secreting chemokines such as CXCL13, which is produced mostly by B cells in GB patient samples and is related to enhanced T cell infiltration and improved patient survival (Khan et al., 2020).

Anti-CD20 antibodies like as rituximab have been studied in clinical trials for the reduction of B cells in GB. Combination of Anti-CD20 antibodies with traditional chemotherapy medicines such as temozolomide has increased progression-free survival. Rituximab has also been demonstrated to diminish B cell infiltration in the GB microenvironment and increase immunotherapy effectiveness (Wintterle et al., 2003).

2.2.5 Natural -killer cell

NK cells are innate immune cells that help the body defend against viruses and tumors. NK cells are present in the tumor microenvironment in GB but are frequently functionally compromised (Vivier et al., 2008). NK cells have been demonstrated in studies to infiltrate glioblastomas and may contribute to tumor management via a variety of methods, including the direct killing of tumor cells and activation of other immune cells (Yang et al., 2010). However, NK cells, like other immune cells, can be suppressed within the glioblastoma microenvironment by factors such as immune checkpoint molecule upregulation and immunosuppressive cell accumulation (Hasmim et al., 2015). Tumor cells can cause NK cell dysfunction through a variety of methods, including activating ligand downregulation and inhibitory ligand overexpression (Fujita et al., 2011). Immunosuppressive substances in the tumor microenvironment, such as TGF-β and interleukin-10 (IL-10) (Ho and Ho, 2021), can also limit NK cell activity.

2.2.6 Dendritic cells

Dendritic cells (DCs) are important components of the immune response and have been linked to glioblastoma (GB) tumor microenvironment. Recent research has shown that DCs can interact with other immune cells in the GB microenvironment, boosting the growth of regulatory T cells (Tregs) through TGF-mediated signaling (Carmeliet and Jain, 2000). DCs release VEGF-A, which promotes tumor development and angiogenesis in GB (Plate et al., 1992b). The presence of DCs in the GB microenvironment implies requires a better understanding into their interactions with other immune cells, that may lead to better treatment methods. Boosting anti-tumor immunity of DCs

while suppressing their pro-tumor actions can be an effective strategy for GB therapy.

2.2.7 Myeloid-derived suppressor cells

MDSCs, a diverse population of immature myeloid cells that limit the function of immune effector cells. Several studies have shown that MDSCs promote tumor growth and invasion via a variety of mechanisms, including cytokine and growth factor secretion, immune effector cell suppression, and angiogenesis stimulation. MDSCs secrete IL-6 by activating the signal transducer and activator of transcription 3 (STAT3) signaling pathway, promoting tumor growth and invasion. MDSCs also inhibit NK cell activity by upregulating PD-L1 expression (Eichler et al., 2011).

Depleting MDSCs in the tumor microenvironment can increase the activity of immune effector cells while decreasing tumor development and invasion. In a mouse model of GB, all-trans retinoic acid (ATRA)-mediated MDSC reduction enhanced T cell infiltration and decreased tumor development (Sun et al., 2021). Similarly, targeting S100 Calcium Binding Protein A9 (S100A9), which is expressed by MDSCs, inhibited tumor development and invasion in a mouse model of GB (Hynes, 2002).

2.3 Non immune cells in glioblastoma micro-environment

2.3.1 Endothelial cells

Endothelial cells present in the tumor microenvironment play an important role in supporting glioblastoma development and invasion (Reardon et al., 2017). Endothelial cells are important for angiogenesis, which is the development of new blood vessels from pre-existing ones and is a characteristic of glioblastoma growth. These cells have high quantities of pro-angiogenic factors including VEGF, which promote blood vessel creation as well as glioblastoma cell survival and invasion (Silva et al., 2008). Endothelial cells can also influence the immune response by secreting immunosuppressive factors like TGF-β and expressing immunological checkpoint molecules like PD-L1 that decrease T cell activation and proliferation. Endothelial cells can also modify the extracellular matrix (ECM) of glioblastoma tumors, allowing glioblastoma cells to migrate and invade (Tawi et al., 2021).

Several strategies have been developed to target endothelial cells in glioblastoma therapy. One such strategy is to use monoclonal antibodies or small molecule inhibitors to limit VEGF signaling and hence reduce angiogenesis. Another strategy is to target endothelial cell survival and migratory pathways such as PI3K/Akt and mTOR (Charles et al., 2012). However, these approaches have limitations and can interfere with normal endothelial cell functions, resulting in negative outcomes (Liang et al., 2014). Immunotherapy is another intriguing strategy that targets the immune regulatory activities of endothelial cells. Anti-PD-L1 antibodies have shown potential therapeutic effects in glioblastoma tumors by increasing T-cell infiltration and activation. In preclinical investigations, combining anti-PD-L1 treatment with other immune checkpoint inhibitors, such as anti-cytotoxic T-lymphocyte–associated antigen 4 (anti-CTLA-4), yielded encouraging outcomes (Cekanaviciute et al., 2014). However, more research is needed to develop safe and effective therapeutic strategies for glioblastoma tumors that target endothelial cells.

2.3.2 Astrocytes

Astrocytes, the most common glial cells in the central nervous system, have been revealed to play an important role in glioblastoma tumor microenvironment. Glioblastoma tumor-induced astrocyte activation can increase tumor growth. Activated astrocytes release cytokines and growth factors that promote glioblastoma cell proliferation and invasion. Astrocyte activation has also been linked to a poor prognosis in glioblastoma patients (Olea-Flores et al., 2020). Astrocytes can produce immunomodulatory substances such transforming growth factor- (TGF-β) and interleukin-10 (IL-10), which dampen the immune response to glioblastoma cells. Furthermore, astrocytes can inhibit the activity of immune cells involved in anti-tumor immunity, such as T-cells and NK-cells (Farin et al., 2006).

Astrocytes, in addition to immunological regulation, can enhance angiogenesis in the glioblastoma microenvironment. Astrocytes also have the ability to produce vascular endothelial growth factor (VEGF), a critical regulator of angiogenesis, and express integrins as well as extracellular matrix proteins that aid in the formation and stabilization of blood vessels (Nagy et al., 2010). Astrocytes have also been found to contribute to drug resistance in glioblastoma tumors by secreting factors that protect glioblastoma cells from chemotherapy. Additionally, astrocytes can form a physical barrier between glioblastoma cells and chemotherapy agents, preventing them from reaching the tumor cells. They can also activate signaling pathways that promote drug resistance in glioblastoma cells (Zhao et al., 2008). Understanding the role of astrocytes in glioblastoma tumor microenvironment is essential for the development of effective treatments for this devastating disease.

2.3.3 Neurons

In recent research, neurons in the GB microenvironment have been identified as a potential contributor to tumor formation. Glutamate and substance P, for example, have been shown to promote GB cell motility and invasion. It has been demonstrated that the synthesis of chemicals like brain-derived neurotrophic factor (BDNF) by neurons can promote cancer growth by boosting angiogenesis (Venkatesh et al., 2017).

Neurons in the GB microenvironment are not passive bystanders; rather, they engage in active interactions with glioblastoma cells. Glioblastoma cells on the other hand promote the formation of synapses between neurons, resulting in enhanced neuronal activity (Venneti et al., 2015). Neurons, have been shown to alter glioblastoma cell behaviour through the synthesis of BDNF and neuregulin-1 (NRG1) (Venkataramani et al., 2019). Recent research has shown that glioblastoma cells can form direct synapses with neurons, allowing impulses to be transmitted between the 2 cell types (Lu et al., 2012).

The interaction of neurons and glioma cells involves complex signaling pathways (Venkatesh et al., 2019). The binding of BDNF to its receptor TrkB on glioblastoma cells, for example, has been shown to promote tumor development and invasion by activating many signaling pathways such as PI3K/AKT, MEK/ERK, and PLC. Similarly, binding of NRG1 to its receptor ErbB3 on glioblastoma

cells has been shown to increase cancer cell survival and invasion via the PI3K/AKT and MEK/ERK pathways (Kermani et al., 2005).

The discovery of neurons' participation in the GB microenvironment has significant implications for GB treatment (Zhang et al., 2008). In preclinical studies, blocking BDNF signaling was shown to reduce GB development and invasion. Inhibiting NRG1 signaling also improves glioblastoma cell susceptibility to radiation treatment (Zhang et al., 2014). Targeting neuronal signaling pathways, could therefore emerge as a novel therapeutic strategy for GB.

3 Single-cell sequences in GBM

Single-cell sequencing has revolutionized our understanding of the complex genetic heterogeneity driving tumor growth by providing a means of analyzing genomes, transcriptomes, and epigenomes at the individual cell level. It reveals a level of complexity that was previously unattainable by identifying cellular heterogeneity, which is frequently hidden in hybrid sample sequencing carried out conventionally (Risau, 1997). Concurrently, the Tumor Microenvironment (TME) becomes apparent as a crucial element in the emergence, progression, and reaction to treatment of tumors. A paradigm shift in TME analysis has been brought about by the application of single-cell sequencing, which has revealed the immune cells' differentiation pathways and heterogeneity as well as the pan-cancer immune microenvironment blueprint, providing prognostic value for tumor prognosis. This collaboration offers a singular chance to analyze the molecular processes driving the genesis and spread of tumors (Hanahan and Folkman, 1996). Advances in TME analysis and single-cell sequencing have shown great promise recently, with applications ranging from clinical translation to cancer research. Through single-cell transcriptome sequencing and spatial transcriptome combination, the previously underappreciated presence of tumor-associated fibroblasts (CAFs) in glioblastoma (GBM) has been revealed, challenging the presumption and advancing our knowledge of GBM (Ferrara and Kerbel, 2005). Understanding the fibrocytes that promote tumor growth improves our understanding of GBM and opens the door to more intelligent treatment approaches. Given that tumor cells can adapt to changes in their environment brought about by drugs, it is critical to comprehend the unique differentiation processes that these cells go through to develop targeted therapies that are effective (Navin et al., 2011).

4 Mechanisms pertaining to progression of GB

4.1 Angiogenesis in GB

Angiogenesis is a critical process for the development and maintenance of blood vessels in various tissues, and its dysregulation has been implicated in the progression of multiple diseases, including cancer and inflammation (Puram et al., 2017; Jain et al., 2023). The angiogenesis induced neovascularization in tumors is critical for providing required nutrients and oxygen to fast growing GB cells. Angiogenesis in the GB micro-environment is modulated by several growth factors that include vascular endothelial growth factor (VEGF), hepatocyte growth factor (HGF), Fibroblast growth factor (FGF), Platelet-derived growth factor (PDGF), Transforming growth factors (TGF-β), Matrix metalloproteinase (MMPs) and Angiopoietins (Angs) as depicted in Figure 3.

4.1.1 Vascular endothelial growth factors

Vascular endothelial growth factors (VEGFs) and receptors (VEGFRs) play critical roles in vasculogenesis and angiogenesis (Quail and Joyce, 2017). Endothelial cell proliferation and survival are largely driven by the ERK, neuropilin-1 (NRP1), and PI3K/Akt pathways, which are triggered by a variety of signaling intermediates (Takahashi et al., 2001). Endothelial cell migration is regulated by several mechanisms that frequently converge on PI3K stimulation, resulting in the activation of Rho family G proteins. VEGF can also attach to NRP1 on endothelial cells, boosting VEGF binding to VEGFR2 and magnifying its pro-angiogenic effects (Garrido-Urbani et al., 2009). MMPs are upregulated by VEGFA predominantly through Akt-dependent activation of -catenin and nuclear factor kappa B (NFκ-B) and ROS-mediated mechanisms (Van Hinsbergh and Koolwijk, 2008).

Following the discovery of VEGF as a key regulator of pathologic angiogenesis and tumor growth in glioblastoma, VEGF and VEGFR inhibitors have been developed (Gerstner et al., 2009). The first anti-angiogenic medication approved for cancer therapy was bevacizumab, a human monoclonal antibody that precisely recognizes and inhibits VEGF-A (Vredenburgh et al., 2007). However, resistance mechanisms such as the activation of alternative angiogenic pathways and the recruitment of pro-angiogenic immune cells have limited anti-angiogenic therapy's clinical effectiveness in glioblastoma (Gilbert et al., 2014).

4.1.2 Fibroblast growth factors

FGFs are a class of growth factors that govern angiogenesis and have been linked to the development of GB. FGFs bind to four tyrosine kinase receptors (FGFR1-4) on the cell surface, activating a variety of signaling pathways such as PI3K, PLC, mitogen-activated protein kinases (MAPK), signal transducers and activators of transcription (STATs), and protein kinase C (PKC). These mechanisms increase cell proliferation, survival, and migration, which are required for tumor angiogenesis (Hadari et al., 2001). FGF expression is elevated in glioblastoma and is associated with tumor grade and patient prognosis. FGFs enhance angiogenesis by boosting endothelial cell proliferation and migration (Udayakumar et al., 2002), triggering the production of pro-angiogenic molecules such as VEGF, and affecting extracellular matrix remodeling during angiogenesis (Takahashi et al., 1992). Because of FGF's crucial involvement in glioblastoma tumor angiogenesis, treatments targeting FGF signaling pathways, such as FGFR inhibitors and combination therapies targeting FGF and other pro-angiogenic pathways such as VEGF, have been developed (Shah et al., 2008; Koch et al., 2012).

4.1.3 Platelet-derived growth factor

Platelet-derived growth factor (PDGF) family members include PDGF-AA, AB, BB, CC, and DD, which activate intracellular

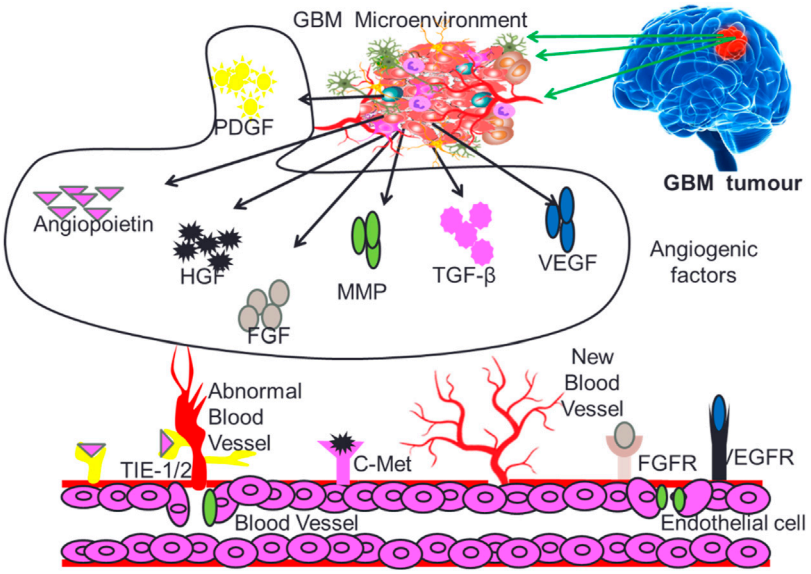

FIGURE 3
Different types of growth factors supporting GB tumor growth and proliferation.

signaling pathways such as Ras-MAPK, PI3K, and PLCg (Vredenburgh et al., 2007) to kick-start the cell cycle, DNA synthesis, mitosis, cell migration, and chemotaxis (Galanis et al., 2018). GB is characterized by elevated PDGF and PDGFR expression. Preclinical investigation in rats and marmosets revealed that PDGF overexpression, particularly PDGFB and PDGFA play an important role in the genesis and progression of GB (Saha and Giri, 2017). Furthermore, it has been demonstrated that low molecular weight PDGF receptor kinase inhibitors effectively reverse the transformed phenotype and inhibit tumor growth *in vivo*. In GB, PDGF/PDGFR targeting has shown promising therapeutic outcomes (Xu et al., 2015). PDGF genes express differently in glial cells and endothelial cells in GB micro-environment, while PDGFR is preferentially expressed in GB stem cells, encouraging their self-renewal and invasion (Ozawa et al., 2014). Endo-MT and VEGFR-2 down-expression are regulated by the PDGF/NF-B/Snail axis in GB, resulting in resistance to anti-angiogenic treatment. Inhibiting PDGF signaling improves the sensitivity of anti-VEGF/VEGFR therapy in GB, allowing for the creation of more effective treatment regimens (Uhrbom et al., 2004). PDGF-D is a potent growth factor for human GB cells, and HIF1 plays an important role in the constitutive activation of the AKT signaling pathway in GB by regulating the expression of PDGF-D and its receptor, PDGFR. Inhibition of HIF1α disrupts the HIF1α-PDGF-D-PDGFRα feedforward axis, leading to the abolishment of AKT pathway activation and a potentially effective therapeutic approach for GB treatment (Liu et al., 2018).

4.1.4 Hepatocyte growth factor

Hepatocyte growth factor (HGF), also known as scatter factor (SF), is a heparin-binding mesenchyme-derived cytokine that has been linked to glioblastoma multiforme (GB) angiogenic process. HGF/SF has been established in recent investigations to play an important role in GB tumor angiogenesis by boosting endothelial cell proliferation, migration, and survival (Peng et al., 2021).

HGF/SF is a strong mitogen that promotes endothelial cell growth. The binding of HGF/SF to its receptor, c-MET, stimulates multiple downstream signaling pathways that promote cell proliferation, including the PI3K-AKT, RAS-ERK, and JAK-STAT pathways. HGF/SF has been demonstrated to increase endothelial cell proliferation in GB by activating the PI3K-AKT and RAS-ERK pathways (Trusolino and Comoglio, 2002).

The hepatocyte growth factor/scatter factor (HGF/SF) has been linked to the control of angiogenesis through the overexpression of VEGF, a powerful pro-angiogenic factor, and the reduction of thrombospondin 1 (TSP-1), an endogenous regulator of angiogenesis. This dual method of action shows that HGF/SF is important in balancing pro- and anti-angiogenic factors in the tumor microenvironment (Olmez et al., 2018).

4.1.5 Angiopoietins (Angs)

Angiopoietins (Angs) are a protein family that binds to the Tie-2 receptor and play an important role in GB angiogenesis. Angiopoietins are classified into four kinds, each with distinct and opposing actions on the vasculature (Knowles et al., 2009). Angiopoietin-1 (Ang-1) promotes endothelial cell survival, proliferation, migration, and tube formation by activating the Tie2 receptor tyrosine kinase and stabilizing blood vessels. It also stimulates the recruitment of pericytes and smooth muscle cells to the vessel wall, which helps to stabilize it. Ang-1 causes new vessel development with angiogenic activities independent of VEGF and stabilizes them via reciprocal interactions between the endothelium and the surrounding extracellular matrix (Suri et al., 1996a; Suri et al., 1996b).

Ang-1 and Ang-2 are key Ang family members that connect to the Tie-2 receptor on endothelial cells. Ang-1 promotes blood vessel stabilization, whereas Ang-2 promotes vascular remodeling by

destabilizing blood vessels and inducing sprouting angiogenesis (Daly et al., 2006a). Ang 2 also stimulates downstream signaling pathways that induce angiogenesis, such as AKT and ERK (Ricci-Vitiani et al., 2010). The invasiveness of gliomas is linked to Ang-2 upregulation. Inhibiting Ang-2 expression can reduce glioma invasiveness and avoid an anti-VEGF therapeutic escape mechanism. Dual suppression of the VEGF and angiopoietin-TIE2 signaling pathways is thought to be a potential treatment option for recurrent GB (Kienast et al., 2010). The role of Ang-1 in GB angiogenesis on the other hand is controversial, with some studies showing that it can suppress GB angiogenesis by stabilizing blood vessels and reducing vessel permeability (Huang et al., 2010).

4.1.6 Transforming growth factors (TGF-β)

The TGF- family of structurally similar polypeptides regulate several pro-tumorigenic processes, including proliferation, apoptosis, differentiation, epithelial-mesenchymal transition (EMT), and angiogenesis. TGF-β signaling can activate downstream effectors that govern cellular activities such as the canonical Smad pathway, which includes the Wnt, Notch, Hippo, Hedgehog, and JAK-STAT pathways, as well as non-Smad pathways such as PI3K-Akt, MAPK, and Rho GTPases (Akwii et al., 2019).

The key process of epithelial-mesenchymal transition (EMT) promotes the growth of GB. E2 and TGF-β have been found to suppress the expression of the estrogen receptor (ER) and Smad2/3. TGF-β causes Smad2 phosphorylation and subsequent nuclear translocation, which is blocked by E2. Both E2 and TGF- β have been discovered to elicit EMT-related cellular processes such as morphological alterations, actin filament reorganization, and mesenchymal marker expression (N-cadherin and vimentin). Interestingly, co-treatment with E2 and TGF- β has been shown to inhibit EMT activation (Daly et al., 2006b).

TGF- β is linked with a poor prognosis in GB and promotes the production of pro-angiogenic factors such as VEGF, FGF, and PDGF-β (Itoh et al., 2018). TGF-β1 enhances glioma-induced angiogenesis via the JNK pathway in zebrafish embryo/xenograft glioma models (Li and Flavell, 2008). Crosstalk between TGF-β and VEGF/PLGF signaling has been demonstrated to exhibit both pro- and anti-angiogenic actions in human brain-derived microvascular endothelial cells (hCMECs) and glioblastoma-derived endothelial cells (GMECs). TGF-β increases VEGF and PlGF mRNA and protein expression in glioma cells, resulting in pro-angiogenic effects. Exogenous TGF-β, on the other hand, inhibits endothelial characteristics and causes endothelial-mesenchymal transition (EndoMT) in hCMEC and GMEC (Liu et al., 2012).

4.1.7 Matrix metalloproteinases

Matrix metallopeptidases (MMPs) are a class of structurally conserved zinc-dependent endopeptidases generated by tumor cells that play a crucial role in tumor development invasion, metastasis, and angiogenesis in the central nervous system through participating in the breakdown of extracellular matrix macromolecules such as angiogenesis and cytokine activation. MMPs stimulate endothelial cell invasion by destroying the vascular basement membrane and ECM (Hernández-Vega and Camacho-Arroyo, 2021). They also promote pericyte proliferation and activation, as well as their migration to newly formed vasculature, resulting in vascular stabilization (Chamberlain, 2013). MMP-9-mediated VEGF release from the matrix has been shown in multiple transgenic mice models that triggers angiogenic switching in pre-malignant tumors (Krishnan et al., 2015).

Guanylate-binding proteins 5 (GBP5) mediated activation of MMP3 plays an important role in the development and invasion of glioblastoma (GB). GBP5 has been demonstrated to activate the Src/ERK1/2 MAPK pathway in GB cells, resulting in the production of matrix metalloproteinase-3 (MMP3). According to research, MMP3 is overexpressed in gliomas and contributes to the aggressiveness of GB. As a result, the GBP5/Src/ERK1/2/MMP3 axis has been postulated as a possible therapeutic target for GB (Sternlicht and Werb, 2001; Bassiouni et al., 2021).

5 Therapeutic implications in GB

GB treatment is particularly challenging due to its intra-tumor heterogeneity wherein the cells have differences in characteristics at molecular levels which is further complicated by genetic and epigenetic changes that promote evasion of standard treatment procedures. Neoplastic cells demonstrate the quality to adjust to their surrounding environment and accordingly alter their microenvironment for their advantage. This complexity leads to the need for varying therapeutic strategies which can act together to provide a meaningful therapeutic response. GB patients are basically treated by surgical exclusion of the neoplastic lesion usually followed by chemotherapy and radiation therapy. With the advent of modern research, a number of new techniques have been put forward towards the treatment of GB patients (Pombo Antunes et al., 2020) There are new approaches to the problem of BBB blockage, but before they are used in clinical settings, their feasibility must be confirmed.

5.1 Adaptive T cells

The most common chemotherapeutic agent is temozolomide, a DNA methylator that causes DNA cross-linking. Adaptive T cells therapies which include IL13Rα2-CAR-T cells, IL13Rα2 is known to promote tumor regression in glioma and few other tumor models. With the increase in malignancy grade expression of IL13Rα2 is a prognostic indicator for poor patient survival (Chantrain et al., 2006).In recent times personalized cancer therapy is emerging as a preferred therapy for cancer treatment. One such method is treating cancer-bearing host with Cytokine-induced killer (CIK) immune cells which can direct an anticancer activity. Cytokine-induced killer (CIK) cells are major histocompatibility (MHC)-unrestricted cytotoxic lymphocytes that can be produced *in vitro* from peripheral blood mononuclear cells and can also be cultured with the addition of interferon (IFN)-γ, interleukin (IL)-2, and CD3 monoclonal antibody (CD3mAb). (Brown et al., 2013). The use of immunotherapy, to provide anti-tumor immune response is surely an area of active research towards the treatment of glioblastoma.

Promising survival advantages were reported in both *in vitro* and in xenograft models when CAR-T treatment targeting CD276 was used (Wang et al., 2014). A unique understanding of the combination of anti-CD276 and anti-angiogenesis revealed by

using antibody–drug conjugates to ablate CD276+glioma cells concurrently impairing tumour vascular, which was reinforced by the confirmation that CD276 was positively correlated with VEGFA and MMP2. In patients with GBM, CAR-T cells that target EGFRvIII, HER2, and IL-13Rα2 have demonstrated a good safety profile and therapeutic effects.

5.2 Checkpoint Inhibitor

In the physiologic state, immune checkpoints play a major role in the sustainable balance of immune modulation in order to prevent autoimmune disorders. Immune checkpoints are the key regulators of the immune system that are expressed by T effector cells, antigen-presenting cells (APCs), and myeloid-derived cells in the normal immune system. When these checkpoints are engaged, they reduce immune activity by inducing T-cell anergy and apoptosis. Programmed death ligand 1 (PD-L1) mediated immune evasion plays a major role in neoplastic growth. Programmed death 1(PD1) and its ligand PDL1 regulate the proliferation and activation of T cells. Blockage of immune checkpoints with monoclonal antibodies has emerged as a promising new approach for the treatment of glial neoplasms. Previous studies on murine glioma models show improved survival with the use of checkpoint inhibitors that suggest immune checkpoint blockade can play an important role in treatment options for GB. (Berghoff et al., 2015; Nehama et al., 2019).

In a phase I trial, the co-inhibitory molecule T cell immunoglobulin and mucin domain-containing protein 3 (TIM-3), which is expressed on immune cells, is being investigated for its inhibition in relation to anti-PD1 medications for a variety of tumour types, including GB. Lymphocyte activation gene 3 (LAG-3) served as an early indicator of exhausted T cells, suggesting that early anti-LAG-3 medication therapy may be beneficial. A phase I trial is being conducted to examine the effects of anti-LAG-3 treatment alone or in conjunction with anti-PD1 treatment for patients with recurrent GBM (Reardon et al., 2021). AntiTIGIT drugs are direct inhibitors of T-cell proliferation and improve the anti-tumor immune response in many pre-clinical studies as a monotherapy or in combination with PD-1 and TIM-3 inhibitors. T cell immunoreceptor with Ig and ITIM domains (TIGIT) is an inhibitory receptor expressed on several types of lymphocytes. Anti-TIGIT treatment is reported to be currently in phase I clinical development for recurrent GBM in a multicenter trial in combination with antiPD-1 drugs (Lim et al., 2017).

Nivolumab is a fully human immunoglobulin G4 monoclonal antibody that targets the programmed death-1 (PD-1) immune checkpoint receptor (Zhang et al., 2018). Ipilimumab, a human IgG1 monoclonal antibody, is directed against CTLA-4, a critical immune checkpoint molecule known to be overexpressed on the membranes of Treg and downregulates the function of the effector cells. By increasing this inhibitory effect, ipilimumab stimulates the immune system and enhances its reaction against the tumor (Reardon et al., 2020). Pembrolizumab, which is a human anti-PD-1 antibody has shown antitumor activity with a favorable safety profile and has also been approved by the US Food and Drug Administration (FDA) as monotherapy across a number of tumor types (Youssef and Dietrich, 2020).

5.3 Angiogenesis inhibitors

It is now known that VEGF, also referred to as VEGF-A is an important regulator of angiogenesis. Human anti VEGF monoclonal antibody like (rhuMab VEGF; bevacizumab; Avastin) binds with VEGF with a very similar to that of the original antibody (Kd ~0.5 nM) and thereby prevents its interaction with VEGF receptor tyrosine kinases VEGFR1 and VEGFR2 on the surface of endothelial cells. (Burns et al., 2016).

5.4 Vaccine approach

Dendritic cell (DC) vaccines are potentially effective in the treatment of GB, though their development is quite a challenging process requiring elaborate facilities to safely extract and pulse DCs with the tumor components. This limits the ability of DC vaccines to be rapidly scaled for broader utilization. Similar to DC vaccines, peptide vaccines are made from the tumor associated antigens. However, unlike DC vaccines that are personalized therapies, peptide vaccines are produced centrally. Thus, peptide vaccines can be distributed to different medical facilities more quickly, which makes them a viable strategy for multicenter glioma immune treatment trials.

A well-known target for peptide vaccines is the epidermal growth factor receptor (EGFR), which is a receptor tyrosine kinase that is highly expressed in glioblastoma. In GB, the most frequent mutation of EGFR is the EGFRvIII truncated variant that aids signaling independent of ligands. Constitutively active kinase activity and the existence of distinct amino acid sequences at newly formed mutation-induced junctions are the outcomes of an in-frame deletion of EGFR exons 2 through 7. EGFRvIII therefore promotes glioma tumors. This makes EGFRvIII an important target for immune therapy, as it is a tumor-specific target driver of the malignancy and is expressed on the cell surface. (Ferrara et al., 2004).

Rindopepimut is a 14-mer peptide conjugated to the immunogenic carrier protein keyhole limpet hemocyanin (KLH) that spans the mutation site of EGFRvIII (PEPvIII: NH2-Leu-Glu-Glu-Lys-Lys-Gly-Asn-Tyr-Val-Val-Thr-Asp-His-Cyt-COOH) (Garima et al., 2022). Also known as CDX-110, it targets the EGFR deletion mutation EGFRvIII, consisting of an EGFRvIII-specific peptide conjugated to keyhole limpet hemocyanin. Rindopepimut is under phase 3 clinical trials in glioblastoma patients (Swartz et al., 2014). The vaccine is injected intradermally leading to antigen recognition by antigen-presenting cells (APCS) and its presentation to T-cells cytotoxic and T-lymphocyte (CTL) T-cells which in turn activate B-cells that produce antibodies against EGFRvIII in the tumor. CTLs have the ability to cross the blood-brain barrier and target GB cells with EGFRvIII mutation on the surface. This activation of T-cells and CTLs leads to an anti-tumor response (Weller et al., 2017).

Tumour necrosis factor superfamily receptor abundant on T cells and glucosecorticoid-induced TNFR-related protein (GITR) has showed potential as an immunotherapy target. An

agonistic antibody against GITR has been reported to inhibit Tregs in a number of models and has been addressed in glioma. Granzyme B (GrB) expression by Tregs was significantly reduced by peripheral treatment, whereas GrB expression by Tregs was also selectively depleted by intratumoral treatment, primarily by FcγR-mediated destruction. Anti-GITR treatment results in the enhanced survival and functionality of dendritic cells (DCs). (Guo et al., 2015).

5.5 Signaling pathway targets

Genomic analysis of glioblastoma revealed several signaling pathways and gene alterations that are critical for the development and progression of GB. The conversion of sphingomyelin to ceramide which is regulated by the enzyme sphingomyelin phosphodiesterase 1 (SMPD1) is one such pathway with SMPD1 being a potential drug target for GB. The highly brain-penetrant antidepressant fluoxetine has an inhibitory effect on SMPD1 activity, thereby killing GBMs by inhibiting the epidermal growth factor receptor (EGFR) signaling and activation of lysosomal stress mechanisms. (Miska et al., 2016; Lynes et al., 2018).

Nonsteroidal anti-inflammatory drugs (NSAIDs) act as a cell proliferation inhibitor by suppressing Wnt/b-catenin/Tcf signaling in many human malignancies. Studies have revealed that NSAIDs diclofenac and celecoxib are potential therapeutic agents that target glioblastoma cells by downregulating the activation of Wnt/b-catenin/Tcf signaling (Bi et al., 2021; Ulrich et al., 2006; mT hun et al., 2002).

Tumor cells induce vasogenic edema by releasing VEGF which induces increased vascular permeability in the tumor microenvironment. Dexamethasone, a synthetic glucocorticoid, counteracts this process by acting on glucocorticoid receptors, thereby decreasing both VEGF expression by tumor cells and VEGF sensitivity of the endothelial target cells (Sareddy et al., 2013).

Micheliolide (MCL) derivative 9-oxomicheliolide, has a strong anticancer activity towards GB in mice, with its rate of tumor inhibition comparable to clinical drug temozolomide. The mode of action of 9-oxomicheliolide is apparently through inhibitory effects on NF-κB and STAT3 signaling pathways as well as induction of cell apoptosis (Swildens et al., 2022).

The epidermal growth factor receptor-1 (EGFR) is a protein tyrosine kinase that can be activated by both epidermal growth factor (EGF) and tumor growth factor-α (TGF-α). Reports suggest that there is an upregulation of EGFR receptors in glioblastoma patients. (Zeng et al., 2021). Erlotinib is an orally bioavailable reversible competitive inhibitor of the adenosine triphosphate region of the EGFR tyrosine kinase domain. The FDA has approved erlotinib for use as a second and third-line treatment for non-small cell (NSCL) cancer (Wong et al., 1987).

Integrins are transmembrane αβ heterodimers; in humans, there are at least 18 α and 8 β subunits identified, resulting in 24 heterodimers. Members of this family are found in chicken, mammals, and zebrafish, as well as lower eukaryotes, including sponges, the nematode *Caenorhabditis elegans* (two α and one β subunits, which generate two integrins) and the fruitfly *Drosophila melanogaster* (five α and one β, which generate five integrins) (De Groot et al., 2008).

In a phase I trial, individuals with reccurent GBM showed excellent tolerance to cediranib plus celenigitide, a selective integrin inhibitor that targets αvβ3 and αvβ. Cilengitide (CGT) has a moderate efficacy in a phase II study and can bind with avβ3 and αvβ5 to be transported and stored in reccurentGBM cells (Takada et al., 2007). It has been reported that intravenously injected nanoparticles enhance drug penetration into the central nervous system by raising the permeability of the blood-brain barrier. In addition to preventing medication exposure to off-target tissues, encapsulating CGT in a well-designed nanocarrier can postpone drug clearance and enable prolonged or triggered release. This is especially important for CGT therapy since it can prolong its circulation duration, achieve more favorable pharmacokinetics, and lessen its non-specific effects on healthy cells, making the possibility of safer and more effective cancer treatment possible (Yang et al., 2022).

5.6 Oncolytic virus

Because of their modest pathogenic effect, oncolytic viruses (OVs) have antineoplastic roles by selectively infecting and killing cancer cells while sparing healthy ones. Furthermore, OVs may be able to change the immunosuppressive Tumor Microenvironment (TME) to an immunocompetent one. In fact, OV has the ability to carry a transgene and releases tumour antigens (Zhao et al., 2016).

DNX-2401 is a replicative engineered oncolytic adenovirus that consists of two stable genetic changes in the adenovirus genome for selectively and efficiently infecting and replicateing retinoblastoma pathway deficient such as tumor cells (Ma et al., 2023). Preclinical studies on DNX-2401 has demonstrated to be effective against glioma xenograft mouse models received through intratumoral injections of the virus by direct oncolysis in addition to eliciting antitumor immune responses. Phase I trials were carried in GB patients. For patients with recurrent GB or gliosarcoma, DNX2401 in combination with pembrolizumab, an anti-PD-1 antibody, is being tested in a phase II trial (Jiang et al., 2014).

Recombinant Lerapolturev (PVSRIPO), a rhinovirus chimaera derived from poliovirus (PV), is a new intratumoral immunotherapy that is non-neurovirulent. According to trial data in patients with rGBM, PVSRIPO monotherapy has a higher long-term survival rate. PVSRIPO targets CD155, the PV receptor, which is expressed in APC and solid tumours. In TME APC, PVSRIPO infection causes non-lethal persistent infection but inflammatory-mediated tumour cell death. Tumour antigen-specific T cell activation and recruitment result from this which is enhanced by immunologic recall to intratumoral replicating virus from previous vaccination. Type I/III interferon-dominant inflammation follows (Sloan et al., 2021).

5.7 Combination therapy

Numerous pharmacological compounds that are known to affect the Tumor micro environment or have an impact on GB cells are currently being used in clinical practice for a variety of illnesses. Small-molecule inhibitors are intended to prevent tumour growth, survival, angiogenesis, and metastasis by blocking signalling pathways. In clinical trials, tyrosine kinase inhibitors (TKIs) have been evaluated as monotherapies for individuals with GB; nevertheless, their therapeutic impact has been limited (Kim and

TABLE 2 List of Therapeutic agents and their targets in treating GB.

Therapeutics	Mode of action	Treatment effect	Studied in	Clinical trials	Author
Adaptive T cells					
IL13Rα2-CAR-T cells	Targets CAR T cells possessing a mutated form of IL-13 in the CAR construct (Thaci et al., 2014)	Feasible and safe with clinical safe reported in human pilot study (Brown et al., 2015)	Humans	phase I safety and feasibility trial (Brown et al., 2022)	Thaci et al. (2014) Brown et al. (2015) Brown et al. (2022)
cytokine-induced killer (CIK) Immunotherapy	Cytokine-induced killer cells therapy for newly diagnosed GB. (Kong et al., 2017)	Neutropenia events, pneumonia and aute renal failure (Kong et al., 2017)	Humans	Phase III RCT (Kong et al., 2017)	Kong et al. (2017)
Checkpoint Inhibitor					
Pembrolizumab	Anti-programmed death 1 (PD-1) immune checkpoint inhibitor (Reardon et al., 2021)	Rash, proteinuria, fatigue, increased alanine aminotransferase, and hypertension (Reardon et al., 2021; Sahebjam et al., 2021)	Humans	phase II RCT (Nayak et al., 2021)	Reardon et al. (2021); Sahebjam et al. (2021), Lakshmi N, et al., 2021
Nivolumab	Antibody targeting the programmed death-1 (PD-1) immune checkpoint receptor. (Reardon et al., 2020)	Fatigue, Increased alanine aminotransferase, Headache, Increased lipase, Pulmonary embolism (Reardon et al., 2020)	Humans	phase III RCT (Reardon et al., 2020)	Reardon et al. (2020)
Ipilimumab	Checkpoint inhibitor acting against the CTLA-4 protein (Youssef and Dietrich, 2020)	fatigue and diarrhea (Youssef and Dietrich, 2020)	Humans	FDA approved (Brown et al., 2020)	Youssef Dietrich (2020) Brown et al. (2020)
Bevacizumab	Binds to vascular endothelial growth factor A (VEGF-A) and prevents its interaction with VEGF receptor tyrosine kinases VEGFR1 and VEGFR2 on the surface of endothelial cells, (Ferrara et al., 2004)	reduced interstitial edema and interstitial hypertension (Ferrara et al., 2004)	Humans	FDA approved (Wu et al., 2021)	Ferrara et al. (2004), Wu et al. (2021)
Vaccine					
Rindopepimut	Targets treatment of EGFRvIII-positive GB. (Weller et al., 2017)	fatigue, rash, nausea, pruritus, and headache (Weller et al., 2017)	Humans	phase III RCT (Schuster et al., 2015)	Weller et al. (2017) Schuster et al. (2015)
Signaling Pathway targets					
9 - oxo mic. heliolide	Inhibitor of NF-κB and STAT3 signaling pathways, along with induction effects of cell apoptosis. (Sahebjam et al., 2021)	Not known	Mice	Not known	Zeng et al. (2021)
Erlotinib	reversible competitive inhibitor of the adenosine triphosphate region of the EGFR tyrosine kinase domain (De Groot et al., 2008)	rash, fatigue and diarrhea (De Groot et al., 2008)	Humans	phase II study (De Groot et al., 2008)	de Groot et al. (2008)
NSAIDs— diclofenac and celecoxib	Wnt signaling inhibitor (Sareddy et al., 2013)	Not known	Humans	More prospective investigation of the effect of NSAID is required (Bruhns et al., 2018)	Sareddy et al. (2013) Bruhns et al. (2018)
Dexamethasome	Cell cycle progression Inhibitor through down-regulating of cyclin D1 and inhibition of ERK1/2 phosphorylation. (Liu et al., 2009; Kostaras et al., 2014)	myopathy, abnormal glucose metabolism, gastrointestinal complications, irritability, anxiety, insomnia, pneumonia infection (Swildens et al., 2022)	Humans	Not known	Liu et al. (2009)
	Reduces number of macrophages and T cells in GB microenvironment.				Swildens et al. (2022) Kostaras et al. (2014)

(Continued on following page)

TABLE 2 (*Continued*) List of Therapeutic agents and their targets in treating GB.

Therapeutics	Mode of action	Treatment effect	Studied in	Clinical trials	Author
	Dexamethasone removes checkpoint inhibitor-induced antitumor effects in glioblastoma. (Burns et al., 2016)				
Cilengitide (CGT)	Integrin inhibitor that targets αvβ3 and αvβ	No significant adverse events, and no patients developed intracranial hemorrhage (Zhao et al., 2016)	Humans	phase II study (195)	Zhao et al. (2016) Reardon et al. (2021)

Ko, 2020). TKI and CAR T cell combinations have demonstrated synergistic results in the treatment of other solid cancer types, making them a good option to consider in GBM patients (Wu et al., 2019). A chemical involved in cell-cell adhesion called protein phosphatase 2A (PP2A) is inhibited by the tiny molecule LB-100. Combination with LB-100 can improve the effectiveness of CAIX-specific CAR T cell therapy in both *in vivo* and *in vitro* GBM models (Brown et al., 2016; Cui et al., 2019).

Combination of DNX-2401 and TMZ for newly diagnosed GB, temozolomide (TMZ), an alkylating drug, is a part of the conventional therapy regimen. Promoter methylation is known to play an epigenetic role in TMZ chemosensitivity by suppressing O6-methylguanine-DNA methyltransferase (MGMT) (Dunn et al., 2009).Pre-clinically, it was demonstrated that DNX-2401 infection decreased the IC50 of TMZ and MGMT levels in human GBM cell lines (U87 and T98G) *in vitro* (Alonso et al., 2007). Combination treatment with DNX-2401 and TMZ greatly increased the length of survival in an immunodeficient mice model of GBM xenograft. Later research by Kleijn et al. demonstrated that the combination was similarly effective in immunocompetent mouse models of GBM.These investigations served as justification for the DNX-2401 and TMZ combination therapy Phase I trial, which is currently taking place in Spain for recurrent glioblastoma (Kiyokawa and Wakimoto, 2019).

For a long time, researchers have been looking at using adenovirus vectors carrying the HSV thymidine kinase gene (HSV-tk) as a treatment for GBM. When a nucleoside analogue prodrug, like ganciclovir, is administered systemically to tumour cells after adenoviral transduction of HSV-tk, it phosphorylates the prodrug, stops DNA replication, and causes cell death in proliferating tumour cells as well as nearby cells through the bystander effect. Tumour neoantigens are released when cancer cells die, and this triggers cellular immune responses that fight the malignancy (Barba et al., 1994; Perez-Cruet et al., 1994). Table 2.

6 Conclusion

Despite considerable progress in the understanding of molecular mechanisms and signaling molecules that regulate stemness, invasion and proliferation in the GB micro-environment, the prognosis still remains poor resulting in high recurrence and mortality. This requires further research on identification of upstream targets that trigger conversion of normal cells to cancer phenotypes. Since the downstream regulators of GB like VEGF or immune responses have a constitutive role at the system level, scope of intervention is limited. Identification of molecular targets and mechanisms that are exclusive to GB and its micro-environment holds the key to effective treatment modalities. With the advent of personalized medicine, the therapeutic strategies also need to be upgraded to individual centric rather than population centric approaches. Considering the wide variability in pro-carcinogenic factors amongst patients, personalized approaches could probably result in better patient outcome (Buckley, 1929; Sachs, 1954; Jelsma and Bucy, 1967; Edland et al., 1971; Ramsey and Brand, 1973; Rosenblum et al., 1973; Tani et al., 1973; Marton et al., 1974; Yung et al., 1976; Heiss, 1978; Morantz et al., 1979; Neuwelt et al., 1980; Otsuka et al., 1984; Jacobs et al., 1986; Ellemann et al., 1988; Plate et al., 1992a; Shweiki et al., 1992; MURATA et al., 1993; Tada et al., 1994; Miescher et al., 1997; Liau et al., 2000; Hao et al., 2002; Rodrigues et al., 2010; Reardon and Cheresh, 2011).

Author contributions

DT: Writing–original draft. LP: Writing–original draft. SB: Supervision, Writing–review and editing. KB: Conceptualization, Writing–review and editing.

Funding

The author(s) declare that no financial support was received for the research, authorship, and/or publication of this article.

Conflict of interest

The authors declare that the research was conducted in the absence of any commercial or financial relationships that could be construed as a potential conflict of interest.

Publisher's note

All claims expressed in this article are solely those of the authors and do not necessarily represent those of their affiliated organizations, or those of the publisher, the editors and the reviewers. Any product that may be evaluated in this article, or claim that may be made by its manufacturer, is not guaranteed or endorsed by the publisher.

References

Achkova, D., and Maher, J. (2016). Role of the colony-stimulating factor (CSF)/CSF-1 receptor axis in cancer. *Biochem. Soc. Trans.* 44 (2), 333–341. doi:10.1042/BST20150245

Agarwal, S., Sane, R., Oberoi, R., Ohlfest, J. R., and Elmquist, W. F. (2011). Delivery of molecularly targeted therapy to malignant glioma, a disease of the whole brain. *Expert Rev. Mol. Med.* 13, e17. doi:10.1017/S1462399411001888

Akwii, R. G., Sajib, M. S., Zahra, F. T., and Mikelis, C. M. (2019). Role of Angiopoietin-2 in vascular physiology and pathophysiology. *Cells* 8, E471. doi:10.3390/cells8050471

Alban, T. J. (2018). *Targeting immune suppression in glioblastoma*. Case Western Reserve University.

Alonso, M. M., Gomez-Manzano, C., Bekele, B. N., Yung, W. A., and Fueyo, J. (2007). Adenovirus-based strategies overcome temozolomide resistance by silencing the O6-methylguanine-DNA methyltransferase promoter. *Cancer Res.* 67 (24), 11499–11504. doi:10.1158/0008-5472.CAN-07-5312

Barba, D., Hardin, J., Sadelain, M., and Gage, F. H. (1994). Development of anti-tumor immunity following thymidine kinase-mediated killing of experimental brain tumors. *Proc. Natl. Acad. Sci.* 91 (10), 4348–4352. doi:10.1073/pnas.91.10.4348

Bassiouni, W., Ali, M. A., and Schulz, R. (2021). Multifunctional intracellular matrix metalloproteinases: implications in disease. *FEBS J.* 288 (24), 7162–7182. doi:10.1111/febs.15701

Berghoff, A. S., Kiesel, B., Widhalm, G., Rajky, O., Ricken, G., Wöhrer, A., et al. (2015). Programmed death ligand 1 expression and tumor-infiltrating lymphocytes in glioblastoma. *Neuro-oncology* 17 (8), 1064–1075. doi:10.1093/neuonc/nou307

Berghoff, A. S., Kiesel, B., Widhalm, G., Wilhelm, D., Rajky, O., Kurscheid, S., et al. (2017). Correlation of immune phenotype with IDH mutation in diffuse glioma. *Neuro-oncology* 19 (11), 1460–1468. doi:10.1093/neuonc/nox054

Bi, J., Khan, A., Tang, J., Armando, A. M., Wu, S., Zhang, W., et al. (2021). Targeting glioblastoma signaling and metabolism with a re-purposed brain-penetrant drug. *Cell. Rep.* 37 (5), 109957. doi:10.1016/j.celrep.2021.109957

Bikfalvi, A., da Costa, C. A., Avril, T., Barnier, J. V., Bauchet, L., Brisson, L., et al. (2023). Challenges in glioblastoma research: focus on the Tumor Microenvironment: (Trends in Cancer, 9:1 p:9-27, 2023). *Trends cancer* 9, 692. doi:10.1016/j.trecan.2023.02.006

Brown, C. E., Alizadeh, D., Starr, R., Weng, L., Wagner, J. R., Naranjo, A., et al. (2016). Regression of glioblastoma after chimeric antigen receptor T-cell therapy. *N. Engl. J. Med.* 375 (26), 2561–2569. doi:10.1056/NEJMoa1610497

Brown, C. E., Badie, B., Barish, M. E., Weng, L., Ostberg, J. R., Chang, W. C., et al. (2015). Bioactivity and safety of il13rα2-redirected chimeric antigen receptor CD8+ T cells in patients with recurrent glioblastoma. *Clin. cancer Res.* 21 (18), 4062–4072. doi:10.1158/1078-0432.CCR-15-0428

Brown, C. E., Rodriguez, A., Palmer, J., Ostberg, J. R., Naranjo, A., Wagner, J. R., et al. (2022). Off-the-shelf, steroid-resistant, IL13Rα2-specific CAR T cells for treatment of glioblastoma. *Neuro-oncology* 24 (8), 1318–1330. doi:10.1093/neuonc/noac024

Brown, C. E., Warden, C. D., Starr, R., Deng, X., Badie, B., Yuan, Y. C., et al. (2013). Glioma IL13Rα2 is associated with mesenchymal signature gene expression and poor patient prognosis. *PloS one* 8 (10), e77769. doi:10.1371/journal.pone.0077769

Brown, N. F., Ng, S. M., Brooks, C., Coutts, T., Holmes, J., Roberts, C., et al. (2020). A phase II open label, randomised study of ipilimumab with temozolomide versus temozolomide alone after surgery and chemoradiotherapy in patients with recently diagnosed glioblastoma: the Ipi-Glio trial protocol. *BMC cancer* 20, 198–205. doi:10.1186/s12885-020-6624-y

Bruhns, R. P., James, W. S., Torabi, M., Borgstrom, M., Roussas, A., and Lemole, M. (2018). Survival as a function of nonsteroidal anti-inflammatory drug use in patients with glioblastoma. *Cureus* 10 (9), e3277. doi:10.7759/cureus.3277

Buckley, R. C. (1929). Tissue culture studies of the glioblastoma multiforme. *Am. J. pathology* 5 (5), 467–472.5.

Burns, M. C., O'donnell, A., and Puzanov, I. (2016). Pembrolizumab for the treatment of advanced melanoma. *Expert Opin. orphan drugs* 4 (8), 867–873. doi:10.1080/21678707.2016.1191348

Hasmim, W. L. (2015). *Optimisation of immune effector function within the tumor microenvironment*. Doctoral dissertation, University College Cork.

Cai, J., Zhang, W., Yang, P., Wang, Y., Li, M., Zhang, C., et al. (2015). Identification of a 6-cytokine prognostic signature in patients with primary glioblastoma harboring M2 microglia/macrophage phenotype relevance. *PloS one* 10 (5), e0126022. doi:10.1371/journal.pone.0126022

Carmeliet, P., and Jain, R. K. (2000). Angiogenesis in cancer and other diseases. *nature* 407 (6801), 249–257. doi:10.1038/35025220

Cekanaviciute, E., Dietrich, H. K., Axtell, R. C., Williams, A. M., Egusquiza, R., Wai, K. M., et al. (2014). Astrocytic TGF-β signaling limits inflammation and reduces neuronal damage during central nervous system Toxoplasma infection. *J. Immunol.* 193 (1), 139–149. doi:10.4049/jimmunol.1303284

Chamberlain, M. C. (2013). Treatment of newly diagnosed malignant glioma in the elderly people: new trials that impact therapy. *Int. J. Clin. Pract.* 67 (12), 1225–1227. doi:10.1111/ijcp.12258

Chang, K., Zhang, B., Guo, X., Zong, M., Rahman, R., Sanchez, D., et al. (2016). Multimodal imaging patterns predict survival in recurrent glioblastoma patients treated with bevacizumab. *Neuro-oncology* 18 (12), 1680–1687. doi:10.1093/neuonc/now086

Chantrain, C. F., Henriet, P., Jodele, S., Emonard, H., Feron, O., Courtoy, P. J., et al. (2006). Mechanisms of pericyte recruitment in tumour angiogenesis: a new role for metalloproteinases. *Eur. J. Cancer* 42 (3), 310–318. doi:10.1016/j.ejca.2005.11.010

Charles, N. A., Holland, E. C., Gilbertson, R., Glass, R., and Kettenmann, H. (2012). The brain tumor microenvironment. *Glia* 60 (3), 502–514. doi:10.1002/glia.21264

Chen, Z., Feng, X., Herting, C. J., Garcia, V. A., Nie, K., Pong, W. W., et al. (2017). Cellular and molecular identity of tumor-associated macrophages in glioblastoma. *Cancer Res.* 77 (9), 2266–2278. doi:10.1158/0008-5472.CAN-16-2310

Cui, J., Zhang, Q., Song, Q., Wang, H., Dmitriev, P., Sun, M. Y., et al. (2019). Targeting hypoxia downstream signaling protein, CAIX, for CAR T-cell therapy against glioblastoma. *Neuro-oncology* 21 (11), 1436–1446. doi:10.1093/neuonc/noz117

Daly, C., Pasnikowski, E., Burova, E., Wong, V., Aldrich, T. H., Griffiths, J., et al. (2006a). Angiopoietin-2 functions as an autocrine protective factor in stressed endothelial cells. *Proc. Natl. Acad. Sci.* 103 (42), 15491–15496. doi:10.1073/pnas.0607538103

Daly, C., Pasnikowski, E., Burova, E., Wong, V., Aldrich, T. H., Griffiths, J., et al. (2006b). Angiopoietin-2 functions as an autocrine protective factor in stressed endothelial cells. *Proc. Natl. Acad. Sci.* 103 (42), 15491–15496. doi:10.1073/pnas.0607538103

Daneman, R., and Prat, A. (2015). The blood–brain barrier. *Cold Spring Harb. Perspect. Biol.* 7 (1), a020412. doi:10.1101/cshperspect.a020412

De Groot, J. F., Gilbert, M. R., Aldape, K., Hess, K. R., Hanna, T. A., Ictech, S., et al. (2008). Phase II study of carboplatin and erlotinib (Tarceva, OSI-774) in patients with recurrent glioblastoma. *J. neuro-oncology* 90, 89–97. doi:10.1007/s11060-008-9637-y

Dunn, J., Baborie, A., Alam, F., Joyce, K., Moxham, M., Sibson, R., et al. (2009). Extent of MGMT promoter methylation correlates with outcome in glioblastomas given temozolomide and radiotherapy. *Br. J. cancer* 101 (1), 124–131. doi:10.1038/sj.bjc.6605127

Edland, R. W., Javid, M., and Ansfield, F. J. (1971). Glioblastoma multiforme: an analysis of the results of postoperative radiotherapy alone versus radiotherapy and concomitant 5-fluorouracil (a prospective randomized study of 32 cases). *Am. J. Roentgenol.* 111 (2), 337–342. doi:10.2214/ajr.111.2.337

Eichler, A. F., Chung, E., Kodack, D. P., Loeffler, J. S., Fukumura, D., and Jain, R. K. (2011). The biology of brain metastases—translation to new therapies. *Nat. Rev. Clin. Oncol.* 8 (6), 344–356. doi:10.1038/nrclinonc.2011.58

Ellemann, K., Christensen, L., Gjerris, F., Briand, P., and Kruse-Larsen, C. (1988). Glucocorticoid receptors in glioblastoma multiforme: a new approach to antineoplastic glucocorticoid therapy. *Acta Neurochir.* 93, 6–9. doi:10.1007/BF01409894

Farin, A., Suzuki, S. O., Weiker, M., Goldman, J. E., Bruce, J. N., and Canoll, P. (2006). Transplanted glioma cells migrate and proliferate on host brain vasculature: a dynamic analysis. *Glia* 53 (8), 799–808. doi:10.1002/glia.20334

Fecci, P. E., Mitchell, D. A., Whitesides, J. F., Xie, W., Friedman, A. H., Archer, G. E., et al. (2006). Increased regulatory T-cell fraction amidst a diminished CD4 compartment explains cellular immune defects in patients with malignant glioma. *Cancer Res.* 66 (6), 3294–3302. doi:10.1158/0008-5472.CAN-05-3773

Ferrara, N., Hillan, K. J., Gerber, H. P., and Novotny, W. (2004). Discovery and development of bevacizumab, an anti-VEGF antibody for treating cancer. *Nat. Rev. Drug Discov.* 3 (5), 391–400. doi:10.1038/nrd1381

Ferrara, N., and Kerbel, R. S. (2005). Angiogenesis as a therapeutic target. *Nature* 438 (7070), 967–974. doi:10.1038/nature04483

Fujita, M., Kohanbash, G., Fellows-Mayle, W., Hamilton, R. L., Komohara, Y., Decker, S. A., et al. (2011). COX-2 blockade suppresses gliomagenesis by inhibiting myeloid-derived suppressor cells. *Cancer Res.* 71 (7), 2664–2674. doi:10.1158/0008-5472.CAN-10-3055

Galanis, E., Anderson, S. K., Miller, C. R., Sarkaria, J. N., Jaeckle, K., Buckner, J. C., et al. (2018). Phase I/II trial of vorinostat combined with temozolomide and radiation therapy for newly diagnosed glioblastoma: results of Alliance N0874/ABTC 02. *Neuro-oncology* 20 (4), 546–556. doi:10.1093/neuonc/nox161

Garg, A. D., Vandenberk, L., Van Woensel, M., Belmans, J., Schaaf, M., Boon, L., et al. (2017). Preclinical efficacy of immune-checkpoint monotherapy does not recapitulate corresponding biomarkers-based clinical predictions in glioblastoma. *Oncoimmunology* 6 (4), e1295903. doi:10.1080/2162402X.2017.1295903

Garima, G., Thanvi, S., Singh, A., and Verma, V. (2022). Epidermal growth factor receptor variant III mutation, an emerging molecular marker in glioblastoma multiforme patients: a single institution study on the Indian population. *Cureus* 14 (6), e26412. doi:10.7759/cureus.26412

Garrido-Urbani, S., Jemelin, S., Deffert, C., Carnesecchi, S., and Basset, O. (2009). *Targeting vascular NADPH oxidase 1 blocks tumor angiogenesis through a*.

Gerstner, E. R., Duda, D. G., Di Tomaso, E., Ryg, P. A., Loeffler, J. S., Sorensen, A. G., et al. (2009). VEGF inhibitors in the treatment of cerebral edema in patients with brain cancer. *Nat. Rev. Clin. Oncol.* 6 (4), 229–236. doi:10.1038/nrclinonc.2009.14

Gilbert, M. R., Dignam, J. J., Armstrong, T. S., Wefel, J. S., Blumenthal, D. T., Vogelbaum, M. A., et al. (2014). A randomized trial of bevacizumab for newly diagnosed glioblastoma. *N. Engl. J. Med.* 370 (8), 699–708. doi:10.1056/NEJMoa1308573

Gomez-Zepeda, D., Taghi, M., Scherrmann, J. M., Decleves, X., and Menet, M. C. (2019). ABC transporters at the blood–brain interfaces, their study models, and drug delivery implications in gliomas. *Pharmaceutics* 12 (1), 20. doi:10.3390/pharmaceutics12010020

Gregoriadis, G. (2008). Liposome research in drug delivery: the early days. *J. Drug Target.* 16 (7-8), 520–524. doi:10.1080/10611860802228350

Guo, G., Gong, K., Wohlfeld, B., Hatanpaa, K. J., Zhao, D., and Habib, A. A. (2015). Ligand-independent EGFR signaling. *Cancer Res.* 75 (17), 3436–3441. doi:10.1158/0008-5472.CAN-15-0989

Hadari, Y. R., Gotoh, N., Kouhara, H., Lax, I., and Schlessinger, J. (2001). Critical role for the docking-protein FRS2 alpha in FGF receptor-mediated signal transduction pathways. *Proc. Natl. Acad. Sci.* 98 (15), 8578–8583. doi:10.1073/pnas.161259898

Hanahan, D., and Folkman, J. (1996). Patterns and emerging mechanisms of the angiogenic switch during tumorigenesis. *Cell.* 86 (3), 353–364. doi:10.1016/s0092-8674(00)80108-7

Hao, C., Parney, I. F., Roa, W. H., Turner, J., Petruk, K. C., and Ramsay, D. A. (2002). Cytokine and cytokine receptor mRNA expression in human glioblastomas: evidence of Th1, Th2 and Th3 cytokine dysregulation. *Acta neuropathol.* 103, 171–178. doi:10.1007/s004010100448

Heiss, W. D. (1978). Chemotherapy of malignant gliomas: comparison of the effect of polychemo-and CCNU-therapy. *Acta Neurochir.* 42, 109–115. doi:10.1007/BF01406637

Hernández-Vega, A. M., and Camacho-Arroyo, I. (2021). Crosstalk between 17β-estradiol and TGF-β signaling modulates glioblastoma progression. *Brain Sci.* 11 (5), 564. doi:10.3390/brainsci11050564

Ho, R. L., and Ho, I. A. (2021). Recent advances in glioma therapy: combining vascular normalization and immune checkpoint blockade. *Cancers* 13 (15), 3686. doi:10.3390/cancers13153686

Huang, H., Bhat, A., Woodnutt, G., and Lappe, R. (2010). Targeting the ANGPT–TIE2 pathway in malignancy. *Nat. Rev. Cancer* 10 (8), 575–585. doi:10.1038/nrc2894

Hussain, S. F., Yang, D., Suki, D., Aldape, K., Grimm, E., and Heimberger, A. B. (2006). The role of human glioma-infiltrating microglia/macrophages in mediating antitumor immune responses. *Neuro-oncology* 8 (3), 261–279. doi:10.1215/15228517-2006-008

Hynes, R. O. (2002). Integrins: bidirectional, allosteric signaling machines. *Cell.* 110 (6), 673–687. doi:10.1016/s0092-8674(02)00971-6

Itoh, Y., Saitoh, M., and Miyazawa, K. (2018). Smad3–STAT3 crosstalk in pathophysiological contexts. *Acta biochimica biophysica Sinica* 50 (1), 82–90. doi:10.1093/abbs/gmx118

Jacobs, S. K., Wilson, D. J., Kornblith, P. L., and Grimm, E. A. (1986). *In vitro* killing of human glioblastoma by interleukin-2-activated autologous lymphocytes. *J. Neurosurg.* 64 (1), 114–117. doi:10.3171/jns.1986.64.1.0114

Jain, R. K., Di Tomaso, E., Duda, D. G., Loeffler, J. S., Sorensen, A. G., and Batchelor, T. T. (2007). Angiogenesis in brain tumours. *Nat. Rev. Neurosci.* 8 (8), 610–622. doi:10.1038/nrn2175

Jain, S., Rick, J. W., Joshi, R. S., Beniwal, A., Spatz, J., Gill, S., et al. (2023). Single-cell RNA sequencing and spatial transcriptomics reveal cancer-associated fibroblasts in glioblastoma with protumoral effects. *J. Clin. Investigation* 133 (5), e147087. doi:10.1172/JCI147087

Jelsma, R., and Bucy, P. C. (1967). The treatment of glioblastoma multiforme of the brain. *J. Neurosurg.* 27 (5), 388–400. doi:10.3171/jns.1967.27.5.0388

Jiang, H., Clise-Dwyer, K., Ruisaard, K. E., Fan, X., Tian, W., Gumin, J., et al. (2014). Delta-24-RGD oncolytic adenovirus elicits anti-glioma immunity in an immunocompetent mouse model. *PloS one* 9 (5), e97407. doi:10.1371/journal.pone.0097407

Jiao, S., Xia, W., Yamaguchi, H., Wei, Y., Chen, M. K., Hsu, J. M., et al. (2017). PARP inhibitor upregulates PD-L1 expression and enhances cancer-associated immunosuppression. *Clin. Cancer Res.* 23 (14), 3711–3720. doi:10.1158/1078-0432.CCR-16-3215

Kermani, P., Rafii, D., Jin, D. K., Whitlock, P., Schaffer, W., Chiang, A., et al. (2005). Neurotrophins promote revascularization by local recruitment of TrkB+ endothelial cells and systemic mobilization of hematopoietic progenitors. *J. Clin. investigation* 115 (3), 653–663. doi:10.1172/JCI22655

Khan, S., Mittal, S., McGee, K., Alfaro-Munoz, K. D., Majd, N., Balasubramaniyan, V., et al. (2020). Role of neutrophils and myeloid-derived suppressor cells in glioma progression and treatment resistance. *Int. J. Mol. Sci.* 21 (6), 1954. doi:10.3390/ijms21061954

Kienast, Y., Von Baumgarten, L., Fuhrmann, M., Klinkert, W. E., Goldbrunner, R., Herms, J., et al. (2010). Real-time imaging reveals the single steps of brain metastasis formation. *Nat. Med.* 16 (1), 116–122. doi:10.1038/nm.2072

Kim, G., and Ko, Y. T. (2020). Small molecule tyrosine kinase inhibitors in glioblastoma. *Archives pharmacal Res.* 43, 385–394. doi:10.1007/s12272-020-01232-3

Kioi, M., Vogel, H., Schultz, G., Hoffman, R. M., Harsh, G. R., and Brown, J. M. (2010). Inhibition of vasculogenesis, but not angiogenesis, prevents the recurrence of glioblastoma after irradiation in mice. *J. Clin. investigation* 120 (3), 694–705. doi:10.1172/JCI40283

Kiyokawa, J., and Wakimoto, H. (2019). Preclinical and clinical development of oncolytic adenovirus for the treatment of malignant glioma. *Oncolytic virotherapy* 8, 27–37. doi:10.2147/OV.S196403

Knowles, L. M., Stabile, L. P., Egloff, A. M., Rothstein, M. E., Thomas, S. M., Gubish, C. T., et al. (2009). HGF and c-Met participate in paracrine tumorigenic pathways in head and neck squamous cell cancer. *Clin. Cancer Res.* 15 (11), 3740–3750. doi:10.1158/1078-0432.CCR-08-3252

Koch, C., Fielding, A. J., Brodhun, F., Bennati, M., and Feussner, I. (2012). Linoleic acid positioning in psi factor producing oxygenase A, a fusion protein with an atypical cytochrome P450 activity. *FEBS J.* 279 (9), 1594–1606. doi:10.1111/j.1742-4658.2011.08352.x

Kong, D. S., Nam, D. H., Kang, S. H., Lee, J. W., Chang, J. H., Kim, J. H., et al. (2017). Phase III randomized trial of autologous cytokine-induced killer cell immunotherapy for newly diagnosed glioblastoma in Korea. *Oncotarget* 8 (4), 7003–7013. doi:10.18632/oncotarget.12273

Kostaras, X., Cusano, F., Kline, G. A., Roa, W., and Easaw, J. (2014). Use of dexamethasone in patients with high-grade glioma: a clinical practice guideline. *Curr. Oncol.* 21 (3), 493–503. doi:10.3747/co.21.1769

Krishnan, S., Szabo, E., Burghardt, I., Frei, K., Tabatabai, G., and Weller, M. (2015). Modulation of cerebral endothelial cell function by TGF-β in glioblastoma: VEGF-dependent angiogenesis versus endothelial mesenchymal transition. *Oncotarget* 6 (26), 22480–22495. doi:10.18632/oncotarget.4310

Lamszus, K., Ulbricht, U., Matschke, J., Brockmann, M. A., Fillbrandt, R., and Westphal, M. (2003). Levels of soluble vascular endothelial growth factor (VEGF) receptor 1 in astrocytic tumors and its relation to malignancy, vascularity, and VEGF-A. *Clin. Cancer Res.* 9 (4), 1399–1405. PMID: 12684411.

Li, M. O., and Flavell, R. A. (2008). TGF-beta: a master of all T cell trades. *Cell.* 134 (3), 392–404. doi:10.1016/j.cell.2008.07.025

Li, Y., Li, A., Glas, M., Lal, B., Ying, M., Sang, Y., et al. (2011). c-Met signaling induces a reprogramming network and supports the glioblastoma stem-like phenotype. *Proc. Natl. Acad. Sci.* 108 (24), 9951–9956. doi:10.1073/pnas.1016912108

Liang, J., Piao, Y., Holmes, L., Fuller, G. N., Henry, V., Tiao, N., et al. (2014). Neutrophils promote the malignant glioma phenotype through S100A4. *Clin. cancer Res.* 20 (1), 187–198. doi:10.1158/1078-0432.CCR-13-1279

Liau, L. M., Black, K. L., Martin, N. A., Sykes, S. N., Bronstein, J. M., Jouben-Steele, L., et al. (2000). Treatment of a glioblastoma patient by vaccination with autologous dendritic cells pulsed with allogeneic major histocompatibility complex class I–matched tumor peptides: case report. *Neurosurg. focus* 9 (6), 1–5. doi:10.3171/foc.2000.9.6.9

Lim, M., Ye, X., Piotrowski, A. F., Desai, A. S., Ahluwalia, M. S., Walbert, T., et al. (2017). Updated phase I trial of anti-LAG-3 or anti-CD137 alone and in combination with anti-PD-1 in patients with recurrent GBM. *J. Clin. Oncol.* 38, 15.

Liu, C., Liu, X. N., Wang, G. L., Hei, Y., Meng, S., Yang, L. F., et al. (2017). A dual-mediated liposomal drug delivery system targeting the brain: rational construction, integrity evaluation across the blood–brain barrier, and the transporting mechanism to glioma cells. *Int. J. nanomedicine* 12, 2407–2425. doi:10.2147/IJN.S131367

Liu, H., Huang, X., Wang, H., Shen, A., and Cheng, C. (2009). Dexamethasone inhibits proliferation and stimulates SSeCKS expression in C6 rat glioma cell line. *Brain Res.* 1265, 1–12. doi:10.1016/j.brainres.2009.01.050

Liu, Q., Zhang, Y., Mao, H., Chen, W., Luo, N., Zhou, Q., et al. (2012). A crosstalk between the Smad and JNK signaling in the TGF-β-induced epithelial-mesenchymal transition in rat peritoneal mesothelial cells. *PloS one* 7 (2), e32009. doi:10.1371/journal.pone.0032009

Liu, T., Ma, W., Xu, H., Huang, M., Zhang, D., He, Z., et al. (2018). PDGF-mediated mesenchymal transformation renders endothelial resistance to anti-VEGF treatment in glioblastoma. *Nat. Commun.* 9 (1), 3439. doi:10.1038/s41467-018-05982-z

Louis, D. N., Perry, A., Wesseling, P., Brat, D. J., Cree, I. A., Figarella-Branger, D., et al. (2021). The 2021 WHO classification of tumors of the central nervous system: a summary. *Neuro-oncology* 23 (8), 1231–1251. doi:10.1093/neuonc/noab106

Louveau, A., Smirnov, I., Keyes, T. J., Eccles, J. D., Rouhani, S. J., Peske, J. D., et al. (2015). Structural and functional features of central nervous system lymphatic vessels. *Nature* 523 (7560), 337–341. doi:10.1038/nature14432

Lu, K. V., Chang, J. P., Parachoniak, C. A., Pandika, M. M., Aghi, M. K., Meyronet, D., et al. (2012). VEGF inhibits tumor cell invasion and mesenchymal transition through a MET/VEGFR2 complex. *Cancer Cell.* 22 (1), 21–35. doi:10.1016/j.ccr.2012.05.037

Lynes, J., Sanchez, V., Dominah, G., Nwankwo, A., and Nduom, E. (2018). Current options and future directions in immune therapy for glioblastoma. *Front. Oncol.* 8, 578. doi:10.3389/fonc.2018.00578

Ma, R., Li, Z., Chiocca, E. A., Caligiuri, M. A., and Yu, J. (2023). The emerging field of oncolytic virus-based cancer immunotherapy. *Trends Cancer* 9 (2), 122–139. doi:10.1016/j.trecan.2022.10.003

Mantovani, A., Sica, A., Sozzani, S., Allavena, P., Vecchi, A., and Locati, M. (2004). The chemokine system in diverse forms of macrophage activation and polarization. *Trends Immunol.* 25 (12), 677–686. doi:10.1016/j.it.2004.09.015

Martin, M., Vermeiren, S., Bostaille, N., Eubelen, M., Spitzer, D., Vermeersch, M., et al. (2022a). Engineered Wnt ligands enable blood-brain barrier repair in neurological disorders. *Science* 375 (6582), eabm4459. doi:10.1126/science.abm4459

Martin, M., Vermeiren, S., Bostaille, N., Eubelen, M., Spitzer, D., Vermeersch, M., et al. (2022b). Engineered Wnt ligands enable blood-brain barrier repair in neurological disorders. *Science* 375 (6582), eabm4459. doi:10.1126/science.abm4459

Marton, L. J., Heby, O., and Wilson, C. B. (1974). Increased polyamine concentrations in the cerebrospinal fluid of patients with brain tumors. *Int. J. Cancer* 14 (6), 731–735. doi:10.1002/ijc.2910140606

Miescher, G. C., Taylor, V., Olivieri, G., Mindermann, T., Schröck, E., and Steck, A. J. (1997). Extensive splice variation and localization of the EHK-1 receptor tyrosine kinase in adult human brain and glial tumors. *Mol. Brain Res.* 46 (1-2), 17–24. doi:10.1016/s0169-328x(96)00268-9

Miska, J., Rashidi, A., Chang, A. L., Muroski, M. E., Han, Y., Zhang, L., et al. (2016). Anti-GITR therapy promotes immunity against malignant glioma in a murine model. *Cancer Immunol.* 65, 1555–1567. Immunotherapy. doi:10.1007/s00262-016-1912-8

Mo, F., Pellerino, A., Soffietti, R., and Rudà, R. (2021). Blood–brain barrier in brain tumors: biology and clinical relevance. *Int. J. Mol. Sci.* 22 (23), 12654. doi:10.3390/ijms222312654

Morantz, R. A., Wood, G. W., Foster, M., Clark, M., and Gollahon, K. (1979). Macrophages in experimental and human brain tumors: part 2: studies of the macrophage content of human brain tumors. *J. Neurosurg.* 50 (3), 305–311. doi:10.3171/jns.1979.50.3.0305

mT hun, M. J., Henley, S. J., and Patrono, C. (2002). Nonsteroidal antiinflammatory drugs as anticancer agents: mechanistic, pharmacologic, and clinical issues. *J. Natl. Cancer Inst.* 94, 252–266. doi:10.1093/jnci/94.4.252

Murata, J. I., Sawamura, Y., Tada, M., Sakuma, S., Sudo, M., Aida, T., et al. (1993). Human glioblastoma cells produce granulocyte-macrophage colony-stimulating factor *in vitro*, but not *in vivo*, without expressing its receptor. *Neurol. medico-chirurgica* 33 (9), 603–609. doi:10.2176/nmc.33.603

Nagy, J. A., Chang, S. H., Shih, S. C., Dvorak, A. M., and Dvorak, H. F. (2010). Heterogeneity of the tumor vasculature. *InSeminars thrombosis hemostasis* 36 (03), 321–331. doi:10.1055/s-0030-1253454

Navin, N., Kendall, J., Troge, J., Andrews, P., Rodgers, L., McIndoo, J., et al. (2011). Tumour evolution inferred by single-cell sequencing. *Nature* 472 (7341), 90–94. doi:10.1038/nature09807

Nayak, L., Molinaro, A. M., Peters, K., Clarke, J. L., Jordan, J. T., de Groot, J., et al. (2021). Randomized phase II and biomarker study of pembrolizumab plus bevacizumab versus pembrolizumab alone for patients with recurrent glioblastoma. *Clin. Cancer Res.* 27 (4), 1048–1057. doi:10.1158/1078-0432.CCR-20-2500

Nehama, D., Di Ianni, N., Musio, S., Du, H., Patané, M., Pollo, B., et al. (2019). B7-H3-redirected chimeric antigen receptor T cells target glioblastoma and neurospheres. *EBioMedicine* 47, 33–43. doi:10.1016/j.ebiom.2019.08.030

Neuwelt, E. A., Frenkel, E. P., Diehl, J., Vu, L. H., Rapoport, S., and Hill, S. (1980). Reversible osmotic blood-brain barrier disruption in humans: implications for the chemotherapy of malignant brain tumors. *Neurosurgery* 7 (1), 44–52. doi:10.1227/00006123-198007000-00007

Olea-Flores, M., Juárez-Cruz, J. C., Zuñiga-Eulogio, M. D., Acosta, E., García-Rodríguez, E., Zacapala-Gomez, A. E., et al. (2020). New actors driving the epithelial–mesenchymal transition in cancer: the role of leptin. *Biomolecules* 10 (12), 1676. doi:10.3390/biom10121676

Olmez, I., Zhang, Y., Manigat, L., Benamar, M., Brenneman, B., Nakano, I., et al. (2018). Combined c-Met/Trk inhibition overcomes resistance to CDK4/6 inhibitors in glioblastoma. *Cancer Res.* 78 (15), 4360–4369. doi:10.1158/0008-5472.CAN-17-3124

Ostrom, Q. T., Cioffi, G., Gittleman, H., Patil, N., Waite, K., Kruchko, C., et al. (2019). CBTRUS statistical report: primary brain and other central nervous system tumors diagnosed in the United States in 2012–2016. *Neuro-oncology* 21, v1–v100. doi:10.1093/neuonc/noz150

Otsuka, S. H., Handa, H., Yamashita, J., Suda, K., and Takeuchi, J. (1984). Single agent therapy of interferon for brain tumours: correlation between natural killer activity and clinical course. *Acta Neurochir.* 73, 13–23. doi:10.1007/BF01401780

Ozawa, T., Riester, M., Cheng, Y. K., Huse, J. T., Squatrito, M., Helmy, K., et al. (2014). Most human non-GCIMP glioblastoma subtypes evolve from a common proneural-like precursor glioma. *Cancer Cell.* 26 (2), 288–300. doi:10.1016/j.ccr.2014.06.005

Parrish, K. E., Pokorny, J., Mittapalli, R. K., Bakken, K., Sarkaria, J. N., and Elmquist, W. F. (2015). Efflux transporters at the blood-brain barrier limit delivery and efficacy of cyclin-dependent kinase 4/6 inhibitor palbociclib (PD-0332991) in an orthotopic brain tumor model. *J. Pharmacol. Exp. Ther.* 355 (2), 264–271. doi:10.1124/jpet.115.228213

Pellegatta, S., Valletta, L., Corbetta, C., Patanè, M., Zucca, I., Riccardi Sirtori, F., et al. (2015). Effective immuno-targeting of the IDH1 mutation R132H in a murine model of intracranial glioma. *Acta neuropathol. Commun.* 3 (1), 4–2. doi:10.1186/s40478-014-0180-0

Peng, G., Wang, Y., Ge, P., Bailey, C., Zhang, P., Zhang, D., et al. (2021). The HIF1α-PDGFD-PDGFRα axis controls glioblastoma growth at normoxia/mild-hypoxia and confers sensitivity to targeted therapy by echinomycin. *J. Exp. Clin. Cancer Res.* 40 (1), 278–294. doi:10.1186/s13046-021-02082-7

Perez-Cruet, M. J., Trask, T. W., Chen, S. H., Goodman, J. C., Woo, S. L., Grossman, R. G., et al. (1994). Adenovirus-mediated gene therapy of experimental gliomas. *J. Neurosci. Res.* 39 (4), 506–511. doi:10.1002/jnr.490390417

Philipsen, M. H., Hansson, E., Manaprasertsak, A., Lange, S., Jennische, E., Carén, H., et al. (2023). Distinct cholesterol localization in glioblastoma multiforme revealed by mass spectrometry imaging. *ACS Chem. Neurosci.* 14, 1602–1609. doi:10.1021/acschemneuro.2c00776

Plate, K. H., Breier, G., Weich, H. A., and Risau, W. (1992a). Vascular endothelial growth factor is a potential tumour angiogenesis factor in human gliomas *in vivo*. *Nature* 359 (6398), 845–848. doi:10.1038/359845a0

Plate, K. H., Breier, G., Weich, H. A., and Risau, W. (1992b). Vascular endothelial growth factor is a potential tumour angiogenesis factor in human gliomas *in vivo*. *Nature* 359 (6398), 845–848. doi:10.1038/359845a0

Pombo Antunes, A. R., Scheyltjens, I., Duerinck, J., Neyns, B., Movahedi, K., and Van Ginderachter, J. A. (2020). Understanding the glioblastoma immune microenvironment as basis for the development of new immunotherapeutic strategies. *Elife* 9, e52176. doi:10.7554/eLife.52176

Puram, S. V., Tirosh, I., Parikh, A. S., Patel, A. P., Yizhak, K., Gillespie, S., et al. (2017). Single-cell transcriptomic analysis of primary and metastatic tumor ecosystems in head and neck cancer. *Cell.* 171 (7), 1611–1624. doi:10.1016/j.cell.2017.10.044

Quail, D. F., and Joyce, J. A. (2017). The microenvironmental landscape of brain tumors. *Cancer Cell.* 31 (3), 326–341. doi:10.1016/j.ccell.2017.02.009

Quintero-Fabián, S., Arreola, R., Becerril-Villanueva, E., Torres-Romero, J. C., Arana-Argáez, V., Lara-Riegos, J., et al. (2019). Role of matrix metalloproteinases in angiogenesis and cancer. *Front. Oncol.* 9, 1370. doi:10.3389/fonc.2019.01370

Ramsey, R. G., and Brand, W. N. (1973). Radiotherapy of glioblastoma multiforme. *J. Neurosurg.* 39 (2), 197–202. doi:10.3171/jns.1973.39.2.0197

Rana, R., Kumari, B., Kumari, J., and Ganguly, N. K. (2019). Glioblastoma diagnostics and prognostic biomarkers: current status in medicine and exosome derivation. *Curr. Med. Res. Pract.* 9 (2), 65–73. doi:10.1016/j.cmrp.2019.03.001

Reardon, D. A., Brandes, A. A., Omuro, A., Mulholland, P., Lim, M., Wick, A., et al. (2020). Effect of nivolumab vs bevacizumab in patients with recurrent glioblastoma: the CheckMate 143 phase 3 randomized clinical trial. *JAMA Oncol.* 6 (7), 1003–1010. doi:10.1001/jamaoncol.2020.1024

Reardon, D. A., and Cheresh, D. (2011). Cilengitide: a prototypic integrin inhibitor for the treatment of glioblastoma and other malignancies. *Genes. & cancer* 2 (12), 1159–1165. doi:10.1177/1947601912450586

Reardon, D. A., Kim, T. M., Frenel, J. S., Simonelli, M., Lopez, J., Subramaniam, D. S., et al. (2021). Treatment with pembrolizumab in programmed death ligand 1–positive recurrent glioblastoma: results from the multicohort phase 1 KEYNOTE-028 trial. *Cancer* 127 (10), 1620–1629. doi:10.1002/cncr.33378

Reardon, D. A., Lassman, A. B., Van Den Bent, M., Kumthekar, P., Merrell, R., Scott, A. M., et al. (2017). Efficacy and safety results of ABT-414 in combination with radiation and temozolomide in newly diagnosed glioblastoma. *Neuro-oncology* 19 (7), 965–975. doi:10.1093/neuonc/now257

Rehman, A. U., Omran, Z., Anton, H., Mély, Y., Akram, S., Vandamme, T. F., et al. (2018). Development of doxorubicin hydrochloride loaded pH-sensitive liposomes: investigation on the impact of chemical nature of lipids and liposome composition on pH-sensitivity. *Eur. J. Pharm. Biopharm.* 133, 331–338. doi:10.1016/j.ejpb.2018.11.001

Ricci-Vitiani, L., Pallini, R., Biffoni, M., Todaro, M., Invernici, G., Cenci, T., et al. (2010). Tumour vascularization via endothelial differentiation of glioblastoma stem-like cells. *Nature* 468 (7325), 824–828. doi:10.1038/nature09557

Risau, W. (1997). Mechanisms of angiogenesis. *Nature* 386 (6626), 671–674. doi:10.1038/386671a0

Rodrigues, J. C., Gonzalez, G. C., Zhang, L., Ibrahim, G., Kelly, J. J., Gustafson, M. P., et al. (2010). Normal human monocytes exposed to glioma cells acquire myeloid-derived suppressor cell-like properties. *Neuro-oncology* 12 (4), 351–365. doi:10.1093/neuonc/nop023

Rosenblum, M. L., Reynolds, A. F., Smith, K. A., Rumack, B. H., and Walker, M. D. (1973). Chloroethyl-cyclohexyl-nitrosourea (CCNU) in the treatment of malignant brain tumors. *J. Neurosurg.* 39 (3), 306–314. doi:10.3171/jns.1973.39.3.0306

Sachs, E. (1954). The treatment of glioblastomas with radium. *J. Neurosurg.* 11 (2), 119–121. doi:10.3171/jns.1954.11.2.0119

Saha, J., and Giri, K. (2017). Molecular phylogenomic study and the role of exogenous spermidine in the metabolic adjustment of endogenous polyamine in two rice cultivars under salt stress. *Gene* 609, 88–103. doi:10.1016/j.gene.2017.02.001

Sahebjam, S., Forsyth, P. A., Tran, N. D., Arrington, J. A., Macaulay, R., Etame, A. B., et al. (2021). Hypofractionated stereotactic re-irradiation with pembrolizumab and bevacizumab in patients with recurrent high-grade gliomas: results from a phase I study. *Neuro-oncology* 23 (4), 677–686. doi:10.1093/neuonc/noaa260

Sareddy, G. R., Kesanakurti, D., Kirti, P. B., and Babu, P. P. (2013). Nonsteroidal anti-inflammatory drugs diclofenac and celecoxib attenuates Wnt/β-catenin/Tcf signaling pathway in human glioblastoma cells. *Neurochem. Res.* 38, 2313–2322. doi:10.1007/s11064-013-1142-9

Schuster, J., Lai, R. K., Recht, L. D., Reardon, D. A., Paleologos, N. A., Groves, M. D., et al. (2015). A phase II, multicenter trial of rindopepimut (CDX-110) in newly diagnosed glioblastoma: the ACT III study. *Neuro-oncology* 17 (6), 854–861. doi:10.1093/neuonc/nou348

Shah, K., Hingtgen, S., Kasmieh, R., Figueiredo, J. L., Garcia-Garcia, E., Martinez-Serrano, A., et al. (2008). Bimodal viral vectors and *in vivo* imaging reveal the fate of human neural stem cells in experimental glioma model. *J. Neurosci.* 28 (17), 4406–4413. doi:10.1523/JNEUROSCI.0296-08.2008

Shonka, N., Piao, Y., Gilbert, M., Yung, A., Chang, S., DeAngelis, L. M., et al. (2013). Cytokines associated with toxicity in the treatment of recurrent glioblastoma with aflibercept. *Target. Oncol.* 8, 117–125. doi:10.1007/s11523-013-0254-0

Shweiki, D., Itin, A., Soffer, D., and Keshet, E. (1992). Vascular endothelial growth factor induced by hypoxia may mediate hypoxia-initiated angiogenesis. *Nature* 359 (6398), 843–845. doi:10.1038/359843a0

Silva, R., D'Amico, G., Hodivala-Dilke, K. M., and Reynolds, L. E. (2008). Integrins: the keys to unlocking angiogenesis. *Arteriosclerosis, thrombosis, Vasc. Biol.* 28 (10), 1703–1713. doi:10.1161/ATVBAHA.108.172015

Singh, S., Deora, H., Neyaz, A., Das, K. K., Mehrotra, A., Srivastava, A. K., et al. (2021). Trends in clinico-epidemiology profile of surgically operated glioma patients in a tertiary care center over 12 years—through the looking glass. *Egypt. J. Neurosurg.* 36 (1), 32–38. doi:10.1186/s41984-021-00118-w

Singla, A. K., Madan, R., Gupta, K., Goyal, S., Kumar, N., Sahoo, S. K., et al. (2021). Clinical behaviour and outcome in pediatric glioblastoma: current scenario. *Radiat. Oncol. J.* 39 (1), 72–77. doi:10.3857/roj.2020.00591

Sloan, A. E., Buerki, R. A., Murphy, C., Kelly, A. T., Ambady, P., Brown, M., et al. (2021). *LUMINOS-101: phase 2 study of PVSRIPO with pembrolizumab in recurrent glioblastoma*.

Sternlicht, M. D., and Werb, Z. (2001). How matrix metalloproteinases regulate cell behavior. *Annu. Rev. Cell. Dev. Biol.* 17 (1), 463–516. doi:10.1146/annurev.cellbio.17.1.463

Sun, C., Zheng, X., Sun, Y., Yu, J., Sheng, M., Yan, S., et al. (2021). Identification of IGF2BP3 as an adverse prognostic biomarker of gliomas. *Front. Genet.* 12, 743738. doi:10.3389/fgene.2021.743738

Suri, C., Jones, P. F., Patan, S., Bartunkova, S., Maisonpierre, P. C., Davis, S., et al. (1996a). Requisite role of angiopoietin-1, a ligand for the TIE2 receptor, during embryonic angiogenesis. *Cell.* 87 (7), 1171–1180. doi:10.1016/s0092-8674(00)81813-9

Suri, C., Jones, P. F., Patan, S., Bartunkova, S., Maisonpierre, P. C., Davis, S., et al. (1996b). Requisite role of angiopoietin-1, a ligand for the TIE2 receptor, during embryonic angiogenesis. *Cell.* 87 (7), 1171–1180. doi:10.1016/s0092-8674(00)81813-9

Swartz, A. M., Li, Q. J., and Sampson, J. H. (2014). Rindopepimut: a promising immunotherapeutic for the treatment of glioblastoma multiforme. *Immunotherapy* 6 (6), 679–690. doi:10.2217/imt.14.21

Swildens, K. X., Sillevis Smitt, P. A., Van Den Bent, M. J., French, P. J., and Geurts, M. (2022). The effect of dexamethasone on the microenvironment and efficacy of checkpoint inhibitors in glioblastoma: a systematic review. *Neuro-Oncology Adv.* 4 (1), vdac087. doi:10.1093/noajnl/vdac087

Tada, M., Diserens, A. C., Desbaillets, I., and de Tribolet, N. (1994). Analysis of cytokine receptor messenger RNA expression in human glioblastoma cells and normal astrocytes by reverse-transcription polymerase chain reaction. *J. Neurosurg.* 80 (6), 1063–1073. doi:10.3171/jns.1994.80.6.1063

Takada, Y., Ye, X., and Simon, S. (2007). The integrins. *Genome Biol.* 8, 215–219. doi:10.1186/gb-2007-8-5-215

Takahashi, J. A., Fukumoto, M., Igarashi, K., Oda, Y., Kikuchi, H., and Hatanaka, M. (1992). Correlation of basic fibroblast growth factor expression levels with the degree of malignancy and vascularity in human gliomas. *J. Neurosurg.* 76 (5), 792–798. doi:10.3171/jns.1992.76.5.0792

Takahashi, T., Yamaguchi, S., Chida, K., and Shibuya, M. (2001). A single autophosphorylation site on KDR/Flk-1 is essential for VEGF-A-dependent activation of PLC-γ and DNA synthesis in vascular endothelial cells. *EMBO J.* 20 (11), 2768–2778. doi:10.1093/emboj/20.11.2768

Tani, E., Nishiura, M., and Higashi, N. (1973). Freeze-fracture studies of gap junctions of normal and neoplastic astrocytes. *Acta neuropathol.* 26, 127–138. doi:10.1007/BF00697748

Tawi, H. A., Forsyth, P. A., Hodi, F. S., Lao, C. D., Moschos, S. J., Hamid, O., et al. (2021). *Efficacy and safety of the combination of nivolumab (NIVO) plus ipilimumab (IPI) in patients with symptomatic melanoma brain metastases*. CheckMate 204.

Thaci, B., Brown, C. E., Binello, E., Werbaneth, K., Sampath, P., and Sengupta, S. (2014). Significance of interleukin-13 receptor alpha 2–targeted glioblastoma therapy. *Neuro-oncology* 16 (10), 1304–1312. doi:10.1093/neuonc/nou045

Trusolino, L., and Comoglio, P. M. (2002). Scatter-factor and semaphorin receptors: cell signalling for invasive growth. *Nat. Rev. cancer* 2 (4), 289–300. doi:10.1038/nrc779

Udayakumar, T. S., Stratton, M. S., Nagle, R. B., and Bowden, G. T. (2002). Fibroblast growth factor-1 induced promatrilysin expression through the activation of extracellular-regulated kinases and STAT3. *Neoplasia* 4 (1), 60–67. doi:10.1038/sj.neo.7900207

Uhrbom, L., Nerio, E., and Holland, E. C. (2004). Dissecting tumor maintenance requirements using bioluminescence imaging of cell proliferation in a mouse glioma model. *Nat. Med.* 10 (11), 1257–1260. doi:10.1038/nm1120

Ulrich, C. M., Bigler, J., and Potter, J. D. (2006). Non-steroidal antiinflammatory drugs for cancer prevention: promise, perils and pharmacogenetics. *Nat. Rev. Cancer* 6, 130–140. doi:10.1038/nrc1801

Van Hinsbergh, V. W., and Koolwijk, P. (2008). Endothelial sprouting and angiogenesis: matrix metalloproteinases in the lead. *Cardiovasc. Res.* 78 (2), 203–212. doi:10.1093/cvr/cvm102

Vegliante, M. C., Mazzara, S., Zaccaria, G. M., De Summa, S., Esposito, F., Melle, F., et al. (2022). NR1H3 (LXRα) is associated with pro-inflammatory macrophages, predicts survival and suggests potential therapeutic rationales in diffuse large b-cell lymphoma. *Hematol. Oncol.* 40 (5), 864–875. doi:10.1002/hon.3050

Venkataramani, V., Tanev, D. I., Strahle, C., Studier-Fischer, A., Fankhauser, L., Kessler, T., et al. (2019). Glutamatergic synaptic input to glioma cells drives brain tumour progression. *Nature* 573 (7775), 532–538. doi:10.1038/s41586-019-1564-x

Venkatesh, H. S., Morishita, W., Geraghty, A. C., Silverbush, D., Gillespie, S. M., Arzt, M., et al. (2019). Electrical and synaptic integration of glioma into neural circuits. *Nature* 573 (7775), 539–545. doi:10.1038/s41586-019-1563-y

Venkatesh, H. S., Tam, L. T., Woo, P. J., Lennon, J., Nagaraja, S., Gillespie, S. M., et al. (2017). Targeting neuronal activity-regulated neuroligin-3 dependency in high-grade glioma. *Nature* 549 (7673), 533–537. doi:10.1038/nature24014

Venneti, S., Dunphy, M. P., Zhang, H., Pitter, K. L., Zanzonico, P., Campos, C., et al. (2015). Glutamine-based PET imaging facilitates enhanced metabolic evaluation of gliomas *in vivo*. *Sci. Transl. Med.* 7 (274), 274ra17. 274ra17-. doi:10.1126/scitranslmed.aaa1009

Vivier, E., Tomasello, E., Baratin, M., Walzer, T., and Ugolini, S. (2008). Functions of natural killer cells. *Nat. Immunol.* 9 (5), 503–510. doi:10.1038/ni1582

Vredenburgh, J. J., Desjardins, A., Herndon, J. E., II, Dowell, J. M., Reardon, D. A., Quinn, J. A., et al. (2007). Phase II trial of bevacizumab and irinotecan in recurrent malignant glioma. *Clin. Cancer Res.* 13 (4), 1253–1259. doi:10.1158/1078-0432.CCR-06-2309

Wainwright, D. A., Balyasnikova, I. V., Chang, A. L., Ahmed, A. U., Moon, K. S., Auffinger, B., et al. (2012). Ido expression in brain tumors increases the recruitment of regulatory T cells and negatively impacts survival. *Clin. cancer Res.* 18 (22), 6110–6121. doi:10.1158/1078-0432.CCR-12-2130

Wang, G., Zhang, J., Hu, X., Zhang, L., Mao, L., Jiang, X., et al. (2013). Microglia/macrophage polarization dynamics in white matter after traumatic brain injury. *J. Cereb. Blood Flow Metabolism* 33 (12), 1864–1874. doi:10.1038/jcbfm.2013.146

Wang, M., Cao, J. X., Pan, J. H., Liu, Y. S., Xu, B. L., Li, D., et al. (2014). Adoptive immunotherapy of cytokine-induced killer cell therapy in the treatment of non-small cell lung cancer. *PloS one* 9 (11), e112662. doi:10.1371/journal.pone.0112662

Weller, M., Butowski, N., Tran, D. D., Recht, L. D., Lim, M., Hirte, H., et al. (2017). Rindopepimut with temozolomide for patients with newly diagnosed, EGFRvIII-expressing glioblastoma (ACT IV): a randomised, double-blind, international phase 3 trial. *Lancet Oncol.* 18 (10), 1373–1385. doi:10.1016/S1470-2045(17)30517-X

Wen, L., Tan, Y., Dai, S., Zhu, Y., Meng, T., Yang, X., et al. (2017). VEGF-mediated tight junctions pathological fenestration enhances doxorubicin-loaded glycolipid-like nanoparticles traversing BBB for glioblastoma-targeting therapy. *Drug Deliv.* 24 (1), 1843–1855. doi:10.1080/10717544.2017.1386731

Wintterle, S., Schreiner, B., Mitsdoerffer, M., Schneider, D., Chen, L., Meyermann, R., et al. (2003). Expression of the B7-related molecule B7-H1 by glioma cells: a potential mechanism of immune paralysis. *Cancer Res.* 63 (21), 7462–7467.

Wong, A. J., Bigner, S. H., Bigner, D. D., Kinzler, K. W., Hamilton, S. R., and Vogelstein, B. (1987). Increased expression of the epidermal growth factor receptor gene in malignant gliomas is invariably associated with gene amplification. *Proc. Natl. Acad. Sci.* 84 (19), 6899–6903. doi:10.1073/pnas.84.19.6899

Wu, W., Klockow, J. L., Zhang, M., Lafortune, F., Chang, E., Jin, L., et al. (2021). Glioblastoma multiforme (GBM): an overview of current therapies and mechanisms of resistance. *Pharmacol. Res.* 171, 105780. doi:10.1016/j.phrs.2021.105780

Wu, X., Luo, H., Shi, B., Di, S., Sun, R., Su, J., et al. (2019). Combined antitumor effects of sorafenib and GPC3-CAR T cells in mouse models of hepatocellular carcinoma. *Mol. Ther.* 27 (8), 1483–1494. doi:10.1016/j.ymthe.2019.04.020

Xu, B., Luo, Y., Liu, Y., Li, B. Y., and Wang, Y. (2015). Platelet-derived growth factor-BB enhances MSC-mediated cardioprotection via suppression of miR-320 expression. *Am. J. Physiology-Heart Circulatory Physiology* 308 (9), H980–H989. doi:10.1152/ajpheart.00737.2014

Yang, I., Han, S. J., Kaur, G., Crane, C., and Parsa, A. T. (2010). The role of microglia in central nervous system immunity and glioma immunology. *J. Clin. Neurosci.* 17 (1), 6–10. doi:10.1016/j.jocn.2009.05.006

Yang, K., Wu, Z., Zhang, H., Zhang, N., Wu, W., Wang, Z., et al. (2022). Glioma targeted therapy: insight into future of molecular approaches. *Mol. Cancer* 21 (1), 39–32. doi:10.1186/s12943-022-01513-z

Youssef, G., and Dietrich, J. (2020). Ipilimumab: an investigational immunotherapy for glioblastoma. *Expert Opin. Investigational Drugs* 29 (11), 1187–1193. doi:10.1080/13543784.2020.1826436

Yung, W. K., Steward, W., Marks, J. E., Griem, M. L., and Mullan, J. F. (1976). Glioblastoma multiforme: treatment with radiation and triiodothyronine. *Int. J. Radiat. Oncol. Biol. Phys.* 1 (7-8), 645–650. doi:10.1016/0360-3016(76)90146-2

Zeng, B., Cheng, Y., Zheng, K., Liu, S., Shen, L., Hu, J., et al. (2021). Design, synthesis and *in vivo* anticancer activity of novel parthenolide and micheliolide derivatives as NF-κB and STAT3 inhibitors. *Bioorg. Chem.* 111, 104973. doi:10.1016/j.bioorg.2021.104973

Zhang, M., Behbod, F., Atkinson, R. L., Landis, M. D., Kittrell, F., Edwards, D., et al. (2008). Identification of tumor-initiating cells in a p53-null mouse model of breast cancer. *Cancer Res.* 68 (12), 4674–4682. doi:10.1158/0008-5472.CAN-07-6353

Zhang, Q., Bi, J., Zheng, X., Chen, Y., Wang, H., Wu, W., et al. (2018). Blockade of the checkpoint receptor TIGIT prevents NK cell exhaustion and elicits potent anti-tumor immunity. *Nat. Immunol.* 19 (7), 723–732. doi:10.1038/s41590-018-0132-0

Zhang, Y., Yang, P., and Wang, X. F. (2014). Microenvironmental regulation of cancer metastasis by miRNAs. *Trends Cell. Biol.* 24 (3), 153–160. doi:10.1016/j.tcb.2013.09.007

Zhao, D., Najbauer, J., Garcia, E., Metz, M. Z., Gutova, M., Glackin, C. A., et al. (2008). Neural stem cell tropism to glioma: critical role of tumor hypoxia. *Mol. Cancer Res.* 6 (12), 1819–1829. doi:10.1158/1541-7786.MCR-08-0146

Zhao, Y. Z., Lin, Q., Wong, H. L., Shen, X. T., Yang, W., Xu, H. L., et al. (2016). Glioma-targeted therapy using Cilengitide nanoparticles combined with UTMD enhanced delivery. *J. Control. Release* 224, 112–125. doi:10.1016/j.jconrel.2016.01.015

Zhou, W., Ke, S. Q., Huang, Z., Flavahan, W., Fang, X., Paul, J., et al. (2015). Periostin secreted by glioblastoma stem cells recruits M2 tumour-associated macrophages and promotes malignant growth. *Nat. Cell. Biol.* 17 (2), 170–182. doi:10.1038/ncb3090

Zou, Y., Sun, X., Yang, Q., Zheng, M., Shimoni, O., Ruan, W., et al. (2022). Blood-brain barrier–penetrating single CRISPR-Cas9 nanocapsules for effective and safe glioblastoma gene therapy. *Sci. Adv.* 8 (16), eabm8011. doi:10.1126/sciadv.abm8011

frontiers | Frontiers in Pharmacology

TYPE Technology and Code
PUBLISHED 11 April 2024
DOI 10.3389/fphar.2024.1375112

Check for updates

OPEN ACCESS

EDITED BY
Claudia Carbone,
University of Catania, Italy

REVIEWED BY
Xiaodong Lu,
Emory University, United States
Mariana Magalhães,
University of Coimbra, Portugal

*CORRESPONDENCE
Lei Han,
superhanlei@hotmail.com
Zhenyu Zhang,
fcczhangzy1@zzu.edu.cn

†These authors have contributed equally to this work

RECEIVED 23 January 2024
ACCEPTED 18 March 2024
PUBLISHED 11 April 2024

CITATION
Li Z, Wei C, Zhang Z and Han L (2024), ecGBMsub: an integrative stacking ensemble model framework based on eccDNA molecular profiling for improving IDH wild-type glioblastoma molecular subtype classification. *Front. Pharmacol.* 15:1375112. doi: 10.3389/fphar.2024.1375112

COPYRIGHT
© 2024 Li, Wei, Zhang and Han. This is an open-access article distributed under the terms of the Creative Commons Attribution License (CC BY). The use, distribution or reproduction in other forums is permitted, provided the original author(s) and the copyright owner(s) are credited and that the original publication in this journal is cited, in accordance with accepted academic practice. No use, distribution or reproduction is permitted which does not comply with these terms.

ecGBMsub: an integrative stacking ensemble model framework based on eccDNA molecular profiling for improving IDH wild-type glioblastoma molecular subtype classification

Zesheng Li[1†], Cheng Wei[1†], Zhenyu Zhang[2*] and Lei Han[1*]

[1]Tianjin Neurological Institute, Key Laboratory of Post-Neuro Injury, Neuro-Repair and Regeneration in Central Nervous System, Ministry of Education and Tianjin City, Tianjin Medical University General Hospital, Tianjin, China, [2]Department of Neurosurgery, The First Affiliated Hospital of Zhengzhou University, Zhengzhou, Henan, China

IDH wild-type glioblastoma (GBM) intrinsic subtypes have been linked to different molecular landscapes and outcomes. Accurate prediction of molecular subtypes of GBM is very important to guide clinical diagnosis and treatment. Leveraging machine learning technology to improve the subtype classification was considered a robust strategy. Several single machine learning models have been developed to predict survival or stratify patients. An ensemble learning strategy combines several basic learners to boost model performance. However, it still lacked a robust stacking ensemble learning model with high accuracy in clinical practice. Here, we developed a novel integrative stacking ensemble model framework (ecGBMsub) for improving IDH wild-type GBM molecular subtype classification. In the framework, nine single models with the best hyperparameters were fitted based on extrachromosomal circular DNA (eccDNA) molecular profiling. Then, the top five optimal single models were selected as base models. By randomly combining the five optimal base models, 26 different combinations were finally generated. Nine different meta-models with the best hyperparameters were fitted based on the prediction results of 26 different combinations, resulting in 234 different stacked ensemble models. All models in ecGBMsub were comprehensively evaluated and compared. Finally, the stacking ensemble model named "XGBoost.Enet-stacking-Enet" was chosen as the optimal model in the ecGBMsub framework. A user-friendly web tool was developed to facilitate accessibility to the XGBoost.Enet-stacking-Enet models (https://lizesheng20190820.shinyapps.io/ecGBMsub/).

KEYWORDS

brain tumor, IDH wild-type glioblastoma, eccDNA, machine learning, ensemble model, molecular subtype

1 Introduction

Glioblastoma (GBM) is a type of notorious intracranial tumor with low survival rates and high heterogeneity and recurrence rates. The standard treatment strategy involves surgery, radiation, and chemotherapy. While standard treatment can effectively alleviate symptoms, the overall survival of patients remains unsatisfactory (Lu et al., 2022; Schaff and Mellinghoff, 2023). In past decades, high-throughput omics data revealed heterogeneous genetic/genomic/epigenetic landscapes and prompted individual therapies based on molecular subtypes. In 2010, Verhaak et al. identified four GBM subtypes, including classical (CL), mesenchymal (MES), neural (NE), and proneural (PN) (Verhaak et al., 2010). Because PN contributes to a more favorable outcome while the MES subtype relates to dismal survival, numerous studies have focused on them (Yan et al., 2022; Qiu et al., 2023). However, the above-mentioned finding might be largely attributed to the favorable outcome of IDH mutant GBMs, which are consistently classified as PN. According to the fifth edition of the WHO Classification of Tumors of the Central Nervous System (WHO CNS5), the definition of GBM was augmented with genetic modifiers (e.g., GBM and IDH-wildtype) (Louis et al., 2021). In 2017, Wang et al. defined three IDH wild-type GBM subtypes based on the gene expression profile, including CL, MES, and PN, which are tightly related to the tumor immune environment (Wang et al., 2017). Their findings might aid in precision immunotherapy medicine. However, two potential issues need to be further improved. First, most clinicians are not familiar with the analysis of sequence data, which prevents them from calculating the patient's molecular subtype based on gene expression information. Second, extrachromosomal genetic elements play a key role in regulating gene expression, but their roles in the identification of molecular subtypes have not been fully considered.

Extrachromosomal circular DNA (eccDNA) plays diverse roles in healthy bioprocesses and cancer progression. EccDNAs are mostly shorter than 1 kb. In contrast, a special subtype of eccDNA is named extrachromosomal DNA (ecDNA) and is much larger (50kb–5 Mb) (Yi et al., 2022). Although ecDNAs play an important role in cancer, the larger size makes it challenging for enrichment and identification, setting up a barrier for research. Compared with ecDNAs, eccDNAs with smaller sizes exhibit more promise serving as biomarkers. A previous study reported that eccDNAs in maternal plasma represent prospective circulating nucleic acid biomarkers to improve early diagnosis and management (Sin et al., 2020; Sin et al., 2021). Here, we adapt the Circle-seq to specifically enrich extrachromosomal circular DNA from GBM tumor tissues and adjacent non-tumor tissues. Circle-seq can effectively capture eccDNAs, although it is challenging to capture megabase-sized ecDNAs.

Leveraging machine learning to decode the underlying links in multi-omics biological data has been popular (Sin et al., 2021; Greener et al., 2022). Machine learning is a robust tool for tackling challenging data (Greener et al., 2022). Stacking ensemble is a strategy that combines the predictions of multiple base models to create an ensemble model with more robust performance. Here, we developed "ecGBMsub," a stacking ensemble framework based on eccDNA molecular profiling, which may provide a convenient tool for clinicians to identify the IDH wild-type GBM subtypes and reveal the underlying links between GBM subtype evaluation and eccDNA biology.

We used nine machine learning algorithms to fit base models on the training set. Then, the five optimal base models on cross-validation (CV) were selected to create the stacking ensemble framework, ecGBMsub. The optimal stacking ensemble model, named XGBoost.Enet-stacking-Enet, exhibited robust performance in the prediction of all IDH wild-type GBM molecular subtypes. We conducted a model interpretability analysis using SHAP to understand the decision-making process. Finally, we developed a web tool and deployed the machine learning model on the web tool. Our studies might help clinicians predict molecular subtypes in patients with IDH wild-type GBM.

2 Materials and methods

2.1 Sample acquisition and diagnosis

GBM tumors and adjacent tissues (three pairs) were collected from First Affiliated Hospital of Zhengzhou University. Following WHO CNS5 standards, the initial histopathological diagnosis is conducted at the institution that collects the tissue. To ensure consistency across samples, in-house neuropathologists reviewed the initial diagnosis. This study was approved by the hospital's institutional review board, and written informed consent was obtained from all patients. The clinical data for the samples are listed in Supplementary Table S1.

2.2 Circle-seq and data analysis

Circle-seq analysis based on clinical samples was performed by CloudSeq Biotech Inc. (Shanghai, China). The detailed procedure was previously reported (Møller et al., 2015; Møller et al., 2018). The edgeR (v0.6.9) software was used to normalize and calculate fold changes and *p*-values between two groups/samples to screen differentially expressed eccDNAs. Gene annotation of differential eccDNAs was performed using bedtools software (v2.27.1).

2.3 Data collection criteria and preprocess

The inclusion criteria for datasets were 1) that they contained IDH wild-type GBM and 2) that they contained classical, mesenchymal, and proneural molecular subtype information. Three datasets met the criteria and were enrolled in this study. The number of IDH wild-type GBM samples in these cohorts was as follows: TCGA-GBM (n = 114), CGGA301 (n = 89), and G-SAM (n = 283). The TCGA-GBM RNA-seq raw count was downloaded from the TCGA portal (https://portal.gdc.cancer.gov/) and converted to transcripts per kilobase million (TPM), followed by log-2 transformation. The G-SAM dataset was accessed from the European Genome Phenome Archive (EGA; EGAD00001007860) (Draaisma et al., 2020; Hoogstrate et al., 2023). The CGGA301 dataset was accessed from the Chinese Glioma Genome Atlas (CGGA, http://www.cgga.org.cn/) (Zhao et al.,

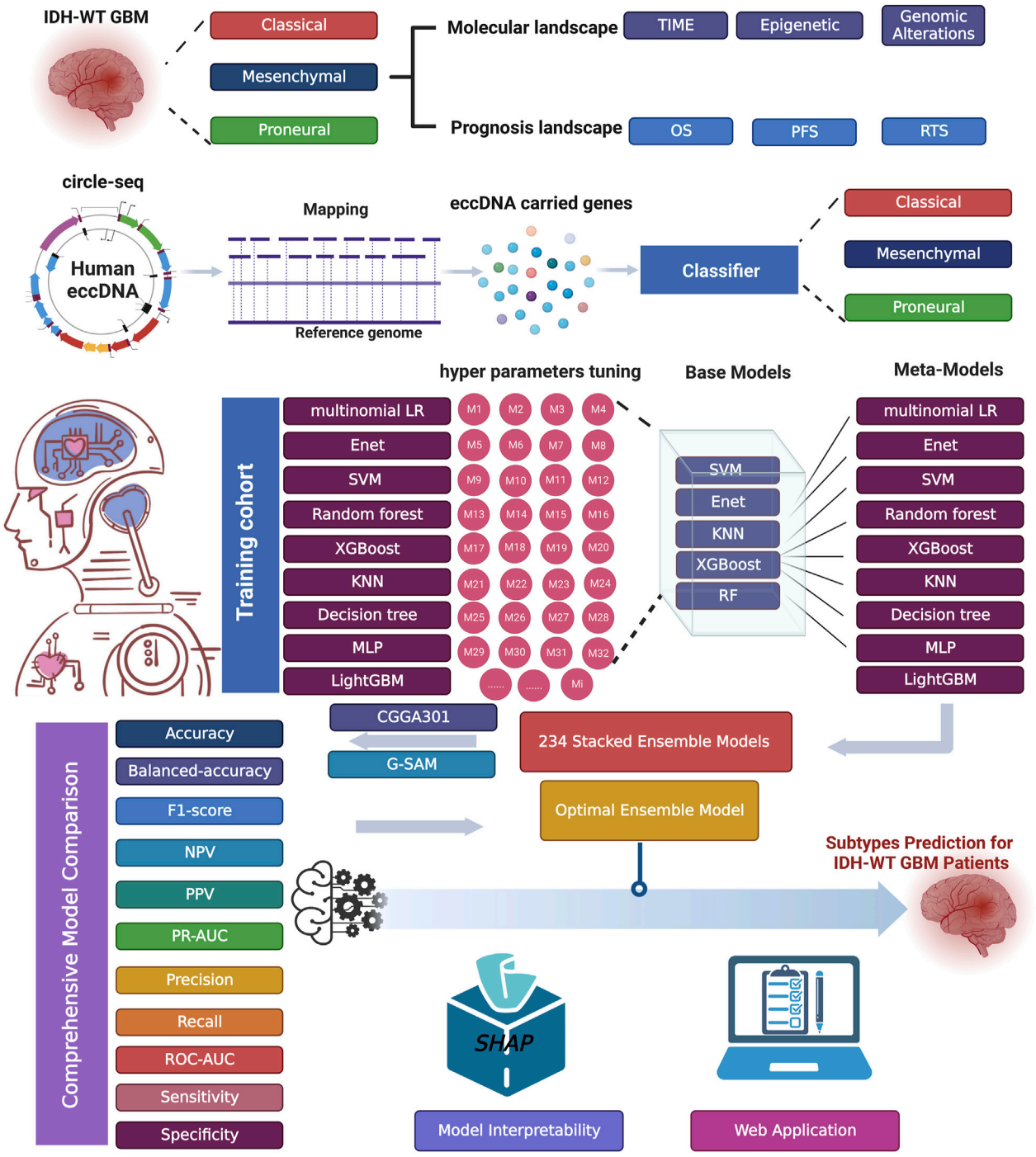

FIGURE 1
The workflow of this study.

2021). The ComBat algorithm was utilized to remove batch effects from nonbiological technical biases between different cohorts (Supplementary Figure S1). Somatic mutation and copy number segment data were downloaded from cBioPortal (https://www.cbioportal.org/) and FireBrowse (http://firebrowse.org/), respectively. TCGA was set as the training set, while the others (CGGA301 and G-SAM) were used for independent test datasets.

2.4 Molecular landscape analysis

The immune signatures were obtained from previous studies (Lu et al., 2021). The R package "GSVA" was used to calculate the score of immune signature gene sets in each sample. The R package "RTN" was used to construct transcriptional regulatory networks (regulons). The activities of regulons (transcription factors) that

were associated with GBM progression and the regulators that were relevant to cancerous histone modification were calculated. Specifically, the transcriptome expression profile was analyzed using mutual information analysis and Spearman rank-order correlation to determine the potential associations between regulators and potential targets. Permutation analysis was applied to eliminate associations with an FDR >0.00001. Unstable associations were removed through a bootstrapping strategy of 1,000 resamplings with a consensus bootstrap greater than 95%. The weakest associations in the triangles of two regulators and common targets were removed. A two-sided GSEA was used to estimate the activity of each regulon.

2.5 Framework of ecGBMsub

Numerous studies have demonstrated that ensemble models might exhibit higher performance under certain situations than single models. Unlike other ensemble strategies, such as bagging and boosting, a stacking strategy creates a hybrid model by combining the strengths of different predictive models. The workflow of ecGBMsub development includes the fit, evaluation, and selection of base models, the generation of new feature vectors, the selection of meta-models with an enumeration method, and the selection of the optimal model by comprehensive evaluation. The workflow of this study is shown in Figure 1.

2.5.1 Base model construction

Nine machine learning algorithms, including multinomial logistic regression, decision tree (DT), random forest (RF), extreme gradient boosting (XGBoost), multilayer perceptron (MLP), elastic net (Enet), support vector machine (SVM), light gradient boosting machine (LightGBM) and K-nearest neighbor (KNN), were performed to fit models based on 5-fold CV on the training cohort.

2.5.2 Evaluation and selection of base models

Base learner accuracy and diversity were vital to the performance of the ensemble model. A comprehensive evaluation involving multiple metrics was performed. We used accuracy, balanced accuracy, F1-score, NPV, PPV, PR-AUC, precision, recall, ROC-AUC, sensitivity, and specificity in CV as statistics to ensure the robustness of base models. Finally, SVM, Enet, KNN, XGBoost, and RF were determined to be the best-performing base models.

2.5.3 New feature vector generation

The new feature vector was created using predicted probabilities (PPs) of five optimal base models. The new feature vector was defined as [PPs(SVM), PPs(Enet), PPs(KNN), PPs(XGBoost), PPs(RF)]^T, where PPs i) is the PPs based on the optimal base model i.

2.5.4 Meta-model selection with enumeration method

Nine machine learning algorithms, including multinomial logistic regression, DT, RF, XGBoost, MLP, Enet, SVM, LightGBM, and KNN, were used as meta-models. In the enumeration framework, the five base models were randomly combined to generate 26 different combinations, and then nine algorithms were used to build a meta-model, resulting in 234 stacking models. In total, 243 types of models, including 234 stacking ensemble models and nine base models, were created in the ecGBMsub framework.

2.5.5 Selection of optimal model by comprehensive evaluation

The performance of all models in ecGBMsub was evaluated and compared using 11 standard performance metrics for the classification problem: accuracy, balanced accuracy, F1-score, NPV, PPV, precision, recall, PR-AUC, ROC-AUC, sensitivity, and specificity. Finally, the stacking model, named XGBoost.Enet-stacking-Enet, was chosen as the optimal model in the ecGBMsub framework. XGBoost.Enet-stacking-Enet refers to a two-layer stacking model, of which the optimal XGBoost and Enet models are the base learner, and the Enet model is the meta-learner.

2.5.6 Hyperparameter settings

The base model employs 5-fold cross-validation along with Bayesian optimization to improve its performance. The stacking ensemble model leverages bootstrap resampling in combination with Bayesian optimization to enhance performance. The hyperparameter tuning metrics were set as balanced accuracy. During Bayesian optimization, the maximum number of iterations is set to 50. If there is no performance improvement within 10 consecutive iterations, the process is terminated early. The bootstrap resampling times are set to 10. The hyperparameter tuning process is shown in Supplementary Figure S2.

2.6 Statistical analysis

The statistical tests were conducted by R4.2.2, including the Kruskal–Wallis test for comparisons among multiple groups of continuous variables, Fisher's exact test for categorical data, and the log-rank test for Kaplan–Meier curves. For unadjusted comparisons, statistical significance was defined as $p < 0.05$.

3 Results

3.1 Prognostic landscape of IDH wild-type GBM subtypes

Most of the patients in the G-SAM database received standard treatment, while the treatment approaches of patients in the TCGA group were diverse. Therefore, the G-SAM database was selected for the survival analysis. To standardize the survival analysis candidates, the patients were filtered according to the following criteria: 1) IDH wild-type; 2) underwent temozolomide chemotherapy combined with radiotherapy after surgical resection. Patients meeting both criteria were retained for survival analysis (n = 260). The mesenchymal subtype in the G-SAM cohort had the most unfavorable overall survival (OS), progression-free survival (PFS), and post-relapse treatment survival (RTS) of all the subtypes (all pairwise comparisons, $p = 0.004$; $p = 0.02$; $p < 0.001$, Figures 2A–C). RTS refers to the survival time after the patient's tumor recurred and

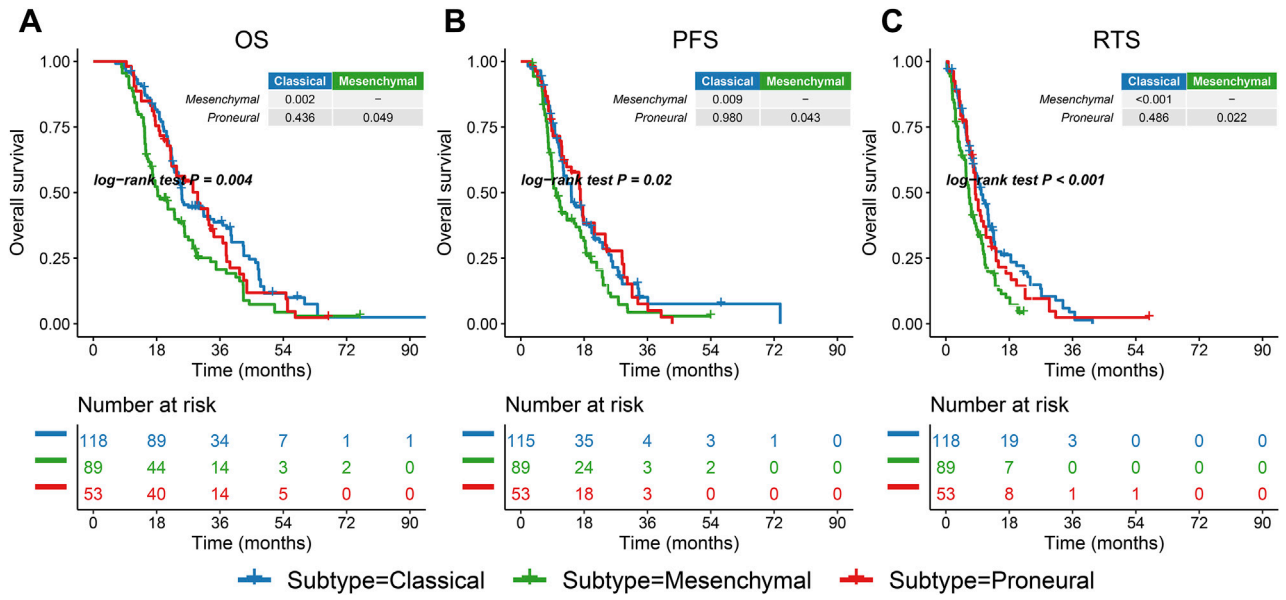

FIGURE 2
Prognostic landscape of three IDH wild-type GBM subtypes. **(A–C)** Kaplan–Meier curves of overall survival (OS), progression-free survival (PFS), and post-relapse treatment survival (RTS) log-rank test for 260 IDH wild-type GBM patients classified by subtypes.

received treatment. Thus, different subtypes imply different prognostic landscapes, which emphasizes the importance of accurate prediction of subtypes.

3.2 Molecular landscape of IDH wild-type GBM subtypes

As cancer immunity plays a pivotal role in tumor progression, we hypothesized that the tumor immune microenvironment (TIME) of the mesenchymal subtype may be different from that of the other subtypes. Thus, the immune cell infiltration status was investigated in two cohorts (TCGA and G-SAM). Specifically, we quantified the infiltration levels of 24 microenvironment cell types and the expression of immune checkpoints in IDH wild-type GBM samples. In the TCGA and G-SAM cohorts, the analysis of immune signature expression levels suggested that immunocyte infiltration was dramatically higher in the mesenchymal subtype (Figure 3A; Supplementary Figure S3A). Compared to the other subtypes, the mesenchymal subtype exhibited a relatively higher expression of checkpoints that represent potential targets for immunotherapy (Lu et al., 2021), including *CD247* (*CD3*), *CTLA4* (*CD152*), *IDO1*, *IL10*, *PDCD1*, *PDCD1LG2* (*PDL2*), and *TNFRSF9* (*CD137*) in the TCGA cohort and *CD247* (*CD3*), *CD274* (*PDL1*), *CD276*, *CTLA4* (*CD152*), *IDO1*, *IL10*, *PDCD1* (*PD1*), *PDCD1LG2* (*PDL2*), and *TNFRSF9* (*CD137*) in the G-SAM cohort (Supplementary Figure S3B). Additionally, the mesenchymal subtype exhibited higher immune and stromal scores (Figure 3A; Supplementary Figure S3C), which confirms the feasibility of microenvironment-targeted therapy for patients with the mesenchymal subtype.

To further explore the epigenetic landscape of IDH wild-type GBM, we analyzed GBM-specific regulon activity and potential regulators relevant to cancerous histone modification (Li et al., 2016; Sharpe and Baskin, 2016; Luedi et al., 2018; Chen et al., 2019; Yang et al., 2021; Tsai et al., 2022; Yuan et al., 2022; Dai et al., 2023; Kosti et al., 2023; Mao et al., 2023; Yao and Wang, 2023). Surprisingly, the regulon activity was tightly associated with IDH wild-type GBM subtypes. The patterns of regulon activity were different in three subtypes. The mesenchymal subtype exhibits high activity of *POU2F2*, *SPP1*, *CEBPD*, and *CEBPB*, while the classical subtype was distinctly associated with high activity of *POU3F2* and *TCF3* (Figure 3B). The regulation activity patterns associated with histone modification among the three subtypes were also different, emphasizing that epigenetic networks might play a pivotal role in defining these molecular subtypes. Compared with classical and proneural subtypes, the mesenchymal subtype exhibited lower cancerous histone modification activity in the TCGA cohort (Figure 3B). Therefore, epigenetic regulation of the mesenchymal subtype may be primarily influenced by transcription factor activity rather than chromatin accessibility.

To investigate the genomic heterogeneity of three IDH wild-type GBM subtypes further, the genomic alteration landscape was systematically characterized in the TCGA cohort (Figure 4A). There was no significant difference in tumor mutation burden (TMB) among subtypes (p = 0.14, Figure 4B). The fraction genome altered (FGA) and fraction genome gain/loss (FGG/FGL) among the three subtypes did not show differences (Figure 4C).

Notably, we found that the classical and mesenchymal subtypes exhibited higher *EGFR* mutation frequencies than the proneural subtype. The *NF1* was exclusively mutated in mesenchymal subtype (Figure 4A). Wang et al. reported that *NF1* deficiency drives the infiltration of tumor-associated macrophages/microglia (Wang et al., 2017). Therefore, *NF1* mutations may contribute to a tumor-promoting immune microenvironment in the mesenchymal subtype. Meanwhile, the proneural subtype exhibited higher 4q12-amplification, 12q14.1-amplification, and lower 9p21.3-deletion than

10.3389/fphar.2024.1375112

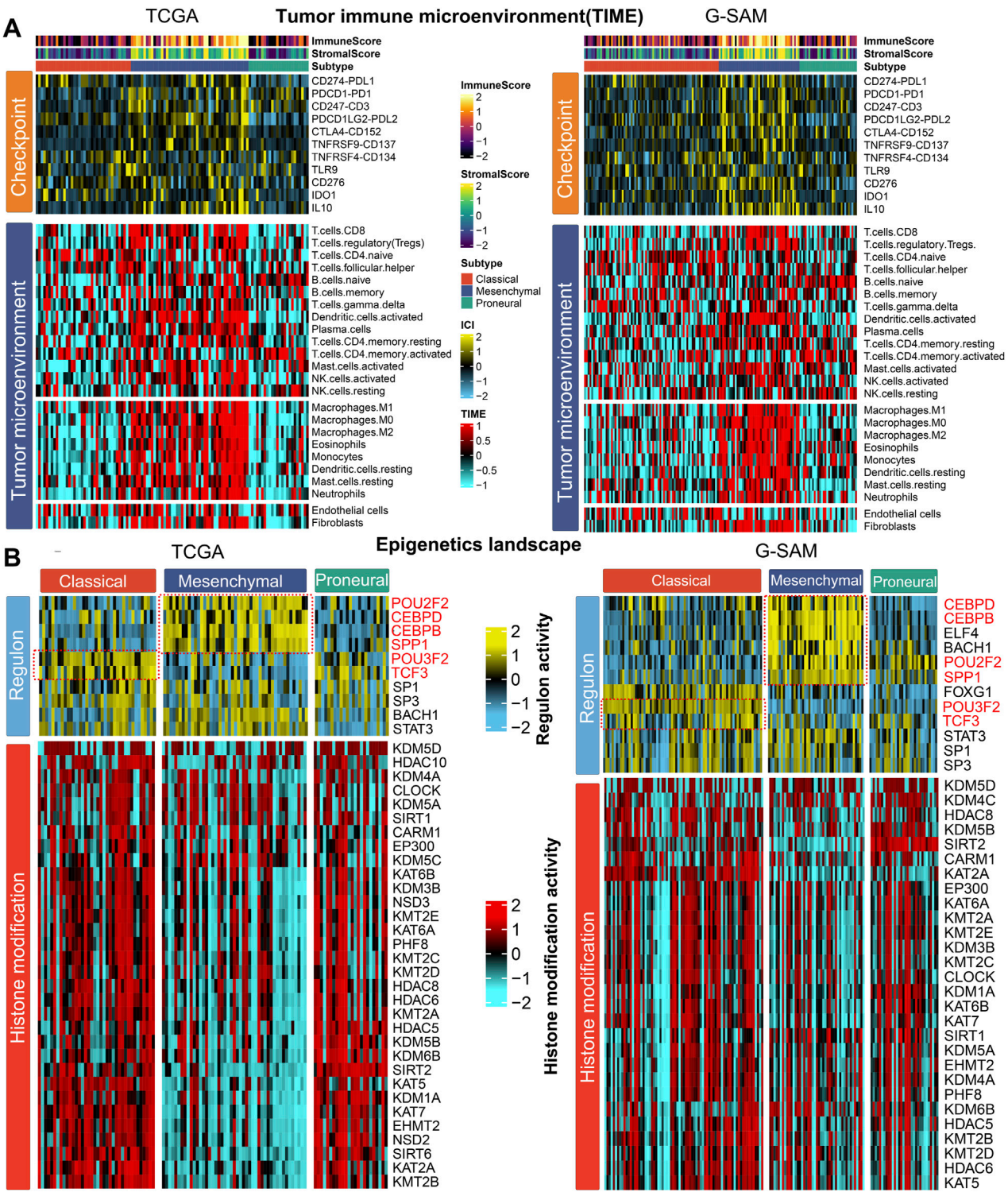

FIGURE 3
Molecular landscape of three IDH wild-type GBM subtypes. **(A)** Tumor immune microenvironment (TIME): heatmap showing the immune profile in the IDH wild-type GBM subtypes (TCGA for left; G-SAM for right), with the top panel showing the expression of genes involved in immune checkpoint targets and the bottom panel showing the enrichment level of 24 microenvironment cell types. The immune enrichment score and stromal enrichment score are annotated at the top of the heatmap. **(B)** Epigenetic landscape: heatmap showing regulon activity profiles for GBM transcription factors (top panel) and potential regulators associated with histone modification (bottom panel) in the IDH wild-type GBM subtypes (TCGA on the left; G-SAM on the right).

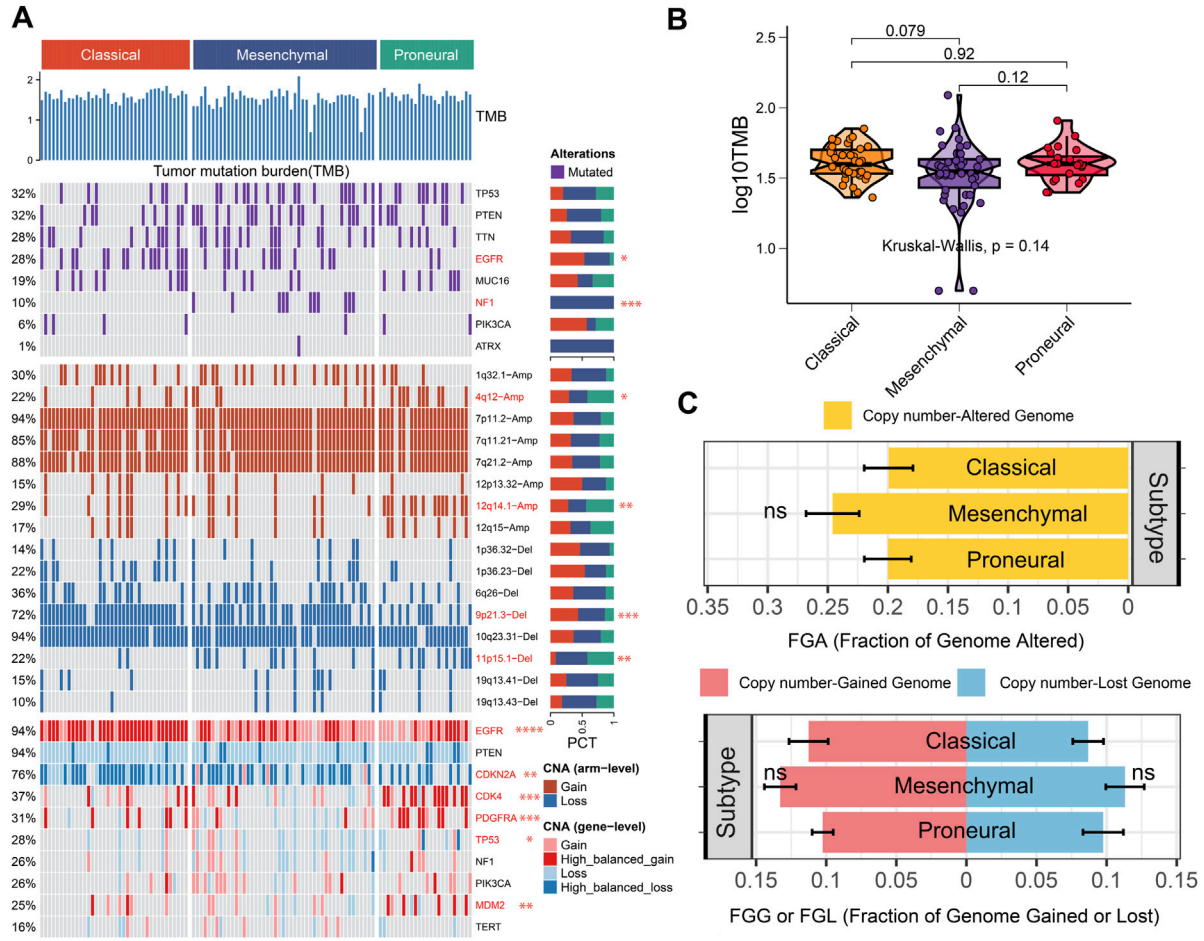

FIGURE 4
Genomic alteration landscape of three IDH wild-type GBM subtypes. **(A)** Genomic alteration landscape in the three IDH wild-type GBM subtypes. **(B)** Tumor mutation burden (TMB) in different subtypes. **(C)** Distribution of fraction genome altered (FGA) and fraction genome gain/loss (FGG/FGL) in the three IDH wild-type GBM subtypes. Bar charts are presented as the mean ± standard error of the mean. * ($p < 0.05$), ** ($p < 0.01$), and *** ($p < 0.001$), ns ($p > 0.05$).

other subtypes. The classical subtype exhibited lower 11p15.1-deletion than other subtypes. Alterations in these chromosomal arms may serve as biomarkers for subtype identification. Additionally, *EGFR* showed a more high-balanced gain in the classical subtype than other subtypes, which is consistent with previous studies (Verhaak et al., 2010). EGFR tyrosine kinase inhibitor (TKI) might exhibit better benefits for patients in the classical subtype. *CDKN2A* showed more high-balanced loss in the classical and mesenchymal subtypes than in the proneural subtype. Nathanson et al. reported that *CDKN2A* deletion remodels lipid metabolism, thereby priming GBM for ferroptosis (Minami et al., 2023). Drugs targeting lipid metabolism and enhancing the ferroptosis process may be more suitable to benefit patients with the classic or the mesenchymal subtypes. The *CDK4*, *PDGFRA*, and *MDM2* showed more high-balanced gain in the proneural than the other subtypes, which provided potential individualized targets for patients in the proneural subtype (Figure 4A). Meanwhile, some inhibitors that might aid in clinical administration have been developed, including CDK4/6 inhibitors, PDGFRA inhibitors, and MDM2 inhibitors. Therefore, considering genetic alterations in clinical administration may be the key to achieving precision medicine among different subtypes.

3.3 Feature selection and base model construction

A total of 924 differentially expressed eccDNAs carrying protein-coding genes were identified in GBM core tissues and adjacent tissues with a cut-off criteria of |FC (fold change)| >2 and $p < 0.05$. Among them, 371 eccDNAs were upregulated, and 553 were downregulated in the GBM tumor core tissues (Supplementary Table S2). Finally, 717 protein-coding genes carried by differentially expressed eccDNAs were included in three data sets (TCGA, CGGA301, and G-SAM). The 717 protein-coding genes mentioned above are original features and will be used for subsequent analysis.

Two machine learning algorithms, including SVM-RFE and varSelRF, were used for feature selection. When faced with redundant features, SVM-RFE generally exhibits higher robustness because it considers the interactions between the features. The varSelRF algorithm is based on multiple decision trees with non-linear modeling capabilities. The rationality of these two methods is that they can provide feature screening at different levels and perspectives. Finally, a total of 29 independent

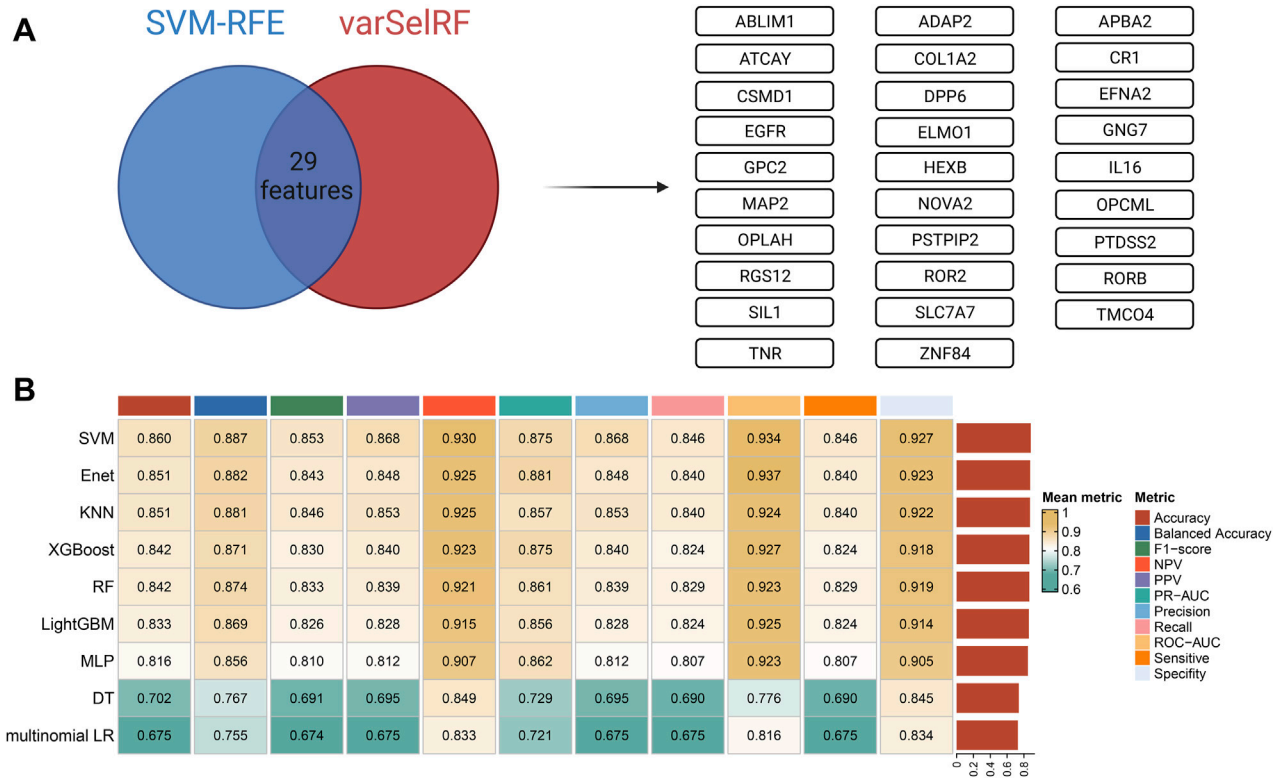

FIGURE 5
Feature selection and base model construction and comparison. **(A)** Feature selection: the SVM-REF and varSelRF algorithms were used for feature selection, and 29 features were retained. **(B)** Base model construction and comparison: nine machine learning algorithms were used to fit models based on 5-fold cross-validation (CV) on the training cohort (TCGA). The performance of each model on CV was comprehensively evaluated.

features were obtained based on two algorithms, including *ABLIM1*, *ADAP2*, *APBA2*, *ATCAY*, *COL1A2*, *CR1*, *CSMD1*, *DPP6*, *EFNA2*, *EGFR*, *ELMO1*, *GNG7*, *GPC2*, *HEXB*, *IL16*, *MAP2*, *NOVA2*, *OPCML*, *OPLAH*, *PSTPIP2*, *PTDSS2*, *RGS12*, *ROR2*, *RORB*, *SIL1*, *SLC7A7*, *TMCO4*, *TNR*, and *ZNF84* (Figure 5A).

Nine machine learning algorithms, including multinomial logistic regression, DT, RF, XGBoost, MLP, Enet, SVM, LightGBM, and KNN, were used to fit base models on the training set (TCGA cohort). The optimal hyperparameters on the CV of each base model are shown in Supplementary Table S3. The nine models with optimal hyperparameters were comprehensively evaluated on CV. Eleven metrics were calculated for model evaluation, including accuracy, balanced accuracy, F1-score, NPV, PPV, PR-AUC, precision, recall, ROC-AUC, sensitivity, and specificity. Finally, the mean metric was calculated as the average of each metric on CV (Figure 5B). SVM, Enet, KNN, XGBoost, and RF were the top five optimal base models among these models.

3.4 Construction of stacking ensemble models and selection of optimal model by comprehensive evaluation

We randomly combined the five optimal base models, which generated 26 types of different combinations. Then, the new feature vector was created using the predicted probabilities (PPs) of 26 combinations. For example, for the combination of SVM. Enet. KNN. XGBoost. RF, the new feature vector was defined as [PPs(SVM), PPs(Enet), PPs(KNN), PPs(XGBoost), PPs(RF)]^{T}, where PPs i) is the PPs based on the optimal base model i. Next, the meta-models were fitted based on the new feature vector. Here, nine types of machine learning algorithms, including multinomial logistic regression, DT, RF, XGBoost, MLP, Enet, SVM, LightGBM, and KNN, were set as meta-models to fit the two-layer stacking ensemble models. Finally, 234 stacking ensemble models were generated.

The 243 models, including 234 stacking ensemble models and nine base models, were comprehensively evaluated on the G-SAM and CGGA301 test cohorts. The mean metric was calculated by the mean value of each metric on the two test sets. The XGBoost.Enet-stacking-Enet stacking ensemble model exhibits a robust performance among all metrics on test sets (Figure 6).

3.5 Evaluation of XGBoost.Enet-stacking-Enet

An ROC curve and a confusion matrix were used for the performance evaluation of XGBoost.Enet-stacking-Enet. ROC curves can exhibit the model's classification ability across each

10.3389/fphar.2024.1375112

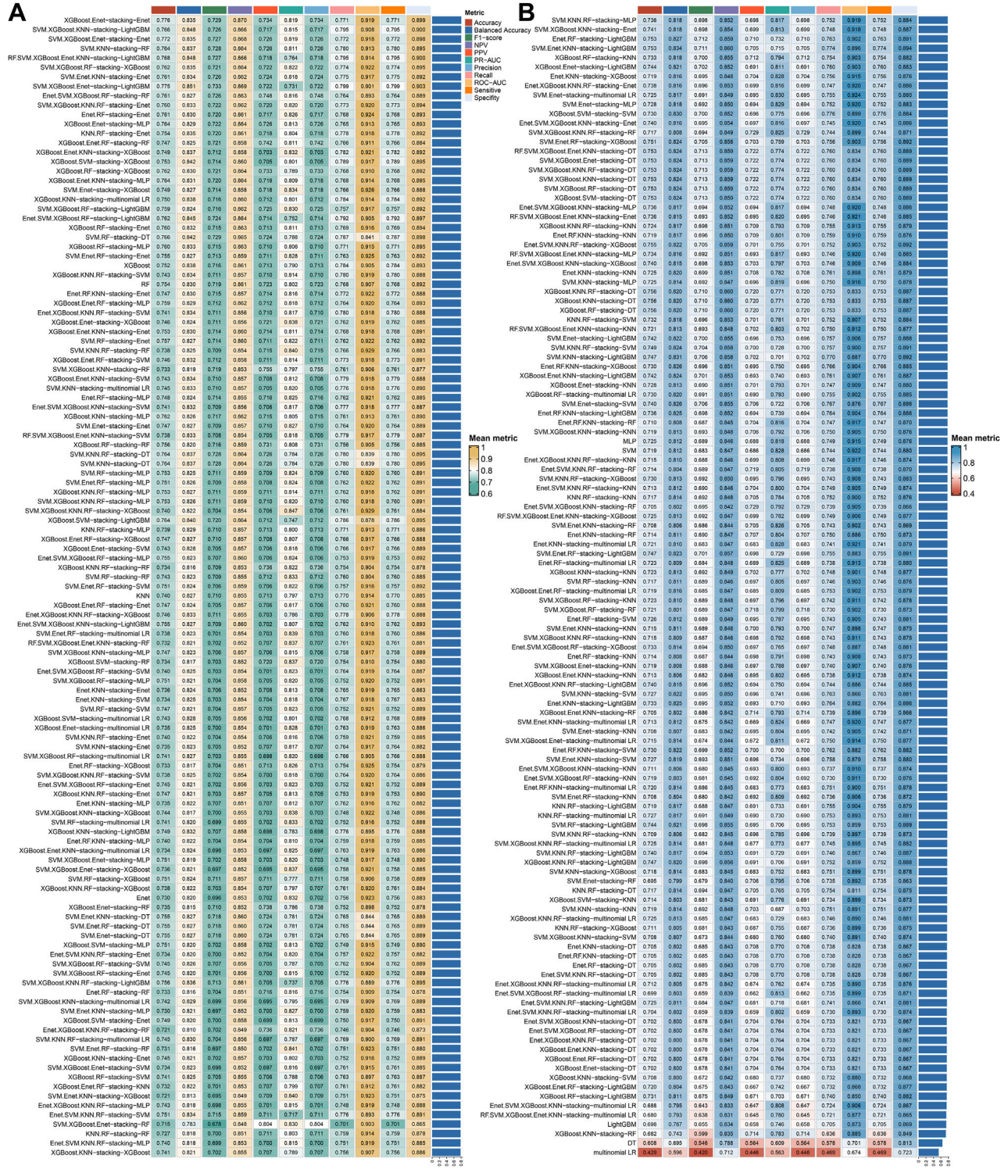

FIGURE 6
Integrative construction of stacking ensemble models and model comparison. A total of 243 models, including 234 stacking ensemble models and nine base models, were comprehensively evaluated on two test cohorts. The metric values were calculated by the mean values of the G-SAM and CGGA301 cohorts. **(A)** The top 121 models ranked by mean metric. **(B)** The 122–243 models ranked by mean metric.

class. The confusion matrix provides detailed class-level performance metrics. The macro average method was used to calculate the area under the curve (ROC-AUC) of the model on each class. This approach calculates and averages the AUC for each class to obtain an averaged ROC-AUC. In this way, we can evaluate the performance of each class equally without suffering from class

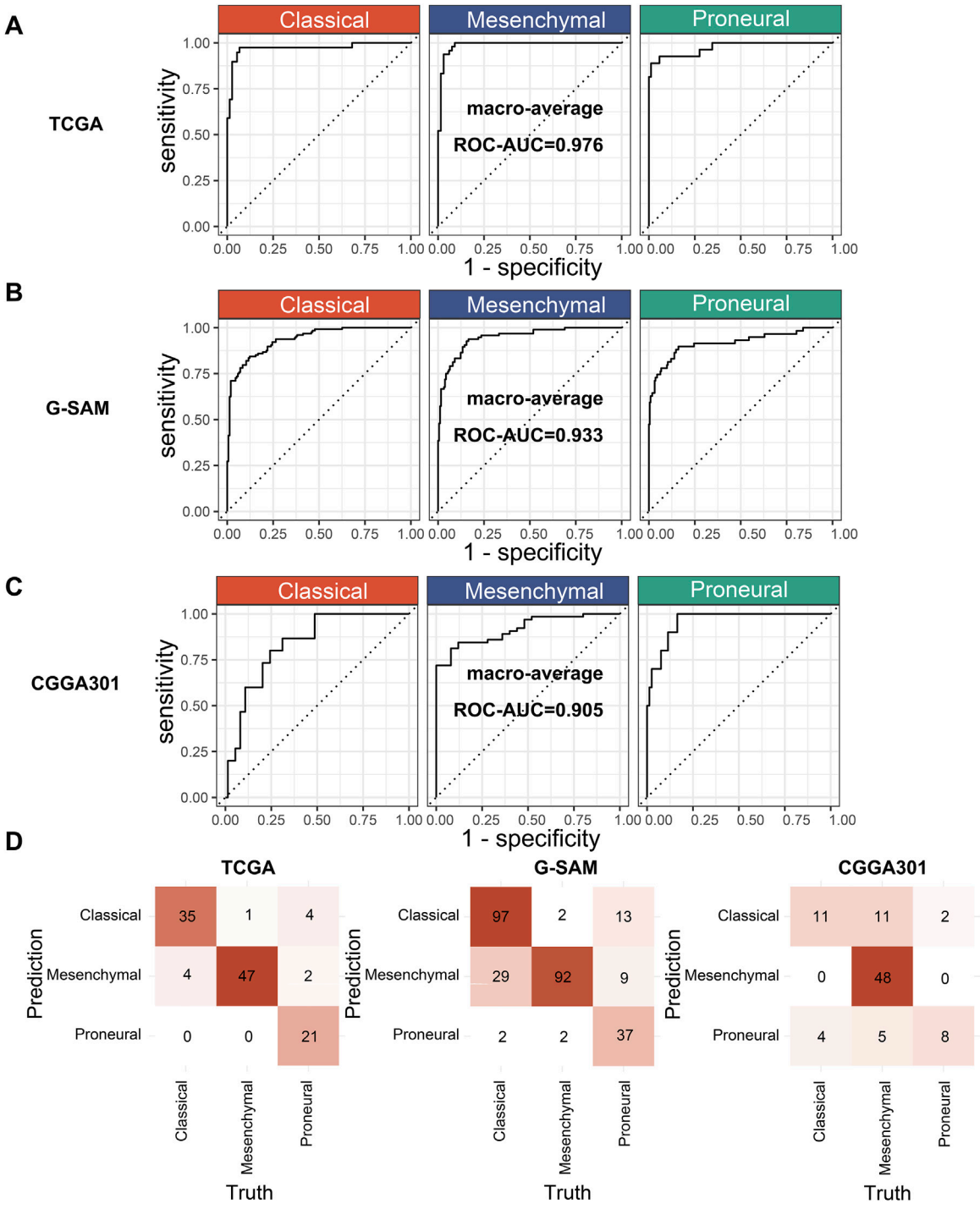

FIGURE 7
Performance evaluation of the optimal model. **(A)** ROC curves of the XGBoost.Enet-stacking-Enet model in the training cohort (TCGA). **(B, C)** ROC curves of the XGBoost.Enet-stacking-Enet model in the test cohort (G-SAM, CGGA301). **(D)** Confusion matrix of the XGBoost.Enet-stacking-Enet model on the training and test cohorts.

imbalance. The macro-averaged ROC-AUC values were 0.976 in the TCGA cohort, 0.933 in the G-SAM cohort, and 0.905 in the CGGA301 cohort, respectively (Figures 7A–C). The confusion matrix consists of rows representing the true classes and columns representing the model's predicted classes. Overall, the XGBoost.Enet-stacking-Enet model performed well on both the training and test sets (Figure 7D).

3.6 Interpretability analysis of XGBoost.Enet-stacking-Enet

Shapley additive explanations (SHAP) is widely used to explain machine learning model predictions. Here, SHAP was used to perform an interpretability analysis of XGBoost.Enet-stacking-Enet. First, the feature importance analysis was performed by

10.3389/fphar.2024.1375112

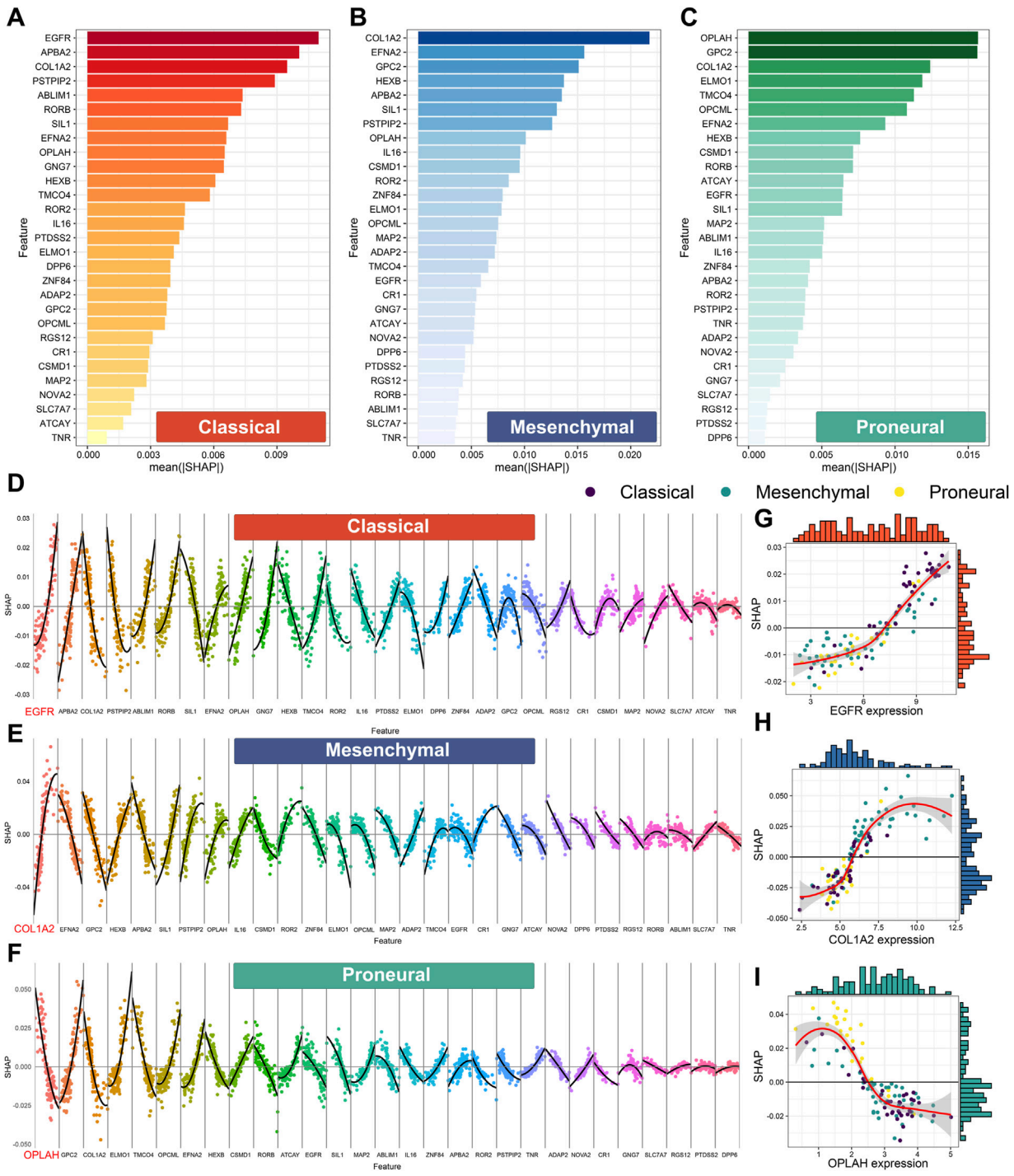

FIGURE 8
Feature importance based on Shapley additive explanation (SHAP) analysis of the XGBoost.Enet-stacking-Enet model. Feature importance for the prediction of the classical subtype **(A)**, the mesenchymal subtype **(B),** and the proneural subtype **(C)**. The features are ranked from most important to least important on the vertical axis, ordered from top to bottom. The horizontal axis shows the mean absolute SHAP values in all samples in the TCGA cohort. The higher absolute SHAP values mean higher importance. Feature contribution for the prediction of the classical subtype **(D)**, mesenchymal subtype **(E),** and proneural subtype **(F)**. The non-linear relationship between the expression level of EGFR **(G)**, COL1A2 **(H)**, OPLAH **(I),** and SHAP value. The horizontal axis represents the feature expression values of each feature ordered from low to high in each feature. SHAP values are presented on the vertical axis. A SHAP value higher than 0 implicates positive contributions to the corresponding subtype prediction, and SHAP values less than 0 indicate negative contributions to the corresponding subtype prediction.

calculating the mean absolute SHAP value. For the prediction of classical, mesenchymal, and proneural subtypes, the expression levels of *EGFR*, *COL1A2,* and *OPLAH/GPC2* play the most important roles (Figures 8A–C).

Next, we explored the contributional directions of features for each subtype. The high expression level of *EGFR* might contribute to the classical subtype (Figure 8D). Meanwhile, the high expression level of *COL1A2* and *GPC2* might contribute to mesenchymal and proneural subtypes, respectively (Figures 8E,F). Notably, the correlations between some features and prediction outcomes were non-linear, which confirmed the ability of XGBoost.Enet-stacking-Enet to capture non-linear relationships. For example, the expression levels of *EGFR*, *COL1A2,* and *OPLAH* have a non-linear relationship with outcomes (Figures 8G–I).

3.7 Establishment of web tool based on the XGBoost.Enet-stacking-Enet model

To support intelligent automated decision-making and make it easier for clinicians to use the model, we developed a web tool (https://lizesheng20190820.shinyapps.io/ecGBMsub/). This web tool will promote the practice of precision medicine for IDH wild-type GBM patients, ultimately improving patients' quality of life and treatment outcomes.

4 Discussion

IDH wild-type GBM intrinsic subtypes have been linked to different genomic landscapes, epigenetic landscapes, treatment benefits, and tumor immune microenvironments (Figures 2–4). Accurately identifying molecular subtypes is pivotal to better understanding the biological characteristics of IDH wild-type GBM, thereby developing more personalized treatment administration. Our previous study demonstrated that eccDNA plays an important role in predicting the grade and prognosis of glioma patients and the recurrence of GBM (Li et al., 2023). Here, we would like to further explore the potential of eccDNA in the identification of IDH wild-type GBM molecular subtypes.

In this study, we have successfully identified differentially expressed eccDNAs between IDH wild-type GBM tumor tissues and para-tumor tissues through Circle-seq sequencing. Simultaneously, it was discovered that these differentially expressed eccDNAs carried several protein-coding genes. Currently available IDH wild-type GBM datasets with subtype information were collected. A novel stacked ensemble machine learning framework, ecGBMsub, was developed by integrating multiple machine learning algorithms. Following a comprehensive model evaluation and comparison, the XGBoost.Enet-stacking-Enet model was determined to be the optimal model (Figure 6). The XGBoost.Enet-stacking-Enet is a two-layer stacking ensemble model, utilizing the XGBoost and Enet models with optimal hyperparameters as base models and Enet as the meta-model. The meta-model takes the PPs of the base model as input and allows the generation of new PPs, thus integrating the advantages of different models. As expected, this model exhibits robust performance in predicting molecular subtypes in IDH wild-type GBM patients (Figure 7). To better understand how XGBoost.Enet-stacking-Enet achieves predictions for each subtype, a model interpretability analysis was conducted using SHAP to help explain the decision-making process for molecular subtype identification (Figure 8). To enhance the model's clinical applicability, a website tool was developed, and the machine learning model was deployed on the website. This facilitates easy access for clinicians to leverage our model for molecular subtype prediction in IDH wild-type GBM patients.

Compared with previous models, the XGBoost.Enet-stacking-Enet stacking ensemble model exhibits three main advantages. First, our model was validated in two large-scale independent cohorts, ensuring its generalization ability. Munquad et al. developed a biologically interpretable deep learning framework based on a convolutional deep neural network (CDNN) for subtype classification (Munquad et al., 2022). Their model integrated transcriptome and methylome to accurately predict molecular subtypes. However, their model was trained and validated on a single-center cohort and lacked external validation. Second, the XGBoost.Enet-stacking-Enet model exhibits better interpretability, aiding us to better understand the decision-making process. Mao et al. developed a CDNN to classify samples (Mao et al., 2022). However, their models suffer from poor interpretability and limited clinical translation potential. Third, we developed a website tool to deploy machine learning models to make it easier for clinicians to access. Ensenyat-Mendez et al. developed GBM subtype classifiers based on transcriptomic and epigenomic using random forest and nearest shrunken centroid algorithms (Ensenyat-Mendez et al., 2021). Tang et al. leveraged extreme gradient boosting (XGBoost) to develop a classifier to predict the molecular subtypes of GBM (Tang et al., 2021). The two models mentioned above have not been deployed on web tools, making them inconvenient for clinicians to use.

The innovation of this model lies in two key points: 1) the source of its features and 2) the model stacking strategy. Our features were obtained from eccDNA molecular profiling. We first revealed the underlying correlation between eccDNA and the molecular subtypes of IDH wild-type GBM. A stacking ensemble strategy was developed based on enumeration. The ecGBMsub framework maximizes the advantages of stacking ensemble models by integrating diverse base models and meta-models to capture complex relationships within datasets. The framework enhances model stability, especially when dealing with challenging datasets such as imbalanced or high-dimensional data.

However, there are some limitations. First, the eccDNAs identified by Circle-seq sequencing need to be further experimentally verified to eliminate false positive effects. Likewise, there may be eccDNAs that are not detected by Circle-seq due to false negative effects. More advanced sequencing methods and computational biology tools are needed to fully corroborate and supplement our detected eccDNA molecules. Second, all data are sourced from public datasets, and a large-scale in-house cohort is needed to further verify the robustness of the model. Third, to confirm that eccDNA molecules play a role in subtype transformation, *in vitro* and *in vivo* experiments that target specific eccDNA molecules are needed. Finally, our models are trained and tested based on the transcription profile of the genes carried by eccDNA, which can be attributed to the lack of a large

eccDNA molecular profile cohort. In the future, artificial intelligence models based on eccDNA's DNA molecular profiling should be developed. Such models might be capable of monitoring the emergence and evolution of eccDNAs during disease progression to achieve much-needed patient stratification.

Data availability statement

The original contributions presented in the study are included in the article/Supplementary Material, further inquiries can be directed to the corresponding authors.

Ethics statement

The studies involving humans were approved by the institutional Ethics Review Board of First Affiliated Hospital of Zhengzhou University. The studies were conducted in accordance with the local legislation and institutional requirements. The participants provided their written informed consent to participate in this study.

Author contributions

ZL: formal analysis, methodology, visualization, and writing–original draft. CW: conceptualization, validation, and writing–original draft. ZZ: funding acquisition, resources, and writing–review and editing. LH: funding acquisition, supervision, and writing–review and editing.

Funding

The author(s) declare financial support was received for the research, authorship, and/or publication of this article. The project was supported by grants (No. 81773187; No. 82273493) from the National Nature Science Foundation of China. The project was sponsored by the Tianjin Health Research Project (TJWJ2023ZD001) and the Natural Science Foundation of Henan Province for Excellent Young Scholars (No. 232300421057). The project was also supported by the Ji nan Clinical Medical Science and Technology Innovation Plan project (202134059).

Acknowledgments

Figure 1 was created with BioRender.com. This study makes use of data generated for the G-SAM dataset. We thank Youri Hoogstrate for the warm help.

Conflict of interest

The authors declare that the research was conducted in the absence of any commercial or financial relationships that could be construed as a potential conflict of interest.

Publisher's note

All claims expressed in this article are solely those of the authors and do not necessarily represent those of their affiliated organizations, or those of the publisher, the editors, and the reviewers. Any product that may be evaluated in this article, or claim that may be made by its manufacturer, is not guaranteed or endorsed by the publisher.

Supplementary material

The Supplementary Material for this article can be found online at: https://www.frontiersin.org/articles/10.3389/fphar.2024.1375112/full#supplementary-material

References

Chen, P., Zhao, D., Li, J., Liang, X., Li, J., Chang, A., et al. (2019). Symbiotic macrophage-glioma cell interactions reveal synthetic lethality in PTEN-null glioma. *Cancer Cell* 35 (6), 868–884. doi:10.1016/j.ccell.2019.05.003

Dai, Y., Wang, Z., Xia, Y., Li, J., Wu, Y., Wang, Y., et al. (2023). Integrative single-cell and bulk transcriptomes analyses identify intrinsic HNSCC subtypes with distinct prognoses and therapeutic vulnerabilities. *Clin. Cancer Res.* 29 (15), 2845–2858. doi:10.1158/1078-0432.CCR-22-3563

Draaisma, K., Chatzipli, A., Taphoorn, M., Kerkhof, M., Weyerbrock, A., Sanson, M., et al. (2020). Molecular evolution of IDH wild-type glioblastomas treated with standard of care affects survival and design of precision medicine trials: a report from the eortc 1542 study. *J. Clin. Oncol.* 38 (1), 81–99. doi:10.1200/JCO.19.00367

Ensenyat-Mendez, M., Íñiguez-Muñoz, S., Sesé, B., and Marzese, D. M. (2021). iGlioSub: an integrative transcriptomic and epigenomic classifier for glioblastoma molecular subtypes. *BioData Min.* 14 (1), 42. doi:10.1186/s13040-021-00273-8

Greener, J. G., Kandathil, S. M., Moffat, L., and Jones, D. T. (2022). A guide to machine learning for biologists. *Nat. Rev. Mol. Cell Biol.* 23 (1), 40–55. doi:10.1038/s41580-021-00407-0

Hoogstrate, Y., Draaisma, K., Ghisai, S. A., van Hijfte, L., Barin, N., de Heer, I., et al. (2023). Transcriptome analysis reveals tumor microenvironment changes in glioblastoma. *Cancer Cell* 41 (4), 678–692.e7. doi:10.1016/j.ccell.2023.02.019

Kosti, A., Chiou, J., Guardia, G. D. A., Lei, X., Balinda, H., Landry, T., et al. (2023). ELF4 is a critical component of a miRNA-transcription factor network and is a bridge regulator of glioblastoma receptor signaling and lipid dynamics. *Neuro Oncol.* 25 (3), 459–470. doi:10.1093/neuonc/noac179

Li, R., Li, Y., Hu, X., Lian, H., Wang, L., and Fu, H. (2016). Transcription factor 3 controls cell proliferation and migration in glioblastoma multiforme cell lines. *Biochem. Cell Biol.* 94 (3), 247–255. doi:10.1139/bcb-2015-0162

Li, Z., Wang, B., Liang, H., Li, Y., Zhang, Z., and Han, L. (2023). A three-stage eccDNA based molecular profiling significantly improves the identification, prognosis assessment and recurrence prediction accuracy in patients with glioma. *Cancer Lett.* 574, 216369. doi:10.1016/j.canlet.2023.216369

Louis, D. N., Perry, A., Wesseling, P., Brat, D. J., Cree, I. A., Figarella-Branger, D., et al. (2021). The 2021 WHO classification of tumors of the central nervous System: a summary. *Neuro Oncol.* 23 (8), 1231–1251. doi:10.1093/neuonc/noab106

Lu, G., Wang, X., Li, F., Wang, S., Zhao, J., Wang, J., et al. (2022). Engineered biomimetic nanoparticles achieve targeted delivery and efficient metabolism-based synergistic therapy against glioblastoma. *Nat. Commun.* 13 (1), 4214. doi:10.1038/s41467-022-31799-y

Lu, X., Meng, J., Su, L., Jiang, L., Wang, H., Zhu, J., et al. (2021). Multi-omics consensus ensemble refines the classification of muscle-invasive bladder cancer with stratified prognosis, tumour microenvironment and distinct sensitivity to frontline therapies. *Clin. Transl. Med.* 11 (12), e601. doi:10.1002/ctm2.601

Luedi, M. M., Singh, S. K., Mosley, J. C., Hassan, I. S. A., Hatami, M., Gumin, J., et al. (2018). Dexamethasone-mediated oncogenicity *in vitro* and in an animal model of glioblastoma. *J. Neurosurg.* 129 (6), 1446–1455. doi:10.3171/2017.7.JNS17668

Mao, X. G., Xue, X. Y., Lv, R., Ji, A., Shi, T. Y., Chen, X. Y., et al. (2023). CEBPD is a master transcriptional factor for hypoxia regulated proteins in glioblastoma and augments hypoxia induced invasion through extracellular matrix-integrin mediated EGFR/PI3K pathway. *Cell Death Dis.* 14 (4), 269. doi:10.1038/s41419-023-05788-y

Mao, X. G., Xue, X. Y., Wang, L., Lin, W., and Zhang, X. (2022). Deep learning identified glioblastoma subtypes based on internal genomic expression ranks. *BMC Cancer* 22 (1), 86. doi:10.1186/s12885-022-09191-2

Minami, J. K., Morrow, D., Bayley, N. A., Fernandez, E. G., Salinas, J. J., Tse, C., et al. (2023). CDKN2A deletion remodels lipid metabolism to prime glioblastoma for ferroptosis. *Cancer Cell* 41 (6), 1048–1060.e9. doi:10.1016/j.ccell.2023.05.001

Møller, H. D., Mohiyuddin, M., Prada-Luengo, I., Sailani, M. R., Halling, J. F., Plomgaard, P., et al. (2018). Circular DNA elements of chromosomal origin are common in healthy human somatic tissue. *Nat. Commun.* 9 (1), 1069. doi:10.1038/s41467-018-03369-8

Møller, H. D., Parsons, L., Jørgensen, T. S., Botstein, D., and Regenberg, B. (2015). Extrachromosomal circular DNA is common in yeast. *Proc. Natl. Acad. Sci. U. S. A.* 112 (24), E3114–E3122. doi:10.1073/pnas.1508825112

Munquad, S., Si, T., Mallik, S., Das, A. B., and Zhao, Z. (2022). A deep learning-based framework for supporting clinical diagnosis of glioblastoma subtypes. *Front. Genet.* 13, 855420. doi:10.3389/fgene.2022.855420

Qiu, W., Xiao, Z., Yang, Y., Jiang, L., Song, S., Qi, X., et al. (2023). USP10 deubiquitinates RUNX1 and promotes proneural-to-mesenchymal transition in glioblastoma. *Cell Death Dis.* 14 (3), 207. doi:10.1038/s41419-023-05734-y

Schaff, L. R., and Mellinghoff, I. K. (2023). Glioblastoma and other primary Brain malignancies in adults: a review. *JAMA* 329 (7), 574–587. doi:10.1001/jama.2023.0023

Sharpe, M. A., and Baskin, D. S. (2016). Monoamine oxidase B levels are highly expressed in human gliomas and are correlated with the expression of HiF-1α and with transcription factors Sp1 and Sp3. *Oncotarget* 7 (3), 3379–3393. doi:10.18632/oncotarget.6582

Sin, S. T. K., Ji, L., Deng, J., Jiang, P., Cheng, S. H., Heung, M. M. S., et al. (2021). Characteristics of fetal extrachromosomal circular DNA in maternal plasma: methylation status and clearance. *Clin. Chem.* 67 (5), 788–796. doi:10.1093/clinchem/hvaa326

Sin, S. T. K., Jiang, P., Deng, J., Ji, L., Cheng, S. H., Dutta, A., et al. (2020). Identification and characterization of extrachromosomal circular DNA in maternal plasma. *Proc. Natl. Acad. Sci. U. S. A.* 117 (3), 1658–1665. doi:10.1073/pnas.1914949117

Tang, Y., Qazi, M. A., Brown, K. R., Mikolajewicz, N., Moffat, J., Singh, S. K., et al. (2021). Identification of five important genes to predict glioblastoma subtypes. *Neurooncol Adv.* 3 (1), vdab144. doi:10.1093/noajnl/vdab144

Tsai, Y. T., Lo, W. L., Chen, P. Y., Ko, C. Y., Chuang, J. Y., Kao, T. J., et al. (2022). Reprogramming of arachidonate metabolism confers temozolomide resistance to glioblastoma through enhancing mitochondrial activity in fatty acid oxidation. *J. Biomed. Sci.* 29 (1), 21. doi:10.1186/s12929-022-00804-3

Verhaak, R. G. W., Hoadley, K. A., Purdom, E., Wang, V., Qi, Y., Wilkerson, M. D., et al. (2010). Integrated genomic analysis identifies clinically relevant subtypes of glioblastoma characterized by abnormalities in PDGFRA, IDH1, EGFR, and NF1. *Cancer Cell* 17 (1), 98–110. doi:10.1016/j.ccr.2009.12.020

Wang, Q., Hu, B., Hu, X., Kim, H., Squatrito, M., Scarpace, L., et al. (2017). Tumor evolution of glioma-intrinsic gene expression subtypes associates with immunological changes in the microenvironment. *Cancer Cell* 32 (1), 42–56. doi:10.1016/j.ccell.2017.06.003

Yan, T., Tan, Y., Deng, G., Sun, Z., Liu, B., Wang, Y., et al. (2022). TGF-β induces GBM mesenchymal transition through upregulation of CLDN4 and nuclear translocation to activate TNF-α/NF-κB signal pathway. *Cell Death Dis.* 13 (4), 339. doi:10.1038/s41419-022-04788-8

Yang, R., Wang, M., Zhang, G., Li, Y., Wang, L., and Cui, H. (2021). POU2F2 regulates glycolytic reprogramming and glioblastoma progression via PDPK1-dependent activation of PI3K/AKT/mTOR pathway. *Cell Death Dis.* 12 (5), 433. doi:10.1038/s41419-021-03719-3

Yao, J., and Wang, L. (2023). Integrin α3 mediates stemness and invasion of glioblastoma by regulating POU3F2. *Curr. Protein Pept. Sci.* 24 (3), 247–256. doi:10.2174/1389203724666230224115459

Yi, E., Chamorro González, R., Henssen, A. G., and Verhaak, R. G. W. (2022). Extrachromosomal DNA amplifications in cancer. *Nat. Rev. Genet.* 23 (12), 760–771. doi:10.1038/s41576-022-00521-5

Yuan, F., Cong, Z., Cai, X., Zhu, J., Yuan, L., Wang, Y., et al. (2022). BACH1 as a potential target for immunotherapy in glioblastomas. *Int. Immunopharmacol.* 103, 108451. doi:10.1016/j.intimp.2021.108451

Zhao, Z., Zhang, K. N., Wang, Q., Li, G., Zeng, F., Zhang, Y., et al. (2021). Chinese glioma genome Atlas (CGGA): a comprehensive resource with functional genomic data from Chinese glioma patients. *Genomics Proteomics Bioinforma.* 19 (1), 1–12. doi:10.1016/j.gpb.2020.10.005

Oncology Reviews

SYSTEMATIC REVIEW
published: 19 April 2024
doi: 10.3389/or.2024.1374513

Efficacy and Safety of Vaccines After Conventional Treatments for Survival of Gliomas: A Systematic Review and Meta-Analysis

*Elnaz Amanzadeh Jajin[1], Saeed Oraee Yazdani[2], Alireza Zali[2] and Abolghasem Esmaeili[1]**

[1]Department of Biology, Faculty of Sciences, University of Isfahan, Isfahan, Iran, [2]Functional Neurosurgery Research Center, Shohada Tajrish Comprehensive Neurosurgical Center of Excellence, Shahid Beheshti University of Medical Sciences, Tehran, Iran

Background: Malignant gliomas are known with poor prognosis and low rate of survival among brain tumors. Resection surgery is followed by chemotherapy and radiotherapy in treatment of gliomas which is known as the conventional treatment. However, this treatment method results in low survival rate. Vaccination has been suggested as a type of immunotherapy to increase survival rate of glioma patients. Different types of vaccines have been developed that are mainly classified in two groups including peptide vaccines and cell-based vaccines. However, there are still conflicts about which type of vaccines is more efficient for malignant glioma treatment.

Methods: Phase I/II clinical trials which compared the efficacy and safety of various vaccines with conventional treatments were searched in databases through November 2022. Overall survival (OS) rate, progression free survival (PFS), and OS duration were used for calculation of pooled risk ratio (RR). In addition, fatigue, headache, nausea, diarrhea, and flu-like syndrome were used for evaluating the safety of vaccines therapy in glioma patients.

Results: A total of twelve articles were included in the present meta-analysis. Comparison of OS rate between vaccinated groups and control groups who underwent only conventional treatments showed a significant increase in OS rate in vaccinated patients (I^2 = 0%, RR = 11.17, 95% CI: 2.460–50.225). PFS rate was better in vaccinated glioma patients (I^2 = 83%, RR = 2.87, 95% CI: 1.63–5.03). Assessment of safety demonstrated that skin reaction (I^2 = 0.0%, RR = 3.654; 95% CI: 1.711–7.801, *p*-value = 0.0058) and flu-like syndrome were significantly more frequent adverse effects win vaccinated groups compared to the control group. Subgroup analysis also showed that vaccination leads to better OS duration in recurrent gliomas than primary gliomas, and in LGG than HGG (*p*-value = 0). On the other hand, personalized vaccines showed better OS duration than non-personalized vaccines (*p*-value = 0).

Conclusion: Vaccination is a type of immunotherapy which shows promising efficacy in treatment of malignant glioma patients in terms of OS, PFS and duration of survival. In

OPEN ACCESS

Edited by:
Deepa Kushwaha,
Rare Genomics Institute,
United States

Reviewed by:
Mariana Magalhães,
University of Coimbra, Portugal
Javier Retamales,
Grupo Oncológico Cooperativo Chileno de Investigación, Chile

***Correspondence**
Abolghasem Esmaeili,
abesmaeili@yahoo.com

Received: *22 January 2024*
Accepted: *04 March 2024*
Published: *19 April 2024*

Citation:
Amanzadeh Jajin E, Oraee Yazdani S, Zali A and Esmaeili A (2024) Efficacy and Safety of Vaccines After Conventional Treatments for Survival of Gliomas: A Systematic Review and Meta-Analysis. Oncol. Rev. 18:1374513. doi: 10.3389/or.2024.1374513

addition, AFTV, peptide, and dendritic cell-based vaccines are among the most efficient vaccines for gliomas. Personalized vaccines also showed considerable efficacy for glioma treatments.

Keywords: glioma, vaccine, overall survival, progression free survival, personalized vaccine

INTRODUCTION

Glioma is the most prevalent brain tumor that leads to death a few months after appearance, so that its median survival duration is 14.5 months [1]. Gliomas are classified based on the genetic profiles and variations into four different grades among which grade I/II are known as low grade glioma (LGG) and grades III/IV are known as malignant or high-grade glioma (HGG) [2]. Based on 2021 classification of gliomas, this group of tumors include CNS WHO grade 2 (Oligodendroglioma and Diffuse astrocytoma), grade 3 (Anaplastic oligodendroglioma and Anaplastic astrocytoma), and grade 4 (Glioblastoma and Astrocytoma) [3].

Management of glioma treatment develops several challenges for not only healthcare systems, but also for physicians, pharmacists, and researchers because of short survival duration and low overall survival (OS) rate [4]. Accordingly, finding effective therapeutic methods is necessary to increase OS rate and duration in glioma patients. The conventional therapeutic methods for this cancerous disease include surgery followed by temozolomide (TMZ), mTOR inhibitors, tyrosine kinase inhibitors, IDH (Isocitrate dehydrogenase) targeted therapy, and radiotherapy (RT). However, none of these methods are known as successful treatment method for increasing OS in glioma patients [5].

Accordingly, novel treatment methods are introduced for gliomas along with advancements in genomics studies and development of various targeted therapies for this disease. Vaccines are used as novel therapeutics to target specific tumor antigens and induce immune response via T cells in cancer microenvironment [6]. Several types of cancer vaccines have been introduced for cancer treatment so far, among which dendritic cell-based and peptide-based vaccines can be mentioned as the most popular ones. Dendritic cell-based vaccines are developed based on their potential of beginning primary immune response by antigen presentation, specifically in cancers [7, 8]. Peptide vaccines are produced using immunogenic tumor associated antigens (TAA) which are isolated from tumors and initiate immune response via activating T-cells leading to the lysis of cancer cells [9]. However, the main aim of developing new types of vaccines is to induce T-cell immunity and localization of this immune response to the tumor site [10]. In addition, personalized vaccines are known as promising candidates to overcome the challenges for cancer vaccination. Development of personalized vaccines have gained great attention, since it is possible to consider genetics differences of individuals in vaccine design and improve efficacy of vaccines in induction of immune response after conventional treatments and increase survival duration [11].

On the other hand, vaccines have shown promising effect on treatment of malignant gliomas because of their potential to pass through blood brain barrier (BBB) and provide targeted therapy while induce immunogenicity. Peptide-based vaccines, heat-shock protein vaccines, dendritic cell vaccines are among the most common vaccines produced for treatment of malignant glioma [6]. The use of other types of vaccines such as tumor initiating cell, B Cell Hybridoma, autologous formalin fixed vaccines, etc., has been suggested for treatment of gliomas [12–16]. On the other hand, personalized vaccines including modified genes are considered as the novel treatment which trigger genetic variations in individuals with malignant glioma [17]. These vaccines are manufactured using the genetics and epigenetics information of subjects and it is aimed to increase OS and PFS rate in glioma patients more than conventional methods of treatment and non-personalized vaccines [18].

Considering the aggressive nature of glioma tumors and the low survival rate using conventional treatment, it is important to develop novel treatment methods such as immunotherapies and vaccines to improve management of glioma patients and increase their survival. In this regard, it seems necessary to evaluate efficacy and safety of studied vaccines to compare different types of vaccines and their effects on survival od glioma patients. Based on our knowledge, no meta-analysis has been conducted for evaluation of pooled efficacy and safety of glioma vaccines and also subgroup analysis for comparison of various vaccine types. In this regard, we aim to compare efficacy and safety of studied vaccines in published articles of performed clinical trials with conventional therapeutic methods of glioblastoma. We believe that the results will provide information helpful about vaccine compartments and the outcomes of patients that can be used for designing more efficient vaccines in the future. In addition, we aim to compare the efficacy of personalized and non-personalized vaccines using survival duration in the present meta-analysis.

METHODS

Search Strategy

We followed the strategy of Preferred reporting Initiative for Systematic review and Meta-analysis (PRISMA) guidelines in the present meta-analysis. Searching publications was done in PubMed, Cochrane Library, Embase, and ClinicalTrials.gov initiating from November 2022 and ended in March 2023. We used keywords including “glioblastoma,” “GBM,” “glioma,” “brain tumor,” “vaccine,” “dendritic cell,” “peptide vaccine,” cancer vaccine,” and “personalized” in different combinations. There was no limitation on the publication date in the screening process. In order to have a comprehensive search, the reference

lists of found publications were reviewed. Two reviewers performed searching process independently and the final lists were checked while any disagreement between them was solved by a third reviewer.

Inclusion and Exclusion Criteria

Inclusion criteria for this meta-analysis included: 1- patients diagnosed with glioma (Grade I, II, III and IV glioma patients), 2- glioma patients treated with vaccines following surgery, chemotherapy, and radiotherapy, 3- clinical trials, 4- control or historical control groups availability, 5- control groups treatment with convention treatments, 6- overall survival (OS) rate and duration report, 7- follow-up period of at least 2 years, 8- studies published in English.

The studies which 1. were duplicates, conference letters, registered trials with no published articles, letters, or articles with no available full text, 2. were animal or cell culture studies, were excluded from this study. In case of any disagreements between researchers regarding the inclusion and exclusion criteria, it was resolved by discussing details and agreement was obtained.

Data Extraction

Data was extracted from the finally included studies independently by two different authors. Any disagreement between authors was resolved with the presence of third author and the process continued after achieving the agreement. Author name, year, number of patients in control and vaccine groups, age, sex, overall survival rate (OS), progression free survival (PFS) rate, survival duration, tumor grade, primary or recurrent tumor, and vaccine cycles were the collected characteristics. After data collection, differences were assessed and discussed to reach agreement. For those studies which used historical control, the references were also evaluated and used for direct data extraction.

Quality Assessment

Considering the potential errors caused by study design and implementation that can influence the quality of results in systematic review, quality of assessment is performed to reduce the risk of bias as much as possible. The risk of bias of included studies were evaluated for phase I/II clinical trials using Cochrane risk of bias tool, The Risk of Bias in Non-randomized Studies—Of Interventions (ROBINS-I). For quality assessment, the questions in seven domains including "Bias due to confounding," "Bias in selection of participants into the study," "Bias in classification of interventions," "Bias due to deviations from intended interventions," "Bias due to missing data," "Bias in measurement of outcomes," "Bias in selection of the reported results," and overall bias. In order to achieve an exact judgment about the studies, we referred the guidelines of ROBINS-I tool [19].

Data Analysis

Data analysis was performed using Rstudio and R (version: 4.2.1). Various packages including metaforest (version: 0.3.1), dmetar (version: 0.9000), meta (version: 6.2-0), and metafor (version: 2) were used in order to perform meta-analysis and drawing graphs. Risk Ratio (RR) was used for comparison of efficacy of vaccines to the control groups using OS rate and PFS rate as continuous data. In addition, standard mean difference (SMD) was used to compare survival duration between vaccinated and control groups. In addition, survival duration was used for subgroup meta-analyses. The significance level for effect sizes for all assessments was considered as $p < 0.05$. In addition, heterogeneity was assessed using Dixons Q-test and the *I*-squared (I^2) statistical tests. In case no heterogeneity was found in the results ($I^2 < 50\%$, $p \leq 0.1$), the fixed model was used for meta-analysis; whereas if the heterogeneity was high ($I^2 < 50\%$, $p \leq 0.05$), the random effect model was applied. In the following, we used subgroup analysis. The funnel plot was used for assessment of publication bias via the signs of asymmetry. Sensitivity analysis was used to evaluate the stability of the results that determines the effect of removal of each study on the meta-analysis results.

RESULTS

Eligible Studies

Searching for eligible studies was done in databases (Embase, PubMed, Google Scholar, and ClinicalTrials.gov) and it yielded 346 studies, primarily. Duplicates exclusion was performed before screening leading to the removal of 193 articles. Abstract screening of remaining 153 records led to removal of 100 of them because there were no full text articles available (10 records), registered clinical trials but no articles published (66 records), and studies on vaccines of cancers other than glioma (24 records). The methodology of remaining 53 articles were reviewed and studies without measurable results and outcomes, or those which did not complete the trial were excluded. Finally, 12 phase I/II clinical trials met all the inclusion criteria and included in the present meta-analysis [12–16, 20–28]. The process of article selection was performed based on the PRISMA flow as shown in **Figure 1**.

Characteristics Collection

A total of 289 patients with glioma from different grades [68 low grade glioma (LGG), 221 high grade glioma (HGG)] were included in this study, among which 52 were recurrent and 237 were primary cases. The average Karnofsky Performance Status (KPS) of patients was 70%, while patients received normal treatments including surgery followed by radiotherapy and chemotherapy before receiving vaccines dosage. Vaccine dosage and administration showed a wide variety between included studies, so that injection cycles were variable between 1 and 20 times and similarly the duration of vaccination were variant between 1 and 24 weeks. In all included studies, vaccination was initiated at least 2 weeks after completion of routine treatments. The follow-up period after vaccination was different between 40 and 240 weeks, however, 2 years (96 weeks) follow-up was applied in most of

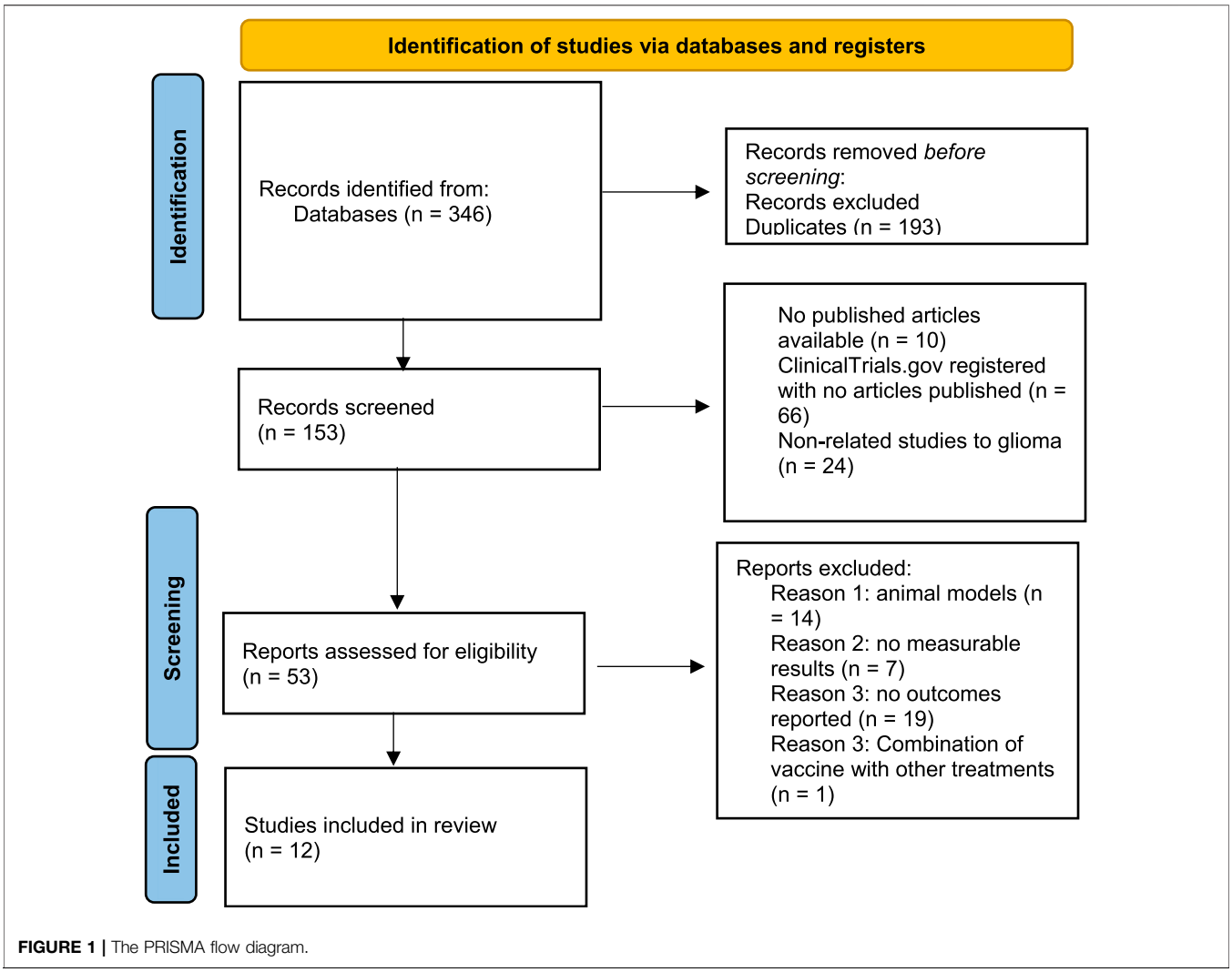

FIGURE 1 | The PRISMA flow diagram.

the studies. No limitations were considered for publication date of included studies. According to the results of primary statistical analysis, no significant difference was found between age and sex of subjects between the included studies (**Table 1**).

Quality Assessment of Included Studies

Since all the included studies were Phasel/ll CTs, ROBINS-I tool was used for quality assessment of 13 included studies. Seven studies used historical controls as the control groups, while the remaining 5 studies had control groups. In none of the studies, randomization process was mentioned for group deviations, while all participants were aware of their treatment process. In terms of outputs, OS rate was reported in all 12 studies, but PFS rate was reported in 9 of included studies. Detailed information is mentioned in **Table 1**. In addition, adverse effects reported in included studies were not the same in all studies and accordingly, the adverse effects which were mentioned in more than two studies were used for safety assessment (**Figure 2**).

Efficacy

OS

The rate of OS was used to evaluate the efficacy of vaccination in the included studies within 2 years follow-up. Accordingly, OS rate for 2 years follow-up was extracted for the studies which reported even longer follow-up time. Results of the meta-analysis revealed a median heterogeneity rate (I^2 = 52.3%), while the risk ratio (RR) was obtained equal to 2.283 (95% CI: 1.671–3.118) indicating that vaccination leads to increase in the number of survived patients within 2 years follow-up significantly (p-value < 0.0001) (**Figure 3A**). Assessment of RR for each of included studies revealed that highest RR was found for [22] (RR = 11.17, 95% CI: 2.460–50.225) who reported 37.5% of OS rate after 2-year follow-up and 18% OS rate after 5-year follow-up, and lowest RR was obtained for [16] (RR = 1.380, 95% CI: 0.936–2.035) who reported 27% OSR after 2 years follow-up.

PFS

In addition, progression free survival (PFS) rate was used to evaluate the efficacy of vaccination in recurrence of glioma.

TABLE 1 | Collected characteristics from included studies.

Row	Study	Sample size	Mean age	Sex (Male %)	WHO grade	Primary or recurrent	Prior treatment	Vaccine type	Follow-up duration (Weeks)	2 years OS rate (%) Intervention/ Control	Control
1	Terasaki, 2011	12	61	74.95	I/II	Recurrent	RT/TMZ RT/ACNU RT/ACNU/VCR Repeat Surgery, TMZ	Peptide/PM	96	83/26	573 [42]
2	Schijns, 2015	9	50.1	55.5	III/IV	Recurrent	RT TMZ Bevacizumab (Avastin)	Gilovac/PM	40	77/10	39 [43]
3	Ishikawa, 2007	5	50.41	33.3	III/IV	Recurrent	Surgery ACNU	AFTV	96	40/0	7
4	Moviglia, 2008	4	52.6	58.3	III/IV	Recurrent	Surgery, RT	glioms ma cell B-lymphocyte hybrid (TBH) mixed lymphocyte culture (MLC)	96	35/0	8
5	Sampson, 2009	12	43.75	66.6	III/IV	Primary	RT, TMZ, CW	DC	240	50/42	1578 [44]
6	Chang, 2011	16	44.5	47.05	III/IV	Recurrent	Surgery	DC	138	37.5/3.2	63
7	Cho, 2011	12	52.11	44	III/IV	Primary	Surgery, CCRT, Temadol	DC	132	44.4/18.75	16
8	Phuphanich, 2013	20	44.2	60	III/IV	Primary/ Recurrent	Surgery, RT, TMZ, Avastin	DC	160	55.6/0	—
9	Ishikawa, 2014	24	48	70.8	I/II	Primary	Surgery, RT, TMZ	AFTV	96	50/24	40 [45]
10	Wen, 2019	75	57.4	54.3	III/IV	Primary	RT, TMZ	DC/PM	48	21/3	43
11	Hu, 2021	36	54	64.35	I/II	Primary/ Recurrent	Surgery, RT, TMZ	DC	15	92/42 () 100/42 ()	369 [46]
12	Bota, 2022	60	59	70	III/IV	Primary	Surgery, TMZ, bevacizumab	TIC/PM		27/15	833 [47] 458 [48] 978 [49] 573 [50]

Abbreviations: ACNU, nimustine hydrochloride; TMZ, temozolomide; RT, radiation therapy; VCR, vincristine; PM, personalized Medicine; PR, partial response; NC, no change; PD, progressive disease; DC, dendritic cell-based vaccine; NR, not reported; AFTV, autologous formalin fixed tumor vaccine; CW, carmustine wafer; CCRT, combined chemotherapy and radiotherapy; TIC, tumor initiating cell.

According to the results, pooled RR of PFS rate for nine studies was obtained as 2.866 (95% CI: 1.634–5.028), meaning that PFS rate in patients treated with vaccines after conventional treatment within 2 years follow up was significantly higher than patients who were treated only with conventional treatments (p-value < 0.001), though heterogeneity for this analysis was high (I^2 = 83.3%) (**Figure 3B**).

Survival Duration

Survival duration was also used for meta-analysis and evaluate the efficacy of studied vaccines. Standard mean difference (SMD) was used to compare survival duration between vaccinated and control or historical control groups for each study and pooled SMD was obtained as 6.845 (95% CI: 2.676–11.014). This result shows a significant positive effect of vaccination on survival time in comparison with patients who underwent only conventional treatment (p-value < 0.001) (**Figure 3C**). According to the results, the biggest SMD was reported by [12] as 8.904, [21] as 8.594, and [23] as 8.179, who reported the highest survival duration as 25, 28.19, and 38.4 months, respectively.

Safety

Safety assessment was performed in this meta-analysis using the rate of Grade 1–3 of Treatment Related Adverse Events (TRAEs) including fever, headache, flu-like symptoms, lymphopenia, injection site reactions, vomiting, and diarrhea. The extracted data for safety assessment has been summarized in **Table 2**.

Meta-analysis of skin reaction after vaccination showed low between-study heterogeneity (I^2 = 0.0%). The pooled RR for skin reaction was higher than control groups (RR = 3.654; 95% CI: 1.711–7.801), and it was statistically significant (p-value = 0.0058) (**Figure 4A**). Assessment of pooled RR for flu-like syndrome revealed low between-study heterogeneity (I^2 = 0.0%), while this adverse effect was significantly higher in vaccinated groups compared to the control groups (RR = 5.21, 95% CI: 2.691–10.086) (p-value = 0.0009) (**Figure 4B**). RR was also calculated for lymphopenia which was considered as a serious

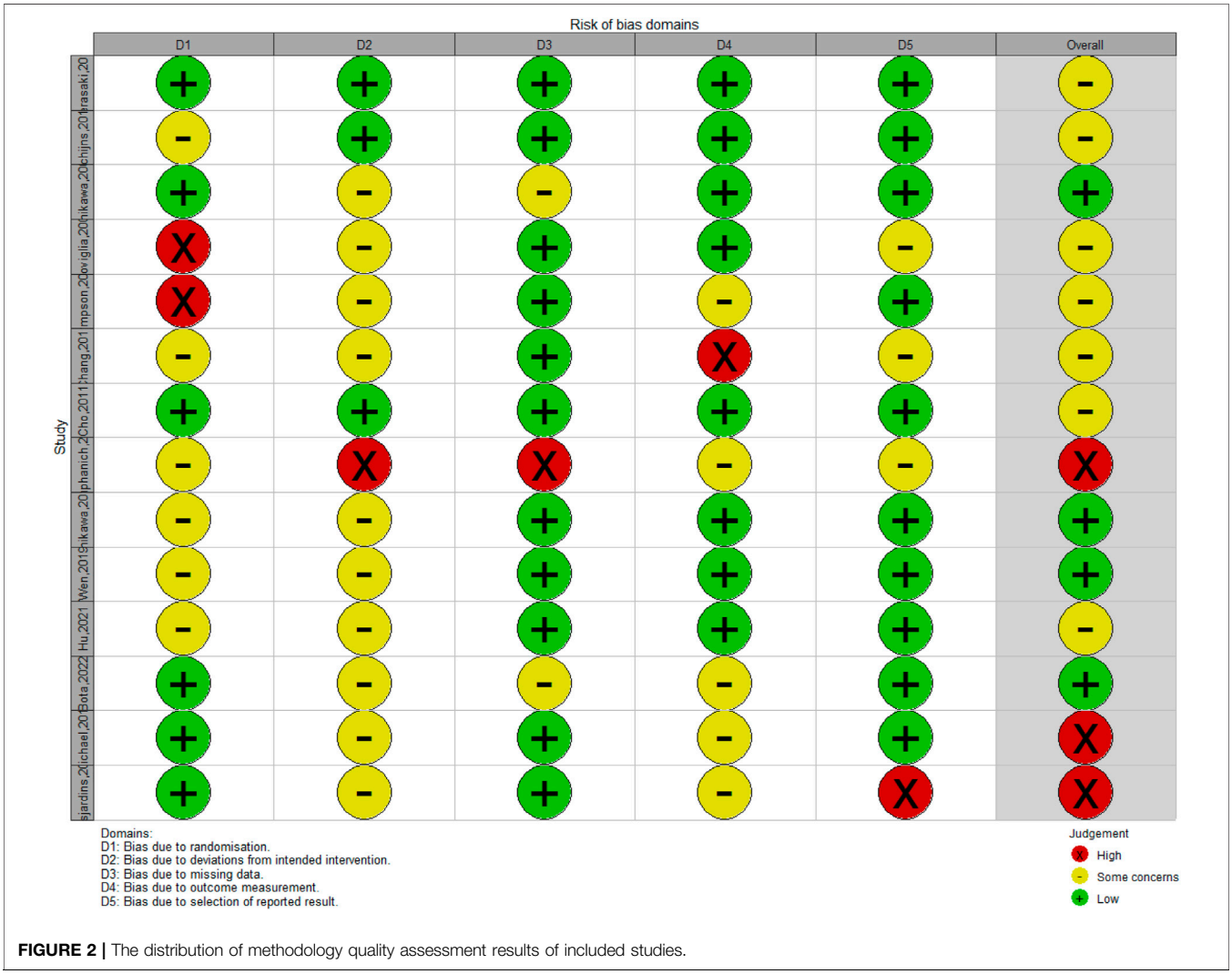

FIGURE 2 | The distribution of methodology quality assessment results of included studies.

problem after vaccination and the results revealed high between-study heterogeneity (I^2 = 91.4%). The obtained results demonstrated that gastrointestinal symptoms do not appear significantly more frequent than the control group (RR = 21.962, 95% CI: 0.322–1497.67) (p-value = 0.112) (**Figure 4C**).

Subgroup Analysis

Sensitivity analysis results did not demonstrate significant differences omitting each of studies. Accordingly, subgroup analysis was performed based on all the factors that have the potential to influence the results of efficiency of the vaccines. Subgroup analysis was performed based on the different factors including vaccine type, glioma grade, primary or recurrent tumor, and personalized vaccine characteristics.

Vaccine Type

In the subgroup of vaccine type, mean survival duration was compared between vaccinated and control groups in four subgroups including peptide, AFTV, DC, and other (including Gliovac, B cell hydroma, and tumor initiating cell). The pooled SMD for peptide, DC, and other subgroups revealed that vaccination increased survival duration in all subgroups (22.75, 2.96, and 2.41, respectively) (p-value < 0.01); however, although pooled SMD for AFTV showed increase in mean survival time, the difference was not statistically significant (SMD = 4.72, p-value = 0.1) (**Figure 5A**).

Tumor Type

The subgroup analysis was performed to assess the efficacy of vaccination on primary and recurrent tumors, separately. According to the results, pooled SMD for recurrent subgroup was highly effective (SMD = 8.148) and this effect was statistically significant (p-value < 0.01). The results of this subgroup analysis for primary tumors showed smaller SMD (SMD = 2.41) than recurrent subgroup, but it was still significant (p-value = 0), indicating that vaccination is also effective for primary tumors (**Figure 5B**). These results mean that vaccination leads to

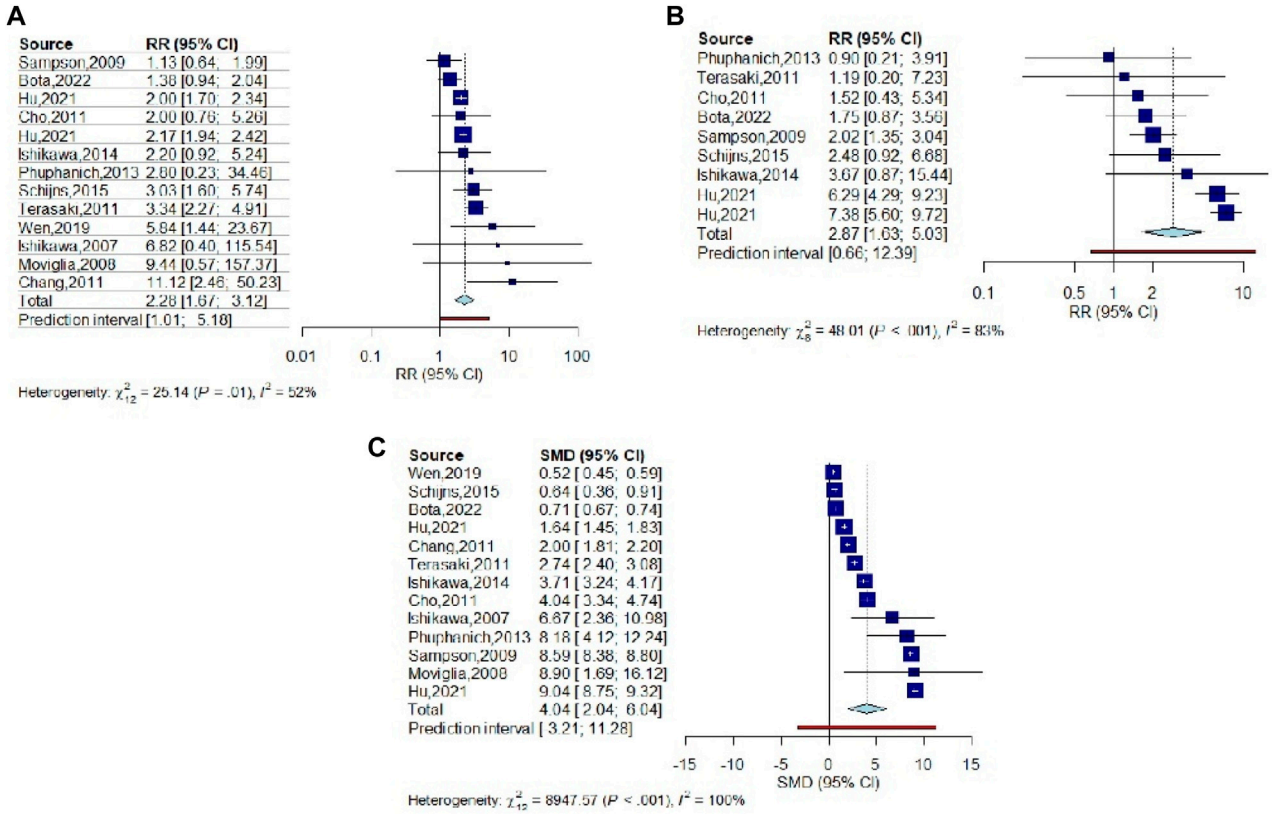

FIGURE 3 | Forest plot for RR of OS rate in vaccinated glioma patients. **(A)** Meta-analysis of OS rate for 2 years follow-up (RR: 2.283, 95% CI: 1.671–3.118), **(B)** Meta-analysis of PFS rate for 2 years follow-up (RR: 2.866, 95% CI: 1.634–5.028), and **(C)** Meta-analysis of survival duration for vaccinated GBM patients compared to unvaccinated patients (SMD: 6.845, 95% CI: 2.676–11.014).

TABLE 2 | Adverse events reported in the included studies.

Study	Flu-like symptoms (%)	Encephalopathy	Headache (%)	Skin reactions (%)	Gastrointestinal (%)	Lymphopenia (%)	Pruritus (%)
Terasaki, 2011	NR	NR	NR	50, Grade 1 33.3 Grade 2 16.7, Grade 3	NR	16.7 Grade 1	16.7, Grade 2
Schijns, 2015	NR	NR	22	60, Grade 1	NR	NR	NR
Ishikawa, 2007	66.7, Grade 2	NR	NR	22.2, Grade 2	NR	NR	NR
Moviglia, 2008	50, Grade 1	16.7, Grade 1 33.4, Grade 2 16.7, Grade 4	NR	NR	NR	NR	NR
Sampson, 2009	NR	NR	NR	33.3, Grade 1	NR	NR	NR
Chang, 2011	NR	NR	NR	NR	NR	29.5, Grade 1 and 2 29.5, Grade 3 and 4	NR
Cho, 2011	NR	NR	NR	NR	NR	5.9, Grade 1	NR
Phuphanich, 2013	36, Grade 1	NR	NR	9, Grade 1	18, Grade 2	NR	18, Grade 2
Ishikawa, 2014	2, Grade 1	NR	NR	21, Grade 1 and 2	7, Grade 1 and 2	8, Grade 1 and 2	2.8, Grade 1
Wen, 2019	NR	57.5, Grade 2 and 3	8.8, Grade 1	NR	21.3, Grade 1	NR	NR
Hu, 2021	16.7, Grade 1 and 2	NR	NR	50, Grade 1 and 3	2.8, Grade 1	NR	NR
Bota, 2022	54.4, Grade 1 and 2	36.8, Grade 1 and 2	NR	15.8, Grade 1 and 2	38, Grade 1 and 2	NR	10.5, Grade 1

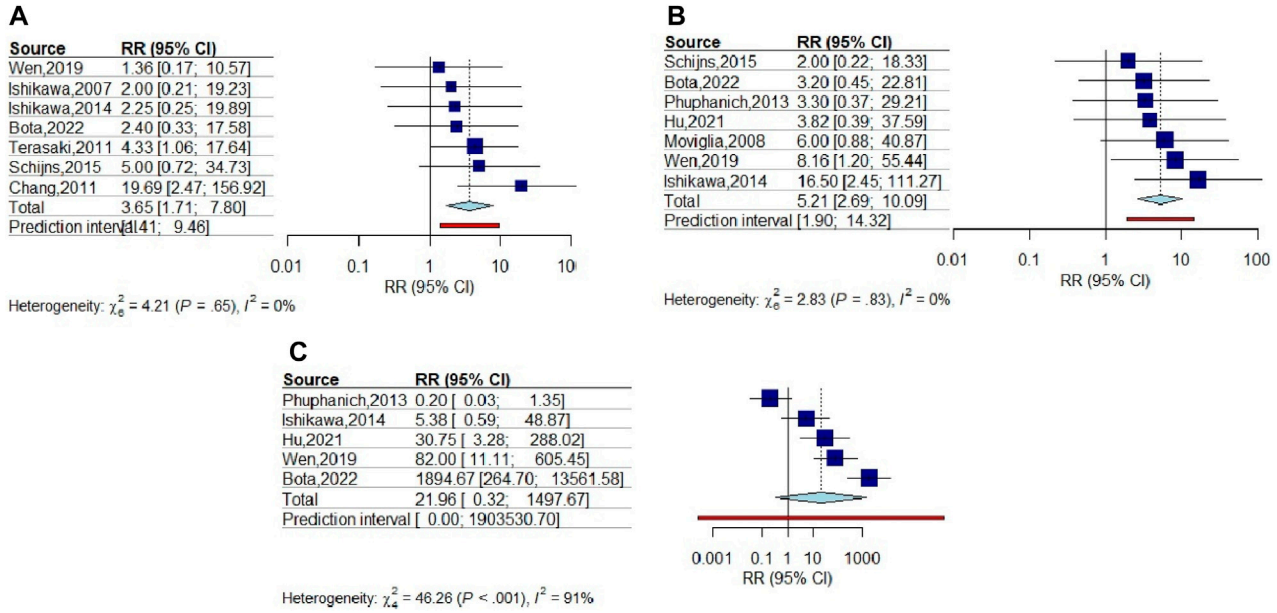

FIGURE 4 | Forest plots of skin reaction, flu-like syndrome, and gastrointestinal symptoms after vaccination of glioma patients. **(A)** Meta-analysis of skin reaction (RR = 3.654; 95% CI: 1.711–7.801), **(B)** Meta-analysis of flu-like syndrome (RR = 5.21, 95% CI: 2.691–10.086), and **(C)** Meta-analysis of lymphopenia (RR = 21.962, 95% CI: 0.322–1497.67). For all the analyses, the significance level of $p \leq 0.05$ was considered.

drastically longer survival duration in recurrent glioma patients compared to those who undergone only conventional treatments.

Glioma Grade

Assessment of vaccination efficacy based on the tumor grade was also performed. For this analysis, WHO grade I/II glioma were classified in low grade glioma (LGG) group and WHO grade III/IV were classified in the high-grade glioma (HGG) group. The results of SMD for survival duration showed that in HGG subgroup, vaccination has led to increase in survival duration (SMD = 14.09, p-value < 0.01) more effectively than LGG subgroup (SMD = 1.45, p-value < 0.01). Noteworthy, the pooled SMD for both groups are statistically significant (**Figure 5C**).

Personalized Approach

The efficacy assessment of vaccines which were manufactured based on personalized approaches was performed in PM subgroup analysis. The results of this subgroup analysis demonstrated that PM vaccines lead to longer survival duration than control groups who underwent only conventional treatments (SMD = 6.13, p-value < 0.01); however, the pooled SMD for non-PM vaccines was slightly smaller than PM vaccines but it also demonstrated statistically significant effect on survival duration (SMD = 4.34, p-value < 0.01) (**Figure 5D**).

Publication Bias

Funnel plot analysis for assessment of vaccine effectiveness on the OS rate and PFS rate showed a significant asymmetric distribution (**Figures 6A, B**). The Egger linear regression test results revealed no potential publication bias for OS rate (I^2 = 49.84%, H^2 = 1.99, R^2 = 57.87%) and PFS rate (I^2 = 67.11%, H^2 = 3.04, R^2 = 0.00%) between included studies.

DISCUSSION

Based on our knowledge, the present meta-analysis is the first one which evaluates the effectiveness of various types of vaccines against gliomas. Although it has been mentioned that immunotherapy using vaccines is an effective method for gliomas, there are still uncertainties about their efficacy and advantages above conventional treatments [17]. Previous reviews have discussed the efficacy of glioma vaccines in terms of immune responses and cytotoxicity and the need for longer terms of assessments and larger populations are emphasized [29]. In general, the pooled RR in this study showed that not only 2-year OS rate, but also PFS rate in vaccinated groups was significantly higher than conventional treatments. In addition, we showed that OS rate of vaccinated patients, without considering the type of vaccine, was higher than patients treated using conventional methods.

Peptide vaccines are known as effective candidates for glioma immunotherapy, because they can be used for specific targets in cells such as mutated and overexpressed genes and result in improved prognosis in malignant glioma [30, 31]. The previous studies showed that targeting key oncogenes in malignant gliomas as an effective immunotherapy method for longer survival duration and higher OS rate while mild adverse effects are observed after vaccination [32]. Our results of subgroup analysis showed that peptide vaccines result in a

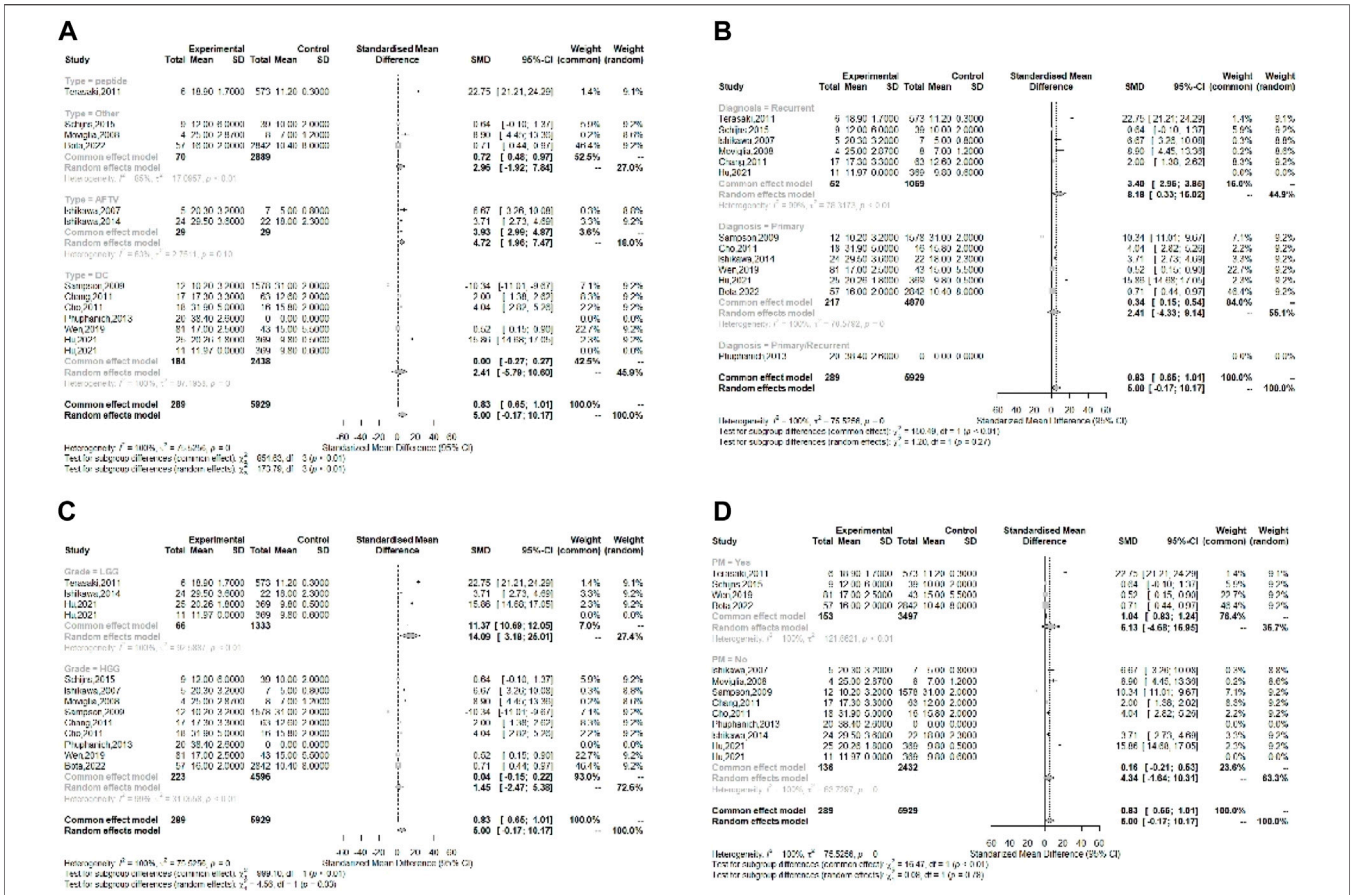

FIGURE 5 | Subgroup Forest plot of OS duration based on the subgroups including **(A)** Vaccine types (peptide (SMD = 22.75), AFTV (SMD = 4.72), DC (SMD = 2.41), and others (SMD = 2.69), **(B)** Tumor diagnosis (Primary (SMD = 8.18) and Recurrent (SMD = 2.41)), **(C)** Tumor Grade (HGG (SMD = 14.09) and LGG (SMD = 1.45)), and **(D)** Personalized approach for vaccine production (Personalized (SMD = 6.13), and Non-Personalized (SMD = 4.34)).

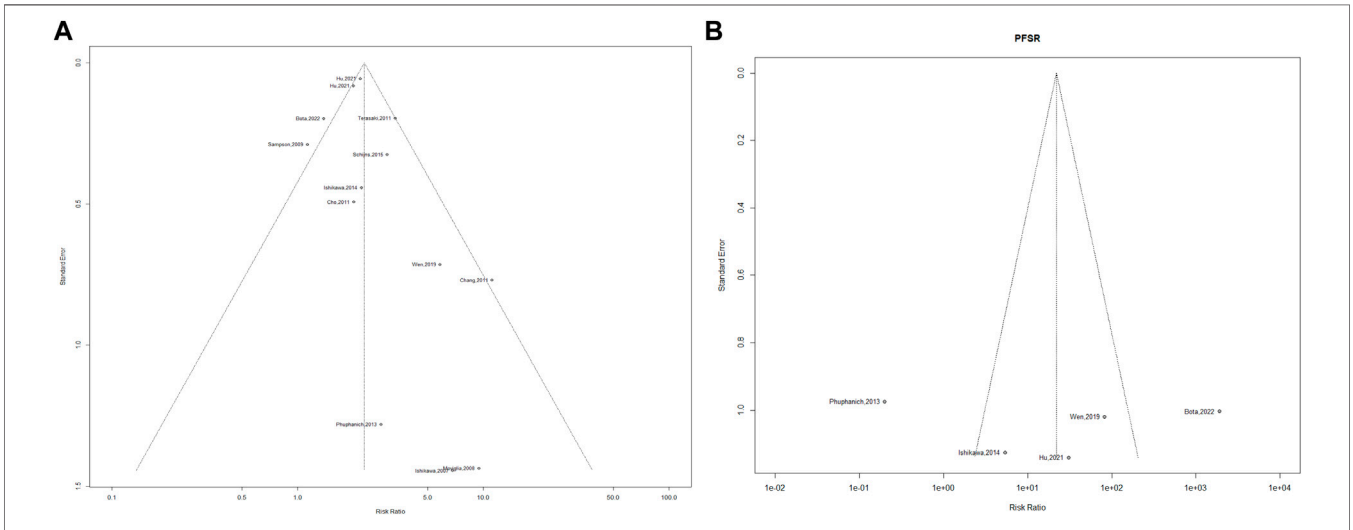

FIGURE 6 | Publication bias. **(A)** OS, Beggs test, *p*-value = 0.032, **(B)** PFS, Beggs test, *p*-value = 0.390.

significantly longer survival duration in comparison with patients treated only with usual methods. Noteworthy, designing peptide vaccines using novel methods such as machine learning and deep learning algorithms along with specific delivery systems for these vaccines in order to increase the immunogenicity still remain as challenging concerns about peptide vaccines [33]. Considering the potential of peptide vaccines, designing personalized peptide vaccines via genomics data of patients seems a necessity in cancer vaccines which should be focused on more [34].

Dendritic cell vaccines are known as promising vaccines for induction of immune response in glioma cells and also increase their sensitivity for chemotherapy [35]. In this regard, Wang et al. meta-analyzed six clinical trials to evaluate the efficacy of dendritic cell-based vaccines for malignant glioma and their results showed longer survival duration and 2 years survival rate for vaccinated patients [36]. The efficacy of antigen pulsed dendritic cell was meta-analyzed for HGG patients and their results showed no improvement in neither KPS performance nor lymphocytes percentages, while INFγ showed higher level in DC treated patients [37]. The results of this study challenged the results of previous meta-analysis and led to rise more uncertainties in terms of DC-based vaccines. However, a current meta-analysis showed efficacy of DC therapy for malignant gliomas and immune responses via induction of $CD8^+$ T cells, while they also reported fatigue as most common adverse effects of this treatment method [38]. Considering that these studies focused on only DC-based therapies, these vaccines were not compared to other vaccines before. Our results of subgroup analysis showed that although DC-based vaccines are among the most common vaccines against malignant glioma, but the increase in survival duration in DC-based vaccine group was smaller than other vaccine types. Accordingly, it seems that more clinical trials with larger populations are required to compare the effects of these vaccines with other types of vaccines.

The effectiveness of autologous formalin fixed vaccines has been shown for various cancers such as hepatocellular carcinoma, breast cancer, etc. The results of these studies showed promising efficacy for AFTV for treatments of cancers and especially metastatic cancers which lead to higher OS and PFS rates. In the present meta-analysis, AFTV showed large increase in OS and PFS rates and also leads to longer survival duration. Comparison of AFTV with other vaccines showed better effect on survival duration than CD-based vaccines and other vaccines which included B cell Hydroma and TIC vaccines. Altogether, these findings shed light on the more efficient compartments of the vaccines on the survival of glioma patients. On the other hand, the results obtained in all types of studies showed better OS rate than conventional treatments. These findings show the potential of vaccines to be added to the conventional treatment process of glioma patients in order to increase survival duration of patients. However, more studies and phase II and pahseIII clinical trials are required to show the reliability of vaccines in terms of efficacy and safety using bogger populations.

In terms of safety, meta-analysis of adverse effects including flu-like syndrome, gastrointestinal symptoms, and skin reaction for vaccination in comparison with patients who underwent only usual treatments showed that the frequency of skin reaction and flu-like syndrome was not significantly more in vaccinated patients than control groups. However, gastrointestinal symptoms showed higher prevalence in vaccinated patients in comparison with control groups. Considering that vomiting and diarrhea can lead to serious problems in glioma patients and disturb vaccination process, improvement of vaccines formulation in order to reduce gastrointestinal symptoms seems necessary for future vaccines.

Personalized medicine, as the novel and growing area in medicine, is known as a hope for development of efficient treatment methods for cancer treatment. Personalized vaccines are designed based on the genomics data of each patient and show efficacy and safety for patients [39]. Despite the glory of personalized medicine, the application of this immunotherapy method has several challenges such as optimized dosage, potential adverse effects, factors influencing immune response, etc [40]. Accordingly, lots of uncertainties arise related to personalized vaccines. In the present study, we performed a subgroup analysis to compare the effect of conventional vaccines and personalized vaccines on the survival duration in glioma patients. The results showed that although the number of studies which used personalized vaccines and accordingly, the number of subjects were less than conventional vaccines, but pooled SMD for personalized vaccines was higher than conventional vaccines. Noteworthy, these results obtained for a heterogenous vaccines group including DC-based, AFTV, and peptide vaccines. Therefore, we claim that personalized vaccines show promising effects on survival duration in glioma patients; however, we propose studying the effect of personalized vaccines on larger populations in randomized clinical trials to compare various types of personalized vaccines in terms of efficacy and safety.

We faced limitations in terms of number of subjects enrolled in the included studies, comparison of present results with historical controls. Considering that included studies were mainly in early phase clinical trials, this limitation caused a challenge in terms of study population. In addition, not all the included studies reported adverse effects. It is suggested to add all types of adverse effects into the studies in the future and report all versions of adverse effects. In addition, it is important to consider the severity and frequency of the adverse effects of vaccines in the future studies, since almost all mentioned studies reported the number of patients who showed or did not show adverse effects. It has been mentioned that using vaccines against glioma has shown efficacy; however, conducting phase III clinical trials which bring certainty into the field of vaccine therapy for glioma is necessary [34, 41]. In addition, since vaccination is a type of immunotherapy, lymphocyte percentage data and other related assessments of immunogenicity of vaccines were rarely considered in the assessed studies, while it seems highly important for

comparison of vaccines and their efficacy. It remains as another question which should be addressed in the future clinical trials. We suggest more studies in the future based on the findings of the present meta-analysis to compare different vaccine types or compartments of vaccines on the survival duration of glioma patients. We believe that our findings are highly valuable for future studies, but more comprehensive studies with larger populations are required to prove the results of the present systematic review and meta-analysis.

CONCLUSION

In conclusion, the present meta-analysis explains the efficacy and safety of available vaccines and personalized vaccines for treatment of malignant glioma patients in comparison with patients who underwent only conventional treatments including RT, chemotherapy, or TMZ after surgery. We also showed higher efficacy of personalized vaccines than conventional vaccines in increasing OS in glioma patients. Peptide vaccines and dendritic cell-based vaccines are among the most popular vaccines for malignant glioma, but novel vaccines are also being developed with high efficacy. Based on the results of this meta-analysis, designing personalized vaccines and evaluation of efficacy for vaccine treatments in Phase III clinical trials are suggested.

DATA AVAILABILITY STATEMENT

Data presented in this article was extracted from articles and they were used for meta-analysis in this systematic review and meta-analysis. Accordingly there is no repository or link for this data. The articles used in this study are listed in the article.

AUTHOR CONTRIBUTIONS

All authors listed have made a substantial, direct, and intellectual contribution to the work and approved it for publication.

FUNDING

The authors declare that no financial support was received for the research, authorship, and/or publication of this article.

CONFLICT OF INTEREST

The authors declare that the research was conducted in the absence of any commercial or financial relationships that could be construed as a potential conflict of interest.

REFERENCES

1. Ostrom QT, Bauchet L, Davis FG, Deltour I, Fisher JL, Langer CE, et al. The Epidemiology of Glioma in Adults: A "State of the Science" Review. *Neuro-Oncology* (2014) 16(7):896–913. doi:10.1093/neuonc/nou087
2. Louis DN, Ohgaki H, Wiestler OD, Cavenee WK, Burger PC, Jouvet A, et al. The 2007 WHO Classification of Tumours of the Central Nervous System. *Acta Neuropathologica* (2007) 114(2):97–109. doi:10.1007/s00401-007-0243-4
3. Huang LE. Impact of CDKN2A/B Homozygous Deletion on the Prognosis and Biology of IDH-Mutant Glioma. *Biomedicines* (2022) 10(2):246. doi:10.3390/biomedicines10020246
4. Khan MN, Sharma A, Pitz M, Loewen S, Quon H, Poulin A, et al. High-Grade Glioma Management and Response Assessment—Recent Advances and Current Challenges. *Curr Oncol* (2016) 23(4):383–91. doi:10.3747/co.23.3082
5. Śledzińska P, Bebyn M, Furtak J, Koper A, Koper K. Current and Promising Treatment Strategies in Glioma. *Rev Neurosciences* (2022) 34:483–516. doi:10.1515/revneuro-2022-0060
6. Oh T, Sayegh ET, Fakurnejad S, Oyon D, Lamano JB, DiDomenico JD, et al. Vaccine Therapies in Malignant Glioma. *Curr Neurol Neurosci Rep* (2015) 15:508–7. doi:10.1007/s11910-014-0508-y
7. Zhong H, Shurin MR, Han B. Optimizing Dendritic Cell-Based Immunotherapy for Cancer. *Expert Rev Vaccin* (2007) 6(3):333–45. doi:10.1586/14760584.6.3.333
8. Yamanaka R. Dendritic-Cell-And Peptide-Based Vaccination Strategies for Glioma. *Neurosurg Rev* (2009) 32(3):265–73. doi:10.1007/s10143-009-0189-1
9. Schneble E, Clifton GT, Hale DF, Peoples GE. Peptide-Based Cancer Vaccine Strategies and Clinical Results. *Methods Mol Biol* (2016) 1403:797–817. doi:10.1007/978-1-4939-3387-7_46
10. Vermaelen K. Vaccine Strategies to Improve Anti-Cancer Cellular Immune Responses. *Front Immunol* (2019) 10:8. doi:10.3389/fimmu.2019.00008
11. Ye T, Li F, Ma G, Wei W. Enhancing Therapeutic Performance of Personalized Cancer Vaccine via Delivery Vectors. *Adv Drug Deliv Rev* (2021) 177:113927. doi:10.1016/j.addr.2021.113927
12. Moviglia GA, Carrizo AG, Varela G, Gaeta CA, de Lima AP, Farina P, et al. Preliminary Report on Tumor Stem Cell/B Cell Hybridoma Vaccine for Recurrent Glioblastoma Multiforme. *Hematology/oncology Stem Cel Ther* (2008) 1(1):3–13. doi:10.1016/s1658-3876(08)50054-9
13. Terasaki M, Shibui S, Narita Y, Fujimaki T, Aoki T, Kajiwara K, et al. Phase I Trial of a Personalized Peptide Vaccine for Patients Positive for Human Leukocyte Antigen–A24 With Recurrent or Progressive Glioblastoma Multiforme. *J Clin Oncol* (2011) 29(3):337–44. doi:10.1200/jco.2010.29.7499
14. Cho D-Y, Yang WK, Lee HC, Hsu DM, Lin HL, Lin SZ, et al. Adjuvant Immunotherapy With Whole-Cell Lysate Dendritic Cells Vaccine for Glioblastoma Multiforme: A Phase II Clinical Trial. *World Neurosurg* (2012) 77(5–6):736–44. doi:10.1016/j.wneu.2011.08.020
15. Ishikawa E, Muragaki Y, Yamamoto T, Maruyama T, Tsuboi K, Ikuta S, et al. Phase I/IIa Trial of Fractionated Radiotherapy, Temozolomide, and Autologous Formalin-Fixed Tumor Vaccine for Newly Diagnosed Glioblastoma. *J Neurosurg* (2014) 121(3):543–53. doi:10.3171/2014.5.jns132392
16. Bota DA, Taylor TH, Piccioni DE, Duma CM, LaRocca RV, Kesari S, et al. Phase 2 Study of AV-GBM-1 (A Tumor-Initiating Cell Targeted Dendritic Cell Vaccine) in Newly Diagnosed Glioblastoma Patients: Safety and Efficacy Assessment. *J Exp Clin Cancer Res* (2022) 41(1):344–9. doi:10.1186/s13046-022-02552-6
17. Dai X, Jiang W, Wang W, Zhao S. Drug or Vaccine? Selecting the Appropriate Treatment for Malignant Glioma Patients. *Drugs* (2010) 70:1477–86. doi:10.2165/11538040-000000000-00000
18. Londhe VY, Date V. Personalized Neoantigen Vaccines: A Glimmer of Hope for Glioblastoma. *Expert Rev Vaccin* (2020) 19(5):407–17. doi:10.1080/14760584.2020.1750376
19. Sterne J. A. C. H. J., Higgins J, Reeves B. *A Cochrane Risk of Bias Assessment Tool: For Non-Randomized Studies of Interventions*. United States Environmental Protection Agency (EPA): ACROBAT-NRSI (2014). p. 24 (Version 1.0).
20. Ishikawa E, Tsuboi K, Yamamoto T, Muroi A, Takano S, Enomoto T, et al. Clinical Trial of Autologous Formalin-Fixed Tumor Vaccine for Glioblastoma

Multiforme Patients. *Cancer Sci* (2007) 98(8):1226–33. doi:10.1111/j.1349-7006.2007.00518.x
21. Sampson JH, Archer GE, Mitchell DA, Heimberger AB, Herndon JE, Lally-Goss D, et al. An Epidermal Growth Factor Receptor Variant III-Targeted Vaccine Is Safe and Immunogenic in Patients With Glioblastoma Multiforme. *Mol Cancer Ther* (2009) 8:2773–9. doi:10.1158/1535-7163.mct-09-0124
22. Chang C-N, Huang YC, Yang DM, Kikuta K, Wei KJ, Kubota T, et al. A Phase I/II Clinical Trial Investigating the Adverse and Therapeutic Effects of a Postoperative Autologous Dendritic Cell Tumor Vaccine in Patients With Malignant Glioma. *J Clin Neurosci* (2011) 18(8):1048–54. doi:10.1016/j.jocn.2010.11.034
23. Phuphanich S, Wheeler CJ, Rudnick JD, Mazer M, Wang H, Nuño MA, et al. Phase I Trial of a Multi-Epitope-Pulsed Dendritic Cell Vaccine for Patients With Newly Diagnosed Glioblastoma. *Cancer Immunol Immunother* (2013) 62:125–35. doi:10.1007/s00262-012-1319-0
24. Schijns VEJC, Pretto C, Devillers L, Pierre D, Hofman FM, Chen TC, et al. First Clinical Results of a Personalized Immunotherapeutic Vaccine Against Recurrent, Incompletely Resected, Treatment-Resistant Glioblastoma Multiforme (GBM) Tumors, Based on Combined Allo-And Auto-Immune Tumor Reactivity. *Vaccine* (2015) 33(23):2690–6. doi:10.1016/j.vaccine.2015.03.095
25. Löhr M, Freitag B, Technau A, Krauss J, Monoranu CM, Rachor J, et al. High-Grade Glioma Associated Immunosuppression Does Not Prevent Immune Responses Induced by Therapeutic Vaccines in Combination With T Reg Depletion. *Cancer Immunol Immunother* (2018) 67:1545–58. doi:10.1007/s00262-018-2214-0
26. Wen PY, Reardon DA, Armstrong TS, Phuphanich S, Aiken RD, Landolfi JC, et al. A Randomized Double-Blind Placebo-Controlled Phase II Trial of Dendritic Cell Vaccine ICT-107 in Newly Diagnosed Patients With Glioblastoma. *Clin Cancer Res* (2019) 25(19):5799–807. doi:10.1158/1078-0432.ccr-19-0261
27. Wang Q-T, Nie Y, Sun SN, Lin T, Han RJ, Jiang J, et al. Tumor-Associated Antigen-Based Personalized Dendritic Cell Vaccine in Solid Tumor Patients. *Cancer Immunol Immunother* (2020) 69:1375–87. doi:10.1007/s00262-020-02496-w
28. Hu JL, Omofoye OA, Rudnick JD, Kim S, Tighiouart M, Phuphanich S, et al. A Phase I Study of Autologous Dendritic Cell Vaccine Pulsed With Allogeneic Stem-Like Cell Line Lysate in Patients With Newly Diagnosed or Recurrent Glioblastoma. *Clin Cancer Res* (2022) 28(4):689–96. doi:10.1158/1078-0432.ccr-21-2867
29. Yan Y, Zeng S, Gong Z, Xu Z. Clinical Implication of Cellular Vaccine in Glioma: Current Advances and Future Prospects. *J Exp Clin Cancer Res* (2020) 39(1):257–18. doi:10.1186/s13046-020-01778-6
30. Huang Y, Wang Y, Huang Z. A Specific Peptide Vaccine Against IDH1 (R132H) Glioma. *Neurosci Bull* (2022) 38(2):223–5. doi:10.1007/s12264-021-00791-9
31. Yokota C, Kagawa N, Takano K, Chiba Y, Kinoshita M, Kijima N, et al. Maintenance of WT1 Expression in Tumor Cells Is Associated With a Good Prognosis in Malignant Glioma Patients Treated With WT1 Peptide Vaccine Immunotherapy. *Cancer Immunol Immunother* (2022) 71(1):189–201. doi:10.1007/s00262-021-02954-z
32. Fenstermaker RA, Ciesielski MJ, Qiu J, Yang N, Frank CL, Lee KP, et al. Clinical Study of a Survivin Long Peptide Vaccine (SurVaxM) in Patients With Recurrent Malignant Glioma. *Cancer Immunol Immunother* (2016) 65:1339–52. doi:10.1007/s00262-016-1890-x
33. Liu W, Tang H, Li L, Wang X, Yu Z, Li J. Peptide-Based Therapeutic Cancer Vaccine: Current Trends in Clinical Application. *Cel Prolif* (2021) 54(5):e13025. doi:10.1111/cpr.13025
34. Sasada T, Yamada A, Noguchi M, Itoh K. Personalized Peptide Vaccine for Treatment of Advanced Cancer. *Curr Med Chem* (2014) 21(21):2332–45. doi:10.2174/0929867321666140205132936
35. Luptrawan A, Liu G, Yu JS. Dendritic Cell Immunotherapy for Malignant Gliomas. *Rev Recent Clin Trials* (2008) 3(1):10–21. doi:10.2174/157488708783330530
36. Wang X, Zhao HY, Zhang FC, Sun Y, Xiong ZY, Jiang XB. Dendritic Cell-Based Vaccine for the Treatment of Malignant Glioma: A Systematic Review. *Cancer Invest* (2014) 32(9):451–7. doi:10.3109/07357907.2014.958234
37. Cao J-X, Zhang XY, Liu JL, Li D, Li JL, Liu YS, et al. Clinical Efficacy of Tumor Antigen-Pulsed DC Treatment for High-Grade Glioma Patients: Evidence From a Meta-Analysis. *PloS one* (2014) 9(9):e107173. doi:10.1371/journal.pone.0107173
38. Shamshiripour P, Nikoobakht M, Mansourinejad Z, Ahmadvand D, Akbarpour M. A Comprehensive Update to Dendritic Cell Therapy for Glioma: A Systematic Review and Meta-Analysis. *Expert Rev Vaccin* (2022) 21(4):513–31. doi:10.1080/14760584.2022.2027759
39. Sahin U, Türeci Ö. Personalized Vaccines for Cancer Immunotherapy. *Science* (2018) 359(6382):1355–60. doi:10.1126/science.aar7112
40. Shemesh CS, Hsu JC, Hosseini I, Shen BQ, Rotte A, Twomey P, et al. Personalized Cancer Vaccines: Clinical Landscape, Challenges, and Opportunities. *Mol Ther* (2021) 29(2):555–70. doi:10.1016/j.ymthe.2020.09.038
41. Maxwell R, Luksik AS, Garzon-Muvdi T, Lim M. The Potential of Cellular-And Viral-Based Immunotherapies for Malignant Glioma–Dendritic Cell Vaccines, Adoptive Cell Transfer, and Oncolytic Viruses. *Curr Neurol Neurosci Rep* (2017) 17:50–12. doi:10.1007/s11910-017-0754-x
42. Stupp R, Hegi ME, van den Bent MJ, Mason WP, Weller M, Mirimanoff RO, et al. Changing Paradigms—An Update on the Multidisciplinary Management of Malignant Glioma. *The Oncologist* (2006) 11(2):165–80. doi:10.1634/theoncologist.11-2-165
43. Barker FG, Chang SM, Gutin PH, Malec MK, McDermott MW, Prados MD, et al. Survival and Functional Status After Resection of Recurrent Glioblastoma Multiforme. *Neurosurgery* (1998) 42(4):709–19. doi:10.1097/00006123-199804000-00013
44. Curran WJ, Scott CB, Horton J, Nelson JS, Weinstein AS, Fischbach AJ, et al. Recursive Partitioning Analysis of Prognostic Factors in Three Radiation Therapy Oncology Group Malignant Glioma Trials. *JNCI: J Natl Cancer Inst* (1993) 85(9):704–10. doi:10.1093/jnci/85.9.704
45. Iversen TZ, Brimnes MK, Nikolajsen K, Andersen RS, Hadrup SR, Andersen MH, et al. Depletion of T Lymphocytes Is Correlated With Response to Temozolomide in Melanoma Patients. *Oncoimmunology* (2013) 2(2):e23288. doi:10.4161/onci.23288
46. Reardon DA, Brandes AA, Omuro A, Mulholland P, Lim M, Wick A, et al. Effect of Nivolumab vs Bevacizumab in Patients With Recurrent Glioblastoma: The CheckMate 143 Phase 3 Randomized Clinical Trial. *JAMA Oncol* (2020) 6(7):1003–10. doi:10.1001/jamaoncol.2020.1024
47. Gilbert MR, Wang M, Aldape KD, Stupp R, Hegi ME, Jaeckle KA, et al. Dose-Dense Temozolomide for Newly Diagnosed Glioblastoma: A Randomized Phase III Clinical Trial. *J Clin Oncol* (2013) 31(32):4085–91. doi:10.1200/jco.2013.49.6968
48. Chinot OL, Wick W, Mason W, Henriksson R, Saran F, Nishikawa R, et al. Bevacizumab Plus Radiotherapy–Temozolomide for Newly Diagnosed Glioblastoma. *New Engl J Med* (2014) 370(8):709–22. doi:10.1056/NEJMoa1308345
49. Gilbert MR, Dignam JJ, Armstrong TS, Wefel JS, Blumenthal DT, Vogelbaum MA, et al. A Randomized Trial of Bevacizumab for Newly Diagnosed Glioblastoma. *New Engl J Med* (2014) 370(8):699–708. doi:10.1056/NEJMoa1308573
50. Stupp R, Mason WP, van den Bent MJ, Weller M, Fisher B, Taphoorn MJ, et al. Radiotherapy Plus Concomitant and Adjuvant Temozolomide for Glioblastoma. *New Engl J Med* (2005) 352(10):987–96. doi:10.1056/NEJMoa043330

Copyright © 2024 Amanzadeh Jajin, Oraee Yazdani, Zali and Esmaeili. This is an open-access article distributed under the terms of the Creative Commons Attribution License (CC BY). The use, distribution or reproduction in other forums is permitted, provided the original author(s) and the copyright owner(s) are credited and that the original publication in this journal is cited, in accordance with accepted academic practice. No use, distribution or reproduction is permitted which does not comply with these terms.

Frontiers in Pharmacology

Explores the interactions between chemicals and living beings

The most cited journal in its field, which advances access to pharmacological discoveries to prevent and treat human disease.

Discover the latest Research Topics

See more →

Frontiers

Avenue du Tribunal-Fédéral 34
1005 Lausanne, Switzerland
frontiersin.org

Contact us

+41 (0)21 510 17 00
frontiersin.org/about/contact